



IntechOpen

**Nuclear Power**  
Deployment, Operation and Sustainability

*Edited by Pavel Tsvetkov*





---

# **NUCLEAR POWER – DEPLOYMENT, OPERATION AND SUSTAINABILITY**

---

Edited by **Pavel V. Tsvetkov**

## **Nuclear Power - Deployment, Operation and Sustainability**

<http://dx.doi.org/10.5772/704>

Edited by Pavel Tsvetkov

### **Contributors**

Takashi Kamei, Tamás János Katona, Rick Demmer, Dietmar Moeller, Rolf Bielecki, Behnam Taebi, Jacob Jacobson, Steven Piet, Gretchen Matthern, Vasily Glebov, Edward Kryuchkov, Anatoly Shmelev, Vladimir Apse, Gennadiy Kulikov, Sergey Masterov, Pavel V. Tsvetkov, E.G. Kulikov, Hiroki Shiotani, Kiyoshi Ono, Takashi Namba, Alexandru Cecal, Doina Humelnicu, Hadi Hamidian, Ying Fan, Lei Zhu, Zhaolin Wang, Greg Naterer, Michael Zentner, Magdi Ragheb, Steven R. Sherman, Collin Knight, Kazuo Furukawa, You-Shao Wang, Marcello De Falco, Gaetano Iaquaniello, Annarita Salladini, Martin Kalinowski, Sarah Von Kaminietz

### **© The Editor(s) and the Author(s) 2011**

The moral rights of the and the author(s) have been asserted.

All rights to the book as a whole are reserved by INTECH. The book as a whole (compilation) cannot be reproduced, distributed or used for commercial or non-commercial purposes without INTECH's written permission.

Enquiries concerning the use of the book should be directed to INTECH rights and permissions department ([permissions@intechopen.com](mailto:permissions@intechopen.com)).

Violations are liable to prosecution under the governing Copyright Law.



Individual chapters of this publication are distributed under the terms of the Creative Commons Attribution 3.0 Unported License which permits commercial use, distribution and reproduction of the individual chapters, provided the original author(s) and source publication are appropriately acknowledged. If so indicated, certain images may not be included under the Creative Commons license. In such cases users will need to obtain permission from the license holder to reproduce the material. More details and guidelines concerning content reuse and adaptation can be found at <http://www.intechopen.com/copyright-policy.html>.

### **Notice**

Statements and opinions expressed in the chapters are these of the individual contributors and not necessarily those of the editors or publisher. No responsibility is accepted for the accuracy of information contained in the published chapters. The publisher assumes no responsibility for any damage or injury to persons or property arising out of the use of any materials, instructions, methods or ideas contained in the book.

First published in Croatia, 2011 by INTECH d.o.o.

eBook (PDF) Published by IN TECH d.o.o.

Place and year of publication of eBook (PDF): Rijeka, 2019.

IntechOpen is the global imprint of IN TECH d.o.o.

Printed in Croatia

Legal deposit, Croatia: National and University Library in Zagreb

Additional hard and PDF copies can be obtained from [orders@intechopen.com](mailto:orders@intechopen.com)

Nuclear Power - Deployment, Operation and Sustainability

Edited by Pavel Tsvetkov

p. cm.

ISBN 978-953-307-474-0

eBook (PDF) ISBN 978-953-51-6045-8



# We are IntechOpen, the world's leading publisher of Open Access books Built by scientists, for scientists

4,000+

Open access books available

116,000+

International authors and editors

120M+

Downloads

151

Countries delivered to

Our authors are among the  
Top 1%

most cited scientists

12.2%

Contributors from top 500 universities



WEB OF SCIENCE™

Selection of our books indexed in the Book Citation Index  
in Web of Science™ Core Collection (BKCI)

Interested in publishing with us?  
Contact [book.department@intechopen.com](mailto:book.department@intechopen.com)

Numbers displayed above are based on latest data collected.  
For more information visit [www.intechopen.com](http://www.intechopen.com)





# Meet the editor



Dr. Tsvetkov is a faculty member at the Department of Nuclear Engineering, Texas A&M University. His research program is focused on high-fidelity predictive engineering of complex systems. System analysis and optimization methods for complex engineered systems enable development of advanced sustainable nuclear energy technologies towards “environmentally benign” system design and deployment. The integrated systems approach makes it possible to optimize choices for the system as a whole. Specific areas of investigative emphasis include nuclear system design, symbiotic nuclear energy systems, waste minimization, HTGRs and co-generation systems, and direct nuclear energy conversion systems. Dr. Tsvetkov leads and actively participates in numerous collaborative research projects as well as international educational programs. He has authored and co-authored more than 150 publications.



---

# Contents

---

**Preface XIII**

**Part 1 Nuclear Power Deployment 1**

Chapter 1 **Nuclear Naval Propulsion 3**  
Magdi Ragheb

Chapter 2 **Assessment of Deployment  
Scenarios of New Fuel Cycle Technologies 33**  
J. J. Jacobson, G. E. Matthern and S. J. Piet

Chapter 3 **The Investment Evaluation of Third-Generation  
Nuclear Power - From the Perspective of Real Options 69**  
Ying Fan and Lei Zhu

Chapter 4 **Characteristic Evaluation and  
Scenario Study on Fast Reactor Cycle in Japan 91**  
Hiroki Shiotani, Kiyoshi Ono and Takashi Namba

Chapter 5 **Nuclear Proliferation 113**  
Michael Zentner

Chapter 6 **Ethics of Nuclear Power: How to  
Understand Sustainability in the Nuclear Debate 129**  
Behnam Taebi

**Part 2 Operation and Decommissioning 151**

Chapter 7 **Long-Term Operation of VVER Power Plants 153**  
Tamás János Katona

Chapter 8 **A Novel Approach to Spent Fuel Pool Decommissioning 197**  
R. L. Demmer

Chapter 9 **Post-Operational Treatment of  
Residual Na Coolant in EBR-II Using Carbonation 211**  
Steven R. Sherman and Collin J. Knight

**Part 3 Environment and Nuclear Energy 241**

- Chapter 10 **Carbon Leakage of Nuclear Energy – The Example of Germany 243**  
Sarah von Kaminietz and Martin Kalinowski
- Chapter 11 **Effects of the Operating Nuclear Power Plant on Marine Ecology and Environment - A Case Study of Daya Bay in China 255**  
You-Shao Wang
- Chapter 12 **Microbial Leaching of Uranium Ore 291**  
Hadi Hamidian

**Part 4 Advances in Nuclear Waste Management 305**

- Chapter 13 **Storage of High Level Nuclear Waste in Geological Disposals: The Mining and the Borehole Approach 307**  
Moeller Dietmar and Bielecki Rolf
- Chapter 14 **Isotopic Uranium and Plutonium Denaturing as an Effective Method for Nuclear Fuel Proliferation Protection in Open and Closed Fuel Cycles 331**  
Kryuchkov E.F., Tsvetkov P.V., Shmelev A.N., Apse V.A., Kulikov G.G., Masterov S.V., Kulikov E.G. and Glebov V.B

**Part 5 Thorium 363**

- Chapter 15 **Implementation Strategy of Thorium Nuclear Power in the Context of Global Warming 365**  
Takashi Kamei
- Chapter 16 **Thorium Fission and Fission-Fusion Fuel Cycle 383**  
Magdi Ragheb
- Chapter 17 **New Sustainable Secure Nuclear Industry Based on Thorium Molten-Salt Nuclear Energy Synergetics (THORIMS-NES) 407**  
Kazuo Furukawa, Eduardo D. Greaves,  
L. Berrin Erbay, Miloslav Hron and Yoshio Kato

**Part 6 Advances in Energy Conversion 445**

- Chapter 18 **Water Splitting Technologies for Hydrogen Cogeneration from Nuclear Energy 447**  
Zhaolin Wang and Greg F. Naterer
- Chapter 19 **Reformer and Membrane Modules (RMM) for Methane Conversion Powered by a Nuclear Reactor 467**  
M. De Falco, A. Salladini, E. Palo and G. Iaquaniello

Chapter 20	<b>Hydrogen Output from Catalyzed Radiolysis of Water</b>	<b>489</b>
	Alexandru Cecal and Doina Humelnicu	





---

## Preface

---

We are fortunate to live in incredibly exciting and incredibly challenging time. The world is rapidly growing; country economies developing at accelerated growth rates, technology advances improve quality of life and become available to larger and larger populations. At the same time we are coming to a realization that we are responsible for our planet. We have to make sure that our continuous quest for prosperity does not backfire via catastrophic irreversible climate changes, and depleted or limited resources that may challenge the very existence of future generations. We are at the point in our history when we have to make sure that our growth is sustainable. Energy demands due to economic growth and increasing population must be satisfied in a sustainable manner assuring inherent safety, efficiency and no or minimized environmental impact. New energy sources and systems must be inherently safe and environmentally benign.

These considerations are among the reasons that lead to serious interest in deploying nuclear power as a sustainable energy source. Today's nuclear reactors are safe and highly efficient energy systems that offer electricity and a multitude of co-generation energy products ranging from potable water to heat for industrial applications. At the same time, catastrophic earthquake and tsunami events in Japan resulted in the nuclear accident that forced us to rethink our approach to nuclear safety, design requirements and facilitated growing interests in advanced nuclear energy systems, next generation nuclear reactors, which are inherently capable to withstand natural disasters and avoid catastrophic consequences without any environmental impact.

This book is one in a series of books on nuclear power published by InTech. It consists of six major sections housing twenty chapters on topics from the key subject areas pertinent to successful development, deployment and operation of nuclear power systems worldwide:

### **Nuclear Power Deployment**

1. Nuclear Naval Propulsion
2. Deployment Scenarios for New Technologies
3. The Investment Evaluation of Third-Generation Nuclear Power - from the Perspective of Real Options
4. Characteristic Evaluation and Scenario Study on Fast Reactor Cycle in Japan

5. Nuclear Proliferation
6. Ethics of Nuclear Power: How to Understand Sustainability in the Nuclear Debate

#### **Operation and Decommissioning**

7. Long-Term Operation of VVER Nuclear Power Plants
8. Novel, In-situ Spent Fuel Pool Decommissioning
9. Post-Operational Treatment of Residual Na Coolant in EBR-II Using Carbonation

#### **Environment and Nuclear Energy**

10. Carbon Leakage of Nuclear Energy – The Example of Germany
11. Effects of the Operating Nuclear Power Plant on Marine Ecology & Environment- a Case Study of Daya Bay in China
12. Microbial Leaching of Uranium Ore

#### **Advances in Nuclear Waste Management**

13. Storage of High Level Nuclear Waste in Geological Disposals: The Mining and the Borehole Approach
14. Isotopic Uranium and Plutonium Denaturing as an Effective Method for Nuclear Fuel Proliferation Protection in Open and Closed Fuel Cycles

#### **Thorium**

15. Implementation Strategy of Thorium Nuclear Power in the Context of Global Warming
16. Thorium Fission and Fission-Fusion Fuel Cycle
17. New Sustainable Secure Nuclear Industry Based on Thorium Molten-Salt Nuclear Energy Synergetics (THORIMS-NES)

#### **Advances in Energy Conversion**

18. Water Splitting Technologies for Hydrogen Cogeneration from Nuclear Energy
19. Reformer and Membrane Modules (RMM) for Methane Conversion Powered by a Nuclear Reactor
20. Hydrogen Output from Catalyzed Radiolysis of Water.

Our book opens with the section on general aspects of nuclear power deployment. Later sections address selected issues in operation and decommissioning, economics and environmental effects. The book shows both advantages and challenges emphasizing the need for further development and innovation. Advances in nuclear waste management and thorium-based fuel cycles lead to environmentally benign nuclear energy scenarios and ultimately, towards nuclear energy sustainability. Improvements in applications and efficiency of energy conversion facilitate economics competitiveness of nuclear power.

With all diversity of topics in 20 chapters, the nuclear power deployment, operation and sustainability is the common thread that is easily identifiable in all chapters of our book. The “system-thinking” approach allows synthesizing the entire body of provided information into a consistent integrated picture of the real-life complex engineering system – nuclear power system – where everything is working together.

The goal of the book is to bring nuclear power to our readers as one of the promising energy sources that has a unique potential to meet energy demands with minimized environmental impact, near-zero carbon footprint, and competitive economics via robust potential applications. Continuous technological advances will lead towards sustainable nuclear energy via closed fuel cycles and advanced energy systems.

The book targets everyone as its potential readership groups - students, researchers and practitioners - who are interested to learn about nuclear power. The idea is to facilitate intellectual cross-fertilization between field experts and non-field experts taking advantage of methods and tools developed by both groups. The book will hopefully inspire future research and development efforts, innovation by stimulating ideas.

We hope our readers will enjoy the book and will find it both interesting and useful.

**Pavel V. Tsvetkov**  
Department of Nuclear Engineering  
Texas A&M University  
United States of America



# **Part 1**

## **Nuclear Power Deployment**



# Nuclear Naval Propulsion

Magdi Ragheb

*Department of Nuclear, Plasma and Radiological Engineering  
University of Illinois at Urbana-Champaign  
216 Talbot Laboratory, Urbana, Illinois  
USA*

## 1. Introduction

The largest experience in operating nuclear power plants has been in nuclear naval propulsion, particularly aircraft carriers and submarines. This accumulated experience may become the basis of a proposed new generation of compact-sized nuclear power plants designs. The mission for nuclear powered submarines is being redefined in terms of signal intelligence gathering and special operations. The nuclear powered vessels comprise about 40 percent of the USA Navy's combatant fleet, including the entire sea based strategic nuclear deterrent. All the USA Navy's operational submarines and over half of its aircraft carriers are nuclear-powered.

The main considerations here are that nuclear powered submarines do not consume oxygen like conventional power plants, and that they have large endurance or mission times before fuel resupply; limited only by the available food and air purification supplies on board. Another unique consideration is the use of High Enriched Uranium (HEU) to provide a compact reactor system with enough built-in reactivity to overcome the xenon reactor dead time for quick restarts and long fuel burnup periods between refuelings.

During World War II, submarines used diesel engines that could be run on the water surface, charging a large bank of electrical batteries. These could later be used while the submarine is submerged, until discharged. At this point the submarine had to resurface to recharge its batteries and become vulnerable to detection by aircraft and surface vessels. Even though special snorkel devices were used to suck and exhaust air to the submarine shallowly submerged below the water's surface, a nuclear reactor provides it with a theoretically infinite submersion time. In addition, the high specific energy, or energy per unit weight of nuclear fuel, eliminates the need for constant refueling by fleets of vulnerable tankers following a fleet of surface or subsurface naval vessels. On the other hand, a single refueling of a nuclear reactor is sufficient for long intervals of time.

With a high enrichment level of 93 percent, capable of reaching 97.3 percent in  $U^{235}$ , modern naval reactors, are designed for a refueling after 10 or more years over their 20-30 years lifetime, whereas land based reactors use fuel low-enriched to 3-5 percent in  $U^{235}$ , and need to be refueled every 1-1 1/2 years period. New cores are designed to last 50 years in carriers and 30-40 years in submarines, which is the design goal of the Virginia class of submarines. Burnable poisons such as gadolinium or boron are incorporated in the cores. These allow a high initial reactivity that compensates for the build-up of fission products poisons over the

core lifetime, as well as the need to overcome the reactor dead time caused by the xenon poison changes as a result of operation at different power levels.

Naval reactors use high burn up fuels such as uranium-zirconium, uranium-aluminum, and metal ceramic fuels, in contrast to land-based reactors which use uranium dioxide,  $UO_2$ . These factors provide the naval vessels theoretical infinite range and mission time. For all these considerations, it is recognized that a nuclear reactor is the ideal engine for naval propulsion.

A compact pressure vessel with an internal neutron and gamma ray shield is required by the design while maintaining safety of operation. Their thermal efficiency is lower than the thermal efficiency of land based reactors because of the emphasis on flexible power operation rather than steady state operation, and of space constraints. Reactor powers range from 10 MWth in prototypes to 200 MWth in large subsurface vessels, and 300 MWth in surface ships.

Newer designs use jet pump propulsion instead of propellers, and aim at an all electrical system design, including the weapons systems such as electromagnetic guns.

## 2. Historical evolution

In the USA, initially the General Electric (GE) Company developed a liquid metal reactor concept; and the Westinghouse Company, a pressurized water reactor concept. Each company built an Atomic Energy Commission (AEC) owned and financed development laboratory. Westinghouse used the site of the Allegheny County Airport in a suburb of Pittsburgh, Pennsylvania for what became known as the Bettis Atomic Power Laboratory. GE built the Knolls Atomic Power Laboratory in the state of New York.

The Westinghouse program used pressurized water as the coolant. It revealed how corrosive hot water could be on the metal cladding surrounding the fuel. It realized that the use of zirconium resisted such corrosion. The pure metal was initially used as the cladding for the fuel elements, to be later replaced by a zirconium alloy, Zircaloy that improved its performance. Zirconium has a low neutron absorption cross section and, like stainless steel, forms a protective, invisible oxide film on its surface upon exposure to air. This oxide film is composed of zirconia or  $ZrO_2$  and is on the order of only 50 to 100 angstroms in thickness. This ultra thin oxide prevents the reaction of the underlying zirconium metal with virtually any chemical reagent under ambient conditions. The only reagent that will attack zirconium metal at room temperature is hydrofluoric acid, HF, which will dissolve the thin oxide layer off of the surface of the metal and thus allow HF to dissolve the metal itself, with the concurrent evolution of hydrogen gas.

Jules Verne, the French author in his 1870 book: "20,000 Leagues Under the Sea," related the story of an electric submarine. The submarine was called the "Nautilus," under its captain Nemo. Science fiction became reality when the first nuclear submarine built by the USA Navy was given the same name. Construction of the Nautilus (SSN-571) started on June 14, 1952, its first operation was on December 30, 1954 and it reached full power operation on January 13, 1955. It was commissioned in 1954, with its first sea trials in 1955. It set speed, distance and submergence records for submarine operation that were not possible with conventional submarines. It was the first ship to reach the North Pole. It was decommissioned in 1980 after 25 years of service, 2,500 dives, and a travelled distance of 513,000 miles. It is preserved at a museum at Croton, Connecticut, USA.





Fig. 1. The "Nautilus", the first nuclear powered submarine (Photo: USA Navy).

An experimental setup designated as the S1W prototype was built for the testing of the Nautilus's nuclear reactor at the Idaho National Laboratory (INL) in 1989. The section of the hull containing the reactor rested in a "sea tank" of water 40 feet deep and 50 feet in diameter. The purpose of the water was to help the shielding designers study the "backscatter radiation" that might escape the hull, scatter off the water, and reflect back into the living quarters of the ship.

The reactor for the Nautilus was a light water moderated, highly enriched in  $U^{235}$  core, with zirconium-clad fuel plates. The high fuel enrichment gives the reactor a compact size, and a high reactivity reserve to override the xenon poison dead time. The Nautilus beat numerous records, establishing nuclear propulsion as the ideal driving force for the world's submarine fleet. Among its feats was the first underwater crossing of the Arctic ice cap. It traveled 1,400 miles at an average speed of 20 knots. On a first core without refueling, it traveled 62,000 miles. Another nuclear submarine, the Triton reenacted Magellan's trip around the Earth. Magellan traveled on the surface, while the Triton did it completely submerged.

### 3. Reactor design concepts

There have been more reactor concepts investigated in the naval propulsion area by different manufacturers and laboratories than in the civilian field, and much can be learned from their experience for land applications, particularly for small compact systems. According to the type of vessel they power, they have different first letter designations: A for Aircraft carrier, C for Cruiser, D for Destroyer and S for Submarine. They are also designated with a last letter according to the designer institution or lead laboratory: B for Bechtel, C for Combustion Engineering, G for General Electric and W for Westinghouse. A middle number between the first and last letter refers to the generation number of the core design. For instance, the A1B is the first generation of a core design for aircraft carriers with Bechtel operating the lead laboratory for the design.

Naval reactors designs use boron as a burnable neutron poison. The fuel is an alloy of 15 percent zirconium and 85 percent uranium enriched to a level of about 93 percent in  $U^{235}$ . The burnable poisons and high enrichment allow a long core lifetime and provide enough

reactivity to overcome the xenon poisoning reactor dead time. An axial direction doping provides a long core life, and a radial doping provides for an even power and fuel burnup distributions.

### 3.1 STR or S1W pressurized water reactor design

The Westinghouse Electric Corporation under contract to the USA Navy constructed, tested and operated a prototype Pressurized Water Reactor (PWR) submarine reactor plant. This first reactor plant was called the Submarine Thermal Reactor (STR). On March 30, 1953, the STR was brought to power for the first time. In 1953 it achieved a 96 hours sustained full power run simulating a crossing of the Atlantic Ocean. The second S1W core sustained in 1955 an 66-day continuous full power run, simulating a high speed run twice around the globe.

The STR was redesigned as the first generation submarine reactor S1W, which reached criticality on March 30, 1953, was the prototype of the USS Nautilus (SSN 571) reactor and was followed in the middle to late 1950s by the Aircraft carrier reactor A1W, the prototype for the aircraft carrier USS Enterprise plant. Westinghouse's Bettis Atomic Power Laboratory was assigned the responsibility for operating the reactor it had designed and built, hence the W in the name.

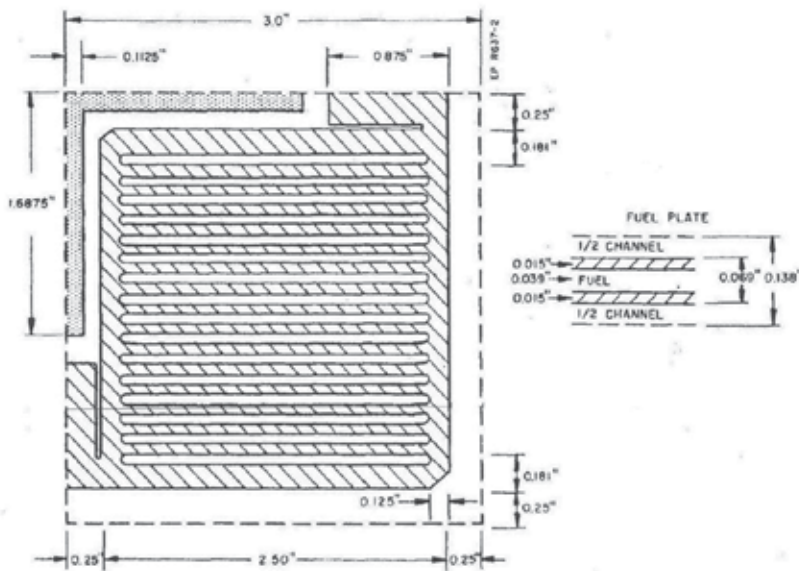


Fig. 2. Plate fuel element configuration (Ragheb, 2011).

The fuel elements are sandwich plates made of U and Zr and clad in Zr. The maximum temperature in the fuel was 645 °F and the sheath temperature was 551 °F with an average cycle time of 600 hours or just  $600 / 24 = 25$  days. The reactor temperature is limited by the pressure needed to prevent boiling, necessitating high pressure vessels, piping and heat exchangers. The steam was generated at a relatively low pressure. A high level of pumping power was required, and the fuel was costly. However this design presented few hazards, was proven in service, and an expensive moderator was not needed.

The S1C reactor used an electric drive rather than a steam turbine like in the subsequent S5W reactor design rated at 78 MWth and a 93 percent U<sup>235</sup> enriched core that was the standard in the 1970s. The S6G reactor plant was rated at 148 MWth and the D2W core was rated at 165 MWth. The S6G reactor is reported to be capable of propelling a Los Angeles class submarine at 15 knots or 27.7 km/hr when surfaced and 25 knots or 46.3 km/hr while submerged. The Sea Wolf class of submarines was equipped with a single S6W reactor, whereas the Virginia class of submarines is equipped with an S9G reactor.

It is worth noting that the higher achievable submerged speed is partly due to the absence of wave friction resistance underwater, suggesting that submarine cargo ships would offer a future energy saving alternative to surface cargo ships.

### **3.2 Large ship reactors, A1W-A, A1W-B prototype plants**

The A1W (Aircraft carrier, 1st prototype, Westinghouse) plant consisted of a pair of prototype reactors for the USS Enterprise USA Navy nuclear-powered aircraft carrier. Located at the Naval Reactors Facility, the two PWRs designated A and B, were built within a portion of a steel hull. The plant simulated the Enterprise's engine room. The A1W plant was the first in which two reactors powered one ship propeller shaft through a single-gear turbine propulsion unit. As the Navy program evolved, new reactor cores and equipment replaced many of the original components. The Navy trained naval personnel at the A1W plant and continued a test program to improve and further develop its operational flexibility.

The A1W prototype plant was started in 1956 for surface ships using two PWRs. The plant was built as a prototype for the aircraft carrier USS Enterprise (CVN 65), which was the first nuclear-powered aircraft carrier. Power operation of the A1W plant started in October of 1958. In the A1W and A2W designs, the coolant was kept at a temperature between 525-545 °F or 274-285 °C. In the steam generators, the water from the feed system is converted to steam at 535 °F or 279 °C and a pressure of about 600 psi or 4 MPa. The reactor coolant water was circulated by four large electric pumps for each reactor. The steam was directed from each steam generator to a common header, where the steam is then sent to the main engine, electrical generators, aircraft catapult system, and various auxiliaries. The main propulsion turbines are double ended, in which the steam enters at the center and divides into two opposing streams. The main shaft was coupled to a reduction gear in which the high rotational velocity of the turbine shaft is stepped down to a usable rotational rate for ship propulsion.

In the A3W reactor design used on the USS John F. Kennedy a 4-reactor plant is used. In the A4W design with a life span of 23 years on the Nimitz Class carriers only two reactors per ship are used with each providing 104 MWth of power or 140,000 shaft HP. The A1B is also a two reactor design for the Gerald R. Ford class of carriers.

### **3.3 SIR or S1G intermediate neutron flux beryllium sodium cooled reactor**

This reactor design was built by the General Electric (GE) Company, hence the G designation. The neutron spectrum was intermediate in energy. It used UO<sub>2</sub> fuel clad in stainless steel with Be used as a moderator and a reflector. The maximum temperature in the fuel could reach 1,700 +/- 300 °F with a maximum sheath temperature of 900 °F, with a cycle time of 900 hours or 900 / 24 = 37.5 days.

A disadvantage is that the coolant becomes activated with the heat exchangers requiring heavy shielding. In addition Na reacts explosively with water and ignites in air, and the fuel element removal is problematic. On the other hand, high reactor and steam temperatures can be reached with a higher thermal efficiency. A low pressure is used in the primary system.

Beryllium has been used as a moderator in the Sea Wolf Class of submarines reactors. It is a relatively good solid moderator, both from the perspectives of slowing down power and of the moderating ratio, and has a very high thermal conductivity. Pure Be has good corrosion resistance to water up to 500 °F, to sodium to 1,000 °F, and to air attack to 1,100 °F. It has a noted vapor pressure at 1,400 °F and is not considered for use much above 1,200 °F even with an inert gas system. It is expensive to produce and fabricate, has poor ductility and is extremely toxic necessitating measures to prevent inhalation and ingestion of its dust during fabrication.

A considerably small size thermal reactor can be built using beryllium oxide as a moderator. It has the same toxicity as Be, but is less expensive to fabricate. It can be used with a sodium cooled thermal reactor design because BeO is corrosion resistant to sodium. It has similar nuclear properties to Be, has a very high thermal conductivity as a ceramic, and has a good resistance to thermal shock. It can be used in the presence of air, Na and CO<sub>2</sub>. It is volatile in water vapor above 1,800 °F. In its dense form, it resists attack by Na or the Na-K alloy eutectic, which remains liquid at room temperature, at a temperature of 1,000 °F. BeO can be used as a fuel element material when impregnated with uranium. Low density increases its resistance to shock. A BeO coating can be applied to cut down on the fission products release to the system.

The USS Seawolf submarine initially used a Na-cooled reactor that was replaced in 1959 by a PWR to standardize the fleet, because of superheater bypass problems causing mediocre performance and as a result of a sodium fire. The steam turbines had their blades replaced to use saturated rather than superheated steam. The reactor was housed in a containment vessel designed to contain a sodium fire.

The eighth generation S8G reactor was capable of operating at a significant fraction of full power without reactor coolant pumps. The S8G reactor was designed by General Electric for use on the Ohio Class (SSGN/SSBN-726) submarines. A land based prototype of the reactor plant was built at Knolls Atomic Power Laboratory at Ballston Spa, New York. The prototype was used for testing and crew training throughout the 1980s. In 1994, the core was replaced with a sixth generation S6W Westinghouse reactor, designed for the Sea Wolf Class submarines.

### **3.4 Experimental Beryllium Oxide Reactor, EBOR**

The Experimental Beryllium Oxide Reactor (EBOR)'s objective was to develop beryllium oxide as a neutron moderator in high-temperature, gas-cooled reactors. The project was cancelled in 1966 before construction was complete. Among the reasons for the cancellation was the encouraging progress achieved, concurrent with the EBOR construction, in developing graphite as a moderator. This reduced the importance of developing beryllium oxide as an alternate. No uranium fuel ever was loaded into the EBOR and it never operated or went critical before the program was cancelled.

### **3.5 SC-WR super critical water reactor**

The Super Critical Water Reactor (SC-WR) was considered with an intermediate energy neutron spectrum. The fuel was composed of UO<sub>2</sub> dispersed in a stainless steel matrix. It

consisted of 1 inch square box with parallel plates and sine wave filters with a type 347 stainless steel cladding 0.007 inch thick. The maximum temperature in the fuel reached 1,300 °F with an average cycle time of 144 hours or  $144 / 24 = 6$  days.

The materials for high pressure and temperature and the retention of mechanical seals and other components caused a service problem. The water coolant reached a pressure of 5,000 psi. The high pressure and temperature steam results in a high cycle efficiency, small size of the reactor with no phase change in the coolant.

### **3.6 Organic Moderated Reactor Experiment, OMRE**

The Organic Cooled and Moderated Reactor has been considered as a thermal neutron spectrum shipboard power plant. The Terphenyl waxy organic coolant was considered promising because it liquefied at high temperatures but did not corrode metals like water. Also, it operated at low pressure, significantly reducing the risk of coolant leak and loss of coolant through depressurization. A scaled-up reactor, the Experimental Organic Cooled Reactor, was built in anticipation of further development of the concept.

The rectangular-plates fuel clad in aluminum can be natural uranium since the organic coolant can have good moderating properties. The cladding temperature can reach 800 °F with an average cycle time of 2,160 hours or  $2,160 / 24 = 90$  days. The overall heat transfer coefficient of the coolant is low with the formation of polymers under irradiation that require an adequate purification system. The perceived advantages are negligible corrosion and the achievement of low pressure at a high temperature.

A Diphenyl potential coolant broke down under irradiation. The hydrogen in the compound turned into a gas, forming bubbles. The bubbles reduced the moderator density and made it difficult to maintain the chain reaction. The initially clear liquid turned into a gummy and black breakup product. No uranium fuel ever was loaded into the reactor and it never operated or went critical before the program was cancelled.

### **3.7 Lead-bismuth cooled fast reactors**

The alpha class of Russian submarines used an alloy of Pb-Bi 45-50 percent by weight cooled fast reactors. The melting point of this alloy is 257 °F. They faced problems of corrosion of the reactor components, melting point, pump power, polonium activity and problems in fuel unloading. Refueling needed a steam supply to keep the liquid metal molten. Bismuth leads to radiation from the activated products, particularly polonium. An advantage is that at decommissioning time, the core can be allowed to cool into a solid mass with the lead providing adequate radiation shielding. This class of submarine reactors has been decommissioned.

### **3.8 Natural circulation S5G prototype**

The S5G was the prototype of a PWR for the USS Narwhal. It was capable of operating in either a forced or natural circulation flow mode. In the natural circulation mode, the cooling water flowed through the reactor by natural convection, not by pumps. Use of natural circulation instead of pumps reduced the noise level in the submarine. To prove that the design concept would work in an operating ship at sea, the prototype was built in a submarine hull section capable of simulating the rolling motion of a ship at sea. The S5G continued to operate as part of the Navy's nuclear training program until that program was reduced after the end of the Cold War.

The S5G reactor had two coolant loops and two steam generators. It had to be designed with the reactor vessel situated low in the ship hull and the steam generators high in order for natural circulation of the coolant to be developed and maintained using the chimney effect. It was largely a success, although the design never became the basis for any more fast attack submarines besides the Narwhal. The prototype testing included the simulation of the engine room of an attack submarine. By floating the plant in a large pool of water, the whole prototype could be rotated along its long axis to simulate a hard turn. This was necessary to determine whether natural circulation would continue even during hard maneuvers, since natural circulation is dependent on gravity.

The USS Narwhal had the quietest reactor plant in the USA naval fleet. Its 90 MWth reactor plant was slightly more powerful than the other fast attack USA nuclear submarines of that era such as the third generation S3G and the fifth generation S5W. The Narwhal contributed significantly to the USA effort during the Cold War. With its quiet propulsion and the pod attached to its hull, it used a towed sonar array and possibly carried a Remotely Operated Vehicle (ROV) for tapping into communication cables and maintaining a megaphones tracking system at the bottom of the oceans.

It was intended to test the potential contribution of natural circulation technology to submarine noise suppression by the avoidance of forced flow pump cooling. The reactor primary coolant pumps are one of the primary sources of noise from submarines in addition to the speed reduction gearbox and cavitation forming collapsing bubbles from the propeller. The elimination of the coolant pumps and associated equipment would also reduce mechanical complexity and the space required by the propulsion equipment. The S5G was the direct precursor to the eighth generation S8G reactor used on the Ohio class ballistic missile submarines; a quiet submarine design.

The S5G was also equipped with coolant pumps that were only needed in emergencies to attain high power and speed. The reactor core was designed with very smooth paths for the coolant. Accordingly, the coolant pumps were smaller and quieter than the ones used by the competing S5W core, a Westinghouse design, and were also fewer in number. In most situations, the submarine could be operated without using the coolant pumps, useful for stealth operation. The reduction in the electrical requirements enabled this design to use only a single electrical turbine generator plant.

The S8G prototype used natural circulation allowing operation at a significant fraction of full power without using the reactor pumps, providing a silent stealth operation mode. To further reduce engine plant noise, the normal propulsion setup of two steam turbines driving the propeller screw through a reduction gear unit was changed instead to one large propulsion turbine without reduction gears. This eliminated the noise from the main reduction gears, but at the expense of a large main propulsion turbine. The turbine was cylindrical, about 12 feet in diameter and 30 feet in length. This large size was necessary to allow it to rotate slowly enough to directly drive the propulsion screw and be fairly efficient in the process.

### **3.9 Fail-safe control and load-following S7G design**

The S7G core was controlled by stationary gadolinium-clad tubes that were partially filled with water. Water was pumped from the portion of the tube inside the core to a reservoir above the core, or allowed to flow back down into the tube. A higher water level in the tube within the core slowed down the neutrons allowing them to be captured by the gadolinium tube cladding rather than the uranium fuel, leading to a lower power level.

The design constituted a unique fail-safe control system. The pump needed to run continuously to keep the water level pumped down. Upon an accidental loss of pump power, all the water would flow back into the tube, shutting down the reactor.

This design also had the advantage of a negative reactivity feedback and a load-following mechanism. An increase in reactor power caused the water to expand to a lower density lowering the power. The water level in the tubes controlled the average coolant temperature, not the reactor power. An increase in steam demand resulting from opening the main steam throttle valves would automatically increase reactor power without action by the operator.

### **3.10 S9G high energy density core**

The S9G is a PWR built by General Electric with increased energy density, and new plant components, including a new steam generator design featuring improved corrosion resistance and a reduced life cycle cost. This reactor in the Virginia Class SSN-774 submarines is designed to operate for 33 years without refueling and last the expected 30 year design life of a typical submarine. It produces about 40,000 shaft horsepower, or about 30 MWth of power.

The higher power density decreases not only the size of the core, but also enhances quiet operation through the elimination of bulky control and pumping equipment. It would be superior to any Russian design from the perspective of noise reduction capability, with 30 units planned to be built. The core for a contemplated New Attack Submarine is expected to last for the operational life of the ship. The design goals include eliminating the need for a refueling, will reduce life cycle costs, cut down the radiation exposure of shipyard staff, and lessen the amount of radioactive waste generated. This is possible because of many developments such as the use of advanced computers to perform three-dimensional nuclear, thermal, and structural calculations; further exploitation of a modified fuel process; and better understanding of various reactor technologies which permits more highly optimized designs. Performance improvements are gained through advances in such areas as thermal hydraulics and structural mechanics, and by optimizing reactor-to-systems interfaces.

The new reactor with increased energy density has new plant components, such as a new concept steam generator, with improved corrosion resistance and reduced life-cycle costs. The new steam generators allow greater plant design flexibility and decreased construction costs due to a smaller size, spatial orientation, and improved heat transfer efficiency which reduces coolant flow requirements. They alleviate the corrosion concerns encountered in existing designs of steam generators, while reducing component size and weight and providing greater flexibility in the overall arrangement.

## **4. Commercial nuclear ships**

The USA built one single nuclear merchant ship: the Savannah. It was designed as a national showpiece, and not as an economical merchant vessel. For compactness, the steam generators and steam drums surround the reactor core. This Integral Design configuration also provides shielding for the crew. It was retired in 1970.

The 630-A reactor, a low-power critical experiment, was operated at the Idaho National Laboratory (INL) to explore the feasibility of an air-cooled, water-moderated system for nuclear-powered merchant ships. Further development was discontinued in December 1964 when decisions were made to lower the priority of the entire nuclear power merchant ship program.

Nuclear Ice Breakers like the Russian Lenin and the Arktica were a good success, not requiring refueling in the arctic regions. The Otto Hahn bulk ore carrier was built by Germany. It operated successfully for ten years. The Mutsu was an oceanographic research vessel built in Japan in 1974. Due to a design flaw causing a radiation leakage from its top radiation shield, it never became fully operational. The Sturgis MH-1A was a floating nuclear power plant ship. It was carrying a 45 Megawatts Thermal (MWth) PWR providing remote power supplies for the USA Army.

Reactor type	Rated power	
	shaft horse power, [shp]	[MW]*
A2W	35,000	26.1
A4W/A1G	140,000	104.4
C1W	40,000	29.8
D2G	35,000	26.1
S5W	15,000	11.2
S5G	17,000	12.7
S6W	35,000	26.1
S8G	35,000	26.1
S9G	40,000	29.8

\*1 shp = 745.6999 Watt = 0.7456999 kW

Table 1. Power ratings of naval reactor designs.

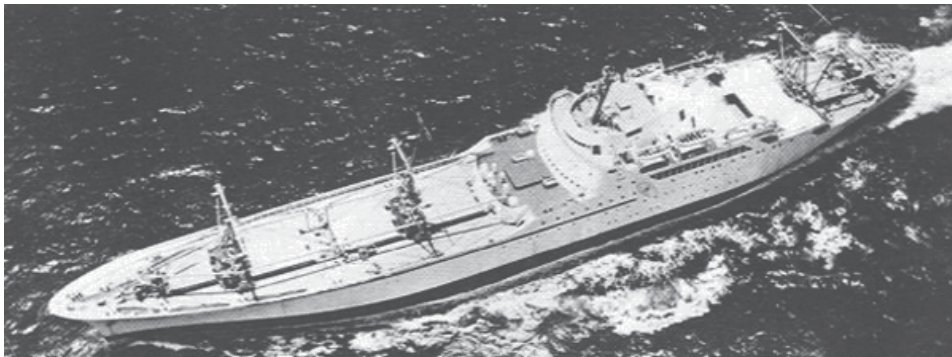


Fig. 3. The Savannah, the first USA merchant ship.

## 5. Power plant configurations

The nuclear navy benefited the civilian nuclear power program in several ways. It first demonstrated the feasibility of the PWR concept, which is being currently used in the majority of land based power reactors worldwide. Second, naval reactors accumulated a large number of operational experience hours, leading to improvements in the land based reactors. The highly trained naval operational crews also become of great value to the civilian nuclear utilities providing them with experienced staffs in the operation and management of the land based systems.



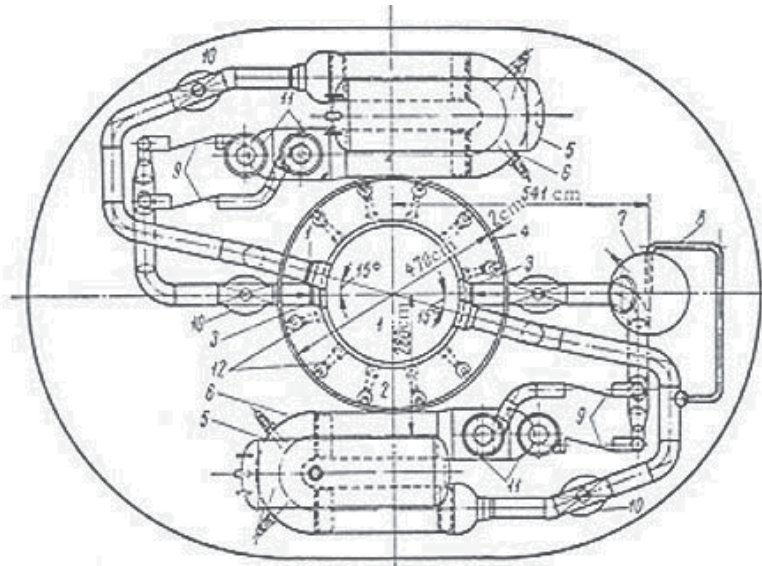


Fig. 4. The loop-type naval reactor design for the nuclear ship Savannah. The reactor core is surrounded by the heat exchangers and the steam drums providing a compact shielding design. The horizontal steam generator was replaced by a vertical tube steam generator and an integrated system in subsequent designs. 1: Reactor core, 2: Water shield, 3: Coolant inlet, 4: Pb Shield layer, 5: Steam drum, 6: Heat exchanger, 7: Pressurizer, or volume compensator, 8: Equalizer line, 9: Cutoff channel, 10: Gate valve, 11: Coolant pumps, 12: Instrumentation channel. (Broder, 1970).

Land based reactors differ in many ways from naval reactors. The thermal power of land based reactors is in the range of 3,000 MWth or higher. In contrast, a submarine reactor's power is smaller in the range of the hundreds of MWths. Land based systems use uranium fuel lightly enriched to the 3-5 percent range. This low level enrichment was imposed on the designers of land-based reactors to primarily avoid the circulation of highly enriched fuel. It is an impediment since it forces the use of a large volume for the core, increases the capital cost and hence the cost of the electricity produced. Highly enriched fuel at the 93-97 percent level is used in naval reactors to provide enough reactivity to override the xenon poison dead time, compactness as well as provide higher fuel burnup and the possibility for a single fuel loading over the useful service time of the powered ship.

Table 2 shows the composition of highly enriched fuel used in nuclear propulsion as well as space reactor designs such as the SAFE-400 and the HOMER-15 designs (Poston, 2002). Most of the activity is caused by the presence of  $U^{234}$ , which ends up being separated with the  $U^{235}$  component during the enrichment process. This activity is primarily alpha decay and does not account for any appreciable dose. Since the fuel is highly purified and there is no material such as fluorine or oxygen causing any  $(\alpha, n)$  reactions in the fuel, the alpha decay of  $U^{234}$  does not cause a neutron or gamma ray dose. If uranium nitride (UN) is used as fuel, the interaction threshold energy of nitrogen is well above the alpha emission energies of  $U^{234}$ . Most of the dose prior to operation from the fuel is caused by  $U^{235}$  decay gammas and the spontaneous fission of  $U^{238}$ . The total exposure rate is 19.9 [ $\mu$ Röntgen / hr] of which the gamma dose rate contribution is 15.8 and the neutron dose rate is 4.1.

Isotope	Composition (percent)	Activity (Curies)	Decay Mode	Exposure Rate Contribution [ $\mu\text{R}/\text{hr}$ ]
$\text{U}^{234}$	0.74	6.1	Alpha decay	unappreciable
$\text{U}^{235}$	97.00		Decay gammas	appreciable
$\text{U}^{238}$	2.259		Spontaneous fissions	appreciable
$\text{Pu}^{239}$	0.001		Alpha decay	unappreciable
Total		6.5		19.9

Table 2. Composition of highly enriched fuel for naval and space reactors designs (Poston, 2002).

Reactor operators can wait for a 24 hours period; the reactor dead time, on a land based system for the xenon fission product to decay to a level where they can restart the reactor. A submarine cannot afford to stay dead in the water for a 24 hour period if the reactor is shutdown, necessitating highly enriched fuel to provide enough high reactivity to overcome the reactor dead time effect. A nuclear submarine has the benefit of the ocean as a heat sink, whereas a land based reactor needs sufficiently large water reservoirs to be available for its safety cooling circuits

For these reasons, even though the same principle of operation is used for naval and land based reactor designs, the actual designs differ substantially. Earlier naval reactors used the loop type circuit for the reactor design for the Savannah reactor. There exists a multitude of naval reactor designs. More modern designs use the Integral circuit type.

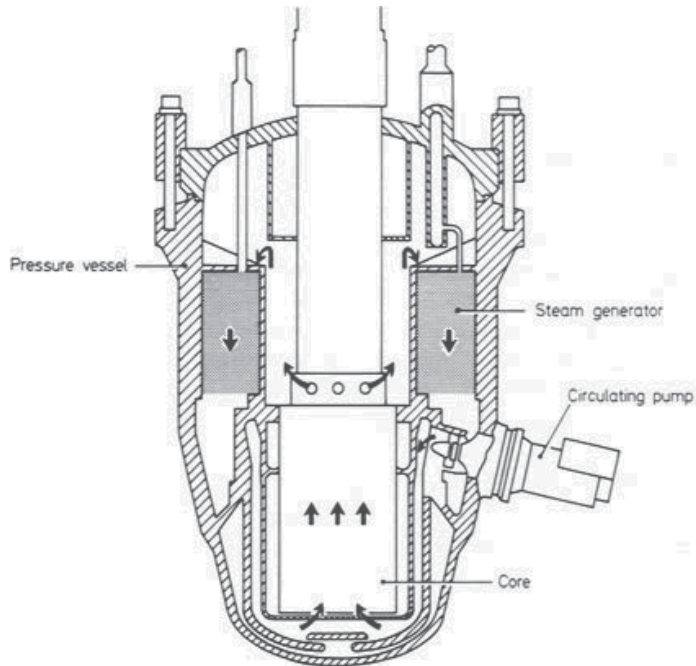


Fig. 5. Integral type of naval reactor vessel (Collier, 1987).

Because of the weight of the power plant and shielding, the reactor and associated steam generation equipment is located at the center of the ship. Watertight bulkheads isolating the reactor components surround it. The greater part of the system is housed in a steel containment, preventing any leakage of steam to the atmosphere in case of an accident. The containment vessel for the Savannah design consisted of a horizontal cylindrical section of 10.7 meters diameter, and two hemispherical covers. The height of the containment was 15.2 meters. The control rod drives are situated in a cupola of 4.27 m in diameter, on top of the containment. The containment vessel can withstand a pressure of 13 atm. This is the pressure attained in the hypothetical maximum credible accident, or design-basis accident. It is postulated as the rupture of the primary loop and the subsequent flashing into steam of the entire coolant volume.

The secondary shielding consists of concrete, lead, and polyethylene and is positioned at the top of the containment. A prestressed concrete wall with a thickness of 122 cm surrounds the lower section of the containment. This wall rests on a steel cushion. The upper section of the secondary shielding is 15.2 cm of lead to absorb gamma radiation, and 15.2 cm of polyethylene to slow down any leaking neutrons. The space between the lead plates is filled with lead wool. The lead used in the shielding is cast by a special method preventing the formation of voids and inhomogeneities.

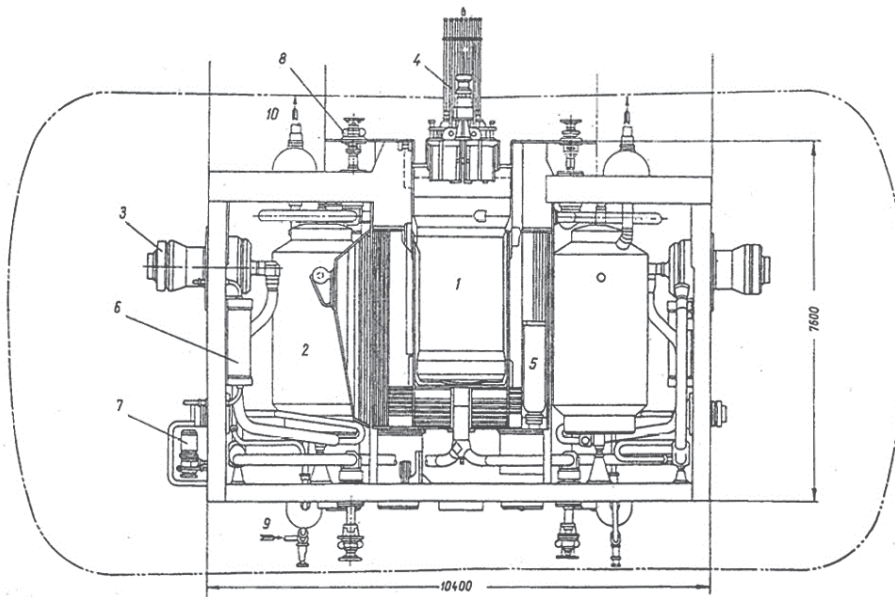


Fig. 6. Layout of the OK-150 plant. 1: Reactor, 2: Steam generator, 3: Main circulation pumps, 4: Control rod drives mechanism, 5: Filter, 6: Cooler, 7: Emergency cooling pump, 8: Primary circuit pressure relief valve, 9: Feedwater inlet, 10: Steam outlet (Reistad et. al., 2006).

The polyethylene sheets are spaced so as to allow thermal expansion. Thick collision mats consisting of alternate layers of steel and wood are placed on the sides of the containment. The effective dose rate at the surface of the secondary sheet does not exceed 5 cSv (rem)/year. The containment is airtight. Personnel can remain in it for up to 30 minutes after reactor shutdown and the radiation level would have fallen to less than 0.2 cSv (rem)/hr.

The primary shielding is here made of an annular water tank that surrounds the reactor and a layer of lead attached to the outer surface of the tank, to minimize space. The height of the tank is 5.2 m, the thickness of the water layer, 84 cm, and the thickness of the lead is 5-10 cm. The weight of the primary shields is 68.2 tons, and with the water it is 118.2 tons. The weight of the containment is 227 tons. The secondary shielding weights 1795 tons consisting of: 561 tons of ordinary concrete, 289 tons of lead, 69 tons of polyethylene, and 160 tons of collision mats. The latter consist of 22 tons of wood and 138 tons of steel. The shielding complex is optimized to minimize the space used, while providing low radiation doses to the crew quarters. It is comparatively heavy because of the use of lead and steel, and is complicated to install.

The Integral circuit design offers a substantial degree of inherent safety since the pumps; the steam generators and reactor core are all contained within the same pressure vessel. Since the primary circulating fluid is contained within the vessel, any leaking fluid would be contained within the vessel in case of an accident. This also eliminates the need for extensive piping to circulate the coolant from the core to the steam generators. In loop type circuits, a possibility exists for pipe rupture or leakage of the primary coolant pipes. This source of accidents is eliminated in an integral type of a reactor (Collier, 1987).

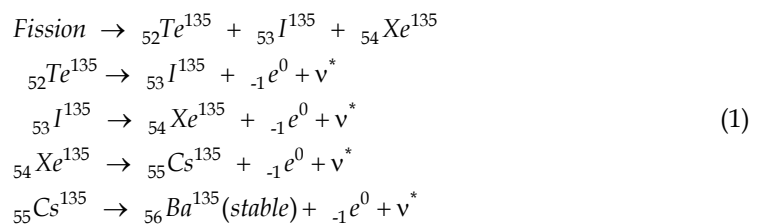
## 6. Xenon generation

The fission process generates a multitude of fission products with different yields (Lamarsh, 1983). Table 3 shows some of these fission products yields resulting from the fission of three fissile isotopes:

Isotope	${}_{92}\text{U}^{233}$	${}_{92}\text{U}^{235}$	${}_{94}\text{Pu}^{239}$
${}_{53}\text{I}^{135}$	0.04750	0.06390	0.06040
${}_{54}\text{Xe}^{135}$	0.01070	0.00237	0.01050
${}_{61}\text{Pm}^{149}$	0.00795	0.01071	0.01210

Table 3. Fission products yields from thermal 2200 m/sec neutrons,  $\gamma_i$  [nuclei/fission event] (Lamarsh, 1983).

The most prominent of these fission products from the perspective of reactor control is  ${}_{54}\text{Xe}^{135}$ . It is formed as the result of the decay of  ${}_{53}\text{I}^{135}$ . It is also formed in fission and by the decay of the tellurium isotope:  ${}_{52}\text{Te}^{135}$ . This can be visualized as follows:



The half lives of the components of this chain are shown in Table 4. The end of the chain is the stable isotope  ${}_{56}\text{Ba}^{135}$ . Because  ${}_{52}\text{Te}^{135}$  decays rapidly with a half life of 11 seconds into  ${}_{53}\text{I}^{135}$ , one can assume that all  ${}_{53}\text{I}^{135}$  is produced directly in the fission process.

Denoting  $I(t)$  as the atomic density of iodine in [nuclei/cm<sup>3</sup>],  $\psi$  as the thermal neutron flux [n / (cm<sup>2</sup>.sec)] one can write a rate equation for the iodine as:

$$\begin{aligned} \frac{dI(t)}{dt} &= [\text{rate of formation of iodine from fission}] \\ &\quad - [\text{rate of radioactive transformations of iodine}] \\ \frac{dI(t)}{dt} &= \gamma_I \Sigma_f \psi - \lambda_I I(t) \end{aligned} \quad (2)$$

where:  $\gamma_I$  is the fission yield in [nuclei/fission event],

$\Sigma_f$  is the thermal fission cross section in [cm<sup>-1</sup>],

$\lambda_I$  is the decay constant in [sec<sup>-1</sup>], with  $\lambda_I = \frac{\ln 2}{T_{1/2}}$ ,  $T_{1/2}$  is the half life.

Isotope	Half Life, $T_{1/2}$
<sup>52</sup> Te <sup>135</sup>	11 sec
<sup>53</sup> I <sup>135</sup>	6.7 hr
<sup>54</sup> Xe <sup>135</sup>	9.2 hr
<sup>55</sup> Cs <sup>135</sup>	2.3x10 <sup>6</sup> yr
<sup>56</sup> Ba <sup>135</sup>	Stable

Table 4. Half lives of the isotopes in the xenon decay chain.

A rate equation can also be written for the xenon in the form:

$$\begin{aligned} \frac{dX(t)}{dt} &= [\text{rate of formation of xenon from fission}] \\ &\quad + [\text{rate of formation of Xe from the transformation of the Iodine}] \\ &\quad - [\text{rate of radioactive transformations of xenon}] \\ &\quad - [\text{rate of disappearance of xenon (X) through neutron absorptions}], \end{aligned} \quad (3)$$

or :

$$\frac{dX(t)}{dt} = \gamma_X \Sigma_f \psi + \lambda_I I(t) - \lambda_X X(t) - \sigma_{aX} \psi X(t)$$

where  $\sigma_{aX}$  is the thermal microscopic absorption cross section for xenon equal to  $2.65 \times 10^6$  [b].

The large value of the absorption cross section of Xe, and its delayed generation from iodine, affect the operation of reactors both under equilibrium and after shutdown conditions.

## 7. Iodine and xenon equilibrium concentrations

Under equilibrium conditions, the rate of change of the iodine as well as the xenon concentrations is zero:

$$\frac{dI(t)}{dt} = \frac{dX(t)}{dt} = 0 \quad (4)$$

This leads to an equilibrium concentration for the iodine as:

$$I_0 = \frac{\gamma_I \Sigma_f \Psi}{\lambda_I} \quad (5)$$

The equilibrium concentration for the xenon will be:

$$X_0 = \frac{\gamma_X \Sigma_f \Psi + \lambda_I I_0}{\lambda_X + \sigma_{aX} \Psi} \quad (6)$$

Substituting for the equilibrium concentration of the iodine, we can write:

$$X_0 = \frac{(\gamma_X + \gamma_I) \Sigma_f \Psi}{\lambda_X + \sigma_{aX} \Psi} \quad (7)$$

## 8. Reactivity equivalent of xenon poisoning

Ignoring the effects of neutron leakage, since it has a minor effect on fission product poisoning, we can use the infinite medium multiplication factor for a poisoned reactor in the form of the four factor formula (Ragheb, 1982):

$$k = \eta \epsilon p f \quad (8)$$

and for an unpoisoned core as:

$$k_0 = \eta \epsilon p f_0 \quad (9)$$

We define the reactivity  $\rho$  of the poisoned core as:

$$\rho = \frac{k - k_0}{k} = \frac{\Delta k}{k} = \frac{f - f_0}{f} = 1 - \frac{f_0}{f} \quad (10)$$

In this equation,

$\eta = \frac{\nu \Sigma_f}{\Sigma_{aF}}$ , is the regeneration factor,

$\epsilon$  is the fast fission factor,

$p$  is the resonance escape probability,

$\nu$  is the average neutron yield per fission event,

$\Sigma_f$  is the macroscopic fission cross section,

$\Sigma_{aF}$  is the macroscopic absorption cross section of the fuel,

$f$  is the fuel utilization factor.

The fuel utilization factor for the unpoisoned core is given by:

$$f_0 = \frac{\Sigma_{aF}}{\Sigma_{aF} + \Sigma_{aM}} \quad (11)$$

And for the poisoned core it is:

$$f = \frac{\Sigma_{aF}}{\Sigma_{aF} + \Sigma_{aM} + \Sigma_{aP}} \quad (12)$$

where:

$\Sigma_{aM}$  is the moderator's macroscopic absorption coefficient,

$\Sigma_{aP}$  is the poison's macroscopic absorption coefficients.

From the definition of the reactivity in Eqn. 10, and Eqns. 11 and 12 we can readily get:

$$\rho = - \frac{\Sigma_{aP}}{\Sigma_{aF} + \Sigma_{aM}} \quad (13)$$

It is convenient to express the reactivity in an alternate form. For the unpoisoned critical core:

$$1 = k_0 = \eta \epsilon p f_0 = \eta \epsilon p \frac{\Sigma_{aF}}{\Sigma_{aF} + \Sigma_{aM}} \quad (14)$$

From which:

$$\Sigma_{aF} + \Sigma_{aM} = \eta \epsilon p \Sigma_{aF} \quad (15)$$

Substituting this value in the expression of the reactivity, and the expression for the regeneration factor, we get:

$$\rho = - \frac{1}{v \epsilon p} \frac{\Sigma_{aP}}{\Sigma_f} \quad (16)$$

For equilibrium xenon:

$$\Sigma_{aP} = \sigma_{aX} X_0 = \frac{(\gamma_X + \gamma_I) \Sigma_f \psi \sigma_{aX}}{\lambda_X + \sigma_{aX} \psi} \quad (17)$$

Inserting the last equation for the expression for the reactivity we get:

$$\rho = - \frac{(\gamma_X + \gamma_I) \psi \sigma_{aX}}{(\lambda_X + \sigma_{aX} \psi) v \epsilon p} \quad (18)$$

Dividing numerator and denominator by  $\sigma_{aX}$  we get:

$$\rho = - \frac{(\gamma_X + \gamma_I) \psi}{\left(\frac{\lambda_X}{\sigma_{aX}} + \psi\right) v \epsilon p} \quad (18)'$$

The parameter:

$$\varphi = \frac{\lambda_X}{\sigma_{aX}} = 0.77 \times 10^{13} \quad (19)$$

at 20 degrees C, and has units of the flux [neutrons/(cm<sup>2</sup>.sec)].

The expression for the reactivity is written in terms of  $\varphi$  as:

$$\rho = - \frac{(\gamma_X + \gamma_I)\psi}{(\varphi + \psi) \nu \epsilon p} \quad (18)''$$

For a reactor operating at high flux,

$$\varphi \approx \psi ,$$

and we can write:

$$\rho = - \frac{(\gamma_X + \gamma_I)}{\nu \epsilon p} \quad (20)$$

### Example

For a reactor fueled with  $U^{235}$ ,  $\nu = 2.42$ ,  $p = \epsilon = 1$ , the value for  $\rho$  for equilibrium xenon is:

$$\rho = - \frac{(0.00237 + 0.06390)}{2.42} = - \frac{0.06627}{2.42} = -0.027384$$

or a negative 2.74 percent.

## 9. Reactor dead time

A unique behavior occurs to the xenon after reactor shutdown. Although its production ceases, it continues to build up as a result of the decay of its iodine parent. Therefore the concentration of the xenon increases after shutdown. Since its cross section for neutrons is so high, it absorbs neutrons and prevents the reactor from being restarted for a period of time denoted as the "reactor dead time."

In a land based reactor, since the xenon eventually decays, after about 24 hours, the reactor can then be restarted. In naval propulsion applications, a naval vessel cannot be left in the water unable to be restarted and vulnerable to enemy attack by depth charges or torpedoes. For this reason, naval reactor cores must be provided with enough reactivity to overcome the xenon negative reactivity after shutdown.

To analyze the behavior, let us rewrite the rate equations for iodine and xenon with  $\psi$  equal to 0 after shutdown:

$$\frac{dI(t)}{dt} = - \lambda_I I(t) \quad (21)$$

$$\frac{dX(t)}{dt} = + \lambda_I I(t) - \lambda_X X(t) \quad (22)$$

Using Bateman's solution (Ragheb, 2011), the iodine and xenon concentrations become respectively:

$$I(t) = I_0 e^{-\lambda_I t} \quad (23)$$

$$X(t) = X_0 e^{-\lambda_X t} + \frac{\lambda_I}{\lambda_I - \lambda_X} I_0 (e^{-\lambda_X t} - e^{-\lambda_I t}) \quad (24)$$



Substituting for the equilibrium values of  $X_0$  and  $I_0$  we get:

$$X(t) = \frac{(\gamma_X + \gamma_I)\Sigma_f\Psi}{\lambda_X + \sigma_{aX}\Psi} e^{-\lambda_X t} + \frac{\gamma_I}{\lambda_I - \lambda_X} \Sigma_f\Psi (e^{-\lambda_X t} - e^{-\lambda_I t}) \quad (25)$$

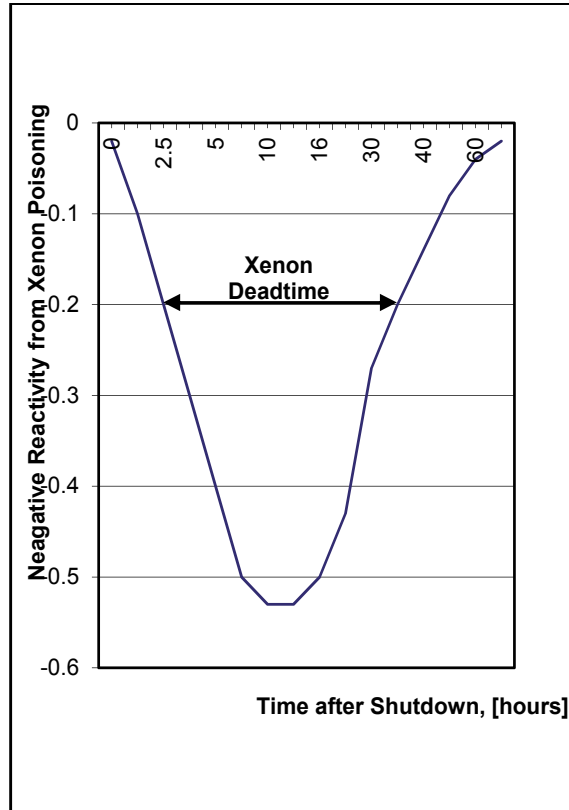


Fig. 7. Negative reactivity due to xenon poisoning. Flux =  $5 \times 10^{14}$  [n/(cm<sup>2</sup>.sec)] (Ragheb, 2011).

The negative reactivity due to xenon poisoning is now a function of time and is given by:

$$\begin{aligned} \rho(t) &= - \frac{1}{v\epsilon p} \frac{\Sigma_{aP}(t)}{\Sigma_f} \\ &= - \frac{1}{v\epsilon p} \frac{\sigma_{aP}X(t)}{\Sigma_f} \\ &= - \frac{\sigma_{aP}\Psi}{v\epsilon p} \left[ \frac{\gamma_X + \gamma_I}{\lambda_X + \sigma_{aX}\Psi} e^{-\lambda_X t} + \frac{\gamma_I}{\lambda_I - \lambda_X} (e^{-\lambda_X t} - e^{-\lambda_I t}) \right] \end{aligned} \quad (26)$$

Figure 7 shows the negative reactivity resulting from xenon after reactor shutdown. It reaches a minimum value, which occurs at 10 hours after shutdown. This post shutdown reactivity is important in reactors that have operated at a high flux level. If at any

time after shutdown, the positive reactivity available by removing all the control rods is less than the negative reactivity caused by xenon, the reactor cannot be restarted until the xenon has decayed. In Fig. 7, at an assumed reactivity reserve of 20 percent, during the time interval from 2.5 hours to 35 hours, the reactor cannot be restarted. This period of 35-2.5 = 32.5 hours is designated as the “Reactor Dead Time.”

This reactor dead time is of paramount importance in mobile systems that may be prone to accidental scrams. This is more important at the end of core lifetime, when the excess reactivity is limited. For this reason, mobile reactors necessitate the adoption of special design features, providing the needed excess reactivity to override the negative xenon reactivity, such as the use of highly enriched cores.

In land based systems such as the Canadian Deuterium Uranium (CANDU) reactor concept, booster rods of highly enriched U<sup>235</sup> are available to override the xenon dead time after shutdown, leading to a higher capacity factor. Power fluctuations induced to follow demand in any power reactor lead to xenon oscillations without any reactor shutdown. The changes of xenon concentrations due to load following are compensated for by adjusting the chemical shim or boron concentration in the coolant, and by control rods adjustments.

## 10. Nuclear navies

The USA nuclear fleet grew rapidly at the height of the East West Cold War in the 1980s. About one fourth of the submarine fleet carried intercontinental ballistic missiles. These can be ejected by the use of compressed air while the submarine is totally submerged, with the rocket engine starting once the missile is above the water surface.

In the Falkland Islands War, a single nuclear British submarine paralyzed the entire Argentinean Naval fleet. It sunk the cruiser “General Belgrano” and forced the Argentine Navy to not deploy out of port.

During the first and second Gulf Wars, and in the Lybia conflict, the USA Navy launched Tomahawk missiles, had unchallenged use of the oceans and protected 85 percent of the war supplies that were transported by ships.

### 10.1 Navy carrier force

The mission of the aircraft carrier force is to provide a credible, sustainable, independent forward presence and a conventional deterrence in peace times. In times of crisis, it operates as the cornerstone of joint and/or allied maritime expeditionary forces. It operates and support air attacks on enemies, protects friendly forces and engages in sustained independent operations in times of war. As an example, the vital statistics of the nuclear Nimitz Class aircraft carrier are:

Power Plant:	Two nuclear reactors, four shafts.
Length:	1,092 feet.
Beam:	134 feet.
Displacement:	97,000 tons at full load.
Speed:	30 knots, 34.5 miles per hour.
Aircraft:	85.
Crew:	500 officers, 5,000 enlisted.

## 10.2 Nuclear submarine force

The USA submarine force maintains its position as the world's preeminent submarine force. It incorporates new and innovative technologies allowing it to maintain dominance throughout the naval battle space. It incorporates the multiple capabilities of submarines and develops tactics for high seas control, land battle support as well as strategic deterrence. It also fills the role of a stealthy signal and intelligence gathering and a full spectrum of special operations and expeditionary missions. It includes forces of ballistic missile submarines (SSBN), guided missile submarines (SSGN), and attack submarines (SSN). The vital statistics of the Ballistic Missile Trident submarines and the guided missiles submarines are:

Armament, SSBN:	Trident missiles.
Armament, SSGN:	154 Tomahawk missiles, 66 Special operation Forces.
Power Plant:	One nuclear reactor, one shaft.
Length:	560 feet.
Beam:	42 feet.
Displacement:	18,750 tons, submerged.
Speed:	20 knots, 23 miles per hour.
Crew:	15 officers, 140 enlisted.

The statistics for the fast attack Los Angeles class submarines are:

Power Plant:	One nuclear reactor, one shaft.
Length:	360 feet.
Beam:	33 feet.
Displacement:	6,900 tons, submerged.
Speed:	25 knots, 28 miles per hour.
Crew:	12 officers, 121 enlisted.

## 10.3 Russian navy

The nuclear Russian navy also reached its peak at the same time as the USA navy. The first of the Typhoon Class 25,000 ton strategic ballistic missile submarines was launched in 1980 from the Severodvinsk Shipyard on the White Sea. In the same year the first Oscar Class guided missile submarine was launched. It is capable of firing 24 long range anti-ship cruise missiles while remaining submerged. Five shipyards produced seven different classes of submarines.

The Delta IV class is nuclear-powered with two VM-4 pressurized water reactors rated at 180 MWth. There are two turbines, type GT3A-365 rated at 27.5MW. The propulsion system drives two shafts with seven-bladed fixed-pitch propellers.

## 10.4 Chinese navy

Five hundred years ago the contender for the dominance of the world's oceans was the Chinese imperial exploration fleet which was at its peak technologically centuries ahead of its competitors. A strategic mistake by its emperor was to neglect its sea access with the result of opening the door to European (The Opium Wars) and then Japanese military intervention and occupation. Being the world's second largest importer of petroleum after the USA, China seeks to protect its energy corridors by sea and free access to Southeast Asia sea lanes beyond the Indochinese Peninsula.

China's naval fleet as of 2008 had 5 nuclear powered fast attack submarines and one ballistic missiles submarine carrying 12-16 nuclear tipped missiles with a range of 3,500 km. This is in addition to 30 diesel electric submarines with 20 other submersibles.

The Chinese submarine fleet is expected to exceed the number of USA's Seventh Fleet ships in the Pacific Ocean by 2020 with the historic patience and ambition to pursue a long term strategy of eventually matching and then surpassing the USA's regional dominance.

## 11. Nuclear cruise missile submarines

The nuclear powered Echo I and II, and the Charlie I and II can fire eight antiship weapons cruise missiles while remaining submerged at a range of up to 100 kilometers from the intended target. These cruise missile submarines also carry ASW and anti-ship torpedoes.

The nuclear cruise missile submarines are meant to operate within range of air bases on land. Both forces can then launch coordinated attacks against an opponent's naval forces. Reconnaissance aircraft can then provide target data for submarine launched missiles.

## 12. Nuclear ballistic missile submarines

Submarine Launched Ballistic Missiles (SLBMs) on Nuclear Powered Ballistic Missile Submarines (SSBNs) have been the basis of strategic nuclear forces. Russia had more land based Intercontinental Ballistic Missiles (ICBMs) than the SLBM forces (Weinberger, 1981).

The Russian ICBM and SLBM deployment programs initially centered on the SS-9 and SS-11 ICBMs and the SS-N-6/Yankee SLBM/SSBN weapons systems. They later used the Multiple Independently targetable Reentry Vehicles (MIRVs) SS-N-18 on the Delta Class nuclear submarines, and the SS-NX-20 on the nuclear Typhoon Class SSBN submarine.

The Russian SLBM force has reached 62 submarines carrying 950 SLBMs with a total of almost 2,000 nuclear warhead reentry vehicles. Russia deployed 30 nuclear SSBNs, and the 20 tube very large Typhoon SSBN in the 1980s. These submarines were capable to hit targets across the globe from their homeports.

The 34 deployed Yankee Class nuclear submarines each carried 16 nuclear tipped missiles. The SS-N-6/Yankee I weapon system is composed of the liquid propellant SS-N-6 missile in 16 missile tubes launchers on each submarine. One version of the missiles carries a single Reentry Vehicle (RV) and has an operational range of about 2,400 to 3,000 kilometers. Another version carries 2 RVs, and has an operational range of about 3,000 kilometers.

The Delta I and II classes of submarines displaced 11,000 tons submerged and have an overall length of about 140 meters. These used the SS-N-8 long range, two stages, liquid propellant on the 12-missile tube Delta I and the 16 missile tube Delta II submarines. The SS-N-8 has a range of about 9,000 kilometers and carries one RV. The SS-N-18 was used on the 16 missile tube Delta III submarines, and has MIRV capability with a booster range of 6,500 to 8,000 kilometers, depending on the payload configuration. The Delta III nuclear submarines could cover most of the globe from the relative security of their home waters with a range of 7,500 kilometers.

The Typhoon Class at a 25,000 tons displacement, twice the size of the Delta III with a length of 170 m and 20 tubes carrying the SS-NX-20 missile each with 12 RVs, has even greater range at 8,300 kms, higher payload, better accuracy and more warheads.

### 13. Nuclear attack submarines

At some time the Russian Navy operated about 377 submarines, including 180 nuclear powered ones, compared with 115 in the USA navy. The Russian navy operated 220 attack submarines, 60 of them were nuclear powered. These included designs of the November, Echo, Victor, and Alfa classes. The Victor class attack submarine, was characterized by a deep diving capability and high speed.

### 14. Alfa class submarines

The Alfa Class submarine is reported to have been the fastest submarine in service in any navy. It was a deep diving, titanium hull submarine with a submerged speed estimated to be over 40 knots. The titanium hull provided strength for deep diving. It also offered a reduced weight advantage leading to higher power to weight ratios resulting in higher accelerations. The higher speed could also be related to some unique propulsion system. The high speeds of Russian attack submarines were meant to counter the advanced propeller cavitation and pump vibration reduction technologies in the USA designs, providing them with silent and stealth hiding and maneuvering.

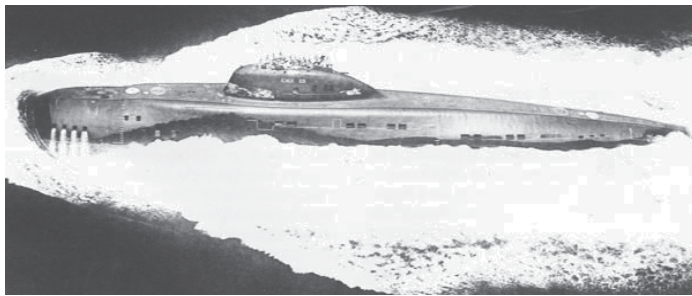


Fig. 8. The Nuclear Powered Russian VICTOR I class Attack Submarine (Weinberger, 1981).

The Alfa Class of Russian submarines used a lead and bismuth alloy cooled fast reactors. They suffered corrosion on the reactor components and activation through the formation of the highly toxic  $\text{Po}^{210}$  isotope. Refueling needed a steam supply to keep the liquid metal molten above 257 °F.

Advantages were a high cycle efficiency and that the core can be allowed to cool into a solid mass with the lead providing adequate radiation shielding. This class of submarines has been decommissioned.

### 15. Seawolf class submarines

The Seawolf class of submarines provided stealth, endurance and agility and are the most heavily armed fast attack submarines in the world.

They provided the USA Navy with undersea weapons platforms that could operate in any scenario against any threat, with mission and growth capabilities that far exceed Los Angeles-class submarines. The robust design of the Seawolf class enabled these submarines to perform a wide spectrum of military assignments, from underneath the Arctic icepack to littoral regions of the world. These were capable of entering and remaining in the backyards of potential adversaries undetected, preparing and shaping the battle space and striking

rapidly. Their missions include surveillance, intelligence collection, special warfare, cruise missile strike, mine warfare, and anti-submarine and anti-surface ship warfare

Builder	General Dynamics, Electric Boat Division.
Power plant	One S6W nuclear reactor, one shaft.
Length	SSN 21 and SSN 22: 353 feet (107.6 meters) SSN 23: 453 feet (138 meters)
Beam	40 feet (12.2 meters)
Submerged Displacement	SSN 21 and SSN 22: 9,138 tons (9,284 metric tons) SSN 23 12,158 tons (12,353 metric tons)
Speed	25+ knots (28+ miles / hour, 46.3+ kilometers / hour)
Crew	140: 14 Officers; 126 Enlisted
Armaments	Tomahawk missiles, MK-48 torpedoes, eight torpedo tubes
Commissioning dates	Seawolf: July 19, 1997 Connecticut: December 11, 1998; Jimmy Carter: February 19, 2005.

Table 5. Seawolf class of submarines technical specifications.

## 16. Ohio class submarines

The Ohio Class submarine is equipped with the Trident strategic ballistic missile from Lockheed Martin Missiles and Space. The Trident was built in two versions, Trident I (C4), which is phased out, and the larger and longer range Trident II (D5), which entered service in 1990. The first eight submarines, (SSBN 726 to 733 inclusive) were equipped with Trident I and the following ten (SSBN 734 to 743) carry the Trident II. Conversion of the four Trident I submarines remaining after the START II Treaty (Henry M. Jackson, Alabama, Alaska and Nevada), to Trident II began in 2000 and completed in 2008. Lockheed Martin produced 12 Trident II missiles for the four submarines.

The submarine has the capacity for 24 Trident missile tubes in two rows of 12. The dimensions of the Trident II missile are length 1,360 cm x diameter 210 cm and the weight is 59,000 kg. The three-stage solid fuel rocket motor is built by ATK (Alliant Techsystems) Thiokol Propulsion. The USA Navy gives the range as “greater than 7,360 km” but this could be up to 12,000 km depending on the payload mix. Missile guidance is provided by an inertial navigation system, supported by stellar navigation. Trident II is capable of carrying up to twelve MIRVs, each with a yield of 100 kilotons, although the SALT treaty limits this number to eight per missile. The circle of equal probability, or the radius of the circle within which half the strikes will impact, is less than 150 m. The Sperry Univac Mark 98 missile control system controls the 24 missiles.

The Ohio class submarine is fitted with four 533 mm torpedo tubes with a Mark 118 digital torpedo fire control system. The torpedoes are the Gould Mark 48 torpedoes. The Mark 48 is a heavy weight torpedo with a warhead of 290 kg, which has been operational in the USA Navy since 1972. The torpedo can be operated with or without wire guidance and the system has active and/or passive acoustic homing. The range is up to 50 km at a speed of 40 knots. After launch, the torpedo carries out target search, acquisition and attack procedures delivering to a depth of 3,000 ft.

The Ohio class submarine is equipped with eight launchers for the Mk 2 torpedo decoy. Electronic warfare equipment is the WLR-10 threat warning system and the WLR-8(V)

surveillance receiver from GTE of Massachusetts. The WLR-8(V) uses seven YIG tuned and vector tuned super heterodyne receivers to operate from 50MHz up to J-band. An acoustic interception and countermeasures system, AN/WLY-1 from Northrop Grumman, has been developed to provide the submarine with an automatic response against torpedo attack.

The surface search, navigation and fire control radar is BPS 15A I/J band radar. The sonar suite includes: IBM BQQ 6 passive search sonar, Raytheon BQS 13, BQS 15 active and passive high-frequency sonar, BQR 15 passive towed array from Western Electric, and the active BQR 19 navigation sonar from Raytheon. Kollmorgen Type 152 and Type 82 periscopes are fitted.

The main machinery is the GE PWR S8G reactor system with two turbines providing 60,000 hp and driving a single shaft. The submarine is equipped with a 325 hp Magnatek auxiliary propulsion motor. The propulsion provides a speed in excess of 18 knots surfaced and 25 knots submerged.

It is designed for mine avoidance, special operations forces delivery and recovery. It uses non acoustic sensors, advanced tactical communications and non acoustic stealth. It is equipped with conformal sonar arrays which seek to provide an optimally sensor coated submarine with improved stealth at a lower total ownership cost. New technology called Conformal Acoustic Velocity Sonar (CAVES) could replace the existing Wide Aperture Array technology and is to be implemented in units of the Virginia Class.

Power Plant	Single S9G PWR Single shaft with pump jet propulsion One secondary propulsion submerged motor
Displacement	7,800 tons, submerged
Length	277 ft
Draft	32 ft
Beam	34 ft
Speed	25+ knots, submerged
Horizontal tubes	Four 21 inches torpedo tubes
Vertical tubes	12 Vertical Launch System Tubes
Weapon systems	39, including: Vertical Launch System Tomahawk Cruise Missiles Mk 48 ADCAP Heavy weight torpedoes Advanced Mobile Mines Unmanned Undersea Vehicles
Special warfare	Dry Deck Shelter
Sonars	Spherical active/passive arrays Light Weight Wide Aperture Arrays TB-16, TB-29 and future towed arrays High frequency chin and sail arrays
Counter measures	1 internal launcher 14 external launchers
Crew	113 officers and men

Table 6. Technical Specifications of the Virginia Class of Submarines.

High Frequency Sonar will play a more important role in future submarine missions as operations in the littorals require detailed information about the undersea environment to support missions requiring high quality bathymetry, precision navigation, mine detection or ice avoidance. Advanced High Frequency Sonar systems are under development and testing that will provide submarines unparalleled information about the undersea environment. This technology will be expanded to allow conformal sonar arrays on other parts of the ship that will create new opportunities for use of bow and sail structure volumes while improving sonar sensor performance.

## 17. Nuclear ice-breakers

Nuclear-powered icebreakers were constructed by Russia for the purpose of increasing the shipping along the northern coast of Siberia, in ocean waters covered by ice for long periods of time and river shipping lanes. The nuclear powered icebreakers have far more power than their diesel powered counterparts, and for extended time periods. During the winter, the ice along the northern Russian sea way varies in thickness from 1.2 - 2 meters. The ice in the central parts of the Polar Sea is 2.5 meters thick on average. Nuclear-powered icebreakers can break this ice at speeds up to 10 knots. In ice free waters the maximum speed of the nuclear powered icebreakers is 21 knots. In 1988 the NS Sevmorpu was commissioned in Russia to serve the northern Siberian ports. It is a 61,900 metric tonnes, 260 m long and is powered by the KLT-40 reactor design, delivering 32.5 propeller MW from the 135 MWth reactor.

Russia operated at some time up to eight nuclear powered civilian vessels divided into seven icebreakers and one nuclear-powered container ship. These made up the world's largest civilian fleet of nuclear-powered ships. The vessels were operated by Murmansk Shipping Company (MSC), but were owned by the Russian state. The servicing base Atomflot is situated near Murmansk, 2 km north of the Rosta district.

Icebreakers facilitated ores transportation from Norilsk in Siberia to the nickel foundries on the Kola Peninsula, a journey of about 3,000 kms. Since 1989 the nuclear icebreakers have been used to transport wealthy Western tourists to visit the North Pole. A three week long trip costs \$ 25,000.

The icebreaker Lenin, launched in 1957 was the world's first civilian vessel to be propelled by nuclear power. It was commissioned in 1959 and retired from service in 1989. Eight other civilian nuclear-powered vessels were built: five of the Arktika class, two river icebreakers and one container ship. The nuclear icebreaker Yamal, commissioned in 1993, is the most recent nuclear-powered vessel added to the fleet.

The nuclear icebreakers are powered by PWRs of the KLT-40 type. The reactor contains fuel enriched to 30-40 percent in U<sup>235</sup>. By comparison, nuclear power plants use fuel enriched to only 3-5 percent. Weapons grade uranium is enriched to over 90 percent. American submarine reactors are reported to use up to 97.3 percent enriched U<sup>235</sup>. The irradiated fuel in test reactors contains about 32 percent of the original U<sup>235</sup>, implying a discharge enrichment of  $97.3 \times 0.32 = 31.13$  percent enrichment.

Under normal operating conditions, the nuclear icebreakers are only refueled every three to four years. These refueling operations are carried out at the Atomflot service base. Replacement of fuel assemblies takes approximately 1 1/2 months.

For each of the reactor cores in the nuclear icebreakers, there are four steam generators that supply the turbines with steam. The third cooling circuit contains sea water that condenses



and cools down the steam after it has run through the turbines. The icebreaker reactors' cooling system is especially designed for low temperature Arctic sea water.

## **18. Discussion: Defining trends**

Several trends may end up shaping the future of naval ship technology: the all electrical ship, stealth technology, littoral vessels and moored barges for power production. Missions of new naval systems are evolving towards signal intelligence gathering and clandestine special forces insertion behind enemy lines requiring newer designs incorporating stealth configurations and operation.

The all-electric ship propulsion concept was adopted for the future surface combatant power source. This next evolution or Advanced Electrical Power Systems (AEPS) involves the conversion of virtually all shipboard systems to electric power; even the most demanding systems, such as propulsion and catapults aboard aircraft carriers. It would encompass new weapon systems such as modern electromagnetic rail-guns and free electron lasers.

Littoral vessels are designed to operate closer to the coastlines than existing vessels such as cruisers and destroyers. Their mission would be signal intelligence gathering, stealth insertion of Special Forces, mine clearance, submarine hunting and humanitarian relief. Unmanned Underwater Vehicles (UUVs), monitored by nuclear-powered Virginia Class submarines would use Continuous Active Sonar (CAS) arrays which release a steady stream of energy, the sonar equivalent of a flashlight would be used as robots to protect carrier groups and turning attacking or ambushing submarines from being the hunters into being the hunted.

### **18.1 All electric propulsion and stealth ships**

The CVN-21's new nuclear reactor not only will provide three times the electrical output of current carrier power plants, but also will use its integrated power system to run an Electro Magnetic Aircraft Launch System (EMALS) to replace the current steam-driven catapults, combined with an Electromagnetic Aircraft Recovery System (EARS). To store large amounts of energy, flywheels, large capacitor banks or other energy storage systems would have to be used.

A typical ship building experience involved the design conversion of one class of submarines to an all-electric design. The electric drive reduced the propulsion drive system size and weight; eliminating the mechanical gearbox. However, the power system required extensive harmonic filtering to eliminate harmonic distortion with the consequence that the overall vessel design length increased by 10 feet.

Tests have been conducted to build stealth surface ships based on the technology developed for the F-117 Nighthawk stealth fighter. The first such system was built by the USA Navy as "The Sea Shadow." The threat from ballistic anti ship missiles and the potential of nuclear tipped missiles has slowed down the development of stealth surface ships. The USA Navy cut its \$5 billion each DDG-1000 stealth destroyer ships from an initially planned seven to two units.

Missile defense emerged as a major naval mission at the same time that the DDG-1000's stealth destroyer design limitations and rising costs converged, all while shipbuilding

budgets were getting squeezed. The SM-3 Standard missile, fired only by warships, is the most successful naval missile defense system; having passed several important trials while other Ballistic Missile Defense, BMD weapons are under testing. The ballistic-missile threat is such that the USA Navy decided it needed 89 ships capable of firing the SM-3 and that the DDG-1000 realistically would never be able to fire and guide the SM-3 since the stealth destroyer is optimized for firing land-attack missiles not Standard missiles.



Fig. 9. The DDG-1000 stealth destroyer is optimized for firing land-attack missiles; not Ballistic Missile Defense, BMD missiles. The Raytheon Company builds the DDG-1000's SPY-3 radar, and Bath Iron Works, the Maine shipyard builds the DDG-1000. (Source: Raytheon).

The USA Navy has 84 large surface combatants, split between Arleigh-Burke Class destroyers and the Ticonderoga Class cruisers, capable of carrying the combination of Standard missiles and the BMD capable Aegis radar. The DDG-1000 cannot affordably be modified to fire SM-3s. So the Navy needs another 12 SM-3 "shooters" to meet the requirement for missile defense, and there was no time to wait for the future CG-X cruiser. With new amphibious ships, submarines, carriers and Littoral Combat Ships in production alongside the DDG-1000s, there was no room in the budget for five extra DDG-1000s.

### 18.2 Multipurpose floating barges

The vision of floating barges with nuclear reactors to produce electrical power for industrial and municipal use, hydrogen for fuel cells, as well as fresh desalinated water at the shores of arid areas of the world may become promising future prospects. The electricity can be used to power a new generation of transportation vehicles equipped with storage batteries, or the hydrogen can be used in fuel cells vehicles. An urban legend is related about a USA Navy nuclear submarine under maintenance at Groton, Connecticut, temporarily supplying the neighboring port facilities with electricity when an unexpected power outage occurred. This would have required the conversion, of the 120 Volts and 400 Hz military electricity standard to the 10-12 kV and 60 Hz civilian one. Submarines tied up at port connect to a

connection network that matches frequency and voltage so that the reactors can be shut down. The two electrical generators on a typical submarine would provide about  $3 \text{ MWe} \times 2 = 6 \text{ MWe}$  of power, with some of this power used by the submarine itself. In case of a loss of local power, docked vessels have to start their reactors or their emergency diesel generators anyway.

The accumulated experience of naval reactors designs is being as the basis of a trend toward the consideration of a new generation of modular compact land-based reactor designs.



Fig. 10. The Phalanx radar-guided gun, nicknamed as R2-D2 from the Star-Wars movies, is used for close-in ship defense. The radar controlled Gatling gun turret shooting tungsten armor-piercing, explosive, or possibly depleted uranium munitions on the USS Missouri, Pearl Harbor, Hawaii. (Photo: M. Ragheb).

## 19. References

- Ragheb, Magdi, "Lecture Notes on Fission Reactors Design Theory," FSL-33, University of Illinois, 1982.
- Lamarsh, John, "Introduction to Nuclear Engineering," Addison-Wesley Publishing Company, 1983.
- Murray, Raymond L., "Nuclear Energy," Pergamon Press, 1988.
- Collier, John G., and Geoffrey F. Hewitt, "Introduction to Nuclear Power," Hemisphere Publishing Corp., Springer Verlag, 1987.

Broder, K. K. Popkov, and S. M. Rubanov, "Biological Shielding of Maritime Reactors," AEC-tr-7097, UC-41, TT-70-5006, 1970.

Weinberger, Caspar, "Soviet Military Power," USA Department of Defense, US Government Printing Office, 1981.

Reid, T. R., "The Big E," National Geographic, January 2002.

Poston, David I. , "Nuclear design of the SAFE-400 space fission reactor," Nuclear News, p.28, Dec. 2002.

Reistad, Ole, and Povl L Olgaard, "Russian Power Plants for Marine Applications," NKS-138, Nordisk Kernesikkerhedsforskning, April 2006.

Ragheb, Magdi, "Nuclear, Plasma and Radiation Science, Inventing the Future," <https://netfiles.uiuc.edu/mragheb/www>, 2011.

# Assessment of Deployment Scenarios of New Fuel Cycle Technologies

J. J. Jacobson, G. E. Matthern and S. J. Piet

*Idaho National Laboratory  
United States*

## 1. Introduction

There is the beginning of a nuclear renaissance. High energy costs, concern over fossil fuel emissions, and energy security are reviving the interest in nuclear energy. There are a number of driving questions on how to move forward with nuclear power. Will there be enough uranium available? How do we handle the used fuel, recycle or send to a geologic repository? What type of reactors should be developed? What type of fuel will they need?

## 2. Why assess deployment scenarios?

Nuclear fuel cycles are inherently dynamic. However, fuel cycle goals and objectives are typically static.<sup>1,2,3</sup> Many (if not most) comparisons of nuclear fuel cycle options compare them via static time-independent analyses. Our intent is to show the value of analyzing the nuclear fuel cycle in a dynamic, temporal way that includes feedback and time delays.

Competitive industries look at how new technology options might displace existing technologies and change how existing systems work. So too, years of performing dynamic simulations of advanced nuclear fuel cycle options provide insights into how they might work and how one might transition from the current once-through fuel cycle.

Assessments can benefit from considering dynamics in at least three aspects – A) transitions from one fuel cycle strategy to another, B) how fuel cycles perform with nuclear power growth superimposed with time delays throughout the system, and C) impacts of fuel cycle performance due to perturbations.

To support a detailed complex temporal analysis of the entire nuclear fuel cycle, we have developed a system dynamics model that includes all the components of the nuclear fuel cycle. VISION tracks the life cycle of the strategic facilities that are essential in the fuel cycle such as, reactors, fuel fabrication, separations and repository facilities. The facility life cycle begins by ordering, licensing, construction and then various stages of on-line periods and finally decommission and disposition. Models need to allow the user to adjust the times for various parts of the lifecycle such as licensing, construction, operation, and facility lifetimes. Current energy production from nuclear power plants in the once through approach is linear. Uranium is mined, enriched, fabricated into fuel, fed to nuclear reactor, removed from a nuclear reactor and stored for future disposal. This is a once through cycle, with no real “cycle” involved. Future fuel cycles are likely to be real cycles where nuclear fuel and other materials may be reused in a nuclear reactor one or more times. This will increase the

dependency among the steps in the process and require a better understanding of the technical limitations, the infrastructure requirements, and the economics. All three of these elements are time dependent and cyclical in nature to some degree. Understanding how these elements interact requires a model that can cycle and evolve with time – a dynamic model. Understanding these new fuel cycles also requires extrapolation beyond current fuel cycle operating experience. The goal is not to be able to predict the exact number or size of each of the elements of the fuel cycle, but rather to understand the relative magnitudes, capacities, and durations for various options and scenarios. A systems-level approach is needed to understand the basics of how these new fuel cycles behave and evolve.

### 3. Vision nuclear fuel cycle model

The Verifiable Fuel Cycle Simulation (VISION) model was developed and is being used to analyze and compare various nuclear power technology deployment scenarios<sup>4</sup>. The scenarios include varying growth rates, reactor types, nuclear fuel and system delays. Analyzing the results leads to better understanding of the feedback between the various components of the nuclear fuel cycle that includes uranium resources, reactor number and mix, nuclear fuel type and waste management. VISION links the various fuel cycle components into a single model for analysis and includes both mass flows and decision criteria as a function of time.

This model is intended to assist in evaluating “what if” scenarios and in comparing fuel, reactor, and fuel processing alternatives at a systems level. The model is not intended as a tool for process flow and design modeling of specific facilities nor for tracking individual units of fuel or other material through the system. The model is intended to examine the interactions among the components of the nuclear fuel system as a function of time varying system parameters; this model represents a dynamic rather than steady-state approximation of the nuclear fuel system.

#### 3.1 VISION introduction

VISION tracks the flow of material through the entire nuclear fuel cycle. The material flows start at mining and proceed through conversion, enrichment, fuel fabrication, fuel in and out of the reactor and then used fuel management, either recycling, storage, or final waste disposition. Each of the stages in the fuel cycle includes material tracking at the isotopic level, appropriate delays and associated waste streams. VISION is able to track radioactive decay in any module where the material resides for a minimum of a year.

VISION also tracks the life cycle of the strategic facilities that are essential in the fuel cycle such as, reactors, fuel fabrication, separations, spent fuel storage and conditioning and repository facilities. The life cycle begins by ordering, licensing, construction and then various stages of on-line periods and finally decommission and disposition. The model allows the user to adjust the times for various parts of the lifecycle such as licensing time, construction time and active lifetime.

VISION calculates a wide range of metrics that describe candidate fuel cycle options, addressing waste management, proliferation resistance, uranium utilization, and economics. For example, waste metrics include the mass of unprocessed spent fuel, mass in storage, final waste mass and volume, long-term radiotoxicity, and long-term heat commitment to a geologic repository. Calculation of such metrics requires tracking the flow of 81 specific isotopes and chemical elements.<sup>5</sup>

Figure 1 is a schematic of a nuclear fuel cycle, which is organized into a series of modules that include all of the major facilities and processes involved in the fuel cycle, starting with

uranium mining and ending with waste management and disposal. The arrows in the diagram indicate the mass flow of the material. Not shown, but included in each module within the model, are the information and decision algorithms that form the logic for the mass flow in VISION. The mass flows are combined with waste packaging data to provide insight into transportation issues of the fuel cycle.

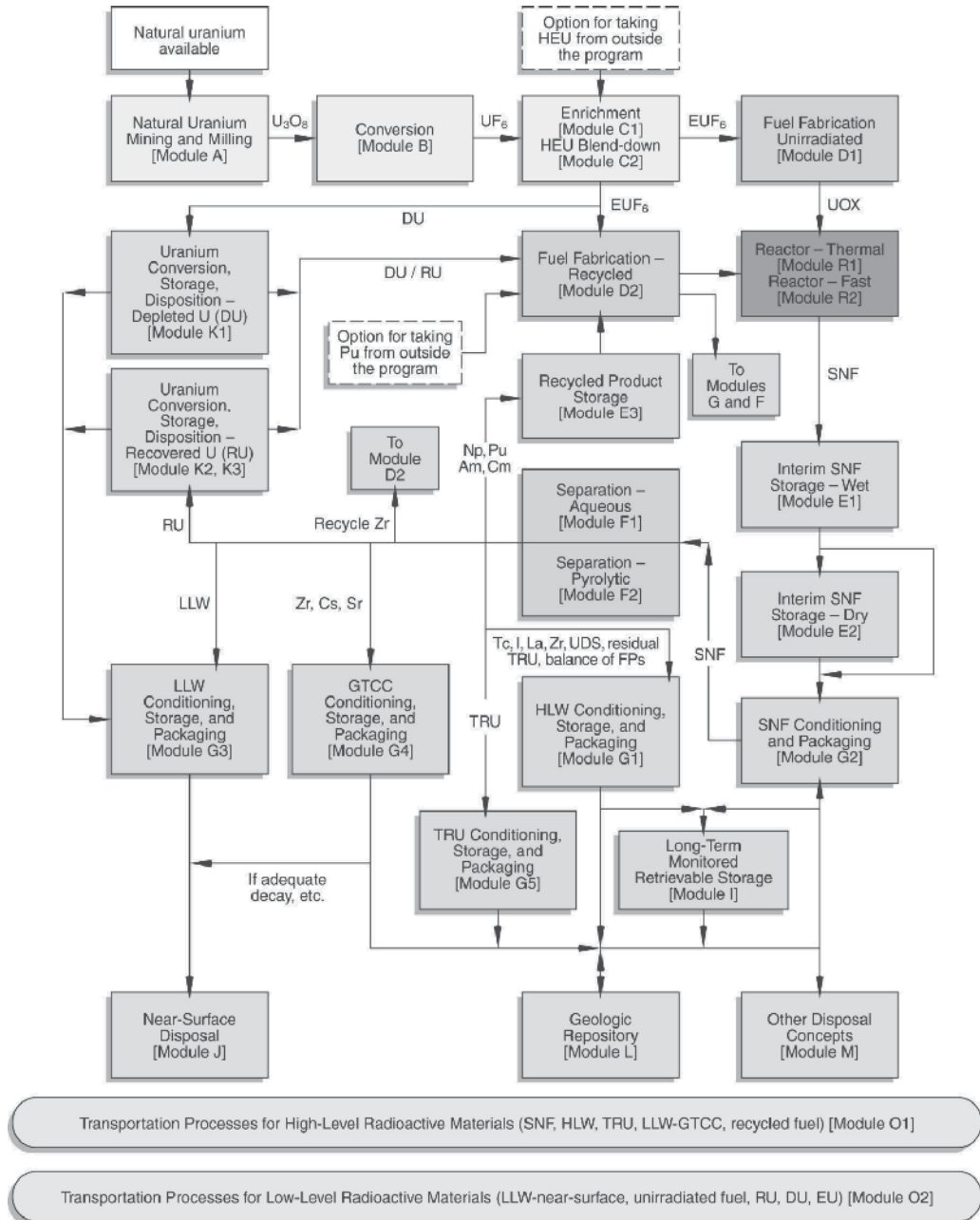


Fig. 1. Schematic of VISION modules representing the nuclear fuel cycle processes and facilities.

### 3.2 VISION functionality

VISION is designed around the methodology of system dynamics. System dynamics is a computer-based method for studying dynamic, problematic behavior of complex systems. The method emerged in the 1960s from the work of Jay Forrester at the Sloan School of Management at Massachusetts Institute of Technology. A detailed description of the system dynamics approach was first given in "Principles of Systems".<sup>6</sup> VISION is designed to run on a desktop personal computer with run times less than 10 minutes for any single scenario simulated over a 200-year period. Users can run scenarios by selecting pre-defined base cases or by modifying the options that make up a scenario. Currently, there are approximately 60 predefined scenarios available that range from the more simple case of thermal reactors without recycling to more advanced cases that include advanced reactor types such as fast reactors with various recycle options. Results are displayed in a variety of charts and graphs that are part of the interface or the user can open up the Excel charts that include many more tables and charts. The charts include comparative charts of data within the scenario such as the number of light water reactors (LWR) versus Fast Reactors.

VISION simulates the nuclear fuel cycle system with as many of its dynamic characteristics as possible, to name a few, it simulates impacts from delays, isotopic decay, capacity building and fuel availability. The VISION model has three modes of reactor ordering, the first takes a projected energy growth rate and nuclear power market share over the next century and builds reactors in order to meet this demand, second the user can manually set the number of reactors that are ordered each year and lastly, the user can specify an end of the century target in GWe and allow the model to build reactors to meet that projection. Options are included in the model that allow the user to recycle used nuclear fuel with up to 10 different separation technologies, use up to 10 different reactor and fuel types, and have up to 15 different waste management options. The technology performance can be varied each year. The results of the model will help policy makers and industry leaders know and understand the impacts of delays in the system, infrastructure requirements, material flows, and comparative metrics for any combination of advanced fuel cycle scenarios.

The subsections below describe key algorithms and approaches that comprise VISION's functionality. The first several subsections address the issue of when new facilities are ordered. VISION has a complex look-ahead ordering algorithm for new facilities. The user can override this instead and force the model to build facilities by inputting the capacity for each type of facility. The discussion on facility ordering entails subsections on facilities themselves as an introduction, supplies needed for the facility, and outputs from each facility. After ordering facilities, the section turns to energy growth rate, and then the physics issues of which isotopes are tracked in VISION and how VISION uses reactor physics data.

#### 3.2.1 Facilities

The mathematical model for ordering facilities is based upon a demand-supply model, where facilities for one or more stages of the fuel cycle create demand, which is serviced by the supply produced by facilities for another stage. The overall driver triggering the demand is electrical energy growth and nuclear power market share that is expected over the next 200 years.

To further explain the ordering process by way of example, for a closed (recycle) fuel cycle, the future electrical energy demand will require increased supply of electrical energy. If this supply is not adequate, new nuclear power plants will need to be built. In turn, this will



result in an increased demand for fuel fabrication services. If supply and usable inventory is not adequate, new fuel fabrication plants will be built; this will result in an increased demand for separation services. Again, if supply and usable inventory is not adequate, new separation plants will be built, which will result in an increased demand for used fuel. If supply and usable inventory is not adequate for this, new nuclear power plants will be built, bringing us back to the beginning of the cycle.

Note that a circular logic has developed, where we started with building new nuclear power plants due to electrical demand and return to this at the end due to used fuel demand. This implies that some decisions, e.g., mix of light water reactor multiple fuels (LWRmf) (multiple fuels means uranium oxide (UOX), mixed oxide (MOX) or inert matrix fuel (IMF)) and fast consumer/breeder reactor (FBR) or conversion ratio of FBR, must be made such that the starting and ending states are consistent. In order to prevent a mismatch of fuel available for advanced reactors which rely on used fuel from LWR and LWRmf reactors for their fuel supply, a predicted used fuel calculation must be performed at the time of ordering reactors that will inform the system how much used fuel is available for use in advanced reactors.

This demand function looks a certain number of years into the future ( $t + \Delta t^x$ ), where  $t$  is the current time and  $\Delta t^x$  is the time it takes to license and build a supply facility of type "x." The demand function also projects out to the year  $t'$ , where  $t'$  is the year that demand facilities utilize the services provided by supply facilities.

The demand function (Eq. 1) is as follows:

$$D_{t+\Delta t^x}^x = \sum_{y, t' \geq t+\Delta t^x} \gamma_{t' \rightarrow t+\Delta t^x}^{y \rightarrow x} N_{t'}^y C_{t'}^y \quad (1)$$

$D_t^x$  - Demand rate for time period "t" for service or product of facility of type "x" based on the number of type "y" facilities that are operating at time period  $t'$ .

$N_{t'}^y$  - Number of operating facilities of type "y" at time  $t'$  that require the service from type "x" facility. This includes planned facilities and those now operating at "t" that will continue to operate at  $t'$ .

$C_{t'}^y$  - Expected capacity factor for facilities of type "y" at time  $t'$ .

$\gamma_{t' \rightarrow t+\Delta t^x}^{y \rightarrow x}$  - Conversion factor that converts the demand rate for time period  $t'$  for service or product of facility "y" into a demand rate for time period " $t + \Delta t^x$ " for service or product of facility "x" that will service facility "y." It is assumed that the product or service of facility "x" can be produced over one time period, e.g., one year, which implies  $\gamma_{t' \rightarrow t+\Delta t^x}^{y \rightarrow x}$  only takes on a nonzero value for one value of  $t'$  when  $t' - (t + \Delta t^x) =$  time to start offering/production of service/product of facility "x" to have completed, i.e., manufactured + delivered + stored, for facility "y."

The supply function takes the number of operating facilities and their respective availabilities and determines how much available supply of a certain service via production there is in the system. The supply function (Eq. 2) is as follows:

$$S_{t+\Delta t}^x = \beta^x N_{t+\Delta t}^x C_{t+\Delta t}^x \quad (2)$$

$S_{t+\Delta t}^x$  - Rated supply rate of product at “ $t + \Delta t$ ” that can be produced by type “ $x$ ” facility.

$N_{t+\Delta t}^x$  - Number of operating facilities of type “ $x$ ,” including planned facilities and those now operating who at “ $t + \Delta t$ ” will continue to operate.

$C_{t+\Delta t}^x$  - Capacity factor of facility type “ $x$ ” that is in operation.

$\beta^x$  - Converts the number of facilities of type “ $x$ ” into a supply rate of type “ $x$ .”

The capacity factor,  $C_{t+\Delta t}^x$ , is a user defined function which typically depends on maturity level of the technology. For instance, capacity factor for LWR’s is set at around 90%, for new Fast Reactor’s it would probably be set closer to 80%. Such choices are made by the user.

In order to get the current demand, or the demand for services that the system is currently requesting, simply take Equation 1 and set  $\Delta t^x$  equal to zero. This will make the demand function equal to the current demand to produce a product or service. This demand (Eq. 3) will be labeled  $\hat{D}_t^x$  for further use in the methodology.

$$\hat{D}_t^x = \sum_{y, t' \geq t} \gamma_{t' \rightarrow t}^{y \rightarrow x} N_{t'}^y C_{t'}^y \quad (3)$$

In order to get the current supply, simply set the  $\Delta t^x$  in Equation 2 equal to zero. This will cause the equation to only use the facilities that are in operation at the current time “ $t$ .” The current supply (Eq. 4) will be labeled  $\hat{S}_t^x$  for further use in the methodology.

$$\hat{S}_t^x = \beta^x N_t^x A_t^x \quad (4)$$

The actual available output of facilities is based on the capacity factor of the facilities of type “ $x$ .” The capacity factor (Eq. 5) will change automatically for the system as new facilities come online and start requesting services. The capacity factor is a user defined value that is typically adjusted upward as more facilities come on line from an initial low capacity factor representing new types of facilities to a theoretical high value for facility with years of operational experience.

$$O_t^x = \beta^x N_t^x C_t^x \quad (5)$$

$O_t^x$  - Actual output of facility of type “ $x$ ” at time “ $t$ .”

$\beta^x$  - Converts the number of facilities of type “ $x$ ” into a supply rate of type “ $x$ .”

$C_t^x$  - Capacity factor for facilities of type “ $x$ ” at time “ $t$ .”

In order to implement this methodology, a projected energy demand growth and used fuel prediction is calculated in order to determine the number and type of reactors that can come online. The model looks ahead a prescribed number of years (the longest construction time of all of the facilities plus time to manufacture and deliver the product) and calculate supply and demand for reactors, fuel fabrication, and separations. At the beginning of the simulation, before the first time step, the model calculates the energy growth for every year of the simulation plus the number of years the model is looking ahead. The growth function (Eq. 6) is as follows:

$$E_t = E_{t-1} * (1 + p_t / 100) \quad (6)$$

where  $E_t$  in (Eq. 6) is the electric demand at year  $t$  and  $p_t$  is the growth percentage at year  $t$ . When the function reaches the last growth rate  $p_{100}$  provided by the input, it will hold that value in order to project out values beyond the 200-year time period.

The next step is to calculate the number of reactors that need to be ordered based on the growth rate and energy gap during the initial look-ahead time. During the initial look-ahead time,  $\Delta t_{look}$ , the model will only build LWRmf reactors because it is assumed that there will not be any FBRs deployed before the initial look-ahead time. The initial number of reactors for each of the look-ahead years is stored in an initialization vector so that at the beginning of the simulation the model will know how many reactors need to come online and when they need to come online. These reactors are then sent to an order rate array ( $\overline{RO}$ ) where they will be stored and called upon when it is time to order reactors. As the model starts, the simulation will progress forward with the  $t$  variable moving one year out for each year of the simulation. Reactors during the initial look-ahead time will be built based on the initial estimate of reactor ordering at the start of the simulation. As the simulation moves forward, new reactors after the initial look ahead years are ordered based on the energy growth rate and energy gap that is predicted in those future years. That is, if the initial look ahead is 20 years, in year 2001 an estimate will be made on energy growth and energy gap in 2021 and reactors will be ordered that will meet that demand.

The model runs for a specified time period – typically, from year 2000 to year 2200. The user can define a growth rate that nuclear power will grow at and allow the model to determine the number of reactors that are ordered to meet the demand or the user can be more specific and specify the reactor numbers. The model allows the user to define which reactor types to activate at specific times throughout the simulation period. In addition, the user can define the specific fuel to use in each reactor type, as well as the separation technology available and the capacities for all facilities in the fuel cycle (i.e., fuel fabrication, separations, etc.).

For each reactor type the user can set a variety of operational parameters, such as thermal efficiency, load factor, power level, and fuel residence time. In addition, the user can also set time parameters, such as reactor construction time, licensing time, reactor lifetime, used fuel wet storage time, separations time, and fuel fabrication time. Additional parameters can be set to adjust fuel fabrication rate, repository acceptance rate, and separations capacity and processing rate. Overall, there are over 200 parameters that the user can set and adjust between simulations. Because of the large number of parameters, there are a number of predefined scenarios that the user can select from a menu. These predefined scenarios set all the parameters for the selected scenario so these cases can be run with minimal effort.

### 3.2.2 Tracked isotopes

VISION tracks mass at an isotopic level, which is valuable from several aspects. First, the model is able to calculate some important metrics, such as, decay heat, toxicity and proliferation resistance. Second, it allows the model to use specific isotopes, such as Plutonium, for flow control in separations and fuel fabrication based on availability of Pu239, Pu240 and Pu241 from separated spent fuel. Lastly, it allows the estimate of isotopic decay whenever the material is residing in storage of at least 1 year.

Table I lists the 81 isotopes that VISION currently tracks the main fuel flow model. For the four radionuclide actinide decay chains ( $4N$ ,  $4N+1$ ,  $4N+2$ ,  $4N+3$ ), it will track all isotopes with half-life greater than 0.5 years, with the exception of 5 isotopes whose inventory

Actinides and Decay Chain		Fission Products		
He4		H3	Other gases	
Pb206	Transition Metals	C14		
Pb207		C-other		
Pb208		Kr81	Inert gases (Group 0)	
Pb210		Kr85		
Bi209		Inert gas other (Kr, Xe)		
Ra226	Group 2A	Rb	Group 1A/2A	
Ra228		Sr90 w/Y90 decay		
Ac227	Actinides	Sr-other	Zirconium	
Th228		Zr93 w/Nb93m decay		
Th229		Zr95 w/Nb95m decay		
Th230		Zr-other	Technetium	
Th232		Tc99		
Pa231		Tc-other		
U232	Uranium	Ru106 w/Rh106 decay	Transition metals that constrain glass waste forms	
U233		Pd107		
U234		Mo-Ru-Rh-Pd-other		
U235		Se79	Other transition metals	
U236		Cd113m		
U238		Sn126 w/Sb126m/Sb126		
Np237	Neptunium	Sb125 w/Te125m decay	Halogens (Group 7)	
Pu238	Plutonium	Transition Metal-other (Co-Se, Nb, Ag-Te)		
Pu239		I129		
Pu240		Halogen-other (Br, I)		
Pu241		Cs134		Group 1A/2A
Pu242		Cs135		
Pu244		Cs137 w/Ba137m decay		
Am241	Americium	Cs-other	Lanthanides	
Am242m		Ba		
Am243		Ce144 w/Pr144m/Pr144 decay		
Cm242	Curium	Pm147		
Cm243		Sm146		
Cm244		Sm147		
Cm245		Sm151		
Cm246		Eu154		
Cm247		Eu155		
Cm248		Ho166m		
Cm250		LA-other plus Yttrium		
Bk249		Berkelium		
Cf249	Californium			
Cf250				
Cf251				
Cf252				

Table 1. Tracked Isotopes and Chemical Elements

appears never to be significant. For fission products, VISION calculates isotopes found to dominate each possible waste stream, CsSr (Group 1A/2A), halogens, inert gases, transition metals, Zr, Tc, lanthanides, H-3, and C-14. In each case, both key radioactive isotopes and stable mass must be tracked because for the key elements, it is needed to calculate the mass of the key fission product divided by the total mass of that element. For example, to assess the "CsSr" waste option, VISION tracks Sr90 (with Y90 decay energy), Cs134, Cs135, Cs137 (with Ba137m decay energy), stable Rb, other Sr mass, other Cs mass, and stable Ba.

Only isotopes with half-life greater than 0.5 year are candidates for being tracked in fuel cycle simulations. A half year is two VISION time steps when running simulations with the typical 0.25-year time step. Not tracking such short-lived isotopes does not significantly impact mass and radiotoxicity assessments. (Spot checks of gamma and heat indicate the same thing.) Short-lived progeny of other isotopes, however, must be considered. Their heat and decay energy emission must be included when their parent isotopes decay. For example, Y90 decay energy must be included with decay of Sr90.

For actinide and decay chain isotopes, we started with all isotopes with half-life greater than 0.5 year. The behavior of actinide and decay chain isotopes is so complex that we essentially have to include all isotopes with half-life greater than 0.5 years. However, we do discard five of the candidate isotopes (Np235, Np236, Pu236, Cf248, and Es254) because their yield is so low. In subsequent calculations of radiotoxicity, heat, etc, the decay input of those isotopes less than 0.5 years must be accounted for as being in equilibrium with longer-lived parents.

Compared to actinide and decay chain isotopes, the complexity of behavior is less and the number of candidate isotopes is greater for fission products. We started with the set of fission product isotopes previously studied in Advanced Fuel Cycle Initiative (AFCI) system studies and added isotopes (and blocks of "stable" elements) such that the mass and radiotoxicity of each of the candidate waste streams (inert gases, lanthanides, CsSr, transition metal, Tc, halogens) calculated from the reduced set of isotopes and elements was within a few percent of calculations using all the isotopes for UOX at 51 MWth-day/kg-iHM burnup.

The current version of the code evaluates the heat loads, radiotoxicity, proliferation metrics and other parameters at key location in the fuel cycle (repository, dry storage, etc.). For separation and recycle of used thermal fuel, the youngest (shortest time out of the reactor) and then least cycled fuel has priority for the available capacity. The repository capacity can be varied with time, and includes permanent and retrievable capacities, and the rate material can be sent to the repository can also be varied with time. In contrast to separations, the oldest (longest time out of the reactor) and then most cycled fuel has priority for the repository.

### 3.2.3 Neutronics parameters

A key feature of the VISION model is that direct neutronics calculations are not performed within model, which makes it much simpler and more user friendly compared to other fuel cycle system codes that include this type of calculations such as COSI and NFCSIM codes.<sup>8,9</sup>

The neutronics calculations are made external to the model and parameters from those calculations are used as fixed parameters within the model. The important parameters are the composition of fresh and spent fuel that corresponds to a certain type of reactor/fuel, and the initial reactor core loading and the loading per a batch of fuel. More than one composition vector (recipe) can be provided for the same fuel, e.g., in case of recycling in

fast reactors, a non-equilibrium (startup) composition is needed for early cycled fuel and an equilibrium (recycle) composition is needed for fuel cycled greater than or equal to 5 times. Users can input whatever input/output fuel recipes they wish.

Most of our calculations have been done with LWR uranium oxide (UOX) with an initial enrichment of 4.3% U-235 and a discharge burnup of 51,000 MWth-day/tonne-iHM.<sup>10</sup> Other sources of data include Hoffman, Asgari, Ferrer, and Youinou.<sup>11,12,13,14,15,16</sup> The user can alternatively input their own input and output isotopic recipes.

Transmutation in low conversion ratio fast reactor is based on a compact fast burner reactor design that can achieve low conversion ratios.<sup>11</sup> This design is the basis for all transmutation options that used TRU from UOX, MOX or IMF spent fuel into a burner fast reactor in the VISION calculations.

### 3.3 Simulation

The real power of simulation models lies in learning insights into total system behavior as time, key parameters, and different scenarios (e.g. growth rate, reactor type) are considered. This is more valuable (and more credible) than attempting to make design and management decisions on the basis of single-parameter point estimates, or even on sensitivity analyses using models that assume that the system is static. System dynamic models allow users to explore long-term behavior and performance, especially in the context of dynamic processes and changing scenarios. When comparing different management/design scenarios did the system perform better or worse over the long term?

System dynamic models serve many of the same purposes as flight simulators. Indeed, the reason the user input is described as a “cockpit” is that such a model allows the designer/stakeholder to simulate management of the system over time. After repeated simulations, a student pilot gains deeper understanding of how the aircraft systems will respond to various perturbations (none of which will exactly match a real flight) – without the expense and risk of gaining such experience solely in real flights. Instead of simulating an aircraft flight, VISION simulates the nuclear fuel cycle system with as many of its dynamic characteristics as possible. This allows decision makers and developers to learn how the fuel cycle system may respond to time and various perturbations – without having to wait decades to obtain data or risk a system disconnect if a poor management strategy is used. VISION also allows users to test a range of conditions for parameters such as energy growth rate and licensing time which are not controlled by developers of nuclear energy but affect its implementation so that robust and flexible strategies can be identified to address uncertainties. For high-stakes strategy analysis, a system dynamics model, as a result of upfront scientific work, is easier to understand, more reliable in its predictions, and ultimately far more useful than discussion and debate propped up by traditional data analysis techniques such as histograms, Pareto charts and spreadsheets. System Dynamics is an analytical approach that examines complex systems through the study of the underlying system structure. By understanding a system's underlying structure, predictions can be made relative to how the system will react to change.

## 4. Illustrative deployment scenario simulations

The examples in this chapter are based on the following fuel cycles:

- Once through, Light Water Reactor (LWR) with uranium oxide (UOX) fuel at 51 GWth-day/tonne-iHM burnup.

- MOX recycle, Light Water Reactor (LWR) with a combination of mixed oxide fuel (MOX) and uranium oxide fuel (UOX).
- 2-tier, plutonium and uranium from LWR-UOX are first recycled once in LWR as mixed oxide (MOX) fuel. The remaining material and the minor actinides from separation of used LWR-UOX are then recycled in fast reactors.
- 1-tier, transuranic material from LWR-UOX is recycled in fast reactors with a range of transuranic (TRU) conversion ratios (CR) from 0.00 to 1.1. The TRU CR is defined as the production of transuranic material divided by all destruction pathways of transuranic material.

#### 4.1 Illustrative assumptions and input parameters

All of the examples below use the following assumptions:

- Analysis of US domestic systems
- Growth of nuclear energy is flat until 2015, when it resumes growth at an annual rate of 1.75%, resulting in 200 GWe-year of electricity generated in 2060 and 400 GWe-year in 2100. (Current annual output is 86 GWe-year.)
- A centralized facility accepts LWR used fuel for direct disposal starting in 2017 and ending in 2039 for a total of 63,000 MTiHM. For the once-through case, additional used fuel is disposed in generic additional repository capacity when sufficiently cooled (20 years). For the closed fuel cycle cases, additional used fuel is recycled.

The MOX, 2-tier and 1-tier examples also use the following assumptions:

- Separation of LWR used fuel begins in 2020, initially with a small plant (800 MTiHM/year capacity) with additional plants added as needed to work off any excess stores of used fuel by 2100. LWR used fuel is cooled 10 years before shipment for recycling. The TRU from separations is used to make recycle fuel (either MOX-Pu for LWRs or TRU fuel for fast reactors).
- The MOX cycle takes at least 15 years (5 years in the reactor, 10 years cooling) before the used fuel is available for recycle as MOX in thermal reactors or in fast reactors.
- A small fast reactor starts up in 2022 to prove the reactor and transmutation fuel technologies. Follow-on commercial fast reactors use a TRU conversion ratio (CR) of 0.5, metal fuel, and on-site recycling. (Sensitivity studies examine other options.)
  - For the 1-tier scenario, commercial fast reactors follow 10 years later (2032), with construction rates limited for the first decade to allow for learning.
  - For the 2-tier scenario, the MOX cycle takes at least 15 years before the used fuel is available for recycle into fast reactor fuel, so commercial fast reactors are delayed 15 years (to 2047).
- All TRU elements are recovered whenever used fuel is separated. Cesium and Strontium (CsSr) together are separate waste products. Separations losses are defined by the user with the default of 0.1% processing loss.

The once-through scenario provides the basis for comparison with the closed fuel cycle scenarios (fuel recycle). All electricity generation is based on LWRs using standard UOX fuel. The growth curve is depicted in figure 2 and shows the current growth “pause”, with no new reactors until 2015. After 2015, growth is modeled with simple compounding at 1.75%. This growth rate assumes nuclear energy use for electricity only.

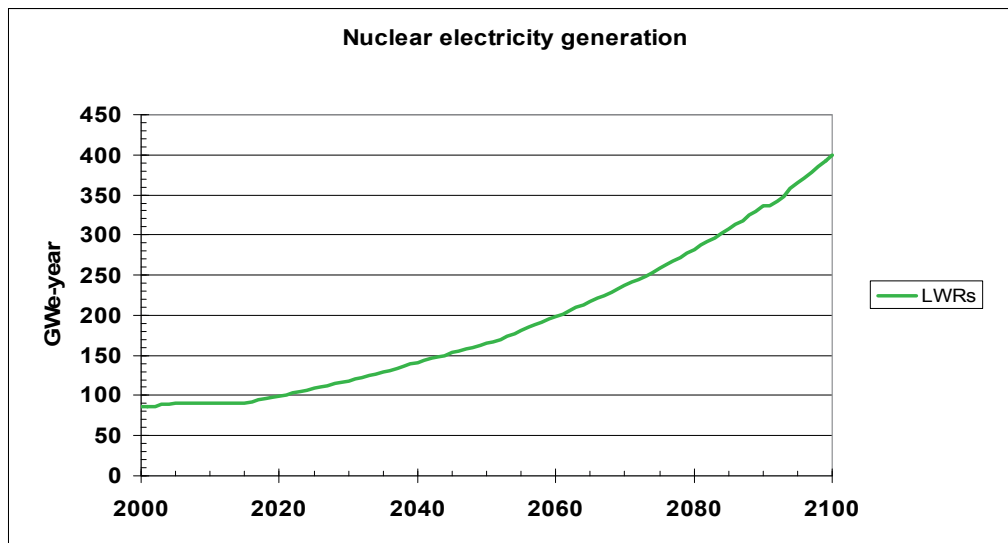


Fig. 2. Nuclear electricity generation for the once-through scenario.

#### 4.2 Where do the transuranics reside?

The location of used fuel for the once-through scenario is shown in figure 3. The used fuel graph shows some used fuel in wet storage and some in dry storage. This is not reflective of actual practice, which will vary at each reactor – it instead reflects the assumption of 10 years of wet storage for cooling before used fuel is moved followed by a minimum 10 years of additional cooling storage before it is emplaced in the repository. The total cooling time from reactor discharge to repository disposal is assumed to be a minimum of 20 years, based on burnup and thermal limits for Yucca Mountain. The “additional repository inventory” reflects how much more used fuel would be available for direct disposal (cooled more than 20 years), without any assumption about where the additional repository capacity would be located. Note the decrease in dry storage between ~2020 and 2040 – this reflects excess fuel in storage today which is transferred to geologic disposal once the initial repository becomes available.

The location of used fuel is very different with the closed fuel cycle. Figure 4 shows the used fuel for the 1-tier scenario, LWR and fast reactors. The 2-tier scenario (LWR-UOX, LWR-MOX, fast reactors) is very similar. When compared to figure 3, there are large differences, with the fuel previously in “additional repository inventory” now recycled.



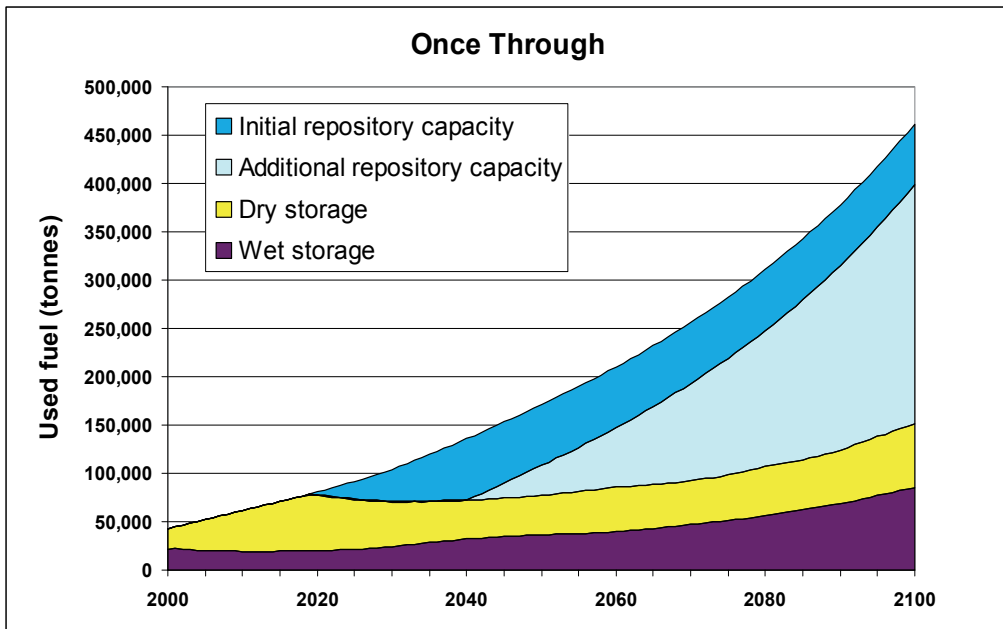


Fig. 3. Used fuel quantities and location in the once-through scenario.

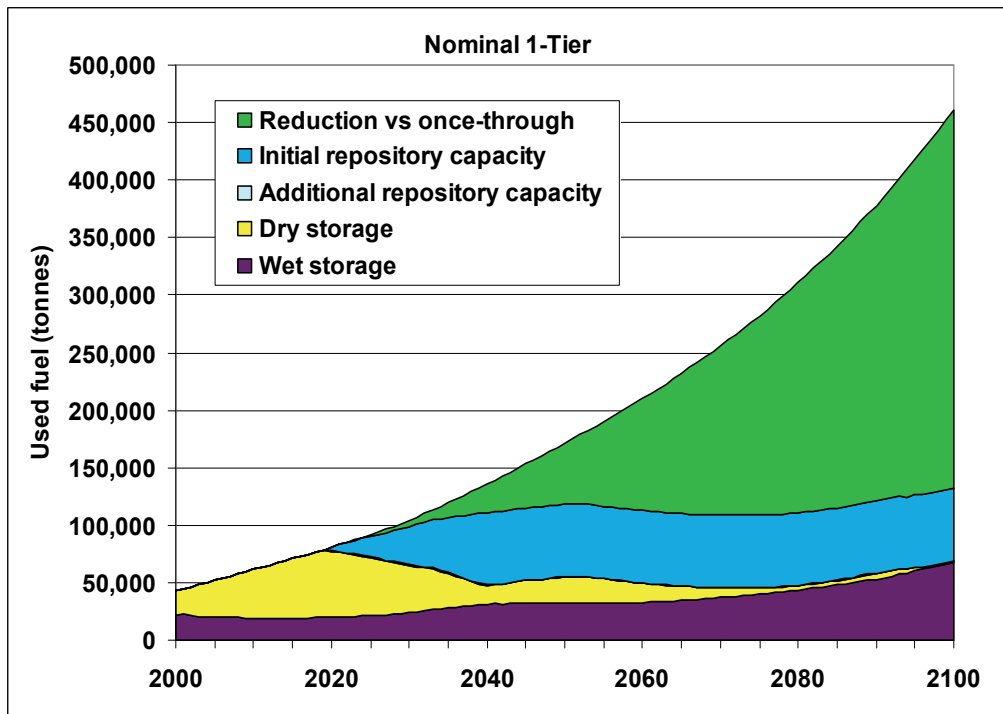


Fig. 4. Used fuel quantities and location in the 1-tier scenario.

### 4.3 How quickly new fuels and reactors penetrate the fuel cycle?

The closed fuel cycle scenarios follow the same growth curve as shown in Figure 2, except the reactor fleet is a combination of UOX and MOX fueled LWRs or a combination of LWRs and fast reactors. Figure 5 shows electricity generation based on fuel type, with the yellow area representing the fast reactor generation and the other areas representing LWR generation using both standard UOX and MOX (in the 2-Tier scenario).

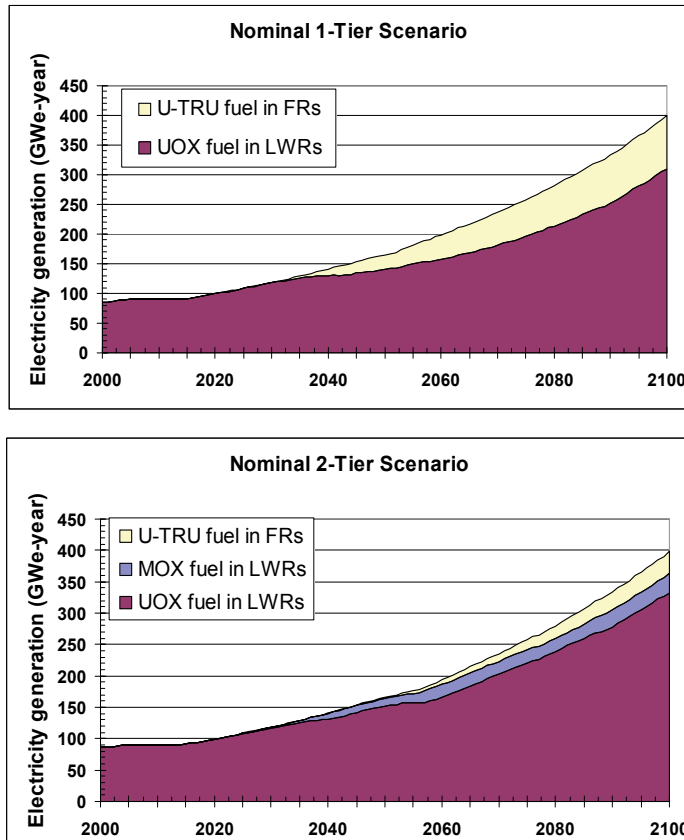


Fig. 5. Electricity generation for 1-tier and 2-tier scenarios as a function of fuel and reactor type.

Figure 6 shows the new fast reactor electricity generation projected for the closed fuel cycle scenarios, as well as the portion of total nuclear-generated electricity coming from the fast reactor fraction of the fleet. The 2-tier scenario includes fewer fast reactors and the reactors start up later due to the impact of the MOX pass in the thermal reactors. The MOX pass delays the availability of TRU for the fast reactors. The MOX pass also reduces the TRU available to the fast reactors through two mechanisms. First, some TRU is consumed in the MOX reactors – approximately two-thirds of a tonne per GWe-year. Second, the electricity produced from MOX offsets electricity from UOX, avoiding the generation of an additional quarter tonne of TRU. When these two mechanisms are combined, the amount of TRU eventually supplied to the fast reactors is reduced by almost a tonne per MOX-fueled GWe-year.

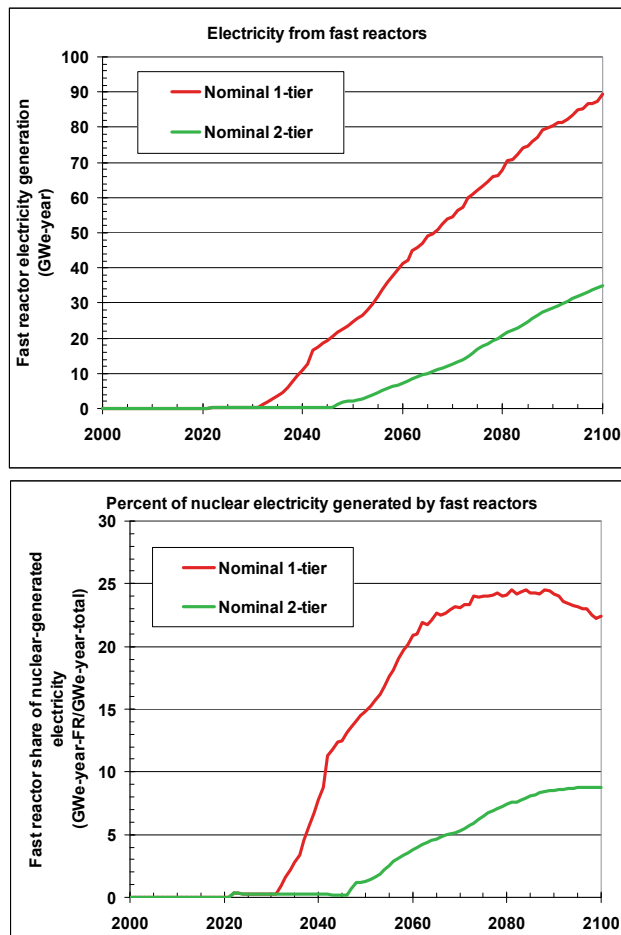


Fig. 6. Fast reactor electricity generation in absolute and percentage terms for 1-tier and 2-tier scenarios.

The portion of fast reactors for the 1-tier case levels out near 25% (and may be decreasing) as excess LWR used fuel is worked off and the fast reactors reach a dynamic equilibrium with the LWRs. This number is much lower than what is calculated by a simple static material balance (36%). This is an important finding from the transitional analysis, as it substantially reduces the number of fast reactors required for a “balanced” system.

The difference is due to several factors:

- The amount of TRU needed to start up a fast reactor is much greater than what is needed to keep it going. This includes the first core, as well as 100% of the initial refueling needs (until used fast reactor fuel can be recycled). The static analysis assumes the fast reactors already have their initial cores and most of their refueling needs are met by recycling of their own used fuel, with only ~20% coming as new makeup fuel from the LWRs.
- The fast reactors are using TRU generated at least 10 years earlier by the LWRs. While the LWR used fuel cools, more LWRs are added, so even without the startup effect the fast reactors would always be “behind”.

- Some amount of TRU is caught up in buffer storage as a hedge against temporary shutdown of the separations or fabrication facilities or the transportation links.

Several factors impact the number of fast reactors added during transition. This section uses the results of sensitivity analyses to show the relative impact of some of the more important factors. The 1-tier nominal scenario is used as the basis of analysis.

For all sensitivity runs, the same assumptions are used as for the nominal case except for the factor being examined and some associated parameters which need to be modified in tandem to keep the model in balance. For example, if a sensitivity analysis involves different values for the total nuclear growth rate, then startup dates for technologies, etc. are kept the same but the total amount of separations will be modified such that excess initial stocks of used fuel are still worked off but there is no excess separations capacity sitting idle due to a lack of feedstock.

The fast burner reactors assumed for the GNEP scenarios require TRU, including large amounts for initial startup and smaller continuing amounts as makeup for refueling. The initial core material for enough fast reactor capacity to produce 1 GWe-year of electricity includes ~7 tonnes of TRU, and additional TRU would be needed for the initial refueling cycles when 100% of the fuel would still come from used UOX. After a few years, the fast reactor fuel could be recycled and the amount of “makeup” fuel from used UOX would drop by ~80%. The annual makeup TRU needed for refueling the same capacity of established fast reactors would be slightly less than half a tonne.<sup>11</sup>

The source for the TRU feedstock is the LWR used fuel, which must be recycled. Assuming all available TRU is used for fast reactors, the reprocessing capacity is the single largest factor impacting fast reactor availability. (The analyses assumed that fuel fabrication was not a constraint.) In the VISION model, if there isn't sufficient TRU to start a fast reactor when a new reactor is needed, then an LWR is built instead. Fig. 7. Figure 7 shows the results of a sensitivity study on used UOX separations capacity – with lower total capacity, there are fewer fast reactors.

The separations capacity analysis is based on UOX at current burnup. Another feedstock consideration is the burnup of the used UOX. If burnup was significantly increased, many fewer tonnes of used fuel would be generated for the same level of electricity generation. However, the amount of TRU per tonne of used fuel would increase. At current burnup, the TRU content in used fuel is ~1.3%. If burnup could be doubled to ~100 GWd/MTiHM then tonnes of used fuel discharged would be cut in half, while the TRU content per tonne would increase to ~2%. Thus the total amount of TRU would decrease, but the amount made available per tonne of separations capacity would increase. The isotopic makeup of the TRU also changes as burnup increases, with less fissile and more non-fissile content. This would equate to somewhat higher TRU content in the fast reactor fuel, so for the same fast reactor capacity slightly more TRU would be needed. (For the 2-tier scenario the impact of isotopic changes on Pu enrichment in MOX fuel would be greater because LWRs are more sensitive to fissile content.)

#### **4.4 Is growth rate important?**

Another major impact on the number of fast reactors is the overall growth rate of nuclear electricity. Higher growth equates to more used fuel, and assuming all available used UOX fuel is reprocessed, to higher numbers of fast reactors. Fig. 8. shows the impact of growth rate on both the total electricity output from fast reactors and the percent output.

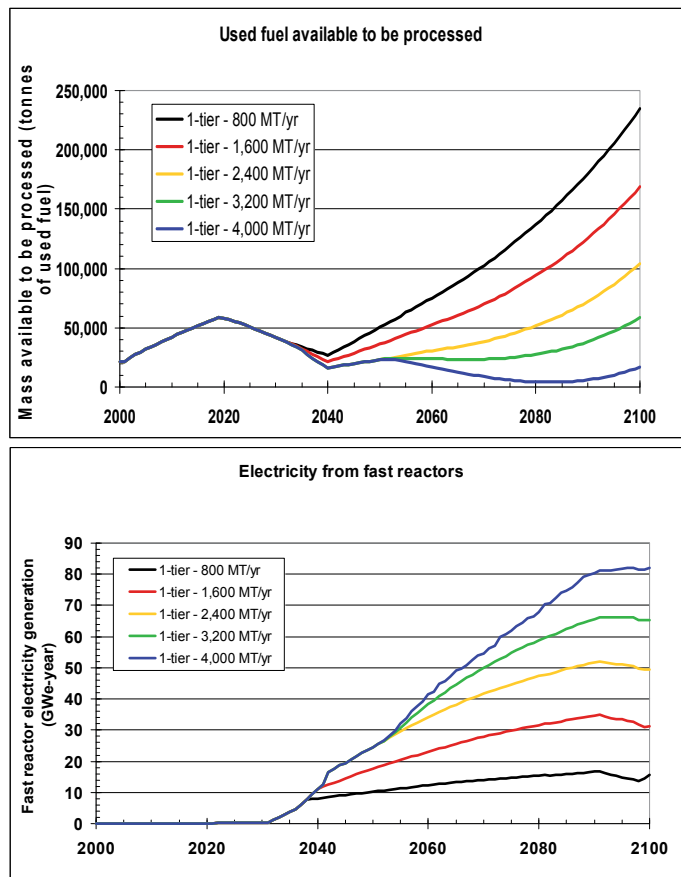


Fig. 7. Impact of varying UOX separations capacity on the amount of fast reactors.

One important finding from dynamic analysis is that as the growth rate increases the absolute level of fast reactors also increases, but the relative amount (percent of the fleet) decreases. This is primarily because the impacts of time lags increase with increasing growth rate (e.g. more LWRs are added while fuel is cooling). This finding has implications on system economics, since the cost of fast reactors is currently projected to be higher than LWRs. At low growth rates, this cost difference will have a greater impact on the overall cost competitiveness of nuclear energy versus other energy sources, but as the growth rate increases, the cost difference due to closing the fuel cycle becomes smaller.

#### 4.5 What is the impact of fast reactor conversion ratio?

The TRU conversion ratio (CR) is calculated as the ratio of TRU produced to TRU consumed during fuel irradiation. Fast burner reactors are defined as having a CR < 1.0. The CR has a large impact on the level of fast reactors for two reasons:

- In the initial core, changes in conversion ratio require virtually no change in TRU content. However, in refueling there is a very large difference. At a CR of 1.0 no additional TRU would be needed, whereas in an equilibrium core at a CR of 0.0, roughly 1 tonne of makeup TRU would be required per GWe-year of generation.

- Since at higher conversion ratios less makeup TRU is needed, more fast reactors can be built from the TRU provided by the LWRs. However, at a constant growth rate, more fast reactors means fewer LWRs, and less TRU generated. Thus at higher CR, while less TRU is consumed, more TRU generation is avoided (by generating electricity using recycle fuels instead of UOX).

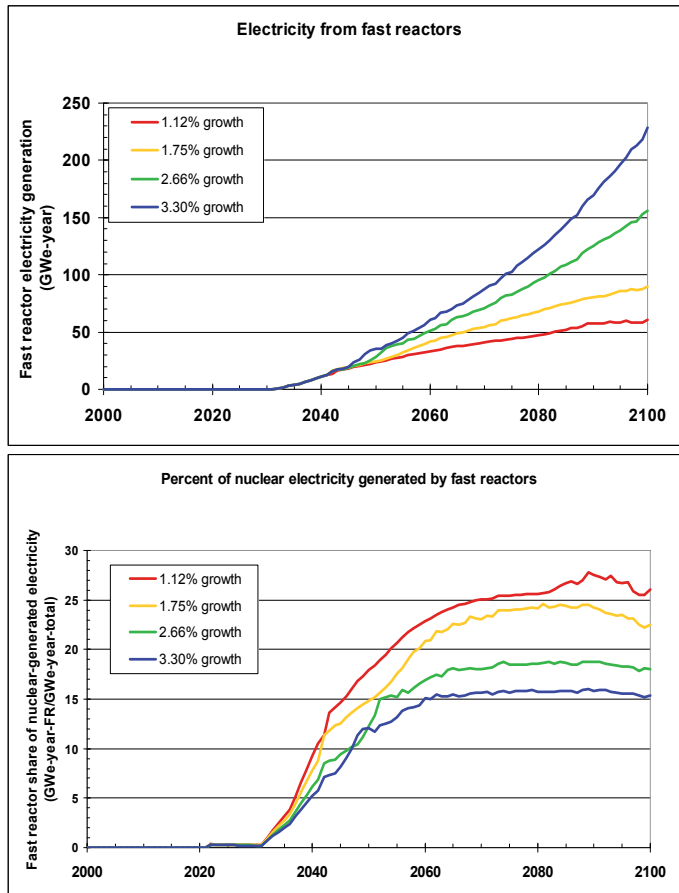


Fig. 8. Fast reactors as a function of growth rate.

Figure 9 shows the impact of conversion ratio on both the total electricity output from fast reactors and the percent output. At higher conversion ratio, both the absolute and relative level of fast reactor generation increases. The reason for this is as the conversion ratio increases, the total amount of TRU consumed plus avoided declines, so on net more TRU is available for more fast reactors.

#### 4.6 What is the impact of fuel cooling times?

Used fuel cooling time is another parameter affecting feedstock availability, and therefore fast reactor capacity. The nominal cases are based on a system that is efficiently functioning by the end of the century – meaning no excess stocks of fuel at intermediate stages in the system, such as the excess fuel currently stored at reactor sites. The used fuel cooling time is

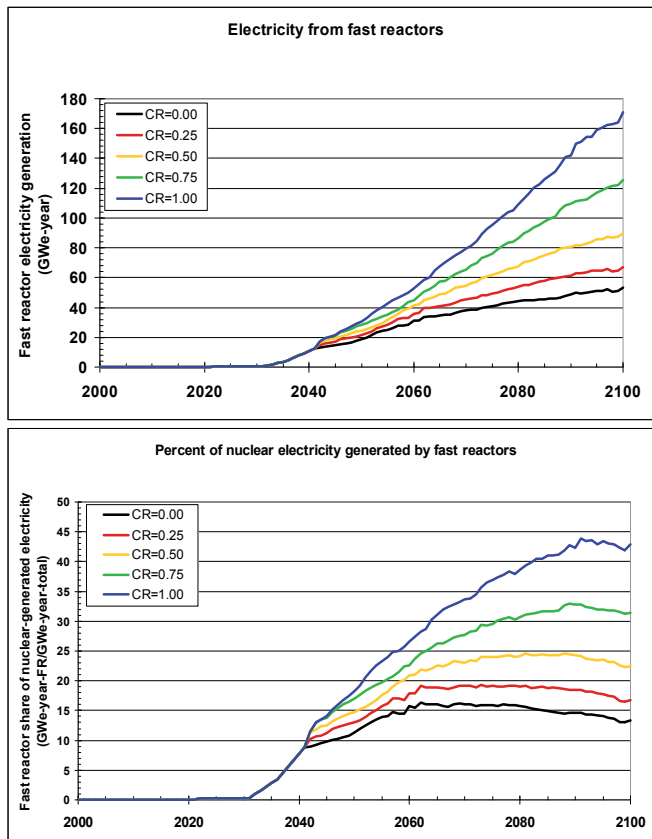


Fig. 9. Fast reactors as a function of conversion ratio.

assumed to be 10 years for LWR fuel (both UOX and MOX). This is based on the decay heat wattage limits of current shipping cask designs, which can accept full loads of used fuel at current burnup approximately 6 or more years after discharge. The value was rounded up, both to account for potential higher burnup and for MOX fuel. However, an "efficiently functioning" system could also be defined with longer cooling times. This would mean more TRU would be tied up in used fuel not yet available for reprocessing, and therefore fewer fast reactors.

Cooling time for fast reactor used fuel is a much larger factor than cooling time for LWR used fuel in determining the number of fast reactors deployed. The nominal case assumes on-site recycling of fast reactor fuel, which means it does not need to cool sufficiently for efficient shipping. For this reason, the assumed cooling time is only 1 year. (An additional year is assumed for separations and fuel fabrication; resulting in 2 years total recycle time.) One alternative is regional or centralized reprocessing of fast reactor fuel. A number of factors may lead to centralized facilities, including economies of scale and fuel type. However, significant transportation considerations must also be considered.

Centralized reprocessing is more likely if an aqueous technology is used, because this technology has significant economies of scale. The overall plant complexity stays fairly constant with size, while the lines, tanks, and other equipment scale up. If an electrochemical (Echem) process is used, there is not as significant a gain in scale economies.

Echem is essentially a batch process with limits on equipment size, so a larger plant would involve more processing stations, and therefore more equipment and complexity. Aqueous processing is usually equated with oxide fuels and Echem with metal fuels - both fuels have been used successfully in fast test reactors. A decision on fuel type for the initial fast reactor has not yet been made, as more information is needed.

Fast reactor fuel produces higher levels of decay heat per MTiHM than LWR UOX fuel. The fresh fuel has a high percentage of TRU, including plutonium-238 (Pu-238), americium-241 (Am-241) and curium-244 (Cm-244). Used fuel has large percentages of both TRU and fission products (due to much higher burnup than UOX). The fuel also contains heavy isotopes with high energy decay products, requiring substantial shielding. These properties of fast reactor fuel make shipping more difficult, and longer cooling times or less fuel per shipment may be required.

Figure 10 shows the impact of fast reactor fuel cooling time on the fraction of fast reactors at the end of the century. The impact of fuel type is also shown - oxide fuel has a softer spectrum, allowing for longer fuel cycles but also requiring more TRU to support those cycles, and therefore more initial TRU for startup. However, overall impact of fuel type is minimal when compared to the impact of cooling time.

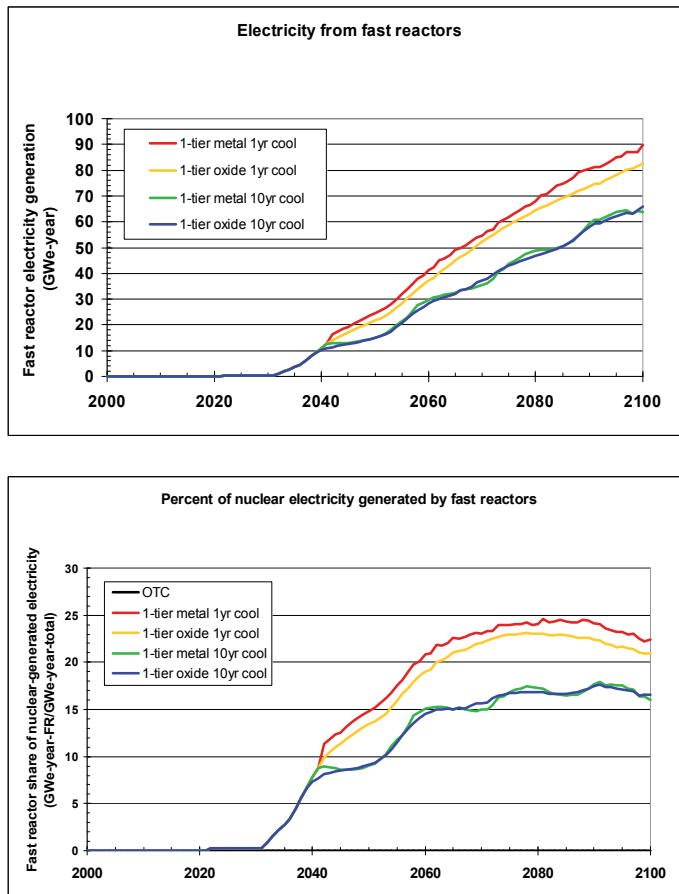


Fig. 10. Impact of cooling time and fuel type on fast reactor level.



#### 4.7 What is the impact of delaying implementation of fast reactors?

The final factor considered in determining the level of fast reactors is the time of introduction of the technology. The 2-tier case has the effect of delaying fast reactor introduction by ~15 years due to the delay in TRU becoming available for fast reactors while it is in the MOX cycle. But the timing of fast reactor introduction could also be later for the 1-tier case. Figure 11 shows the impact of delaying fast reactor introduction by 5, 10 and 15 years, while including the nominal 2-tier case for comparison.

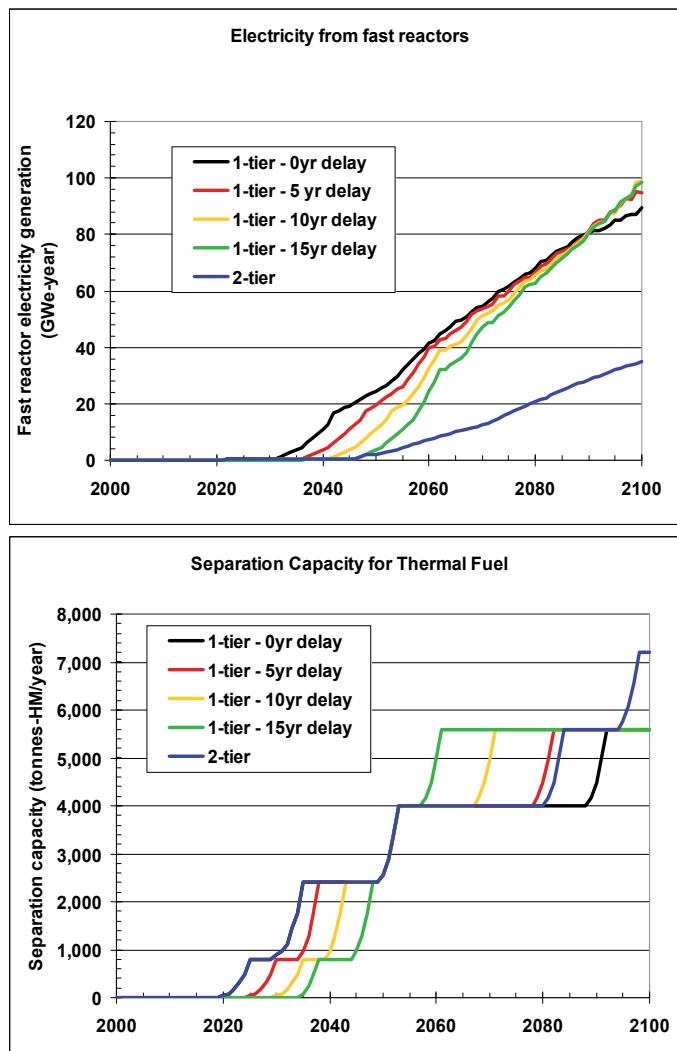


Fig. 11. Impact of delayed fast reactor introduction.

Delaying fast reactor introduction has little long-term impact on the numbers of fast reactors. In fact, there are more fast reactors toward the end of the century than in the nominal scenario. This is due to more TRU being generated by LWRs in the middle of the century (less TRU avoided), providing more feedstock. While initial separations is delayed

(because there are no fast reactors to take the separated TRU), the final separations capacity must be brought on line sooner to achieve the elimination of excess used fuel by 2100. Stores of cooled fuel are twice to three times as high throughout much of the century.

## 5. Lessons from dynamic analyses

Fuel cycle system analyses can be either static or dynamic; they each have value. Static equilibria are easier to calculate, to understand, and to use to compare options. By static equilibria, we mean the system is not changing. For example, static equilibria can include constant time lags for used fuel cooling but not technology changes, deployment, displacement, etc. Dynamic simulations are more realistic.<sup>17</sup> The 2005 AFCI objectives provided to Congress<sup>1</sup> and recent U.S. comparisons<sup>2,3</sup> are primarily static in nature.

Consider three examples of the differences between static and dynamic. First, assume in fast reactors that zirconium (fast reactor metal fuel alloy) and steel (fast reactor metal fuel cladding) are recycled. At static equilibrium, the only required makeup zirconium and steel would be the small amount required to balance processing losses. However, in a dynamic analysis with increasing numbers of fast reactors, zirconium and steel would be required to supply the new fast reactors. The amount of makeup material required would increase as either the growth rate or recycle time lag from fuel fabrication back around to new fuel fabrication increase.

The second example is system evolution. A static equilibrium analysis tells us little about how to manage the system; or, how the system can evolve from one strategy to another. A dynamic analysis or simulation provides some insights into the sequencing of events. Understanding the true system evolution requires a fully time dependent calculation, as provided by system analysis models such as VISION. Under some circumstances, a system establishes a “dynamic equilibrium” in which the relative relationship among parts of the system is fairly constant, but the entire system continues to grow.

The third example is economics. A static equilibrium is appropriate when discount rates, the time value of money, and cash flows are not addressed. If the time value of money is accounted for, then cash flows that lead others are given greater weight; cash flows that lag others are given less weight.

### 5.1 Deployment

All advanced fuel cycles require separation of used UOX fuel. All simulation results depend not only on when the first UOX separation plant starts, but also its capacity. In the simulations presented here, the first separation plant starts in 2020 at 800 tonnes-iHM/yr. It also matters how soon a second UOX separation plant might be deployable. In these simulations, the second plant starts in 2030 at 1600 tonnes-iHM/yr. Consider that the U.S. is currently accumulating used UOX at ~2000 tonnes-iHM/yr and there are few proposals that the first UOX plant be that large. So, just to build capacity equal to the anticipated UOX discharge rate in 2020-2030, multiple separation plants will be required and simulation results depend on how soon that is possible.

All advanced fuel cycles require new fuels that recycle some or all of the transuranic material. Many options require new types of reactors. In most simulations, commercial fast reactor deployment starts in 2032 (1-tier) or 2047 (2-tier). Simulation results also depend on how soon new technologies can be deployed, not just when deployment starts. For example,

many of the calculations in this report constrain fast reactor deployment to 1 GWe of capacity/yr for 5 years, followed by 2 GWe/yr for 5 years. MOX or fast reactor deployment is also constrained by availability of recycled material, which is in turn constrained by deployment of UOX separation capacity. Reactor deployment can also be constrained in low nuclear growth scenarios because new reactors are not built until existing reactors retire. This growth constraint does not occur at 1.75%/yr growth assumed in most of the calculations. Many of the same reactor deployment constraints would hold for fuel fabrication capacity but in the current simulations fuel fabrication capacity was not constrained.

Changes in fuel cycle technology combinations (reactors, fuels, separation, waste forms, waste disposal sites) take decades to be significantly manifest in system-level parameters such as uranium utilization or used fuel inventories in wet storage. That is, the fuel cycle has long response times. Reasons include new technologies take decades to deploy and it can take a decade for fuel to go once around the recycle loop.

The sequence of deployment of new fuel cycle technologies is generally constrained. An obvious example is that MOX fuel in LWRs cannot occur before LWR UOX separation begins. Proper sequencing of technology and facility deployments is a contributor to the long response times.

The adaptability, resilience, and robustness (versus fragility) of fuel cycle options vary. For example, LWRs with MOX are robust in the sense that if MOX fuel is unavailable, one can use enriched UOX without hesitation; enriched UOX fuel is typically assumed to be a "commodity" without dependence on unique facilities. A burner fast reactor is "fragile" in that it requires separated TRU for both startup and throughout its operating life, making it dependent on sources of used fuel, separation of that used fuel, and fabrication of new fuel – which are likely to each be unique facilities that must be deployed in sequence and matched in capacity size to avoid choke points and excessive stockpiles. The adaptability of new reactors is enhanced (at a cost) to the extent that multiple fuel types or fuel compositions are considered in reactor design and licensing, e.g., LWR UOX versus MOX or varying conversion ratio fast reactors.

## 5.2 Waste management

Our first observation is that one way to reduce waste burden is not to make the waste. Reactors fueled with enriched uranium are net producers of TRU (TRU CR>1),<sup>1</sup> while reactors fueled with recycled TRU may be net producers (CR>1) or consumers (CR<1). Fig. 12 shows the reduction of TRU inventory this century as a function of fast reactor TRU CR for 1-tier dynamic simulations. TRU reduction occurs for two reasons; one is consumption of TRU in fast reactors. (In other simulations, TRU is consumed in thermal reactors.) The other is avoidance of TRU production by displacing reactors with net TRU

---

<sup>1</sup>The TRU conversion ratio is TRU production/destruction. CR=1 means the output TRU content equals the input TRU content. Systems with uranium fuel thus create TRU. For systems operating with TRU fuel, the TRU CR is often numerical similar to the fissile breeding ratio as U238 (non-TRU, fertile) is converted to TRU, which is mostly fissile. Indeed, as the TRU CR increases, it approaches the fissile breeding ratio as a higher fraction of the produced TRU is Pu239, which is fissile. As an example of the difference between TRU conservation ratio and fissile breeding ratio, note that conversion of Pu240 to Pu241 does not impact the TRU conversion ratio but does impact fissile breeding ratio. The AFCI program tended to use TRU conversion ratio rather than fissile breeding ratio as relatively more indicative of waste management and proliferation resistance/physical protection issues.

production (such as LWR-UOX) with other reactors and fuels. As an example, a CR=1 fast reactor is not a net consumer of TRU; but the more electricity generated by such reactors, the less that must be generated by LWR-UOX and therefore significant TRU production is avoided.

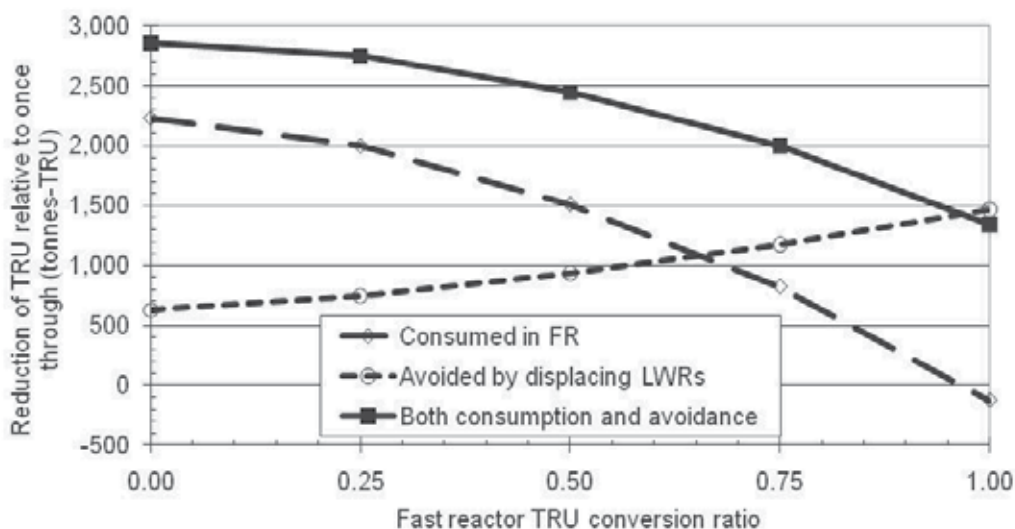


Fig. 12. Consumption and avoidance of TRU, both reduce TRU inventories.

Below CR=1, there is more uranium recovered from separation of used fuel (“recovered uranium”) than used; it goes into storage. Similarly, uranium depleted by enrichment (“depleted uranium”) is not used and goes to storage. Above CR=1, both recovered uranium and depleted uranium is eventually used. In the analyses and results presented below, for CR<1; RU and DU are considered in storage and are not included in either the active or waste inventories.

Below CR=1, the introduction of fast reactors does not increase the production of TRU this century relative to the once through fuel cycle. This cross-over point between increasing versus decreasing TRU this century depends on many parameters, notably the nuclear power growth rate. In all cases, it takes a CR significantly greater than one before there is a net TRU production by the fleet this century.

The second waste management observation is that the radiotoxicity results depend strongly on which transuranics are recycled, processing loss rates, and the time at which radiotoxicity is to be evaluated. Individual isotopes vary as to their contribution (per mass) to radiotoxicity. Consider the example in fig. 13. It shows that if UOX-51 is not recycled or if only uranium from UOX-51 is recycled; the radiotoxicity stays above natural uranium ore until ~300,000 years; there is no reduction in the radiotoxicity source term. If 99% to 100% of the uranium and plutonium are recycled, the radiotoxicity remains above natural uranium ore until 10,000 to 20,000 years; a reduction of LTR-1000 by factors of 7.9 to 8.5. U and Pu constitute 94.6% of used UOX-51 or 99.89% of the heavy metal in used UOX-51. (Of used UOX-51, 0.1% is minor actinides and 5.3% is fission products.) If 99%/99.5%/99.9%/100% of uranium, neptunium, plutonium, americium, curium, and californium are recycled, the LTR-1000 is reduced by factors of 100/200/950/20000; and the time to reach uranium ore

drops to 2000/700/400/300 years. A recent NEA study<sup>17</sup> shows similar trends. At very long times, even the longest-lived minor actinides decay into uranium isotopes and their progeny so that the two “no MA recycled” curves actually increase back toward 1.0 (natural uranium) as the uranium progeny isotopes such as Po210 grow in.

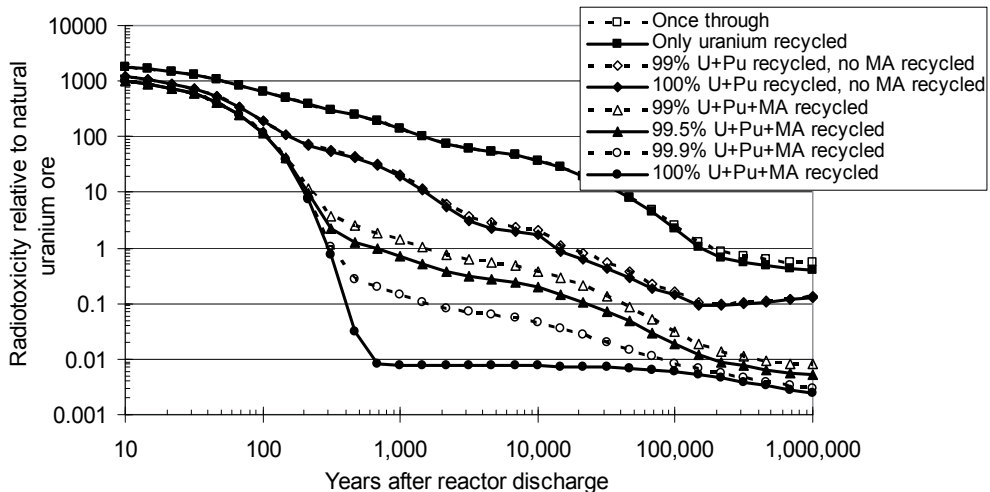


Fig. 13. Radiotoxicity of residual waste from 5-year old UOX-51 as function of minor actinide (MA) recycling.

The third waste management observation is that significant material accumulates throughout the system during recycling; thus, achievement of high waste management benefits depends on continuation of recycling. Don't stop!

The metric is the long-term decay heat emitted by material from 50 to 1500 years; this is a rough approximation of the long-term thermal response in a repository.<sup>18</sup> It is the same concept as the “decay heat integral”.<sup>17</sup> We call it a “commitment” because once emplaced, the energy that will be deposited has been committed; this is analogous to the concept of “dose commitment”; radioactivity taken into the human body commits the body to receiving a dose integrated over time. The heat units are energy (GWth-yr), heat rate (GWth) integrated over time (years). Figure 14 shows the heat commitment in a 1-tier CR=0.50 case. The heat commitment in 2100 would be 86 GWth-yr with the once through fuel cycle; adoption of 1-tier CR=0.50 recycling reduces that to 47 GWth-yr. So, if recycling were to stop in 2100 and all the material in the system went to a repository, the heat-commitment improvement factor to the repository would be only  $1.8=86/47$ .

Relative to used fuel and HLW, there is nil heat commitment in depleted uranium (DU), recovered uranium (RU), low-level waste (LLW), or even TRU waste. (There is little TRU waste in these scenarios; virtually all TRU-containing waste is considered HLW.) But, there is 7 GWth-yr in decay heat storage (CsSr). So, if recycling were to stop in 2100 and that material were not sent to a repository, the improvement factor would increase from 1.8 to  $2.1 = 86/(47-7)$ .

If recycling continues beyond 2100, the 39 GWth-yr active material in the system (reactor, wet storage, separation, fabrication) and 0.8 GWth-yr in dry storage avoid going to the repository. The repository only has 0.2 GWth-yr, so the maximum improvement factor

could approach  $430 = 86/0.2$ ; this is an overestimate because some of the 40 GWth-yr (active, dry) will end up in the repository as recycling continues.

Consider if the material in decay storage is sent to a repository. Then, the repository heat commitment is 7.2 GWth-yr instead of 0.2 GWth-yr and the maximum improvement factor, even if recycling continues, would be  $86/7.2 = 12$ . Again, this is an overestimate because some of the 40 GWth-yr in active systems would eventually go to the repository.

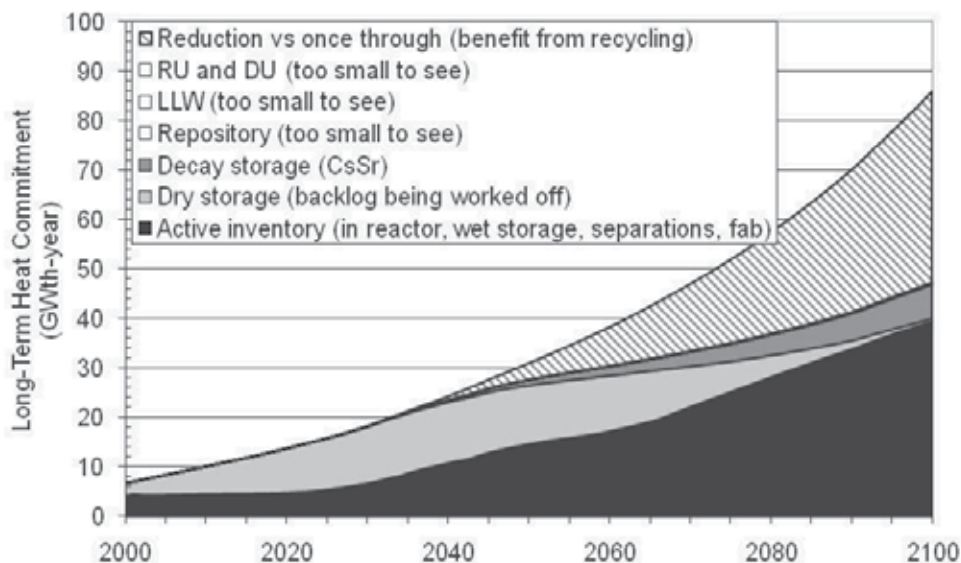


Fig. 14. Long-term heat commitment for 1-tier CR=0.50 fast reactor case.

So, achieving high improvements in repository heat commitment requires continuation of recycling, recycle of Pu and MA, and use of decay storage for CsSr.

The fourth observation is that uranium dominates the mass of the system. Figure 15 shows the composition of the mass in the system for a 1-tier case over the simulation time. The mass at the end of the simulation is dominated by DU and RU; the mass of fuel products and total waste is small. This case uses CR=0.50 fast reactors. To help understand this, consider the static equilibrium in figure 16. At CR=0.50 only 1.3% of the RU and none of the DU is used as fuel. (Uranium in discharged fast reactor fuel is assumed recycled into new fast reactor fuel.) Use of RU increases to 4.2% at fast reactor CR=0.75. At CR=0.986, all of the RU is used but only some of the DU is used. Above TRU CR=0.9985, all of the RU and DU is used as fuel (other than processing losses). Dynamic simulations show somewhat worse results than figure 15 because of the time lags involved in building and operating fast reactors in a growing system, i.e., LWRs are built first and their TRU is used to fuel later fast reactors.

The final waste management observation is that one must put TRU “in play” in order to reduce waste burdens. Use it to lose it. TRU that is sitting in storage does not help reduce waste burdens, except in so far as high-heat load isotopes decay; the notable example is Cs137 and Sr90 with ~30-year half-lives. Similarly, the holdup of transuranic material in the system impacts system performance so that short time lags, e.g., when facilities are co-located instead of at different locations, can lead to faster waste management benefits via

consumption and avoidance of TRU at a given TRU CR. Certainly the rate of TRU consumption from the standpoint of an individual reactor depends on the reactor power and CR; however, from the standpoint of the entire fleet, the rate of TRU consumption and avoidance additionally depends on how fast TRU-consuming reactors (burner FR in this instance) displace TRU-producing reactors (LWRs in this instance), how quickly discharged fuel can be separated and recycled material re-inserted into reactors. Figure 17 shows the impact of increasing the “wet” storage time from 1 to 10 years for a 1-tier CR=0.50 fast reactor case, approximating a shift from onsite to offsite separation and fuel fabrication. The total time from reactor discharge to reinsertion changes from 2 to 11 years.

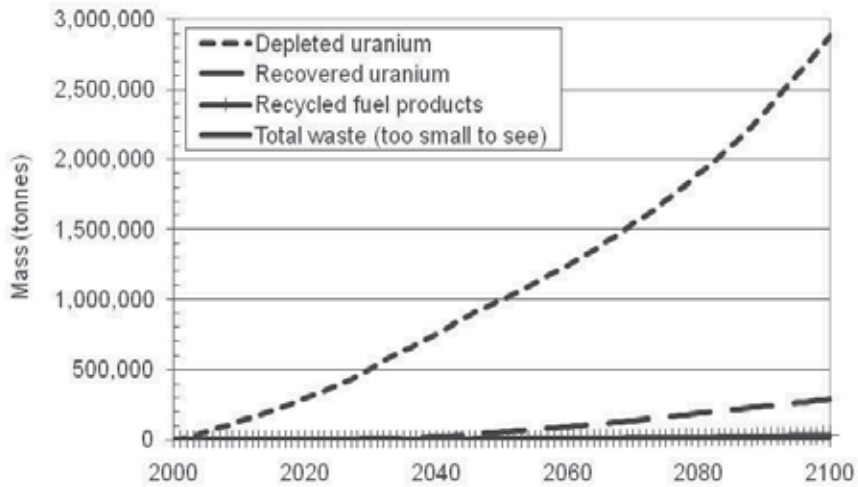


Fig. 15. Waste, uranium, and fuel product mass for a 1-tier recycle case, CR=0.50 fast reactors, no packaging included.

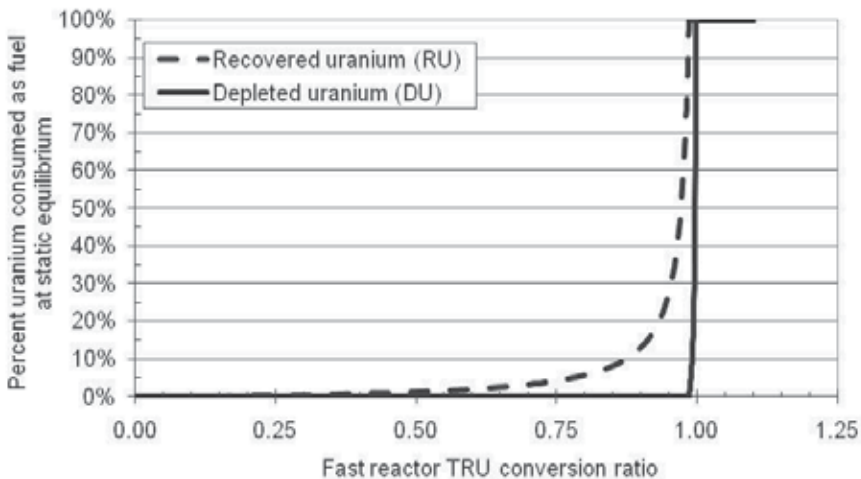


Fig. 16. Percent of RU and DU from LWRs used as fast reactor fuel with fast reactors and LWRs in static equilibrium.

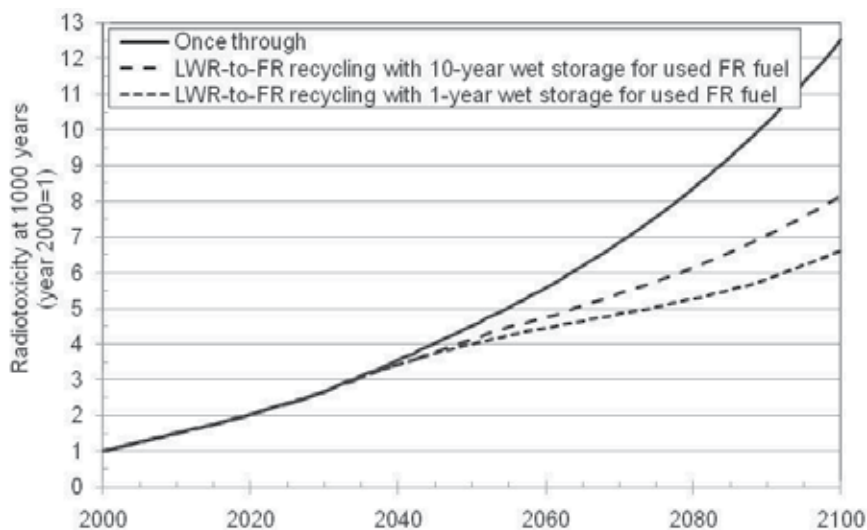


Fig. 17. Long-term radiotoxicity of 1-tier fast reactor CR=0.50 with either 1 or 10 year “wet” cooling before a year of separation and fuel fabrication.

### 5.3 Uranium utilization

To start, consider the range of estimates of world uranium resources in Table II relative to the 2006 production rate of 40,000 tonne-U.<sup>19</sup> The current nuclear power production rate would exhaust total estimated conventional resources (16,000,000 tonnes-U) in 400 years. That time scale can drop to within a century with modest nuclear power growth, but extend many centuries if unconventional resources become practical.

Conventional resources	Reference	Tonnes-U
Reasonably assured resource, <\$130/kg-U	Redbook <sup>19</sup>	3.3e6
Inferred resources, <\$130/kg-U	Redbook <sup>19</sup>	2.1e6
Prognosticated resources, <\$130/kg-U	Redbook <sup>19</sup>	2.8e6
Speculative resources, <\$130/kg-U	Redbook <sup>19</sup>	4.8e6
Total estimated conventional resources		
Above 4 categories, <\$130/kg-U	Redbook <sup>19</sup>	1.3e7
Above 4 categories, plus “cost range unassigned”	Redbook <sup>19</sup>	1.6e7
Undiscovered + known, <\$130/kg-U	Herring <sup>20</sup>	1.5e7
Undiscovered + known, <\$130/kg-U	Steyn <sup>21</sup>	1.6e7
Unconventional resources	Reference	Tonnes-U
Uranium in sandstone deposits	Herring <sup>20</sup>	1.8e8
Uranium in volcanic deposits	Herring <sup>20</sup>	2.0e9
Uranium from seawater	Herring <sup>20</sup>	4.2e9
Uranium in phosphate deposits	Herring <sup>20</sup>	8.0e11

Table 2. World Potential Uranium Resources



Nuclear fuel isotopes are either fissile or fertile; fissile isotopes are much more readily consumed. The only fissile isotope in nature is U-235, which is 0.7% of uranium ore. The only fertile isotopes in nature are U-238 (99.3% of uranium ore) and Th-232 (100% of thorium ore). To extend ore utilization substantially above 0.7%, one must convert or "breed" fertile to fissile isotopes. Fertile U-238 can be bred to fissile Pu-239, called the uranium-plutonium fuel cycle (or plutonium for short). Fertile Th-232 can be converted to fissile U-233, called the thorium-uranium fuel cycle (or thorium for short). The ratio of producing fissile isotopes (from fertile) to consuming fissile isotopes is called the fissile breeding ratio. A ratio greater than 1 means that more fissile isotopes are bred than consumed, shifting the limiting resource from fissile isotopes to fertile isotopes.

All current U.S. reactors have fissile breeding ratio less than 1 and thus use less than 1% of the original uranium ore. Recycling in such reactors is not sufficient to break 1% because their fissile breeding ratios remain below 1. When the fissile breeding ratio is greater than 1, the uranium (or thorium) utilization can exceed 1%. There are exotic concepts in which maximize in-situ breeding without recycling used fuel, it advanced materials can be developed, these may achieve ~10% uranium utilization. With recycling of used fuel in breeder reactors, uranium and thorium utilization can approach 100%, subject to processing losses.

Accomplishing 50-100x improvement in uranium utilization means near total replacement of LWRs (or other thermal reactors) with fast reactors. For example, if 10% of the reactor fleet remains LWRs with UOX fuel with 90% of the electricity from fast breeder reactors, the maximum uranium utilization improvement is 10x. Such substantial infrastructure change from LWRs to FRs is notoriously difficult.<sup>22</sup> As most of the U.S. LWR fleet is moving toward a 60-year reactor lifetime, such a replacement of LWRs will take at least 6 decades from the operation of the last LWR. As an example, if fast breeder reactor deployment requires 2 decades from first deployment to 100% of new construction (i.e. allowing 2 decades for industrial scale-up and market penetration); it will be 2120 before the last LWR retires. Predicting uranium resources so far in advance is questionable.

The above example assumes that the fast breeder reactors can grow faster than nuclear power growth during its market penetration from 0 to 100%, followed by continued breeder growth at the nuclear power growth rate once it reaches 100% of new construction. The rate of breeder deployment is constrained by fuel supply, which we have tended to assume is transuranic material recycled from LWRs and fast reactors once operating, rather than high enriched uranium (~30% U235).

We have derived the required TRU conversion ratio, such that LWR are not required to supply TRU to a growing fleet of fast reactors:

$$CR = e^{m(t_F + t_R)} \quad (7)$$

where  $m$  is the growth rate;  $t_F$  is the time for cooling, separation, and fuel fabrication;  $t_R$  is the time in reactor. Thus,  $t_F + t_R$  is the total turnaround time. As an example, if  $m=0$ , then  $CR=1$  and the system is in balance with no LWRs. Or, if one wants  $m>0$ , then  $CR>1$ . The higher the desired growth rate, the higher the required CR.

In addition, because new fast reactors (growing at rate  $m$ ) must have  $t_R - 1$  additional years' worth of fuel to start up, equation 1 must be multiplied by another term.<sup>2</sup>

<sup>2</sup>A core contains  $t_R$  years worth of fuel, with 1 year's worth added each year. At startup, there is therefore an extra  $t_R-1$  that must be provided.

$$CR = e^{m(t_F + t_R)} (1 + m(t_R - 1)) \quad (8)$$

At a nominal growth rate of 1.75%/yr, the time lags in the system are important. If  $t_F = 2$  (example for onsite recycling) and  $t_R = 4$ , then  $CR = 1.17$  is required. If  $t_F = 11$  (example for offsite recycling) and  $t_R = 4$ , then  $CR = 1.36$  is required.

Fig. 18 shows the required CR as function of desired growth rate and turnaround time. The minimum turnaround time is probably ~5 years (1-year cooling, separation, fabrication and 4 years in reactor).

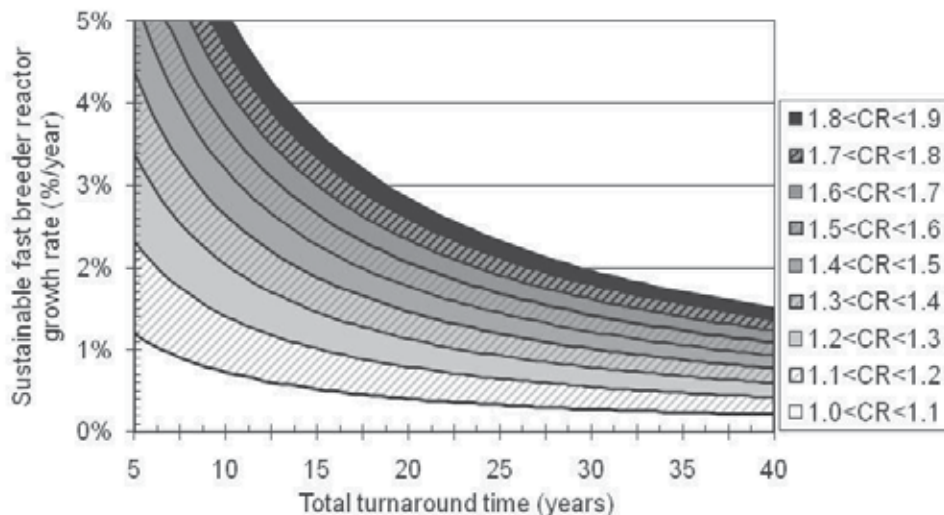


Fig. 18. Required fast reactor TRU conversion ratio at dynamic equilibrium, as a function of growth rate and turnaround, ignoring displacement of pre-existing LWRs or TRU stockpiles.

The theoretical maximum CR is ~1.9 because Pu239 dominates fission in a fast reactor and it yields 2.9 neutrons/fission. One neutron must induce the next fission, leaving 1.9 to make more transuranic material from U238.<sup>3</sup> Neutron yields vary slightly by isotope, e.g., 2.4 for U235, 2.9 for Pu241, and 3.2 for Am242m, so the exact theoretical maximum could be slightly different than 1.9. Of course, as neutron leakage and neutron capture by fuel and non-fuel core material is accounted for, the practical maximum conversion ratio will be significantly lower than 1.9. For example, if that maximum is considered to be 1.5, then the maximum rate of breeder reactor introduction can be 4.7% with 6-year turnaround (onsite recycling), but only 2.3% with 15-year turnaround (offsite recycling). The holdup of transuranic material in the system impacts system performance so that short time lags, e.g., when facilities are co-located instead of at different locations, can lead to faster system evolution.

<sup>3</sup> The theoretical maximum is actually smaller than 1.9 because some neutrons absorbed into fuel necessarily lead to  $(n, \gamma)$  reactions instead of  $(n, \text{fission})$ . However, some of the  $(n, \gamma)$  products and their successors will fission, so the reduction of the maximum below 1.9 is somewhat complicated and beyond the scope of this illustrative calculation.

### 5.4 Proliferation resistance and physical protection

Barriers to acquisition of a nuclear weapon/explosive are called “proliferation resistance” for a host nation of nuclear facilities and “physical protection” for a subnational or terrorist group. An evaluation methodology should include the four stages toward a weapon – (1) diversion (if host nation) or theft (if subnational), (2) transportation, (3) transformation, and (4) weapon fabrication and indicate how the various indicators are to be combined.

First, observe that although there is significant reduction of TRU relative to once through (avoided and consumed), there remains significant TRU material throughout a fuel cycle system. Figure 19 illustrates that there is substantial reduction of TRU material relative to once-through (via avoidance and consumption) but also that there is substantial TRU in many parts of the system.

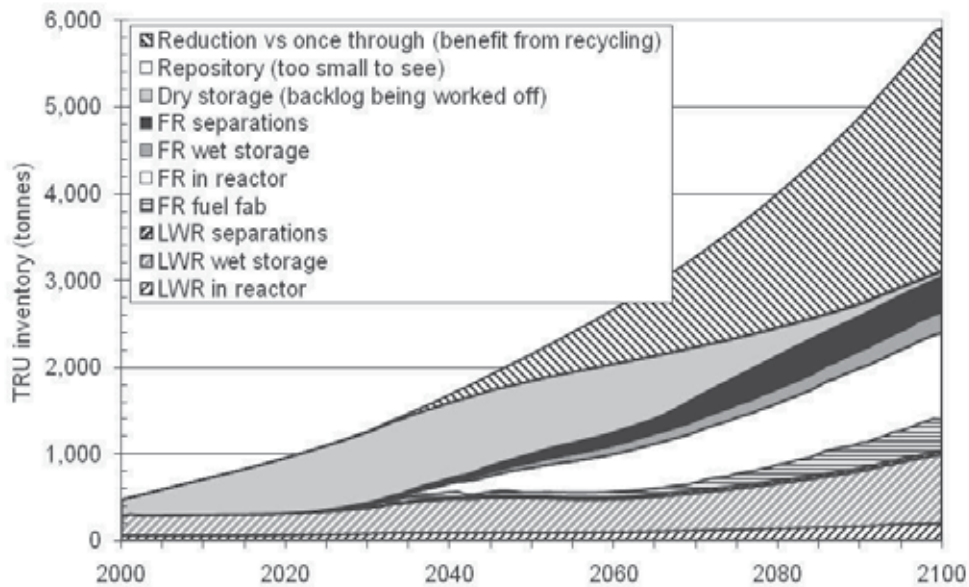


Fig. 19. Location of TRU material in a 1-tier recycle case.

The second proliferation resistance observation is that the mass flow of material through separations can vary significantly both quantitatively and by type of separation, independent of separation efficiency. Figure 20 shows the total mass sent through separations (the sum of the flow tonnes-TRU/yr times the number of years) as a function of fast reactor conversion ratio for a 1-tier simulation; this figure keeps the fast reactor fuel constant (metal) with onsite processing. As CR increases, there are fewer LWRs hence less processing of used LWR fuel; but there are more fast reactors and more processing of fast reactor fuel. These may be of different technologies and the siting strategy could differ, e.g., large centrally located aqueous separation of used UOX fuel versus at-reactor electrochemical separation of used fast reactor metal fuel. In such cases, the proliferation risk posed by different technologies and locations would vary.

The third proliferation resistance observation is that the recycled material composition will change significantly with time. Figure 21 shows evolution of the recycle mix as TRU material is repeatedly recycled, in this case as mixed oxide fuel in LWRs.<sup>12</sup> This calculation

uses heterogeneous inert matrix fuel (IMF)<sup>4</sup> to keep the material fissile, i.e., each recycle is a mixture of fresh UOX and IMF made with TRU recovered from the previous recycle. The figure shows that the Cm and Cf isotopes, which emit high numbers of neutrons, increase up to four orders of magnitude between the first recycle and equilibrium. Figure 21 compares MOX and metal fast reactor fuel (at CR=0.75, comparable to the CR of MOX) at the first and equilibrium recycle. Both MOX-TRU and FR-TRU evolve considerably from the first to the equilibrium recycle. FR-TRU has higher Pu content but lower amounts of the highest TRU isotopes (Cf) that tend to dominate neutron emission.

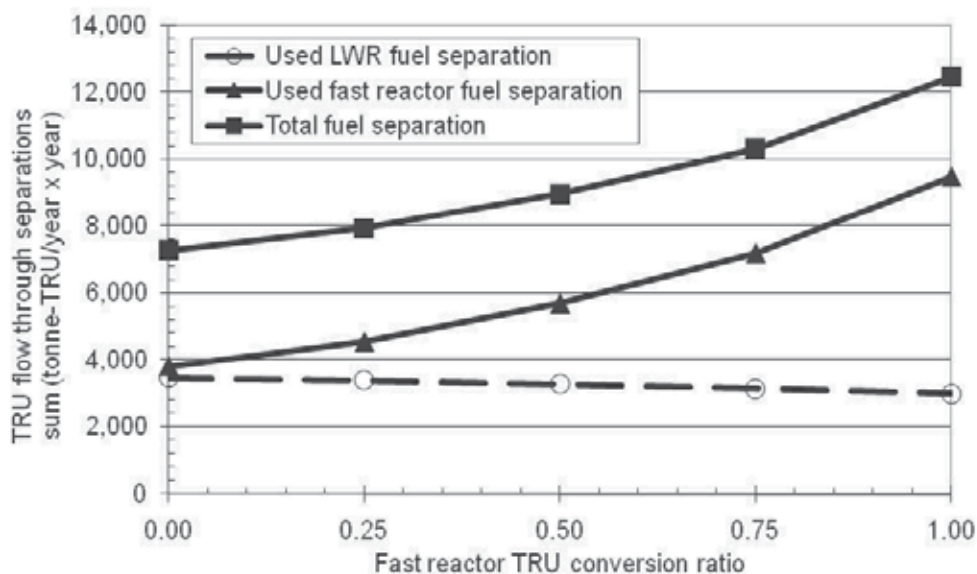


Fig. 20. Total mass of TRU material sent through separations in 1-tier recycle case as a function of fast reactor TRU conversion ratio; metal fuel, on-site processing assumed.

Figure 22 shows that MOX-TRU and FR-TRU vary little after the first recycle (square data points), with major differences only in the Cf isotopes. (Composition impacts many areas, not just proliferation and physical security.) At equilibrium recycle (circle data points), MOX-TRU and FR-TRU differ less than an order of magnitude below Cm244, about an order of magnitude from Cm244 to Cm248 and over an order of magnitude for the Cf isotopes. High gamma emitting isotopes are found throughout the actinide chain and therefore the total gamma comparison between MOX-TRU and FR-TRU is merely an order of magnitude. The highest neutron emitters are located at the top of the TRU chain and therefore the neutron emission comparison between MOX-TRU and FR-TRU grows over an order of magnitude. Still, both MOX and FR at equilibrium have higher gamma and neutron emission than either has at the start of recycling.

The fourth and final proliferation resistance observation is that the quality of Pu does not change dramatically throughout the century. The quality of Pu measured as the fraction of

<sup>4</sup> MOX fuel has U and one or more TRU elements mixed in each fuel pellet and fuel pin. A homogeneous IMF fuel has only TRU. A heterogeneous IMF fuel is a mix of IMF fuel pins and UOX fuel pins.

Pu-239 to total Pu in the system only changes from 0.55 (once through) to ~0.50 for the two recycle cases.

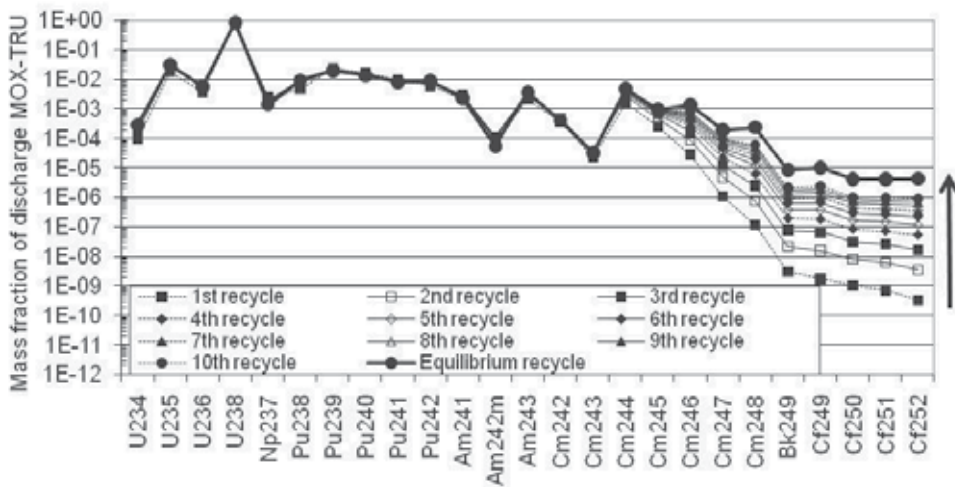


Fig. 21. Isotopic mix for discharged MOX-TRU as a function of how many times transuranic material is. Transmutation data from ref. 16.

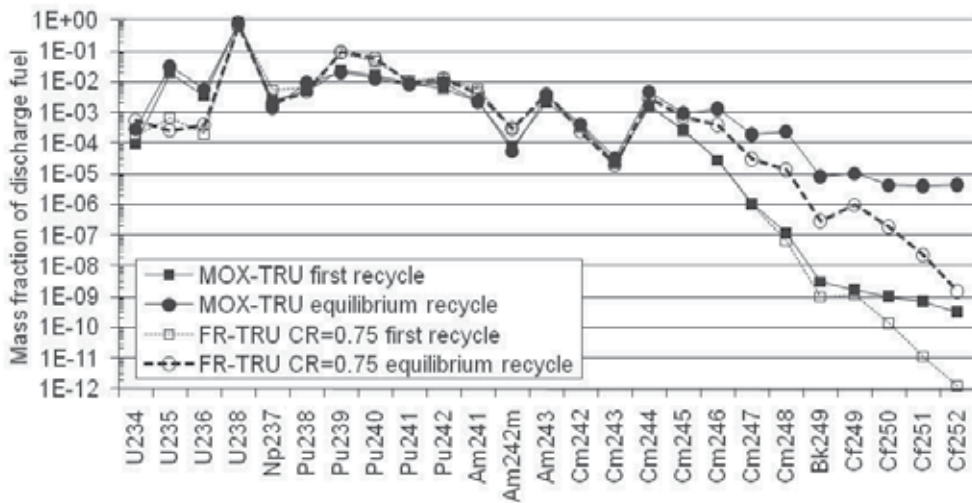


Fig. 22. Isotopic mix for discharged MOX-TRU and FR-metal-TRU for first and equilibrium recycle. Transmutation data from ref. 12 and 16.

### 5.5 Economics

In any area of technology, the cheapest situation occurs when raw materials are very low cost and one is allowed to just walk away from waste. As raw material cost increases, the incentive to recycle materials increase. As waste disposal costs increase, the incentive to reduce, re-use, and recycle increases.

Unsurprisingly, therefore, for nuclear fuel cycles, there are major uncertainties associated with the future cost of uranium (or thorium), any waste repository, and any new technologies (reactors, fuels, separation, waste forms) that may be involved. Were uranium and waste disposal inexpensive, it would be difficult to economically justify new technologies.

The average cost of electricity from current U.S. nuclear power plants is less than \$0.018/kilowatt-hour or 18 mills/kilowatt-hour (18 mills/kW-hr) because their capital costs have mostly been depreciated. Cost projections for new plants in the next decade range from 47 to 71 mills/kW-hr which include capital recovery. Fuel cycle costs are about 6 mills/kW-hr. Of this, 1 mill/kW-hr is the fee currently paid by U.S. utilities to the Federal government for future geologic disposal, covering projected disposal costs.

To date, estimates of the cost of relatively traditional alternative fuel cycle options (most uranium cost increases, Yucca Mtn repository, and GNEP technology options) suggest uncertainties of a few mills/kW-hr, and possible increased cost (relative to once through) ranging from zero to a few mills/kW-hr, or 0-10% of total nuclear energy cost.

The first is that dynamic versus static will impact economic assessments. A static equilibrium is appropriate when discount rates, the time value of money, and cash flows are not addressed. A dynamic equilibrium comes closer to cash flows if the time value of money is accounted for as costs that lead others are given greater weight; cash flows that lag others are given less weight. Table III lists key lead and lag items in dynamic equilibria. For example, one builds LWRs relatively early in the process of generating electricity; therefore, when time value of money is considered, the relative contribution of LWRs to total cost increases. Conversely, fast reactors and waste disposal are bought relatively late; therefore, their relative contribution to total cost decreases.

	Leading Purchase relatively soon	Lagging Purchase relatively late
Increase or decrease when shifting from static to dynamic equilibrium	Increase, hence factor might be more important than predicted by static equilibrium	Decrease, smaller impact than might be predicted by static equilibrium
Material inputs	Natural uranium Depleted uranium Enriched uranium Zirconium and steel	
Types of reactors	Number of thermal reactors using uranium oxide fuel	Number of fast reactors Thermal efficiency increases
Types of facilities	Fabrication plants	Separation plants
Material output		Waste disposal

Table 3. Lead and Lag Items in Dynamic Equilibria

The fraction of fast reactors in time will be much lower than predicted by simple “static equilibrium” calculations due to multiple system constraints that impact the amount of TRU available for fueling new reactors at startup. This is illustrated in figure 23.



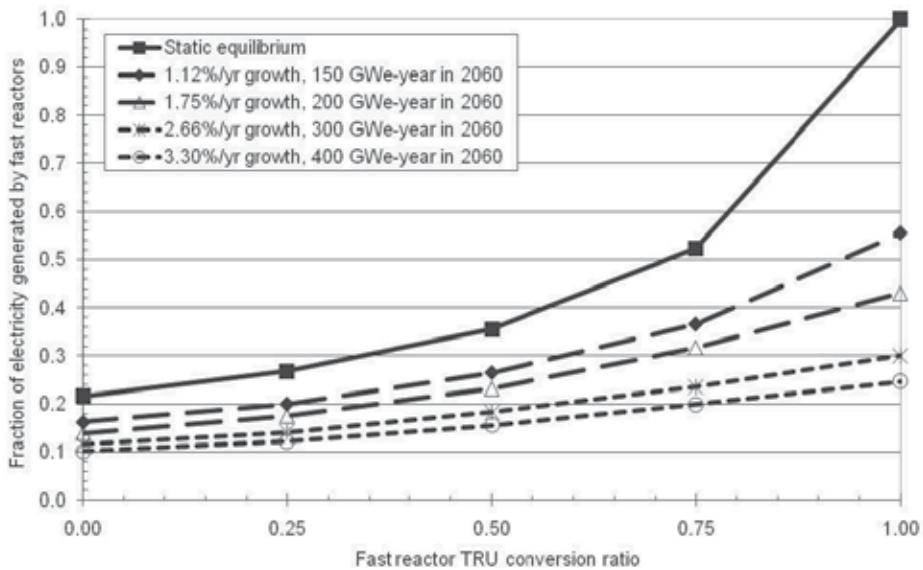


Fig. 23. Fraction of electricity generated by fast reactor at dynamic equilibrium (near 2100) as function of fast reactor TRU conversion rate and nuclear electricity power growth rate, calculations assumed metal fuel and onsite processing.

The final observation is that fuel and separation facilities must accommodate variation in fuel mixture elemental composition. This composition will vary as reactor type, fuel type, burnup, aging of used fuel, number of recycles, separation purity, etc.

## 6. Acknowledgments

This chapter was prepared for the U.S. Department of Energy Office of Nuclear Energy, Science, and Technology under DOE Idaho Operations Office Contract DE-AC07-05ID14517.

## 7. References

- [1] U. S. Department of Energy, Office of Nuclear Energy, Science, and Technology, Report to Congress - Advanced Fuel Cycle Initiative: Objectives, Approach, and Technology Summary, May (2005).
- [2] U. S. Department of Energy, Office of Nuclear Energy, Science and Technology, Advanced Fuel Cycle Initiative (AFCI) Comparison Report, FY 2005, May (2005).
- [3] U. S. Department of Energy, Office of Nuclear Energy, Science, and Technology, Advanced Fuel Cycle Initiative (AFCI) Comparison Report, FY 2006 Update, July (2006).
- [4] J. J. Jacobson, A.M. Yacout, G.E. Matthern, S.J. Piet, D.E. Shropshire, R.F. Jeffers, T. Schweitzer, "Verifiable Fuel Cycle Simulation Model (VISION): A tool for Analyzing Nuclear Fuel Cycle Futures", Nuclear Technology, Volume 172, Number 2, November 2010.
- [5] S. J. Piet, "Selection of Isotopes and Elements for Fuel Cycle Analysis", Advances in Nuclear Fuel Management IV, April 12-15, 2009.

- [6] J. W. Forrester, *Principles of Systems*, Wright-Allen Press, Inc, 1971.
- [7] Powersim Software AS, Bergen, Norway, [www.powersim.com](http://www.powersim.com).
- [8] J. Grouiller, G. Glamenbaum, B. Sicard, M. Mus, J. Martin, J. Devezeaux de Lavergne, O. Comellini. COSI, A Simulation Software for a Pool of Reactors and Fuel Cycle Plants: Application to the Study of the Deployment of Fast Breeder Reactors. Proceedings of the International Conference on Fast Reactors and Related Fuel Cycles, Kyoto, Japan, October 1991.
- [9] C. G. Bathke and E. A. Schneider. Report of the COSI and NFCSim Benchmark. Los Alamos National Laboratory (2003). LA-UR-03-8051.
- [10] J. A. Stillman, "Homogeneous Recycling Strategies in LWRs for Plutonium, Neptunium, and Americium Management," Argonne National Laboratory, ANL-AFCI-124, August 2004.
- [11] E. A. Hoffman, W. S. Yang, R. N. Hill, Preliminary Core Design Studies for the Advanced Burner Reactor over a Wide Range of Conversion Ratios, ANL-AFCI-177, September 29, 2006.
- [12] E. A. Hoffman, "Updated Design Studies for the Advanced Burner Reactor over a Wide Range of Conversion Ratios," Argonne National Laboratory report, ANL-AFCI-189, May 31 (2007).
- [13] E. A. Hoffman, "FY09 ANL AFCI Transmutation Studies," Argonne National Laboratory report, ANL-AFCI-271, August 31 (2007).
- [14] M. Asgari, B. Forget, S. Piet, R. Ferrer, S. Bays, Computational Neutronics Methods and Transmutation Performance Analyses for Light Water Reactors, INL/EXT-07-12472, March 2007.
- [15] R. M. Ferrer, M. Asgari, S. E. Bays, B. Forget, "Fast Reactor Alternative Studies: Effects of Transuranic Groupings on Metal and Oxide Sodium Fast Reactor Designs," INL/EXT-07-13236, September 2007.
- [16] G. Youinou and S. Bays, "Homogeneous recycling of Pu or Pu with Minor Actinides in PWRs loaded with MOX-UE fuel (MOX with U-235 enriched U support), INL/EXT-09-16091, AFCI-SYSA-TRAN-SS-RT-2009-000055, June (2009).
- [17] OECD Nuclear Energy Agency, Nuclear Fuel Cycle Transition Scenario Studies Status Report (2009).
- [18] S. J. PIET, G. E. Matthern, J. J. Jacobson, C. T. Laws, L. C. Cadwallader (INL), A. M. Yacout, R. N. Hill (ANL), J. D. Smith, A. S. Goldmann, G. Bailey (SNL), "Fuel Cycle Scenario Definition, Evaluation, and Trade-offs," INL report, INL/EXT-06-11683, August (2006).
- [19] OECD Nuclear Energy Agency and International Atomic Energy Agency, Uranium 2007: Resources, Production and Demand, NEA No. 6345 (2008).
- [20] J. S. Herring, "Uranium and Thorium Resources," in *The Encyclopedia of Energy*, Cutler J. Cleveland, editor in chief, Academic Press, (2004).
- [21] J. J. Steyn, "Uranium Resources: Need For 21st Century Advanced Fuel Cycles," Energy Resources International, Inc., NEI International Fuel Seminar (2003).
- [22] D. J. Rose, *Learning About Energy*, Plenum Press, New York (1986).



# The Investment Evaluation of Third-Generation Nuclear Power - From the Perspective of Real Options

Ying Fan and Lei Zhu

*Center for Energy and Environmental Policy research, Institute of Policy and  
Management, Chinese Academy of Sciences, Beijing  
China*

## 1. Introduction

The continued growth of world's population and gradual increase of people's living standards in developing countries have sped up the exhaustion of fossil fuels and caused large amount of greenhouse gas emissions. Although renewable energy sources (e.g. wind energy, solar energy, hydro energy and biomass energy) have developed rapidly in recent years, limitations existing in these energy sources (e.g. non-continuous electricity supply of wind and solar power generation, resource constraints for hydro power and biomass energy etc.) still set barriers to launching application in large scale and fulfilling world's energy demand in near future.

Currently, great attention has been paid to nuclear technology. It has been widely accepted around the world that nuclear power is a clean energy option which causes zero-emissions of SO<sub>2</sub>, NO<sub>x</sub>, smoke dust and carbon. A safely-operating nuclear power plant with strict radiation monitoring and risk management system will have little impacts on its surroundings, and the effects of radiation dose on citizens near the plant will be lower than 1% of underground natural radiation. The development of nuclear energy can broaden the energy sources in energy industry, ease the limitations of fossil fuel supply, and reduce the environmental pollution caused by fossil fuel combustion. The development of nuclear technology will also have significant impacts on greenhouse gas emission reduction.

Asia has become the largest market for nuclear power after remarkable growth has emerged to its economies in the last decade, especially in China and India. The enjoyment of rapid economic development in Asian countries also brings the booming of energy consumption. On one hand, considering large fluctuation of international fossil energy prices (e.g. oil prices) in recent years and lack of effective energy supply, Asian countries have to face more serious energy security situations; On the other hand, the consumption of fossil energy has caused severe environmental pollutions and large amount of greenhouse gas emissions, in the case of renewable energy development barriers, Asian countries need to find other new, clean, stable and extensive energy resource to meet their domestic energy demand. Nuclear power is regarded as a trustworthy way to enhance Asian countries' energy security and becomes a preferred-choice in their energy options.

As the world's largest developing country which is struggling with limited energy resources, growing energy demand, increasing dependence on imported oil, deteriorating

environment, and enormous greenhouse gas emission, China has taken nuclear power as one of main directions in future energy development to cope with serious threats on domestic energy security. China's power generation portfolio aims to gradually reduce the proportion of coal-fired power in the total power-generation mix and to promote the diversification of electrical energy sources, the power industry's 'Eleventh Five-Year Plan' (NDRC, 2007) has been proposed to optimize the development of nuclear power. Furthermore, the objective of 'Mid and Long-term Nuclear Power Development Plan' (NDRC, 2007) is to achieve a new capacity of 40 GW Nuclear Power in the year 2020, which will account for 4% of total generating capacity. At the end of 2009, China has owned the largest scale of nuclear power plants under construction over the world, and the plants in progress have reached 21.92 GW with a total of 20 units.

After the development of first two generations of nuclear power, China proposed to pioneer the demonstration and deployment of third-generation nuclear power with advanced reactors (Generation III nuclear reactor) in order to further enhance the level of self-developed nuclear power technology. The third-generation reactors have: 1) a standardized, simpler and more rugged design for each type to expedite licensing; 2) higher availability and longer operating life expectancy; 3) comparatively lower possibility of core melt accidents; 4) resistance to serious damages; 5) higher burning temperature to reduce fuel use and the amount of waste and burnable absorbers to extend fuel life. In 2007, as one of the Generation III nuclear reactor technologies on basis of a comprehensive technology transfer, Westinghouse AP1000 has been selected by China National Nuclear Cooperation to build four nuclear reactors in two demonstration projects in Zhejiang Sanmen and Shandong Haiyang. Currently, nuclear reactors built in Zhejiang Sanmen are the only third-generation nuclear power units in the world.

## **2. Uncertainties of China's third-generation nuclear power technology investment**

Some scholars have already studied the third-generation nuclear power from different perspectives. Yim (2006) has discussed the relationship between the future expansion of nuclear power and the prospect for world nuclear nonproliferation, he concludes that the development of nuclear power and expansion of advanced nuclear technology will not result in nuclear proliferation. Popa-Simil (2008) has proposed that the micro-bead heterogeneous fuel mesh gives the fission products the possibility to acquire stable conditions outside the hot zones without spilling and the high temperature fission products free fuel with near perfect burning, which is important to the future of nuclear power development. Marcus (2008) has studied the characteristics of advanced nuclear reactor in order to extensive demands worldwide, including the role of nuclear power in the world power generation, introduction of innovative nuclear technologies, nuclear path forward and international initiatives of advanced nuclear technologies. Tronea (2011) has discussed the European quest for standardisation of nuclear power reactors, including nuclear power design, new reactors standard and nuclear safety. Yan et.al (2011) has introduced the development of nuclear power and third-generation nuclear power demonstration projects in China, and they also have forecasted the future demand of uranium fuel in China.

In the study of the economics of nuclear power, Kessides (2010) has discussed nuclear power investment from the perspective of economic risks and uncertainties. He points out that several elements should be considered in nuclear power valuation, including

environmental benefits of nuclear power investments (the contribution of greenhouse gas emissions), fuel costs, costs of radioactive waste disposal, risks associated with radio activity release from all fuel cycle activity, with the capital or nuclear power construction costs with the greatest importance. However, as a technology that is currently in the research and development stage, China is facing numerous uncertainties in demonstration and deployment of third-generation nuclear power, including:

1. The uncertainty from the technology itself. As a large-scale and capital-intensive technology, third-generation nuclear power is still in the development and demonstration stage which exhibiting unsolved technology uncertainties. During the technology deployment process, uncertainties around the technology mainly come from the plant design and construction, reactor installation, and equipment commissioning. And this corresponds to the uncertainties of investment cost and construction period which are in need for technology deployment.
2. It is claimed in the design that the operating costs of third-generation nuclear power will be equal or even lower than that of second-generation. It should be noted that nuclear fuel cost has accounted for a large proportion in nuclear power operating costs. Currently, the price of nuclear fuel is relatively stable because uranium resources in each country are under government control, as more nuclear power plants will be put into use in the coming future, increasing demand of uranium resources worldwide may result in price increasing and fluctuation. This will add more price risk to generating cost.
3. Although the design of third-generation nuclear power is much safer than first two generations, because the lack of actual operational experiments, the potential risk of radiation can not be completely under control. China's National Nuclear Security Regulations require the Probabilistic Safety Assessment (PSA) must be carried out by all nuclear power plants. Nuclear accidents are unexpected events with small probability, and previous studies in nuclear power valuation have not considered the impacts of nuclear accidents and losses (or damage) caused by nuclear plants operation.
4. The uncertainty in electricity price mechanism. Currently, China's electricity price of nuclear power is set by the government, which is a cost-benefit pricing mechanism and each nuclear power plant has its own constant electricity price. So the electricity prices vary a lot among different nuclear plants. With the continuous electricity market reform, the electricity price will be gradually pushed forward to market-oriented. One important feature of electricity price marketization is "price bidding" among different kinds of power plants. Liberalized electricity price will be affected by seasonal demand for electricity, fuel price changes, and other factors. And thus it is uncertain. Electricity price mechanism and price level will directly affect the valuation of third-generation nuclear power investment.
5. Regarding climate policy, nuclear power can be viewed as an emission reduction option. Compared to thermal power with identical installed capacity, the operation of nuclear power does not produce greenhouse gas emissions, but this part of emission reduction can not be verified in current Clean Development Mechanism (CDM). So the application of nuclear power can not have Certification Emission Reduction (CER) and trade in CDM. In fact, the nuclear industry is promoting nuclear power CDM credits. If nuclear power can be included in Clean Development Mechanism, the uncertainties in climate policy and trading mechanism of CDM (Bilateral or Unilateral) will also affects the investment of third-generation nuclear power.

As NPV based evaluation method can not fully catch the impacts of these uncertainties on nuclear power investment, it is necessary to develop a proper method to handle such kinds of uncertainties to evaluate the demonstration and deployment of third-generation nuclear power plants in China.

Real options approach is suitable for evaluation of large-scale investment projects with great uncertainties. Brennan and Schwartz (1985) first introduced a real options approach to natural-resource investment decisions. After that, real options approach has been applied more frequently in the evaluation of energy investment (Paddock et. al, 1988, Smith and Nau, 1995, Smith and McCardle, 1998, 1999, Fan and Zhu, 2010). For power investment projects, real options approach can consider the uncertainties of the market environment, generating fuel prices, environmental factors, electricity demand and supply and so on (Venetsanos et.al, 2002, Davis and Owens, 2003, Siddiqui et. al, 2007, Abadie and Chamorro, 2008a, 2008b, Fuss et.al, 2008, Fleten and Näsäkkälä, 2009). Therefore, the real options approach would be useful for evaluation of advanced generating technologies. In the valuation of nuclear investment, Gollier et. al (2005) apply real options approach with the consideration of electricity price uncertainty to compare the critical value between flexible sequence of small nuclear power plants and a nuclear power plant of large capacity. They show that the option value of modularity has a sizeable effect on the optimal dynamic strategy of the producer, particularly in terms of the optimal timing of the decision to invest in the first module.

This paper applies real options theory with Monte Carlo method to establish a nuclear power investment evaluation model, incorporating the world's first third-generation nuclear power project-Sanmen nuclear power plant in Zhejiang province, to evaluate the value of third-generation nuclear power plant from the perspective of power generation enterprises. Several technical and economic uncertainty factors (deployment cost, generating cost and nuclear accident), and two price mechanisms (electricity price and CDM) have been considered in the model and it is solved by Least Squares Monte Carlo (LSM) method. As the model can be used as a policy analysis tool, under a given period of nuclear power operation, first we have evaluated the value of Sanmen third-generation nuclear power plant in current constant electricity price set by the government to see whether it is worth investing or not. Then the impacts of different electricity and CDM mechanisms on the valuation of third-generation nuclear power have been discussed. And we have also analyzed the acceptable level of investment cost for third-generation nuclear power in China.

### 3. Model description and parameter settings

As stated above, Sanmen third-generation nuclear power project has been chosen for evaluation object, the model established here is based on real options theory with Monte Carlo method and solved by Least Squares Monte Carlo (LSM) simulation. The valuation includes nuclear power plant construction period and operation period. As a large-scaled investment project, it will take time to complete nuclear power investment. And the power generation enterprise has the right to exercise the abandon option to terminate the nuclear project in the investment stage. So at each step of the investment stage, the enterprise can re-evaluate the nuclear project to decide whether to continue or abandon the investment. Assuming the total period for nuclear power construction and operation is  $T$  years, for the purpose of valuation we divide the  $T$  years into  $N$  periods, each with a length of

$\Delta t = T / N$ , and define  $t_n = n\Delta t$ ,  $n = 0, 1, \dots, N$ . All the units for the parameters described below is displayed in table 1.

### 3.1 Modeling third-generation nuclear power operation

At nuclear power plant operation period, first it is in need to calculate the cash flow during nuclear power operation. Assuming at any period  $t_n$ , the generating capacity of third-generation nuclear power is  $Q_{Elec}(t_n)$ , and all the electricity generated by nuclear power can be sold to grid. Considering the possibility of nuclear accident, after nuclear power investment has been completed, the cash flow  $CF(t_i)$  earned by the power enterprise through electricity selling from nuclear power at  $t_i$  period should be:

$$CF_{Nu}(t_i) = [P_{Nu}(t_i) + P_C(t_i) - C_{Nu}(t_i) - R_w] \cdot Q_{Elec}(t_i) \cdot (1 - Tax) - \Delta q$$

Where  $P_{Nu}(t_i)$  is the electricity price;  $P_C(t_i)$  is the carbon price under CDM, and if nuclear power can not be included in CDM, this term will be 0;  $C_{Nu}(t_i)$  is the nuclear generating cost;  $Tax$  denotes the income tax for power generation enterprise;  $R_w$  represents the cost for nuclear waste disposal; and  $\Delta q$  is the impact of nuclear accident.

At any period  $t_i$  after accomplishment of nuclear power investment, the value  $V_{Nu}(t_i)$  for enterprise operating the nuclear power plant is:

$$V_{Nu}(t_i) = \sum_{n=i}^N e^{-r(t_n - t_i)} CF_{Nu}(t_n)$$

And  $r$  is the risk free rate.

During nuclear power plant operation period, we have considered the impact of three electricity price mechanism, two CDM price mechanism, generating cost (uranium fuel price) uncertainty, and unexpected events with small possibility on the nuclear power plant operating cash flow and value.

First, we can assume nuclear generating cost following a geometric Brownian motion:

$$C_{Nu}(t_{i+1}) = C_{Nu}(t_i) \exp(\alpha_C \Delta t + \sigma_C (\Delta t)^{1/2} \varepsilon_C)$$

Where  $\varepsilon_C$  is a normally distributed random variable with mean of 0 and standard deviation equivalent to 1; and  $\alpha_C$  and  $\sigma_C$  represent the drift and variance parameters of the nuclear generating cost, respectively.

Nuclear accidents are unexpected events with small possibility. Here we apply a Poission process to describe the unexpected events (nuclear accidents) during nuclear power plant operation period. Let  $q$  be a Poission process, then we have:

$$\Delta q = \begin{cases} 0, & \text{Probability: } 1 - \lambda \Delta t \\ u = \begin{cases} u_S, \text{Probability: } \eta_S \\ u_M, \text{Probability: } \eta_M \\ u_L, \text{Probability: } \eta_L \end{cases}, & \text{Probability: } \lambda \Delta t \end{cases}$$

Where  $\lambda$  is the average probability for the unexpected events (nuclear accidents), and at any time horizon  $\Delta t$ , the probability of nuclear accidents happen will be  $\lambda \Delta t$  and the

probability of nuclear accidents do not happen will be  $1 - \lambda\Delta t$ ;  $u$  represents the damage or loss caused by nuclear accidents during nuclear operation, and  $\eta_S + \eta_M + \eta_L = 1$ .

Considering different level of nuclear accidents will cause different damage or loss, we define three levels of nuclear accidents which correspond to different probability:

1. Minor accident, the probability is  $\eta_S$ , there is a small loss  $u_S$  for nuclear power plant and it will not affect plant operation.
2. Moderate accident, the probability is  $\eta_M$ , there is a moderate loss  $u_M$  for nuclear power plant. And the plant will pause power generation in next two years in order to have necessary reactor security maintenance and monitoring nuclear leak, which  $Q_{Elec}(t_{x+1}) = Q_{Elec}(t_{x+2}) = 0$ .
3. Serious accident, the probability is  $\eta_L$ , there is a severe loss of  $u_L$  for nuclear power plant. And the plant will be shut down permanently, which  $Q_{Elec}(t_{x+1}) = Q_{Elec}(t_{x+2}) = \dots = Q_{Elec}(t_N) = 0$ .

For electricity price, three forms of price mechanism have been taken in to account in this paper, which are shown as follows:

1. The electricity price follows cost-benefit pricing mechanism and is set by the government, it is a constant price mechanism in which  $P_{Nu}(t_{i+1}) = P_{Nu}(t_i)$ .
2. The electricity price is still under government control but has a constant growth rate at each period, it is a constant growth price mechanism in which  $P_{Nu}(t_{i+1}) = P_{Nu}(t_i)\exp(\alpha_p\Delta t)$ .
3. The electricity price is liberalized as electricity marketization. Assuming the liberalized electricity price follows a geometric Brownian motion

$$P_{Nu}(t_{i+1}) = P_{Nu}(t_i)\exp(\alpha_p\Delta t + \sigma_p(\Delta t)^{1/2}\varepsilon_p)$$

Where  $\varepsilon_p$  is a normally distributed random variable with mean of 0 and standard deviation equivalent to 1; and  $\alpha_p$  and  $\sigma_p$  represent the drift and variance parameters of the electricity price, respectively.

For CDM, two following forms of CDM have been modelled in this paper:

1. In bilateral CDM, the carbon price is constant, of which  $P_C(t_{i+1}) = P_C(t_i)$ .
2. In unilateral CDM, referring to previous research related carbon price modeling (Abadie and Chamorro, 2008, Heydari et.al, 2010), assuming the carbon price in unilateral CDM follows a geometric Brownian motion:

$$P_C(t_{i+1}) = P_C(t_i)\exp(\alpha_{p_c}\Delta t + \sigma_{p_c}(\Delta t)^{1/2}\varepsilon_{p_c})$$

Where  $\varepsilon_{p_c}$  is a normally distributed random variable with mean of 0 and standard deviation equivalent to 1; and  $\alpha_{p_c}$  and  $\sigma_{p_c}$  represent the drift and variance parameters of the carbon price, respectively.

### 3.2 Modeling third-generation nuclear power investment

At nuclear power plant construction period, we apply a controlled diffusion process to describe the uncertainty of third-generation nuclear power investment.  $K_{Nu}$  is the expected total investment cost for power generation enterprises to deploy third-generation nuclear

power technology and the total deployment investment remaining at period  $t_i$  is  $K_{Nu}(t_i)$ . Assume that  $K_{Nu}$  follows the controlled diffusion process:

$$K_{Nu}(t_{i+1}) = K_{Nu}(t_i) - I_{Nu}(t_i)\Delta t + \beta[I_{Nu}(t_i)K_{Nu}(t_i)]^{1/2}(\Delta t)^{1/2}\varepsilon_x$$

Where  $\beta$  is a scale parameter representing the uncertainty around  $K_{Nu}$ ;  $\varepsilon_x$  is a normally distributed random variable with mean of 0 and standard deviation equivalent to 1. The variance of  $K_{Nu}$  is  $Var(K_{Nu}) = \left(\frac{\beta^2}{2-\beta^2}\right)K_{Nu}^2$ , whereby uncertainty of third-generation nuclear power technology reduces as  $K_{Nu}$  decreases.

Under the real option analysis framework, the power generation enterprise owns the abandon option during nuclear power plant construction period. At any time period  $t_i$  in construction period, the value of the nuclear power investment opportunity owned by the enterprise is denoted by  $F_{Nu}(t_i)$ . At the time period which nuclear power investment is completed (construction finished), the value of abandon option is equal to nuclear power project value:

$$F_{Nu}(\tau) = V_{Nu}(\tau)$$

At the time period  $t_i$  before investment is completed, the value of the nuclear power investment opportunity that the enterprise owns is equal to:

$$F_{Nu}(t_i) = \max\left\{0, E_{t_i}\left[e^{-r(t_{i+1}-t_i)}F_{Nu}(t_{i+1})\right] - I_{Nu}(t_i)\right\}$$

Where  $E_{t_i}[*]$  is the expected value which the enterprise chooses to hold abandon option and continue to invest in nuclear power plant at the time period  $t_i$ .

### 3.3 LSM Solution to the model

The abandon option  $F_{Nu}(t_i)$  of third-generation nuclear power investment is computed by the Least Squares Monte Carlo (LSM) method. The LSM method was developed for valuing American options and is based on Monte Carlo simulation and least squares regression (Longstaff and Schwartz, 2001; Schwartz, 2004). The model also computes the related greenhouse gas emission reduction which is avoided by applying nuclear power to take place of thermal power. Take  $\tau_g$  to represent the time that the third-generation nuclear power investment is completed in path  $g$ . Thus, the greenhouse gas emission reduction from the adoption of nuclear power during the given observation period can be computed as:

$$ER(g) = e \cdot Q_{Elec} \cdot (T - \tau_g)$$

Where  $ER(g)$  is the emission reduction amount during path  $g$ ;  $e$  is the emission factor for existing thermal power. Taking the average over all the paths, the total emission reduction amount through investing in third-generation nuclear power technology can be obtained. LSM method described has been implemented in Matrix Laboratory (MATLAB), and all solution procedure is vividly described in figure 1.

### 3.4 Model parameters

Table 1 shows the parameter values of the model. The project data related to Sanmen third-generation nuclear power plant mainly derive from public reports. Liberalized electricity price mechanism refers to European electricity market, and the data of uranium price comes from EIA. Some parameter values are estimated in this research due to data lack.

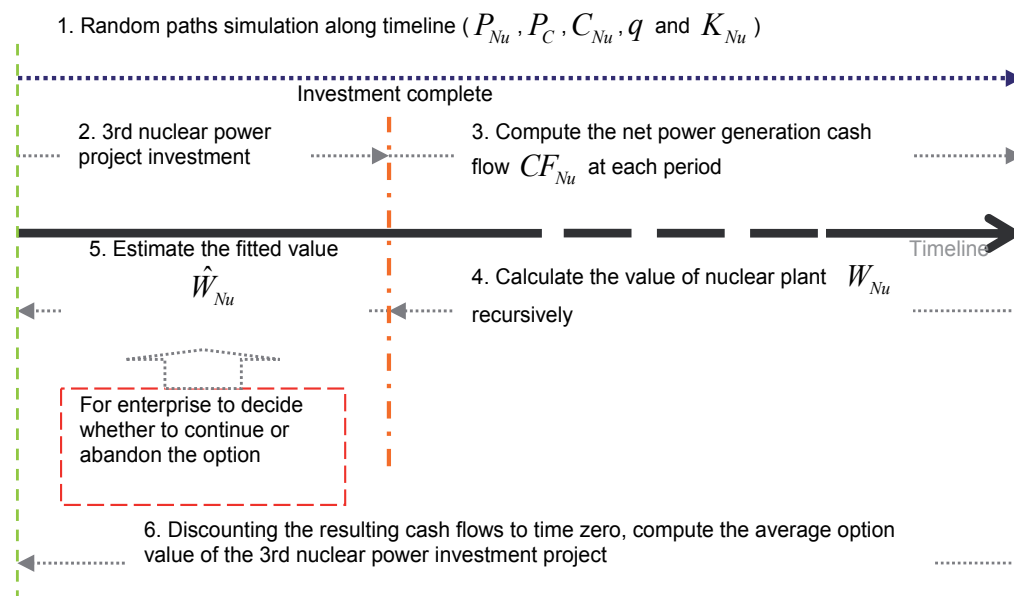


Fig. 1. LSM based Model Solution Procedure

Parameter	Model symbol	Value	Notes
generation capacity	$Q_{Elec}$	$15000 \times 10^6$ kwh	After Sanmen Nuclear Power project phase I has been completed, it will provide the power installed capacity of 2.5 million kilowatts, with a electricity supply of annual 17.5 billion kwh. It is designed to meet new electricity demand in Zhejiang province.
Total investment cost of third-generation nuclear power plant	$K_{Nu}$	$40000 \times 10^6$ yuan	Sanmen Nuclear Power Project will build 2 units with each installed capacity of 1.25 million kilowatts, and the total investment cost is 40 billion.
Initial annual investment cost	$I_{Nu}$	$8000 \times 10^6$ yuan	The time needed for nuclear power construction is generally 5 years. Sanmen Nuclear Power Project has started construction in 2009, and it is expected to be put into in operation in 2014. So the initial investment cost can be set as five years annual investment cost.
Nuclear technology uncertainty	$\beta$	0.5	Here refers to the settings in the research of Schwartz (2003), Dixit and Pindyck (1994).



Parameter	Model symbol	Value	Notes
Nuclear power generating cost	$C_{Nu}$	0.25 yuan/kwh	The data refers to the estimation of uranium generating cost from Zhu and Fan (2010). Set by this study.
Nuclear power generating cost drift rate	$\alpha_C$	0.01/year	
Nuclear power generating cost standard deviation rate	$\sigma_C$	6.24%/year	The data refers to the estimation of uranium generating fuel risk from Zhu and Fan (2010).
Electricity price	$P_{Nu}$	0.45 yuan/kwh	The price level refers to the electricity price set for Tianwan nuclear power plant which is newly put into operation, and this is also the baseline electricity price in our model.
Electricity price drift rate	$\alpha_P$	0.01/year	Set by this study.
Electricity price standard deviation rate	$\sigma_P$	5.00%/year	Set by this study. Considering future economic development in China, the demand for electricity is to some extent rigid, so here we set a low level of price volatility.
Correlation between Electricity price and generating cost	$\rho_{PCNu}$	0.3	Set by this study.
Carbon price	$P_C$	0.12 yuan/kwh	The data refers to the estimation of carbon emission cost from Zhu and Fan (2010). And this is also the baseline carbon price in our model.
Carbon price drift rate	$\alpha_{Pc}$	0.02/year	Set by this study.
Carbon price standard deviation rate	$\sigma_{Pc}$	11.50%/year	The data refers to the estimation of carbon price risk from Zhu and Fan (2009).
Probability of nuclear accident	$\lambda$	0.01%/year	Set by this study.
Probability of minor accident	$\eta_S$	98.90%	Here assume most of the nuclear accident are minor accident
Probability of moderate accident	$\eta_M$	1.00%	Assuming there will be 1.00% the probability to be moderate accident after nuclear accident happened.
Probability of serious accident	$\eta_L$	0.10%	Assuming there will be 0.10% the probability to be serious accident after nuclear accident happened.
Damage or loss of minor accident	$u_S$	$50 \times 10^6$ yuan	The loss for minor accident and it will not affect plant operation.
Damage or loss of moderate accident	$u_M$	$500 \times 10^6$ yuan	The loss for moderate accident, And the plant will pause power generation in next two years in order to have necessary reactor security maintenance

Parameter	Model symbol	Value	Notes
Damage or loss of serious accident	$u_L$	$5000 \times 10^6$ yuan	and monitoring nuclear leak. The loss for serious accident, And the plant will be shut down permanently.
Nuclear waste disposal cost	$Rw$	0.02 yuan/kwh	The cost of nuclear waste disposal is generally account for 10% of total nuclear generating cost.
Riskfree rate	$r$	0.05%	China's long-term deposit interest rate is used as a risk-free rate to represent the discount rate.
Tax rate	$Tax$	25%	Refers to the level of current domestic income tax.
Observation time	$T$	30 year, year 2010-2040	Here we consider the first 30 years of nuclear power plant life, this period is main investment accounting period for nuclear power investment.
Time Step Size in Simulations	$\Delta t$	1 year	
Number of Simulations	$G$	5000	In general, the simulation results will start to convergence when paths more than 1000, so the number of paths simulated in different scenarios are set as 5000.
Emission Factor	$e$	893g CO2/kwh	Emission factor of coal-fired generation comes from IEA (2009). In 2007, CO2 emission per kwh from electricity and heat generation using coal/peat in China is 893g CO2/kwh.

Table 1. Parameters used in the model

Figure 2a and 2b shows the changes of nuclear power generating cost  $C_{Nu}$  and remaining investment cost of third-generation nuclear power plant  $K_{Nu}$  in 250 of 5000 simulation paths. Figure 2c-2e shows once nuclear accident happen, the impact of three levels of nuclear accident on the nuclear power plant operation and cash flow in a single path. A large sample of random routing Monte Carlo simulation can simulate every possible result of cost change, and can better quantify the impact of nuclear accident on the value of third-generation nuclear power plant.

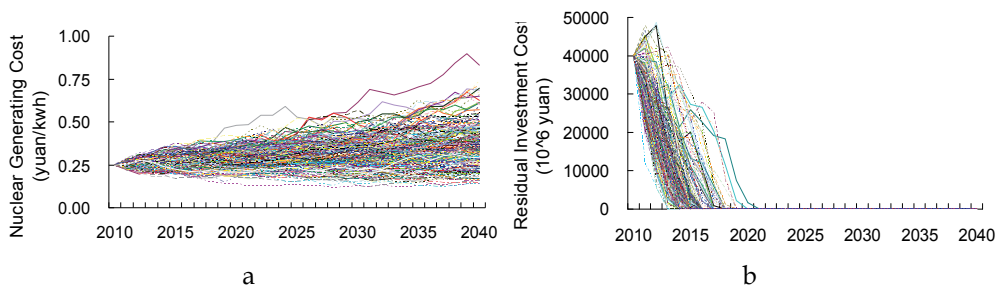


Fig. 2a. Generating cost simulation (Paths:250 of 5000)

Fig. 2b. Residual investment cost simulation (Paths:250 of 5000)

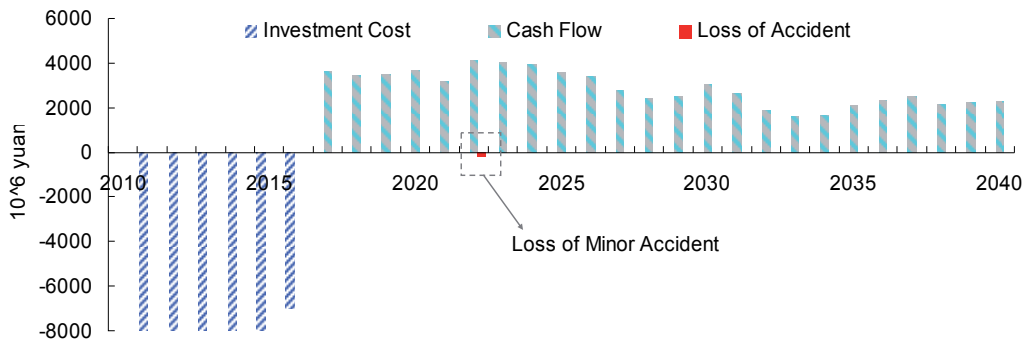


Fig. 2c. Single simulated path of minor nuclear accident

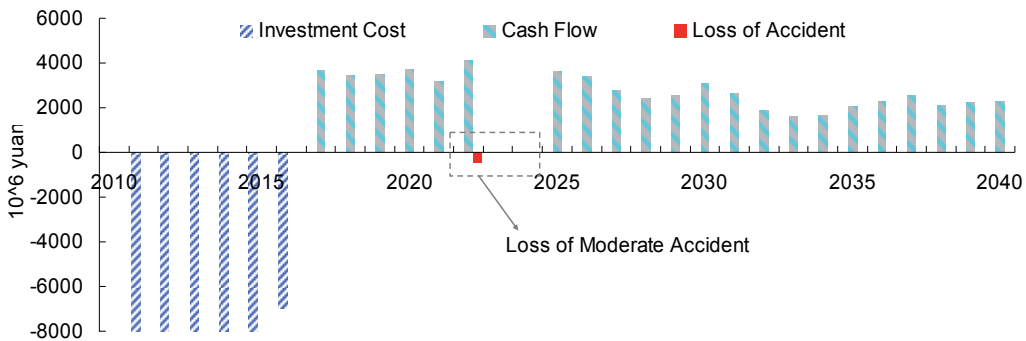


Fig. 2d. Single simulated path of moderate nuclear accident

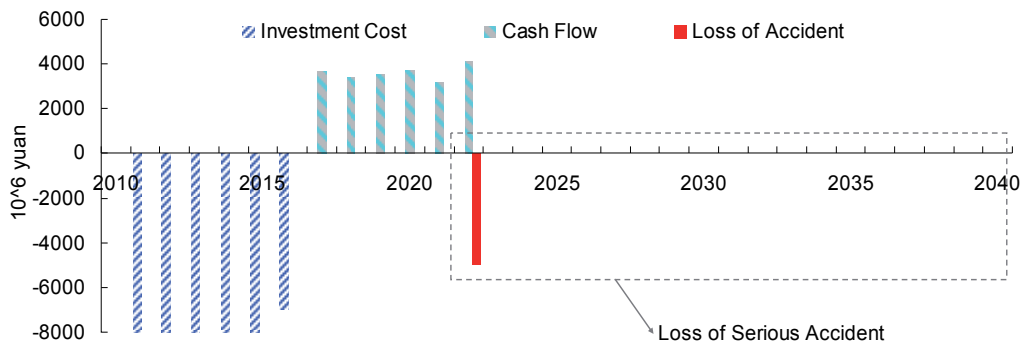


Fig. 2e. Single simulated path of serious nuclear accident

#### 4. Evaluation of third-generation nuclear power investment in China

Take the value of parameters into the model, and simulate the future changes of uncertainty factors according to their initial settings, then we can calculate the nuclear power plant value with abandon option by LSM method. Considering the Randomness of Monte Carlo simulation and in order to have a more accurate result, we have calculated five seeds for each result. And each seed has a result based on 5000 paths simulation with the application of LSM solution. Taking the average of the results in five seeds then we can get the value of third-generation nuclear power plant with abandon option.

For comparisons, we have presented two cases. Case 1 is based on current situation in China that the electricity price of nuclear power is set by the government and nuclear power can not be included in CDM. The constant electricity price set in our model is 0.45yuan/kwh which refers to the electricity price set for Tianwan nuclear power plant, and carbon price is 0. Case 2 sets the electricity price that is liberalized and nuclear power can be included in CDM (unilateral CDM with uncertain carbon price). The initial electricity price is set as 0.45yuan/kwh, and carbon price is 0.12yuan/kwh. See results in table 2.

It can be seen from table 2 that, in Sanmen third-generation nuclear power investment, if the electricity price is set by the government and nuclear power can not join CDM, the value of nuclear power plant is 0 and the investment has been abandoned in all paths. This means, because of high investment cost and uncertainty, under current level of constant electricity price for nuclear power, third-generation nuclear power is not worth investing in China. And if we consider the liberalized electricity price and CDM, the value of nuclear power plant lies between 17979.49 and 18582.92 million yuan, with a mean of 18322.38 million yuan. The percentage of paths abandoned is 0.74%, which is really small. And the CO<sub>2</sub> emission reduction amount is 325.78 million tons CO<sub>2</sub>e. This means under case 2, the investment of third-generation nuclear power is very attractive and with a very small investment risk.

Case 1: Electricity Price Fixed + Without CDM	Seed 1	Seed 2	Seed 3	Seed 4	Seed 5	Average
Nuclear Power Plant Value (Millions RMB)	0	0	0	0	0	0
Percentage of Paths Abandoned	100%	100%	100%	100%	100%	100%
Emission Reduction Amount (Millions tonnes CO <sub>2</sub> e)	0	0	0	0	0	0
Case 2: Electricity Price Uncertain + Unilateral CDM	Seed 1	Seed 2	Seed 3	Seed 4	Seed 5	Average
Nuclear Power Plant Value (Millions RMB)	18297.62	18447.95	18582.92	18303.94	17979.49	18322.38
Percentage of Paths Abandoned	0.72%	0.74%	0.72%	0.52%	1.00%	0.74%
Emission Reduction Amount (Millions tonnes CO <sub>2</sub> e)	325.84	325.91	325.81	326.48	324.85	325.78

Table 2. Nuclear Power Plant Values Results for Different Seeds

In the next, we will further discuss the impacts of three electricity price mechanism, two CDM, and different levels of investment cost on the valuation of third-generation nuclear power investment.

#### 4.1 The impact of three electricity price mechanism

Nuclear power electricity price level is a significant factor in nuclear investment. Our model has introduced three electricity price mechanisms: constant electricity price set by the government, electricity price with constant growth rate, and liberalized electricity price as market-oriented (the price follows stochastic process). This part aims to investigate, under these three electricity price mechanisms, the impact of different level of electricity price on the value of third-generation nuclear power. In constant electricity price mechanism, the price level will increase from 0.45yuan/kwh gradually up to 0.575yuan/kwh. And in constant growth rate and liberalized electricity price mechanism, the initial price level will increase from 0.45yuan/kwh gradually up to 0.575yuan/kwh. See results in figure 3a-3c.

Figure 3a is the trend for the value of third-generation nuclear power changes as electricity price changes. In constant electricity price mechanism, the value of third-generation nuclear power can exceed 0 only when electricity price is 0.575yuan/kwh, and the value is 88.74 million yuan. Compares to 40000 million yuan investment cost for third-generation nuclear power plant, it has very low investment returns. And the electricity price of 0.575yuan/kwh has increased 27.78% than that of Tianwan nuclear power plant, the price level is high. This mean if we wish to make the investment value of third-generation nuclear power exceed 0, the electricity price need to at least increase 30% than that of current price level in Tianwan nuclear power plant.

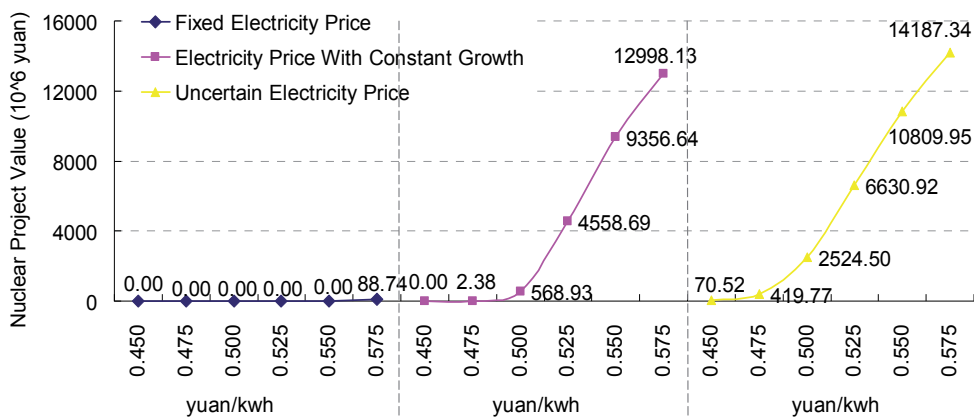


Fig. 3a. Nuclear plant value under 3 electricity price mechanisms

In constant growth rate and liberalized electricity price mechanisms, the value of third-generation nuclear power increases as the initial electricity price level increases. And given the same initial price level, the value in liberalized electricity price mechanism is always higher than that of constant growth rate price mechanism (given the initial electricity price as 0.45yuan/kwh and 0.575yuan/kwh, the value in liberalized electricity price mechanism are 70.52 million yuan and 14187.34 million yuan, which are all larger than 0 and 12998.13 million yuan in that of constant growth rate price mechanism). So in liberalized electricity

price mechanism, future uncertainty in electricity price can indeed increase the value of third-generation nuclear power and make the investment much more attractive.

Figure 3b is the paths abandoned among three electricity price mechanisms. In constant electricity price mechanism, all the paths are abandoned when electricity price level is lower than 0.55yuan/kwh, and the percentage of paths abandoned is 98.8% when the electricity price is 0.55yuan/kwh, which indicates that the investment risk is very high. In constant growth rate and liberalized electricity price mechanisms, the percentage of paths abandoned decreases as the initial electricity price level increases. Take the initial electricity price as 0.45yuan/kwh, the percentage of paths abandoned in constant growth rate and liberalized electricity price mechanisms are 100% and 99.05%. And take the initial electricity price as 0.45yuan/kwh, the percentage of paths abandoned in the two price mechanisms are 0.28% and 2.30%, respectively.

When the initial electricity price is low, the investment risk in constant growth rate mechanism is higher than that of liberalized electricity price mechanism (Take the initial electricity price as 0.475yuan/kwh, the percentage of paths abandoned in constant growth rate price mechanism is 99.93%, which is higher than that of 94.74% in liberalized electricity price mechanism). And when the initial electricity price is high, the investment risk in constant growth rate mechanism is smaller than that of liberalized electricity price mechanism (Take the initial electricity price as 0.55yuan/kwh, the percentage of paths abandoned in constant growth rate price mechanism is 6.55%, which is lower than that of 9.75% in liberalized electricity price mechanism). Though at the same initial price level, the value in liberalized electricity price mechanism is always higher than that of constant growth rate price mechanism, given a higher initial electricity price, the investment risk can be well hedged in constant growth rate price mechanism. This can not happen in liberalized electricity price mechanism because a higher initial electricity price can not fully hedge the uncertainty in future electricity prices. Therefore, the investment risk always exists in liberalized electricity price mechanism.

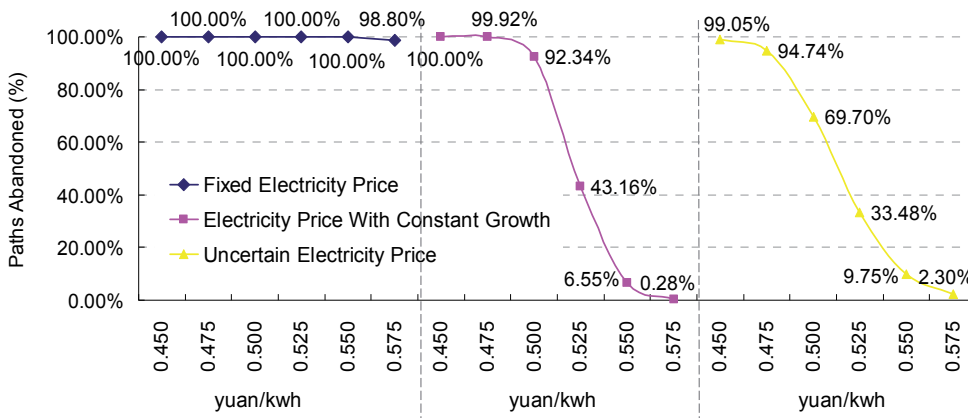


Fig. 3b. Paths abandoned under 3 electricity price mechanisms

Figure 3c is the CO<sub>2</sub> emission reduction amount among three electricity price mechanisms. CO<sub>2</sub> emission reduction amount is negatively correlated to the percentage of paths abandoned. Higher nuclear investment risk will result in lower emission reduction amount. In constant electricity price mechanism, when electricity price level is lower than

0.55yuan/kwh, all the emission reduction amount are all 0 as all the paths are abandoned. When electricity price level is 0.575yuan/kwh, the emission reduction amount is 3.95 million tons CO<sub>2</sub>e as percentage of paths abandoned is 98.8%. In constant growth rate and liberalized electricity price mechanisms, CO<sub>2</sub> emission reduction amount of investing in third-generation nuclear power increases as the initial electricity price level increases.

When the initial electricity price is low, the CO<sub>2</sub> emission reduction amount in constant growth rate mechanism is smaller than that of liberalized electricity price mechanism (Take the initial electricity price as 0.475yuan/kwh, the CO<sub>2</sub> emission reduction amount in constant growth rate price mechanism is 0.26 million tons CO<sub>2</sub>e, which is smaller than that of 17.26 million tons in liberalized electricity price mechanism). And when the initial electricity price is high, the CO<sub>2</sub> emission reduction amount in constant growth rate mechanism is smaller than that of liberalized electricity price mechanism (Take the initial electricity price as 0.55yuan/kwh, the CO<sub>2</sub> emission reduction amount in constant growth rate price mechanism is 306.60 million tons CO<sub>2</sub>e, which is larger than that of 296.19 million tons in liberalized electricity price mechanism). This is mainly because of the changes of investment risks among the two electricity mechanisms.

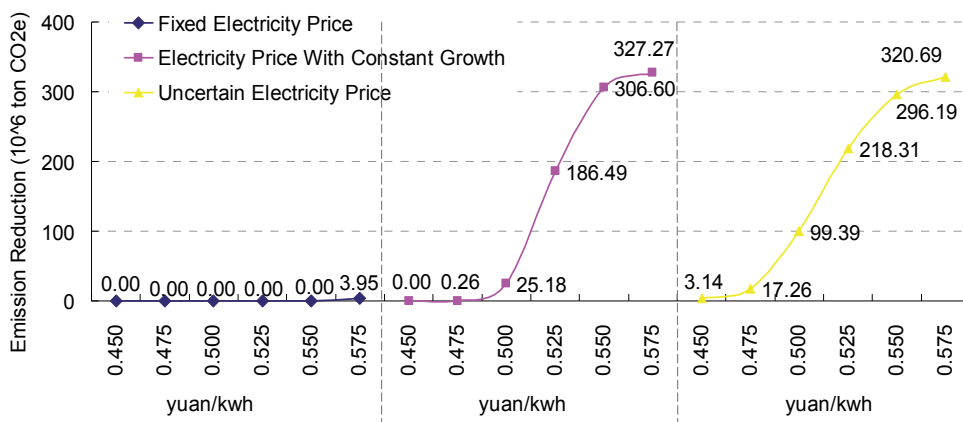


Fig. 3c. Emission reduction amount under 3 electricity price mechanisms

From the results we know that under current domestic constant electricity price level, nuclear power can not be included in CDM, third-generation nuclear power does not worth to invest. And the electricity price need to increase at least 30% than that of current price level in Tianwan nuclear power plant so as to make the investment value of third-generation nuclear power exceed 0. In constant growth rate and liberalized electricity price mechanisms, the value of third-generation nuclear power has increased a lot than that in constant electricity price mechanism. And in liberalized electricity price mechanism, as future uncertainty in electricity price can indeed increase the value of third-generation nuclear power, under this mechanism the value of third-generation nuclear power is the largest, and the investment is the most attractive.

#### 4.2 The impact of two Clean Development Mechanism (CDM)

The nuclear industry is pushing hard to give nuclear power CDM credits. Our model has introduced two forms of CDM, bilateral CDM (constant carbon price) and unilateral CDM (uncertain carbon price). Here we set the electricity price as 0.45yuan/kwh and keep it

constant, the income of nuclear power generation is from two parts, selling electricity plus carbon credit. This part aims to investigate, under two forms of CDM, the impact of different level of carbon price on the value of third-generation nuclear power. In unilateral CDM, the carbon price level will increase from 0 gradually up to 0.125yuan/kwh. And in bilateral CDM, the initial carbon price level will increase from 0 gradually up to 0.125yuan/kwh. See results in figure 4a-4c.

Figure 4a is the trend for the value of third-generation nuclear power changes as carbon price changes. In unilateral CDM, although nuclear power can be included in CDM, the value of third-generation nuclear power still can not exceed 0 when carbon prices are lower than 0.10yuan/kwh. And at the baseline level of carbon price (0.12yuan/kwh) set in our model, the value is only 22.95 million yuan, which is relatively small. In bilateral CDM, at the baseline level of initial carbon price (0.12yuan/kwh), the value of third-generation nuclear power is 7147.07 million yuan, which makes nuclear power more attractive for investment. The value of third-generation nuclear power increases as the initial carbon price level increases, which is similar to that in liberalized electricity price mechanism. But given the same income level, the value in bilateral CDM is much smaller than that in liberalized electricity price mechanism (in bilateral CDM, when the initial income level is  $0.45+0.10=0.55$ yuan/kwh, the value is 2444.34 million yuan, which is much smaller than that of 10809.95 million yuan in liberalized electricity price mechanism with initial electricity price is 0.55yuan/kwh).

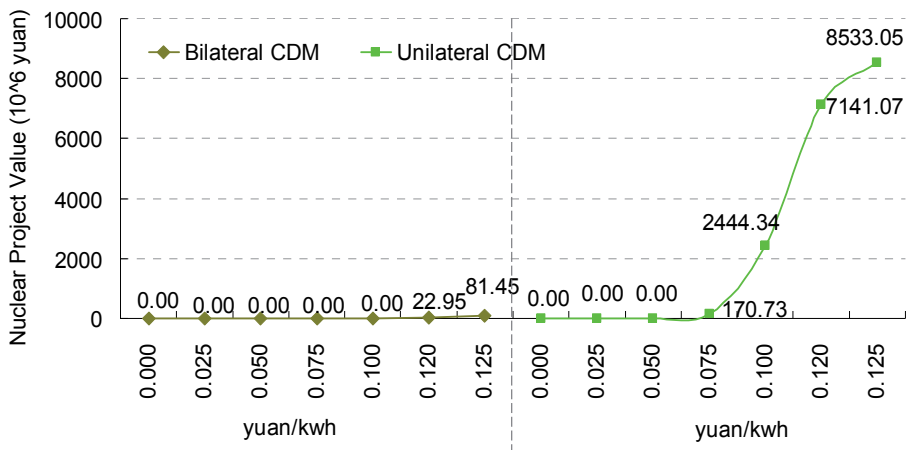


Fig. 4a. Nuclear plant value under 2 CDM mechanisms

Figure 4b presents the paths abandoned among two forms of CDM. In unilateral CDM, the investment risk of third-generation nuclear power is very large. In bilateral CDM, the percentage of paths abandoned decreases as the initial carbon price level increases, which is similar to that in liberalized electricity price mechanism. However, provided in given the same income level, the paths abandoned in bilateral CDM is much larger than that in liberalized electricity price mechanism (in bilateral CDM, when the initial income levels are  $0.45+0.075=0.525$ yuan/kwh and  $0.45+0.125=0.575$ yuan/kwh, the percentage of paths abandoned are 97.72% and 16.40%, which are much larger than that of 33.48% and 2.30% in liberalized electricity price mechanism with initial electricity prices are 0.525yuan/kwh and



0.575yuan/kwh, respectively). This means at the same initial income level, the investment risk in bilateral CDM is always larger than that in liberalized electricity price mechanism.

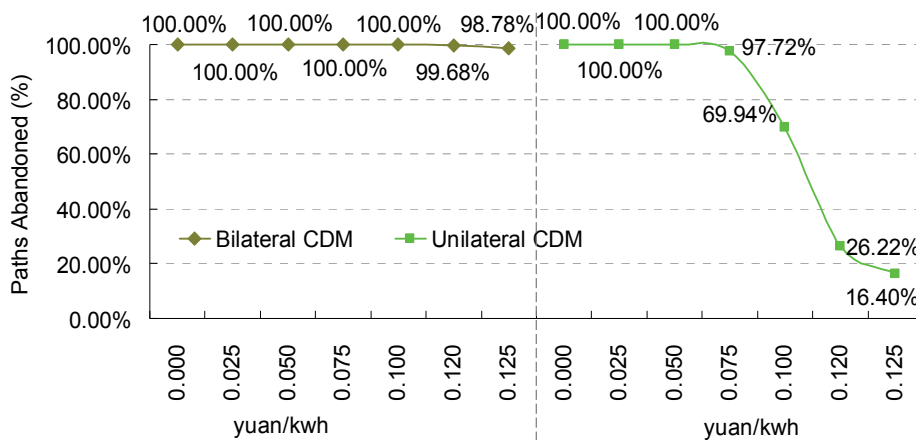


Fig. 4b. Paths abandoned under 2 CDM mechanisms

Figure 4c is the CO2 emission reduction amount among two forms of CDM. In unilateral CDM, the emission reduction amounts are 0 or relatively small because most of the paths are all abandoned. In bilateral CDM, the emission reduction amount increases as the initial carbon price level increases. As given the same initial income level, because the investment risk in bilateral CDM is always larger than that in liberalized electricity price mechanism, so the emission reduction amount in bilateral CDM is always smaller than that in liberalized electricity price mechanism (given the same initial income level as 0.55yuan/kwh, the emission reduction amount in bilateral CDM is 98.70 million tons CO<sub>2</sub>e, which is smaller than that of 296.19 million tons CO<sub>2</sub>e in liberalized electricity price mechanism).

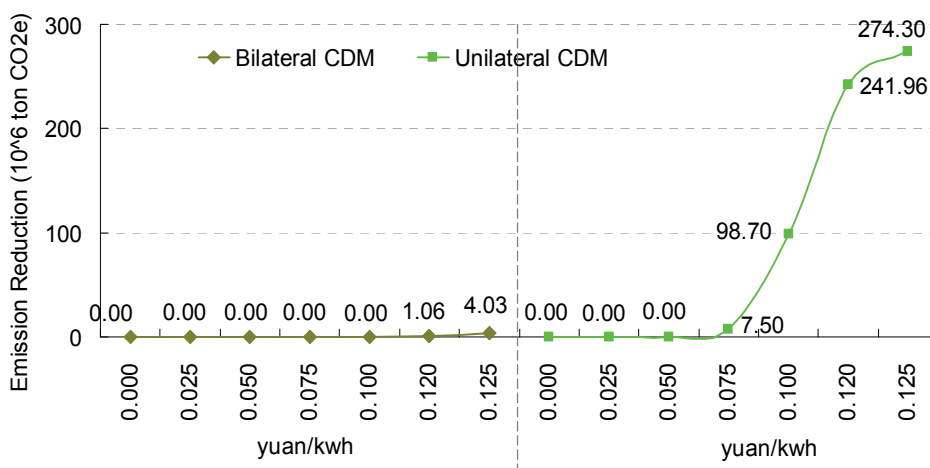


Fig. 4c. Emission reduction amount under 2 CDM mechanisms

From the results we can see that when the carbon price level is low, neither unilateral CDM nor bilateral CDM can increase the attraction of third-generation nuclear power investment. At the baseline carbon price level (0.12yuan/kwh), the carbon credit income in both unilateral CDM and bilateral CDM can increase the value of nuclear power on the basis of constant electricity price (0.45yuan/kwh). And the value will be higher in bilateral CDM. Therefore, if the nuclear power can be included in CDM, we would advise the power generation enterprise to take more efforts in bilateral CDM, but not conservative follow bilateral CDM which is more common for domestic carbon credit sellers. As a result, it can obtain more benefits from carbon credits.

#### 4.3 The impact of different levels of nuclear investment cost

Based on the data from Sanmen third-generation nuclear power plant, the total investment cost is 40000 million yuan with installed capacity of 2500MW (2\*1250MW). And the average unit investment cost is 16000yuan/kw, which is relatively high. High investment cost of third-generation nuclear power will result in great investment risk. This part aims to investigate the impact of investment cost reduction on the valuation of third-generation nuclear power. Here also set the electricity price as 0.45yuan/kwh and remain constant, and nuclear power can not be included in CDM. The investment cost will decrease from 40000 million yuan (16000yuan/kw) gradually down to 25000 million yuan (10000yuan/kw). And 10000yuan/kw is equal to the unit investment cost of domestic second-generation nuclear power plant. See results in figure 5a-5c.

Figure 5a is the trend for the value of third-generation nuclear power changes as investment cost changes. The impact of marginal investment cost reduction on the value of nuclear power shows 'increased first and then decreased' (as total investment cost decrease from 37500 million yuan to 35000 million yuan, the increment of nuclear power value is 2250.96 million yuan; as total investment cost decrease from 35000 million yuan to 32500 million yuan, the increment of nuclear power value is 2700.83 million yuan; as total investment cost decrease from 27500 million yuan to 25000 million yuan, the increment of nuclear power value is 1928.53 million yuan). Consequently, the contribution to nuclear power value from marginal investment cost reduction will decrease when the total investment cost is less than 32500 million yuan.

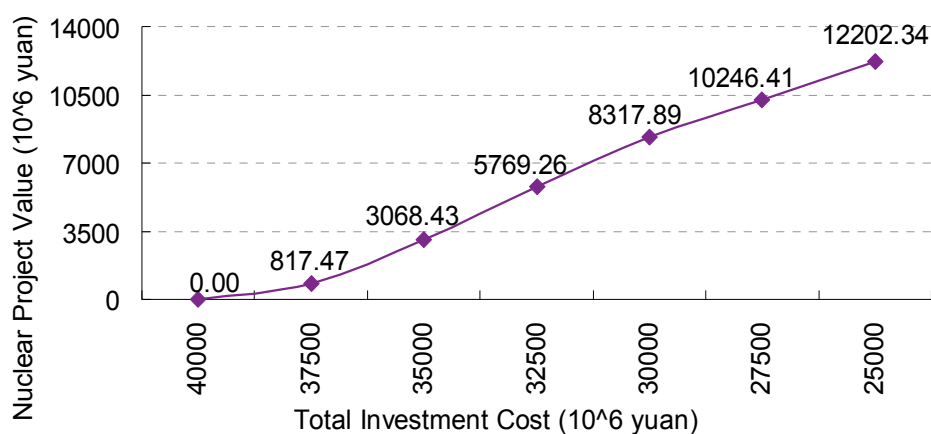


Fig. 5a. Nuclear plant value under different total investment cost

Figure 5b is the trend for the percentage of paths abandoned changes as investment cost changes. The percentage of paths abandoned decreases as third-generation nuclear power investment cost decreases and total investment cost reduction can reduce the investment risk effectively. The percentages of paths abandoned are all less than 5% when total investment cost falls below the level of 30000 million yuan. And as the total investment cost decreased to 25000 million yuan, the percentages of paths abandoned is only 0.26%, the investment risk is very small. The marginal investment risk reduction also shows 'increased first and then decreased' as investment cost decreases, and the contribution to nuclear power investment risk reduction from marginal investment cost reduction decreases when total investment cost falls below 32500 million yuan.

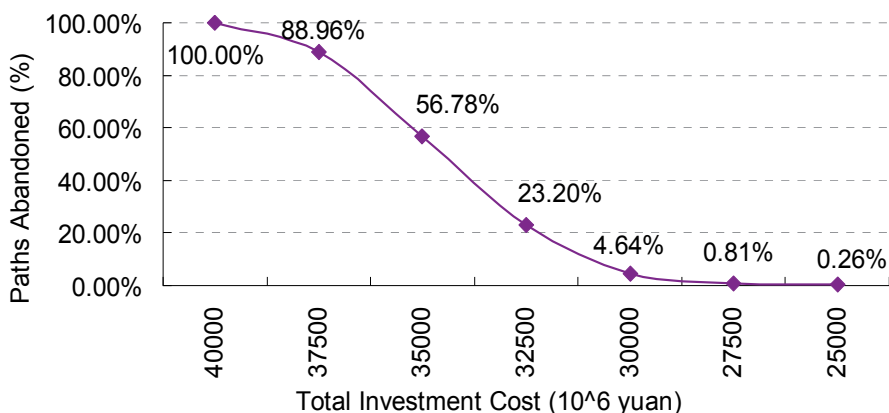


Fig. 5b. Paths abandoned under different total investment cost

Figure 5c is the trend for the CO<sub>2</sub> emission reduction amount as investment cost changes. The emission reduction amount increases and the marginal CO<sub>2</sub> emission reduction amount also shows 'increased first and then decreased' as third-generation nuclear power investment cost decreases. When the total investment cost falls below 30000 million yuan, the CO<sub>2</sub> emission reduction amounts are all larger than 310 million tons CO<sub>2</sub>e, the changes in marginal CO<sub>2</sub> emission reduction amounts are very tiny.

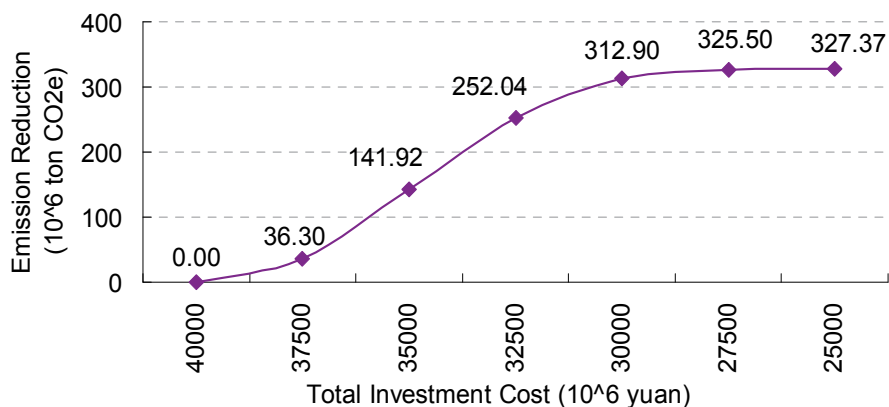


Fig. 5c. Emission reduction amount under different total investment cost

From the results we are informed that under baseline constant electricity price as 0.45yuan/kwh, changes in investment cost have significant impact on the value of third-generation nuclear power. If the total investment cost falls below 30000 million yuan which investment cost per unit is 12000yuan/kw, the investment risk is lower than 5%, implying that the investment is more viable. At this case the investment cost per unit is 1.2 times to that of average unit cost of domestic second-generation nuclear power plant.

## 5. Conclusions and further work

This paper applies real options theory with Monte Carlo method to establish a nuclear power investment evaluation model, incorporating the world's first third-generation nuclear power project-Sanmen nuclear power plant in Zhejiang province to evaluate the value of third-generation nuclear power plant in China. With several technical and economic uncertainty factors (deployment cost, generating cost and nuclear accident) considered in the model, we have investigated the impacts of three electricity price mechanisms, two forms of CDM, and investment cost reduction on the value of Sanmen third-generation nuclear power plant. Based on the result analysis, a couple of conclusions are drawn as follows:

1. Under constant electricity price mechanism, third-generation nuclear power is worth investment if the price refers to the electricity price in Tianwan nuclear power plant. And the electricity price need to at least increase 30% than current price level in Tianwan nuclear power plant so it can make third-generation nuclear power worth to invest. It should be noticed that in liberalized electricity price mechanism, the investment of third-generation nuclear power is more attractive than the other two price mechanisms among all electricity price levels. So the electricity price marketization will be a preferred option to promote the investment in third-generation nuclear power under current investment cost level.
2. Currently nuclear power can not be included in CDM. If the CDM can give nuclear power credit, the selling of carbon credit can increase the income of nuclear power plant, and this will also promote the investment in third-generation nuclear power. Considering the current electricity price is set by the government and remains constant, at baseline carbon price level, CDM has provided another option for power generation enterprise to compensate for the large investment cost of third-generation nuclear power. Based on the comparison between bilateral CDM and unilateral CDM, we would advise the power generation enterprise to take more efforts in bilateral CDM to obtain more benefits from carbon credits.
3. As the world's first third-generation nuclear power project, currently the investment cost of Sanmen nuclear power plant is relatively high. As the value of nuclear power is sensitive to investment cost, under current constant electricity price mechanism, the investment in third-generation nuclear power will be more viable if the total investment cost can be reduced to 1.2 times to that of domestic second-generation nuclear power plant.

Third-generation nuclear power is an advanced generating technology with large uncertainties. Our model still has limitations. Firstly, some data, especially nuclear accidents data in the model, are estimated in this research owing to shortage of actual data supporting. Secondly, the model does not consider any flexibility during the nuclear power operating period and we only consider the abandon option in Sanmen nuclear power plant

first phase project. Actually, the power generation enterprises can decide whether to invest in second phase project based on the judgment of electricity market of nuclear power operation status. As a consequence, taking compound option during nuclear power operational period into our model is one of the most important directions for model improvements. The forementioned issues require emphasizing in future work.

## 6. Acknowledgement

Support from the National Natural Science Foundation of China under Grant No. 70825001 is greatly acknowledged.

## 7. References

- [1] Held, H. et. al. 2008. Efficient climate policies under technology and climate uncertainty. *Energy Economics*, doi:10.1016/j.eneco.2008.12.012.
- [2] Myers, S.C., Turnbull, S.M. 1977. Capital Budgeting and the Capital Asset Pricing Model: Good News and Bad News. *The Journal of Finance*, 32(2): 321-333.
- [3] Ross, S. 1978. A simple approach to the valuation of risky streams. *Journal of Business*, 51(3): 453-475.
- [4] McDonald, R., Siegel, D. 1986. The Value of Waiting to Invest. *Quarterly J. Economics*, 101(4): 707-728.
- [5] Brennan, M.J., Schwartz, E.S. 1985. Evaluating Natural Resource Investments. *J. Business* 58: 135-157.
- [6] Paddock, J.L., Siegel, D.R., Smith, J.L. 1988. Option valuation of claims on real assets: the case of offshore petroleum leases. *Quarterly J. Economics* 103: 479-508.
- [7] Smith, J.E., Nau, R.F. 1995. Valuing Risky Projects: Option Pricing Theory and Decision Analysis. *Management Science*, 41 (5): 795-816.
- [8] Smith, J.E., McCardle, K.F. 1996. Valuing oil properties: integrating option pricing and decision analysis approaches. *Operations Research* 46: 198-217.
- [9] Fan, Y., Zhu, L. 2010. A Real Options Based Study on Overseas Oil Investment and its application in China's Oversea Oil Investment. *Energy Economics*. 32, 627-637.
- [10] Venetsanos, K. et. al. 2002. Renewable energy sources project appraisal under uncertainty: the case of wind energy exploitation within a changing energy market environment. *Energy Policy*, 30(4): 293-307.
- [11] Davis, G., Owens, B. 2003. Optimizing the level of renewable electric R&D expenditures using real options analysis. *Energy Policy*, 31(15): 1589-1608.
- [12] Siddiqui, A.S. et. al. 2007. Real options valuation of US federal renewable energy research, development, demonstration, and deployment. *Energy Policy*, 35(1): 265-279.
- [13] Fuss, S. et. al. 2009. Impact of climate policy uncertainty on the adoption of electricity generating technologies. *Energy Policy*, 37(2): 733-743.
- [14] Blyth, W., Yang, M. 2007. Modeling Investment Risks and Uncertainties with Real Options Approach. Working Paper LTO/2007/WP 01, IEA, Paris.
- [15] Kumbaroğlu, G. et. al. 2008. A real options evaluation model for the diffusion prospects of new renewable power generation. *Energy Economics*, 30(4): 1882-1908.
- [16] Abadie, L.M., Chamorro, J.M.. 2008a. Valuing flexibility: The case of an Integrated Gasification Combined Cycle power plant. *Energy Economics*, 30: 1850-1881.
- [17] Maribu, K.M. et. al. 2007. Distributed energy resources market diffusion model. *Energy Policy*, 35: 4471-4484.

- [18] Siddiqui, A.S., Marnay, C. 2008. Distributed generation investment by a microgrid under uncertainty. *Energy*, 33: 1729-1737.
- [19] Siddiqui, A.S., Maribu, K. 2009. Investment and upgrade in distributed generation under uncertainty. *Energy Economics*, 31: 25-37.
- [20] Abadie, L.M., Chamorro, J.M. 2008b. European CO<sub>2</sub> prices and carbon capture investments. *Energy Economics*, 30: 2992-3015.
- [21] Fuss, S. 2008. Investment under market and climate policy uncertainty. *Applied Energy*, 85: 708-721.
- [22] Fleten, S.E., Näsäkkälä, E. 2009. Gas-fired power plants: Investment timing, operating flexibility and CO<sub>2</sub> capture. *Energy Economics*, doi:10.1016/j.eneco.2009.08.003.
- [23] Heydari et.al, 2010. Real options analysis of investment in carbon capture and sequestration technology. *Computational Management Science*, doi: 10.1007/s10287-010-0124-5.
- [24] Zhou, W. et.al. 2010. Uncertainty modeling of CCS investment strategy in China's power sector. *Applied Energy*, 87: 2392-2400.
- [25] Schwartz, E.S. 2004. Patents and R&D as Real Options. *Economic Notes by Banca Monte dei Paschi di Siena SpA*, 33: 23-54.
- [26] Dixit, A. K. and R. S. Pindyck. 1994. *Investment Under Uncertainty*. Princeton University Press, Princeton, NJ.
- [27] Majd, S., R. S. Pindyck. 1987. Time to build, option value, and investment decisions. *Journal of Financial Economics*. 18 (1): 7-27.
- [28] Bar-Ilan, A., Strange, W.C. 1996. Investment Lags. *The American Economic Review*. 86 (3): 610-622.
- [29] Aguerrevere, F.L. 2003. Equilibrium Investment Strategies and Output Price Behavior: A Real-Options Approach. *Review of Financial Studies*. 16 (4): 1239-1272.
- [30] Pindyck, R.S. 1999. The long-run evolution of energy prices. MIT-CEEPR working papers. <http://mit.dspace.org/handle/1721.1/45087>
- [31] Longstaff, F.A., Schwartz, E.S. 2001. Valuing American Options by Simulation: A Simple Least Square Approach. *The Review of Financial Studies*. 14(1): 113-147.
- [32] Zhu, L., Fan, Y. 2010. Optimization of China's Generating Portfolio and Policy Implications Based on Portfolio Theory. *Energy*. 35: 1391-1402.
- [33] Fan, Y. et.al. 2010. An analysis on Carbon Capture and Storage Technology, Regulations and Its Emission Reduction Potential. *Advances in Climate Change Research*. 5: 362-369. (In Chinese)
- [34] Pindyck, R.S. 1993. Investments of Uncertain Cost. *Journal of Financial Economics*. 34: 53-76.
- [35] Gollier, C. et.al, 2005. Choice of nuclear power investments under price uncertainty: Valuing modularity. *Energy Economics*. 27: 667-685.
- [36] Kessides, I.N..2010. Nuclear power: Understanding the economic risks and uncertainties. *Energy Policy*. 38: 3849-3864.
- [37] International Energy Agency (IEA). 2007. *World Energy Outlook 2007*. OECD/IEA. Paris.
- [38] International Energy Agency (IEA). 2009. *CO<sub>2</sub> Emissions from Fuel Combustion*. Paris.

# Characteristic Evaluation and Scenario Study on Fast Reactor Cycle in Japan

Hiroki Shiotani, Kiyoshi Ono and Takashi Namba  
*Japan Atomic Energy Agency (JAEA)*  
*Japan*

## 1. Introduction

Today, Japanese nuclear energy faces a period of great change. After the start up of plutonium recycling in LWR (light water reactor) and groundbreaking of MOX (Mixed OXide) fuel fabrication plant (J-MOX), Rokkasho reprocessing plant is preparing its operation. Regarding Gen IV nuclear energy system, a joint team of Japan Atomic Energy Agency (JAEA) and the Japan Atomic Power Company (JAPC) and related parties has been conducting Fast Reactor Cycle Technology Development Project (FaCT Project) since 2006. It has been a Japanese political choice to take a step toward Fast Reactor (FR) commercialization in the middle of this century. It will be reviewed by the government of Japan in response to the recent accident at Fukushima Daiichi Nuclear Power Station. In FaCT project, besides the facility design studies and element technology development, the characteristic evaluations and scenario studies have been conducted including the methodology development to confirm and give suggestions on basic directions of the research and development (R&D).

## 2. FaCT project and evaluation tool

In this section, the outline of FaCT project is described including the background Japanese nuclear policies firstly. Then, a new evaluation code developed for FaCT project is described as the basic infrastructure for the strategic studies and evaluations in future Japanese nuclear fuel cycle.

### 2.1 Outline of FaCT project

FR cycle technology is capable of reprocessing spent fuels and utilizing recovered plutonium and uranium as new fuels effectively. It also has the potential to provide Japan with long-term stable energy supply and contribute to reducing the potential harmfulness of radioactive waste. Therefore, with the aim of putting FR cycle technology into practice at an early stage, JAEA, in cooperation with electric utilities, is working on FaCT project which mainly targets a combination of the Sodium-cooled FR with oxide fuel, advanced aqueous reprocessing, and the simplified pelletizing fuel fabrication since 2006. In 2010, taking the transitional period from LWR cycle to FR cycle into consideration, we reviewed and revised the procedures of R&D on reprocessing technology deployment from 2011 onward. Outline of FaCT project is shown in Figure. 1.

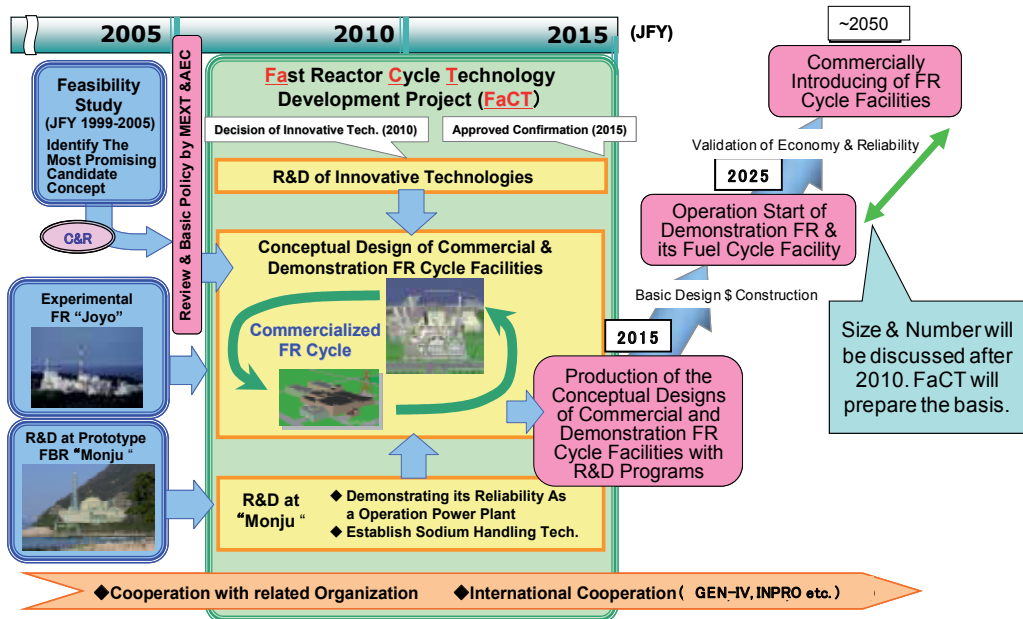


Fig. 1. Outline of FaCT project

The national policy guidelines such as "Energy Basic Plan" articulates that R&D on FR cycle technology should be promoted aiming for the start-up of demonstration FR around 2025 and its introduction on a commercial basis before 2050. Based on these national policies, in 2015, FaCT project aims to present conceptual designs of both commercial and demonstration facilities of FR cycle, which has capability to acquire the feature that next-generation nuclear energy system must fulfill from the viewpoints of safety, economics, environmental impact, resource utilization efficiency and proliferation resistance, and R&D plan towards its commercialization. In order to put those commercial and demonstration facilities in practice, promoting introduction of innovative technology, FaCT project is conducting element technology development and its subsequent design studies which are identified with 13 R&D issues (or 10 techniques regrouped for adoption judgment) on reactor system and 6 R&D issues on reprocessing system and fuel fabrication system respectively. In 2010, the last year of FaCT project phase 1 starting 2006, we carried out the adoption judgment of innovative technologies and the performance criteria assessment of FR cycle system, which reflect the results of the adoption judgment, toward the performance target. These results are being assessed by the Ministry of Education, Culture, Sports, and Technology (MEXT) and the Ministry of Economy, Trade and Industry (METI). Although the future FaCT plan will be reconsidered due to the accident at Fukushima Dai-ichi nuclear power station, we will progress steadily to realize the commercialization of FR and its fuel cycle in around 2050 while enhancing the safety and reliability of the FR cycle concept. Meanwhile, we are also conducting R&D on metal fuel cycle as secondary concept, and plan to carry out from 2011 onward with the international cooperation.

## 2.2 Typical Japanese FR deployment scenario

World's energy consumption is increasing with economic growth and it is expected for nuclear energy to play an important role worldwide to secure the stable energy supply and



to prevent global warming (reduction of greenhouse gas emission) aiming at realization of sustainable growth. The level 7 accident of International Nuclear Event Scale (INES) occurred at the Fukushima Dai-ichi Nuclear Power Station by the massive earthquake in March 11, 2011 in Japan and some countries began to revalidate nuclear plant safety and conduct a review of their nuclear policies. However, in the U.S., large number of nuclear power plants are planned to be built for the first time in 30 years. In India and China, which maintain high rates of economic growth, it is planned to build additional nuclear power plants to raise the entire nuclear capacity up to about 290GWe and 250GWe, respectively by 2050. In Long-term forecasts conducted by major international agencies concerning energy, such as WEO 2009, ETP2008 and ETP2010 by OECD and IEA, it is projected that nuclear energy will expand in the long-term as a countermeasure against global warming with posing scenarios where conventional measure that only focused on controlling global warming will be replaced by the measure that promotes nuclear energy utilization while limiting greenhouse effect gas emission intensively.

Meanwhile, in ‘Basic Energy Plan’ decided by the Japanese Cabinet in June, 2010, it is planned to build at least 14 additional nuclear power plants by 2030, domestic nuclear power plant capacity of about 48.8GWe will rise to about 68GWe. Furthermore, Japan aims at introducing FR cycle on a commercial basis before 2050 as stated in ‘Framework for Nuclear Energy Policy’ decided by the Cabinet in October, 2005 and in ‘Nuclear Energy Nation Plan’ approved by the Atomic Energy Commission in March, 2006. The ‘Basic Energy Plan’ will be reviewed in response to the Fukushima Dai-ich accident. An example of trial calculation is shown in Figure 2, it demonstrates the transition of the nuclear energy composition when FRs (combination of high breeding core with breeding ratio of 1.2 and low breeding core with breeding ratio of 1.03) featured in the FaCT project, are introduced in 2050. Before FR deployment, plutonium recovered from LWR reprocessing plants will be recycled mainly in LWR, and its LWR capacity will be about 10-20GWe. From 2050 onward, if the LWRs with life time of 60 years are replaced by FRs one by one, it takes minimum 60 years for the complete transition from LWR to FR. Or, if the deployment pace of FR becomes slow and it makes the coexistence period of LWR and FR longer, FR cycle can be flexible to deal with the transition from LWR to FR by adjusting FR breeding performance and/or reprocessing plan by itself.

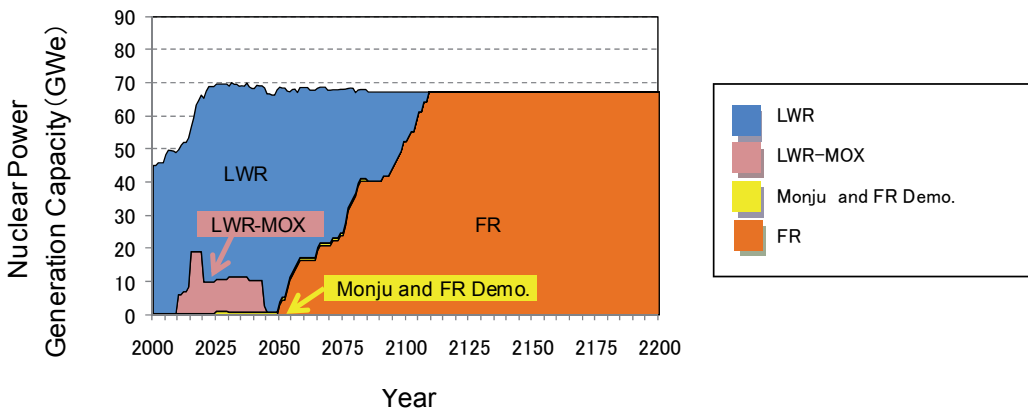


Fig. 2. Long term framework for nuclear energy in Japan (FR deployment in 2050)

Currently, Japan poses basic nuclear scenario where current LWR cycle transitions completely to FR cycle and it is detailed as follows: 1) the period of LWR existence only, 2) the transition period from LWR to FR, and 3) the equilibrium period of FR existence only. Evaluation of equilibrium cycle is targeted to the third, 'FR equilibrium period'. As the 'FR equilibrium period', when only FR cycle and its fuel cycle exist, continues for long period of time, plutonium composition in new fuels and spent fuels of FR, high-level radioactive waste, and economics will converge to a certain equilibrium value and end up being simple phase, that is 'the state of multiple equilibrium cycle'.

### **2.3 Performance evaluation tool both for equilibrium and transient nuclear fuel cycle system**

Regarding the evaluation methodology to seize the comprehensive characteristics of nuclear energy (typically LWR cycle to FR cycle), the methodology is aimed at: 1) performing comprehensive evaluation of nuclear energy business based on both transient period and equilibrium period using the systematically structured data model of nuclear facilities; 2) being a fundamental deliberation evaluation tool providing various information on R&D and design study of nuclear energy system in the future. Evaluating dynamic nuclear energy system in the transient period as well as FR cycle in equilibrium status, we employ time-series evaluation method mainly dealing cash-flow or mass-flow regarding atomic energy directly to reflect transition of target nuclear energy system.

From the view point of economic evaluation, a large-scale calculation system is required because it is necessary to express cash-flow or mass-flow of every facility, such as nuclear power reactor, fuel fabrication facility, reprocessing facility, waste disposal facility, etc. in the life cycle consisting of construction, operation and decommissioning and to calculate the amount of waste or cash-flow from nuclear system overall through adding up those cash-flows or mass-flows.

With the knowledge of management engineering, this method was built based on the concept of supply-chain management (SCM) for nuclear fuel cycle with the consideration of business risk of nuclear fuel cycle which was carried out at the first stage of FS phase II. Using the calculation tool employing time-series multi-dimensional evaluation method basically developed in the final evaluation of FS phase II, we started development of the system intensively and obtained sufficient functions to coordinate evaluation and review the design of FaCT project. Thus the SCM code is at present developed as both performance criteria evaluation tool and detailed transition period evaluation tool.

This method is network-flow type dynamic analysis model to simulate overall nuclear energy business by forming nuclear facilities which makes up nuclear energy system. Object-oriented design and analysis technique was used to enhance the system flexibility and extendibility of the code. It covers almost all the facilities in Japan from the beginning of the nuclear energy utilization and FR cycle equilibrium state in future. It can conduct burnup calculation of nuclear fuel in nuclear power plants as well as decay calculation of nuclear material in fuel cycle facilities including actinides, fission products, and other nuclides although it only uses the ORIGEN-2 code with the libraries based on JENDL-3.3. Although the evaluation started at the present in the figure, it should be started the calculation at the beginning of the use of nuclear energy. With the capability described above, it enables to evaluate both the amounts and compositions of materials/wastes. Furthermore it can assess cost (economic efficiency) at all facilities in Japanese FR deployment scenario (installed capacity) shown as Figure 2.

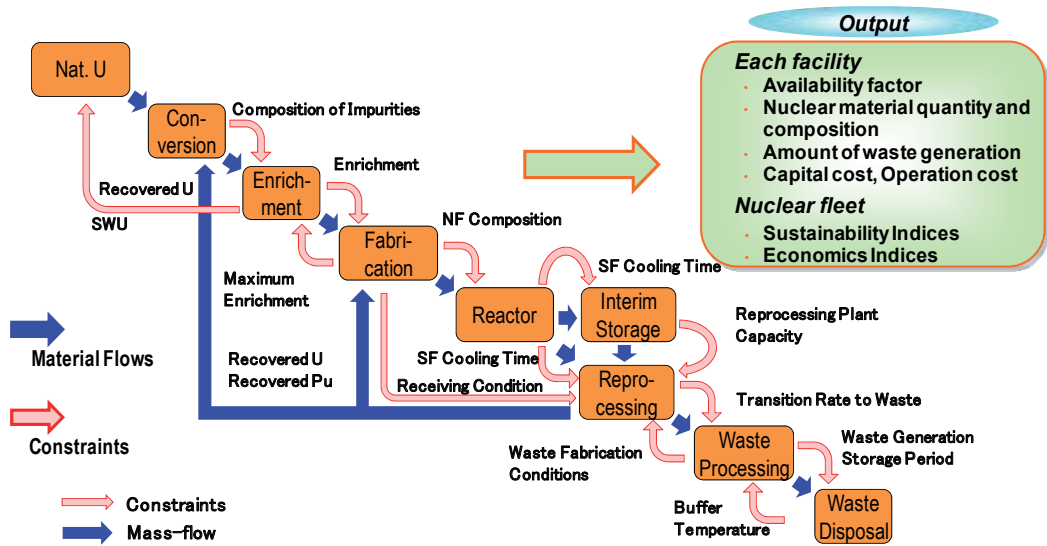


Fig. 3. Nuclear supply chain and SCM code

Figure 3 shows the relationship between the facilities in nuclear fleet. For example, the effects from the differences of breeding ratio of FR, reprocessing plant, and Am-Cm recycling on characteristics from developmental targets influences the material flow from reprocessing plant. With the object oriented design feature and mechanism that conveys information and materials via the interface among highly independent facilities, it is easy to place improvements on a facility by itself according to needs. Furthermore, the SCM code enabled us to simulate nuclear fuel cycle overall in the process of procurement, dispose and transportation of material from the upper to lower facilities without any major change with facility data that indicates basic characteristics of nuclear facilities according to the provided schemes and scenarios as the assumption of analyses by user in timely manners.

### 3. Characteristics evaluation of equilibrium FR cycle and scenario evaluation

In this section, evaluation on Japanese nuclear fleet in FaCT project is described mainly by SCM code. It covers almost all the facilities in Japan from the beginning of the nuclear energy utilization and FR cycle equilibrium state in far future.

#### 3.1 Characteristics evaluation of equilibrium FR cycle

The characteristics evaluations on FR cycle in equilibrium status related to the development target of FaCT project, which are, economics, environment reservation, radioactive waste management, uranium resource utilization efficiency, and proliferation resistance. The recent results of the design studies of FR cycle reflected in the evaluations. In those evaluations, single reactor and related fuel cycle were supposed to be evaluated.

##### 3.1.1 Evaluation method of equilibrium cycle

The characteristics of system will be defined more clearly in its equilibrium state because FR cycle is closed cycle which has limited mutual actions with outside. That means evaluation

of equilibrium cycle is suitable method for conducting comparative evaluations on candidate concepts having different characters with common manner. Furthermore, it requires few preconditions aside from design result of FR cycle since mutual actions (mass balance) with outside of FR cycle are small. Therefore, it will be relatively easy to apply strict methods to evaluate and lessen the uncertainty which affect the characteristics of FR cycle. In mass balance calculation, more sophisticated methods than those used in time-series evaluation are applied and its calculation result is stable. The flexibility of SCM code enabled us to treat FR cycle in equilibrium state and mixture of LWR cycle and FR cycle transient state with unified manner in the same code. We are conducting the evaluations of accumulative natural uranium demand, waste generation and economics for 'the state of multiple equilibrium cycle'.

### 3.1.2 Accumulative natural uranium demand

Although the analysis for cumulative natural uranium demand treats a transient characteristic of nuclear fleet, natural uranium demand evaluation result is written here because it is raised as one of the essential characteristics of FR cycle system. Figure 4 shows Japan's accumulative natural uranium demand of some scenarios, such as 'LWR once through', 'Pu recycling in LWR' and 'FR deployments' in 2040, 2050 and 2060. In the cases of LWR once through and Pu recycling in LWR, accumulative natural uranium demand in the period of 2007 through 2120 will be about 1.5 million tons and 1.15 million tons, respectively. In addition, if FRs with breeding ratio of 1.1 or 1.2 are deployed starting in 2050, all LWRs will be replaced to FRs completely around 2130, enabling accumulative uranium demand to be saturated at about 0.8 million tons level which accounts for 5% of conventional uranium resources (total about 16.7 million tons). Consequently, there will be no need to import natural uranium from other countries. In the case of 'LWR once through' and 'Pu recycling in LWR', it will be required to procure large quantities of uranium even after the late 21<sup>st</sup> century in which fears over depletion of uranium resource will be foreseen worldwide. On the other hand, in 'deployment of FR' case, it will be unnecessary to import uranium and will lead to an enhancing of energy security.

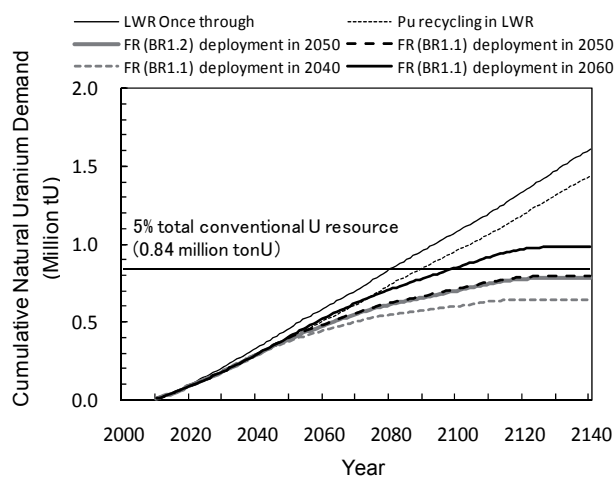


Fig. 4. Accumulative uranium demand in Japan

### 3.1.3 Waste generation

Nuclear energy supply chain is complicated and great deal of radioactive waste is handled in it, thus sufficient safety measure and waste management should be established at the nuclear facilities to prevent from influencing surrounding environment and residents. In particular, we have to address the challenges to treat and dispose HLW generated in reprocessing plant safely. Figure 5 indicates the amount of HLW unit of electricity generated and usable years of final disposal site. In current LWR cycle, HLW, namely vitrified wastes are produced with the amount of 30 canisters during the operation of LWR with 1GWe for a year. While, in the future FR cycle case, it reduces the amount of vitrified waste by 20% compared with the current LWR cycle because of high thermal efficiency of FR and reduction of pyrogenic FP production. By reflecting foundational R&D result concerning FP recycle in addition to the minor actinides recycle, it has possibility to achieve drastic reduction of HLW and longer-use of disposal site. Figure 6 shows chronological changes of potential harmfulness (relative values) of HLW (spent fuel (SF) and vitrified waste) in the same amount of electricity generated for each case. After 1000 years later from being discharged from nuclear reactor, in the vitrified waste produced from 'Pu recycling in LWR' case in which most of uranium and plutonium are recycled, potential harmfulness will be reduced to 1/8 of that of spent fuel which is disposed directly in 'LWR once through' case. Moreover, in FR cycle, minor actinides are also recycled in addition to uranium and plutonium, enabling the potential harmfulness to be reduced to 1/30. Meanwhile, the potential harmfulness of HLWs generated in each case are compared with the potential harmfulness of natural uranium required to produce the same amount of electricity generated as each case, which is indicated by the red dashed horizontal line in Figure 6. It will take 100,000 years for the potential harmfulness of direct disposed spent fuel to reduce to the same level with that from natural uranium, 10,000 years for the vitrified waste from LWR cycle, and a couple of hundred years for the vitrified waste from FR cycle. Recycling minor actinides in FR cycle enables us to reduce the potential harmfulness and environmental burdens caused by HLW.

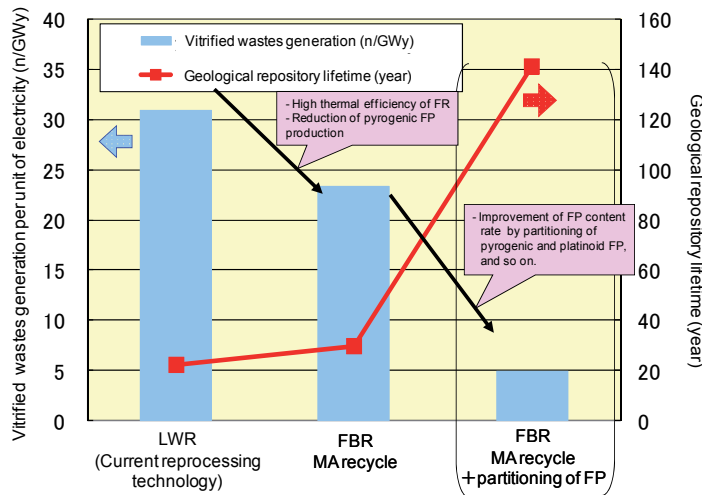


Fig. 5. HLW generation and usable years of final disposal site in Japan

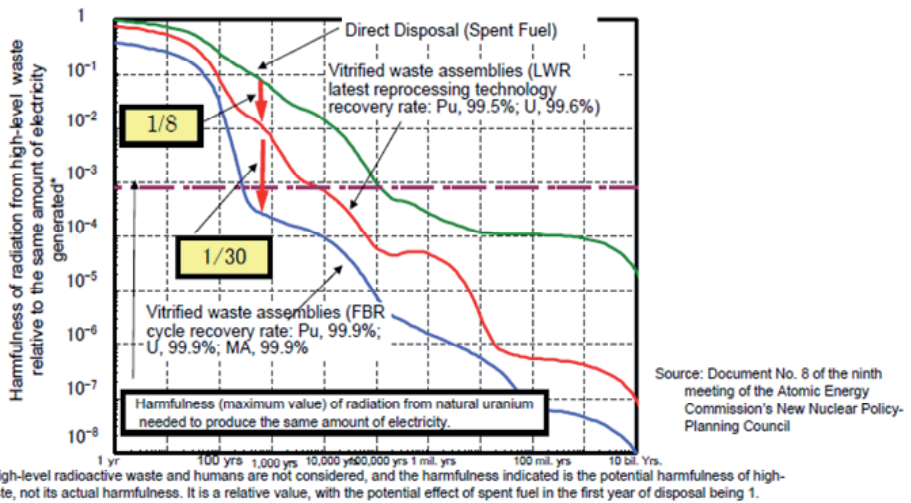


Fig. 6. Harmfulness of HLW (spent fuel and vitrified waste)

**3.1.4 Economics**

We are aiming at economics improvement due to a reduction of amount of material by adoption of innovative technologies toward commercialization before 2050 since FR cycle should be competitive in economy to become basic electric source in the future. Figure 7 shows estimation of the generation costs of current LWR, future LWR and Future FR (breeding ratio of 1.1). The generation cost of future LWR will reduce to 60% of that of current LWR by improvement of capacity factor and reduction in unit construction cost of reactor. If FR (NOAK) provides superior performance as designed, it will be able to compete with future LWR economically by the effect of high thermal efficiency and adoption of high burn-up fuel, although the unit construction cost of reactor may be little higher. The total cost consists of capital cost, operating cost and fuel cost accounting for about a third each. As regard to FR, considering the effect of drop down of capacity factor and increase of the unit fuel cycle cost posed by adoption of alternate technologies on the power generation cost, the power generation cost will be almost the same level as that of current LWR. However, it would appear that the FR cycle compete with the future LWR cycle economically.

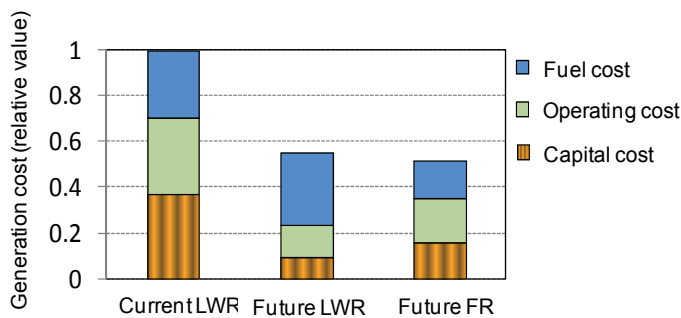


Fig. 7. Comparison of the generation costs between LWR and FR (relative value)



### 3.1.5 Nuclear proliferation resistance

As nuclear materials are used as fuels in nuclear energy, we must sweep away the concerns over nuclear proliferation. Japan has been applied comprehensive safeguards including supplementary protocols and becomes an international model country. In addition, toward a commercialization of FR cycle, it is making effort to lead the future nuclear non-proliferation models by concept study for the process in which uranium will be constantly accompanied by plutonium and minor actinides while developing state-of-art technologies of safeguards and physical protections of nuclear materials. As one of the efforts, we are studying for upgrading reactor cores with effective nuclear proliferation resistance and identified the advantage to material barrier which is one of indexes for nuclear proliferation resistance by evaluating isotope composition of plutonium in its spent blanket fuels. The concepts of upgrading reactor cores with effective nuclear proliferation resistance are listed as follows: the core without radial blanket fuels, the core with radial blanket fuels added by plutonium and that added by minor actinides. Figure 8 shows the three core concepts. Regarding the radial blanket fuels added by plutonium, the ratio of  $^{240}\text{Pu}/\text{Pu}$  total in the radial blanket spent fuels is more than 18% and it meets a criterion for reactor-grade plutonium ( $^{240}\text{Pu}/\text{Pu}$  total > 18%) suggested by Dr. Pellaud. Thus, this design concept alters the plutonium composition to the one without capability being nuclear weapon by adding plutonium into radial blanket fuels, and become the one of measures to enhance the effect of nuclear proliferation resistance.

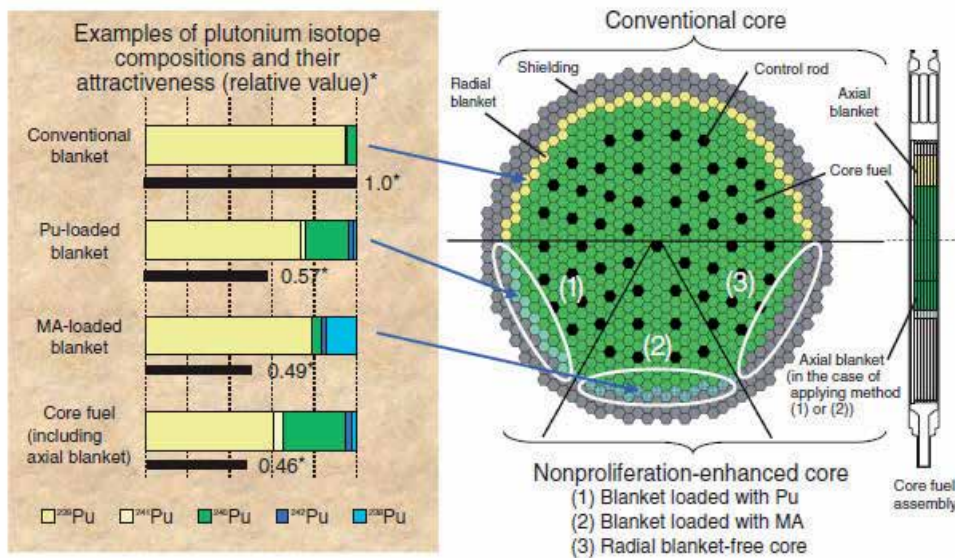


Fig. 8. Three sample core concepts for enhancing the effect of nuclear proliferation resistance (Taken from a figure of “JAEA R&D Review 2010”)

### 3.2 Japanese scenario evaluations with advanced analysis tool

In scenario evaluation, we mainly target at ‘the transition period from LWR to FR’, which is the second item in the three periods indicated in section 3.1.1. LWRs, FRs and their nuclear fuel cycles coexist in this transition period from LWR to FR. For this reason, in the

evaluation of ‘the transition period from LWR to FR’, the results are characterized by the complicated effects of various events and preconditions such as, the FR deployment pace, introduction plan of reprocessing facilities, interim storages of spent fuels, recycle of recovered uranium and so on. In the time-series scenario evaluation, we will optimize the mass-balance among various types of reactors, cycle facilities and fuels and will focus attention on the smooth transition to FR. Since we target at more complex mass-flow comparing to the evaluation of equilibrium cycle, higher leveled and more sophisticated methods must be applied in mass-balance calculation, waste generation, and cash-flow evaluation, etc. In addition, the number of input items and calculation conditions increase and this makes possible for the uncertainty about entire evaluation to be higher than that of equilibrium cycle evaluation. We conduct the evaluations of the changes in nuclear material and radioactive wastes at the same time including plutonium composition, the amount of waste generation and economics on the transition state to the FR cycle.

The scenario analyses were performed to investigate the characteristics of current Japanese nuclear fleet with LWR cycle to the future nuclear fleet with FR cycle. Based on the intensive development of the SCM code to cover both equilibrium and transient status of nuclear fuel cycle, economics, resources, radioactive wastes, and non-proliferation issues and the complex of those issues have been surveyed with consideration of the recent technical progress and events in Japanese society. The authors should begin with the alternation of scenario in recent several years (after the establishment of “Framework for Nuclear Energy Policy” in Japan). Although safety and reliability is raised as one of the important development targets in FaCT project, the consideration of them is not directly reflected in the analyses. Therefore, some important topics in the course of realizing the equilibrium FR cycle state which bring uncertainties to Japanese nuclear fleet were discussed.

### 3.2.1 Basic Japanese scenario evaluations including recent change

The current image of Japanese nuclear energy capacity which is expressed in Framework for Nuclear Energy Policy by Japan Atomic Energy Commission is shown in Figure 9.

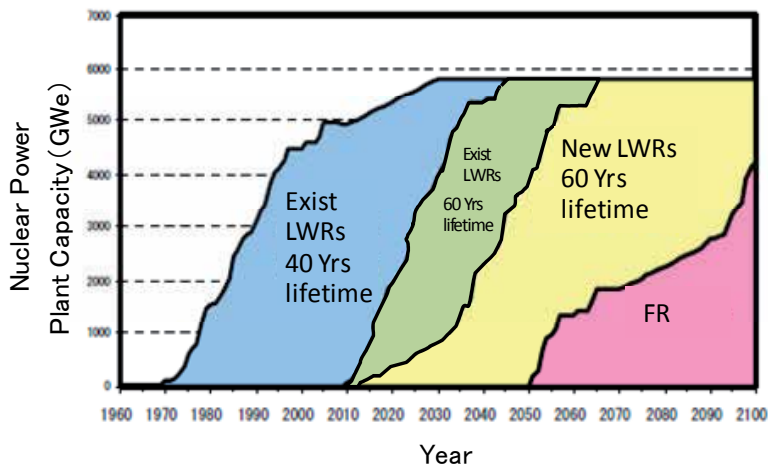


Fig. 9. Nuclear power plant capacity image in the current Framework for Nuclear Energy Policy (Original figure was AEC’s HP: Revised by the authors)



In Figure 9, important points of the nuclear power plant capacity are as follows:

In Japan, the nuclear capacity goal was changed from 58GWe,

The BR=1.1 was supposed for FR for future deployment,

The lifetimes of nuclear power plants were 40 to 60 years,

The reprocessing plants for FR spent fuels will be constructed independently from those for LWR spent fuels.

However, more than five years have passed since the announcement of the current Framework for Nuclear Energy Policy, the circumstances surrounding nuclear fuel cycle including FR cycle also have been changed. The authors discuss several factors which will affect the FR cycle long-term plan and strategy in this section.

First of all, the expectation for nuclear energy has been increased (at least before the accident of Fukushima Daiichi Nuclear Power Station) because it is a just suitable energy to achieve both to urge sustainable economic development and to reduce greenhouse gas emission in the world. In Japan, national energy basic plan published in 2010 insisted that the nuclear energy capacities up to 68GWe by 2030 mainly to meet both of sustainable economic growth and greenhouse gas emission reduction. The increase of the expected nuclear capacity in Japan will urge the breeding needs of FR and related fuel cycle in Japan. Regarding the breeding ratio of FR, BR=1.1 is considered as the reference in the current Framework and FaCT project, but FR with higher BR (ex.BR=1.2) which was described in former section is also important in preparedness for the uncertainties of the fuel cycle operation and the possibility of development toward global standard after the governmental evaluation of FS Phase II. Besides, Japanese government, electricity utilities, and manufacturers are making the concept of the next generation LWRs which has 80 years lifetime with the burnup of more than 70GWd/tHM, etc. Additionally, the study on reprocessing facilities subsequent to Rokkasho-Reprocessing Plant (RRP) has started. In the study, dual-purpose (LWR-SF and FR-SF) reprocessing plants were proposed as well as independent single-purpose (for exclusive use) reprocessing plants. Therefore, the authors tried to include those variations in the analysis cases listed in Table 1.

Case	Capacity (GWe)	Core Fuel	Breeding Ratio	LWR lifetime	Reprocessing Plant mode
Conventional	58	(U, Pu, MA) oxide	1.1 to 1.03	60	Single Use
Recent (Ref.)	68	(U, Pu, MA) oxide	1.1 to 1.03	80	Dual Use
BR=1.2	68	(U, Pu, MA) oxide	1.2 to 1.03	80	Dual Use
60Yrs	68	(U, Pu, MA) oxide	1.1 to 1.03	60	Dual Use
Single Use	68	(U, Pu, MA) oxide	1,1 to 1.03	80	Single Use

Table 1. Analysis cases reflected basic nuclear energy policy change

In those analyses listed in Table 1, the influence of lifetime extension was largest on future scenarios; change in breeding ratio and future nuclear power plant capacity had some influence. The reprocessing plant mode had a relatively smaller influence, on the whole.

The authors would like to start an analysis treated the meaning of the breeding ratio in the recent context of Japan. The result of FS showed that FR with breeder core of BR1.1 will be enough to deploy FRs smoothly in 80 years for future Japan. The lifetime extension of next generation LWRs to 80years helped reduce the breeding requirement of FRs in future Japan.

Figure 10 shows the nuclear capacity in Japan for deployment of FR with BR=1.1 with the 80 years lifetime of LWR. The “Dual Use” means a reprocessing plant can be used both for LWR-SF and FR-SF. On the contrary, “Single Use” means a reprocessing plant can be used only for LWR-SF or FR-SF.

However, if some larger uncertainties are considered in scenario study, FRs with breeder core of BR=1.2 contributes to offset the risk in Japanese nuclear energy system. Smaller number of FRs with breeder core will be needed for future Japan as is shown in Figure 11. Since cash-flow is the basis for all economics evaluation, Figure 12 shows the total cash-flows of FR deployment scenarios with FR of BR=1.1 and BR=1.2 from Japanese nuclear fleet from 2000 to 2200. It can be said that the decrease of total power generation cost was JPY from JPY in BR=1.1 case from BR=1.2, the authors considered the economic merit was not the critical reason to abandon higher breeding ratio, even if the relative low power generation cost for BR=1.1 case acts as an incentive around the deployment stage of FR cycle. Therefore, the room for breeding ratio adjustment corresponds to socio-environment is an evidence of the inherent flexibility in core fuel with fast neutron.

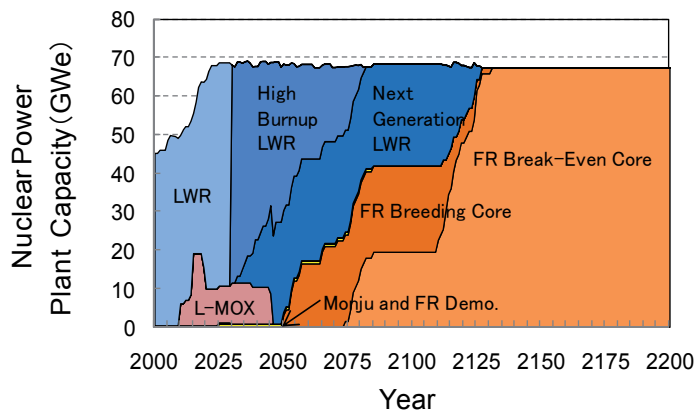


Fig. 10. The nuclear capacity for FR with BR=1.1 with the 80years lifetime of LWR

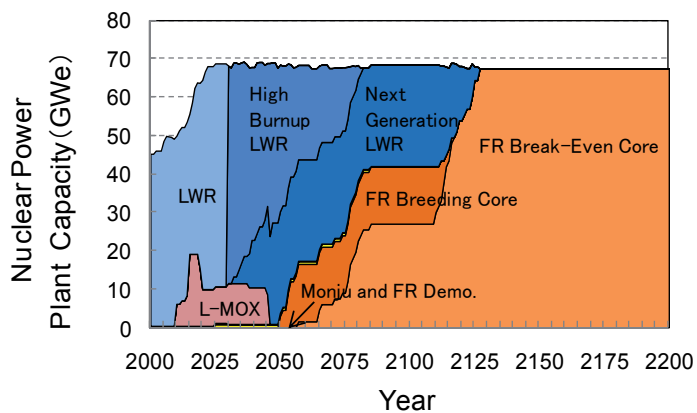


Fig. 11. The nuclear capacity for FR with BR=1.2 with the 80years lifetime of LWR

As the readers can see several peaks and bottoms from the area chart in Figure 13, the realistic cash-flows are different from simple averaged power generation costs (ex. 2.8JPY/kWh for BR=1.1 or 2.6 JPY/kWh for BR=1.03) although they became similar in far future after 2200. The actual dynamic analysis result for electricity generation cost will not usually accord with the simplified or averaged power generation cost of nuclear fleet. In other words, the original cash-flow is the basis of the economic evaluation, it should not be forgotten that simplified electricity generation cost result is basically studied from the ground of cash-flow result in particularly in case of scenario (time-series) evaluation.

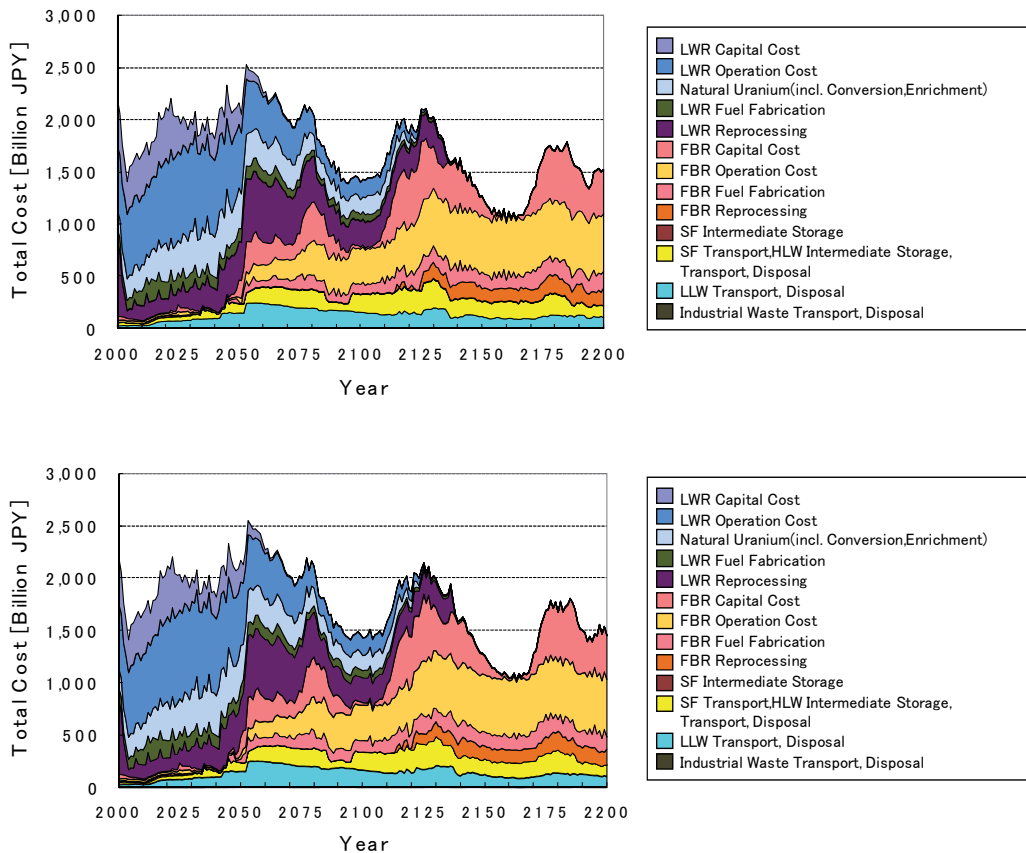


Fig. 12. Total cash-flow of Japanese nuclear fleet for both (BR=1.1 and BR=1.2) cases

### 3.2.2 Radioactive waste management scenario evaluations

Another scenario study results showed that the effects of MA recycling on radioactive waste management in FR cycle (reduction of HLWs generation from FR cycle or reduction of heat emission from HLW in FR cycle to cut disposal area). The effect was described in 3.1.3 for equilibrium state of FR cycle. It is caused partly by the nuclear materials in precedent LWR cycle transferred from LWR cycle to FR cycle. The cases listed in Table 2 were analyzed by SCM code on radioactive wastes (mainly HLW) generation.

Case	Capacity (GWe)	Core Fuel	Breeding Ratio	Reprocessing Plant mode
U-Pu, Single	68	(U, Pu) oxide	1.1 to 1.03	Single Use
U-Pu, Dual	68	(U, Pu) oxide	1.1 to 1.03	Dual Use
TRU, Single	68	(U, Pu, MA) oxide	1.1 to 1.03	Single Use
TRU, Dual	68	(U, Pu, MA) oxide	1.1 to 1.03	Dual Use

Table 2. Analysis cases with/without MA recycling

Since there was little difference in the results between the single use reprocessing plant case and dual use plant case, the authors did not write the concrete case in the following part. Figure 13 shows the radioactive wastes generation from Japanese nuclear fleet in reference case based on the waste management evaluation by SCM code. There are several peaks in the figure which correspond to the major facilities' decommissioning such as LWR reprocessing plants and nuclear power plants. Although the quantity of HLW is small, it requires large scale facility for disposal and usually focused in disposal site finding issue. Therefore, the influence on HLW from MA recycling is investigated in this section.

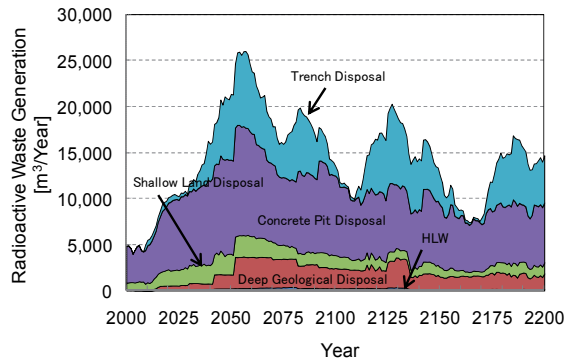


Fig. 13. Radioactive wastes generation from Japanese nuclear fleet

Figure 14 shows the calculated Japanese nuclear power plant capacities according to core type in a typical case without MA recycling. FRs are deployed after 2050 just as same as the reference case explained in 2.2.1. Since the completion of switchover to FR with (U, Pu) oxide cores were delayed several years from the reference case, total transition period is 84 years from the analyses results. It is explained from the internal conversion ratio difference.

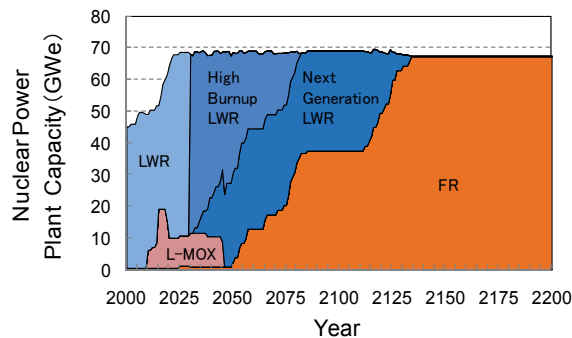


Fig. 14. FR deployment with core of BR=1.1 without MA recycling

When the total Japanese nuclear fleet is considered, MA recycling has the potential to reduce the quantities of HLW from FR cycle system. Because of the difference in fuel cycle and other discrepancies, it is difficult to compare directly the scenarios with or without MA recycling. Comparing the quantities of HLW generation, Figure 15 was obtained. Though there seems to be little difference (the difference is a kind of complex of causes) in HLW generation from Figure 15, it is expected that the area needed for HLW disposal will be reduced as a result of reduction in decay heat from HLW by MA recovery from raffinate in reprocessing plants. Besides that, MA recycling leaves the possibility for further HLW reduction combined with the introduction of high density FP packing in vitrified waste technology. The reduction of HLW generation will be realistic if the high emission heat nuclides are removed from HLW by the recovery of MAs and/or FPs as described in Figure 16. The difference of HLW generation after 2135 in Figure 17 is the combined effect of MA recycling and high density FP packing in vitrified wastes although the fuel cycle schemes are different because of the existence or non-existence of MA recycling.

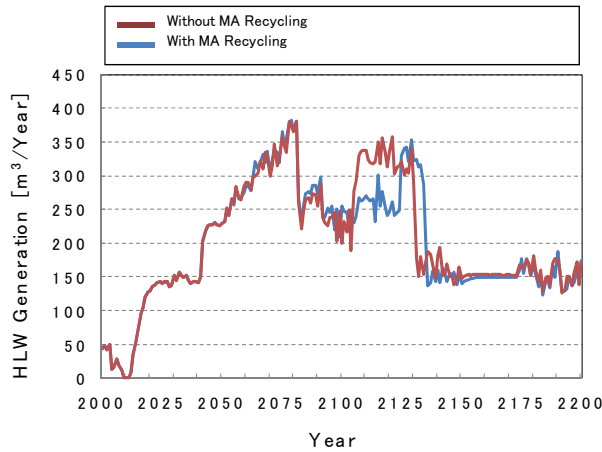


Fig. 15. Comparison of HLW generation from nuclear fleets with and without MA recycling

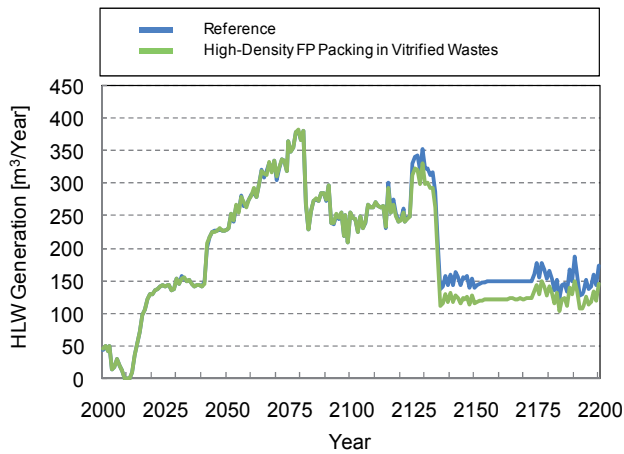


Fig. 16. The effect of MA recycling combined with high-density FP packing in HLW

### 3.2.3 Nuclear non-proliferation scenario evaluations

As for the scenario study related to non-proliferation, the measures to dope MAs in blanket fuel to improve the non-proliferation characteristics of spent blanket fuel have some issue to be resolved to supply sufficient amounts of MAs to all FRs and its fuel cycle system in Japan. On the other hand, although the measure to add Pu in blanket may delay FR deployment in future, it is feasible from both of the viewpoints of material supply and of improving material barrier of spent blanket fuel. There are many ideas to enhance proliferation resistance of FR cycle system.

Case	Core Fuel / Axial Blanket / Radial Blanket	Reprocessing Plant
Depleted Uranium Blanket Fuel	(U, Pu, MA) oxide / U Oxide / U oxide	Single Use
Radial Blanket Free Fuel	(U, Pu, MA) oxide / U Oxide / -	Single/Dual Use
MOX Radial Blanket Fuel	(U, Pu, MA) oxide / U Oxide / (U, Pu) oxide	Single/Dual Use
Radial Blanket Fuel with MA Doping (Mino Actinide)	(U, Pu, MA) oxide / U Oxide / (U, MA) oxide	Single/Dual Use
All MOX Blanket Fuel	(U, Pu, MA) oxide / (U, Pu) oxide / (U, Pu) oxide	Single/Dual Use
All Blanket Fuels with MA Doping (Mino Actinide)	(U, Pu, MA) oxide / (U, MA) oxide / (U, MA) oxide	Single/Dual Use

Table 3. Analysis cases for non-proliferation improvement core

The analysis cases listed in Table 3 reflect the authors' concern on the measures to apply to the Pu in blanket SF of FR. In Case-1, called the "Radial Blanket Free Core" concept, the radial blanket is replaced by a steel reflector, In Case-2, the radial blanket is fabricated with Pu in low isotope enrichment so that the plutonium produced in the radial blanket will have a low-fissile ratio. In Case-3 the radial blanket fuel is doped MA, which reduces the attractiveness because of the heat generation from Pu-238. The maximum MA ratio of new core fuel was assumed to be 5wt% which was almost recovered from spent LWR fuels although the MA ratio of new core fuel in the equilibrium state FR cycle. In Case-4, the radial blanket is fabricated with Pu in low isotope enrichment so that the plutonium produced in the radial blanket will have a low-fissile ratio. In Case-5 the radial blanket fuel is doped MA, which reduces the attractiveness because of the heat generation from Pu-238. The maximum MA ratio of new core fuel was assumed to be 5wt% which was almost recovered from spent LWR fuels although the MA ratio of new core fuel of FR in the equilibrium state is considered as about one per cent.

The nuclear power plant capacities of all MOX blanket fuel case and all blanket fuel with MA doping case are shown in Figure 17 and figure 18, respectively. No severe influence on smooth introduction of FRs was seen from the analyses. The authors tried to confirm the effect of Pu addition to blanket fuel through the analyses with SCM code. Dr. Pellaud defined the plutonium including more than 18% of Pu-240 as "reactor grade" (RG-Pu) as it was explained in 3.1.6. Plutonium in LWR SF meets this RG-Pu condition; it has been used

globally in commercial manner under the appropriate nuclear material control and management. If the idea that proliferation resistance target of future nuclear energy system should fulfil a kind of “Pareto criterion” in material attractiveness is true, FR cycle system which uses RG-Pu achieves the target. The transition of Pu240/Pu in blanket SF in “All MOX blanket core” case is shown in Figure 19. The Pu240/Pu keeps more or equal than 18% in general during the lifetime of the reactor though the option somewhat sacrifices the speed of FR deployment.

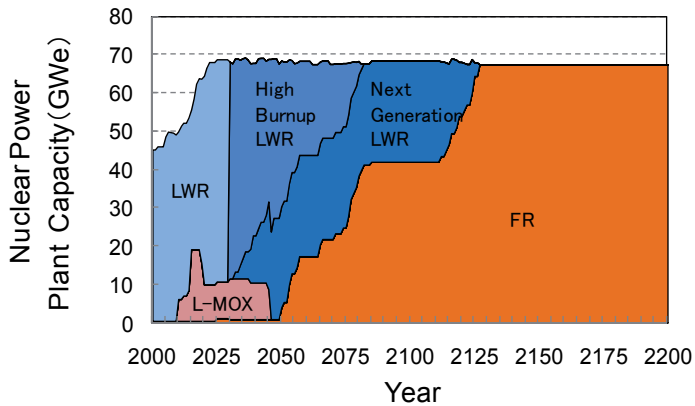


Fig. 17. FR deployment scenario for all MOX blanket case

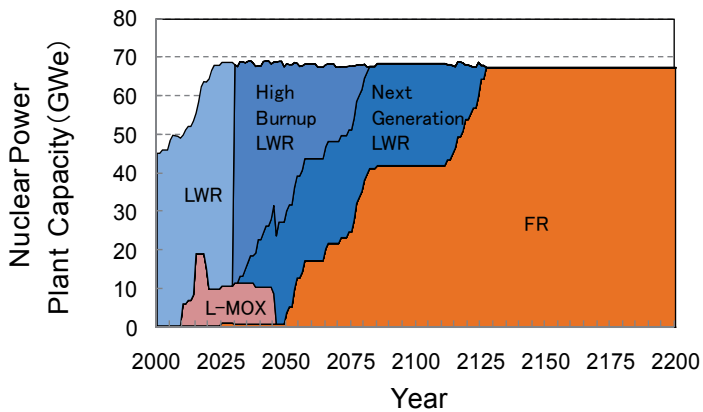


Fig. 18. FR deployment scenario for in all blankets with MA doping case

Pu isotope content in blanket SF during the transition period from LWR to FR in all MA doping blanket fuel case is shown in Figure 20. As for the period when FRs with radial blanket are installed (before 2090), it looks difficult to meet Kessler’s criteria because of the shortage of MAs supply to dope blanket fuels. Regarding heat emission from radial blanket assemblies, it reached around the boundary condition (2.6kW/Assembly) for the design study in FaCT project. Meanwhile, FRs without radial blanket increase after 2090; although the quantity of MAs are enough for the criteria, it may need additional measure for high decay heat emission from radial blanket assemblies because of the recovered MAs with high

decay heat in FR cycle. Though only an example scenario is provided here, it can be said that the measure to improve proliferation resistance of blanket SF by MA doping should be careful for both proliferation resistance requirements and realistic constraints of fuel cycle operation at the same time.

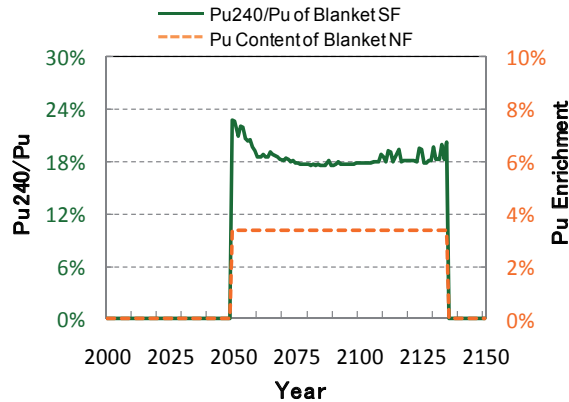


Fig. 19. Pu 240/Pu in blanket SF of all MOX blanket fuel case

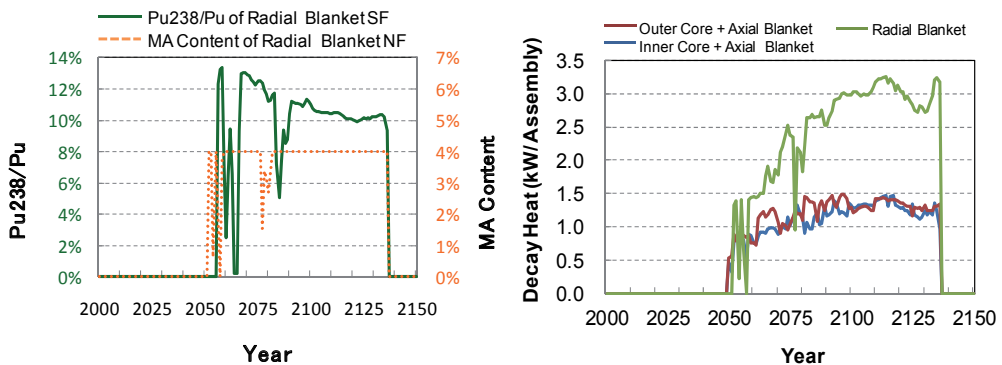


Fig. 20. Pu 238/Pu of blanket SF and decay heat emission from assemblies in all blanket fuels with MA doping case

In general, the measure except for “all blanket with MA” case in this scenario study to improve proliferation resistance of blanket spent fuel in FR can achieve their purposes unless they are reviewed from broader feasibility including R&D difficulties, adverse effect on economics, and other logistics issues, etc. Accordingly, it should be paid attention to the by-effects described above in case such measures are applied as a practical manner in future.

### 3.2.4 Advanced topics and latest situation of Japanese nuclear energy

The authors will explain the more realistic supposition in the scenario analyses with the Pu possession by utility companies. Furthermore, a scenario study for the influence of accident in Fukushima Daiichi occurred after a gigantic earthquake hit several prefectures in eastern part of Japan in March, 2011.



Conventional scenario analyses usually consider the Japanese nuclear power plants as one block; therefore, they ignore both the property right of nuclear material and/or constraints based on the matter of contracts between companies in general. Regarding the detailed analysis dealing Pu recycling in LWR with full MOX core at Ohma by J-Power, the analysis tool can reflect plutonium transfer contracts between J-power and 7 electric utilities (Tohoku, Tokyo, Chubu, Hokuriku, Chugoku, Shikoku, and Kyushu) for the initial loading core. If the future Pu balance was considered from worm’s-eye view, such kinds of transfers should be counted. An example of rough estimation of Pu transfers during “Pu recycling in LWR period” in Japan between electricity utilities by SCM code was shown in Figure 21. Besides the Pu demands in Figure 22, other Pu is needed for FR deployment and running stock for operation from the discrepancy of recovered Pu and Pu demand for Pu recycling in LWR. J-power may have to gather Pu from other electricity utilities for Pu recycling in Ohma plant.

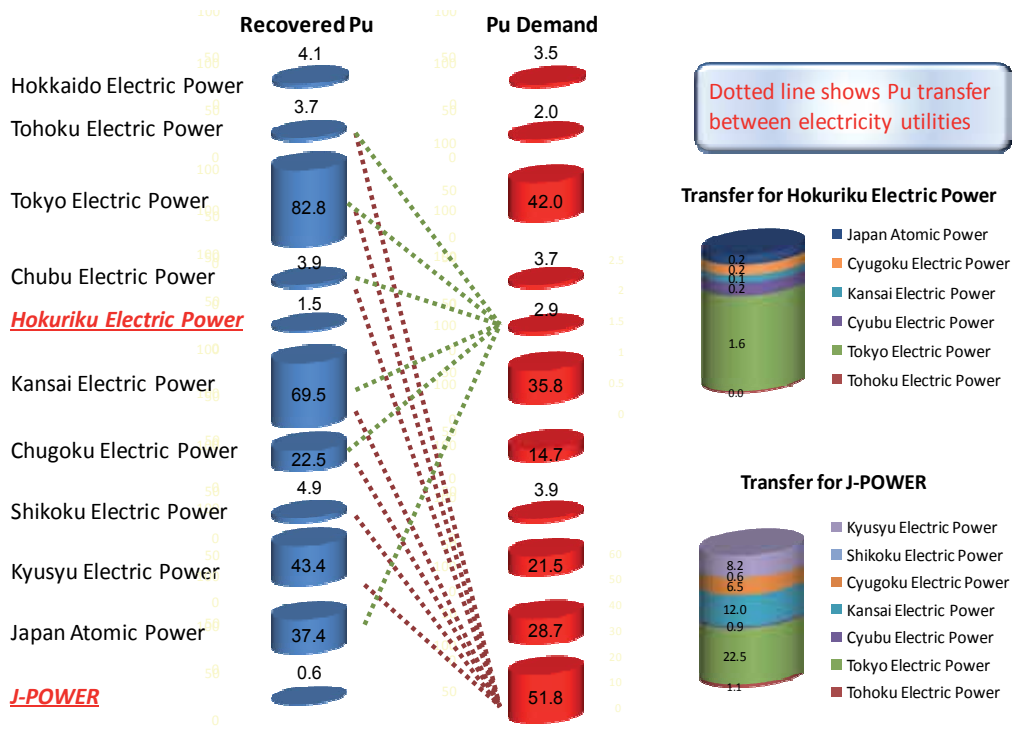


Fig. 21. Example of Pu transfer estimation during “plutonium recycling in LWR” period in Japan

A larger earthquake ever recorded in Japanese history hit northern eastern part of Japan on March 11, 2011, the record-breaking tsunami occurred subsequent to the earthquake caused severe accident of Fukushima Daiichi Nuclear Power Station. Concerning the influence of the accident on Japanese nuclear policies, it is too early to say something definitive because the accident has not finalized yet and the governmental argument on future energy policies has not started. Presently, the authors can suggest the role and flexibility of FR cycle according to the series of analyses by SCM code with the following assumptions:

The nuclear power plants involved in Fukushima Daiichi accident (Fukushima-1 No.1 to NO. 4) will not restart,

Though new nuclear power plants will not be constructed in new locations, the existing nuclear power plants other than listed above will be replaced by new nuclear power plants.

The breeding requirement for FR cycle system will be reduced under the assumption of both withdrawals from several nuclear power plants and deployment of next generation LWRs with longer plant lifetime. The result also indicated that FR cycle will be FR with break-even core from the beginning of installation without rapid breeding needs. It will curb fuel cycle cost through the reduction of mass-flow by the usage of high burnup fuel. The flexibility of breeding capability in FR leads us to adapt both higher nuclear capacity and lower nuclear capacity to some extent by giving weight to economics or breeding in the coexistence of LWR and FR nuclear fleet in transient state.

#### **4. Conclusion**

The authors tried to provide overall path to nuclear energy system with FR and related fuel cycle facilities firstly. Along with to the R&D effort to improve economic competitiveness, safety and reliability, and several ideas for future uncertainties the fissile material breeding ability of FR cycle system and the potential of FR core with fast neutron to burn broader isotopes, FR is major option for electricity supply for future Japan.

Secondly, the recent achievement in SCM code as the system dynamic analysis tool in FaCT project. Because of the sufficient flexibility of the newly developed analysis code based on object-oriented design, it can meet both “single plant characteristic evaluation” and “Japanese whole nuclear fleet scenario study until 22nd century”. The code will be used as an infrastructure of future nuclear energy system in Japan.

In addition to the fact that a nuclear energy system development usually needs a long lead-time for decades, it was important that the development of the current LWR cycle and R&Ds may have an influence on successive nuclear energy system including FR cycle through the supply chain of nuclear energy system. Nuclear energy utilization and development become a matter of argument in reaction to the occurrence of Fukushima Daiichi’s accident, it should be keep in mind that today’s decision on the directions of nuclear energy R&D under influence of the fresh memory of accident may make a difference in far future as well as that in immediate future.

#### **5. Acknowledgment**

The authors would like to express their deep gratitude to both Mr. Heta and Mr. Yasumatsu of NESI Inc. for their contribution for the various works. The authors also would like to express admiration for Mr. Ishii and other members of Mizuho Information and Research for their high performance in the development of the analysis code.

## 6. References

- Grover R. B. and Chandra S. (2004). A Strategy for Growth of Electrical Energy in India, DAE Report No.10
- Japan Atomic Energy Agency. (2011), JAEA R&D Review 2010, What Core Design Prevents Nuclear Proliferation? –Commercial FBR Core Study Focusing on a Material Barrier-, 12, (CD-ROM)
- Japan Atomic Energy Agency/Japan Atomic Power Company. (2009), Fast Reactor Cycle Technology Development Project (FaCT Project) – Phase I (Interim Report) –, JAEA-Evaluation-2009-003, (May 2009) (in Japanese)
- Japan Atomic Energy Commission. (2005), Framework for Nuclear Energy Policy, (October 2005)
- Japan Atomic Energy Commission. (2010), Appropriateness of the „Plutonium Utilization Plans (FY2010)“ Announced by Electric Utilities and the IAEA, (March 2010), AEC HP , Apr 12, 2011, Available from:  
<[http://www.aec.go.jp/jicst/NC/about/kettei/seimei/100323\\_e.pdf](http://www.aec.go.jp/jicst/NC/about/kettei/seimei/100323_e.pdf)>
- Kawashima, K. et al. (2010). Fast reactor Core Design Considerations from Proliferation Resistance Aspects, *Proceedings of FR09*, Kyoto, Japan, December 7-11, 2009
- Ministry of Economy, Trade and Industry. (2010), Basic Energy Plan (June 2010), pp. 27, 31, 32 (in Japanese)
- Ministry of Economy, Trade and Industry. (2010), FY2010 Electric Power Supply Plan (March 2010) (in Japanese)
- Ministry of Education, Trade and Technology. (2010), Seinoumokuhyou no tasseido hyouka (1)-(3), MEXT HP, April 12, 2011, Available from:  
[http://www.mext.go.jp/b\\_menu/shingi/chousa/kaihatu/008/shiryo/\\_\\_icsFiles/afieldfile/2010/12/28/1300643\\_1.pdf](http://www.mext.go.jp/b_menu/shingi/chousa/kaihatu/008/shiryo/__icsFiles/afieldfile/2010/12/28/1300643_1.pdf),  
[http://www.mext.go.jp/b\\_menu/shingi/chousa/kaihatu/008/shiryo/\\_\\_icsFiles/afieldfile/2010/12/28/1300643\\_2.pdf](http://www.mext.go.jp/b_menu/shingi/chousa/kaihatu/008/shiryo/__icsFiles/afieldfile/2010/12/28/1300643_2.pdf),  
[http://www.mext.go.jp/b\\_menu/shingi/chousa/kaihatu/008/shiryo/\\_\\_icsFiles/afieldfile/2010/12/28/1300643\\_3.pdf](http://www.mext.go.jp/b_menu/shingi/chousa/kaihatu/008/shiryo/__icsFiles/afieldfile/2010/12/28/1300643_3.pdf)
- Nuclear energy subcommittee of Electricity Industry Committee of Advisory Committee for Natural Resources and Energy in Ministry of Economy, Trade and Industry. (2006), Japan's Nuclear Energy National Plan (August 2006), pp. 63 (in Japanese)
- OECD/IEA. (2008), Energy Technology Perspectives 2008
- OECD/IEA. (2009). World Energy Outlook 2009
- OECD/IEA. (2010). Energy Technology Perspectives 2010
- OECD/NEA & IAEA. (2010). Uranium 2009: Resources, Production and Demand
- Ohki, S. et al., (2008). FBR core concepts in the FaCT Project in Japan, *Proceedings of Physor '08*, Interlaken, Switzerland, September 14-19, 2008
- Sagayama Y. (2010), Long-term Nuclear Energy Development Scenario for Sustainable Energy Supply, *Electrical Review*, Vol.556 (December 2010) (in Japanese)
- The advisory committee for Natural Resources and Energy's subcommittee to study costs and other issues, The report of the Advisory Committee for Natural Resources and Energy's subcommittee to study costs and other issues, Japan. (2004)(in Japanese).

Xu M. (2005). Status and Prospects of Sustainable Nuclear Power Supply in China, GLOBAL 2005, Tsukuba, Japan, Oct. 9-13 2005

# Nuclear Proliferation

Michael Zentner

*Pacific Northwest National Laboratory  
United States of America*

## 1. Introduction

Early nuclear energy system designs grew out of programs to develop nuclear weapons, and accordingly these systems were optimized to produce weapons usable material. As the nuclear industry matured and the use of nuclear power spread, safety, cost, environmental impact and waste management considerations shaped nuclear energy system designs that were deployed for the purpose of producing electricity. A multi-faceted international nonproliferation regime comprised of treaty commitments and obligations, verification mechanisms, export controls, and diplomatic strategies intended to dissuade States from proliferating has grown (Figure 1). Likewise, measures to prevent theft of nuclear materials by subnational groups have been implemented at both the national and international levels. There has been continuing interest in developing nuclear technologies that would permit the peaceful use of nuclear power without an associated proliferation of nuclear weapons capability. The term “proliferation resistant” was coined to describe technologies that are not suitable for the production of weapons usable material.

Despite this interest in “proliferation resistant technologies,” the reality remains that a truly proliferation-proof nuclear energy system has yet to be discovered. A fuller understanding of the nature of nuclear proliferation would suggest that motivation, underlying political-military ambitions, in some cases domestic political imperatives, are key drivers for proliferation or for decisions not to pursue nuclear weapons development. There is no technological “silver bullet” that will solve the proliferation challenge. Even for technologies that are said to be more difficult to misuse for proliferation purposes, one must recognize that the international transfer of such technology can impart to the recipient technical capabilities and know-how that can be put to use in facilities that could be used to support a nuclear weapons program.

A more productive course of action would be to consider how a particular technology or facility design might lend itself to more effective and efficient forms of international verification by the International Atomic Energy Agency. Beginning early in the 1950s, international safeguards agreements and principles were put in place to make certain that as the use of nuclear power spread it would be used for peaceful purposes only, and if a State were to misuse these technologies it would be detectable so that the international community could take timely action. The more difficult and detectable it was to use a system to make nuclear weapons usable material, the better.

As discussed below, the notion of “proliferation resistance” in this context is more relative, that is, how one system might compare to another. Results of proliferation resistance studies

should not be construed as implying that a particular system is proliferation-proof, nor that features claimed to make a system more proliferation resistant provide a rationale for relaxing: 1) international safeguards for such systems; 2) controls on the export of such systems and related technologies; or 3) the nonproliferation credentials and commitments of the recipient of such technology transfers.



Fig. 1. International safeguards agreements

Nuclear energy system designers and engineers must understand not only how to design and build their systems to make them safe and secure, but also easy to safeguard. In this chapter, we will show how proliferation resistance has been studied, what can be learned from these studies, and how the results can be used in the international community. As already stated, the problem of nuclear proliferation is multi-faceted, with a long and complicated history, and for purposes of this chapter we will focus only on the concept of proliferation resistance.

## 2. Proliferation resistance

The generally accepted definition for *proliferation resistance* is:

*“... that characteristic of a nuclear energy system that impedes the diversion or undeclared production of nuclear material or misuse of technology by States in order to acquire nuclear weapons or other nuclear explosive devices. The degree of proliferation resistance results from a combination of, inter alia; technical design features, operational modalities, institutional arrangements and safeguards measures. Intrinsic proliferation resistance features are those features that result from the technical design of nuclear energy systems, including those that facilitate the implementation of extrinsic measures. Extrinsic proliferation resistance measures are those measures that result from States’ decisions and undertakings related to nuclear energy systems.” (IAEA-STR-332, 2002)*

This definition makes clear that proliferation resistance should be considered a function of the *intrinsic* technical features (facility design and operation) and *extrinsic* properties (implementation of international agreements and safeguards) of a nuclear energy system. The degree of effectiveness of these properties is used to determine a nuclear energy system's proliferation resistance.

Studies of nuclear proliferation can be broadly separated into two distinct categories, as follows:

- *State-level* proliferation studies (e.g., Meyer 1984; Singh & Way 2004; Li et al. 2009, etc.) examine the implications and consequences of State motivations, resources (technical, human, and financial), geostrategic or regional rivalries, and international agreements. Using this information, analysts assess the likelihood that a State will proliferate or attempt to do so.
- *Technical* proliferation studies address elements of Nuclear Energy Systems (NES), focusing on their possible contributions to a nuclear weapons program. Technical studies can range from evaluating an individual facility or unit to examining all elements of a fuel cycle.

This chapter focuses on technical proliferation resistance studies, which can be used to:

- evaluate characteristics of proposed nuclear energy systems that are intended to impede the diversion or undeclared production of nuclear material or the misuse of technology,
- evaluate the vulnerability of proposed NES design and operational features from a proliferation resistance point of view,
- evaluate the applicability and effectiveness of international safeguards measures,
- provide a basis for improving both facility intrinsic features (design options) and extrinsic measures (safeguards) to achieve an appropriate balance, and
- communicate proliferation resistance strengths and weaknesses of the NES to decision makers in a transparent, understandable and meaningful way. (Zentner, et al., 2009)

### 3. Proliferation risk

Although the terms “proliferation resistance” and “proliferation risk” are sometimes used interchangeably, they are not synonymous. Technically, risk can be defined (Kaplan & Garrick, 1981) in terms of a risk “triplet”: 1) *What can go wrong?* 2) *How likely is it?* 3) *What are the consequences?* For proliferation risk, technical proliferation resistance studies answer the first and the third questions, but answering the second—the *likelihood* of the deliberate act of proliferation—is a difficult calculation most suited to State level proliferation studies as described above.

Accordingly, proliferation resistance should be considered a component of proliferation risk, and proliferation resistance studies may be useful to identify means of addressing elements of that risk. The concept of proliferation risk includes much broader political considerations than proliferation resistance, and will not be further addressed here.

### 4. Physical protection

It is important to understand the difference between the concepts of Proliferation Resistance and Physical Protection. *Physical protection* is defined as “that characteristic of an NES that impedes the theft of materials suitable for nuclear explosives or radiation dispersal devices

(RDDs) and the sabotage of facilities and transportation by sub-national entities and other non-Host State adversaries.

The objective of a physical protection system is to minimize the susceptibility to and opportunity for unauthorized removal of nuclear material in use, storage or transport and of sabotage of nuclear material and nuclear facilities. The effectiveness of the system is demonstrated by its capability to prevent the successful execution of a malicious act and to prevent and/or mitigate radiological consequences thereof.

Physical protection concerns are not unique to the nuclear industry. Although what is to be protected; consequences of a successful attack; and approaches for detecting, delaying, and responding to an attack may differ, the same basic principles are applied to protect any important facility against sabotage or theft, whether it is an NES, an oil refinery, a communications center, or a military site (Bari, 2009). Accordingly Physical Protection will not be further addressed in this chapter.

## 5. Studying proliferation resistance

A number of distinct procedures for the study of proliferation resistance exist. Four representative methodologies (TOPS<sup>1</sup>, INPRO<sup>2</sup>, SAPRA<sup>3</sup>, and GEN IV PR&PP WG<sup>4</sup>) are described below. All use the standard definition of proliferation resistance, "... *that characteristic of a nuclear energy system that impedes the diversion or undeclared production of nuclear material or misuse of technology by States in order to acquire nuclear weapons or other nuclear explosive device...*", but take distinctly different approaches.

They can be broadly separated into two classes: multi-attribute utility analyses (MAUA) and pathway analyses. In the first class (TOPS, INPRO, and SAPRA) a set of attributes (i.e., material and technical barriers to proliferation) are identified and relevant values are established for measuring the relevant importance or effectiveness of each barrier against a particular proliferation threat. In the second class (GEN IV PR&PP WG) possible proliferation pathways are postulated involving the diversion of weapons usable material or misuse of technology to produce such material. For each pathway, acquisition scenarios are identified and analyzed, and the resulting outcomes are compared using specified sets of proliferation resistance measures.

### 5.1 Technological Opportunities to Increase the Proliferation Resistance of Global Civilian Nuclear Power Systems (TOPS)

The TOPS Task Force <sup>5</sup> was established in 1999 to "identify near and long-term technical opportunities to increase the proliferation resistance of global civilian nuclear power systems and to recommend specific areas of research that should be pursued to further these goals" (TOPS, 2001). After reviewing several proposed approaches, a MAUA methodology was developed that identifies a set of material and technical attributes considered barriers to proliferation, with relevant importance values. *Material barriers* are properties that affect the

---

<sup>1</sup> TOPS: *Technological Opportunities to Increase the Proliferation Resistance of Global Civilian Nuclear Power Systems*

<sup>2</sup> INPRO: *International Project on Innovative Nuclear Reactors and Fuel Cycles* (IAEA)

<sup>3</sup> SAPRA: *Simplified Approach for Proliferation Resistance Assessment of Nuclear Systems*

<sup>4</sup> GEN IV PR&PP WG: *Generation IV Proliferation Resistance and Physical Protection Working Group*

<sup>5</sup> Created by the U.S. Department of Energy (DOE) Office of Nuclear Energy, Science, and Technology and DOE's Nuclear Energy Research Advisory Committee (NERAC)



desirability or attractiveness of the material as an explosive. *Technical barriers* are those aspects that make it difficult to gain access to materials and/or to use or misuse facilities to obtain weapons-usable materials (Table 1).

Barrier Descriptions		Barriers Considered in each method					
		TOPS	SAPRA				Note
			Diversion	Transport	Transform	Weapon fabricate	
Material	Isotopic	Critical Mass					1
		Isotopic Enrichment					2
		Spontaneous Neutron Generation					
		Heat Generation Rate					
		Radiation					
	Dangerousness (other than irradiation)						
	Chemical						
	Radiological (other than the material)						
	Mass and bulk						
	Physical form						
Detectability							
Technical	Facility unattractiveness						3
	Facility accessibility						
	Available mass						
	Diversion detectability						
	Skill, expertise, knowledge						
	Time						
	Technical difficulty						
	Collusion level						
	Construction detectability						
	Signature of installation						
Extrinsic	Safeguards						
	Access/control/security						
	Location/distance (for transport phase)						

- Notes:**
- 1 - in SAPRA, this barrier is implicitly included in "Mass and Bulk" barrier
  - 2 - Isotopic barrier plays a role only when enrichment is inescapable to obtain direct weapons usable material
  - 3 - In SAPRA, this barrier is implicitly included in other technical barriers linked to the diversion phase, in particular the "technical difficulty" and "accessibility" barriers

Table 1. Comparison of TOPS and SAPRA barriers (Greeneche et al., 2007)

Examples of material barriers used in the original TOPS procedure included material isotopic, radiological, and chemical properties, in addition to mass or bulk. Technical barriers included attractiveness of the facility to a potential weapons program, difficulty of facility access, detectability of proliferator actions, and necessary skills and time needed for the proliferator's actions.

As the use of the TOPS methodology has matured, a variety of approaches has been developed to determine barrier values. For example, in one proliferation resistance study using the TOPS approach (Skutnik et al., 2009), barrier values were developed using a "fuzzy logic" based attributed analysis approach. This technique was intended to overcome the challenges of subjectivity inherent in development of the barrier values. The resulting model was tested by evaluating several reprocessing technologies, and the results were found to generally agree with more structured PR studies.

The TOPS approach forms the basis for a number of advanced assessment methodologies, two of which (INPRO and SAPRA) are described in more detail below.

### **5.2 Simplified Approach for Proliferation Resistance Assessment of Nuclear Systems (SAPRA)**

In 2002, a French nuclear industry working group was formed to select and develop a methodology for assessing the proliferation resistance of nuclear energy systems. The result was a methodology called the *Simplified Approach for Proliferation Resistance Assessment of Nuclear Systems* (SAPRA). SAPRA (Greneche et al., 2007) is an evolutionary approach based on the TOPS methodology, with a number of modifications, additions, and improvements. Table 1 compares the two approaches.

SAPRA separates proliferation into four phases: diversion, transport, transformation, and nuclear weapon fabrication. At each phase, intrinsic and extrinsic barriers to proliferation are identified and scored based on the perceived robustness of the barrier. SAPRA addressed the complete fuel cycle. A panel of experts was assembled to determine the values to be assigned to each of the barriers. The values were then added together to give an aggregate "Proliferation Resistance Index." Using these results the strengths and weaknesses of the various nuclear energy systems studied were identified. SAPRA is unique among most proliferation resistance assessment approaches in that it explicitly includes theft by a State as a possible proliferation threat.

### **5.3 Guidance for the Application of an Assessment Methodology for Innovative Nuclear Energy Systems – Proliferation Resistance (INPRO)**

Beginning in 2002, the IAEA's International Project on Innovative Nuclear Reactors and Fuel Cycles (INPRO) developed a proliferation resistance assessment methodology that is primarily based on a multi-attribute utility analysis approach. The INPRO proliferation resistance approach identifies one *Basic Principle of Proliferation Resistance* with five *User Requirements* for meeting this Principle, along with seventeen indicators with specific criteria and acceptance limits (IAEA, 2007).

The Proliferation Resistance Basic Principle is: "*Proliferation resistance intrinsic features and extrinsic measures shall be implemented throughout the full life cycle for an INS to help ensure that INSs will continue to be an unattractive means to acquire fissile material for a nuclear weapons program. Both intrinsic features and extrinsic measures are essential, and neither shall be considered sufficient by itself.*"

The five Proliferation Resistance User Requirements are:

1. States' commitments, obligations and policies regarding nonproliferation and its implementation should be adequate to fulfil international non-proliferation standards.
2. The attractiveness of nuclear material and nuclear technology in an INS for a nuclear weapons program should be low.
3. Any diversion of nuclear material should be reasonably difficult and detectable.
4. Innovative nuclear energy systems should incorporate multiple proliferation resistance features and measures.
5. The combination of intrinsic features and extrinsic measures, compatible with other design considerations, should be optimized in the design/engineering phase to provide cost-efficient proliferation resistance.

Table 2 (IAEA, 2007) shows User Requirement 3 including the description of the User Requirement, related criteria, indicators, and acceptance limits.

Several studies have been performed to demonstrate the use of the INPRO methodology. An important example is the "INPRO Collaborative Project PRADA: *Proliferation Resistance: Acquisition/Diversion Pathway Analysis*" (Chang & Ko, 2010). In this study of the proposed South Korean DUPIC<sup>6</sup> fuel cycle User Requirements 3 and 4 were evaluated using a modification of the PR&PP pathway analysis methodology (section 5.4). The PRADA study concludes that a multiplicity of barriers is not sufficient to ensure robust proliferation resistance; rather robustness is not a result of the number of barriers or of their individual characteristics but is an integrated function of the whole system.

#### **5.4 Generation IV International Forum Proliferation Resistance and Physical Protection Evaluation Methodology (GEN IV PR&PP WG)**

The Generation IV International Forum<sup>7</sup> (GIF) formed a working group in December 2002 to develop a method for studying proliferation resistance and physical protection of advanced NES to support the proliferation related technology goal of Generation IV (GIF002-00, 2002; PR&PP, 2006) Nuclear Energy Systems (NES): "*Generation IV NESs will increase the assurance that they are a very unattractive and the least desirable route for diversion or theft of weapons-usable materials, and provide increased physical protection against acts of terrorism.*"

After exploring several options, the working group developed a methodology using a pathway analysis approach. The methodology separates pathways into three stages: acquisition, processing, and weaponization. *Weaponization* is normally not further evaluated in these GIF studies. For a proposed NES design, proliferation challenges (or threats) are identified, the NES response to these challenges is analyzed, and outcomes are assessed as a set of proliferation resistance measures for each pathway (Figure 2).

The measures determine: 1) the difficulty of the approach; 2) how long it will take to accomplish the goal; 3) how much it will cost to achieve; 4) how much the safeguards system for the NES will cost; 5) how likely it is that actions in the pathway will be detected; and 6) the material of concern

While developing the methodology, members of the working group performed a number of studies to demonstrate and improve the approach. A PR evaluation of a proposed nuclear energy system consisting of four liquid metal reactors and co-located reprocessing and fuel

---

<sup>6</sup> DUPIC (Direct Use of PWR spent fuel In CANDU reactors)

<sup>7</sup> The Generation IV International Forum is "*a cooperative international endeavor organized to carry out the research and development (R&D) needed to establish the feasibility and performance capabilities of the next generation nuclear energy systems.*" (GIF, 2000)

production facilities (PR&PP, 2009), showed that a study performed early in the conceptual design phase of an NES can provide information useful for ensuring an optimal safeguards system concept and provide a basis for detailed systems design. A PR evaluation (Whitlock, 2010) of an advanced CANDU reactor design (*ACR-1000*) provided useful information to the facility design team and resulted in changes that improved facility safeguards without impacting other design requirements. In another study (Zentner, et al. 2010) a suite of four reactors was evaluated against a common set of proliferation threats, and areas where safeguards approaches and technology can be improved through the use of safeguards-by-design studies were identified.

<b>Basic Principle BP:</b> Proliferation resistance intrinsic features and extrinsic measures shall be implemented throughout the full life cycle for innovative nuclear energy systems to help ensure that INs will continue to be an unattractive means to acquire fissile material for a nuclear weapons program. Both intrinsic features and extrinsic measures are essential, and neither shall be considered sufficient by itself.		
<b>User Requirements (UR)</b>	<b>Criteria (CR)</b>	
	<b>Indicator(IN)</b>	<b>Acceptance Limits (AL)</b>
<b>UR3 Difficulty and detectability of diversion:</b> The diversion of nuclear material (NM) should be reasonably difficult and detectable. Diversion includes the use of an INS facility for the production or processing of undeclared material.	<b>CR3.1</b> quality of measurement	
	<b>IN3.1:</b> Accountability.	<b>AL3.1:</b> Based on expert judgment equal or better than existing designs, meeting international state of practice.
	<b>CR3.2</b> C/S measures and monitoring	
	<b>IN3.2:</b> Amenability for C/S measures and monitoring.	<b>AL3.2:</b> Based on expert judgment equal or better than existing designs, meeting international best practice.
	<b>CR3.3</b> detectability of NM	
	<b>IN3.3:</b> Detectability of NM.	<b>AL3.3:</b> Based on expert judgment equal or better than existing facilities.
	<b>CR3.4</b> facility process	
	<b>IN3.4:</b> Difficulty to modify process.	<b>AL3.4:</b> Based on expert judgment equal or better than existing designs, meeting international best practice.
	<b>CR3.5</b> facility design	
	<b>IN3.5:</b> Difficulty to modify facility design.	<b>AL3.5 = AL3.4</b>
<b>CR3.6</b> facility misuse		
<b>IN3.6:</b> detectability to misuse technology or facilities.	<b>AL3.6 = AL3.4</b>	

Table 2. INPRO User Requirement 3, Difficulty and detectability of diversion

The results of these studies establish that the methodology can usefully frame the evaluation of the proliferation resistance of a variety of nuclear fuel cycles. It can also provide insight into the effectiveness of integrated safeguards, and support the development of improved safeguards to support new NES designs.

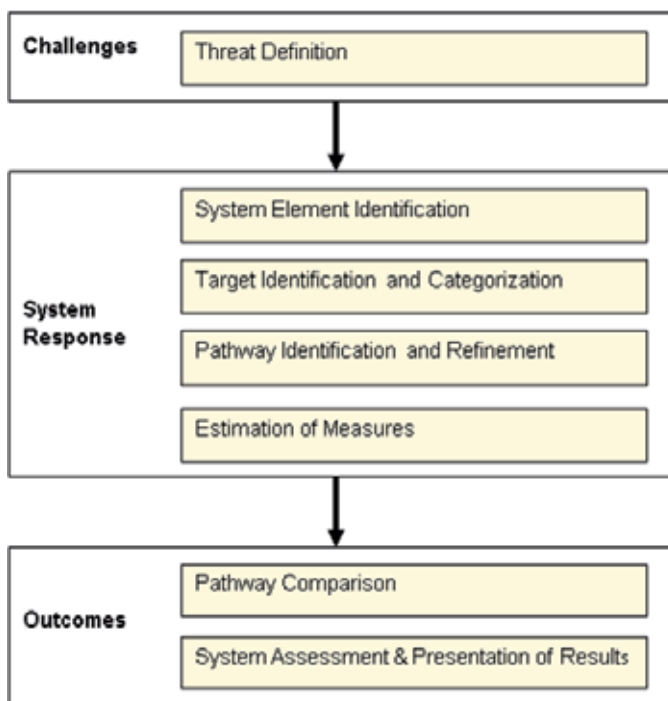


Fig. 2. Framework for the PR&PP Evaluation Methodology

## 6. Usefulness of proliferation resistance studies

The results of proliferation resistance studies can be used by decision-makers at all levels:

- Government officials, including Ministry of Energy, Ministry of Foreign Affairs and legislative officials responsible for program approvals and funding appropriations
- National licensing and regulatory authorities; export control authorities for State exports, imports and indigenous development
- IAEA safeguards authorities and other safeguards inspectorates
- Industrial designers/producers/vendors
- Utility owners and operators (Pomeroy, et al., 2008)

Decisions made by these authorities (Table 3) will set priorities for the activities of the nuclear energy system designers and can help determine the types of technologies and designs to pursue when investing in or building new civil nuclear facilities. Information provided by proliferation resistance assessments, properly used, can: 1) identify potential safeguards issues early in the design process; 2) provide a framework for the selection of design approaches that could make safeguards at the facility more efficient and effective; 3) identify design innovations that could either raise new safeguards issues or lessen cost impacts on the IAEA or the facility operator; and 4) enable the designer to focus on whether

to address new safeguards issues with design modifications that eliminate the issue or with enhanced safeguards measures (Wonder & Hockert, 2011).

<b>Potential Users of a Proliferation Resistance Assessment and Evaluation Methodology</b>	<b>Illustrative Uses of Proliferation Resistance Information</b>
Government officials, including Energy Ministry officials, Foreign Ministry Officials and Legislative officials responsible for program approvals and funding appropriations	<ol style="list-style-type: none"> <li>1. Ensuring provision of sustainable energy supply from safe, secure, economic and proliferation resistant sources.</li> <li>2. Basing nuclear export control decisions on well-understood and assessed proliferation threats</li> </ol>
National licensing and regulatory authorities, and export control authorities, for State exports, State imports and indigenous development	<ol style="list-style-type: none"> <li>1. Developing guidance on and validation of effective and efficient implementation of proliferation resistance/safeguards requirements in design and operation</li> <li>2. Providing basis for cooperation with regional and international safeguards authorities</li> </ol>
IAEA safeguards authorities and other safeguards inspectorates	<ol style="list-style-type: none"> <li>1. Providing understanding of the role of safeguards measures in proliferation resistance</li> <li>2. Ensuring that facility design and operation facilitate the implementation of safeguards</li> </ol>
Industrial designers/producers/vendors	<ol style="list-style-type: none"> <li>1. Employing usable guidance for effective and efficient implementation of proliferation resistance/safeguards requirements in design and operation</li> <li>2. Ensuring that there are transparent acceptance procedures with assessable cost impacts</li> </ol>
Utility owners and operators	<ol style="list-style-type: none"> <li>1. Enhancing public acceptance of nuclear energy production</li> <li>2. Providing transparent means for demonstrating that perceived threats are adequately controlled</li> <li>3. Optimizing extrinsic and intrinsic proliferation resistance measures with facility safety, operations, and cost</li> </ol>

Table 3. Users and Uses of Proliferation Resistance Information (Pomeroy, et al., 2008)

The following section describes how the results of proliferation resistance studies can be used, including discussions concerning nuclear material evaluation, facility safeguardability, and the implementation of safeguards by design.

### 6.1 Nuclear material evaluations

As more work in this area is performed, a number of lessons have been learned and some potential misconceptions have been identified. Experts generally agree that the attractiveness of the nuclear material and nuclear technology in an innovative nuclear system for use in a nuclear weapons program should be low. An important issue under current investigation is the concept of a “proliferation proof” material. Some have proposed that a material could be identified or developed that would be difficult – if not impossible – to use as a weapon or nuclear explosive device because of the material’s isotopic content, its intrinsic radiation field, heat load, or other features. Such material would have minimal safeguards requirements.

A team of specialists from the United States focused on material attractiveness issues from the standpoint of potential usability in a nuclear explosive device. Their studies reviewed a variety of materials associated with existing and proposed reprocessing schemes and nuclear fuel cycles. The research concluded that there are no “silver bullets” in conventional or advanced fuel cycle reprocessing schemes (e.g.; PUREX, UREX, COEX, and pyro-processing). All products from such schemes are potentially attractive for use in a nuclear weapon or nuclear explosive device (Bathke, et al., 2009).

The results of these studies support the assertion that relying on intrinsic features in a nuclear fuel cycle will not be sufficient to ensure that proliferation resistance goals will be met. Effective safeguards are of primary importance to the proliferation resistance of a nuclear energy system, and care must be taken not to construe proliferation resistance as being largely a function of intrinsic measures or as an absolute characteristic in the sense of a nuclear energy system being *proliferation proof*. Consequently, extrinsic features such as international safeguards and other institutional measures such as controls on the export of sensitive enrichment and reprocessing technologies remain essential and cannot be lessened. Rather, it is important to make these measures more effective and cost efficient by improving the “safeguardability” of an NES.

### 6.2 Safeguardability

The fundamental objective of international safeguards is to detect in a timely manner: 1) the diversion of significant quantities of nuclear material from peaceful to non-peaceful uses, and/or 2) possible misuse of nuclear facilities for undeclared purposes. How well and how efficiently an NES meets this objective is defined as its *safeguardability*. Safeguardability can be understood as the extent to which the facility design readily accommodates and facilitates effective and cost-efficient safeguards, that is, effectively integrating a nuclear facility design’s technical features with required safeguards measures.

An important use of the results of proliferation resistance studies is to evaluate and if necessary improve the safeguardability (Bjornard et al., 2009) of an NES by: 1) identifying, evaluating, and optimizing intrinsic barriers in the system design; 2) reviewing and evaluating safeguards measures for cost and effectiveness; and 3) ensuring that safeguards goals can be met. Figure 3 outlines this process.

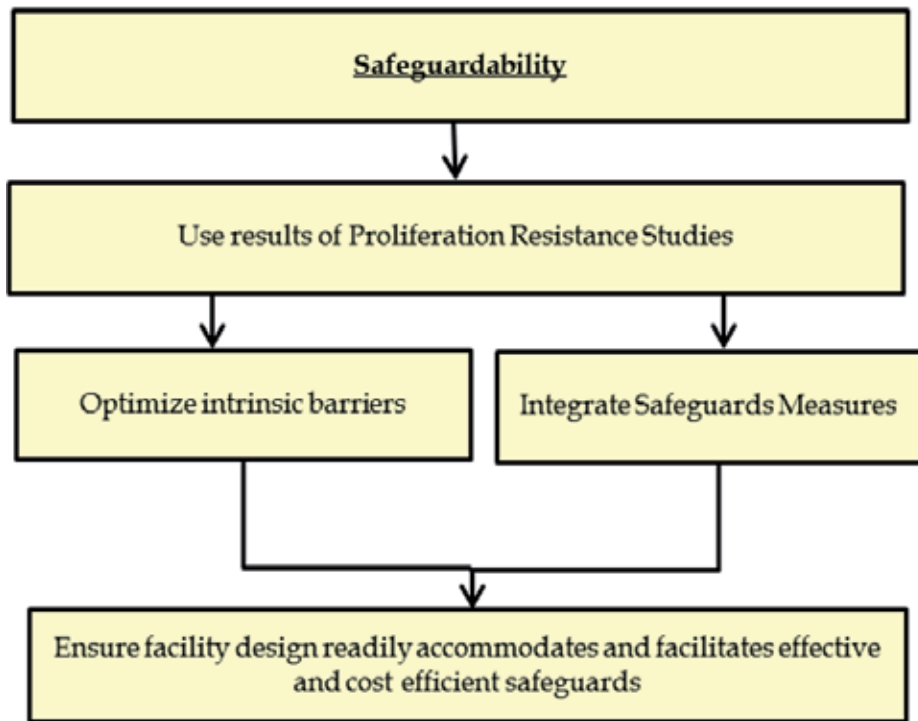


Fig. 3. Elements of safeguardability

Updating and strengthening a structured approach for accomplishing “Safeguards-by-Design” (IAEA, 2009) to help improve the safeguardability of NES facilities is receiving substantial international attention, elements of this activity are discussed further below.

### 6.3 Safeguards-by-Design

The IAEA has described the Safeguards by Design (SBD) concept as an approach in which “international safeguards are fully integrated into the design process of a new nuclear facility from the initial planning through design, construction, operation, and decommissioning” (IAEA, 2009). SBD has taken on a new importance in light of the expected “Nuclear Renaissance” and the requisite expansion of the global reactor fleet with an increased number and variety of reactors and fuel cycles under safeguards. As these new nuclear energy systems are being planned and constructed, it is clear that the IAEA must find ways to optimize its verification activities amidst continuing constraints on the financial and human resources available to it for safeguards. Consequently, the nuclear industry is beginning to address the problem of how it can facilitate the application of IAEA safeguards in a manner that provides benefits to both the IAEA and the facility operator. SBD is intended to help solve this issue by developing a structured approach for designing and incorporating safeguards features into new civil nuclear facilities at the earliest stages in the design process, and designing the facility in such a way that it more readily lends itself to being safeguarded.

Broadly speaking, this effort would involve using safeguardability assessment tools: 1) to aid designers in identifying potential safeguards issues early in the design process; 2) to



provide them with a framework for the selection of facility-specific SBD best practices and lessons learned; and 3) to help them anticipate where innovations in their designs might pose new safeguards issues that might be addressed through changes in the design, or enhancements of accepted safeguards approaches in a manner likely to meet IAEA safeguards requirements while mitigating cost impacts on both IAEA and the facility operator (Wonder & Hockert, 2011). This approach, as laid out in Figure 4, parallels the PR&PP assessment methodology.

Stakeholders responsible for developing and incorporating SBD in the design and construction of new nuclear facilities include those responsible for the design, approval, construction, oversight, operation, and safeguarding of a nuclear facility. These stakeholders include:

- The IAEA
- Owners/operators
- Designers/builders
- Regional or State Systems of Accounting and Control (R/SSAC), and
- Equipment providers.

The future application and development of the concept of SBD is ongoing.

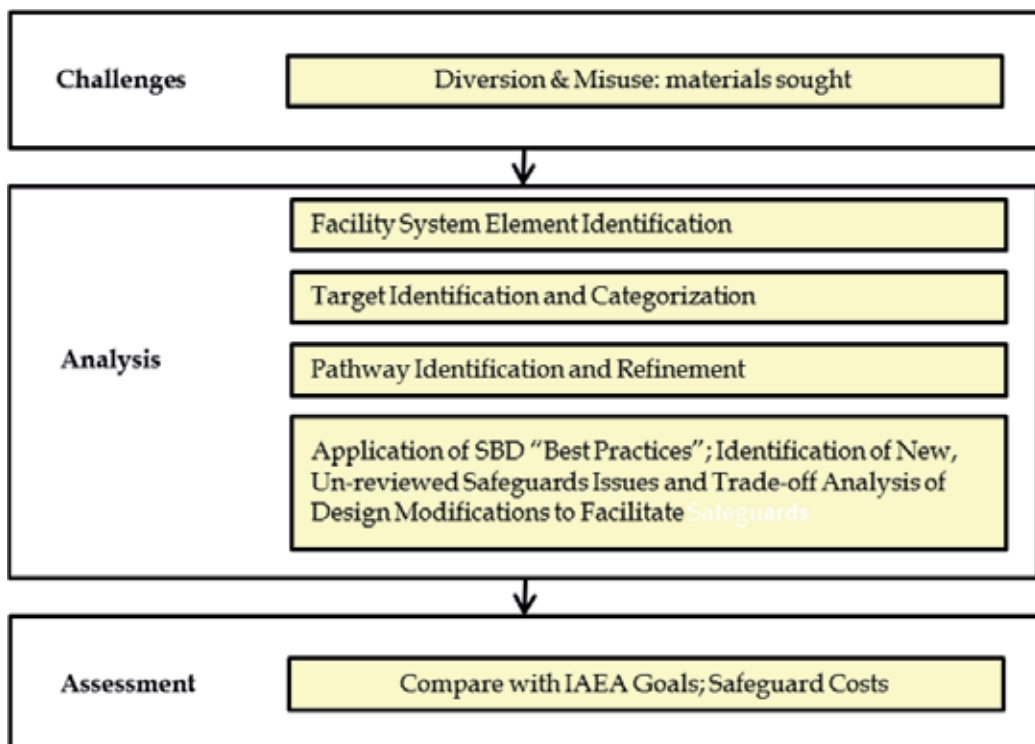


Fig. 4. Safeguards by Design Process (Wonder & Hockert, 2011)

## 7. Conclusion

New approaches for studying proliferation resistance continue to be developed and improved. Their goal is to help ensure that innovative nuclear energy systems are “unattractive and [the] least desirable routes for diversion or development of weapons-usable material.” The “Safeguards-By-Design” approach has become the subject of intense research because it makes use of safeguardability assessment tools such as proliferation resistance studies to improve the design and construction of new facilities in such a way that they will be easier and more cost efficient to safeguard. Stakeholders and decision makers in the nuclear energy field will need to understand, apply, and advance the concepts discussed here to effectively participate in the development of proliferation resistant nuclear facilities in the future.

Inquiry into the nature of proliferation resistance, the utility of different methodologies to study it, and the extent to which proliferation resistance studies offer useful and meaningful answers and insights for decision-makers continues. A growing body of literature is emerging on these subjects, and will continue to grow over the next several years. A new independent evaluation of proliferation resistance and proliferation resistance methodologies by the United States National Academy of Sciences will begin in the summer of 2011. The result will be a report to the U.S. Department of Energy in 2013 that should be particularly valuable in identifying the strengths and limitations of the concept of proliferation resistance and associated methodologies. Recommendations for whether and what types of additional methodology development activities should follow will be an important result of this work.

## 8. References

- Bari, R., (2009) *Proliferation Resistance and Physical Protection (PR&PP) Evaluation Methodology: Objectives, Accomplishments, and Future Directions*, Global 2009, Paris, France
- Bathke, C.; Jarvinen, G.; Wallace, R.; Ireland, J.; Hase, K.; Johnson, M.; Ebbinghaus, B.; Sleaford, B.; Bradley, K.; Charlton, W.; LeBouf, R.; Gariazzo C.; Ford D.; Beard C.; Landsberger S. & Whitaker M. (2007) *Proliferation Resistance Assessment Methodology for Nuclear Fuel Cycles*, *Nuclear Technology*, 157, 1 2007.
- Bjornard, T.; Hebditch, D.; Schanfein, M.; Bari, R. & Peterson, P. (2009) *Improving the Safeguardability of Nuclear Facilities*, *Journal of Nuclear Materials Management*, Summer 2009.
- Chang H. & Ko, W. (2010) *Proliferation Resistance: Acquisition/Diversion Pathway Analysis, Final Report of the INPRO Collaborative Project PRADA*, IAEA, November 2010, Vienna, Austria
- DeMuth, S. & Lockwood, D. (2010) *Safeguards by Design (SBD) for the Next Generation Safeguards Initiative (NGSI)*, IAEA Safeguards Symposium, Vienna, Austria, September 2010
- GIF002-00 (2002) *A Technology Roadmap for Generation IV Nuclear Energy Systems*, U.S. Department of Energy, Nuclear Energy Research Advisory Committee and the Generation IV International Forum, Washington, D.C., December 2002. Accessed March 11, 2011 Available from: <http://www.gen-4.org/Technology/roadmap.htm>

- IAEA, (2007) *Guidance for the Application of an Assessment Methodology for Innovative Nuclear Energy Systems - INPRO Manual Volume 5* (IAEA TECDOC- 1575), Vienna, Austria, 2007
- IAEA (2009), *Facility Design and Plant Operation Features that Facilitate the Implementation of IAEA Safeguards* (IAEA-STR-360), Vienna, Austria, February 2009.
- IAEA STR-332 (2002), *Proliferation Resistance Fundamentals for Future Nuclear Energy Systems* IAEA Department of Safeguards, Vienna, Austria, 2002.
- Greneche, D.; Rouyer, J. & Yazidjian, J. (2007) *Simplified Approach for Proliferation Resistance Assessment of Nuclear Systems - SAPRA, French Working Group on Proliferation Resistance and Physical Protection (GTR3P)*, France, February 2007.
- Kaplan, S. & Garrick, B. (1981) "On the Quantitative Definition of Risk," *Risk Analysis* Volume 1, Issue 1, pages 11-27, March 1981
- Li, J.; Yim, M. & McNelis, D (2009) "An Open Source Based Approach to Predict Nuclear Proliferation Decisions" *Proceedings of the 50th Annual Institute for Nuclear Material Management Meeting*, Tucson, AZ, July 12-16, 2009.
- Meyer, S (1984) *The Dynamics of Nuclear Proliferation*, The University of Chicago Press, Chicago, Illinois.
- Pomeroy G.; Bari, R.; Wonder, E.; Zentner, M.; Haas, E.; Killeen, T. Cojazzi, G., & Whitlock, J. (2008) *Approaches To Evaluation Of Proliferation Resistance Of Nuclear Energy Systems*; *Proceedings of the 49th Annual Institute for Nuclear Material Management Meeting*, Nashville, Tennessee, July 2008.
- PR&PP (2006), *Evaluation Methodology for Proliferation Resistance and Physical Protection of Generation IV nuclear Energy Systems*, Revision 5, November 30, GIF/PRPPWG/2006/005. Accessed March 10, 2011, Available from: <http://www.gen-4.org/Technology/horizontal/PRPPM.pdf>
- PR&PP (2009) 2009 PR&PP Evaluation: ESFR Full System Case Study Final Report GIF/PRPPSG/2009/002, *Proliferation Resistance and Physical Protection Evaluation Methodology Working Group*, June 2009.
- Singh, S. & Way, C. (2004) "The Correlates of Nuclear Proliferation: A Quantitative Test," *Journal of Conflict Resolution*, Vol. 48 (6), December 2004
- Skutnik, S.; Yim, M.; Liy, J.; & McNelisy, D, (2009) *Evaluating Proliferation Resistance and Security Needs of Nuclear Fuel Cycle Technologies through a Fuzzy-Logic Barrier Model*, ; *Proceedings of the 50th Annual Institute for Nuclear Material Management Meeting*, Tucson, Arizona 2009
- TOPS, (2001) *TOPS Task Force on the Nuclear Energy Research Advisory Committee, Technological Opportunities to Increase the Proliferation Resistance of Global Civilian Nuclear Power Systems (TOPS)*, U.S. Department of Energy, 2001.
- Whitlock, J, (2010) *Incorporating the GIF-PRPP Proliferation Resistance Methodology in Reactor Design*; *Proceedings of the 51st Annual Institute for Nuclear Material Management Meeting*, Baltimore, July 11-15, 2010
- Wonder, E. & Hockert, J. (2011), *Facility Safeguardability Analysis*, 33rd ESARDA ANNUAL MEETING, Budapest, Hungary, May 2011

- Zentner, M.; Pomeroy G.; Bari R.; Cojazzi G.; Haas E.; Killeen T.; Peterson P.; Whitlock J. & Wonder, E. (2009) *“Interpretation and Use of the Results of Proliferation Resistance Studies”*, Global 2009, Paris, France
- Zentner, M.; Therios, I.; Bari, R.; Cheng, L.; Yue, M.; Wigeland, R.; Hassberger, J.; Boyer, B. & Pilat, J. (2010) *An Expert Elicitation Based Study of the Proliferation Resistance of a Suite of Nuclear Power Plants*; Proceedings of the 51st Annual Institute for Nuclear Material Management Meeting, Baltimore, Maryland, July 2010

# Ethics of Nuclear Power: How to Understand Sustainability in the Nuclear Debate

Behnam Taebi  
*Delft University of Technology*  
*Netherlands*

## 1. Introduction

With the nuclear accidents in Fukushima Daiichi in Japan, the global public and political debate on nuclear power is rapidly reaching boiling point. On the one hand, it seems that nuclear power is losing public support. Japan intends to review its nuclear policy – one in every eight nuclear reactors is currently in that country – and China have planned one-year moratoriums on new nuclear power constructions. China's position is relevant since the country is set to become a world leader in the next decades: China currently has 13 operational nuclear power reactors, 27 reactors under construction, 50 planned and 110 that are proposed (WNA, 2011). More concretely, pro nuclear stances have led to a loss of political power in Angela Merkel's party in different regions in the recent German elections; Merkel's administration recently decided to phase out all German nuclear reactors (Dempsey & Ewing, 2011). Furthermore, the Swiss government abandoned plans to build new reactors and Italians rejected nuclear energy in a referendum. On the other hand, the extent of our dependency on nuclear power makes one wonder whether we are witnessing the end of the nuclear era; approximately 16% of the world's electricity is currently being produced in nuclear power plants. Perhaps it is more likely that a certain pragmatism with regard to securing domestic energy supplies and curbing carbon dioxide emissions will eventually dominate the debate; see in this connection president Barak Obama's recent plan to cut American oil import and diversify, indeed, in the direction of renewable energy, but to also include nuclear power (Wynn & Doyle, 2011).

Now, more than ever before, there is a need to reflect on the desirability of nuclear power. In such analysis proponents stress the abundant availability of nuclear resources, the ability to produce large amounts of energy with small amounts of fuel and the very low greenhouse gas production levels. It can also make industrialized countries less dependent on conventional energy sources that mainly have to be imported from other parts of the world. The detractors, on the other hand, would emphasize the accident risks of reactors – the unfolding disaster in Japan speaks for itself – the waste transport risks, the proliferation concerns or worries about the possibility that such technology can always be deployed for destructive purposes and, indeed, the matter of what to do with the long-lived radiotoxic waste.

In this paper, I do not intend to get involved in the general desirability debate. I assert that when carefully reflecting on the desirable *energy mix* for the future one needs to consider

nuclear energy in relation to other energy sources. In so doing, we should first be aware of the distinctive aspects of nuclear technology such as the effects that long-lived waste could have upon future generations. We should furthermore include different technological methods or *fuel cycles* in the production process as these methods deal differently with the distinctive aspects. This paper presents this comparison by focusing on the notion of sustainability and its philosophical origins in justice between generations, alternatively known as *intergenerational justice*.

Some people might object that *sustainable nuclear power* is a *contradictio in terminis*. Their objections probably arise from the fact that nuclear power leaves behind highly dangerous toxic waste with tremendous long life-times. This correctly relates to one interpretation of sustainability, but in a comprehensive analysis we need to include all the relevant interpretations. Sustainability could, for instance, also be seen as the endurance of energy resources for future generations. New technology in nuclear power production (i.e. nuclear breeders and multiple recycling of the waste) could facilitate the latter for a very long time. So, nuclear might be unsustainable in one interpretation and sustainable in another; precisely which one should be given priority might emerge after thorough moral analysis. Rather than using *sustainability* as an adjective, this paper sets out to clarify the notion by focusing on how nuclear power production affects the distribution of burdens and benefits over the different generations. Such an analysis can help decision-makers in the making of technically and ethically informed choices, when opting for a certain nuclear fuel cycle. It could also help when comparing nuclear power or, more to the point, a certain nuclear fuel cycle with other energy systems on the basis of the notion of how they affect the interests of people living now and in the future.

The paper consists of seven sections. In Section 2, I will elaborate on the ethical aspects of the notion of sustainable development, arguing that sustainability and intergenerational justice are closely intertwined. This section further elaborates on the question of what we should sustain for posterity. Section 3 focuses on a set of moral values which, together, encompass the value of sustainable development. These moral values will then be operationalized and connected to different steps of nuclear fuel cycles in Section 4. The latter Section further elaborates on the intergenerational conflicts between the values. The role of new technologies will be addressed in Section 5 and Section 6 reviews three challenges when assessing the social and political desirability of nuclear power. The final section concludes the paper with the findings in brief.

## 2. Sustainability and ethics

In the second half of the last century there was growing public awareness of the fact that the earth is a *living space* that we not only share with our ancestors but also with our children and grandchildren and with their offspring. The natural resources upon which our economies heavily depend seem to be running out as a result of the ever-rising world population and industrialization. In addition, the accompanying pollution presents a serious problem; we have been urged by the Club of Rome to consider ‘The Limits to Growth’ (Meadows et al., 1972). So, the technological progress that had once brought wealth and prosperity has come to create concerns for people living now and in the future. These genuine concerns eventually culminated in an Environment and Development report published by a United Nations’ commission with the very telling title ‘Our Common Future’. The first systematic definition of sustainable development emerged as an attempt to

balance economic growth and industrialization on the one hand with environmental damage on the other. Sustainable development as a kind of development that “meets the need of the present without compromising the ability of future generations to meet their own needs” (WCED, 1987, 43) was named after the commission’s chairwoman, the then Norwegian Prime Minister, Gro Harlem Brundtland.

Many of the analyses regarding the desirability of nuclear power seem to revolve around this notion of sustainable development and the specific interpretations made by different scholars and organizations (Elliott, 2007; IAEA, 2006; Turkenburg, 2004). The implicit assumption seems to be that sustainability is synonymous with social and political desirability. Proponents find nuclear energy sustainable as it can produce clean, secure and reliable electricity that does not put the earth’s climate in jeopardy (Bonser, 2002); other enthusiasts have more reservations but maintain that nuclear power can contribute to sustainable development in a “transitional role towards establishing sustainable [renewable] energy systems” (Bruggink & Van der Zwaan, 2002, p.151). The latter endorse the popular opinion that we are facing an “energy gap” in the coming decades which can only be filled with nuclear power (Connor, 2005; Pagnamenta, 2009). The detractors, on the other hand, are utterly resolute in their view that nuclear power is inherently “unsustainable, uneconomic, dirty and dangerous” (GreenPeace, 2006).

Even though Brundtland’s definition has been very influential in the academic and public domain, it requires further clarification, particularly from an ethical point of view. In other words, sustainability is not only a *descriptive* notion, merely stating the facts about the subject of a matter, but also one that should express *normative* opinions about what it is that we *should* sustain, why and how we *should* sustain it and for whom and how long we *should* sustain it (Raffaella et al., 2010). In this paper I will focus on these normative aspects in the case of nuclear power deployment. In the next section, sustainability will be presented as an overarching moral value encompassing certain other values.

Before getting into detailed discussion about what exactly sustainability should protect, let us pause for a moment to elaborate on the philosophical roots of the notion of sustainability. Brundtland’s sustainability is founded on principles of social justice viewed from two main angles: 1) the distribution of wealth among contemporaries or the *spatial* dimension and 2) the distribution of burdens and benefits between generations or the *temporal* dimension. Sustainability also has a third main theme, namely that of the relationship that human beings have with their natural environment which, again, has both a spatial and a temporal dimension. The question of how to value the environment in a moral discussion will be addressed in Section 3.

The two social justice notions that underlie sustainability are referred to as *intragenerational* and *intergenerational* justice. Obviously, in nuclear energy discussions intragenerational justice is relevant, for instance when addressing the question of where to build a nuclear reactor or in connection with issues concerning the distribution of the burdens and benefits between contemporaries; see for instance (Kasperson, 1983; Kasperson & Dow, 2005; Kasperson & Rubin, 1983). In this paper I will mainly focus on the long-term consequences of nuclear power and on the complex questions of intergenerational justice to which that gives rise; in Section 6 I will briefly discuss the issues of intragenerational justice.

## 2.1 Intergenerational justice and nuclear power production

Let me present and briefly discuss the central claim that underlies my analysis, namely that the production of nuclear power creates a problem of intergenerational justice. There are

two intergenerational aspects in nuclear power production that support this claim. Firstly, nuclear energy is produced from a non-renewable resource (uranium) that will eventually be less available to future generations. Stephen Gardiner (2003, 5) refers to this problem as “The Pure Intergenerational Problem” (PIP), which is in fact an exacerbated form of the Tragedy of the Commons, extended over generations. The Tragedy of the Commons is a situation in which various rational agents might be inclined to deplete limited resources on the basis of their own self-interest, while the same action will negatively affect the collective interest. The dilemma was first illustrated in an article compiled by Garrett Hardin, in which he pictured a pasture open to many herdsmen (Hardin, 1968). It is in individual interest of each herder to keep as much cattle as possible on the common ground while in collective terms such a strategy would culminate in the fast depletion of the common. Gardiner extends this argument to include different generations. He imagines a world that consists of temporally distinct groups that can asymmetrically influence each other; “earlier groups have nothing to gain from the activities or attitudes of later groups”. Each generation has access to a diversity of temporally diffuse commodities. It is in the individual interest of each generation to use as many as possible of these commodities, but it is in the collective interest of all temporally diffused generations if earlier generations would avoid depletion. Hence, engaging in activity with these goods poses the problem of justice between generations.

A second intergenerational aspect is the long-term consequences (e.g. pollution) that could be created for future generations, while benefits mainly accrue to the current (and immediately following) generations (Gardiner, 2003). A typical example of this intergenerational problem is the fossil fuel energy consumption situation, which is characterized by predominantly good immediate effects but deferred bad effects in terms of the anthropogenic greenhouse gas emissions that cause climate change. Intergenerational justice and climate change have received increasing attention in the literature in recent years (Athanasίου & Baer, 2002; Gardiner, 2001; Meyer & Roser, 2006; Page, 1999; Shue, 2003). The main rationale behind these discussions is that a change in a climate system that threatens the interests of future generations raises questions concerning justice and posterity.

Alongside the first (depletion) analogy that nuclear power production has with non-replaceable fossil fuel resources, both energy generation methods have potential long-term negative consequences in common. In the case of fossil fuel combustion, it is the emitting of greenhouse gases that can trigger long-term climatic change for posterity, while with nuclear power deployment, it is the creation of long-lived radiotoxic waste that could potentially pose safety and security problems to future generations. What exacerbates this problem is the fact that we – the present generation – are in a beneficial temporal position with regard to not yet existing generations and it is, therefore, quite convenient for us to visit costs on posterity, all of which makes us susceptible to “moral corruption” (Gardiner, 2006).

Intergenerational justice has already been an influential notion in discussions related to nuclear energy, particularly in relation to nuclear waste issues. The International Atomic and Energy Agency (IAEA) has laid down several principles on Radioactive Waste Management, in which concerns about the future were expressed in terms of the “achievement of intergenerational equity”<sup>1</sup> (IAEA, 1995). It was asserted that nuclear waste

---

<sup>1</sup> It should be mentioned that equity entails a narrower notion than justice. However in this paper I do not make a distinction between the two notions.



should be managed in such a way that it “will not impose undue burdens on future generations” (IAEA, 1995, Pr. 5). Many nations agree that this undue burdens clause must be taken to mean that nuclear waste should be disposed of in geological repositories which, it is believed, will guarantee the long-term safety of future generations (NEA-OECD, 1995). I will defer further discussion on this issue to Section 6.

## 2.2 What is it that we should sustain?

The notion of sustainable development implies that there is a certain good that we need to sustain for future generations. I will follow here Brian Barry (1999) in his discussions on the normative aspects of the notion of *sustainable development* and how that relates to the principle of intergenerational justice. Barry argues that there is an entity X which, as we enjoy it, should be *sustained* into the future so that future generations do not fall below our level of X. He then presents principles for the theorems of *fundamental equality*, two of which are the principle of responsibility – “[a] bad outcome for which somebody is not responsible provides a prima-facie case for compensation” – and the principle of vital interests: “locations in space and time do not in themselves affect legitimate claims ... [therefore] the vital interests of people in the future have the same priority as the vital interests of people in the present” (Barry, 1999, p 97-99).

The ensuing question is what this valuable entity of X should be. Barry proposes *opportunity* as a metric of justice: one requirement of justice is that above all else “the overall range of opportunities open to successor generations should not be narrowed” (Barry, 1978, p 243). So, whilst adhering to the guiding principle that we should not narrow the total range of opportunities, I will develop two other sustainability principles that will lead to the matter of how this main principle relates to nuclear power generation, the main rationale being that whenever we find ourselves in a position to *negatively influence the opportunities open to future generations* we should be careful not to narrow these opportunities.

We should recall the two intergenerational aspects of nuclear power production and how they could affect posterity’s equal opportunity. Firstly, we leave behind radiotoxic waste with tremendously long life-time spans. If not properly disposed of, this waste can influence the *vital interests* of future generations and thus also, their equality of opportunity. Hence, the first moral principle I am defending urges us to sustain posterity’s vital interests. Secondly, we are depleting a non-renewable resource, to which posterity has less access. If we assume that well-being significantly relies on the availability of energy resources then we are in a position to influence future opportunity for well-being. From the latter I derive the moral principle that we should sustain future generations’ opportunity for well-being insofar as that can be achieved through the availability of such energy resources. In the following section I will discuss these principles in detail.

## 3. The moral values at stake

So far I have argued that the notion of sustainable development needs further ethical clarification which has been provided in terms of the two moral principles that we have with regard to posterity, namely 1) to sustain future generation’s vital interest and 2) to sustain human well-being in the future. In this section I will elaborate on how to understand these principles in terms of the moral values at stake. But let me first say something about the meaning of *value* and why I intend to approach sustainability from the angle of moral values.

Questions about rightness and wrongness are generally subsumed under the heading of *values*. In everyday life, there are many things we uphold such as honesty and integrity; those things are referred to as values and they inspire social norms in human interaction. Outside this common sense meaning of the term, values are also relevant to many of the choices that we make, also with regard to technology; they reflect our understanding of the rightness and wrongness of those choices. The term value indeed has definitions that extend beyond philosophy and ethics. We find many things such as art and music valuable without making any reference to their moral goodness or rightness; these are indeed non-moral values. The focus of this paper is confined to the moral values that deal with how we want the world to be. In other words, moral values are things worth striving for in order to achieve a good life (Scanlon, 1998, p 78-79). However, we should not confuse values with the personal interests of individuals; values are the general convictions and beliefs that people should hold paramount if society is to be good. Those values in relation to the notion of sustainable development will be reviewed here; what are the things that we find valuable when we refer to sustainability and why do we find them valuable? More importantly, which value should be given priority if different values contradict or cannot be complied with simultaneously?

### 3.1 Sustaining human safety and security and the environment

Let us remind ourselves that one interpretation of sustainable development is that we should sustain the vital interests of future generations. Let us then explore for a moment what exactly is meant by Barry's principle of vital interest and how that relates to the principle that I am defending here. Barry (1999, 105) argues that taking equal opportunity seriously means that "the condition must be such as to sustain a range of possible conceptions of the good life"; such a good life will, in any case, include "adequate nutrition, clean drinking-water, clothing and housing, health care and education". Here my understanding of vital interest is applied to a very specific sense. I argued earlier in this paper that whenever we are in a position to negatively influence future opportunities we should be careful not to narrow those opportunities. One clear way in which we can negatively affect future interest is by inappropriately disposing of nuclear waste. My account of future generation's vital interest relates to the status of the environment and to the safety and security of future generations in so far as they depend on the actions of present generations and how we dispose of our nuclear waste.

Something first has to be said about how to approach issues relating to the environment in a moral discussion. One important issue when addressing 'values' is to determine whether a thing is worth striving for for its own sake or because it serves a greater good. To put this in philosophical terms, we must establish whether something has an *intrinsic* value or whether it has an *instrumental* value, thus requiring reference to an intrinsic value. This discussion is particularly relevant to the way in which we value nature and address human beings' relationships with the natural world. Generally, we can distinguish between two schools of thought: 1) anthropocentrism that situates human beings in the center of ethics; this is alternatively known as human supremacy or human-based ethics and 2) non-anthropocentrism that ascribes an intrinsic value to nature. These discussions relate to one of the central questions in the field of environmental philosophy and it is not my intention to get involved in that debate here. But let me just make one remark.

When it comes to the relationship between humans and non-humans, it is probably uncontroversial to ascribe designations such as moral wrongness; torturing animals is, for

instance, morally wrong. However, our focus in this paper is upon justice to future generations and I follow Barry (1999, p 95) in his suggestion that “justice and injustice can be predicated only of relations among creatures who are regarded as moral equals in the sense that they weigh equally in the moral scales”. Hence, in addressing intergenerational justice in this paper, we refer to the environment with regard to what it means in conjunction with safeguarding the vital interests of human beings. Such considerations would emanate from radiation hazards resulting from possible seepage of radiotoxic material into the environment, which in turn could affect human health and safety. Thus, in the anthropocentric approach adopted in this paper, the moral value of *environmental friendliness* basically relates to the issues that the value of *public health and safety* will raise and so it will be subsumed under the latter value. Indeed, one could defend a non-anthropocentric account of intergenerational justice and separate these two values. However, in discussing the sustainability issues of nuclear power deployment, these environmental concerns relate to exactly the same radiation levels that are relevant when assessing public health and safety issues. The only difference would thus be that an intrinsic value has been ascribed to the environment. In other words, the consequences of radiation in the environment should then be addressed without making reference to what these means for human beings.

#### **Public health & safety (environmental friendliness)**

Sustainability could be taken to relate to human health and safety and to the status of the environment. In its Fundamental Safety Principles, IAEA (2006, p 5) takes safety to “mean the protection of people and the environment against radiation risks”; this definition implies that the IAEA is defending a non-anthropocentric viewpoint. The latter is reiterated in IAEA’s Principles of Radioactive Waste Management, in which one of the key principles relates exclusively to the environment: “[r]adioactive waste shall be managed in such a way as to provide an acceptable level of protection of the environment” (IAEA, 1995, p 5). However, in a temporal sense and when it comes to protecting the future, the principles 5 (the protecting of future generations) and 6 (the burdens on future generations) in the latter IAEA document leave no room for misunderstanding, making it clear that the IAEA’s approach is anthropocentric and solely refers to future generations of human beings who should be protected (IAEA, 1995). The environment thus has here an instrumental value. Safety issues in nuclear power technology include “the safety of nuclear installations, radiation safety, the safety of radioactive waste management and safety in the transport of radioactive material” (IAEA et al., 2006, p 5). The value we link to these concerns is *public health & safety*, which pertains to the exposure of the human body to radiation and the subsequent health effects of radiation.

#### **Security**

*Security* is the next value that will be addressed in this analysis. In the IAEA’s Safety Glossary, nuclear security is defined as “any deliberate act directed against a nuclear facility or nuclear material in use, storage or transport which could endanger the health and safety of the public or the environment” (IAEA, 2007, p.133). One can argue that ‘security’ as defined here also refers to the safety considerations discussed above. We shall, however, keep the value of ‘security’ separate in this analysis so as to be able to distinguish between unintentional and intentional harm. Security also refers to extremely relevant proliferation considerations such as the using and dispersing of nuclear technology for destructive purposes. We define ‘security’ as the protecting of people from the intentional harmful effects of ionizing radiation resulting from sabotage or proliferation.

### 3.2 Sustaining future well-being

So far we have presented three values for sustaining the environment and humankind's safety and security. Another aspect of sustainability links up with the sustaining of human well-being, insofar as it relates to the resources. I will discuss the two values of resource durability and economic viability.

#### Resource durability

Sustainability could be thought to refer to the availability of natural resources and their continuation. Obviously, in discussions on energy production and consumption, the value of *resource durability* plays an important role. Brian Barry presents the theory of intergenerational justice as the appropriate consumption of non-renewable natural resources across time; "later generations should be left no worse off [...] than they would have been without depletion" (Barry, 1989a, p.519) Since it would be irrational to expect the present generation to leave all non-renewable resources to its successors and since replicating such resources is not an option either, Barry (1989a, 519) argues that we need to offer compensation or recompense for depleted resources "in the sense that later generations should be no worse off [...] than they would have been without depletion". We should remember that this reasoning has been presented by Barry in order to keep the range of opportunities open to posterity; "[t]he minimal claim of equal opportunity is an equal claim on the earth's natural resources" (Barry, 1989b, 490). I narrowed down this argument to include only those resources that we might have depleted in the process of nuclear power production. If we now look back on the period of industrial revolution up until the present it would be fairly straightforward to conclude that the availability of energy resources has played a key role in achieving well-being. So I argue that that we should compensate for a reduction in the opportunities for well-being as that can be brought about by energy resources. The value of resource durability is therefore defined as the availability of natural resources for the future or the providing of an equivalent alternative for the same function.

#### Economic viability

Some economists claim that "a development is sustainable if total welfare does not decline along the path" (Hamilton, 2003, p.419) and that "achieving sustainable development necessarily entails creating and maintaining wealth" (Hamilton, 2003, p 419-420).<sup>2</sup> The next value that I shall discuss in relation to sustainability is that of *economic viability*. One might wonder whether economic issues have an inherent moral relevance and whether it is justified to present economic durability as a moral value. On the one hand, one could argue that the safeguarding of the general well-being of society (also, for instance, including issues of health care) has undeniable moral relevance. On the other hand, our understanding of economic viability in this chapter solely relates to the issues that we have presented in relation to nuclear energy production and consumption. With this approach economic aspects do not therefore have any inherent moral relevance; it is what can be achieved with this economic potential that makes it morally relevant. This is why I present the value of economic durability in conjunction with other value. First and foremost, economic viability should be considered in conjunction with resource durability. In that way it relates to the economic potential for the initiation and continuation of an activity that helps in the providing of an alternative for the depleted resources. We will see in the next section that

---

<sup>2</sup> In this paper I do not make a distinction between welfare, well-being and wealth.

economic viability also becomes a relevant notion when we aim to safeguard posterity's safety and security by introducing new technology. In general, economic viability is defined here as the economic potential to embark on a new technology and to safeguard its continuation for the maintaining of the other discussed values.

#### 4. Operationalizing moral values: Assessing existing fuel cycles

Let us first recapitulate the moral values discussed in the preceding section. I argued that above all else, we should sustain *equal opportunity* for future generations. More to the point, we should safeguard posterity's vital interests and the well-being of posterity. To that end, five different interpretations of sustainable development have been presented in terms of five different moral values; the definitions of these values have been summarized in Table 1. In other words, in order to address the sustainability aspects of a certain technology (in our case the sustainability aspects of a certain nuclear fuel cycle), we need to first assess to what extent these values are safeguarded or compromised. To that end, the values should first be *operationalized*, meaning that we should assess the impacts of different stages in the production of nuclear power according to how these values are affected. In this operationalization process, we should take into consideration the fact that the values could relate to the interests of different groups of people belonging to different generations. In the remainder of this section I will first discuss different fuel cycles before going on to elaborate on how to assess the impacts of the fuel cycles according to such values.

Value	Explanation
<b>Environmental friendliness</b>	Preserving the status of nature to safeguard human health and safety
<b>Public health &amp; safety</b>	Protecting people from the accidental and <i>unintentional</i> harmful effects of ionizing radiation
<b>Security</b>	Protecting people from the <i>intentional</i> harmful effects of ionizing radiation arising from sabotage or proliferation
<b>Resource durability</b>	The availability of natural resources for the future or the providing of suitable alternatives
<b>Economic viability</b>	Embarking on a new technology and continuing that activity to safeguard one of the above values

Table 1. Five moral values that together constitute the overarching value of sustainability

##### 4.1 Existing nuclear fuel cycles: open and closed

Generally, there are two main methods, or nuclear fuel cycles, used for the production of nuclear power; namely open and closed fuel cycles. Both fuel cycles have a front-end phase, involving the mining and milling of uranium, enrichment and fuel fabrication, and a back-end phase involving the steps taken after irradiation in the reactor. Both cycles are more or less the same until the moment of initial irradiation in the reactor. I shall start by discussing these fuel cycles from the cutting point of the front-end and the back-end of the cycles, namely from the moment of irradiation in the reactor. What comes out of the nuclear reactor

is not necessarily *waste*; it would be better to refer to it as *spent fuel*. This is because precisely how we deal with this spent fuel determines the type of fuel cycle required. In the open fuel cycle, spent fuel is considered as waste. After irradiation the fuel in the reactor, the spent fuel, will be kept in interim storage on the surface for a couple of decades (basically to let it cool down) and it will then be disposed of in deep underground repositories. Since the fuel will be irradiated only once, this cycle is referred to as a once-through or an open fuel cycle. The disposed of waste should be isolated from the biosphere for the period that it constitutes a radiation risk; for an open fuel cycle this is about 200,000 years. This kind of fuel cycle is sometimes known as the American method, but it is also employed in certain other countries as well, like Sweden. The (black) solid arrows in Fig. 1 represent the open fuel cycle.

In the second method, spent fuel will be *reprocessed*. Reprocessing is a chemical process in which spent fuel can be recycled for two main purposes. Firstly, the still deployable materials in spent fuel (namely uranium and plutonium) will be separated in order to be reinserted into the cycle. That is why this method is called the closed fuel cycle; see in this connection the (red) dotted lines in Fig. 1. Separated uranium can be added at different front-end phases in the open fuel cycle; plutonium can be used to manufacture MOX (Mixed Oxide Fuel), which is a fuel based on a mixture of plutonium and uranium. The second reason for reprocessing is to substantially reduce the volume of the most long-lived type of waste; i.e. the most long-lived materials (again uranium and plutonium) will have been removed. The waste life-time in the closed fuel cycle amounts to about 10,000 years. The closed fuel cycle is more commonly known as the European method, but is also applied in some other countries like Japan. Both fuel cycle types are illustrated in Fig. 1.

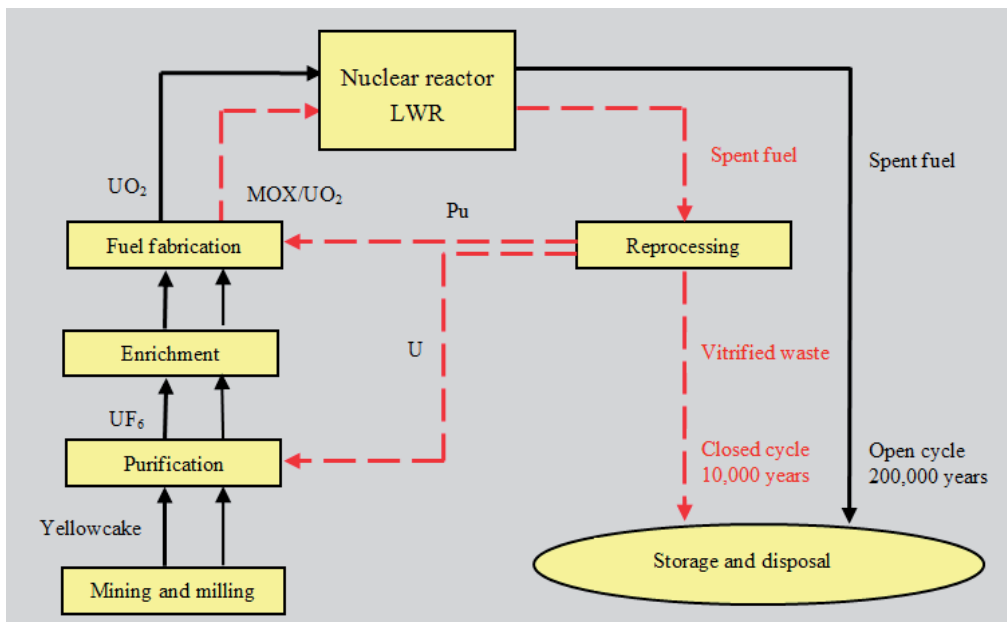


Fig. 1. Schematic representation of open and closed fuel cycles, together with the forecast waste life-times. The black solid lines represent the open fuel cycle and the red dotted lines illustrate the additional steps taken in the closed fuel cycle.

#### 4.2 Operationalization of values: Intergenerational assessment of fuel cycles

It would extend beyond the scope of this work to discuss in detail how the fuel cycles should be assessed according to the values presented, but I will briefly discuss the steps that we need to take in order to operationalize these values. First, we must link the impact of different steps in the fuel cycle to the values presented and evaluate to what extent those impacts are for present and future generations. Let me illustrate this with an example in which we shall operationalize the value 'public health & safety'.

First, when assessing safety issues in an open fuel cycle, we should at least address the following steps that relate in one way or another to the safety issues: 1) mining, milling, enrichment and fuel fabrication, 2) transport of (unused) fuel and spent fuel, 3) reactor operation and decommissioning period, 4) interim storage of spent fuel and 5) final disposal of spent fuel in geological repositories. These impacts have been mapped in Fig. 2.<sup>3</sup> In this figure, it has been assumed that nuclear power production will last for one generation, this is referred to as the Period for which the Activity Lasts (PAL). The first four steps particularly create risks in the short-term, which is slightly longer than the PAL. Especially the decommissioning period and the interim storage of spent fuel will last several decades longer. From the perspective of long-term safety concerns (issue number 5 above), there will be potential burdens after spent fuel has been situated in the geological repositories; these concerns will potentially last for the life-time of the spent fuel, or approximately 200,000 years. So the horizontal black arrow represents these long-term concerns extending into 'Generation n' in the future. Please note that here the value of 'environmental friendliness' is discussed in conjunction with the value of 'public health & safety'.

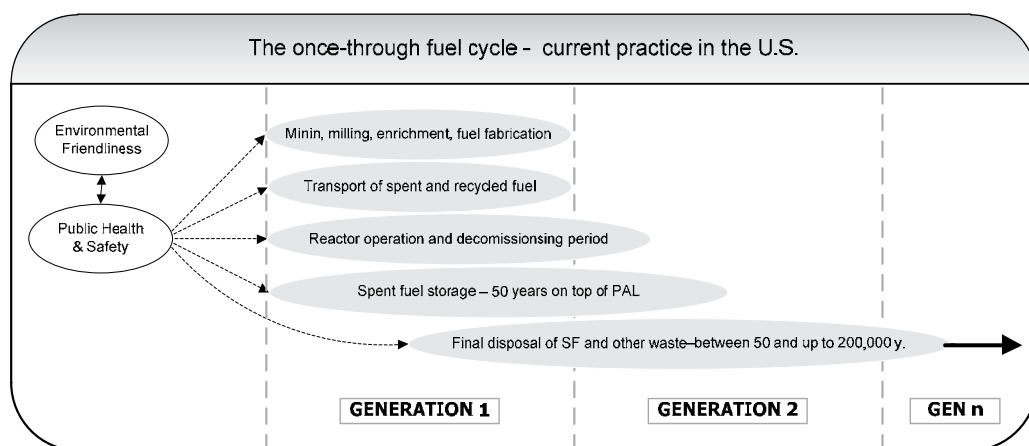


Fig. 2. Relating moral values to concrete fuel cycle steps. PAL stands for the Period for which the Activity Lasts and SF stands for spent fuel. This is a partial representation and a slightly modified version of Figure 3 in (Taebi & Kadak, 2010).

<sup>3</sup> This is a partial representation of a detailed analysis I have made elsewhere together with Andrew Kadak. Readers who are interested could consult this publication for a detailed operationalization of these values in relation to the two existing and the two future nuclear fuel cycles; see (Taebi & Kadak, 2010).

### 4.3 Intergenerational conflicts

Like in the example above, we can operationalize all the values and relate them to the concrete steps in the two fuel cycle. If we now draw a comparable burden-benefit chart for the closed fuel cycle, it should show that the safety concerns for remote future generations will substantially decrease; this is because the waste life-time of the closed cycle will be a factor of 20 less (approximately 10,000 year). From the perspective of future generations, the closed fuel cycle will thus score better on the issue of safety. However, in the short-term and from the perspective of Generation 1, more safety risks will be created since reprocessing is a chemical process that creates different types of nuclear waste that subsequently has to be disposed of (these are mainly different types of waste with shorter lifetimes). Reprocessing plants are furthermore situated in only a few countries, which means that countries that endorse the closed fuel cycle but have no reprocessing plants will be forced to go back and forth with their waste to the country that can do the reprocessing; this creates additional safety risks in relation to transportation. In Europe, the two commercial reprocessing plants are situated in the UK and France. Other European countries that endorse the closed fuel cycle have their waste reprocessed in one of these countries. Another short-term safety concern has to do with the using of plutonium as MOX in fuel. Plutonium is a very dangerous substance when inhaled. See in this connection the concerns that reactor 3 has been raising in the Fukushima Daiichi accident where MOX is being used as fuel in that reactor.

A similar analysis could be presented for the security concerns. Security relates to both *sabotage* and *proliferation* and it could be linked to the following steps in any open fuel cycle: 1) uranium enrichment, 2) reactor operation and the decommissioning period, 3) spent fuel storage and 4) the final disposal of spent fuel. All four issues have to do with the risk of sabotage. Issue number 1 has, in addition, a proliferation aspect as well. The naturally occurring uranium contains different *isotopes*. Since the isotope that is deployable in the conventional reactors ( $^{235}\text{U}$ ) is present in less than 1%, that uranium is enriched in order to make sure that more of that isotope will be present in the fuel. Enriched uranium to 3 (up to 10) percent is usually used for civil energy production purposes. However, the further enriching of uranium (up to 70% and higher) makes it a suitable material for weapon production. The Hiroshima bomb contained about 65 kilogram of 80% enriched uranium.

If we now assess the security concerns of the closed fuel cycle, one important issue will appear in relation to proliferation, namely the issue of the separation of plutonium during reprocessing. In addition to highly enriched uranium, plutonium is also deployable in nuclear weapons; the Nagasaki bomb contained 8 kilograms of weapon-grade plutonium. Plutonium, which usually emanates from civil reactors, is usually of a much lower quality for weapon production, but it does carry serious proliferation risks.<sup>4</sup>

Let us continue with the value of resource durability in our two fuel cycles. If the 2008 uranium consumption rate were continued, there would be enough *reasonably priced uranium* available for approximately 100 years (IAEA-NEA, 2010). Obviously, if many more countries join the nuclear club in the next couple of decades this availability will substantially decrease. It is, however, important to note that this uranium availability constitutes a reference to geological certainty and production costs. If we include estimations of all the available resources (in seawater and in phosphates), this will rise

---

<sup>4</sup>For a more technical discussion on the different isotopes of plutonium and the risk of proliferation, please consult (Taebi, Forthcoming).



significantly (IAEA-NEA, 2010). Yet, the open fuel cycle depletes the resources of reasonably priced uranium much faster. The closed fuel cycle, on the other hand, extends the period of availability of uranium, since reprocessed uranium and plutonium is reused. The conclusion thus seems straightforward. Closed fuel cycles should be preferred from the perspective of resource durability for future generations.

The last issue is the one of economic viability. As stated earlier, reprocessing plants are situated in a very limited number of countries. That is partly because of security concerns in conjunction with proliferation, but what is at least of equal importance, is the fact that reprocessing plants are very expensive. So, for countries with a small number of nuclear reactors, it is not worth while building their own reprocessing plant. Purely from the economic perspective, the open fuel cycle would then be preferred.

Let us now make an overall comparison between the two fuel cycles from the justice angle. From the perspective of the present generation, the open fuel cycle would be preferred, since it creates less safety and security risks and is less costly. The closed fuel cycle is, on the hand, more beneficial from the point of view of future generations, because it reduces the long-term safety concerns of waste disposal and because it helps extend non-renewable resources farther into the future. At the same time, the closed cycle creates more short-term safety and security concerns and economic burdens. This cuts right to the heart of the central issue of this paper, namely that of intergenerational justice. The questions that need to be answered are the following. Does intergenerational justice require that we reduce the waste life-time and enhance the resource availability into the future? If so, are the additional current burdens of the closed fuel cycle sufficiently justified?<sup>5</sup>

## **5. Sustainability as an ethical field of tension: The progress of technology**

When opting for a certain fuel cycle, we first need to express opinions with regard to the moral relevance of the values presented for different generations. After the accidents in Japan, we could for instance conclude that if we want to continue on the nuclear path, we will have to reduce the safety burdens for the present generations as much as possible. So, in terms of our values, we rank the moral relevance of the value of 'public health & safety' in the short-term higher than all of the other values. In such an example, the open fuel cycle with its fewer nuclear activities must be favored. On the other hand, if we now conclude that as producers of nuclear power we are the main ones responsible for reducing its future burdens, we give the same value of 'public health & safety' for future generations higher moral priority; the closed fuel cycle would then become an attractive option.

Then discussion concerning the prioritizing of moral values will gain particular relevance when we come to address technological advancement. Even though technology has no inherent moral value as such, it does enable us to comply better with other moral values. Also in questions regarding the development of new technologies for the future, it is important to be clear on the purpose of this technology, or to put it in philosophical terms, to be clear about which values this technology should improve for which group of people or which generation. Before moving on to discuss new technologies and how they could affect values, let me first say something about the interdependency of these values. Rather than contemplating them in isolation, it is actually the combination of these values which goes towards forming the overarching value of sustainability. We could liken our set of values to

---

<sup>5</sup> See for a detailed discussion of this issue (Taebi & Kloosterman, 2008).

several American football balls held tightly together with springs; see in this connection Fig. 3.<sup>6</sup> Hitting any one of these *balls* will inevitably affect the others in the construction. In other words, by presenting new technology, we might be able to comply better with any one of these values, but we should at the same time evaluate how that would affect the remaining values. This is why I am presenting our set of values as an *ethical field of tension*. Let me explain this by giving an example.

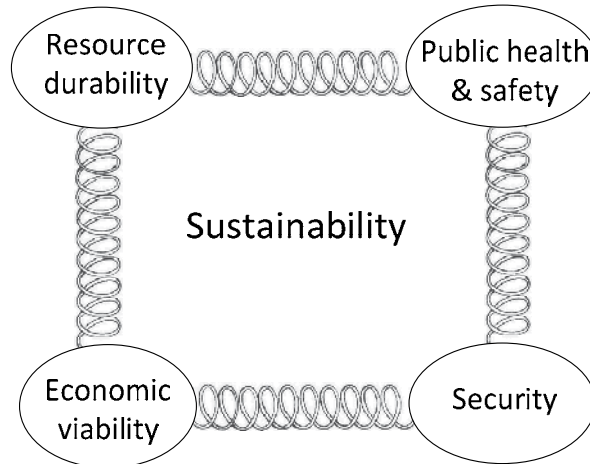


Fig. 3. Schematic representation of sustainability in an ethical field of tension

Due to its radiotoxic nature and extremely long lifetime, nuclear waste is perceived to be the Achilles heel of nuclear energy production. Serious attempts have been made to further reduce its lifetime. A new technology for the latter purpose is that of Partitioning and Transmutation (P&T). This is a complementary method to the closed fuel cycle that involves separating and dividing (partitioning) the materials remaining after reprocessing so that they can afterwards be eliminated (transmuted) in Fast Reactors; these reactors can irradiate the radionuclides that the currently operational thermal reactors cannot irradiate. If completely successful P&T will, it is expected, make the waste lifetime five to ten times shorter when compared to closed fuel cycle waste. After P&T, waste radiotoxicity can decay to a non-hazardous level within the space of hundreds of years, i.e. 500 to 1000 years (KASAM, 2005, Ch 8).

However, P&T is merely a technology that has been scientifically proven at lab level. It still requires decades of development which, in turn, will necessitate serious investments in this technology (NEA-OECD, 2002). Furthermore, the industrialization of P&T requires the building of many more facilities, both nuclear reactors and new reprocessing facilities. All these additional safety, security and economic burdens will have to be borne by contemporaries or at least by those nations that are capable of developing the technology; due to the inherent technological implications and complexity, not all countries will be capable of developing or deploying this technology (IAEA, 2004). To conclude, while P&T is capable of improving the value of 'public health & safety' in the long run, it is

<sup>6</sup>Please note that the value of 'environmental friendliness' has been subsumed under the value of 'public health and safety'.

compromising short-term 'public health & safety' and 'security'. In addition, the economic burdens will mainly be borne by the present and the immediately following generation. In other words, P&T (as an extension to reprocessing) presents an exacerbated form of the intergenerational dilemmas of the closed fuel cycle.<sup>7</sup>

Similarly, we could present fast reactors in the configuration of nuclear breeders in order to breed (make) more fuel than they consume. Breeders are capable of *consuming* the major isotope of uranium (<sup>238</sup>U) that is present for more than 99% in natural uranium. From the point of view of 'resource durability' such a breeder fuel cycle (with multiple recycling) could be very beneficial; we would then use the same natural uranium far more efficiently, all of which would extend the period of its durability. However, from the perspective of short-term concerns such a fuel cycle will bring comparable safety, security and economic burdens to P&T. It is particularly in conjunction with the abundant presence of plutonium and the ensuing proliferation concerns that this cycle method has never attracted serious attention. The term 'plutonium economy' usually refers to the using of plutonium as MOX in a closed fuel cycle and also to a fuel cycle with nuclear breeders.

In short, new technology can contribute to an improvement in moral values. It is therefore important that we include the progress of technology in our moral analysis. For one thing, in a discussion focused on what we *ought to* do for future generations, it is important to first be aware of what we *can* do, technologically speaking. This is the added value of this type of applied ethics in which solutions can be proposed within the realm of *technological realities* and in the light of the progress of technology. For another thing, we should then bring this *solution* back in the ethical field of tension proposed earlier in this chapter. How would the other values be affected by the introduction of this technology? Again, the question of how these values should be ranked in terms of their moral relevance should be determined during public and political discourse.

## 6. Challenges of assessing social and political desirability of nuclear power

In the preceding sections I approached the notion of sustainability as a moral value consisting of several other values. Different nuclear fuel cycles can now be assessed in terms of how well they safeguard or jeopardize these moral values for present and future generations; this gives rise to issues of intergenerational justice. What is now the relationship between these moral discussions and policies? How influential could and should these justice principles be when policy-makers need to deal with serious choices and trade-offs?

I shall elaborate on this issue by giving an example of where tangible nuclear waste management policy and fundamental philosophical discussions on justice to posterity are closely intertwined. The IAEA's principle of avoiding "undue burdens" on future generations is one that has been endorsed by all members of IAEA and it forms part of the current national policies on nuclear waste management. However, what this "undue burdens" clause precisely entails remains a moot point. Indeed, we cannot completely prevent harm to future generations and as the principle implies, there must then be a certain degree of *due burdens* that we are allowed to impose on posterity. It has been argued that

---

<sup>7</sup> The intergenerational distribution of the burdens and benefits of different fuel cycles is more precisely and extensively discussed in a joint paper written with Andrew Kadak (Taebi & Kadak, 2010). The breeder fuel cycle was also assessed in this paper.

this principle is best complied with when we dispose of nuclear waste in geological repositories that are situated a couple of hundred meters underground (NEA-OECD, 1995); the possible harmful consequences of a geological repository in the long run is then tacitly taken to mean *due harm*.

It is the combination of the engineered barrier (i.e. canisters stored in concrete containers) and the natural barrier (i.e. geologic formations) that makes repositories favorable from the point of view of long-term safety (Chapman & McCombie, 2003, 27-31). However, the tremendous long-term uncertainties that repositories bring (Macfarlane & Ewing, 2006) make it difficult to guarantee equal safety for distant future generations (Shrader-Frechette, 1993, 1994; Taebi, Forthcoming). In the case of the Yucca Mountains repositories, once the location had been designated for the permanent disposal of American spent fuel for a million years, an interesting distinction was made between different future people: “a repository must provide reasonable protection and security for the very far future, but this may not necessarily be at levels deemed protective (and controllable) for the current or succeeding generations” (EPA, 2005, 49036). People living in the next 10,000 years deserve a level of protection equal to the current level and the generations belonging to the period extending beyond 10,000 years could conceivably be exposed to a much higher radiation limit. The underlying argument for this distinction is sought in the low degree of predictability for the remote future and the fact that any positive influence on such societies is meaningless, all of which is believed to diminish our responsibility towards future generations.

As a matter of fact, this issue relates to another intergenerational aspect of the notion of sustainability that I was merely hinting at in Section 2, namely that of for whom (and for how long) we should sustain the valuable entity of X? If we now agree that through the inappropriate disposal of nuclear waste, we can affect the vital interests of future generations, and if we again agree that location in time and space does not provide sufficient moral ground for treating people differently (in accordance with Barry’s (1999) principles of fundamental equality), we can now argue that this distinction between different people of the future is ethically problematic. The arguments provided for proposing this distinction are more pragmatic reasons for why we cannot act otherwise than solid moral justifications. The discussions on tangible policies should, therefore, be preceded by the more fundamental discussions on what our relationship with posterity should be.<sup>8</sup>

When addressing the desirability of a certain fuel cycle for the future we should incorporate the social and economic context within which policies are articulated. One possible conclusion to a moral analysis could be that if we decide to continue on the nuclear path, the P&T method as an addition to the closed fuel cycle should be favored, since it has many advantages in terms of substantially reducing the waste lifetime and the potential future burdens.<sup>9</sup> However, as argued in Section 5, the further developing of this method as well as its industrialization will create substantial safety and security burdens for present generations; how can the policy-maker justify these additional burdens? Last but certainly not least, in policy-making there is the question of the legitimacy of the financial efforts that

---

<sup>8</sup> For a detailed discussion on Yucca Mountains Radiation Standards, please see (Vandenbosch & Vandenbosch, 2007). Elsewhere I argue that the proposed distinction must urge us to reconsider other waste management possibilities that could be used to help reduce waste lifetime and potential future burdens (Taebi, Forthcoming).

<sup>9</sup> This argument is extensively defended elsewhere (Taebi, 2011).

are required to make all of this happen. Indeed, these considerations have always been crucial to policy-making and will most probably always remain so. However, what we tend to forget is that our choices today have serious consequences for the interests of the people who happen to come after us. I am therefore endeavoring to shift the focus of the analysis on nuclear energy production and nuclear waste management policies. In other words, since we, the present generation, are enjoying the lion's share of the benefits of nuclear power; justice requires us to remain responsible for its burdens. The challenges mentioned should not, however, be taken too lightly. One important aspect would, for instance, be that of the distribution of these additional burdens among the currently living generations.

A highly relevant question in policy-making is that of whether nuclear power should be considered to be a viable option in the future of energy provision. I started this paper by circumventing this general desirability discussion surrounding nuclear energy. It is, however, worthwhile considering what this analysis can contribute to that public and political discourse. As stated earlier, we should not consider nuclear power in isolation but address its desirability in the broader perspective of the desirable *energy mix*; the moral insights offered here could help one distinguish between different fuel cycles, all of which can facilitate a comparison between a certain nuclear fuel cycle and another specific energy system. We can, for instance, compare the P&T cycle with the waste that remains radiotoxic for a couple of hundred years with a certain fossil fuel system that contributes to a change in the climate system. Such comparisons could be made based on considerations of intergenerational justice, or on how they affect the interests of *both* the present and future generations.

When one compares two non-renewable energy systems, focusing on the intergenerational aspects of sustainability would help us to facilitate a comparison based on moral grounds. We should then distinguish between the nature and longevity of those long-term effects; the latter is, for instance, different for oil and nuclear power both in terms of the type of the consequences and the period for which those consequences will be present. These intergenerational arguments lose, however, relevance when we assess a renewable energy system; there is no depletion of a non-replaceable resource and there are often far fewer, or virtually no more, long-term consequences. Even though renewability is an important aspect of sustainability and – we want to eventually move towards these renewable systems – we should also be aware of the societal and ethical consequences of such energy systems. When addressing the desirability of renewable energy resources, we should instead focus on the spatial aspects of sustainability and on the questions of intragenerational justice that are raised for the generations currently alive. For instance, when assessing the desirability of biofuel there are the issues of land use, water consumption and the possible effects of producing biofuel from food crops that could potentially exacerbate the problem of hunger.<sup>10</sup>

When it comes to comparing different energy systems, we encounter at least two types of implications, namely 1) how to compare different types of burdens and benefits and 2) how to value future burdens and benefits in relation to present burdens and benefits. In economic studies and investment decisions with potential benefits for the future, these issues have been dealt with in *cost-benefit analyses* (CBA) that can be used to identify and quantify different costs and benefits over the course of time. CBA is grounded in the ethical

---

<sup>10</sup> The British Royal Society has represented a comprehensive analysis of how to assess the sustainability of biofuel; see (Pickett et al., 2008).

theory of *utilitarianism* which asserts that the moral worth of any action should be assessed in terms of how it maximizes overall utility (alternatively referred to as well-being or happiness). For the sake of calculation, economists argue that we could express all the costs and benefits in terms of their monetary value. Since the value of different commodities declines over the course of time, the future value of these benefits will be determined on the basis of their present value *discounted* for time.

While CBA and discounting are undisputed<sup>11</sup> and sometimes desirable for certain short-term decisions in policy-making, the whole matter becomes complicated and even controversial when there is more at stake than just monetary costs and benefits, or when we need to account for the detrimental effects and benefits of the distant future. The first issue is the problem of *incommensurability*. How should we incorporate human lives, environmental damage and long-term radiation risks into a CBA? Although there are ways of expressing such concerns in terms of monetary units, all the approaches face the problem of comparing matters that are essentially incomparable. The second issue, accounting for harm and benefit in the distant future, raises questions about the moral legitimacy of discounting (Cowen & Parfit, 1992). Discounting is particularly controversial in the case of non-economic decisions, for example when decisions are made from an intergenerational point of view in the way advocated in this paper (see for an overview (Portney & Weyant, 1999)).

There are many philosophical objections to the applications of a CBA (see for an overview (Hansson, 2007)), but at least two of these objections are worth mentioning here. Firstly, CBAs fail to address the distribution issue between generations and, secondly, if we are to discount risks in the remote future, the policies for mitigating climate change and disposing of nuclear waste will be seriously undermined. The following example may serve to illustrate this: at a discount rate of 5 percent, one death next year becomes *equivalent* to more than a billion deaths in 500 years. It would be outrageous to include such conclusions in the assessment of future risks. In light of the fact that we are considering tremendously long periods of time, discounting – even at a very small rate – will make future catastrophes morally trivial (Parfit, 1983).

To conclude, policy-making on nuclear power production and nuclear waste management needs to include fundamental discussions on our relationship with posterity and to address issues surrounding the distribution of burdens and benefits between generations and also among the present generation. Since economic instruments such as CBA offer no solace, policy-making in nuclear technology should go hand in hand with more fundamental moral discussions.

## 7. Conclusion

Nuclear power production and consumption gives rise to the problem of intergenerational justice as we are using uranium, which is a non-replaceable resource, and as the remaining radiotoxic waste creates potential burdens extending into the very distant future. Since future interest is subject to present action, we have every reason to include posterity's interests in our decision-making in the area of nuclear power production. In my arguments,

---

<sup>11</sup> There are at least two issues that can make short-term CBA problematic. Firstly, the question of how to express the value of goods in terms of money; e.g. what is the economic value of rainforests? Secondly, there is disagreement on the interest rate of discounting when considering future effects; the rate can seriously influence the outcome.

I presented the notion of sustainable development as a moral value and elaborated on its relationship with intergenerational justice. Following Barry, I argued that we should sustain future generation's opportunity for well-being insofar as that can be accomplished with the available energy resources and their vital interests. I then introduced a set of moral values which, in combination with each other, comprise the overarching value of sustainability. The values 'environmental friendliness', 'public health & safety' and 'security' together safeguard the vital interests of future generation; the values 'resource durability' and 'economic viability' help to sustain future well-being.

The impacts of different nuclear fuel cycles were then assessed according to how they affect the values presented. In this operationalization process, we took into consideration the fact that the values could relate to the interests of different groups of people belonging to different generations. The two existing fuel cycles were then compared according to their values; the open fuel cycle could best be associated with short-term benefits and the closed fuel cycle with long-term benefits and the accompanying short-term costs. All of this gives rise to an intergenerational conflict of interests between those alive today and future generations.

The ranking of these values with regard to their moral relevance requires thorough public and political discourse. This is particularly relevant when assessing the desirability of new technology. Even though technology has no inherent moral relevance, it does help improve other values. In a moral discussion on what we *ought to do* for future generations, it is important to first be aware of what we *can do*, technologically speaking. This is the added value of this type of applied ethics in which solutions can be proposed within the realm of *technological realities* and in the light of technological progress. Indeed, the impacts of these new technologies should then be assessed in the ethical field of tension of sustainability, as has been proposed here. It is then worthwhile considering how other values will be affected by the introduction of this technology?

When it comes to policy-making for nuclear power deployment, we need to address several ethical issues regarding our relationship with posterity and the intergenerational distribution of benefits and burdens. Therefore, policies on nuclear power should be accompanied by thorough moral analysis. One possible conclusion arising from such analysis could be that we, the present generations who are enjoying the lion's share of the benefits of nuclear power, should remain responsible for dealing with its waste. This supports the application of P&T that reduces the waste lifetime and therefore also the potential future burdens. Before P&T can be introduced, decades of research and development still need to take place. Several technological challenges, both in the development of reprocessing technologies and in the development of fast reactors still have to be surmounted and the development and ultimate deployment of P&T will create considerable burdens (including certain economic burdens) for contemporaries. So, if the result of the moral discussion is that we want to be able to apply P&T, then this technology should be high on the research agenda so that it can become a serious alternative in the near future; one that is both technically feasible and economically affordable. The decision-maker should be aware of the technological state-of-the-art and of the cost that the development of a certain technology, desirable or not, creates for the present generation. This paper aims to contribute to that awareness.

## 8. References

- Athanasiou, T. & Baer, P. (2002). *Dead heat: Global justice and global warming*. New York: Seven Stories Press.

- Barry, B. (1978). Circumstances of justice and future generations. In B. Barry, & I. Sikora (Eds.), *Obligations to future generations* (pp. 204-248). Philadelphia: Temple University Press.
- Barry, B. (1989a). The Ethics of Resource Depletion. In *Democracy, Power and Justice, Essays in Political Theory* (pp. 511-525). Oxford: Clarendon Press.
- Barry, B. (1989b). Justice as Reciprocity. In *Democracy, Power and Justice, Essays in Political Theory* (pp. 463-494). Oxford: Clarendon Press.
- Barry, B. (1999). Sustainability and Intergenerational Justice. In A. Dobson (Ed.), *Fairness and Futurity: Essays on Environmental Sustainability and Social Justice* (pp. 93-117). New York: Oxford University Press.
- Bonser, D. Nuclear Now for Sustainable Development. In *World Nuclear Association Annual Symposium, London, 4-6 September 2002 2002*
- Bruggink, J. J. C. & Van der Zwaan, B. C. C. (2002). The role of nuclear energy in establishing sustainable energy paths. *International Journal of Global Energy Issues*, 18(2), 151-180.
- Chapman, N. & McCombie, C. (2003). *Principles and Standards for the Disposal of Long-lived Radioactive Wastes* (Waste Management Series, 3 ). Amsterdam: Elsevier.
- Connor, S. (2005, November 29, 2005). Nuclear power: We are heading for an energy gap, but what can fill it? *The Independent*.
- Cowen, T. & Parfit, D. (1992). Against the Social Discount Rate. In P. Laslett, & J. S. Fishkin (Eds.), *Justice Between Age Groups and Generations* (pp. 144-161). New Haven & London: Yale University Press.
- Dempsey, J. & Ewing, J. (2011, May 30, 2011). Germany, in Reversal, Will Close Nuclear Plants by 2022. *The New York Times*.
- Elliott, D. (2007). *Nuclear or not? Does nuclear power have a place in a sustainable energy future?* Hampshire: Palgrave Macmillan.
- EPA (2005). Public Health and Environmental Radiation Protection Standards for Yucca Mountain. 40 CFR Part 197, Part II. Washington D.C.: Office of Radiation and Indoor Air U.S. Environmental Protection Agency.
- Gardiner, S. (2001). The Real Tragedy of the Commons. *Philosophy and Public Affairs*, 30(4), 387-416.
- Gardiner, S. (2003). The Pure Intergenerational Problem. *The Monist*, 86(3), 481-501.
- Gardiner, S. (2006). A Perfect Moral Storm: Climate Change, Intergenerational Ethics and the Problem of Moral Corruption. *Environmental Values*, 15(3), 397-413.
- GreenPeace (2006). *Nuclear Power, Unsustainable, Uneconomic, Dirty and Dangerous, A Position Paper*. Paper presented at the UN Energy for Sustainable Development, Commission on Sustainable Development CSD-14, , New York,
- Hamilton, K. (2003). Sustaining Economic Welfare: Estimating Changes in Total and Per Capita Wealth. *Environment, Development and Sustainability*, 5(3), 419-436.
- Hansson, S. O. (2007). Philosophical Problems in Cost-Benefit Analysis *Economics and Philosophy*, 23(02), 163-183.
- Hardin, G. (1968). The Tragedy of the Commons. *Science*, 162(3859), 1243-1248.
- IAEA-NEA (2010). Uranium 2009: Resources, Production and Demand. *A joint report by the OECD Nuclear Energy Agency and the International Atomic and Energy Agency*. Paris: IAEA and NEA-OECD.
- IAEA (1995). The principles of radioactive waste management. *Radioactive waste safety standards programme*. Vienna: IAEA.



- IAEA (2004). *Technical Implications of Partitioning and Transmutation in Radioactive Waste Management*. Vienna: IAEA.
- IAEA (2006). *Nuclear Power and Sustainable Development*. (pp. 39). Vienna: IAEA.
- IAEA (2007). *IAEA Safety Glossary, Terminology Used in Nuclear Safety and Radiation Protection*. Vienna: IAEA.
- IAEA; Euratom; FAO; IAEA; ILO; IMO, et al. (2006). *Fundamental Safety Principles IAEA Safety Standards Series No. SF1*. Vienna: A joint publication of Euratom, FAO, IAEA, ILO, IMO, OECD-NEA, PAHO, UNEP, WHO
- KASAM (2005). *Nuclear Waste State-of-the-art reports 2004*. In S. Norrby, M. Stenmark, C. R. Brakenhielm, H. Condé, T. L. Andersson, & R. Sandström (Eds.). Stockholm: National Council for Nuclear Waste (KASAM), Sweden.
- Kasperson, R. E. (1983). *Equity Issues in Radioactive Waste Management*. Cambridge, MA: Oelgeschlager, Gunn & Hain Publishers.
- Kasperson, R. E. & Dow, K. M. (2005). Developmental and Geographical Equity in Global Environmental Challenge: A Framework for Analysis. In J. X. Kasperson, & R. E. Kasperson (Eds.), *The social contours of risk: publics, risk communication and the social amplification of risk (volume 1)* (pp. 246-264). London: Earthscan.
- Kasperson, R. E. & Rubin, B. L. (1983). Siting a Radioactive Waste Repository: What Role for Equity? In R. E. Kasperson (Ed.), *Equity Issues in Radioactive Waste Management* (pp. 118-136). Cambridge, MA: Oelgeschlager, Gunn & Hain Publishers.
- Macfarlane, A. & Ewing, R. C. (2006). *Uncertainty underground: Yucca Mountain and the nation's high-level nuclear waste*. Cambridge, MA: MIT Press.
- Meadows, D. H.; Meadows, D. L.; Randers, J. & Behrens, W. W. (1972). *The limits to growth: a report for the Club of Rome's project on the predicament of mankind*: Universe Books New York.
- Meyer, L. H. & Roser, D. (2006). Distributive Justice and Climate Change. The Allocation of Emission Rights. *Analyse & Kritik* 28, 241-267.
- NEA-OECD (1995). *The Environmental and Ethical Basis of Geological Disposal of Long-lived Radioactive Wastes: A Collective Opinion of the Radioactive Waste Management Committee of the Nuclear Energy Agency*. Paris: Nuclear Energy Agency, Organisation for Economic Co-operation and Development.
- NEA-OECD (2002). *Accelerator-driven systems (ADS) and fast reactors (FR) in advanced nuclear fuel cycles: a comparative study*. Nuclear Energy Agency, Organisation for Economic Co-operation and Development.
- Page, E. (1999). Intergenerational Justice and Climate Change. *Political Studies*, 47(1), 53-66.
- Pagnamenta, R. (2009, August 5, 2009). Nuclear power 'needed to fill energy gap'. *The Times*.
- Parfit, D. (1983). Energy Policy and the Further Future: the social discount rate. In D. MacLean, & P. G. Brown (Eds.), *Energy and the Future* (pp. 31-37). Totowa, NJ: Rowman and Littlefield.
- Pickett, J.; Anderson, D.; Bowles, D.; Bridgwater, T.; Jarvis, P.; Mortimer, N., et al. (2008). *Sustainable Biofuels: Prospects and Challenges*. London, UK: The Royal Society.
- Portney, P. R. & Weyant, J. P. (Eds.). (1999). *Discounting and Intergenerational Equity*. Washington DC: Resources for the Future.
- Raffaella, R.; Robison, W. & Selinger, E. (Eds.). (2010). *Sustainability Ethics: 5 questions*. Copenhagen: Automatic Press.

- Scanlon, T. M. (1998). *What We Owe to Each Other*. Cambridge, MA: Belknap Press of Harvard University Press.
- Shrader-Frechette, K. (1993). *Burying Uncertainty: Risk and the Case Against Geological Disposal of Nuclear Waste*: University of California Press.
- Shrader-Frechette, K. (1994). Equity and nuclear waste disposal. *Journal of Agricultural and Environmental Ethics*, 7(2), 133-156.
- Shue, H. (2003). Climate Change. In D. Jamieson (Ed.), *A Companion to Environmental Philosophy* (pp. 449-459). Malden, MA: Blackwell Publishing.
- Taebi, B. (2011). The Morally Desirable Option for Nuclear Power Production. *Philosophy & Technology*, 24(2), 169-192.
- Taebi, B. (Forthcoming). Intergenerational Risks of Nuclear Energy. In S. Roeser, R. Hillerbrand, P. Sandin, & M. Peterson (Eds.), *Handbook of Risk Theory*. Dordrecht: Springer.
- Taebi, B. & Kadak, A. C. (2010). Intergenerational Considerations Affecting the Future of Nuclear Power: Equity as a Framework for Assessing Fuel Cycles. *Risk Analysis*, 30(9), 1341-1362.
- Taebi, B. & Kloosterman, J. L. (2008). To Recycle or Not to Recycle? An Intergenerational Approach to Nuclear Fuel Cycles. *Science and Engineering Ethics*, 14(2), 177-200.
- Turkenburg, W. C. Nuclear energy and sustainable development. In *Innovative Technologies for Nuclear Fuel Cycles and Nuclear Power, 2004* (pp. 45-56)
- Vandenbosch, R. & Vandenbosch, S. E. (2007). *Nuclear Waste Stalemate: Political and Scientific Controversies* (Vol. 61, Vol. 8). Salt Lake City: The University of Utah Press.
- WCED (1987). Our Common Future. In G. H. Brundtland, S. Angelli, S. Al-Athel, & B. Chidzero (Eds.). Oxford: World Commission on Environment and Development (WCED).
- WNA (2011). World Nuclear Power Reactors & Uranium Requirements 2010, Information Paper (2 March 2010). <http://www.world-nuclear.org/info/reactors.html>.
- Wynn, G. & Doyle, A. (2011, April 3, 2011). Pragmatism Influencing Energy Debates. *The New York Times*.

## **Part 2**

# **Operation and Decommissioning**



# Long-Term Operation of VVER Power Plants

Tamás János Katona  
*Nuclear Power Plant Paks Ltd.*  
*Hungary*

## 1. Introduction

The VVER reactors are light-water-moderated and water-cooled i.e. pressurized water reactors (PWRs). The name comes from Russian “водо-водяной энергетический реактор” which transliterates as Vodo-Vodyanoi Energetichesky Reaktor (Water-Water Energetic Reactor WWER but the Russian type acronym VVER is more often used). The VVERs were developed in the 1960s. There are 52 Russian designed VVER-type pressurized water nuclear power plants operating in the world today under of 437 nuclear power plants (for the latest operational statistics VVER plants see IAEA PRIS database [www.iaea.org](http://www.iaea.org)). The cumulative time of safe operation of VVER reactors currently exceeds 1200 reactor-years. The first three VVERs were built in Russia and in Eastern-Germany in 1964-1970 and they were operated up to 1990. The first standard series of VVER have a nominal electrical capacity of 440 MW and the second standard series have the capacity of 1000 MW. There are two basic types of VVER-440 reactors, which are based on different safety philosophies. The VVER-440/230 type is a Generation I design while the VVER-440/213 is representing already the Generation II reactor design with reduced pressure containment. Outside Russia all VVER-440/230 type plants of the standard design are already shut down. There are two specific VVER-440 designs in operation the Loviisa NPP with reduced pressure western type containment and the Armenian Medzamor NPP. In the VVER 1000 MW series, there is a gradual design development through the five oldest plants (small series) while the rest of the operating plants represent the standardised VVER-1000/320 model. The VVER-1000 units commissioned recently and those currently being under construction are improved versions of the VVER-1000/320; for example the Tianwan (China) plant with AES-91 type units and the Kudankulam (India) plant with AES-92 type units. New VVER models e.g. the AES-2006 design is being considered for future bids. The older types of VVER-1000 are of Generation II while the new evolutionary models of large VVER already exhibit Generation III features.

The design operational lifetime of the VVER plants is generally 30 years. Exceptions are only the newly designed and operating VVER-1000 units with 50 or 60 years of designed operational lifetime. A great majority of VVER plants are aged nearing the end of the design-lifetime. Except Russia the VVER operating countries are dependent on nuclear power production for example the Nuclear Power Plant Paks in Hungary provided 40 % of domestic production in 2010. The nuclear power capacities in these countries ensure the necessary diversity of power generation and contribute to the security of supply. Therefore, the VVER owners in Central and Eastern Europe intend to keep their plants in operation via implementing plant lifetime management (PLiM) programmes with the intention of

ensuring safe and financially viable operation in the long term. The PLiM activity and strategy of VVER operators is presented in (Katona, 2010).

The possibility of extension of operational lifetime of VVER-440/213 plants was recognised already in 1992 based on assessment of robustness of the design good technical condition of the plants and synergy between safety upgrading measures and overall condition of the plants (Katona&Bajsz, 1992).

In all VVER operating countries, the lifetime management had the explicit goal of ensuring prolongation of operational lifetime see e.g. (Roesenergoatom, 2003).

The operational license of the four VVER-440/213 units at Paks NPP Hungary is nominally limited to the design lifetime of 30 years. Prolongation by additional 20 years of the operational lifetime is however feasible. The first formal step of licence renewal of Paks NPP has been made in 2008 and the relicensing process is going on.

In Ukraine, the nuclear share in the domestic production of electricity is approximately 48 % while the nuclear power plant comprises 26.6 % of total installed capacity. There is a strong interest to extend the operational lifetime of all Ukrainian NPPs. The operational license of the VVER-440/213 type Units 1 and 2 at Rivne NPP Ukraine has been renewed by additional 20 years under condition of performing safety assessment after ten years of prolonged operation. The extension of operational lifetime is a generic strategy of operators of VVER-440/213 plants in Czech Republic and Slovakia.

The Loviisa NPP in Finland (a non standard VVER-440 design) prolonged the operation up to the next Periodic Safety Review (10 years).

The operational lifetime of the VVER plants in Russia will be extended by 15 to 25 years; the four oldest VVER-440/230 units (Novovoronesh NPP Unit 3 4 Kola NPP Unit 1 and 2) have already received a 15 licence for extended operation. The VVER-440/213 type units (Kola NPP Unit 3 and 4) also prepared to 15 years prolongation of operational licence. Among VVER-1000 plants, the Novovoronesh Unit 5 is prepared to 25 years prolongation of operation after an excessive safety upgrading and modernisation programme.

Increasing the competitiveness by power up-rate is also a general element of industry strategies in all VVER-operating countries. The VVER-440 type units at Loviisa NPP are operated at ~510 MWe power level. At Paks NPP enhancement of the reactor thermal power by 8% increased the power output up-to 500 MW and the commercial competitiveness of the plant. Slovenské Elektrárne also implemented a programme of progressive power up-rate of Bohunice V2 NPP and the net capacity of 472 MW is already achieved. Similar projects are in place at Dukovany NPP in Czech Republic. An 4÷5 % power uprates is planned or under implementation practically at all VVER plants in Russia except the oldest plants which provide approximately 300 MWe extra generating capacity.

VVER operators implemented extensive safety upgrading and modernisation programmes during last decades and achieved an internationally accepted level of safety. Generally, safety deficiencies do not inhibit the long-term operation of the VVER plants.

Considerable progress has been achieved at VVER plants with respect to the improvement of the performance and plant reliability too. The load factor of majority of VVER plants is over 80% at some plants e.g. at Paks and Dukovany NPP it is around 90 %.

In this chapter – after an overview of basic technical features of VVER plants – the development and implementation of PLiM programmes for VVER plants will be presented. The methods for ensuring long-term operation are focused on the type and lifetime limiting ageing/degradation mechanisms of the most important systems structures and components. The integration of the plant activities/programmes into coherent PLiM programme will be

demonstrated taking into account the frame of regulatory requirements regarding long-term operation. The role of the international research and co-operation environment affecting the lifetime management of VVER plants will also be presented. The presentation of the PLiM and long-term operation will focus on the older VVER-440/213 and VVER-1000 type plants. Especially the long-term operation of the VVER-440/213 plants requires specific engineering effort.

The VVER-440/230 plants (Kozloduy NPP Bulgaria and Bohunice V1 NPP Slovakia) being already on permanent shutdown will not be considered. In contrast to this the Kola 1 and 2 and Novovoronezh 3 and 4 units in Russia have already received licences to operate for a further fifteen years after implementation of modernisation and safety enhancement programmes (Rosenergoatom, 2003) to cope with the safety issues relevant for this design (IAEA, 1992). The long-term operation and plant lifetime management of VVER-440/230 plant type is not a generic practice and will be discussed below only to a limited extent.

From the point of view of long-term operation, the newly designed and constructed VVER plants are also of less interest. Obviously, they have been designed and manufactured taking into account the aging lessons learned from the operational experience. The question of longer than designed operation of these plants will be and can be considered after decades of operations.

## 2. Basic idea of long-term operation

The safety of nuclear power plants are determined by the functionality and performance of following systems, structures and components (SSCs):

1. Systems structures and components important to safety that perform the basic safety functions i.e.:
  - a. To ensure integrity of reactor coolant pressure boundary
  - b. To ensure the capability to shut down the reactor cool-down and maintain it in a safe shutdown condition and
  - c. To ensure offsite radioactive exposures less than or comparable to limits specified in the national regulations.
2. Structures and components not important to safety but whose failure impacts safety function: The function of a system structure or component may be compromised by failure of a structure or component not important to safety due to different type of interactions.

The SSCs above are classified into safety classes in accordance with national regulation. The classification of SSCs is usually documented in the Final Safety Analysis Report.

During the total operational lifetime, the performance of the SSCs important to safety has to be assured with prescribed margins. The margins are needed for covering the different type of uncertainties of the design, manufacturing and operation and for the assurance that the SSCs will perform their intended safety function even if an accident happen in the last minute of the operation.

The SSCs can be grouped into three main groups according to the possibility of restoration of the function/performance for the compensation of effect of ageing: long-lived passive non-replaceable or not-to-replace structures and components replaceable SSCs and renewable SSCs.

The functionality/performance of all SSCs will be unambiguously decreasing in time due to ageing all of these components.

The function/performance of the replaceable or renewable SSCs can be restored in proper time, while in case of non-replaceable SSCs the rate of degradation can be influenced via careful operation creation better environmental conditions as that assumed in the design. In some cases, the rate of the degradation can be re-assessed based on new scientific evidences and operational experience. Consequently, the possibility of operation extended over the design lifetime is determined by the ageing and aged condition of long-lived non-replaceable or not-to-replace structures and components (SCs) relevant for safety like reactor pressure vessel containment etc. The functionality and performance of these SCs limit the operational lifetime.

The assurance of intended safety function of replaceable systems, structures and components is also very important and might be critical. However, the assurance of function and performance of that structures systems and components is mainly question of effort and financing and does not limit the operational lifetime.

Off-course the extension of operational lifetime is a business decision of the owners of the plant. From this point of view, the performance and functionality of SSCs important for production also pose limit in time for the extension of operation. The Fig. 1 illustrates the concept outlined above.

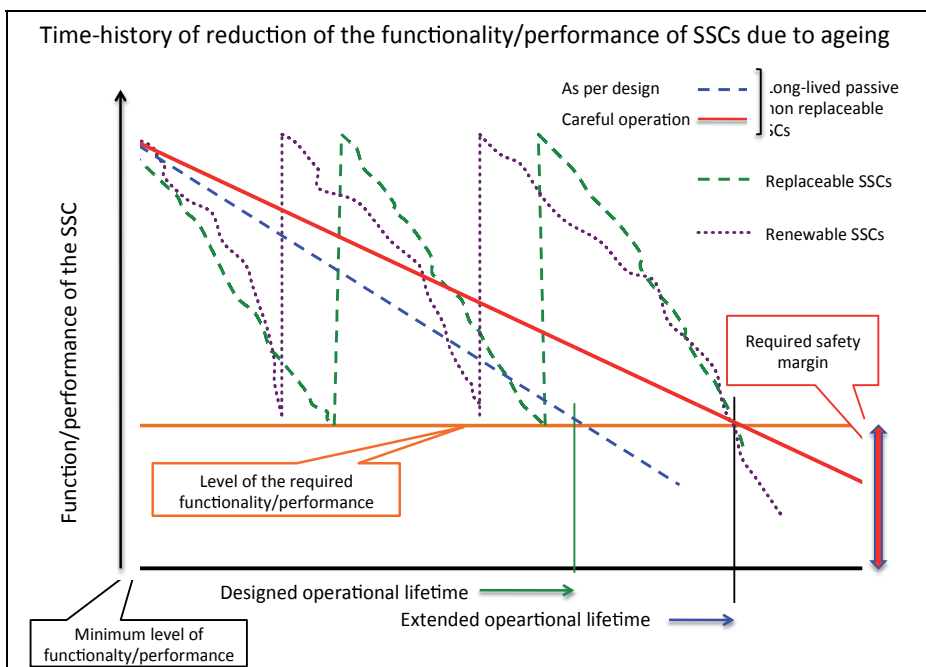


Fig. 1. Why the operational lifetime can be extended?

### 3. Basic features of the VVER design

In the sections below, the basic design characteristics of VVER plants are presented. The design and manufacturing features are also discussed, which are relevant from the point of view of long-term operation (LTO). Safety and compliance with current licensing basis and international requirements are the preconditions for LTO.



### 3.1 The VVER-440 models

#### 3.1.1 Basic design features of the VVER-440

The VVER-440 V-179, V-230 and V-213 plants are equipped with a six-loop VVER-440 reactor. In each loop there are main isolating valves (MIV) on the cold and hot legs, one main circulation pump (MCP) per loop and the horizontal steam generators (SG). The pressurizer with safety valves is connected to the primary loop. The two generations of VVER-440 type reactors have very similar layouts of their primary systems; see Fig. 2. Typical operating parameters are  $T_{\text{hot}}=297^{\circ}\text{C}$   $T_{\text{cold}}=266^{\circ}\text{C}$   $p=12.3\text{ MPa}$  as it shown in Fig. 3. The design bases of the two VVER-440 types (i.e. the 230 and the 213) are essentially different. This has consequences in the design of safety systems and confinement.

There are 16 nuclear power plant units of type VVER-440/213 namely: four in Hungary, four in the Czech Republic and four in Slovakia two in Russia and two in Ukraine. The owners of these plants are preparing for long-term operational life of these units.

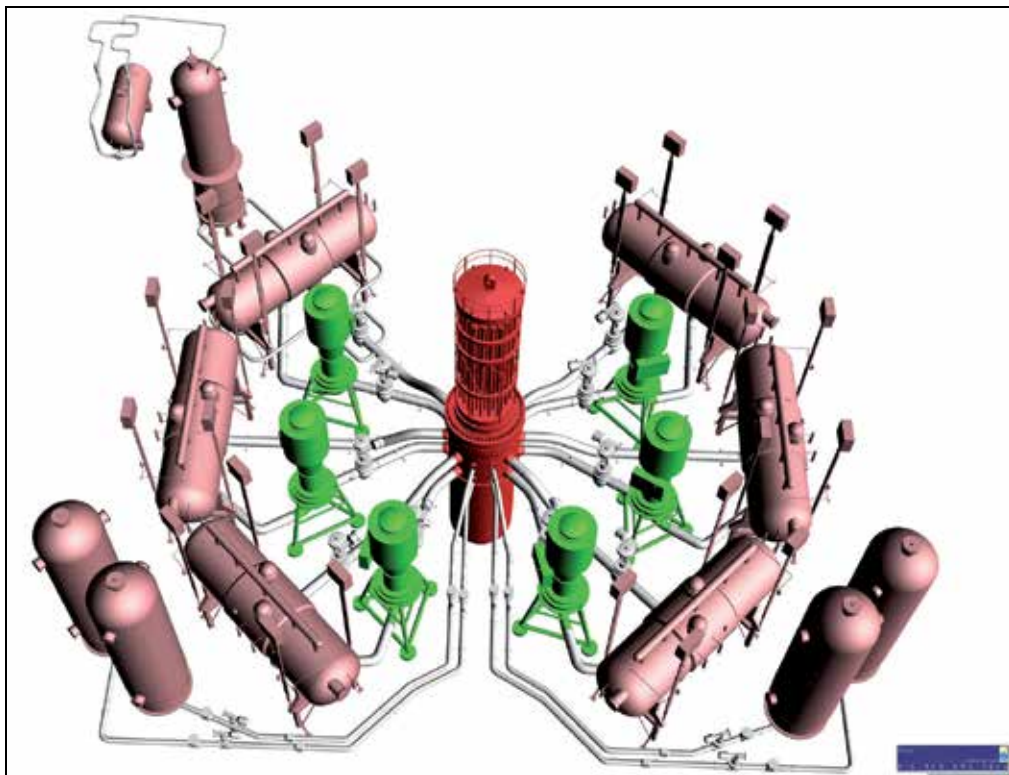


Fig. 2. Layout of the primary system of VVER-440/213 design

The design bases for the VVER-440/213 safety systems are similar to those used in Western PWRs, including the postulating the a double-end guillotine break of the main circulation line in the reactor coolant system. The safety systems exhibit triple redundancy and the reactors have bubbler condenser-type pressure suppression containments capable of withstanding the imposed loads and maintaining containment functionality even following large break LOCA. The VVER-440/213 plants design considered internal and external hazards to some extent. In addition, protection against single failures in the auxiliary and



### 3.1.2 The VVER-440 features relevant for LTO

In case of VVER-440 plant designs, the operational lifetime-limiting structures and components are the containment building, the reactor pressure vessel (RPV) and the steam generator (SG). Contrary to the VVER-1000 and PWRs the steam generators are practically not replaceable in case of VVER-440/213 design.

The ferritic-steel reactor pressure vessel is clad internally with austenitic stainless steel. The reactor pressure vessels are made from low alloy steel (15Cr2MVA; Loviisa 12Cr2MFA) the circumferential submerged arc welding was made using Sv-10CrMoVTi wire. The RPV covered internally by welded clad of two stainless steel layers. The inner layer is a non-stabilised stainless steel (Sv-07Cr25Ni13 similar to AISI 309) and that in contact with the coolant is a niobium stabilised stainless steel (Sv-08Cr19Ni10Mn2Nb (Loviisa Sv-07Cr19Ni10Nb) both equivalent to AISI 347).

From the point of view of longer-term operation, the main deficiency of VVER-440/230 was the high irradiation exposure of the reactor pressure vessel (RPV) wall by fast neutrons and the relatively quick embrittlement of the RPV material. The issue had been aggravated by the lack of a proper RPV surveillance programme at these plants. Several attempts have been made to assess the embrittlement of the base and weld material of those RPVs. For the first generation RPVs essential data for RPV materials, e.g. transition temperature, concentration of copper and phosphorus were absent; archive metal of RPVs was not available. The phosphorus and copper contents in the welds of WVER-440/230 are between 0.030–0.048% and 0.10–0.18% respectively. In the case of VVER-440/213 the same concentrations are in the range of 0.010–0.028 % for P and 0.03–0.18% for Cu (Vasiliev&Kopiev, 2007).

Several measures were implemented for the resolution of the RPV embrittlement issue:

- reduction of the neutron flux on the RPV via low leakage core design dummy shielding assemblies and annealing i.e. affecting the change of material properties
- heating up the water in the emergency core cooling system (ECCS) to lessen thermal shock in a pressurized thermal shock (PTS) situation, steam-line isolation system solutions interlocks, i.e. decreasing the stressors
- introduction of volumetric non-destructive testing for in-service inspection.

Annealing of RPV has been implemented at Loviisa NPP and Kola NPP (also at the shut down plant Buchunice V1). Assessment of annealing effectiveness (level of properties recovering after annealing), determination of re-irradiation re-embrittlement rates after annealing and the behaviour of WVER-440 weld materials showed the real possibilities for recovering RPV toughness properties of irradiated WVER-440 RPV materials. Measures were also taken to improve the knowledge of the vessel material by vessel sampling. Also reducing of neutron irradiation loading of the RPV wall via dummy assemblies around the core was implemented. More detailed description of the RPV neutron irradiation embrittlement issue is provided e.g. in (Erak et al, 2007).

'Extended Surveillance Specimen Programme' was prepared with the aim to validate the results of the standard programme (Kupca, 2006). It was prepared for increasing the accuracy of the neutron fluence measurement, improvement of the determination of the actual temperature of irradiation, fixing the orientation of RPV samples to the centre of the reactor core, minimizing the differences of neutron doses at the Charpy-V notch and crack-opening-displacement specimens and to evaluate any dose rate effects.

For the Mochovce NPP units 1 and 2, a completely new surveillance programme was prepared based on the philosophy that the results of the programme must be available during the whole service life of the NPP. The new advanced surveillance programme deals

with the irradiation embrittlement of the RPV weld area heat affected zone and the RPV austenitic stainless steel cladding, which were not evaluated until this time in the surveillance programmes.

Reactor pressure vessel surveillance programmes became obligatory in all VVER plants that had been commissioned after Units 1 and 2 at Loviisa.

Proper RPV surveillance programmes have been implemented at VVER-440/213 plants outside of former Soviet Union. Since the PTS (pressure-temperature-loading limits) is the lifetime limiting process for the RPV of VVERs, the methodology of PTS evaluation has to be established in the national regulations, which takes into account the applicable best practices, the features of the RPV and the thermal-hydraulic peculiarities of the VVERs. The assumptions of renewed PTS analyses have been confirmed with mixing tests. The embrittlement of the RPV has been controlled via low-leakage core design. Considering the VVER-440/213 plants, annealing of RPV has been implemented at Rivne NPP.

Components of the primary circuit in contact with the primary coolant other than RPV are also made of austenitic stainless steel, i.e. the piping of the primary loop the main circulating pumps gate valves and the emergency and auxiliary systems pipework.

The steam generators in VVER are horizontal (see Fig.4).

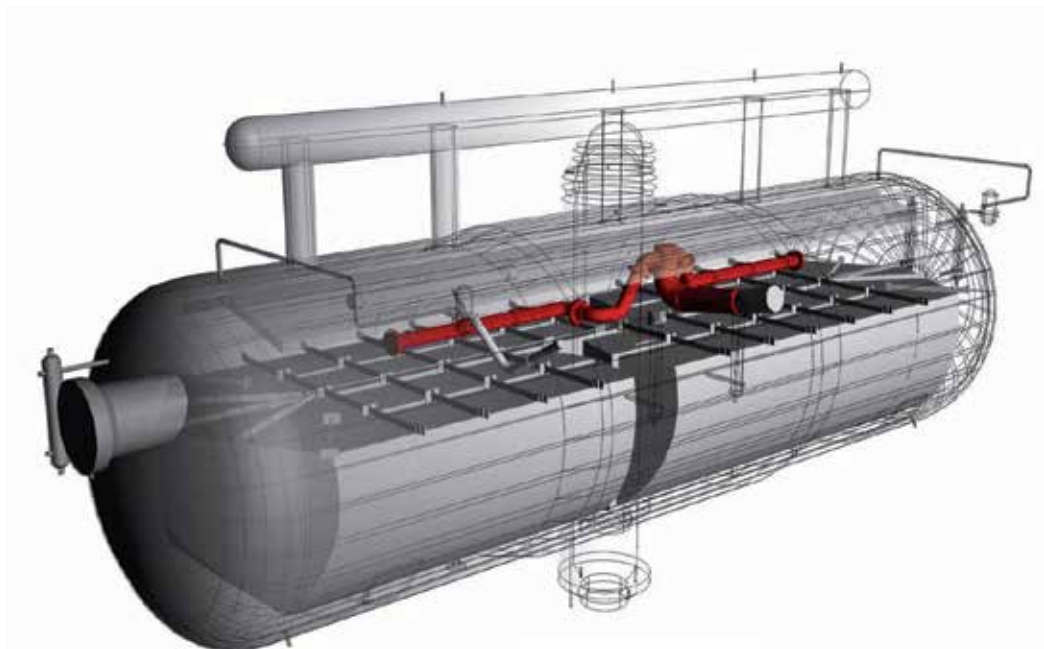


Fig. 4. Steam-generator of VVER-440/213 design

The heat exchanging tubes and the steam generator tube headers (collectors) are manufactured from austenitic stainless steel (18% Cr 10 % Ni stabilized with titanium) in VVERs, instead of the nickel-based alloys (Alloy 600 and 690) and higher chromium-containing alloys (Alloy 800) used in PWR. The material of the SG heat exchanging tubes in VVER-440 is equivalent to AISI 321. The advantages of the VVER horizontal steam generator design are the high reliability absence of vibrations, no accumulation of sludge at the tube sheet and easy to access for the maintenance.

The SG design has positive impact on safety as well, e.g. the design allow reliable natural circulation, effective gas removal, large water inventory and essential thickness of the heat exchanging tubes.

The oldest VVER-440 type steam generators at Novovoronezh NPP unit 3 and 4 are operating already 40 years. Condition of the oldest VVER-440 steam generators at Kola and Novovoronezh plant allows 15 years extension of operation of these plants. According to the operational experience, the feed-water distributor inside the SG shows accelerated ageing due to erosion. These elements were replaced practically at all VVER-440 plants (see the red coloured new distributor in Fig.4).

The experience regarding ageing of VVER steam generators is summarised in the report of the International Atomic Energy (IAEA, 2007). At WWER-440 plants, the lifetime limiting ageing mechanism of the SGs is "Outer Diameter Stress Corrosion Cracking (ODSCC)" of the austenitic stainless steel heat-exchanger tubes. The ODSCC indications appear typically (80%) at the grid structure supporting the tube bundle where the secondary circuit corrosion products with concentrated corrosive agents are deposited. An eddy-current inspection programme is implemented for monitoring the tubes. Samples have been removed from plugged tubes to facilitate investigations of the phenomena. The rate of ODSCC was essentially slowed down by a series of modifications and actions implemented at different plant to different extent.

The measures implemented are as follows:

- Replacement of the condensers: the new condensers have austenitic stainless steel tubes
- Removal of copper and copper-bearing alloys from the secondary circuit
- Replacement of the feed-water distributor (the old one was manufactured from carbon steel)
- Cleaning the heat exchanging surface of the SGs
- Introducing high pH secondary water chemistry
- Replacement of the high-pressure pre-heaters (with erosion-corrosion resistant tubes).

All these measures have been implemented at Paks NPP, which completely changes the conditions and the rate of ODSCC in the SGs. Consequently, a better (i.e. decreasing) plugging trend is experienced, which can also be expected in the long-term. The gaps between the tubes and support grid are still the critical places since remaining corrosion products accumulate there. It is therefore difficult to forecast the ODSCC rate in the gaps and the ageing process has to be well monitored in the future. Under the new conditions, sludge may be accumulated at the bottom area of the SG. An effective method for draining the sludge has to be found. The reserve in heat exchanger surfaces of the SG is relative large (more than 15%). Considering past experience and the recent plugging trend of the heat exchange tubes, none of the SGs would exceed 10% of plugged tubes by the end of 50 years operation due to implemented measures (Katona et al, 2003); see also (Trunov et al, 2006). The number of allowable plugged tubes became more important at the plant where the primary energy output is increased for the power up-rate. Therefore, establishing adequate performance criteria for the steam generators is very important.

The reduced pressure containment of VVER-440/213 is made of reinforced concrete, and steel liner ensures the leak tightness. Therefore, the basic concern regarding containment ageing is the affect of ageing on the containment leak-tightness. The leak rates of VVER-440/213 containment allowed by the design and justified by the regular integral tests equals to 14.7%/day at the post large-break loss-of-coolant accident when the design internal containment pressure equals 2.4 MPa. It is clearly higher at some plants than is allowed for

Western NPP containments. Therefore, the goal of the VVER operators is to improve the leak-tightness. (It should be noted that comparison with Western NPP containments could not be straightforward. In case of design basis accidents the pressure suppression system tends to cause an under-atmospheric pressure rather than overpressure at the time period when the atmosphere of the containment has its highest contents of radioactive aerosols and when the potential for radioactive releases would thus be the highest.) Containment leakage has a complex origin. Investigations carried out at Paks and Buchunice NPP practically from the time of start-up tests shows that the poor sealing of doors and hatches mainly cause the containment leakage. It means that the leakage itself is a maintenance problem rather than an ageing issue.

Some VVER plants are built on relatively soft soil. Geodetic control of the settlement of main building of these plants was started during the construction and it is periodically performed. The phenomena might be a concern when the uneven settlement, i.e. the differential movement causes unaccepted additional deformation of the structures. Experience shows that the differential movement may cause cracks in non-structural masonry walls. Other concern might be, if the non-uniform settlement results in non-allowed tilting of the RPV vertical axis, which would cause problems for control rod drive mechanisms (CRDMs). The operating experience and analysis of settlement with extrapolation to extended operational lifetime is discussed for Paks NPP in (Katona et al, 2009a).

As per operational experience, ageing of both reinforced concrete load bearing structure and liner do not limit the long-term operation of the VVER-440/213 plants.

### **3.2 VVER-1000 model**

#### **3.2.1 Basic design features of the VVER-1000**

The VVER-1000 model exists in several versions. The “small series” plants could be considered as pioneers of this model. The VVER-1000/320 is the large series version of the design. The VVER-1000/320 type plants are operated in Bulgaria, Czech Republic, Russia, Ukraine and China: they were developed after 1975. Modernised versions of VVER-1000 plants are under construction in five countries (Bulgaria, China, India, Iran and Russia).

Regarding lifetime management, the VVER-1000/320 plants have practical importance. The “small series” plants show some specific design features however the lifetime management practice of these plants does not differ essentially from those in the case of the VVER-1000/320 version.

The VVER-1000 is a four loop PWR with horizontal steam generators. Each loop consists of a hot leg, a horizontal steam generator, a main circulating pump and a cold leg. Main isolating valves on the hot and cold legs of each loop equip the non-standard VVER-1000 primary loops. The standard V-320 design and the new clones of the VVER-1000 do not have isolating valves on the primary loops. A pressuriser is connected to the hot leg of one of the loops and the spray line to the cold leg. Operating conditions are  $T_{\text{hot}}=322\text{ }^{\circ}\text{C}$   $T_{\text{cold}}=290\text{ }^{\circ}\text{C}$   $p=15.7\text{ MPa}$ .

The reactor, the primary and safety systems are all placed within a full pressure, dry, pre-stressed concrete containment.

The design bases and the technical solutions applied are very similar to the PWRs operated in Western countries. The safety concerns about the VVER-1000 plants are discussed in detail in IAEA reports; see (IAEA, 1996b) and (IAEA, 2000). The main safety concern regarding the VVER-1000 plants lies in the quality and reliability of the individual equipment especially the instrumentation and control (I&C) equipment. The plant layout

has weaknesses that make the redundant system parts vulnerable to hazardous systems interactions and common cause failures caused by fires internal floods or external hazards. At all plants, many of these deficiencies have been addressed by plant modifications and an acceptable safety level has thus been achieved.

There are several advanced VVER-1000 plants presently under construction and more than 20 new projects of advanced VVER design are under preparation or consideration and several are in the bidding phase. The most advanced versions of VVER design showing features of Generation III reactors are considered for future bids for large generating capacity reactors.

### **3.2.2 Features of VVER-1000 model relevant for LTO**

In case of VVER-1000, the proven design solutions of VVER-440 are implemented like the horizontal steam generator also the concept of the material selection. In the VVER-1000 models, all primary circuit surfaces either are made from or are clad in stainless steel. The 08X18H10T type stainless steel (08Cr18Ni10Ti AISI 321) is used for the core structures, main circulating pumps and steam generator tubing, whilst the main loop pipework and steam generator collectors are manufactured from 10GN2MFA type carbon steel and the cladding is made from 08Cr18Ni10T stainless steel. The pressuriser is also made from 10GN2MFA carbon steel covered by cladding with an inner layer of Sv-07Cr25Ni13 (similar to AISI 309) stainless steel and two layers of Sv-08Cr19Ni10Mn2Nb niobium stabilised stainless steel (similar to AISI 347). The reactor pressure vessel and head are made from the low alloy steel 15Cr2MNFA. The cladding of the reactor head has an inner layer of Sv-07Cr25Ni13 stainless steel and two layers of the niobium stabilised stainless steel Sv-04Cr20Ni10Mn2Nb (again similar to AISI 347). The phosphorus and copper contents in the welds of WWER-1000 are 0.005–0.014% and 0.03–0.08% respectively. The quality of manufacturing and alloy composition ensure the possibility of LTO for VVER-1000 reactors (Vasiliev&Kopiev, 2007).

For newly commissioned WWER-1000 plants and plants in construction, essential modifications of the surveillance programme have been implemented. Specimen containers are located in positions representative for vessel wall conditions at Temelin NPP. Based on the fracture mechanics analysis, it was recommended to heat up the accumulator water to 55°C and to prevent injection of ECCS water with temperatures below 20°C for all the plants. The use of low neutron leakage core loading patterns in WWER-1000 reactors reduces the RPV wall fluences by approximately 30%. It was planned to introduce partial low leakage loading patterns at some plants during 1994 (i.e. fuel assemblies with high burn-up to be placed at the core periphery).

The steam generators for VVER-1000 have been designed on the same principles as in case of VVER-440 plants. However, the SGs at VVER-1000 plants are replaceable.

At some Units throughout the design service life of SG there were problems resulting in necessity of SG replacement.

At the same time, the SGs at some plants can be operated above design service life. As the operating experience shows, the water chemistry of the secondary circuit is the main factor influencing operability of the SG tubing like in the case of VVER-440 plants.

Tube integrity is inspected by eddy current method. The results of eddy current test can be used to determine the plugging criterion for defected tubes. Proper definition of the plugging criterion was an important problem.

The ageing problems of the SGs at VVER-1000 plants are as follows; see (Trunov et al, 2006):



- cracking at headers of the cold collectors of the heat-exchanging tubes
- degradation of the welded zone at hot collector headers
- corrosion of the heat-exchanging tubes
- formation of deposits
- difficulties in measuring and regulating the SG water level.

A study performed in the frame of the International Atomic Energy Agency summarises the status of knowledge on the steam generator ageing (IAEA, 2007).

In VVER-1000 plants, ageing may affect the pre-stressing of the containment. Important ageing mechanisms of the pre-stressed containment and its structural elements, e.g. the tendons anchorages are the relaxation shrinkage creep of steel resulting in loss of pre-stress. Requirements on testing of containment pre-stressing system are defined both by the designer and regulation (Orgenergostroy, 1989a) and (Orgenergostroy, 1989a). The scope of inspection shall be extended if defects are observed and/or average loss of tension force is more than 15%. If additional control verifies obtained results, it is necessary to test 100% of tendons. Tendons with force losses more 15% shall be once again controlled after straining. In the case if a force loss at 24 hours is more than 10% the tendon shall be replaced. In order to enable monitoring of the level of the containment pre-stressing measurement systems are installed permanently on the structure and these systems measure structure deformations and pre-stressing force in the cables.

At VVER-1000 plants, detailed field investigations and analyses have been carried out for the assessment and evaluation of the condition of pre-stressing tendons. There are design solutions for the replacement of tendons. Thus, all existing defects leading to loss of stressing force and rupture of tendons have been avoided.

At some plants, new pre-stressing system and an additional system for automatic control of stressing forces is installed in the bundles.

## **4. Feasibility of long-term operation**

### **4.1 Preconditions and motivations for long-term operation**

Pioneers of the extension of operational lifetime were the VVER-440/213 operators. It was already recognised in 1992 that the favourable characteristics of the VVER-440/213 plants, the comprehensive safety enhancing programme launched and partially already implemented by the operating companies, the operational and maintenance practice of the operator give an opportunity to extend the operation lifetime (Katona&Bajsz, 1992).

Decision on the preparation of feasibility studies for LTO had been based on the recognition of the following VVER features and experiences:

- robust design of VVER-440/213 design
- good plant condition due to well-developed maintenance in-service inspections, careful operation and extensive modernisation and reconstructions
- successful implementation of safety upgrading measures resulting in acceptable level of safety.

Safety of the plants and compliance with international standards have been generally considered as decisive preconditions for long-term operation.

The comprehensive modernisation and safety upgrading programmes implemented by the VVER operators during last two decades resulted in gradual decreasing of the core damage frequency (CDF) of these plants. For example, the level 1 Probabilistic Safety Analysis (PSA) study establishes the resulting CDF for all units at Dukovany NPP between  $1.47 \div 1.67 \cdot 10^{-5}/a$



(Czech Report, 2010). The same achievements are published for other VVER plants in the national reports compiled under Safety Convention; see (Slovak Report, 2010). The CDF for Bohunice V-2 NPP is shown in Fig. 5.

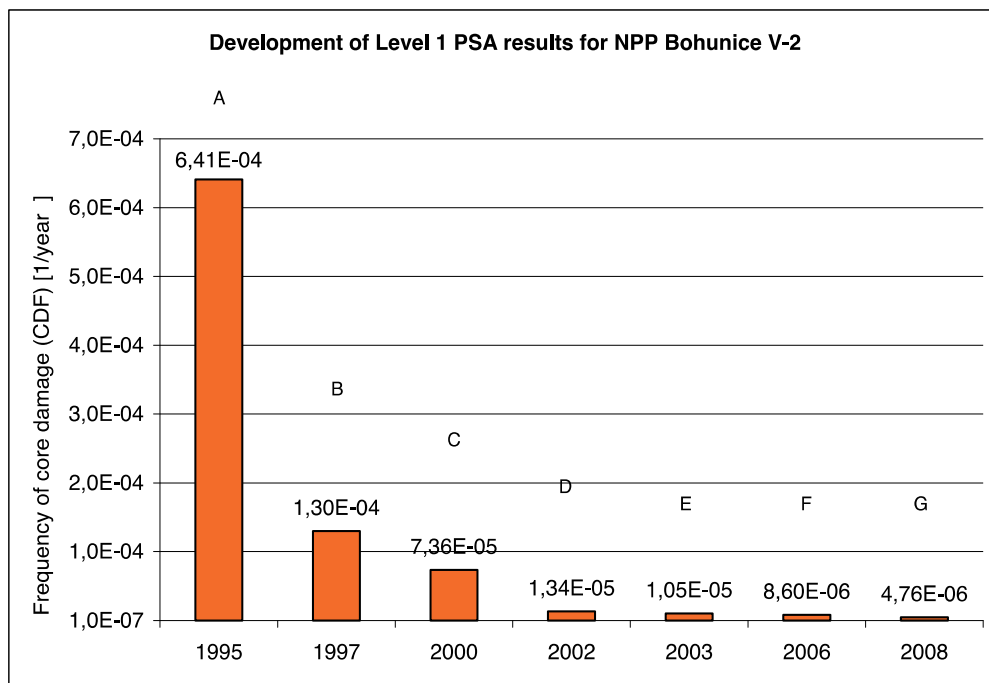


Fig. 5. Decreasing the CDF for Bohunice V-2 NPP due to the implementation of safety upgrading measures (Slovak Report, 2010)

Similar to Slovak and Czech plants results have been achieved at Paks NPP in Hungary too. Extensive modernisation and safety upgrading programme has been implemented in Ukraine (Ukraine, 2011) and Russia (Rosenergoatom, 2003) and Bulgaria (Popov, 2007) too. One of the issues related to the justification of the compliance with current licensing basis at VVERs operated outside of Russia is the lack of the knowledge of design basis, especially the assumptions made by the designer with respect to the ageing mechanisms, stressors and time limits of the safe operation of the components.

The availability of design base information is a current licensing basis requirement.

In the same time knowledge of design base is unavoidable for the preparation of long-term operation and licence renewal especially for the review of time-limited ageing analyses.

Operators of WWER-440/213 units have to perform specific project for the design base reconstitution. The design base reconstitution covers the identification of design base functions values and bounding conditions according to the licensing basis.

Two basic tasks have to be performed while reconstituting the design base:

- collection and review the original design information
- consideration of the changes of the licensing basis since the design and issuance of the operational licence.

The design of VVER-440/213 and the older VVER-1000 plants was generally based on the former USSR regulations of early the seventies:

- General Requirements on Safety of NPP Design, Construction and Operation (OPB- 73) and
- General Safety Rules for Atomic Power Plants (PBYa -74).

OPB-73 marked the beginning of a transition to the generally accepted international practice in nuclear safety (e.g. defence in depth, single failure criterion).

Additional work was needed for the proper definition of design base values and conditions. Design input loads and conditions had to be newly defined for the most important SSC. Information sources for this work were:

- the existing design information
- results of the periodic safety reviews
- current licensing basis compliance check
- transient analyses newly performed for the final safety analysis reports (FSAR)
- operation history.

The design base has to be newly created taking into account all essential changes in the licensing basis. For example, in case of Paks NPP seismic loads were not considered in the design. Current design/licencing base includes safe shutdown earthquake with 0.25 g horizontal acceleration.

The good plant condition and appropriate plant programmes are also preconditions for long-term operations. Especially the surveillance of the RPV embrittlement and monitoring of the condition of long-lived passive structures and components are of interest. The most important ageing management (AM) activities are performed at the VVER plants from the very beginning of the operation. The early AM activity was focused on the known degradation of main SSCs like reactor pressure vessel (RPV) embrittlement or on issue cases, e.g. leaking of the confinement due to the liner degradation outer surface corrosion of the steam generator heat-exchange tubes. Most of early AM programmes were state-of-the-art as for example the RPV surveillance programme. In the course of the first periodic safety reviews, the scope of most critical for operational lifetime SSCs and the dominating ageing mechanisms were defined.

Adequate assessment of the aged condition and forecast of safe lifetime of SCs can only be performed if the ageing process is monitored properly from the very beginning of the operation. The operational history of SCs has to be documented in sufficient details for performing the trending.

Availability of a state-of-the-art FSAR and its regular updating is required for the control of compliance with CLB and configuration management.

The national regulation allowing the approval of the prolongation of the operation beyond designed operational lifetime is also an unambiguous condition of the long-term operation. The legislative framework of regulatory approval of long-term operation in the VVER operating countries is based either on the periodic safety review or on the formal licence renewal.

There are several non-technical conditions, which affected the strategy of VVER operators and motivated the decision on LTO. The positive international tendencies with regard to long-term operation of existing nuclear power generation capacities stimulate the LTO of VVERs too. (This tendency might be changed by the nuclear accident following the Great Tohoku earthquake in Japan March 2011.) Accumulation of the experiences and scientific evidences for justification of longer than designed operation of NPPs provides good basis also for LTO of the VVER. Good market positions of NPPs overall in the VVER operating countries and high level of public acceptance and positive public attitude towards operation of NPPs in these countries.

The intention to prolong the operational lifetime of existing NPPs was also motivated by very low probability for the extension of nuclear power capacity in late nineties since all trials for launching new nuclear projects failed and several projects have been stopped and frozen already for long time.

#### 4.2 The feasibility study

The main goal of the feasibility studies was the preparation of the final owners decision regarding LTO and licence renewal. Simultaneously, the authorities in the VVER operating countries started the preparation of regulations on long-term operation and licencing.

According to (Katona et al, 2001) the feasibility was checked from technical and safety point of view via:

- assessment of plant safety and overall technical condition
- forecast for the lifetime expectations of non-replaceable structures and components
- assessment of the effectiveness of the plant operational and maintenance practice
- evaluation of the safety level of the plant and forecast for the extent of future safety upgrading measures based on the international tendencies in the R&D and development of regulations
- effort needed for ensuring the safety and operational performance scheduled replacements reconstructions

Logic followed in the feasibility study is shown in Fig.6.

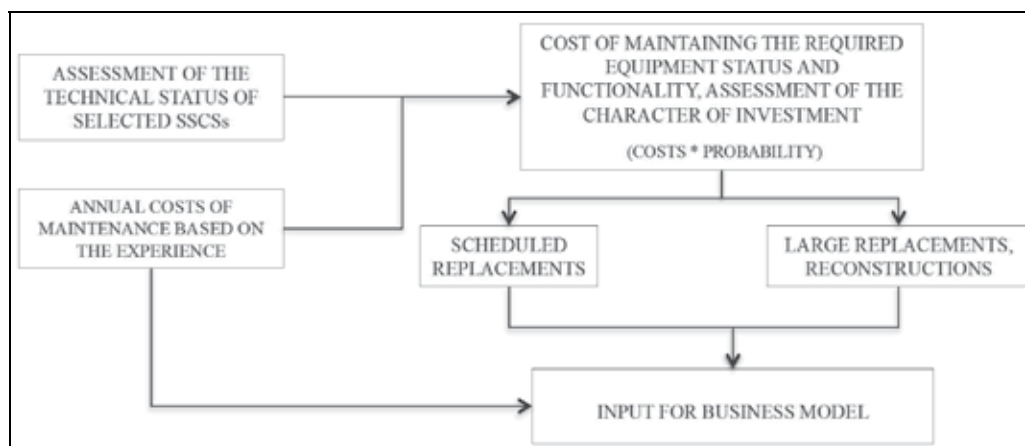


Fig. 6. Logic followed in the feasibility study

It has been found that there is no technical or safety limitation to the 50 years of operation of the Paks NPP. In case of most systems and equipment, the monitoring maintenance and regular renewal practice of the plant allows for the lifetime extension without outstanding costs. There is a well defined number of SSCs only, which require extensive reconstruction and investment as the possibility of compensating for the effects of ageing is limited or a significant moral ageing can be expected. In case of some SSCs, capacity expansion might be needed (e.g. radioactive waste storage tanks).

Findings related to the reactor vessels and steam generators had been dealt with specific attention since these are in case of VVER-440/213 the real lifetime limiting components. As for the reactor vessels of VVER-440/213 at Paks NPP, the embrittlement due to fast neutron

irradiation of the reactor pressure vessels material was found the dominant ageing process. The condition of the RPV was different at different plants. While performing the feasibility study, the condition of RPV at Paks NPP was found that the RPVs of Unit 3 and 4 could be operated without extra measures even at 50 years. It was found that the water in the emergency core cooling (ECC) tanks should be heated up in order to decrease stress levels caused by pressurized thermal shock (PTS) transients. For this purpose, cost-effective technical solutions were already available. At Unit 1 in case of the 50-year lifetime in addition to the ECC heating-up the annealing of the welded joint No. 5/6 close to the core had been considered with 50% probability. It has to be mentioned that these conclusions were revised later on the basis of more sophisticated analyses.

In case of VVER-440/213, the steam generators are not replaceable in a practically reasonable way. Therefore, the steam generators are as critical as the reactor pressure vessels from the point of view of lifetime limits of the safe operation of the plant. A forecast of the expected change of the steam generator performance has to be made based on the plugging rate.

In case of VVER-1000, the reactor pressure vessel and the containment are the real lifetime limiting SCs since the steam-generator is replaceable.

Simultaneously with the assessment of the plant condition and lifetime expectations of the most important non-replaceable structures and components, the evaluation of the effort of the scheduled replacements, safety upgrading measures and reconstructions the costs for maintaining the required plant condition and sustaining the capability of operating company had to be assessed. These data had been used for input of business evaluation of the LTO. Simplified presentation of the business model is shown in Fig.7. Several options might be been investigated: 0, 10, 20 and 30 years of prolongation of operation beyond the licenced 30 years. The results of the study determined the objective of the PLiM.

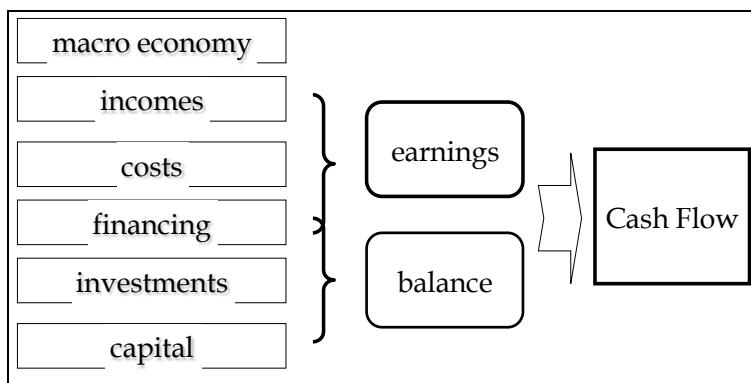


Fig. 7. The business model

Similar to the study presented above has been made for Dukovany NPP in the Czech Republic (Kadecka, 2007) and (Kadecka, 2009).

### 4.3 Synergy between long-term operation and safety upgrading and modernisations

There is a synergy between the long-term operation and different plant actions and measures implemented for safety upgrading, power up-rate, improving reliability and plant programmes. This will be shown below based on (Katona, 2006).

Implementation of the safety-upgrading programme for ensuring the compliance with national and international requirements is a precondition for LTO. In the same time, the safety is the most important aspect of public acceptance. The operator commitment in relation of safety is and will be the decisive point of judgement of the public.

Most of the safety upgrading measures results in positive technical effect too. Due to these modifications, the safety systems or their essential parts had been practically renewed, reconstructed. Consequently, large part of safety systems is not aged. In some cases, safety-upgrading measures have direct influence on the lifetime limiting processes. For example, the new relief valves installed on the pressurizer for the cold over-pressurisation protection eliminate the danger of brittle fracture of the reactor vessel.

Some of the VVER plants implemented extensive seismic upgrading programme involving addition of large number of new seismic fixes and other strengthening measures; see papers in (IAEA, 1993). Fixing the building structures, the anchorages equipment, cabinets and racks, also the structural support of cable trays can be considered as reconstruction of these SCs.

The most important economical condition for long-term operation is the preserving of the present cost advantage of nuclear electricity generation within the market conditions. Exploiting reserves and advantageous features of the VVER-440/213 reactors the electrical output of the plants can be safely increased up-to approximately 500 MWe by improvement of the efficiency of the secondary circuit/turbine and increasing reactor thermal power via implementation of modernised fuel assemblies. Obviously, the power up-rate should not result in a decrease of the plant safety level and should not cause stressors of ageing which affect the lifetime extension perspectives and the plant availability.

The frequently criticised obsolete I&C systems were replaced at VVER plants. The new I&C systems have proper environmental qualification. Beside of the obsolescence, the lack of environmental qualification was the basic issue in case of the old systems practically at all plants.

The major causes of the steam generator heat exchange tube local corrosion is the high concentration level of corrosion activators (chloride ions, sulphates, copper oxides etc.) in the secondary circuit and in the hidden surfaces at the secondary side of the SGs. This is critical in case of VVER-440 hence the steam generators are practically not replaceable. For limitation of the local corrosion, the high level of deposition on the tube surfaces should be eliminated. Most important measure implemented was the replacement the main turbine condenser for example at Paks NPP (Katona et al, 2005). Contrary to the old condensers with copper alloy tube bundle, the new condensers with stainless steel tubing allowed the introduction of the high pH water regime in the secondary circuit providing better operational condition for components of the feed water system and for the generators as well.

## **5. System for ensuring long-term operation**

### **5.1 Concept for ensuring longer term operation**

Safe and economically reasonable prolongation of operation of VVER type plants (and any other old vintage plant) should be not limited to the formal regulatory or re-licensing aspects; it has to be considered in broader context (Katona&Rátkai, 2008) and (Katona et al, 2009). It requires a comprehensive engineering practice, which integrates

- up-to date knowledge on aging phenomena

- vigilance through condition monitoring /aging management
- ability to recognize the unexpected phenomenon when it arises
- a consequent application of best practices
- feedback of experiences
- proper consideration of VVER-440/V213 features
- graded approach in accordance with safety relevance and plant lifetime limiting character of the given structure/component and ageing process;

A comprehensive plant approach to LTO means:

- All systems, structures and components have to be covered by certain plant programme (ageing management preventive maintenance scheduled replacement etc.). In case of safety classified SSCs, plant programmes and practice should comply with regulation; in case of non safety classified one, the complexity of programme depend on the importance of SSCs regarding power production, e.g. preventive maintenance and in some cases even run to failure concept might be applied.
- All ageing processes have to be considered.
- All plant activities have to be considered i.e. the routine activities should be integrated with those specific to LTO utilizing the synergy between them.

The concept is illustrated in Fig.8.

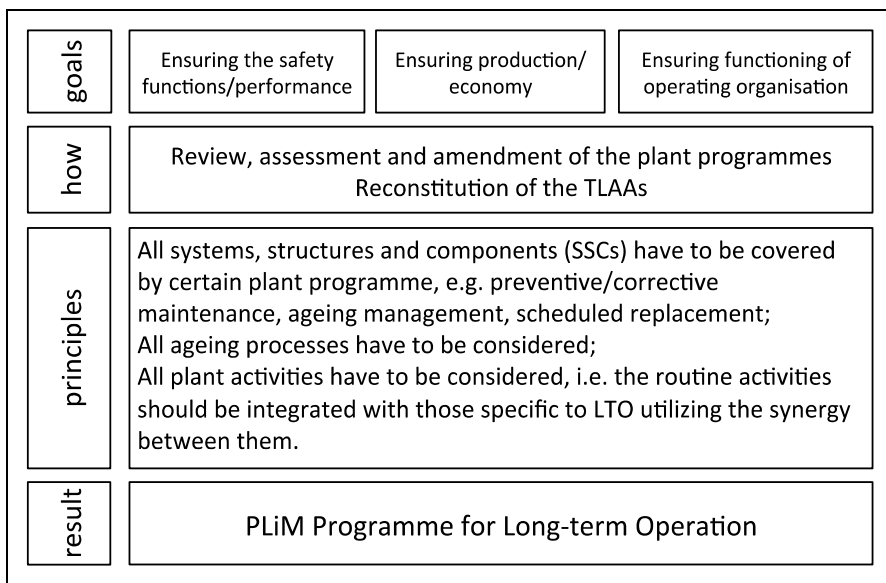


Fig. 8. Concept for preparation of the LTO and LR

## 5.2 Scope of systems structures and components to be considered in LTO

Plant Lifetime Management (PLiM) is complex programme for ensuring safe and long-term production of electrical energy. The scope of LTO should cover the SSCs relevant to safety SSCs important for production and conditions for functioning of operational organisation. PLiM is focusing on ageing on the economically optimal way of ensuring required condition of the plant while ensuring the safety. Practically all SSCs of the plants are within the scope of the PLiM. However, these components can be divided into two categories:

Category 1 – long-lived non-replaceable components as well as those which replacement will makes the LTO economically not reasonable. These components are the RPV, SG, Main Coolant Pump, main circulation pipeline containment cables and most of the buildings etc. The required condition of these SSCs is ensured via ageing management or justified by time limited ageing analyses and environmental qualification validated for the extended time of operation. The method for scoping and screening for ageing management is presented in Section 7.1.

Category 2 – includes all SSCs except for those of Category 1. The required condition of these SSCs is ensured via plant maintenance and scheduled replacement programmes.

The scope of PLiM for LTO is broader than the scope for justification of the safety of the long-term operation developed for obtaining the regulators approval. The regulatory review and approval is focusing on the safety related SSCs and on the plant programmes for ensuring their functioning and performance over the extended operational lifetime. The scope of regulatory approval is presented in the sections below.

### 5.3 Methods for ensuring required functionality/performance

#### 5.3.1 The system for ensuring required plant condition

The control of performance and safety functions shall be ensured by certain plant programme or justified by analysis. The system is illustrated in Fig.9 based on Hungarian Regulatory Guide 4.12; see (Katona, 2010).

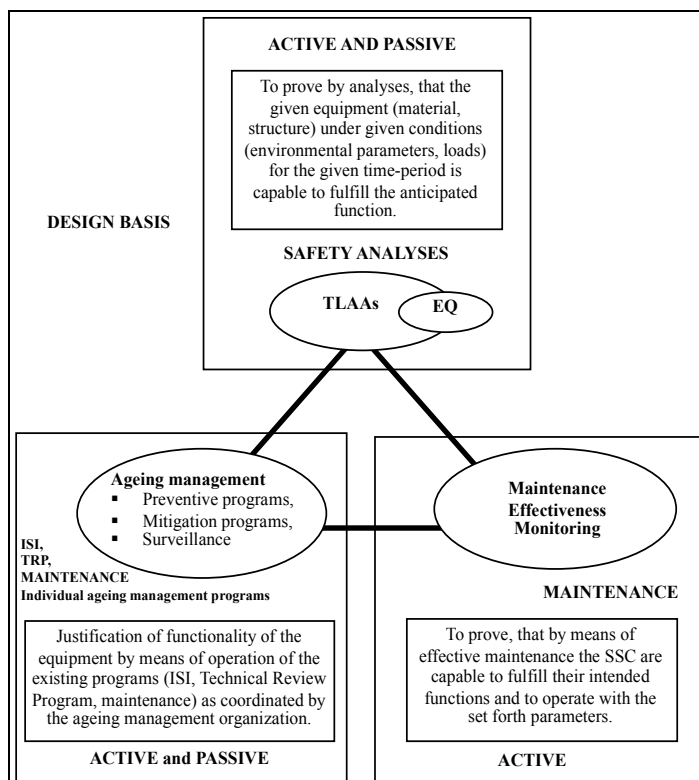


Fig. 9. System for ensuring required safety function and performance of the plant

The possible plant programmes are the ageing management programmes, routine plant surveillance, in-service inspection, testing and monitoring programmes, the maintenance programmes and the scheduled replacement and reconstruction programmes.

Routine plant programmes can be credited after review and justification of effectiveness.

The criteria of adequacy of existing plant programmes with regard to LTO are presented in Section 7.

The adequacy of TLAAs has to be reviewed and demonstrated while entering into LTO; see section 8.

Usually, ageing management programmes ensure the performance and function of passive long-lived SCs. Some VVER operators, such as Hungary, ageing management deals with passive components and structures only, since the active components and systems are addressed by the maintenance rule. There are VVER operating countries where the ageing management deals with both active and passive components and structures.

Plant may select and optimise the methods applied for particular SSCs while the plant practice should be gapless, i.e. all SSCs and degradation mechanisms affecting the safety functions should be covered by the system. However, in case of structures and components of high safety relevance, regulation requires performance of dedicated ageing management programmes. In case of systems working in harsh environment, dedicated programme for maintaining of environmental qualification is required.

### 5.3.2 Environmental qualification

Performance and functioning of active systems can be tested during the operation and can be ensured via maintenance under maintenance rule (MR), i.e. evaluation and assessment of the effectiveness of the maintenance along safety criteria and/or via implementation of the programme for maintaining the environmental qualification (EQ).

Environmental qualification should be implemented especially for I&C equipment, which shall operate in harsh environment.

When the older VVER-440 and VVER-1000 NPPs were built, large part of the originally installed electrical and I&C equipment did not have initial qualification or the qualification was not certified properly. The issue was recognised already in the first reviews for safety; see (IAEA, 1992) (IAEA, 1996a) (IAEA, 1996b) and (IAEA, 2000).

The resolution of the issue can be made in two steps:

- restoring the initial qualification
- maintaining the qualified condition of the equipment.

The maintenance of the qualification means:

1. Control of the capability of equipment to fulfil its safety function through:
  - a. periodic testing of systems and components
  - b. testing of the equipment following maintenance
  - c. results of service routes by maintenance personnel
  - d. diagnostics measurements;
2. Development and implementation of scheduled replacement programme taking into account the requirements for environmental qualification while purchasing the new equipment;
3. Preventive maintenance of the equipment;

The environmental qualification should be reviewed and validated for the extended operational lifetime. There are different possible outcomes of the review:

- The qualification remains valid for the period of long-term operation.



- The qualification has been projected to the end of the period of long-term operation.
- The effects of ageing on the intended function(s) have to be adequately managed for the period of long-term operation via introducing new ageing management programme.
- There is a need for replacement of the equipment.

The plant activity regarding the environmental qualification is a specific TLAA review and revalidation task.

### 5.3.3 Maintenance

According to the logic outlined above, the required condition and functioning of (mainly) active systems and components can be ensured via maintenance or programme for maintaining environmental qualification and/or condition-dependent scheduled replacements.

The plant maintenance programme can be credited as adequate tool for ensuring long-term operation after reviewing and justification of its effectiveness.

Proper procedure has to be in place for monitoring the effectiveness of the maintenance. The monitoring shall demonstrate that the performed maintenance activity ensures the meeting of maintenance objectives set for the SSCs in scope of the maintenance programme and shall provide the necessary information for the improvement of the programme if deviations are detected.

The procedure for monitoring the effectiveness of maintenance should be applied using graded approach depending on the risk-relevance of the SSCs. The risk significance has been defined quantitatively by probabilistic safety analysis (PSA) or qualitatively by expert judgement.

Beyond identification and repair of actual and possible failures, the maintenance process includes other support activities such as in-service inspection and testing, evaluation of maintenance results and monitoring of meeting the maintenance criteria.

These criteria or objectives of the maintenance can be the following:

- Availability
- Success of starting tests
- Failure frequency experienced during tests
- Opening-closing time closing compactness
- Quantity of delivered medium delivery head deviation from the recorded characteristic
- Failure frequency
- Measurement and operation accuracy
- Success of overloading tests
- Repetitive failures that can be prevented by maintenance
- Violation of the Technical Limits and Specifications or being under its effect.

In some countries, e.g. in Hungary the maintenance effectiveness monitoring (MEM) is an adaptation of 10CFR50.65 for the WWER-440/213 design features and Hungarian regulatory environment and plant practice (Katona&Rátkai 2010). There are two basic methods applied in the monitoring:

- deterministic method, i.e. control of maintenance via testing/measuring performance parameters of component
- probabilistic method, i.e. assessing the effectiveness of maintenance via comparison of reliability/availability parameters on the level of component/system or plant.

Performance parameters are defined in accordance with safety class and risk significance.

The deterministic method is based on ASME OM Code. For example, in case of pumps the performance criteria to be checked are the head flow-rate and vibration level. Plant level deterministic performance parameters are for example the capacity factor thermal efficiency of the unit leakage of the containment (%/day).

Risk significance and the probabilistic performance criteria are set based on PSA. Those SSCs are high risk significant, which are in 90% cut set having high contribution to core damage frequency (CDF) or high Fussel-Vessely rank. Performance criteria are based on the reliability/unavailability of performing safety function. System level performance parameters are for example failure rates per demand (failure/start) or run failure rate (failure/time) during operation. Plant level performance parameters are the CDF or some selected contributors to the CDF and other safety factors (unplanned reactor scrams or safety system actuations per year).

The MEM is under implementation at Paks NPP. For the implementation of ASME OM Code, the existing in-service and post-maintenance testing programmes of the Paks NPP have to be modified and amended. Probabilistic performance criteria are under development now. It is expected that the MEM will improve the safety factors and capacity factors for the plant while the maintenance effort will be optimal. MEM is a prerequisite for license renewal in Hungary since it provides the assurance for the functioning of active components.

#### **5.4 Regulatory requirements regarding justification and approval of LTO**

Generally, PLiM is not regulated in VVER operated countries. However, the effectiveness of ensuring the safety functions and plant performance is subject of periodical safety reviews. Contrary to PLiM, the long-term operation beyond the originally licensed or designed term needs well-defined justification and regulatory approval; see e.g. (Svab, 2007).

According to (OECD NEA, 2006) and (IAEA, 2006) there are two principal regulatory approaches to LTO depending on the legislation regarding the operational licence.

The operational licence in VVER operating countries is either limited or unlimited in time.

In those countries where the operational licence has a limited validity in time formal renewal of the operational licence is needed. These are Russia and Hungary where the operational licence is limited to the design lifetime namely 30 years. In these countries, the regulation prescribes the conditions for licence renewal.

In Hungary, the national rules for licence renewal have been developed based on the U.S. Nuclear Regulatory Commission licence renewal rule. In Russia, the rules defined within the context with national regulation.

The control of the compliance with current licensing basis can be maintained via

- Final Safety Analysis Report (FSAR) and its annual update
- Periodic Safety Review (PSR) every ten years
- other regulatory tools including Maintenance Rule (MR) inspections etc.

Within the frames of the Periodic Safety Report:

- a. It shall be certified that the technical conditions of the buildings and equipment of the unit as well as the standard and conditions of operation fulfil the safety requirements and the contents of the regulatory licence;
- b. The current condition of the plant shall be assessed considering the ageing of the SSCs as well as all internal and external factors that influence the safe operation of the facility in the future;

- c. The current characteristics of the plant shall be compared with the regulations considered as up-to-date in international practice and the deviations limiting the safe operability shall be defined according to the regulations considered as up-to-date;
- d. The risk factors revealed based on Items b) and c) shall be ranked and a corrective action program shall be created in order to increase the level of safety.

If the PSR is the basis of the approval for LTO it has to have an extended scope compared to the previous PSR.

The PSR for approving LTO has to include the following tasks:

- comprehensive assessment of the condition of the plant
- review of the plant programmes especially the ageing management activity and
- revalidation of time-limiting ageing analyses for safety relevant long-lived and passive SCs.

The LR is focusing on the ageing of the long-lived passive SCs and revalidation of TLAAs while the performance of active systems and components is controlled in accordance to the maintenance rule and via programmes for maintaining the environmental qualification.

The logic of the justification of the application is shown in Fig.10.

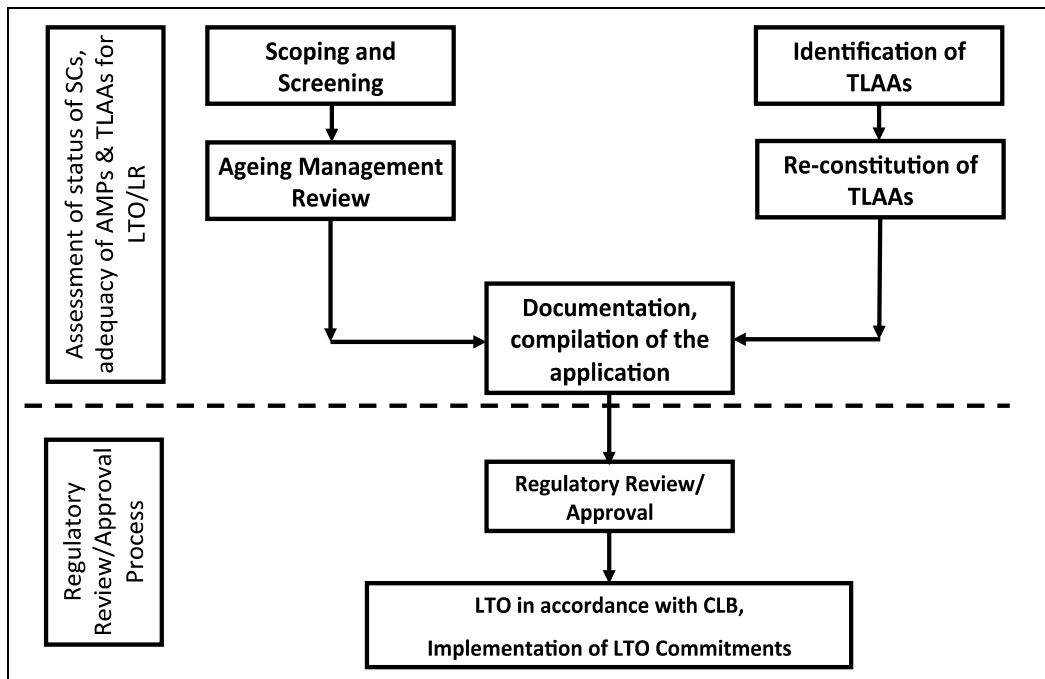


Fig. 10. Logic of the justification of licence renewal application

In the VVER operating countries, licensing of extended operation is rather complex it requires obtaining the environmental licence for extended term of operation and other permissions. This system of licensing is shown in Fig.11.

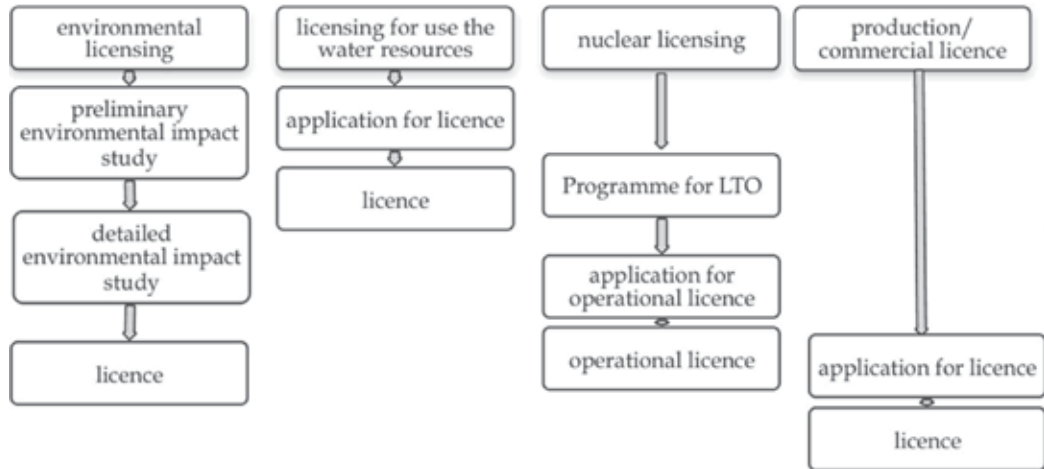


Fig. 11. Flowchart for licensing of extended operational lifetime

## 6. Review of the plant condition

Independent from the regulatory framework for approval of LTO, plant actual condition has to be reviewed and assessed. In the framework of licence renewal, the review of plant condition is part of the integrated plant assessment. In case of periodic safety review, the review of the plant condition is the review area of the safety factor 2 in accordance with IAEA Safety Guide NS-G-2.10 (IAEA, 2003).

The goal of the review is to evaluate and demonstrate the good health and their function and performance in line with requirements.

The scope of the review covers the following SSCs:

1. SSCs with highest safety importance – safety class 1 2 and 3;
2. those non-safety SCs which can jeopardize the safety functions;
3. non-safety related SSCs which can jeopardize the environment (non-nuclear pipelines and tanks for storing different chemical substances);
4. SSCs important for production (turbine cooling water distribution panels etc.).

The review of plant condition is based on the information related to the health of components from the following sources:

- results of operational information records of the operational events;
- failure data root-cause analysis failure statistics;
- outage and maintenance records.

The evaluation can result in:

- modification of the maintenance procedures;
- modification of the periods of the maintenance;
- introducing new diagnostic measures in order to determine the necessary additional actions;

- performing additional evaluation of the situation;
- modifications e.g. implementation new sealing;
- replacement of the component for a different type.

The inspection program for safety class 1 SCs is the most rigorous one. It includes the following:

- data of the non-destructive testing of the SCs;
- evaluation of the results of the in-service inspections;
- evaluation of the results/findings of the maintenances;
- evaluation of the results of the ageing management programs;
- evaluation of failure data and other lifetime information;
- evaluation of operational information.

The non-destructive testing is a regular activity at the power plants. However, in the frame of the plant review for the justification of LTO some additional tests might be necessary. Individual programs can be useful and developed for the Class 1 SCs, i.e. for the reactor main isolation valves (if exist), main pipelines of primary loops, steam generators and pressurizer.

In case of groups (2)-(4) of SCs listed above, the methodology of the inspection for reviewing the plant condition is based practically on the information sources as in case of the group (1). However, the review method is the visual on-site inspection. Application of the graded approach is useful, i.e. in case of higher importance or safety relevance the inspection has to be performed for each particular item while the review can be limited to the inspection of a representative sample of the commodity. The selection of the representative sample has to be made taking into account the type material dominating degradation mechanism environmental stressors etc.

There are very trivial questions or aspects to be checked during the inspections for example:

- symptoms of leakages
- condition of the insulation;
- condition of painting;
- condition of surfaces without painting;
- condition of welding;
- condition of component at junction point of different materials;
- condition of bolted joints etc.

After performing all of the on-site inspections, the findings have to be evaluated and the corrective measures have to be identified. The information obtained has to be taken into account while reviewing the ageing management programmes and TLAAAs.

## 7. Ageing management

Ageing management programmes (AMPs) might be preventive, mitigating of consequences of ageing or slowing down the process like the chemistry programmes.

There are programmes for monitoring of the condition and/or performance of SCs assuming that effective measures might be implemented for compensating the ageing effect and ensuring the required function.

The attributes of ageing management programmes are defined by the national regulations and the IAEA Safety Guide NS-S-G.12 (IAEA, 2009). All these definitions are similar to each other and to the definition given by the NUREG-1801 (US NRC, 2010).

According to the flowchart in Fig.10, the plant has to define the scope of its ageing management and has to review the adequacy of the existing programmes.

Plant routine programmes e.g. the in-service inspection programme might be credited as adequate for ensuring the safety of the LTO if they can be qualified by the review.

## 7.1 Scope of the ageing management

### 7.1.1 Generic approach

Scope of ageing management programmes covers all safety-classified passive, long-lived structures and components, which have to perform intended safety function during operational lifetime. These are the safety and seismic classified SCs. Those non-safety structures and components have to be included into the scope failure of which may inhibit/affect the safety functions.

Depending on the national regulation, the definition of the scope, of ageing management may vary. The scope of AMPs can be extended to the components and equipment having high operational value too.

The starting point of the process is the definition of the safety and seismic classified SSCs. From that scope the SSCs have to be screened those, which are active and short-lived, i.e. in the scope of maintenance and scheduled replacement. The long-lived SCs requiring environmental qualification fall also out. The logic of the definition of the final scope of ageing management after scoping and screening is shown in Fig.12. Furthermore, and it is not indicated in the Fig.12 those SCs have to be also excluded, long-term operation of which will be justified via revalidation of TLAAAs only. A very similar flowchart is given in (IAEA, 2007).

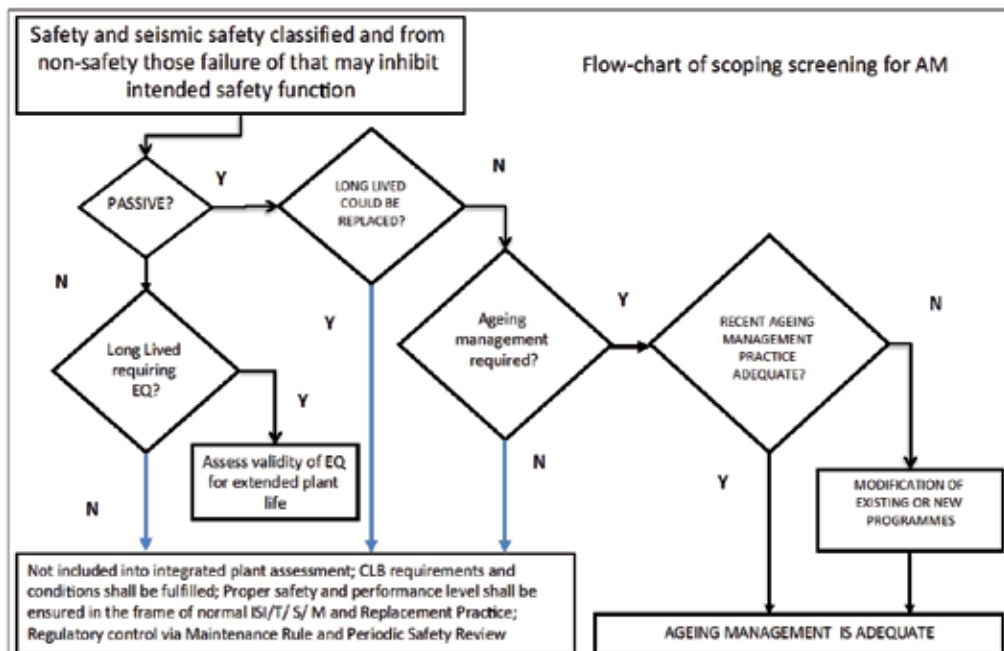


Fig. 12. Flowchart for scoping and screening for ageing management and AM review

Typical set of SCs within the scope of ageing management are as shown in the Table 1; see (Katona et al, 2005) and (Katona et al, 2009b):

SCs within the scope of AM	
Reactor pressure vessel (RPV)	Pressurizer
Reactor vessel internals	Hydro-accumulators and other SSCs of ECCS
Reactor vessel supports	Pumps valves and piping of safety classes 2 and 3
Control Rod Driving Mechanisms	Emergency diesel-generator
Reactor cooling system (RCS)	Containment isolation valves
Piping connected to RCS	Feed-water piping pumps valves
Steam generator	Safety related heat exchangers
Main circulating pump	Piping and component supports
Main gate valves	Containment ventilation system

Table 1. SCs within the scope of ageing management

The IAEA Safety Guide on ageing management interpret the scope of AM including all systems structures and components relevant to safety (IAEA, 2009). Some VVER operating countries ageing management deals with both active and passive components and structures.

### 7.1.2 Specific features of the VVER-440/213 plants

First essential peculiarity of VVER-440/213 design is related to the extreme large number of safety-classified systems structures and components. In case of Paks NPP, the number of SSCs within Safety Classes 1-3 is over hundred thousand because of design features and methodology of safety classification.

The number of passive long-lived of SCs is also very large. After screening out the active and short-lived systems from the total safety classified SSCs approximately 38000 mechanical 6500 electrical and 2000 structural SCs have been identified to be in scope.

This magnitude of the scope multiplies all the ageing management effort of the plant. Methods should be applied for reasonable management of this large scope, e.g. careful structuring is required for effective organisation of ageing management and proper IT tools have to be developed for support of organisation of ageing management and dealing with information related to condition of the SCs (Katona et al, 2008).

## 7.2 Structuring of ageing management programmes

The VVER plants developed different types and system of ageing management programmes e.g.:

1. Plant overall AMP.
2. AMPs addressing a degradation mechanism.
3. Structure or component oriented AMP.

### 7.2.1 Plant overall AMP

Plant overall AMP can be developed and implemented for definition of the goals of the operating company distribution of the responsibilities and organizational performance and policy level activities definition of the structure of the system for ensuring the required plant condition, i.e. the implementation of the concept shown in Fig.9. Several VVER operating countries have utility or even industry level or umbrella type ageing management programmes like Ukraine. The plant level programme has to be deduced from the overall one furthermore the unit level programme from the plant level one. The plant overall AMP also includes the categorisation of the SCs in accordance to the safety relevance importance and complexity. Considering the structuring and organisation of AMPs, graded approach

should be applied according to the safety relevance of the given structure or component and plant lifetime limiting character of the given ageing mechanisms.

### 7.2.2 AMPs addressing a degradation mechanism

AMPs addressing a particular degradation mechanism are listed in the Table2.

### 7.2.3 Structure or component oriented AMP

Applying the graded approach the SCs can be separated into two categories:

1. Highly important from safety point of view items with complex features and ageing mechanisms;
2. Items, e.g. pipelines pipe elements valves heat exchangers which have the same type safety class identical design features materials operating circumstances dominating ageing mechanism could be grouped into commodity groups and for each commodity group a designated AMPs should be implemented.

The highly important SCs like reactor pressure vessel together with internals components of main circulating loop (SCs of Safety Class 1 and some SCs of Class 2) can have dedicated individual AMPs, which are composed from several programmes, each of them is addressing one of the degradation mechanism critical location.

A structure or component oriented AMP is effective for determining the actual condition of specific structure or component or part of a complex SCs (control rod drives) for example:

- a. Reactor pressure vessels
- b. Steam generators
- c. Reactor pressure vessel internals
- d. Pressurizers
- e. Main circulation pipeline
- f. Main coolant pumps
- g. Main gate valves

There are items, e.g. pipelines pipe elements (elbows T-pieces) valves heat exchangers, which can be grouped into commodity groups according to type material working environment. The SSC within a group have the same degradation mechanism and about the same operational and maintenance history. It is very reasonable to develop specific ageing management programmes addressing ageing of commodity groups. The definition of the commodity groups is performed applying the attributes given in the Table 3 in all reasonable combinations.

AMPs addressing a particular degradation mechanism	
Low-cycle fatigue	Thermal ageing
Irradiation damage	Stress corrosion
Boric acid corrosion	Wear
Local corrosion	General corrosion
Irradiation assisted stress corrosion	Loosening
Swelling	High-cycle fatigue
Thermal stratification fatigue	Erosion
Erosion-corrosion	Microbiological corrosion
Water hammer	Groundwater corrosion
Deposition	

Table 2. AMPs addressing a particular degradation mechanism



Safety classification	Type of SSC	Medium	Material
Safety Class 1	Valve body	Borated water	Stainless
Safety Class 2	Pump body	Prepared water	steel
Safety Class 3	Pipe and pipe elements	River/see water	Cast
Non-safety class failure of which may inhibit intended safety function	Heat exchanger	Steam gas-steam mixture	stainless steel
	Tank	Acid or alkali	Carbon steel
		Oil other	

Table 3. Attributes for the definition of commodity groups

### 7.2.4 VVER-440/213 example – AM for civil structures

The VVER-440/213 design is very much differing from the usual architecture of PWRs. In case of Paks NPP practically all building structures at the plant are within the scope. Most of these building structures are complex and heterogeneous from the point of view of structural design, layout, manufacturing and construction of members, material composition and contact with environment (Katona et al, 2009a). In case of Paks NPP it would be difficult to adopt the AMPs described in GALL Report (US NRC, 2010) where nine groups of building structures seven groups of structural components are defined, and ten ageing management programmes cover the whole scope. At Paks NPP, the large number and variety of building structures and structural components requires establishment of a hierarchical structure of ageing management programmes. The type A programmes have been developed for the SCs shown in Table 4.

SCs addressed by A-type AMP	
foundations	reactor support structure
reinforced concrete structural members	equipment foundations
steel and reinforced concrete water structures	carbon and stainless steel liners
prefabricated panels	masonry walls
earth structures	doors and hatches steel-structures
cable and pipe supports	paintings and coatings
penetrations	fire protection structures
main building settlement	support structures of cabinets
sealing's and isolation	corrosion in boric acid environment.

Table 4. SCs addressed by A-type AMP

These programmes are related to specific structures, i.e. structural commodities or specific ageing mechanisms (e.g. building settlement due to soft soil conditions). The control of leak-tightness of the containment is also an A type programme which is related to the containment only.

The buildings having identified safety functions are composed from structural commodities. Using the type A programmes for specific structures (commodities) 30 programmes of type B have been composed which covers all plant building structures. These AMPs contain the identification of ageing effects and mechanisms to be managed the lists and details of the proper application of AMPs of type "A" to be applied while managing the ageing of the given building. The "B" type AMP also contains logistical type information since the accessibility of certain buildings is limited.

### 7.3 Steps of the development of AMP

Practically the first step of the procedure of the development of the ageing management programme is the scoping-screening presented in Section 7.1 above. In strict sense the AMP can be developed in following sequence:

1. Identification of degradation mechanisms and locations susceptible to ageing
2. Identification of the mitigation and preventive measures
3. Identification of the parameters to be controlled
4. Definition of the method for the detection of ageing effects
5. Definition of the monitoring trending condition evaluation
6. Definition of the acceptance criteria
7. Identification of the corrective actions
8. Organising the administrative control
9. Organising the operational experience feedback

In the reality, the development is some kind of iterative process and steps are overlapping, as it will be shown below.

#### 7.3.1 Identification of ageing mechanisms

The development of AMPs has to be started with the identification of the ageing mechanisms critical locations and effect of the ageing on the intended safety function. In case of AMP to be developed for a complex structure or component like reactor or steam generator, several mechanisms and critical locations can be identified. The material conditions and stressors are considered at this step of the AMP development. Examples for the mechanisms are listed in the Table 2.

In fact, the structuring of the ageing management programmes and the identification of the commodities depend from the identification of ageing mechanisms.

For example, a commodity group can be defined as follows, see Table 3: “Safety Class 3” + “Piping and pipe elements” + working in “prepared water” (e.g. feed-water line) + “carbon steel”. As per experience, the dominating ageing mechanism of this group is the flow-accelerated corrosion (FAC), which is a degradation process resulting in wall thinning of piping vessels heat exchanger and further equipment made of carbon and low alloy steel. This degradation mechanism of the identified commodity group should be addressed by proper AMP which can be developed, e.g. via application of COMSY system (Zander, Nopper, Roessner, 2007) used by several VVER operators.

#### 7.3.2 Preventing measures

The second step of the development of the AMPs is the identification of the means of preventing or controlling of the ageing. For example, the corrosion phenomena on the internal surfaces can be slowed down via adequate water chemistry parameters. General corrosion and soil corrosion may be reduced by coatings and ensuring the undamaged state of the coatings. The most effective way of avoiding boric acid corrosion is the timely detection and effective termination of leakages onto carbon steel elements, which are the subject of walk down inspections.

#### 7.3.3 Parameters to be controlled

Identification of the parameters allowing the control of the degradation process is essential part of AMP development. Some parameters are indicating the evolution of degradation

directly e.g. the wall thickness of piping. The water chemistry parameters can be used as indirect controlling parameters of all internal surface corrosion mechanisms.

#### **7.3.4 Definition of the method for the detection of ageing effects**

Most of the postulated ageing effects and their occurrence can be detected during the execution of the current programs of the plant as follows:

- Non-destructive testing performed in the frame of in-service inspection programs;
- Visual inspections performed in the frame of maintenance programs;
- Visual structural inspections;
- Walk-down inspections.

#### **7.3.5 Monitoring trending condition evaluation**

Definition of the methods for monitoring, trending and condition evaluation is the fifth step in the development of the AMPs. For example, the monitoring of the trend of fast neutron fluence absorption in the critical components of the reactor pressure vessel is one of the most important indirect ageing management elements. The monitoring of load cycles defined during design and of their parameters belongs to the ageing management of fatigue degradation mechanism. The monitoring of the number and growth of crack-indications found during material inspections and visual inspections in the frame of in-service inspection can be assigned to each local degradation phenomenon. The monitoring and trending of the value of wall thickness reduction could be taken into account in the case of degradation forms with general material loss. In the case of heat exchangers, the monitoring of the number of plugged tubes can be considered also as an ageing management program element.

#### **7.3.6 Acceptance criteria**

The acceptance criteria are expressed as a limit value for the controlled parameter of the ageing. The limit value corresponds to the performance or functioning with required margin, see Fig.1. Acceptance criteria have to be defined for each component or commodity for each degradation mechanism in relation with fulfilment of intended safety function. The acceptance criteria can be derived from stress calculations in case of allowable wall thickness of piping or fatigue calculation regarding allowable load cycles. The acceptance criteria for degradation phenomena entailing decrease of the brittle toughness are determined by the relevant TLAA analysis results. The compliance criteria for water chemistry parameters are defined in the relevant chemistry instructions.

#### **7.3.7 Corrective actions**

The damages not complying with the acceptance criterion should be repaired if it is possible. In case of fatigue  $CUF > 1.0$  appropriate fatigue monitoring focused in-service inspection programme can be implemented.

#### **7.3.8 Administrative control**

The administrative and organisation arrangements have to be defined for the performance of ageing management programmes. Appropriate plant procedures have to ensure the planning staffing performing documenting and management control of the AMPs. Proper

system for documentation and reporting has to be established. Proper quality assurance plan has to be also developed for AMPs.

### **7.3.9 Operational experience feedback**

A system for the verification of the effectiveness of AMPs and feedback of experience has to be in place at plants. In the case of the found damages, the degradation mechanism should be identified and then it should be evaluated whether the given degradation mechanism is properly managed by the AMPs.

### **7.3.10 Crediting the existing plant programmes**

Review of the existing plant programmes can qualify these programmes for adequate for ageing management. For example, the following programmes can be classified as AMPs or part of AMPs:

- Preventive and predictive maintenance programme can be considered to be part of AMP because it is one of the solutions of ageing mitigation and it is also necessary for AM to obtain information on carried out preventive maintenance of SCs
- In-service inspection programme
- Functional Testing Programme – for active components if they are in the scope of AM.

## **7.4 Review of the AMPs**

The nine generic attributes of an effective ageing management programme against which each ageing management programme should be evaluated are see (IAEA, 2009):

1. Scope of the ageing management programme based on understanding of the ageing
2. Preventive actions to minimize and control the ageing degradation
3. Detection of the ageing effects
4. Monitoring and trending of the ageing effects
5. Mitigating the ageing effects
6. Acceptance criteria
7. Corrective actions
8. Operating experience feedback and feedback of R&D results
9. Quality management

The attributes above are for checking whether all steps for development of AMPs discussed above have been done properly and the practical effectiveness of AMPs ensure the intended safety functions and LTO goals.

## **8. Analyses of ageing processes**

### **8.1 TLAAs and their role of the in justification for LTO**

Although the wording is sometimes different, the term “time-limited ageing analyses” is understood by the VVER operators in a very similar way as it is defined in US NRC Code of Federal Regulation 10CFR Part 54 Requirements for Renewal of Operating Licenses for Nuclear Power Plants. The role of the review and revalidation of the TLAAs in the justification of LTO is also the same as in the international practice.

The TLAAs are those calculations and analyses that:

1. Involve systems structures and components within the scope of LTO;
2. Consider the effects of aging;

3. Involve time-limited assumptions defined by the current operating term for example in case of VVERs considered 30 years;
4. Were determined to be relevant by the licensee in making a safety determination;
5. Involve conclusions or provide the basis for conclusions related to the capability of the system structure and component to perform its intended functions; and
6. Are contained or incorporated by reference in the CLB..."

Existing TLAAs should be reviewed and revalidated with assumed extended time of plant operation. The evaluation of each identified TLAA should justify that the safety function of the SC will remain within design safety margins during the period of LTO.

The plants have to demonstrate either in the frame of the PSR or in the licence renewal application that:

- The analysis remains valid for the period of long-term operation;
- The analysis has been projected to the end of the period of long-term operation; or
- The effects of ageing on the intended function(s) will be adequately managed for the period of long-term operation.

There are three possibilities for validation of the TLAAs:

- It is possible to extend the validity the TLAAs;
- It is possible to remove the conservatism used in the TLAA analysis by less conservative assumptions and methods for analysis. It practically means to perform a new analysis.
- It is possible to demonstrate that measures will be introduced during the extended service life which will control the ageing processes and ensure the intended safety function.

## 8.2 The scope of the required analyses

The identified TLAAs cover the usual areas as fatigue calculations assessment of embrittlement changes of material properties etc. However, the scope of TLAAs in case of some VVERs is differing from the usual one either because of the peculiarities of the design or because of national regulation. For example, in case of Paks NPP, the scope of fatigue calculations is extended to the Safety Class 1 and 2 piping and components, and the analysis of thermal stratification is included. Regarding RPV, besides of PTS analysis, the limits and conditions of safe operation, i.e. the p-T curve has to be re-analysed in the frame of revalidation of TLAAs.

## 8.3 The issue of the TLAAs

Review and validation of TLAAs is a rather complex task for majority of VVER plants. The issue is related to the availability of design base information and incompleteness of the delivered design documentation. Often the results of the analyses are known only; in some cases, the analyses are presumably obsolete.

The TLAAs have to be reviewed and verified for most important structures and components by control calculations using state-of-the-art methods. In many cases, the analyses have to be newly performed in accordance with the recent requirements.

Development of methodology of TLAA reconstitution and definition of the way of adaptation of ASME Boiler & Pressure Vessel Code Section III (ASME BPVC) for a Soviet designed plant has been reported in (Katona, Rátkai, Pammer, 2007) and (Katona, Rátkai, Pammer, 2011). Hungarian regulations require application of state-of-the-art methods codes

and standards while performing the time-limiting ageing analyses. ASME BPVC edition 2001 had been selected for the reconstitution of TLAAAs and associated strength verification. The code selection requires understanding of both the Russian (Soviet) design standards and the ASME BPVC code. Different studies were performed for ensuring the adequacy of ASME BPVC implementation for VVER-440/213.

Calculations were performed for 50 years extended operational lifetime with additional margin of 10 years.

Comparing the practice of different VVER operating countries probably the most complex cases are the Eastern-European VVER-440/213 plants since these plants have to solve the issue indicated. The case of Paks NPP Hungary will be discussed below based on the (Katona et al, 2010).

### 8.3.1 Mechanical components

For justification of safety of long-term operation, the scope of TLAAAs to be reconstructed or newly performed covers the Class 1 and 2 mechanical components. Examples of the calculations/analyses are as follows:

*Low cycle fatigue analysis for Safety Class 1 and 2 piping and mechanical components:*

ASME BPVC was adapted for the calculations; see (Katona, Rátkai, Pammer, 2011). This task also includes identification of needs for fatigue monitoring. Part of the analyses has already been performed. This justified the operability of the Class 1 and 2 piping and components for 50+10 years.

There are only a few non-compliances found.

Most critical ones are the high stresses in the body and sealing block of the main circulating pumps. These however could be managed via focused non-destructive examination programs.

*Analysis for thermal ageing of Class 1 and 2 components:*

This task focuses on components manufactured from 15Ch2MFA 22K 08Ch18N9TL casted stainless steel materials and on welds (Sv04Ch19H11M3 EA400/10T Sv10ChMFT IONI 13/55), which are sensitive to thermal embrittlement.

Change of crack propagation resistance due to thermal embrittlement has been evaluated. Significant changes of material properties due to thermal embrittlement are expected in case of ferrit-pearlit materials or casted stainless steel above 220°C operational temperature.

Only a few components comply with these conditions at Paks NPP.

According to fatigue analyses, there are no cases where crack propagation due to fatigue might be expected. The analysis performed for the main gate valve casted stainless steel body shows that crack propagation should not be expected even if the J-R curve for C8 steel is changing due to embrittlement and a crack is postulated.

*Analysis of thermal stratification for Class 1 and 2 pipelines:*

A measuring system was operated at Paks NPP Unit 1 pressurizer surge line in 2000-2001. Assessment of measured data shows significant thermal stratification (110°C), which moved periodically from the pressurizer to the hot leg. This temperature swing was kept by the swing of water level control in the pressurizer during the heat-up and cool-down. During normal operation, the temperature differences were decreased to a negligible level.

A similar temperature monitoring system is operating on both legs of surge line at Unit 3 since 2007. Evaluation of the measured data and the subsequent fatigue analysis justify the long-term operation for the pressurizer surge lines.

Other pipelines have also been identified where thermal stratification might be the case, e.g. the pipelines connecting the coolant cleaning system No 1 to the primary system the pipeline of passive emergency core cooling system the feed water system pipeline and also the auxiliary emergency feed water pipelines. Experience gained at other VVER-440/213 plants (Mochovce and Dukovany NPP) has been taken into account while the pipelines of interest have been identified. Implementation of monitoring programs is going on at these pipelines with temperature and displacement measurements.

*High cycle fatigue analysis of flow-induced vibration of internal structures of the steam generator tubes:*

This analysis shows that the flow-induced vibration of the heat-exchanging tubes does not cause significant stresses compared to those due to operational loads. Taking into account 60 years of operation and 108% of reactor thermal power the CUF is equal to 0.027 due to vibration even if a pipe wall thinning of 50% is assumed.

*Analysis of the corrosion of piping wall:*

The question is whether the erosion-corrosion allowance applied in the design provides sufficient margin for 50+10 years of operation. The analyses are supported by the data obtained from the erosion-corrosion program, which was implemented practically from the start of operation of the plant. The measured/observed rate of wall thinning is compared to those postulated in the design.

Few cases are expected only where the existing corrosion-erosion monitoring program using COMSY software has to be extended.

*Analysis for material property change of the steam generator tubes:*

The main finding of the study is that the thermal ageing of 08H18N10T material of heat exchanging tubes is negligible at operating temperatures ~290°C. Similar results were obtained from the destructive testing of piping of RBMK reactors made from the same material and working at the same operational temperatures. The material properties provided by the manufacturer can be used while selecting the standardized fatigue curves for the heat exchanging tubes. Results of laboratory tests show that there is no change in the fatigue crack propagation rate due to long-term operation at 288°C; see (NPO Hidropress, 2007).

An operational time of 60 years is justified with this respect.

*Crack propagation analysis of detected defects in Class 1 and 2 components:*

The results of the analyses show that the detected defects are not critical from crack propagation point of view. The retrospective sampling performed for the RPV analysis does not lead to fracture mechanical consequences. The qualification defect sizes of non-destructive testing are also found adequate. The size of acceptable defects should also be reduced in the cases of cracks through cladding and of the longitudinal welds of steam generators. In the frame of this task, the embedded cracks in the heat affected zone below the RPV cladding, which are caused by inter-granular segregation will be analysed.

### **8.3.2 Reactor pressure vessel and internals**

For the justification of operability of RPV and RPV internals for extended operational lifetime, the following analyses have to be performed:

*PTS analyses for RPV*

The structural integrity against brittle fracture of the RPV is ensured if the factual ductile-brittle transition temperature (DBTT) of its critical components is less than the maximum

allowable component-specific DBTT. The analysis is based on the comparison of the static fracture toughness of the material and stress intensity factor calculated from the given loading situation (Linear Elastic Fracture Mechanics or LEFM concept).

Steps of the analysis are as follows:

- Identification of the critical components of the RPV: These are the parts of RPV belt line region (base metal circumferential weld No. 5/6 heat affected zone of the weld cladding) as well as the other circumferential welds of the RPV including the nozzle region.
- Selection of the PTS initiating events: Beyond the PTS initiating events selected on the basis of engineering judgment (LOCAs, stuck open pressurizer safety or relief valve, primary to secondary leakage accidents, etc.) additional transients are also considered if the frequency of occurrence is higher than  $10^{-5}/a$ .
- Thermal-hydraulic calculations: These calculations provide the temperature fields in the down-comer distribution of heat transfer coefficient and pressure of reactor coolant as a function of time.
- Calculations of neutron fluences: Based on core configurations implemented so far and planned to be implemented in the future calculations using KARATE core design code (Kereszturi et al, 2010) and MCNP code (Breismeister, 2000) were performed. End-of-life fluences (for 50 and 60 operating years) are calculated for the RPV wall as well as for the surveillance position. Neutron dosimetry results have been used to verify the calculations.
- Temperature and stress field calculations: Temperature distribution in the RPV wall is determined for the analysed transient as a function of the coolant temperature and heat transfer coefficient between coolant and wall. Deformation and stress fields occurring because of the temperature transient and pressure inside the vessel are determined by solving the system of equations of elasticity (and/or plasticity).
- Fracture mechanics calculations.

Temperature deformation and stress fields are determined using axial-symmetric and/or simplified 3D models with global meshing and without crack; deformation and stress fields are determined based on linear deformation theory using linear-elastic material model.

A full-scope 3D FEM calculation should be used for those cases where the calculation outlined above would show that any transient could challenge the RPV integrity. In this case the FEM mesh contains a crack model with local meshing; determination of deformation and stress fields is based on theory of large deformations using elastic-plastic material models and von Mises theory; the stress intensity factor is determined from J-integral based on the theory of virtual crack increment.

Transients with annual frequency  $\geq 10^{-5}/a$  have been analysed using the LEFM approach. For the two most significant transients further analyses have been conducted applying the Nonlinear Fracture Mechanics theory (Elastic Plastic Fracture Mechanics) to verify the results coming from the LEFM approach. This double check justified the appropriate conservatism of the LEFM approach.

The conclusion of the analyses is that the RPVs at Paks NPP can be safely operated for at least 60 years. For the sake of completeness of the studies, some additional analyses are still going on regarding for PTS sequences initiated by internal fires flooding and earthquakes under shutdown conditions.



The neutron fluences also have to be modified taking into account the new fuel design introduced after power up-rate. These additional studies are not expected to change the conclusion.

#### *Definition of pressure-temperature (p-T) limit curves of RPV*

The Hungarian Authority issued recently a new guideline to replace the old and quite conservative procedure for performing the RPV p-T calculation. The old procedure considered the residual stresses with very high safety margin similarly to PTS calculations while the new guideline reduces this conservatism according to the present international practice. This new guideline will be the basis of calculations performed for the Unit 1 RPV. This task is interrelated to the tasks for review and justification of operational limits and conditions of the VVER-440/213 units at Paks NPP.

#### *Analysis of fracture toughness of structures within the reactor pressure vessel*

According to the preliminary results, the irradiation-assisted stress corrosion cracking and void swelling may be of interest. The stud joints fixing the polygon mantle to the core basket are the critical structures in case of both ageing mechanisms. The stress corrosion cracks might be initiated at the flange between the cap and threaded part of the bolt. The position of the cap may indicate the swelling.

Considering the radiation and temperature the segment No. 18 of the core basket is the most demanded. Measures can be identified after visual inspection of the core basket and review of inspection procedure.

The possibility of implementation of non-destructive volumetric test method for the bolts is also considered. With respect to the void swelling possibility of implementation of ultrasonic measurements as well as gamma heating and a replacement program are being investigated.

### **8.3.3 Analyses related to operational limits and conditions**

Review of Final Safety Analyses Report and reconstruction of design bases, which has been performed at Paks NPP, resulted into recognition of need for justification of operational limits and conditions related to certain ageing phenomena via adequate thermo-hydraulic stress and fracture mechanics analyses. These analyses have been included into the scope of TLAAAs required for the justification of long-term operation of Paks NPP. The task also includes the justification for modification of the limits and conditions in accordance with operational needs allowing rapid temperature changes in certain cases. The temperature measurements and the temperature rate control methodology have also been reviewed and amended.

Following analyses have been performed:

- confirmation of permissible cooling down heating up rates for the primary and secondary circuits
- analyses for confirmation of operational limits and conditions for the operational transients.

Analysis has been performed for the following components:

- RPV, RPV-head and RPV-flange;
- Primary side steam generator elements;
- Secondary side steam generator elements;
- Main isolating valve;
- Main circulating pump;
- Pressurizer tank;

- Hydro-accumulators and their valves;
- Main steam system;
- Heat removal system.

The cases analysed are:

- The Normal Start-up Cycle
- The Normal Shutdown Cycle
- The Cycle Start-up from Operational Mode D
- The Rapid Cool-down Cycle
- Pressurizer Flow at Start-up
- The Pressurizer Flow at High Temperature Difference
- Injection at High Temperature Difference.

The main findings can be summarized as follows:

- The calculations performed for the given temperatures temperature rates and processes justify the adequacy of the limits and conditions defined by the designer.
- In case of injection into the pressurizer in accordance with existing limitation on temperature, the margin to allowable stress (3Sm) is minimal and the number of allowable cycles is rather small (6500) therefore monitoring of cycles shall be established.
- In case of rapid cool-down process a leakage of the inner sealing ring may occur, which can be controlled by leakage detection. Since the flanges of MIV are welded together, this will not result in leakage to the hermetic compartment.
- During the rapid cool-down process (70°C/h cooling rate to reach the 150°C state) leakage may appear in the collector assemblies of the steam generators. However, the rapid cool-down may cause only the loosening of the inner sealing ring of the collector assemblies. Therefore, no primary coolant will get over to the secondary side.

According to existing prescriptions for the control of the heat-up and cool-down rates, the temperature has to be measured every minute and averaged over subsequent time-intervals of 19 minutes. The rate for the control has to be defined by taking the difference of the actual and the previous average temperature values. Compliance with hourly rate limit is ensured if the temperature change is less than 6.3°C for heat-up and 9.5°C for cool-down per every 19 minute interval. The performed analyses show that for certain components it is necessary to introduce ten minute averaging intervals with limitations of 33°C and 5°C per ten minutes corresponding to the rates of 20°C/hour and 30°C/hour respectively. The occasional applicability of the processes in primary system with rates 40°C/h for heat-up and 60°C/h for cool-down and for the rate of temperature change in the pressurizer is 80°C/h have been justified as an amendment to the existing procedures. In these cases, the sudden temperature change should be avoided by appropriate temperature control.

The methodology of calculations was based on the adaptation of ASME BPVC. For the calculation of temperature transients in the primary system the RELAP5/mod3.3 code was used. Specific thermo-hydraulic model was developed for accident analyses. This model consists of detailed model of the primary system the heat removal system and the automatic control system and it takes into account the operator's actions during the heat-up and cool-down processes. The thermo-hydraulic model and the calculation method have been verified via comparison of the calculated transient time histories with the measured ones.

### **8.3.4 Containment civil structures and structural components**

Taking into account the specific features of the VVER-440/213 design of civil structures and the lack/missing of analyses performed by the designer eight analysis tasks were identified

as necessary for the justification of long-term operation of Paks NPP. Necessity of the performance of the stress calculations for the validation of the rather sparse information available for containment and other safety-classified structures were also recognized. Considering their content these calculations are not typical TLAAAs. However, without sufficient information on the design of civil structures, the newly performed TLAAAs would not have the design basis.

The scope includes the following tasks:

- Analysis of buildings classified into safety category for the verification of the design.
- Fatigue analysis for the containment penetrations;
- Fatigue analysis for the hermetic liner of the containment (welding transition welding area of anchors);
- Fatigue analysis for the liner of the spent fuel pool (welding transition welding area of anchors);
- Stress and fatigue analysis for the safety classified crane in the reactor hall with capacity of 250/32/2 tons;

In case of Paks NPP, there are several design-specific TLAAAs of the main reactor building for example:

- Fatigue analysis of the containment for increased pressure level during integral leak-tightness tests;
- Analysis of main reactor building settlement.

The allowable leakage value of the VVER-440/213 containment is 14.7 per cent per day at the design pressure of 2.5 bars. Each of the containments was tested at this design pressure in the start-up phase. The pressure of the yearly leakage tests is 1.2 bar and tests at a pressure of 1.7 bars are carried out during the outages. The leakage value for the nominal pressure of 2.5 bars is calculated via extrapolation from the leak-rate results of tests. This practice has been criticised regarding correctness of the leak-rate extrapolated from the measured ones. Therefore, investigations of enhancement of the test pressure level has been proposed. Nevertheless, the recent reduced pressure test procedure has obvious advantages compared to the tests at enhanced pressure level: the time needed for the low-pressure test is short and the load on containment structures is moderate. In the on-going analyses the test procedure covers all aspects of interest: Correctness of the leak-rate defined via testing, the time consumption and the costs of the tests, and the fatigue due to cyclic loads are being considered and evaluated. According to the results of leak-tests, the correct leakage values at the nominal pressure of 2.5 bars can be determined from the results of test out at considerably lower pressure values. This statement is based on analyses of numerous tests including the results of test carried out at the design pressure of 2.5 bars at Unit 2 in 2008.

Regarding Paks NPP, the analysis of settlement of the main building complex has been identified as a TLAA since an excessive inclination of the main building complex due to differential settlement may result in non-allowed tilting of the RPV vertical axis, which may cause problems with the control rods. Additionally, an excessive inclination can cause extreme local loading as well, resulting in degradations of the building. It has to be mentioned that the VVER-440/213 type units at Paks NPP have twin-unit-design, i.e. two main reactor buildings separated by a dilatation gap are built-up on a common base-mat. Detailed settlement control was started during the construction period of Paks NPP. The measured results are to be evaluated and reported annually. A prolonged in time

consolidation process was observed in case of the main reactor buildings the settlement of which is continuing. The phenomenon is related to the seasonal variation of the water level of the river Danube, which may reach a value of 9 meters. This variation of the river water level influences the ground-water level. According to the data measured in the wells at and around the plant site, the ground-water level follows the variation of the water level in the Danube with a certain time delay. The water-table fluctuations influence the stress-deformation conditions in the subsoil. This can explain the successive settlement of the raft foundation as measured during the past years. The settlement at Unit 4 is somewhat larger than at Units 1-3, which is due to the slight inhomogeneity of the subsoil and the highest alteration of the level of the water table occurring near Unit 4.

Detailed analyses have been performed for the subsidence and differential settlements of the main reactor buildings for the end-of-life situation taking into account the static loading (immediate settlement) ground-water fluctuation seismic settlement dynamic settlement due to machinery and tectonic subsidence. The calculation model and procedure has been calibrated to the measured time-history of subsidence. An adequate constitutive model has to be defined for the soil, which includes the development of a non-linear hardening model and proper definition of the decay curve for cyclic loading due to ground-water fluctuation based on soil tests results.

Regarding the long-term operation, the analyses show that a value of differential settlement that may cause non-allowed tilting of the RPV axis due to the inclination of the building should not be expected. The structural integrity of the foundation and the containment part of the main building structures is not affected by the settlement and it is not expected because of further subsidence.

### **8.3.5 Basic findings of the revalidation/reconstitution of the TLAAs**

Dedicated ageing management programs already control some of the processes addressed by the presented above time-limited ageing analyses, e.g. process of settlement of the main building erosion-corrosion of piping wall.

The results of the above analyses show that only a few non-compliances or lifetime-limiting cases have been found and all of them can be managed by the extension/amendment of the existing ageing management programs and/or other plant programs.

For example, regarding RPV and internals the stud joints fixing the polygon mantle to the core basket are the critical structures from the point of view of irradiation-assisted stress corrosion cracking and void swelling. In order to manage these mechanisms, review and extension of the present programs are going on.

Regarding operational limits and conditions in case of injection into the pressurizer, the margin to allowable stresses is minimal and the number of allowable cycles is rather small. Consequently, the number of cycles should be monitored. It was also found that during certain heat-up and cool-down processes the averaging intervals of the temperature measurements have to be modified at certain components.

With respect to the containment civil structures, the existing ageing management program should be extended for managing the change of material properties of heavy concrete structures and to the corrosion of steel liner on heavy concrete surface.

Regarding electrical and I&C components, cases were found where new ageing management programs are to be introduced or replacement of the equipment is needed.

## 9. Conclusions

A complex picture of ensuring and justification of long-term operation of VVER plants is given in the Chapter; especially the VVER-440/213 model is discussed in details.

In VVER operating countries, proper regulatory framework and comprehensive plant lifetime management system have been developed for ensuring the safety of long-term operation of VVER-440 and VVER-1000 type plants. Detailed studies and already approved cases of prolongation of the plant operational lifetime are demonstrating the feasibility of long-term operation of VVER plants.

Generally accepted principles for safety have been followed while developing plant systems which ensure that any SSCs will be covered by some of the plant programmes and within the frame of LTO Programme all conditions of safe operation will be ensured. Significant for safe long-term operation structures systems and components are identified. Proper level of understanding of the ageing phenomena is reached and adequate ageing management programmes were developed for ensuring the required status and intended function for long-term. Revalidation of time-limited ageing analyses also justify the safety of long-term operation, which is completed by the monitoring of maintenance on performance criteria combined with the maintenance of environmental qualification and replacement/reconstruction programmes.

Best international practice and state-of-the-art methodologies have been applied while performing the particular tasks for preparation and justification of long-term operation and license renewal. However, as it has been demonstrated any good examples and experiences should be adapted in creative way taking into account the design features national regulations and existing plant practice.

This way the strategy of VVER operators to operate safely as long as possible and economically reasonable at higher power level will be ensured.

## 10. References

- Breismeister, J.F. (2000). MCNPMTM – A General Monte Carlo N-Particle Transport Code – Version 4C LA-13709-M 2000
- Czech Report (2010). The Czech Republic National Report under the Convention on Nuclear Safety Ref. No. 7972/2010 [http://www.sujb.cz/docs/CZ\\_NR\\_2010\\_final.pdf](http://www.sujb.cz/docs/CZ_NR_2010_final.pdf)
- Erak, D.Yu. et al (2007). Radiation embrittlement and neutron dosimetry aspects in WWER-440 reactor pressure vessels life time extension, *Second IAEA International Symposium on Nuclear Power Plant Life Management*, 15-18 October 2007 Shanghai China
- IAEA (1992). Ranking of safety issues for WWER-440 model 230 nuclear power plants IAEA-TECDOC-640 IAEA Vienna
- IAEA (1993). Proceedings of the SMiRT-12 Conference Seminar No. 16 on Upgrading of Existing NPPs with 440 and 1000 MW VVER type Pressurized Water Reactors for Severe External Loading Conditions. 23-25 August 1993 IAEA Vienna Austria
- IAEA (1996a). Safety issues and their ranking for WWER-440 model 213 nuclear power plants IAEA-EBP-WWER-03 IAEA Vienna
- IAEA (1996b). Safety issues and their ranking for WWER-1000 model 320 nuclear power plants IAEA-EBP-WWER-05 IAEA Vienna

- IAEA (2000). Safety issues and their ranking for WWER-1000 model “small series” nuclear power plants IAEA-EBP-WWER-14 IAEA Vienna
- IAEA (2003). Periodic Safety Review of Nuclear Power Plants Safety Guide Safety Standards Series No. NS-G-2.10 International Atomic Energy Agency Vienna 2003
- IAEA (2006). Plant Life Management for Long Term Operation of Light Water Reactors: Principles and Guidelines. Technical Reports Series No. 448. IAEA Vienna
- IAEA (2007). Safety Aspects of Long term Operation of Water Moderated Reactors IAEA-EBP-SALTO IAEA July 2007 Vienna
- IAEA (2007). Strategy for Assessment of WWER Steam Generator Tube Integrity IAEA-TECDOC-1577 IAEA Vienna 2007
- IAEA (2008). SALTO Guidelines. Guidelines for Peer Review of Long Term Operation and Ageing Management of Nuclear Power Plants. IAEA Services Series No. 17. Vienna International Atomic Energy Agency.
- IAEA (2009). Ageing Management for Nuclear Power Plants IAEA Safety Standards Series No. NS-G-2.12 International Atomic Energy Agency Vienna 2009 (ISBN:978-92-0-112408-1)
- Kadečka, P. (2007). Effective long term operation for Dukovany NPP, *Second IAEA International Symposium on Nuclear Power Plant Life Management*, 15-18 October 2007 Shanghai China
- Kadečka, P. (2009). New PLiM program for Czech NPPs Proceedings of 2009 ASME Pressure Vessels and Piping Division Conference, July 26-30 2009, Prague, Czech Republic
- Katona, T., Bajsz, J. (1992). Plex at Paks - making a virtue out of necessity. *Nuclear Engineering International* 37:(455) pp. 27-31.
- Katona, T. (2006). Core tasks of long-term operation and their relation to plant processes at Paks NPP, *PLIM + PLEX*, 10-11 April 2006 Paris France
- Katona, T. et al (2005). Key Elements of the Ageing Management of the VVER-440/213 type Nuclear Power Plants In: *18th International Conference on Structural Mechanics in Reactor Technology (SMiRT 18)*. Beijing, China 2005.08.07-2005.08.12. Paper D02-4.
- Katona, T. (2010). Plant life management practices for water-cooled water moderated reactors (VVER) In: *Understanding and mitigating ageing in nuclear power plants*, Woodhead Publishing ISBN 978 1 84569 511 8
- Katona, T. et al (2001). Future of the Paks Nuclear Power Plant Lifetime-Management and Lifetime-Extension. In: *Lifetime management: Proceedings of the 21st ESReDA seminar*, Erlangen, Germany 2001.11.05-2001.11.06. Luxembourg: Office for Official Publications of the European Communities pp. 21-36.(ISBN:92-894-5665-5)
- Katona, T. et al (2003). Main features of design life extension of VVER-440/213 units NPP Paks Hungary, *ICONE 11th International Conference on Nuclear Engineering*, Tokyo, Japan, April 20-23 2003
- Katona, T. et al (2009a). Assessment and Management of Ageing of Civil Structures of Paks NPP. In: *Proceedings of the ASME Pressure Vessels and Piping Conference. ASME 2009: Sustainable Energy for the Third Millennium*. Prague, Czech Republic, 2009.07.26-2009.07.30. American Society of Mechanical Engineers p. CD-ROM. Paper PVP2009-77513. (ISBN:9780791838549)
- Katona, T. et al (2009b). Extension of Operational Life-Time of VVER-440/213 Type Units at Paks Nuclear Power Plant In: *Proceedings of the ASME Pressure Vessels and Piping Conference. ASME 2009: Sustainable Energy for the Third Millennium*, Prague,

- Czech Republic 2009.07.26-2009.07.30. American Society of Mechanical Engineers, p. CD-ROM. Paper PVP2009-77911. (ISBN:9780791838549))
- Katona, T. et al (2010). Time-limited Ageing Analyses for Justification of Long-Term Operation of Paks NPP. In: *ASME International Mechanical Engineering Congress and Exposition*. Vancouver Kanada 2010.11.12-2010.11.18. Paper IMECE2010-40201. (ISBN:978-0-7918-3891-4)
- Katona, T., Rátkai, S. (2008). Extension of Operational Life-Time of VVER-440/213 Type Units at Paks Nuclear Power Plant. *Nuclear Engineering and Technology* 40:(4) pp. 269-276. (2008)
- Katona, T., Rátkai, S. (2010). Programme of Long-term Operation of Paks Nuclear Power Plant. In: Transactions of ENC 2010: *European Nuclear Conference 2010*, Barcelona, Spain 2010.05.30-2010.06.02. Paper A0114. (ISBN:978-92-95064-09-6)
- Katona, T., Rátkai, S., Pammer, Z. (2007). Reconstitution of Time-limited Ageing Analyses for Justification of Long-Term Operation of Paks NPP. In: *19th International Conference on Structural Mechanics in Reactor Technology (SMiRT 19)*. Toronto Kanada 2007.08.12. Paper D02/2-1.
- Katona, T., Rátkai, S., Pammer, Z. (2011). Reconstitution of time-limited ageing analyses for justification of long-term operation of Paks NPP, *Nuclear Engineering and Design*, Volume 241 Issue 3 (March 2011) pp. 638-643
- Kereszturi, A. et al (2010) General features and validation of the recent KARATE-440 code system, *International Journal of Nuclear Energy Science and Technology* 2010 - Vol. 5 No.3 pp. 207-238
- Kupca, L. (2006). Irradiation Embrittlement Monitoring Programs of RPV's in the Slovak Republic NPP's, *14th International conference on nuclear engineering (ICONE 14)*, Miami FL (United States) 17-20 Jul 2006
- NPO Hidropress (2007) Steam Generator PGV-213. Analysis of Material Properties of Steam Generator Tubes. (In Russian). NPO Hidropress Report No. U213D3 2007.
- OECD NEA (2006). Nuclear Power Plant Life Management and Longer-term Operation *OECD Publishing*, NEA No. 6105. ISBN: 9789264029248 OECD Code: 662006111P1.
- Orgenergostroy (1989a). Instruction of technical servicing for standardized units VVER-1000 NPP type B-320 containment pre-stressed system, Moscow, 1989
- Orgenergostroy (1989b). Instruction of technical servicing for main series (non-standardized) units VVER-1000 NPP type 302338 and 187 containment pre-stressed system, Moscow, Orgenergostroy, 1989
- Popov, V. (2007). The large projects at Kozloduy NPP – with focus on long time operation and ageing management *Second IAEA International Symposium on Nuclear Power Plant Life Management* 15-18 October 2007 Shanghai China
- Rosenergoatom (2003). Safety enhancement and lifetime extension of the power unit 1 of Kola NPP, Summary Report, Moscow, 2003
- Slovak Report (2010). National Report of the Slovak Republic Compiled in Terms of the Convention on Nuclear Safety June 2010  
[http://www.ujd.gov.sk/files/dokumenty/NS\\_NS\\_2010.pdf](http://www.ujd.gov.sk/files/dokumenty/NS_NS_2010.pdf)
- Šváb, M. (2007). Regulatory approach to the long-term operation of Czech Nuclear Power Plants *Second IAEA International Symposium on Nuclear Power Plant Life Management* 15-18 October 2007 Shanghai China.

- Trunov, N. B. et al (2006). Consideration of Field Experience in Developing New Projects of Steam Generators for Nuclear Power Stations Equipped with VVER Reactors, *Thermal Engineering* 2006 Vol 53 No 1 pp. 37-42
- Trunov, N. B. et al (2006). WWER Steam Generators Tubing Performance and Aging Management *14th international conference on nuclear engineering (ICONE 14)* Miami FL (United States) 17-20 Jul 2006
- U.S. NRC (2010). Generic Aging Lessons Learned (GALL) Report – Final Report (NUREG-1801 Revision 2)
- Ukraine (2011). Состояние работ по реализации «Комплексной программы работ по продлению срока эксплуатации действующих энергоблоков атомных станций» [http://www.energoatom.kiev.ua/ru/Length\\_extension?\\_m=pubs&\\_t=rec&id=25436](http://www.energoatom.kiev.ua/ru/Length_extension?_m=pubs&_t=rec&id=25436)
- Vasiliev, V. G., Kopiev, Yu.V. (2007). WWER pressure vessel life and ageing management for NPP long term operation in Russia *Second IAEA International Symposium on Nuclear Power Plant Life Management* 15-18 October 2007 Shanghai China
- Zander, A., Nopper, H., Roessner, R. (2007). COMSY - A Software Tool for PLIM + PLEX with Integrated Risk-Informed Approaches *Transactions SMiRT 19* Toronto August 2007 Paper # D02/4



# A Novel Approach to Spent Fuel Pool Decommissioning

R. L. Demmer

*Idaho National Laboratory, Idaho Falls, Idaho  
USA*

## 1. Introduction

A novel underwater strategy was developed at the INL as an interim action to reduce the hazards associated with maintaining excess SFPs containing water, sludge and other debris. It is estimated that hundreds of these facilities exist around the world. They present a hazard to the environment in that they often leak and may spread contamination. In some cases the pools were maintained to prevent airborne contamination risks if the sides become dry, or to shield a “bathtub ring” (or other debris on the bottom of the pool) of highly radioactive material just below the water’s surface. The INL strategy was to vacuum the pool, scrub the sides, filter the water and coat the entire pool to reduce the risks associated with these hazards. Extending this strategy to the more challenging decommissioning of the INTEC-603 pool, with extensive underwater scanning and grouting was a natural progression of the hazard reduction actions.

The underwater coating and cleaning strategy was subsequently found to be of interest in the commercial NPP arena for a deactivation project at the Dresden Nuclear Power Station Unit 1. This project became a cooperative effort between Exelon and Idaho National Laboratory (INL), with shared project planning, equipment, and documentation. The approach was to apply the underwater coating process pioneered at INL. It was successfully modified and deployed by the Dresden Unit 1 SFP team.

The Dresden Station Unit 1 is one of the first commercial nuclear reactors commissioned in the United States. Unit 1 was placed into commercial operation on August 1, 1960, and became the first commercial nuclear power plant built by private industry. It is situated approximately 50 miles southwest of Chicago near the confluence of the Des Plaines and Kankakee Rivers. It shares this site with two other NPPs, Dresden Units 2 and 3.

Unit 1 is a General Electric-designed Boiling Water Reactor. It was originally engineered for a power output of 630 MWt, and this was later increased to 700 MWt, which generated 210 MW of electricity. Unit 1 had a history of minor steam leaks and erosion in steam piping. It operated until 1978, when it was shut down for retrofitting. Following the Three Mile Island incident in 1979, additional regulations were issued, and a decision was made not to restart Unit 1. The plant was subsequently licensed to possess radioactive material but not to operate and its designation was changed to a SAFSTOR configuration, a Nuclear Regulatory Commission (NRC) interim decommissioning designation. Chemical decontamination of the primary system was completed in 1984. According to an NRC report, the remainder of the

decommissioning work has been delayed until the other operating units reach the end of their lifetime (US NRC, 2005).

In 2004, a decision was made by Exelon management to reduce the risk of fuel pool leakage by cleaning, draining, and coating the SFP. The Unit 1 tritium groundwater monitoring program indicated that there may have been leakage from the Unit 1 pools. Since that initial indication there has been no further signs of any significant leakage, and the tritium monitoring will continue to be used to provide indication of any possible leakage until all the water is drained from the pools. Recent incidents of SFP leakage, particularly at the Indian Point and Connecticut Yankee NPPs, underscore the necessity of this concern. In the spring of 2004, a conceptual plan was developed to remove the water, process it in the water treatment facility for Units 2 and 3, seal the basin, and thus reduce the SFP leakage risk and maintenance requirements.

Exelon contacted INL because of their newly developed method of successful SFP decommissioning. INL is a Department of Energy (DOE)-owned, contractor-operated nuclear energy development laboratory located 45 miles west of Idaho Falls, Idaho. During 50 years of nuclear research, INL built several SFPs, four of which were scheduled for decommissioning by 2004. These included the Test Area North (TAN) 607 Pool, the Materials Test Reactor (MTR) 603 Canal, the Power Burst Facility (PBF) 620 Canal, and the Idaho Nuclear Technology Engineering Center (INTEC) 603 Overflow Pit. Decommissioning the large TAN-607 SFP was completed ahead of schedule and for less cost than using traditional practices. The size and condition of the INL pools are shown in Table 1 (Whitmill, 2003).

Pool Designation	Volume	Dimensions	Average Water Contamination
TAN 607	2,948,400 l	14.6 x 21.3 x 7.3 m deep	1E-3 uCi/L
MTR 603	446,040 l	33.5 x 2.4 x 5.5 m deep	4E-2 uCi/L
PBF 620	94,500 l	2.4 x 4.9 x 6.1 m deep	1E-3 uCi/L
INTEC 603 (Overflow Pit)	43,470 l	1.8 x 2.4 x 5.2 m deep	4E-2 uCi/L

Table 1. INL Spent Fuel Pools Completing Underwater Clean and Coat Processes.

## 2. The INL approach

Cleaning and coating an SFP using the underwater coating process requires extensive environmental, safety, and health (ES&H) documentation and engineering efforts. The set of procedures, permits, and safety analyses for the TAN-607 SFP fills four large binders. Members of INL management reviewed these preparations and procedures during an assessment prior to commencing the fieldwork. An underwater team with nuclear reactor experience, Underwater Engineering Services (UES), was contracted to perform the cleaning and coating work, as shown in Figure 1. Emergency procedures were well-documented and reviewed in a pre-job briefing each workday, and work was coordinated through the facility management. During each shift of underwater diving, an INL senior management representative supervised the contractor's conformance with the safety procedures.

One major component of INL's preparation was to develop an "As-Low-As-Reasonably-Achievable" (ALARA) package. Due to the highly-radioactive nature of certain portions of the TAN-607 pool, the work processes and procedures were scrutinized to meet the tightest

level of radiological control. Essentially no portion of the work was left to chance in terms of potential skin contamination or overt radiation exposure. This was integrated with the training and experience of the underwater diver's program.



Fig. 1. Diver at INL completing entry into basin for underwater cleaning and coating.

The INL tested 14 different epoxy-based coatings to determine their conformance to SFP requirements (Tripp, 2004). The following criteria were used to evaluate the coatings:

- Ease of application
- Strong adhesion to carbon steel, brick, concrete block, and stainless steel
- No negative effect on water quality
- No hazardous residues left behind
- Proven in other underwater applications
- High cross-link density and pigment to withstand radiation and contamination penetration.

The ease of application was addressed in terms of moderate, but not excessive, viscosity, application thickness, and pot life (pot life is the amount of time a catalyzed coating may be used prior to solidifying). These types of coatings are used in naval applications for recoating ship hulls underwater. UES had previously made applications of one particular underwater epoxy coating in which they had high confidence. A test of that type of coating, UT-15 Underwater Epoxy, manufactured by Picco Coatings Co., determined that it was within the acceptable range of requirements for this work.

Fieldwork commenced in the TAN-607 SFP in the spring of 2003. This pool was the largest at INL to be decommissioned in this series. A larger pool, the INTEC-603 main pool (north

middle and south basins) has also been deactivated with a modified underwater approach discussed later in this report. The TAN-607 SFP was viewed as a significant but manageable challenge with application to future larger projects. The TAN-607 SFP had been used for storage of a number of different nuclear fuels, the most notable being the damaged Three Mile Island fuel and core debris, which, consequently, led to increased contamination levels in the pool.

The radiological contamination and exposure controls were managed on a real-time basis. While each section of the SFP had been extensively surveyed using remotely-reporting, submersible, extended-reach AMP-100 radiation probes manufactured by Arrow-Tech Inc., each shift of divers also visually surveyed their work area prior to beginning work. Each diver was outfitted with five redundant, remotely-reporting dosimeters multiplexed to the DMC 2000S, manufactured by Merlin Gerin Co. These instruments were integrated into the “dive station” laptop computer that monitored divers’ dive times. If two of the dosimeter units failed, or if dose readings exceeded the 500 mR/hr alarm set point, the diver was required to move to a lower dose area. Industrial guidelines of three-hour dives were maintained; work below 12.2 m could not exceed 1.5 hours. A team of assistants dressed in anti-contamination clothing and a partially-suited substitute diver were maintained at the entrance to the dive at all times.

The divers averaged 5-8 mR radiation dose per dive and completed 255 dives prior to the only incidence of skin contamination (out of a total of 411 dives for 1673 dive hours on all four basins). In preparation for the dives, foreign objects and as much of the sludge as possible were removed from the pool. This action, along with the shielding properties of the water and the heavy rubber dive suit, resulted in lower radiation doses. Debris removal was first attempted using long-reach extension poles, buckets on tethers, and/or placing highly-radioactive objects in shielded casks. During a pre-job survey of one section in the TAN-607 basin, a highly-radioactive nut reading 90 R/hr, probably debris from the Three-Mile Island accident, was discovered in the area. Work was stopped until a plan could be formulated to remove the item. It was retrieved using 2 m long tongs and placed in a stainless-steel bucket. Work continued after this incident with a renewed emphasis on the pre-job surveys. The process of cleaning and coating the TAN-607 SFP began with treating and cleaning the water. UES provided a multi-purpose underwater filter/pump system, manufactured by Prosser, Co., 9-50134-03X. The water was then treated with a calcium hypochlorite to precipitate soluble contaminants. This was not particularly successful because the water turned an opaque brown and required several days of filtration prior to diver reentry. After cleaning the water, a hydraulic hull-scrubber device, like those used to clean boat hulls, was used to clean the pool walls. A large number of paint blisters were found as the wall scrubbing progressed. Every blister required additional scrubbing with a hard-bristle steel-wire brush, thus slowing the cleaning and coating process significantly. The next step was to vacuum the floor of the pool. The multi-purpose filtration system was used for this as well. A special type of paint roller system was used for underwater application of the epoxy coating, which is shown being applied underwater in Figure 2. The system had two separate pumps for the epoxy resin and hardener, which were pumped through separate hoses to a mixing manifold about 1.5 m from the roller. The roller/extruder system was flexible up to that point, and like a solid wand from there to the roller head.

The first half-hour dive provided several important indications that a successful project was underway. A splash curtain was installed along the area where the diver entered and exited the water, and the wipe down and doffing took place within this area. The diver was rinsed

off as he exited the pool, and then dried off completely with disposable wipes prior to doffing.

Unexpectedly high dose rates were encountered in two work evolutions. One occurred when a particle became lodged in the ridges of the vacuuming hose that the diver used to clean the bottom. A smooth hose was then substituted so that it would be less likely that particles would become lodged in the hose. On a second occasion, the knee areas of the diver became highly contaminated from kneeling in debris on the pool floor. To facilitate removal of this contamination in subsequent dives, the knees and shoes of the diver were covered with duct tape in such a manner that the tape could be easily removed prior to the divers leaving the basin.



Fig. 2. Special two hose roller system used for wall coating at the MTR pool.

Another unexpected problem was instrumentation malfunction in the wet and high-vibration conditions typical during this project. Condensation occurred within some of the radiation detection equipment, particularly the multiplexers. Opening the covers of the dosimeters and letting them dry overnight solved this condensation problem. Some of the wires on the electronic dosimeters were fragile and did not stand up well to the vibration and manipulation of the divers. To address this failure potential, the connection points for the dosimeters were reinforced with electrical tape at the clamp areas, and all the connectors were tightened regularly.

Overall, the TAN-607 SFP project was highly successful and reduced personnel exposure, project length, and cost from the baseline case. It was projected that the radiation exposure to divers cleaning the pool would be 1056 mR; the actual exposure was only 744 mR. The highest dose to any diver was 196 mR, which was well below that anticipated for even a conventional, non-diver baseline approach. Exposure for the support personnel was projected at 200 mR, and was actually only 80 mR. Campbell has shown that the integrated basin deactivation project's scheduled duration (6 months for all four basins, about 5200 worker hours) was reduced by 1.5 months (1200 hours) and the cost by \$200,000 from the \$1.9M baseline estimate (Campbell, 2004).

### 3. In-situ deactivation of spent fuel pools

Following the INL SFP coating, cleaning and water removal projects, the basins were stabilized with backfill (soil, gravel or grout). This strategy was performed within the hazardous waste laws of Idaho as an interim action protective of health and the environment. The low strength grout used at the INL provides the capability of future removal if that were required. Similar strategies performed at other DOE sites are described as In-situ Deactivation (or decommissioning) or ISD. For those other nuclear facilities this strategy is considered a permanent end state (Langton, 2010, Brown, 1992), like entombment of a facility. While the INTEC-603 43,470 l Overflow Pit was briefly described in the previous section of this report as a clean and coat action, the larger INTEC-603 (north, middle and south basins, 4,900,000 l) provides an example of the whole basin stabilization process using grout rather than epoxy coating.

There were three phases in deactivating the INTEC-603 SFP. These phases are: 1) Residual cleanout, 2) Validation and 3) Stabilization of remaining contamination. Each of these phases can be very difficult, time consuming and take several years to complete. In the residual cleanout phase, all the spent fuel is removed, equipment is removed and the sludge is removed. The second phase, the validation phase, involves the thorough investigation of the basin to determine that no nuclear fuel remains. This phase also may include extensive sampling and characterization of residual materials for waste disposal. The last phase, stabilization, involves the addition of grout (or another structural material) that prevents intrusion and subsidence. These phases are not rigid and may be revisited over the course of the project.

Residual cleanout can be a very lengthy and difficult stage of the project. Ideally this stage would be part of the operational or (timely) post-operational function of the pool. If consistency with the operation of the pool can be established, it is more likely that trained operators, somewhat knowledgeable about the types of materials that have been used, will be available to identify and remove the items. It is important to stress the continuity of using operators that were trained during the productive life of the pool. They are a ready source of information and skills that will serve the cleanout and deactivation project. This aids the residual cleanout, especially the removal of all spent nuclear fuel or other highly radioactive materials; certainly a priority step in deactivating the pool.

The INTEC-603 pool required an extensive and challenging residual cleanout phase performed well after the post-operational cleanout. At the other INL SFPs the cleanout performed during deactivation was essentially framed within the coating effort. For the INTEC-603 pool the residual cleanout phase was quite extensive and was a project in itself. This pool had a larger accumulation of sludge (some 50,000 kg) and debris that was several

inches deep. Because the waste was known to contain hazardous constituents (cadmium and lead) a treatability study was performed to determine methods to treat the waste within the Resource Conservation and Recovery Act (RCRA) regulations; the treatment required an engineered grout to encapsulate and stabilize the sludge for disposal. As at other DOE sites, the presence of small bits of residual spent fuel must be taken into account. Thus, a difficult problem of underwater removal and RCRA treatment of highly radioactive sludge becomes even more challenging because of the concern for nuclear criticality.

A system was engineered to remove and treat the sludge in an efficient method that satisfied all the regulatory and safety concerns. A similar sludge cleanout campaign was performed some 20 years prior and a great deal of the technical basis from that previous work was employed during the engineering phase. Essentially the cleanout system was composed of a high-integrity container (HIC) where the sludge was pumped, a integral sacrificial stirring system used to mix the grout in the HIC, and a filtration system in the HIC that separated and returned the water to the basin without the sludge (Croson, 2007). A similar system was used on the Dresden project and is detailed in a following section. Other basin cleanout campaigns had removed and repackaged the spent fuel and removed the fuel storage racks and other in-pool facility equipment at INTEC-603.

The validation phase during the INTEC-603 pool project occurred in parallel with some portions of the cleanout phase. After the racks and equipment were removed, an extensive examination using very sophisticated gamma scanning equipment was employed to map the location and character of the sludge at INTEC-603. In previous INL pools the diver simply surveyed the work area using a remotely reporting instrument prior to starting work each shift. At the Dresden project, the small Remote Underwater Characterization System (RUCS) assisted in the validation role prior to diver entry and cleanup. At the INTEC pool the Multi Detector Basin Scanning Array (Figure 3) was employed as the survey tool. This scanning array is composed of three sections containing gamma detection instruments and is specifically designed to be used with the INTEC-603 crane system and to traverse channels in the pool floor. Since the overall residual cleanout is not complete until the sludge is removed, the validation phase was performed after equipment removal but prior to sludge removal.

In the stabilization phase the grout development, delivery and pool water removal aspects of the INTEC-603 project were revealed. A special grout was formulated with admixtures to have high flowability, cure underwater, be self-leveling and maintain a (low) 1724 kPa strength. After extensive laboratory testing, the grout was prepared on-site in a batch plant and pumped into the basin using 10 cm hoses. Grout was directed into the center of the basin and allowed to flow to the outside. As the grout was injected into the basin, the displaced water was filtered and pumped to the Idaho CERCLA Disposal Facility (ICDF), a large waste water evaporation pond maintained at the INTEC facility. Grout lifts were generally about 60 cm thick, with different sections of the pool (north middle and south) receiving lifts on different days allowing curing of the different sections for at least one day.

#### **4. Deactivating the Dresden Unit 1 SFP**

The decommissioning of Unit 1 actually began more than 25 years prior to the SFP campaign. In 1978, reactor operations were suspended and defueling took place. In 2002, the fuel and fuel pool equipment, such as the racks and accessories, were removed. Some cleaning had been performed in the SFP, but no campaign had been waged to completely gut the pool. When the racks were removed, they were cut off at floor level leaving



protrusions as high as 10 cm. The water quality had deteriorated significantly, and there was no longer any appreciable visibility below the water line.



Fig. 3. Multi Detector Basin Scanning Array for INTEC-603.



The Unit 1 team was planning a cleanup of the SFP using long-handle tools and coating the pool as the water was lowered. This is a conventional method of SFP cleanup, but poses some concerns. The primary concern was the potential for high airborne contamination by allowing contaminated poolsides to be exposed during the draindown. Another concern was the length of time involved in slowly removing water and treating the walls. The disposal of water had to be scheduled with the operating unit's 2/3 treatment system. The availability of the 2/3 system could not be assured over wide periods of time, but could be used on an available space and time campaign basis.

The INL underwater coating process was attractive to the Unit 1 team for a number of reasons. First, INL had no airborne contamination problems during the SFP coating projects. Second, with the underwater coating process, there is little concern about scheduling for draining away the pool water; the water can be taken away at any time after the cleaning and coating are completed without impacting the operating unit or the decommissioning schedule. No strain injuries occurred during the INL decommissioning projects while the extensive use of long-handled, underwater tools to clean and paint the pool had a high risk of these injuries. Using divers allows more successful cleaning of the pool bottom and closer cutting of pool equipment. Previously, cutting was accomplished using long-handled cutting tools that left 10 cm rack stubs. Naturally, the reduced schedule, cost, and radiation dose shown in the TAN-607 SFP project was an advantage.

The Dresden Unit 1 SFP was designed with distinct portions that have different depths, functions, and kinds of equipment. The SFP is "L" shaped with the main body composed of two separate pools—the storage pool and the transfer area. The storage pool is 6.1 x 7.6 x 7.9 m deep and the transfer area is 6.1 x 7.6 x 13.6 m deep. The storage pool had contained spent-fuel racks that had been bolted to the floor, but were previously removed. In the transfer area, fuel could be examined and packaged, and maintenance could be performed on reactor components. These two pools were connected with a gateway that could be closed between them. The transfer area was connected to the reactor compartment by a 2.1 x 4.6 x 18 m transfer channel.

Preparations for the underwater coating process began after Exelon management had reviewed decommissioning options. The underwater coating process is not intuitively safer industrially and radiologically, but is proven by INL to be safer statistically. An independent dive contractor, Underwater Construction Company (UCC), was contracted as a preferred provider in the Exelon nuclear system and was tasked with underwater coating process. UCC had performed similar types of nuclear jobs involving coatings at reactors.

An underwater survey of the SFP was also a key initial activity. The pool condition and remaining items in the pool were documented from previous cleaning efforts, but a current survey and up-to-date pictures or video were not available. INL provided an operator and the RUCS which is essentially a small, tethered submersible tool to provide video and radiation dose measurements. Although the RUCS system was not a calibrated Exelon unit, its dose measurements were adequate for development of the ALARA plan. The RUCS showed that the floor had general dose readings of 2-3 Rem/hr, with hot spots up to 11 Rem/hr, but that the general pool dose was less than 10 mR/hr. The in-depth survey also identified additional items in the pool not previously visible from above.

The Dresden Unit 1 SFP project proceeded in a series of tasks that took more than a year to complete. Table II shows the tasks and associated schedule required to perform this work. Each task is not discussed in detail, but some of the more interesting activities are examined.

The overall project took considerably longer than expected, primarily because of the resource drain caused by scheduled work on other Exelon reactors. Work on operating reactors always took precedence over decommissioning work. This was principally manifested in the non-availability of Radiation and Contamination Technicians (RCTs). Thus, decontamination tasks that were expected to take a few months lasted an entire year.

The most extensive activity involved in the underwater coating process was the water cleanup task. The water in the SFP required treatment for two main reasons: first, there was a considerable amount of algae on the surface, and second, the general water condition was moderately contaminated. The bottom was not visible, and the sides of the pool were essentially invisible below the algae layer. Since visual contact with the diver was required at all times, no diver work could start until the water was treated and visibility was adequately restored. There were other reasons to maintain as much cleanliness in the water as possible as well. Beyond the need for visual contact, higher cleanliness contributed to lower radiation doses and contamination on the diver's suit. This made the job of avoiding skin contamination much easier. Cleaning the water also permitted the water to meet the 2/3 system requirements without further remedial treatment.

The process of cleaning the water required a considerable amount of technology. A specialist in the field, Duratek Inc., was contracted to achieve and maintain water quality. The first step was to "shock" the water with the addition of 10 to 15 parts-per-million (ppm) hydrogen peroxide. The hydrogen peroxide primarily served to kill the algae and bacteria. After the initial injection of the peroxide, the water turned dark brown and remained this color for several weeks. The peroxide injection system allowed the use of ultraviolet light and ion-exchange after a few days, once the algae were destroyed.

A system known as the UFV-100 "Tri-Nuc" Filter System, manufactured by Tri-Nuclear Corporation, was placed in the pool to maintain long-term water quality. The Tri-Nuc is a canister-type, shielded filter about 0.8 m. long and 18 cm in diameter. It is an easily-maintained, self-contained system with a submersible pump. After the peroxide injection and three weeks of Tri-Nuc filter operation, the pool water became clear and maintained clarity throughout the project. Over the course of the project, 50 of the Tri-Nuc filters were used. A skimmer system was added to the Tri-Nuc to clear floating algae debris. The underwater diving contractor provided a separate vacuum/filtering system consisting of a pump and eight-38 cm filters on a manifold (see Figure 3). Though this system helped to maintain water clarity, its primary purpose was to contain the paint chips and floor debris. A "rock catcher" screen was used on the UCC system to prevent larger particles from going through the pump.

Following the filtration and water treatment tasks, the wall and floor surfaces were cleaned and prepared. At the start of each work shift, the work area was surveyed using an underwater dosimeter. The floor surface was thoroughly vacuumed using the UCC vacuuming system. The stubs left from previous fuel rack removal were cut with a plasma torch. These were removed along with other small debris so that the floor area was basically clean and free of obstruction. While the walls of the INL SFPs were cleaned using the hull scrubber, the Unit 1 walls were cleaned using hydrolasing. Hydrolasing uses high-pressure water recycled into the pool to blast off grime and loose paint. If the paint came off or blistered paint was present, the areas were cleaned with a 3M Scotch-Brite® pad prior to recoating.

Several devices were used to afford easier pool access, greater visibility, and reliable diver communication. A portable scaffolding device, much like a window cleaner's or painter's

work platform, was used in the wall-cleaning and coating. It was easily raised or lowered to different work levels. Underwater lights were used to provide the divers with better visibility, and inexpensive underwater cameras were employed by the engineers to supervise progress. Voice communication devices were installed in the divers' helmets. Additionally, each suit was pressure-tested for leaks and thoroughly surveyed for contamination prior to each dive.



Fig. 4. UCC vacuuming filtration system underwater manifold.

The pool and cleanup equipment required some on-site modification during the course of the project. A large water heater was used to raise the water temperature from about 15 to 21°C. This enabled more comfortable diving and ensured that the pool walls were at an appropriate temperature for proper coating adhesion. The paint flow through the system was initially slow and somewhat inefficient, so a heated “trace” line was added to the single delivery hose lines and the paint was reformulated to achieve a lower viscosity. The most serious problem was that the mixing lines were too far from the paint roller head. The paint began solidifying before it reached the roller because of the long mixing time while the resin and hardener traveled through the hose, so the mix point was moved to within 1.2 m of the paint roller head. Heavy, stainless-steel buckets were used to transport floor debris, like nuts, bolts, and pieces of basin equipment. A long-reach pickup device was fabricated from a pair of Vice-Grips. This tool, like the long-handled tongs used at INL, was invaluable for moving radioactive items.

During previous cleanout activities, two large fuel transfer fixtures had not been removed from the lower level of the transfer channel. These fixtures, called “elephant’s feet,” resembled large, inverted flower pots about 1 m in diameter and 2.1 m tall. The project engineers were uncertain whether to cut the elephant feet up and remove them, or to



## 5. Lessons learned

During the SFP deactivation projects (INL and Dresden Unit 1), a number of lessons were learned, the most significant of which are listed below:

- Nuclear trained divers must be used for these projects. There is no substitute for trained and experienced divers. They know the proper contamination control processes for this kind of project and are most effective for difficult operations. These trained individuals will be the key operating personnel when the work goes forward.
- High-quality water treatment systems are required to attain and maintain water clarity and low contamination. This is essential to diver productivity and contamination-free operations.
- In both the TAN and Dresden pools the water turned brown after initial treatment, probably from high mineral and algae content. High concentrations of minerals and algae are common with old spent fuel basins, especially if they have not been under water treatment regimes pending decommissioning. Preparations should be made early to filter the residual mineral/algae that may come from initial water treatment (like chemical “shock” treatments).
- Unusual and unexpected objects (probably highly contaminated) are likely to be found in SFPs. Work areas should be surveyed periodically using the waterproof dosimeters. Some flexibility with special procedures and extended reach tools should be planned into the work. Simple tools like inexpensive underwater cameras and Vice-Grips can be effectively employed.
- Maximizing the use of “off-the shelf” items (such as scaffolding, waterproof lights and cameras and even the marine hull scrubber) reduced the cost of special design and fabrication for some equipment
- Coating areas with loose or blistered paint will significantly slow the project and consume much more of the coating resources. During the INL SFP decommissioning project, the delays were significant, and as much as 50% more paint was required due to blistered paint.
- The RCTs and support personnel should remain consistent over the project. The most capable personnel should be chosen to monitor, clean, and check equipment, and then should be left in place as a dedicated team.
- Epoxy coatings may have complicated application requirements. Ensure that the manufacturer has optimized viscosity for roller application and that temperature requirements are met. Use a two-hose application system if possible.
- After about two years of service, the coating at Dresden became loose in some wall areas. This may point to a lack of “profile” in preparing the wall using a hydrolaser. This did not happen using the hull scrubber at INL. It is recommended that an abrasive technique, like the hull scrubber, be employed in surface cleaning.

## 6. Acknowledgments

This work was supported through funding provided by the U.S. Department of Energy (DOE) to the Idaho National Laboratory, operated by Battelle Energy Alliance, LLC, under DOE Idaho Operations Office Contract DE-AC07-05ID14517. The submitted manuscript was authored by a contractor of the U.S. Government. Accordingly, the U.S. Government retains a nonexclusive, royalty-free license to publish or reproduce the published form of this contribution, or allow others to do so, for U.S. Government purposes.

This information was prepared as an account of work sponsored by an agency of the U.S. Government. Neither the U.S. Government nor any agency thereof, nor any of their employees, makes any warranty, express or implied, or assumes any legal liability or responsibility for the accuracy, completeness, or usefulness of any information, apparatus, product, or process disclosed, or represents that its use would not infringe privately owned rights. References herein to any specific commercial product, process, or service by trade name, trademark, manufacturer, or otherwise, does not necessarily constitute or imply its endorsement, recommendation, or favoring by the U.S. Government or any agency thereof. The views and opinions of authors expressed herein do not necessarily state or reflect those of the U.S. Government or any agency thereof.

The author would like to acknowledge the assistance of the following people: Joseph Panozzo and Raymond Christensen of Exelon Corp, Dr. Steven Bakhtiar and Randall Bargelt of the Idaho National Laboratory

## 7. References

- Brown, G. A., et al, "In Situ Decommissioning – the Radical Approach for Nuclear Power Stations", Proceedings of the Institution of Mechanical Engineers 1847-1996, 1992.
- Campbell, J., "Integrated Basin Closure Subproject Lessons Learned," September 2004.
- Crosen, D. V., et al, "Idaho Cleanup Project CPP-603A Basin Deactivation", Waste Management Conference (WM07) Proceedings, 2007.
- Langton, C. A., et al, "Svannah River site R-Reactor Disassembly Basin In-Situ Decommissioning", Waste Management Conference (WM10) Proceedings, 2010.
- Tripp, J. L., et al, "Underwater Coatings Testing for INEEL Fuel Basin Application for Contamination Control," INEEL/EXT-04-01672 Rev. 0, February 2004.
- United States Nuclear Regulatory Commission (US NRC), *Dresden Unit 1*, <http://www.nrc.gov/info-finder/decommissioning/power-reactor/dresden-nuclear-power-station-unit-1.html>, web page last accessed September 2007.
- Whitmill, L. J., et al, , "Deactivation of INEEL Fuel Pools," INEEL/INT-03-00936 Rev. 0, August 2003.

# Post-Operational Treatment of Residual Na Coolant in EBR-II Using Carbonation

Steven R. Sherman<sup>1</sup> and Collin J. Knight<sup>2</sup>

<sup>1</sup>Savannah River National Laboratory

<sup>2</sup>Idaho National Laboratory

USA

## 1. Introduction

The Experimental Breeder Reactor Two (EBR-II) was an unmoderated, heterogeneous, sodium-cooled fast breeder reactor operated by Argonne National Laboratory – West, now part of the Idaho National Laboratory in southeastern Idaho, USA. It was a pool-type reactor. The reactor core, sodium fluid pumps, and intermediate heat exchanger (IHX) were submerged in a tank of molten sodium, and the exchange of heat from the core was accomplished by pumping molten sodium from the pool through the reactor core, IHX, then back into the pool. Thermal energy from the pool was transmitted in the IHX to a secondary sodium loop, which in turn was used to heat high-pressure steam for electricity production. When it operated, the nominal power output of the reactor was 62.5 MW thermal and approximately 20 MW electrical. The reactor began operation in 1964 and operated until final reactor shutdown in 1994. During its lifetime, the reactor served as a test facility for fuels development, hardware validation, materials irradiation, and system and control theory testing.

From 1994 through 2002, the reactor was de-fueled, systems not essential to reactor or facility safety were deactivated or removed, and the primary and secondary sodium systems were drained of sodium metal. During operation, the sodium pool contained approximately  $3.4 \times 10^5$  liters of molten sodium, and the secondary sodium system contained  $4.9 \times 10^4$  liters. After draining these systems, some sodium metal remained behind in hydraulic low spots and as a coating on exposed surfaces. It is estimated that the EBR-II primary tank contained approximately 1100 liters, and the EBR-II secondary sodium system retained approximately 400 liters of sodium metal after being drained. The sodium metal remaining in these systems after the coolant was drained is referred to as *residual sodium*.

At the end of 2002, the EBR-II facility became a U.S. Resource Conservation and Recovery Act (RCRA) permitted site, and the RCRA permit<sup>1</sup> compelled further treatment of the residual sodium in order to convert it into a less reactive chemical form and remove the by-products from the facility, so that a state of RCRA "closure" for the facility may be achieved (42 U.S.C. 6901-6992k, 2002).

---

<sup>1</sup> Hazardous Waste Management Act (HWMA)/RCRA Partial Permit, EBR-II, EPA ID No. ID489000892, effective December 10, 2002 (Part B).

In response to this regulatory driver, and in recognition of project budgetary and safety constraints, it was decided to treat the residual sodium in the EBR-II primary and secondary sodium systems using a process known as "carbonation." In early EBR-II post-operation documentation, this process is also called "passivation." In the carbonation process (Sherman and Henslee, 2005), the system containing residual sodium is flushed with humidified carbon dioxide ( $\text{CO}_2$ ). The water vapor in the flush gas reacts with residual sodium to form sodium hydroxide ( $\text{NaOH}$ ), and the  $\text{CO}_2$  in the flush gas reacts with the newly formed  $\text{NaOH}$  to make sodium bicarbonate ( $\text{NaHCO}_3$ ). Hydrogen gas ( $\text{H}_2$ ) is produced as a by-product. The chemical reactions occur at the exposed surface of the residual sodium. The  $\text{NaHCO}_3$  layer that forms is porous, and humidified carbon dioxide can penetrate the  $\text{NaHCO}_3$  layer to continue reacting residual sodium underneath. The rate of reaction is controlled by the thickness of the  $\text{NaHCO}_3$  surface layer, the moisture input rate, and the residual sodium exposed surface area.

At the end of carbonation, approximately 780 liters of residual sodium in the EBR-II primary tank (~70% of original inventory), and just under 190 liters of residual sodium in the EBR-II secondary sodium system (~50% of original inventory), were converted into  $\text{NaHCO}_3$ . No bare surfaces of residual sodium remained after treatment, and all remaining residual sodium deposits are covered by a layer of  $\text{NaHCO}_3$ . From a safety standpoint, the inventory of residual sodium in these systems was greatly reduced by using the carbonation process. From a regulatory standpoint, the process was not able to achieve deactivation of all residual sodium, and other more aggressive measures will be needed if the remaining residual sodium must also be deactivated to meet the requirements of the existing environmental permit.

This chapter provides a project history and technical summary of the carbonation of EBR-II residual sodium. Options for future treatment are also discussed.

The information collected during the EBR-II post-treatment operation provides guideposts for engineers who must design future sodium-cooled reactors, or who are tasked with cleaning up shutdown sodium-cooled reactor systems. The single, most important lesson to be imparted to the designers of new sodium-cooled reactor systems is this: design systems so that they can be drained effectively at all points, and avoid the creation of hydraulic low spots and "dead ends" that are inaccessible. Observation of this lesson in future designs will minimize the number and size of residual sodium pockets upon drainage of the sodium coolant and increase the effectiveness of any clean-up method, including carbonation. In addition, post-operation clean-up of new sodium-cooled reactor systems will be safer, faster, and less costly.

Lessons may also be drawn from this work for those who wish to react or remove residual sodium from non-nuclear systems such as coolant pipelines, tanks, and drums. The carbonation method is generally applicable to such systems, and is not specific to nuclear reactors.

## 2. Residual sodium inventory determination

The EBR-II Primary Sodium System consisted of components in the EBR-II Primary Tank and supporting systems that came in contact with the primary sodium coolant (i.e., argon cover gas clean-up system, sodium vapor traps). Figure 1 shows a schematic of the EBR-II Primary Tank, which includes the reactor core. The black arrows in Figure 1 show the flow path for sodium coolant from the pool through the reactor core and back to the pool. A detailed description of EBR-II systems and components may be found in Koch, 2008.



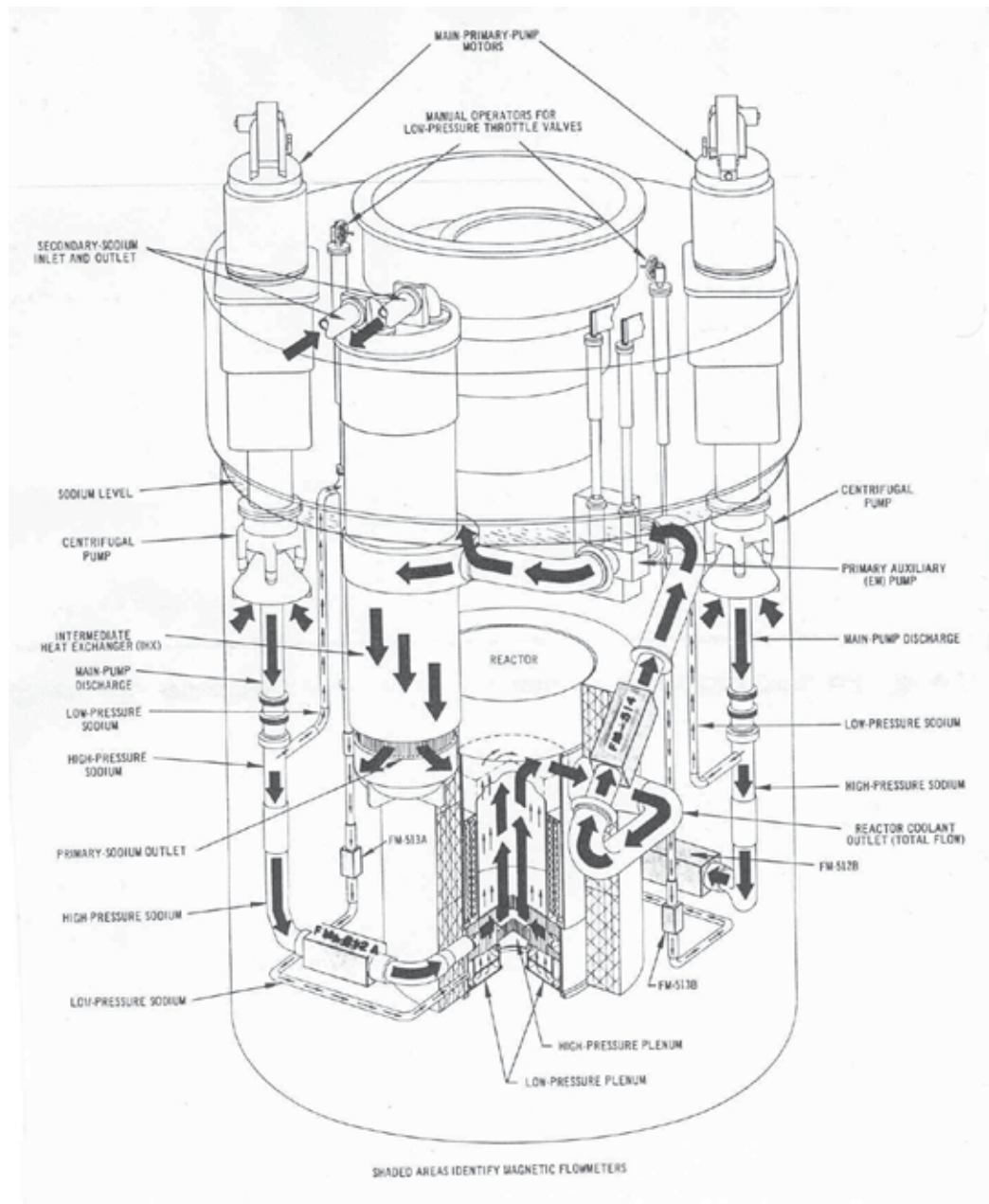


Fig. 1. Schematic of EBR-II Primary Tank and internal systems.

The EBR-II Secondary Sodium System consisted of a network of pipes, steam evaporators, and steam superheaters. In the Secondary Sodium System, molten sodium metal circulated through the IHX in the Primary Tank in order to remove thermal energy from the sodium pool, and then returned to the Secondary Sodium System, where it provided heat to make superheated steam. The system was a closed loop, and sodium metal exiting the Secondary Sodium System was recycled to the IHX.

After shutdown and drainage of the bulk sodium coolant, the Secondary Sodium System delivery/return pipeline was severed from the IHX, and the Secondary Sodium System piping network was re-routed to provide common input and output locations for residual sodium treatment gases. Schematics showing the EBR-II Secondary Sodium System configuration during regular operation and after reactor shutdown are shown in Figures 2 and 3.

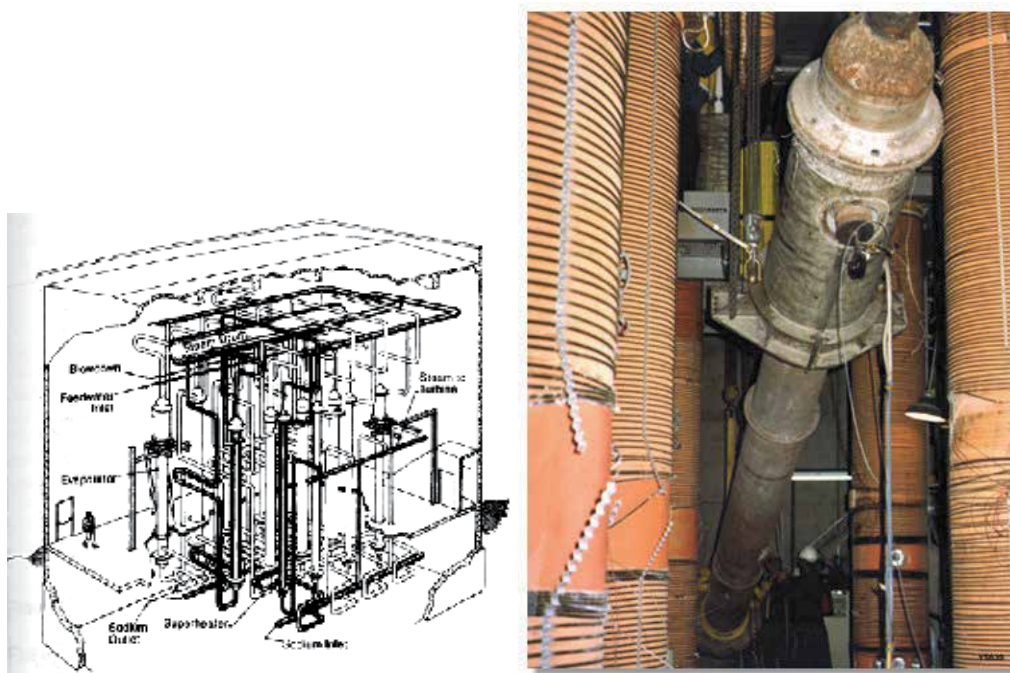


Fig. 2. Schematic and photo of EBR-II Secondary Sodium System as it was configured during regular operations

Determination of the sodium metal inventory during regular operation was relatively easy and straightforward. Operational records were available that provided the amount of sodium metal added to each system before initial reactor start-up. Measurements of the liquid level in the EBR-II Primary Tank and other systems could be tied to these operational records, and the losses of any sodium metal due to the removal of sodium-wetted or sodium-filled components, evaporation of sodium vapor from the pool, and other events, could be correlated to changes in the measured sodium liquid level. All system components were immersed in sodium, and the geometry and configuration of the submerged components had no effect on the determination of the bulk sodium inventory.

After the bulk sodium was drained from these systems, direct observation and measurement of the residual sodium inventory was no longer possible. Residual sodium is not a single entity, and is a collection of localized sodium deposits of heterogeneous depth and physical configuration. The amount of residual sodium at any particular location is highly dependent upon the geometry, elevation, orientation, and configuration of that location. Only a limited number of suspected locations of residual sodium could be visually inspected due to physical access limitations or the presence of radioactive contamination or high radiation fields, and direct measurement of the residual sodium inventory could not be performed.

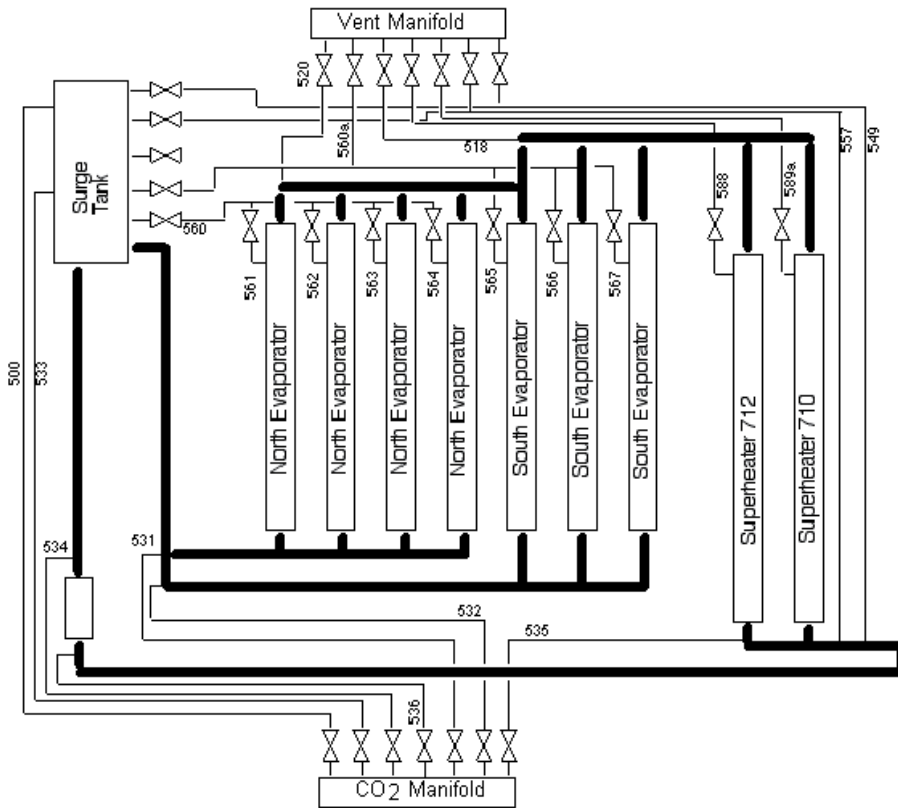


Fig. 3. Schematic of the EBR-II Secondary Sodium System as it was configured during post-operation residual sodium treatment.

An initial estimate of the total residual sodium inventory in these systems was calculated by taking the difference between the known volume of sodium coolant that was present during regular operation, and the amount of sodium collected upon draining the systems. The amount drained from each system, however, was very nearly equal to the known amount of sodium in each system, and only an imprecise determination of residual sodium amounts could be made due to rounding error. By this method, the amount of residual sodium in the Primary Tank and Secondary Sodium System was estimated to be greater than zero and less than 4000 liters and 1000 liters, respectively.

Since fulfillment of the RCRA environmental permit requires that all residual sodium be deactivated or removed, a more precise determination of the starting amount of residual sodium was needed. Assuming a residual treatment process of any kind is monitored and controlled, it should be possible to assess how much sodium has been deactivated or removed at any point in time during the treatment process. This does not, however, provide any measure of how long a treatment process must be performed to reach an end point. For example, if it is known that 500 liters of residual sodium has been deactivated at a certain point in time, what fraction of the total inventory of residual sodium does this represent? Is this 20% of the inventory, or is it 80% of the inventory? Without a more precise point estimate of the initial residual sodium inventory, progress towards an end point can't be

assessed, and the treatment process must be carried out indefinitely until some measured output of the treatment process indicates that a physical end point has been reached.

At worst case, it could have been assumed that the inventory of residual sodium in each system is equal to the upper bound (4000 liters of residual sodium in the Primary Tank and 1000 liters in the Secondary Sodium System), but this likely would have established a treatment target that could never be reached. For example, if the actual residual sodium inventory in the Primary Tank were 2000 liters, and a residual sodium treatment process were applied to it, then the treatment process could potentially be carried out until all 2000 liters of residual sodium were consumed. This would be an excellent result, but the treatment target was established at 4000 liters, and the treatment process would therefore be assessed as being only 50% complete. One could then try to argue with the regulator that the wrong target was chosen and system treatment is complete, but it would be difficult to verify whether this was indeed the case without direct inspection, or whether the treatment method had stopped working for some other reason, and more residual sodium lies within awaiting further treatment.

There is less project risk if the chosen treatment target is less than the actual residual sodium inventory. In this case, achieving less than 100% deactivation of residual sodium is sufficient to achieve project "success", but success would be illusory. Physical evidence from the treatment process would likely indicate that more residual sodium remained in the system being treated after achievement of the project target, and the treatment process would need to be continued anyway until a true endpoint was reached. Extension of the treatment process past the treatment target might then result in increased project costs and schedule delays if the additional treatment work was not planned. Continuing the treatment process past a previously agreed upon target value, however, is more easily acceptable to a regulator, because it would show that the project team was willing to go "above and beyond" the original work scope to achieve environmental goals, and that would reflect more favorably on the clean-up project.

So, there is incentive to choose treatment targets that are less than the upper bounds discussed above, but selection of these targets cannot be done arbitrarily. Project sponsors do not like cost overruns and schedule delays, and will demand a residual sodium inventory estimate that is based on observable data, or that is supported by well-reasoned arguments.

For the EBR-II systems, a mathematical approach was developed for calculating probable residual sodium quantities. The engineering drawings for each system and subsystem were examined, and hydraulic low points were identified. The volume of residual sodium that could be contained in each hydraulic low points was calculated based on the geometry of the location and the presence or absence of drainage points, and the individual volumes were added to calculate the total residual sodium inventory in each system. As a result of this method, the Primary Tank was calculated to contain approximately 1120 liters of residual sodium, and the Secondary Sodium System was determined to contain approximately 400 liters. The detailed calculations are described below.

### **2.1 EBR-II primary tank residual sodium volume determination**

Twenty-four locations were judged likely to contain residual sodium within the Primary Tank. These locations are hydraulic low points, or places where sodium metal may have collected during regular operations but would have failed to drain when the Primary Tank

was emptied. The physical dimensions of each location were then determined from the engineering drawings, and the amount of residual sodium that could have been retained at each location was calculated. The calculated amounts of residual sodium at these locations are shown in Table 1.

For horizontal locations facing upward against gravity, the residual sodium at each location was assumed to have drained to the lowest possible point of drainage, and no blocked drainage points were assumed.

Location	Name	Deposit Volume (L)	Access Limitations?
1	Low pressure plenum	27	No
2	High pressure plenum	125	Yes
3	Inlet pipes to high pressure plenum	117	Yes
4	High pressure plenum inside flow distributing ring	42	No
5	Between blanket lower adapter, sleeve between grid plates	0	Yes
6	Control rod position dummy assembly	0	Yes
7	Inner shield area between inner and outer walls and outlet	11	No
8	Inner shield region between thermal baffle and outer wall	11	Yes
9	Top flange of reactor vessel	15	Yes
10	Reactor cover thermal baffles	11	Yes
11	Sleeves & bellows for gripper, aux. gripper and hold down	11	Yes
12	Sleeves and bellows for control rod drives	8	Yes
13	Guide funnels for control rod drives	38	Yes
14	Outside flow baffle around gripper/hold down	11	Yes
15	Inside flow baffle around gripper/hold down	0	No
16	Recessed area around lifting columns	8	No
17	Safety rod drive lift tubes	1	Yes
18	Transfer arm pedestal	4	Yes
19	Pressure transmitting piping	8	Yes
20	Heater guide funnels	2	Yes
21	Auxiliary pump bellows	2	No
22	Pipe supports	0	No
23	Primary tank bottom	473	No
24	Bottom of Primary Tank cover	189	No
<b>Sub-total, access limitations</b>		364	
<b>Sub-total, no access limitations</b>		752	
<b>Total</b>		1116	

Table 1. Residual sodium locations in the EBR-II Primary Tank.

For vertical surfaces such as the side walls of the Primary Tank, no significant deposits of residual sodium were assumed. This assumption was verified by a video examination of the Primary Tank interior which showed no adhering residual sodium on the side walls of the Primary Tank after the bulk sodium had been drained.

Downward facing horizontal surfaces were generally assumed to be residual sodium-free with the exception of the Primary Tank Cover. The bottom surface of the Primary Tank Cover has a complex geometry, and there were many places for residual sodium to be retained. Also, it was known from regular operating experience that the penetrations in the Primary Tank Cover were slightly cooler than the Primary Tank side walls and submerged components, and residual sodium tended to accumulate at certain locations under the cover due to condensation of sodium vapor and the capture of sodium aerosol.

The largest deposit of residual sodium was on the bottom of the Primary Tank. The depth of residual sodium at this location was determined by calculating the gap space (0.95 cm) between the tank bottom and the bottom of the pump suction that was used to withdraw bulk sodium from the tank. Assuming the Primary Tank bottom is perfectly flat, the volume of residual sodium was calculated by assuming a circular area with a diameter equal to the inner diameter of the Primary Tank minus the projected areas of structures attached to the Primary Tank floor. The Primary Tank had no drain hole, so no further sodium could be drained beyond the lower reach of the pump.

The second largest location for residual sodium is on the bottom of the Primary Tank Cover. No accurate mathematical estimate of residual sodium in this location could be determined, so a guess of 50 gallons (189 liters) was assumed.

The other residual sodium deposits are located in areas that are hydraulic low spots and that have no known drainage points. These areas also include the narrow gap spaces in architectural features that wouldn't have drained well due to surface tension effects, such as the Reactor Cover Thermal Baffles. A detailed examination of engineering drawings of these areas provided the physical dimensions of prospective residual sodium deposits, and the volume of each residual sodium location could be calculated once the dimensions of the locations were known.

After identifying and quantifying residual sodium locations, the locations were also characterized according to their accessibility to the gas space of the Primary Tank. Locations open to the Primary Tank were judged to be completely accessible to any treatment method, while locations with narrow or limited access to the Primary Tank gas space were judged to be only partially accessible, or inaccessible to all but the most severe treatment methods (i.e., filling the Primary Tank with liquid water).

## **2.2 EBR-II secondary sodium system residual sodium volume determination**

An examination of the engineering drawings of the heat exchanger equipment, and a physical examination of the piping network to identify elbows, dead legs, and hydraulic low spots revealed that residual sodium was located throughout the Secondary Sodium System in varying amounts. The largest deposits for residual sodium were identified to reside in the bottom of the steam evaporators and superheaters, and each evaporator and superheater was estimated to contain at least 10 liters of residual sodium. A precise amount of residual sodium could not be determined, but it was estimated that the Secondary Sodium System contained approximately 400 liters of residual sodium based upon these examinations.

Less emphasis was placed on calculating precise residual sodium volumes because the components of the Secondary Sodium System were physically accessible. The progress of

any residual sodium treatment operation or verification of its completion could be checked by cutting open the component or system being treated and examining the contents. Also, if a component or system could not be treated completely using an in-situ method, the component or system could be cut out and dismantled for further treatment at INL's Sodium Component Maintenance Shop (SCMS), a facility used to clean and repair sodium-coated components.

### 3. Selection of residual sodium treatment method

The selection of a residual sodium treatment method was motivated by the requirements of the EBR-II RCRA permit, and the need to maintain a safe work environment while performing residual sodium treatment processes. A RCRA closure permit is a goal-driven document that requires that the permit holder achieve "closure" of the affected system or systems within a defined period of time, usually within 10-20 years of permit issue. The RCRA laws define the closure process as direct removal of RCRA-listed hazardous components, or deactivation (i.e., chemical transformation of a hazardous component into a non-hazardous component) of RCRA-listed components followed by removal of the deactivation products. Once the affected system(s) have been cleaned of hazardous components or deactivation products, an examination of the system by a professional engineer is required to verify the end state. After the inspection step, the affected system(s) is classified as RCRA-closed, and the environmental permit is closed out. Partial closure of a complex system may be performed if a larger system can be divided into smaller, isolated sections that can be treated individually. In cases where complete deactivation or removal cannot be achieved, then the law provides a risk-based closure process that allows some amount of hazardous components or deactivation products to remain in place if the remaining inventory does not pose a risk to human health or the environment. The EBR-II RCRA permit was issued and is administered by the State of Idaho Department of Environmental Quality (Idaho DEQ) on behalf of the U.S. Environmental Protection Agency (U.S. EPA).

In the case of the EBR-II Secondary Sodium System, a RCRA-closed state could be achieved by mechanically extracting the components containing residual sodium (e.g., pipes, tanks, vessels), and treating the pieces one-at-a-time in the on-site Sodium Component Maintenance Shop (SCMS). This approach constitutes a "closure by removal" strategy. Although definitive, it was decided that cutting apart the Secondary Sodium System, packaging and shipping the pieces to the on-site treatment facility, and treating the pieces individually would be too costly in regard to available funding. Also, the dismantling work posed an unacceptably high risk of worker exposure to hazardous chemicals and risk of fire. In addition, the residual sodium in the Secondary Sodium System contains a small amount of tritium, and workers would incur a measurable radiation dose during any dismantling operation.

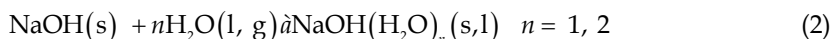
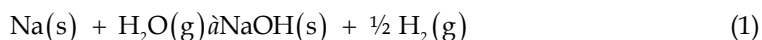
For the EBR-II Primary Tank, a dismantling operation was out of the question due to the presence of a high radiation field and radioactive contamination in the tank. A radiation monitor inserted into the Primary Tank measured a radiation field strength of 50 R/hour just beneath the Primary Tank cover, and higher radiation levels are likely present nearer to the core. Significant sources of radiation in the Primary Tank are Co-60, which is present as fixed contamination in the reactor structural materials, and Na-22, and Cs-137, which are present in the residual sodium.

In-situ treatment methods were then considered. The application of an in-situ treatment method is a "treat, then remove" strategy. The residual sodium in the affected system(s) is reacted in order to transform it into a non-hazardous material, or a less hazardous material, and then the reaction product(s) are removed from the system. Removal of the reaction product(s) is then performed by draining the system if the reaction product is a liquid, or, if the reaction product is a solid, by flushing the system with a solvent in order to dissolve and remove the solid reaction product.

Three in-situ treatment methods were examined in detail, all of which involve the injection of a reacting gas into the system being treated. These methods are the Steam-Nitrogen Process, the Water Vapor Nitrogen (WVN) Process, and the Carbonation Process. The methods were compared on the basis of safety, cost, and schedule. After considerable study and discussion among treatment project engineers, and between treatment project engineers and a sub-set of the engineers who originally designed and built EBR-II, it was decided to pursue carbonation as an in-situ treatment method. A detailed description of these in-situ treatment method, and the selection process, is found in the sub-sections below.

### 3.1 Steam-Nitrogen Process

In the Steam-Nitrogen Process, steam or superheated steam mixed with nitrogen is injected into the system for the purpose of converting residual sodium into sodium hydroxide (NaOH). Hydrogen is also produced. Nitrogen at a concentration of 20-80 vol% is added as a diluent to suppress the potential for a hydrogen fire or explosion. The stoichiometry of this treatment process is shown in Equations 1 and 2.



In Equation 1, sodium metal reacts with steam to form NaOH and hydrogen. Sodium hydroxide is hygroscopic, and absorbs water to form NaOH hydrates, as shown in Equation 2. Pure NaOH melts at 318°C, but sodium hydroxide hydrates for  $n > 2$  are liquid at room temperature. Equation 1 occurs at the exposed residual sodium surface, or at the sodium/NaOH interface after a NaOH surface layer has been established. The treatment rate is generally controlled by the steam feed rate, and rapid treatment of systems (i.e., within hours to days) is possible. Equations 1 and 2 are exothermic, and Equation 1 in particular liberates -184 kJ/mol at standard temperature and pressure. The treatment process is carried out continuously until no hydrogen is generated from the system for a defined period of time (generally greater than 1 hour).

The reaction products, NaOH and NaOH hydrates, are water-soluble, and may be removed from the treated system after the treatment process is complete by flushing the system with liquid water. The water effluent is highly basic and requires neutralization before further treatment and disposal.

The application of this method to residual sodium is characterized by steady periods of smooth operation, interspersed by erratic and spasmodic reaction behavior, as indicated by spikes in system temperature. An example of a temperature spike is shown in Figure 4, which shows the behavior of a steam treatment experiment performed at Argonne National Laboratory (Sherman et al, 2002). In the figure, somewhat steady reaction behavior is experienced between 75 and 250 minutes, and then a spike in hydrogen concentration (bottom curve) and temperature (top curve) occurs in the reaction chamber at 250 minutes.



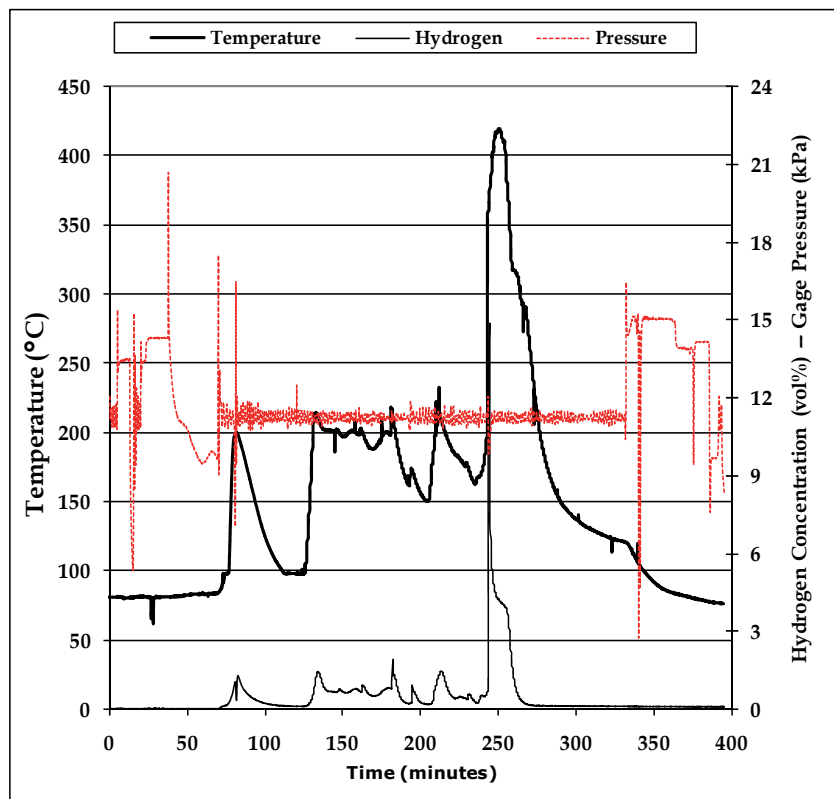


Fig. 4. Measured temperature, guage pressure, and hydrogen concentration in off-gas produced by exposure of sodium metal sample exposed to saturated steam.

Anecdotal evidence seems to indicate that erratic reaction behavior occurs when liquid NaOH hydrates begin to accumulate. The difference in the melting points of pure NaOH and its hydrates, and the strong chemical affinity of sodium metal for water, may lead to the formation of a strong water concentration gradient between the residual sodium surface and the free liquid surface. Once a concentration gradient is established, then circulation of hydrogen bubbles through the liquid layer or other physical disruptions may cause convection within the liquid layer, bringing water-enriched NaOH hydrates in contact with residual sodium, thus causing a sudden acceleration in reaction rate. If the residual sodium temperature is above the melting point of sodium, 97°C, then droplets of liquid sodium, which are less dense, may rise and contact water-enriched NaOH hydrates, which also produces a sudden acceleration in reaction rate.

The frequency of temperature spikes may be reduced by removing liquid reaction products as they form, or by stopping the treatment process periodically to remove liquid pools. Removal of liquid by-products during the reaction process has an added benefit in exposing fresh residual sodium surfaces, and allows for reaction of residual sodium deposits to arbitrary depth. Care must be taken when removing liquid pools, since liquid removal may cause mixing, and this could lead to the uncontrolled reaction behavior that the draining step was intended to prevent.

In spite of these operational instabilities, the Steam-Nitrogen Process is rapid and has been used successfully for many years to deactivate residual sodium in industrial and nuclear

systems. For example, E.I. DuPont de Nemours, Inc., routinely uses the technique to clean residual sodium from sodium transport rail cars and tanker trucks. The Hallam Nuclear Power Facility, a sodium-cooled breeder reactor that operated from 1962 to 1964 in Lancaster County, Nebraska, U.S.A, used superheated steam and nitrogen to deactivate its residual sodium content when the Hallam Reactor was decommissioned (Atomics International, 1970). Superheated steam is being used at the shutdown Fermi 1 Reactor Facility in Frenchtown Charter Township, Michigan, U.S.A. for in-situ cleaning of systems and piping networks containing residual sodium and NaK, and for treatment of sodium-coated components (Goodman, 2009).

### 3.2 Water Vapor Nitrogen (WVN) process

In the Water Vapor Nitrogen (WVN) Process, nitrogen saturated water vapor or nitrogen at less than 100% humidity is injected into the system, and the water vapor in the injection gas reacts with residual sodium to form NaOH, NaOH hydrates, and hydrogen gas. Unlike the Steam-Nitrogen Process, the treatment process is carried out below the boiling point of water and below the melting point of sodium, generally in the temperature range 20-90°C. The treatment rate is influenced by the amount of water vapor in the system, the inventory of water dissolved in the NaOH hydrate layer, and by the thickness of the NaOH and NaOH hydrate layers.

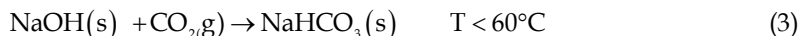
The reaction products, NaOH and NaOH hydrates, are water-soluble, and may be removed from the treated system after the treatment process is complete by flushing the system with liquid water. Effluent from a water flushing step is highly basic due to dissolved NaOH, and generally requires acid neutralization before further treatment and disposal.

Process conditions are selected to minimize the frequency and magnitude of temperature spikes. Water is delivered at a lower concentration to reduce the reaction rate and to allow more heat of reaction to dissipate per unit time. The residual sodium deposits are maintained below the melting point of sodium to minimize intermixing of sodium and water-rich liquids. Though pressure and temperature instabilities may still occur, pools of NaOH hydrates are removed when they accumulate to help prevent reaction instabilities. Like the Steam-Nitrogen Process, the WVN Process is capable of reacting residual sodium deposits to an arbitrary depth.

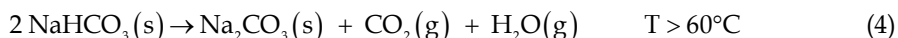
The chief practitioner of the WVN Process in the nuclear area is the United Kingdom Atomic Energy Authority, UKAEA, who is using the technique to clean systems containing residual sodium at its site in Dounreay (Gunn et al., 2009).

### 3.3 Carbonation process

The Carbonation Process is similar in execution to the WVN Process, except nitrogen is replaced with CO<sub>2</sub>, and this replacement greatly changes the process chemistry and characteristics of the treatment process. Like the WVN Process, hydrogen is produced as a by-product of the water-sodium reaction, as shown in Equation 1. Unlike the WVN Process, the CO<sub>2</sub> carrier gas also participates as a reactant. In the presence of CO<sub>2</sub> and at temperatures below 60°C, NaOH produced by the water-sodium reaction is converted into sodium bicarbonate, NaHCO<sub>3</sub>, when it reacts with the CO<sub>2</sub> carrier gas, as shown in Equation 3.



$\text{NaHCO}_3$  does not form liquid hydrates. Above  $60^\circ\text{C}$ ,  $\text{NaHCO}_3$  is unstable and disproportionates into sodium carbonate ( $\text{Na}_2\text{CO}_3$ ),  $\text{CO}_2$ , and water, as shown in Equation 4.



$\text{Na}_2\text{CO}_3$  forms hydrates more readily than  $\text{NaHCO}_3$ , but none of those hydrates are liquids. To avoid the formation of  $\text{Na}_2\text{CO}_3$ , the process is carried out at a temperature below  $60^\circ\text{C}$ . The water content of the  $\text{CO}_2$  carrier gas is maintained at less than 100% humidity to avoid the condensation of liquid water in the system being treated. The treatment rate is influenced by the amount of water vapor in the system being treated, and the thickness of the  $\text{NaHCO}_3$  layer. Since the surface layer is solid, the mass transfer resistance for the diffusion of water vapor to the residual sodium surface is higher than for a liquid surface layer, and the reaction rate quickly becomes surface resistance limited once a  $\text{NaHCO}_3$  surface layer becomes established. Reaction of residual sodium to depths beyond 3-4 cm is possible but is very slow unless the thickness of the intervening  $\text{NaHCO}_3$  layer can be reduced or eliminated.

The reaction products,  $\text{NaHCO}_3$ , is water-soluble, and may be removed from the treated system after the treatment process is complete by flushing the system with liquid water or another suitable solvent. The liquid effluent is only mildly basic, and may not require any further treatment before disposal. In the case that some amount residual sodium remains in the treated system after the Carbonation Process is stopped, the flush liquid would react with residual sodium to form  $\text{NaOH}$ , but this  $\text{NaOH}$  will be buffered to some extent by the presence of dissolved  $\text{NaHCO}_3$ .

$\text{NaHCO}_3$  accumulates as a porous, solid layer on residual sodium surfaces. According to laboratory observations (Sherman et al, 2002), the thickness of the  $\text{NaHCO}_3$  layer is approximately 5 times the thickness of the sodium layer consumed. The volumetric expansion of the surface layer in relation to the volume of residual sodium can cause problems in areas where there is insufficient void space to accommodate growth, such as in small diameter piping. In such places, the void space can become filled with  $\text{NaHCO}_3$ , thus blocking the flow path for humidified  $\text{CO}_2$  at that location. Examples of sodium samples treated with humidified carbon dioxide are shown in Figure 5.



Fig. 5. Sodium samples before (left) and after (right) exposure to humidified  $\text{CO}_2$ . In the figure on the right, the  $\text{NaHCO}_3$  layer is visible as a white layer above darker gray sodium metal.

Unlike the Steam-Nitrogen and WVN Processes, the Carbonation Process is less subject to uncontrolled fluctuations in reaction rate. Under normal operating conditions, moisture does not accumulate in the  $\text{NaHCO}_3$  surface layer, so there is little opportunity for contact between residual sodium and accumulated aqueous solutions. Fluctuations in reaction rate and temperature are still possible if moisture condenses in the system being treated, but this may be avoided by using a sub-saturated treatment gas, or by heating the system that contains residual sodium, so that the atmospheric temperature within the system is higher than the treatment gas.

### 3.4 EBR-II treatment process selection

The process of selecting a treatment method for residual sodium within EBR-II was contentious. One group, composed of the EBR-II reactor designers and former operators, favored the use of the Steam-Nitrogen Process or the WVN Process because these methods promised faster treatment rates and the ability to react residual sodium to greater depths. In addition, the nitrogen-based processes were familiar and backed by experience. They also feared that application of the relatively untested Carbonation Process to EBR-II would place the EBR-II systems into a state in which it would be more difficult and costly to clean up during facility decommissioning than would occur if a nitrogen-based process were used instead. As a back-up strategy, they favored doing nothing as being preferable to application of the Carbonation Process. After all, the empty EBR-II systems were stable and could be maintained indefinitely in this "safe storage" condition as long as required before full funding was available for facility decommissioning.

The other group, composed the engineers and project personnel who were assigned to perform the residual sodium clean-up task, recognized the weight of the first group's recommendations, but were compelled by project requirements and constraints to look for other treatment options. The option of waiting until sufficient funding was available for facility decommissioning was not possible because the RCRA permit compelled treatment. Treatment project funding was insufficient to decommission the facility, and sufficient funding to decommission the facility would not be available for the foreseeable future. The option of using a nitrogen-based process to clean EBR-II systems was studied, but the nitrogen-based methods are subject to fluctuations in temperature and pressure, and the project sponsor, the U.S. Department of Energy, was very risk-averse and had little tolerance for any potential event that might cause harm to personnel or equipment, or lead to an unintentional release of radioactive material to the environment.

A particular project concern with the nitrogen-based processes had to do with the operational characteristics of the method, and the project funding frequency. The project's mandate was to perform residual sodium clean-up *as funding became available*. Full funding was not available at the start of the project, and funding would be provided on a yearly basis across the time span of the project. This meant that there would be periods of activity, followed by periods where the project was waiting for funding and work on the EBR-II systems would cease. The nitrogen-based processes, however, demand a full commitment to the system being treated, and must be carried out to completion once the treatment process is started if system safety is to be maintained. Before a system is treated, it contains only residual sodium, and the configuration is safe and stable. After treatment is completed, the system (presumably) would contain no residual sodium, and the configuration would be safe and stable. During treatment, and in between active treatment periods, the system would be unstable due to the simultaneous presence of residual sodium and liquid NaOH hydrates, and an uncontrolled reaction event could

occur at any time. Although stopping the flow of steam or water vapor to the system stops the active treatment process, a stable configuration is not achieved again until all of the residual sodium inventory is consumed.

The project really needed a residual sodium clean-up method that was capable, stable, and that could be started and stopped at will without creating additional hazards during periods of inactivity. Although untested on a large scale, the Carbonation Process met these criteria. Laboratory work indicated that the method was capable of reacting sodium to depths beyond 3 cm, which is sufficient for a majority of the residual sodium locations in EBR-II. The method was very stable, and did not undergo process variations in temperature and pressure. The  $\text{NaHCO}_3$  layer generated by the treatment process did not accumulate liquid moisture, so that partially treated systems were nearly as safe as untreated systems due to the depletion of residual sodium inventories and the blanketing of residual sodium deposits with a layer of  $\text{NaHCO}_3$ . Also, the concern that application of the Carbonation Process would block access to deeper residual sodium deposits was alleviated by tests that showed that the  $\text{NaHCO}_3$  layer is water-soluble.

In the end, the treatment project team selected the Carbonation Process for these reasons. However, without budget constraints and with greater ability to weather uncontrolled reaction events, the project team might have selected a nitrogen-based process instead. The higher treatment rates and better penetration ability of those methods were recognized, but other project constraints prevented their selection. The Carbonation Process, while slower and less capable of reacting residual sodium to great depths, had many other favorable characteristics, and was compatible with the needs of the treatment project.

#### **4. EBR-II system preparation**

Preparation of the Primary Tank and Secondary Sodium Systems for residual sodium treatment involved installation of a large  $\text{CO}_2$  source tank, piping changes to the Secondary Sodium System, installation of treatment-related equipment and instrumentation, and changeover of the systems' atmospheres from argon to  $\text{CO}_2$ . These preparations are described below.

##### **4.1 $\text{CO}_2$ source tank**

A liquefied  $\text{CO}_2$  tank was installed in between the EBR-II Containment Dome and the Sodium Boiler Building, the building in which the Secondary Sodium System equipment was located (see Figure 2). The tank had a 6400-kg capacity, and was bolted to a concrete pad. The tank was sized to supply pure  $\text{CO}_2$  at a 135 slm (5 standard  $\text{ft}^3/\text{min}$ ) for 2 weeks without refill.

##### **4.2 EBR-II primary tank piping changes**

The EBR-II Primary Tank cover has 58 penetrations or ports through which various instruments, tools, and equipment assemblies were inserted during regular operation of the reactor. One port contained a device called the Failed Fuel Removal System, which had never been used or irradiated. This device was removed from the Primary Tank cover, and a vent pipe was installed in its place. An in-line HEPA filter was also installed to contain any radioactive particulate generated during the treatment process. A schematic of the EBR-II Primary Tank rupture disk and floating head tank remained operational during treatment in order to protect the system against larger overpressure events.

### 4.3 Secondary sodium system piping changes

After the bulk sodium was drained from the Secondary Sodium System, the piping network was altered to allow for the creation of 12 distinct linear flow paths through the system. Without distinct flow paths, sufficient flow of treatment gases through certain pathways could not be guaranteed due to the highly parallel nature of the pipe network. The flow paths were not exclusive, however, and there was some overlap between flow paths. A gas entry manifold was installed that allowed for seven different flow configurations for treatment gas. A vent manifold was also installed. Additional valves and tubing were also installed. The distinct flow paths were created by opening and closing valves in the inlet manifold, the vent manifold, and within the Secondary Sodium System. The exhaust end of the vent manifold was attached to a HEPA filter before exiting to a facility stack. The modified network of valves and pipes is shown in Figure 3.

### 4.4 Additional equipment and instrumentation

#### 4.4.1 Humidification cart

A mobile CO<sub>2</sub> humidification system, the Humidification Cart, was built to facilitate application of humidified CO<sub>2</sub> at multiple locations. The Humidification Cart consists of a 170 liter clear acrylic water tank, four stainless steel frit bubblers, and a collection of Swagelok™ valves and tubing that allow a pressurized supply of CO<sub>2</sub> to be humidified between 0 and 100%. The tank and other equipment are placed on a wheeled platform, which gives it mobility, and the inlet and outlet gas connections are made using flexible tubing. The water tank is equipped with a bayonet heater with thermostatic control. The humidity of the treatment gas is measured using a GE Panametrics Moisture Meter with Remote Moisture Probe, Model #MCHTR-1, which is installed in the CO<sub>2</sub> exit flow path, and the flow rate of CO<sub>2</sub> is measured using a simple glass bead rotometer. A schematic of the Humidification Cart is shown in Figure 6 and images of the Humidification Cart are shown in Figure 7.

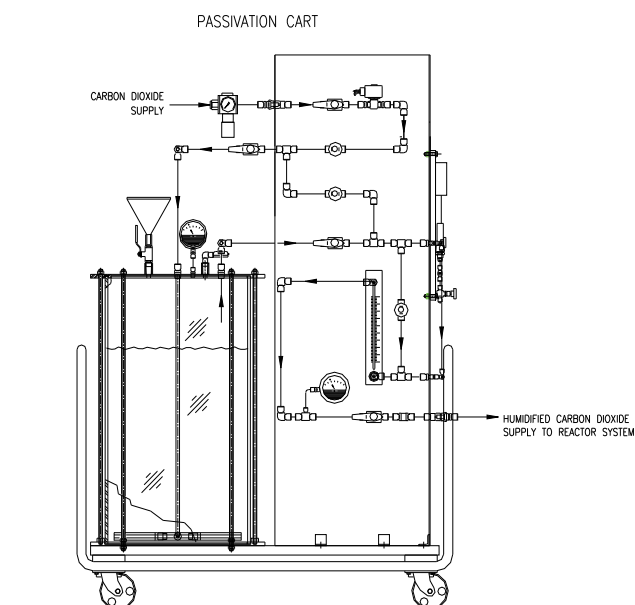


Fig. 6. Schematic of Humidification Cart.



Fig. 7. Photos of the Humidification Cart's acrylic tank and instrumentation/valve panel.

#### 4.4.2 Instrumentation and controls

Instrumentation and controls were installed on the Primary Tank vent line. A 5.08 cm (2") Jordon Mark 518 low pressure spring-loaded mechanical back pressure regulator was installed in order to prevent the back-flow of air from the vent into the EBR-II Primary Tank. The back pressure regulator was normally closed, and opened only when the pressure inside Primary Tank exceeds  $\sim 125$  Pa-gage. A Teledyne Analytical Instruments #326RB oxygen probe was also installed in order to detect air leakage into the Primary Tank, and the monitor was calibrated to read accurately in the range between 0-1 vol%. A Fluid Components International 5.08 cm (2") Model GF92 thermal dispersion mass flow meter with flow transmitter was installed to measure the mass flow rate of the exhaust gas and the exhaust gas temperature. A Teledyne Analytical Instruments #235B thermal conductivity meter was installed to measure the hydrogen concentration in the exhaust gas, and was calibrated to read accurately in the range between 0-4 vol%. A GE Panametrics Moisture Monitor with remote moisture probe, Model #MCHTR-1, was also installed to measure relative humidity of the exhaust gas. The signal outputs from the mass flow meter, oxygen monitor, hydrogen monitor, and humidity monitor were recorded by a facility digital data acquisition system.

The Secondary Sodium System was not as thoroughly instrumented. Oxygen and hydrogen monitors of the same make and model as used on the EBR-II Primary Tank vent line were installed on the Secondary Sodium System vent, and no other instruments or pressure control devices were installed.





Fig. 8. Vent line for EBR-II Primary Tank with installed instrumentation and HEPA filter.

#### **4.5 Changeover of system cover gas from argon to CO<sub>2</sub>**

During regular operation, the EBR-II systems were blanketed with argon to protect the sodium coolant against exposure to oxygen. The Carbonation Process requires an internal atmosphere rich in CO<sub>2</sub>, and so the argon cover gas was changed to CO<sub>2</sub> prior to beginning treatment. The cover gas changeover was accomplished by actively purging the argon blanket with a flow of dry, pure CO<sub>2</sub>. The Primary Tank was purged for 11 days, and the Secondary Sodium System was purged for 4 days with all valves open, at a CO<sub>2</sub> flow rate of 135 standard liters/minute. These purge times were calculated to be sufficient to replace 99% of the argon atmosphere with CO<sub>2</sub> with perfect mixing.

### **5. Carbonation of residual sodium**

The Carbonation Process had never been used before to treat residual sodium within a nuclear reactor's cooling system, and there was no prior operating experience on which to draw. So, the project team decided to pilot the treatment method in the Secondary Sodium System before applying it to the Primary Tank. Although less instrumented, the Secondary Sodium System was accessible, and could be examined to learn more about the in-situ behavior of the treatment method. Also, if the treatment method created some unexpected condition that prevented further in-situ treatment, then the system could be disassembled and treated piecewise at SCMS.

This section describes the application of the Carbonation Process first to the Secondary Sodium System, and then to the Primary Tank.

#### **5.1 Treatment of secondary sodium system**

The treatment of the Secondary Sodium System was performed in two phases. The first phase involved the flow of treatment gas through various paths for time periods ranging



between 1 and 19 days. The second phase involved a longer treatment period for the flow path containing Superheater 712. The flow path containing Superheater 712 was relatively simple with few sections of narrow pipe, and a deep pool (depth > 29 cm) of residual sodium sat in the bottom of Superheater 712, which would allow for a more severe test of the treatment method than would be possible in other parts of the system.

Progress of the treatment process was determined by converting the measured hydrogen concentration data into a molar flow rate, integrating the hydrogen molar flow rate data with respect to time to provide the total amount of hydrogen generated, and then converting this number into the amount of residual sodium consumed using Equation 1. In this calculation, the exhaust gas flow rate was assumed to be equal to the input gas flow rate, and the exhaust gas was assumed to have ideal gas properties. Based on this calculation method, approximately 182 kg (~190 liters) of residual sodium were consumed during treatment of the Secondary Sodium System. This amount is approximately 50% of the starting inventory of residual sodium.

The water level in the humidification cart was also monitored, and the volume of water evaporated was used to calculate an upper bound on the amount of sodium that could be reacted if 100% of the water evaporated from the Humidification Cart were consumed by the water-sodium reaction. This number is only an upper bound, however, since 100% consumption of water vapor becomes unlikely once a  $\text{NaHCO}_3$  surface layer becomes established. Based on this second calculation method, a maximum of approximately 300 kg (~310 liters) of residual sodium could have been consumed during treatment of the Secondary Sodium System. The discrepancy between the hydrogen-based residual sodium estimate and the upper bound estimate would occur if ~1/3 of the water evaporated from the Humidification Cart passed through the Secondary Sodium System without reacting.

### 5.1.1 Secondary sodium system treatment phase one

Phase One treatment of the Secondary Sodium System occurred over 64 days. Treatment occurred by flowing room temperature humidified  $\text{CO}_2$  into the system at a rate of approximately 135 standard liters/minute. A trace of the measured hydrogen concentration in the exhaust gas is shown in Figure 9.

The response of the system during treatment was very stable, and no uncontrolled or runaway reactions occurred due to the build-up of liquid water within the system. The graph shows spikes in hydrogen concentration, but these spikes were aberrations and correspond to time periods when the system valves were changed to alter the flow path of treatment gases. The dip in hydrogen concentration on Day 8 corresponds to a time period when the treatment gas was temporarily changed to dry  $\text{CO}_2$  to put more water in the tank on the humidification cart, and treatment was easily resumed without hysteresis in the system response. The concentration of hydrogen gas remained below 1 vol% during the length of the treatment period, which is below the lower flammability limit of hydrogen in air, 4 vol%. At Day 64, the gas flow was switched back to dry  $\text{CO}_2$  while maintaining a constant flow rate, and the hydrogen concentration in the exhaust gas decayed to 0 vol% as hydrogen was purged from the system.

Table 2 shows the treatment duration per path, and the amount of residual sodium reacted in each pathway based on an integration of the measured hydrogen concentration data. Taking into account the measured hydrogen concentration, approximately 92 kg of residual sodium, or about 95 liters, were consumed during the treatment period. In converting the measured hydrogen concentration into the amount of residual sodium consumed, the

following conditions were applied: constant flow rate of 135 standard liters/minute, ideal gas conditions, and the assumption that 0.5 moles of  $H_2$  are produced for every 1.0 mole of residual sodium consumed.

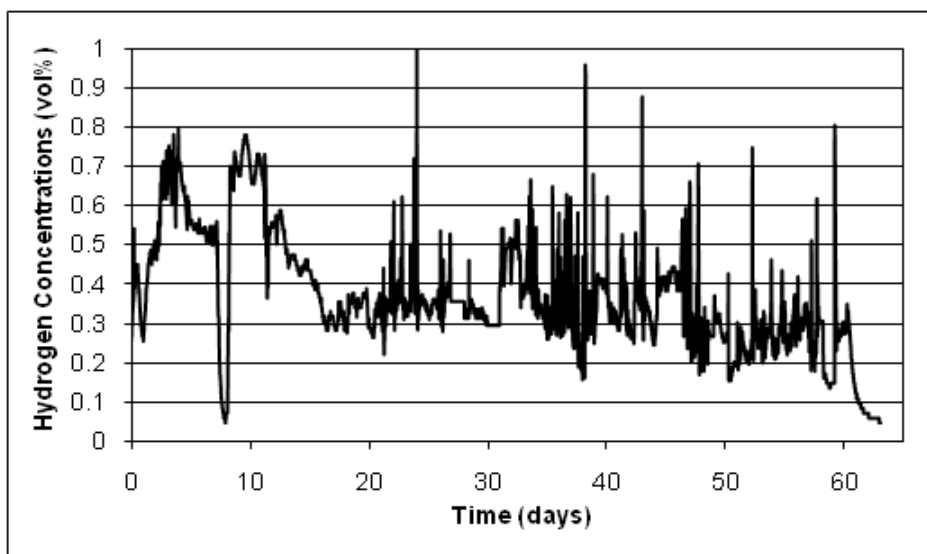


Fig. 9. Measured hydrogen concentration in exhaust gas during treatment of Secondary Sodium System.

Path Name	Treatment Time (days)	Sodium Reacted, kg ( $H_2$ basis)
Surge Tank to Yard Lines	19.0	32
Superheater 712	12.1	21
Secondary Flow Path to Yard Lines	6.9	10
Line Na2-34-557	2.2	2
Major Purge - Superheaters and Evaporators	1.9	2
Superheater 710 Purge	4.1	6
Surge Tank	1.0	1
North Evaporators (4 units)	4.7	7
South Evaporators (3 units)	1.3	1
Line Na2-31-534	1.0	1
Line Na2-31-536	1.0	1
Final Treatment of Surge Tank to Yard Lines	3.8	4
Final Treatment Evaporators, Superheaters, Line Na2-34-520	2.2	3
Final Purge with Dry $CO_2$	2.8	1
Total	64.0	92

Table 2. Summary of treatment times and inventory of reacted residual sodium for Treatment Phase One.

According to the experimental records, approximately 115 liters of water were evaporated during this treatment period, which is enough water to react approximately 145 kg, or about 155 liters, of residual sodium if all of that water came into contact with residual sodium. Since the hydrogen-based residual sodium estimate is less than this number, some amount of water vapor must have passed through the system unreacted. Evidence that water vapor passed through the system unreacted was provided by observing the hydrogen monitoring system. The installed hydrogen monitor required a dry gas feed, and a refrigerated dehumidifier or gas conditioner was used to achieve this. As the treatment operation proceeded, liquid condensate began to accumulate in the gas conditioner's collection bottle, and at an increasing rate, as the treatment process continued. Since the only moisture input stream into the gas conditioner was exhaust gas from the Secondary Sodium System, collection of liquid condensate indicated that the exhaust gas water vapor

### 5.1.2 Secondary sodium system treatment phase two

Phase Two treatment was performed for 72 days, and involved the flow path that included Superheater 712. This flow path had previously been treated for a period of 12 days. The measured hydrogen concentration during this treatment period are shown in Figures 10 and 11. The treatment period is split into two parts, one spanning 8 days, and the other spanning 64 days. This division of the treatment period into two parts was not by design, but was caused by the formation of a blockage in a narrow section of pipe in an elbow at the top of Superheater 712. Physical examination of the blocked location revealed that the narrow pipe section had filled with white powder, which was later revealed by chemical tests to be  $\text{NaHCO}_3$ . After formation of the blockage, a dry  $\text{CO}_2$  flow was initiated through other system pathways to flush hydrogen from the system, and then flexible plastic tubing was installed around the blocked section. Treatment of the Superheater 712 pathway was then resumed.

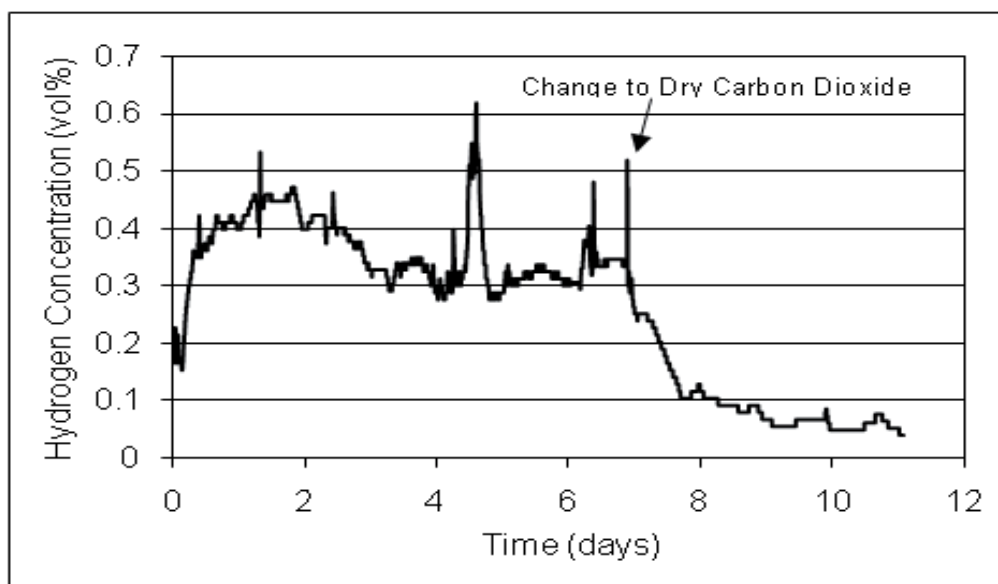


Fig. 10. Measured hydrogen concentration during Phase Two treatment of the Secondary Sodium System, first 8 days.

The treatment process proceeded steadily with no uncontrolled reaction behavior. In Figure 11, there is a large spike in hydrogen concentration on Day 5, but this spike was attributed to a power surge during a lightning storm which tripped the hydrogen monitor, and is not believed to be a true measurement at that point.

According to an integration of the measured hydrogen concentration, approximately 90 kg (< 95 liters) of residual sodium were consumed during Phase Two. Another 115 liters of water were evaporated during the treatment period also, and the excess water vapor was presumed to have been vented in the exhaust gas.

At the end of this treatment phase, the measured hydrogen concentration was still above 0.2 vol%. A treatment endpoint was not reached at the end of Phase Two, and more residual sodium remains in this system that is accessible by the Carbonation Process.

### **5.1.3 Post treatment examination of the secondary sodium system**

A physical examination of Superheater 712 and sections of piping along the Superheater 712 flow path were performed in order to verify the effects of the treatment process. For Superheater 712, the level of residual sodium metal in the bottom of the superheater before and after treatment was determined by hitting the side of the superheater with a hammer and listening for a change in the sound of the hammer blows. According to this test, the residual sodium within the superheater had been reacted to a depth of approximately 2.5 cm. After treatment, a 1.3 cm diameter hole was drilled approximately 25 cm above the measured residual sodium level, and a boroscope was inserted into the superheater to look at the top of the surface layer and other superheater internals. The visual inspection revealed that the surface layer had grown upward in the open space above the residual sodium deposit. A metal support framework affected the growth of the layer, and the layer had expanded upward through the support framework to form white stalagmites. The stalagmites were solid but brittle, and had little mechanical strength when pushed by the boroscope.

In another section of the system, a pipe "T" containing a known amount of residual sodium was drilled and examined using the boroscope. The visual inspection showed a similar looking white layer of material on top of the residual sodium deposit. Residual sodium at this location had also been reacted to a depth of 2.5 cm. Samples of white material obtained at this location were tested chemically by titration and x-ray diffraction, and it was identified as pure  $\text{NaHCO}_3$ .

### **5.1.4 Lessons learned from treatment of secondary sodium system**

The Carbonation Process proved to be a safe and effective means of reacting residual sodium in areas where the residual sodium deposits were shallow, and where there was sufficient void space to accommodate growth of the  $\text{NaHCO}_3$  layer. The behavior of the treatment process in the Secondary Sodium System was similar to what was experienced earlier in the laboratory when test samples were exposed. According to the visual inspections, the method appeared capable of reacting residual sodium to similar depths at widely separated locations, even in complex piping systems. Measurement of hydrogen concentration in the exhaust is the best means available to track treatment progress in systems that cannot be inspected visually during the treatment process. Further treatment of the Secondary Sodium System is needed before RCRA clean closure status may be achieved. Since the treatment process was slow and could be monitored electronically, the process could be operated with minimal supervision and maintenance.

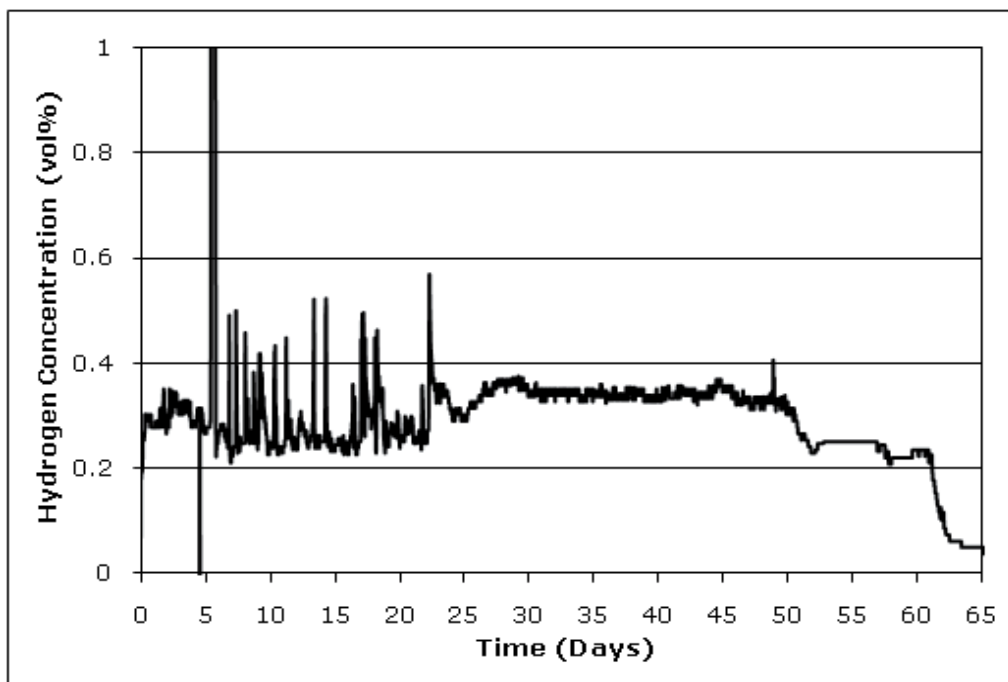


Fig. 11. Measured hydrogen concentration during Phase Two treatment of the Secondary Sodium System, last 64 days.

## 5.2 Treatment of EBR-II primary tank

Treatment of the EBR-II Primary Tank occurred over a cumulative period of approximately 660 days. This treatment period was not continuous, and was interrupted by occasional maintenance periods lasting from days to weeks where the flow of humid carbon dioxide was stopped. During these maintenance periods, the Primary Tank was placed in a no-flow static condition under a dry  $\text{CO}_2$  atmosphere. It is estimated that approximately 760 kg, or 780 liters, of residual sodium was converted into  $\text{NaHCO}_3$  by the Carbonation Process, as determined by an integration of the hydrogen concentration data in the exhaust gas. This amount is approximately 70% of the starting inventory of residual sodium in the EBR-II Primary Tank.

Although the amount of residual sodium consumed could not be verified by visual inspection, integration of the hydrogen concentration data over time provided an indirect method of assessing this number. This calculation was made more accurate by also taking into account the measured exhaust gas mass flow rate, exhaust gas temperature, and the measured concentrations of oxygen and water vapor in the exhaust gas. As was done with the Secondary Sodium System, the exhaust gas was assumed to have ideal gas properties.

The measured reaction rates appear to correspond to treatment rates that would be expected if the following conditions were met: uniform internal distribution of the treatment gas, surface control of the water-sodium reaction rate, and accurate representation of the residual sodium deposit physical geometry and configuration, as described in Section 2.1. A model of the reaction process was prepared to predict treatment rates, and a comparison of the measured and modeled treatment rates showed good agreement, especially after the  $\text{NaHCO}_3$  surface layer becomes established.

### 5.2.1 Initial system treatment

Initially, the EBR-II Primary Tank was treated over a period of 55 days in order to build confidence that the treatment process could be used safely and effectively on the EBR-II Primary Tank. Treatment occurred by flowing either room temperature or heated humidified CO<sub>2</sub> into the system at a rate of approximately 135 standard liters/minute. The treatment gas was introduced to the Primary Tank through a pipe that was inserted through a nozzle in the Primary Tank cover and extending downward to within 0.95 cm from the bottom of the tank. Placement of the pipe exit at the bottom of the tank was believed to enhance gas mixing, since the vent for the tank was installed at the top of the vessel. Figure 12 shows the measured hydrogen concentration and relative humidity in the Primary Tank exhaust gas during the first 55 days of treatment. Initially, the temperature of the water tank was allowed to drift with the temperature of the room. During the last 20 days in the Figure, the water tank was heated to approximately 35-40°C in order to increase the moisture content of the treatment gas. Increasing the water tank temperature resulted in an increase in the measured hydrogen concentration, and also in the relative humidity of the exhaust gas. The drop in hydrogen concentration on Days 20-24 occurred when treatment was temporarily stopped in order to refill the CO<sub>2</sub> supply tank. The treatment gas flow was changed again from humidified CO<sub>2</sub> to dry CO<sub>2</sub> at Day 54, and this change is reflected by the sharp decline in the measured relative humidity and hydrogen concentration on Day 55.

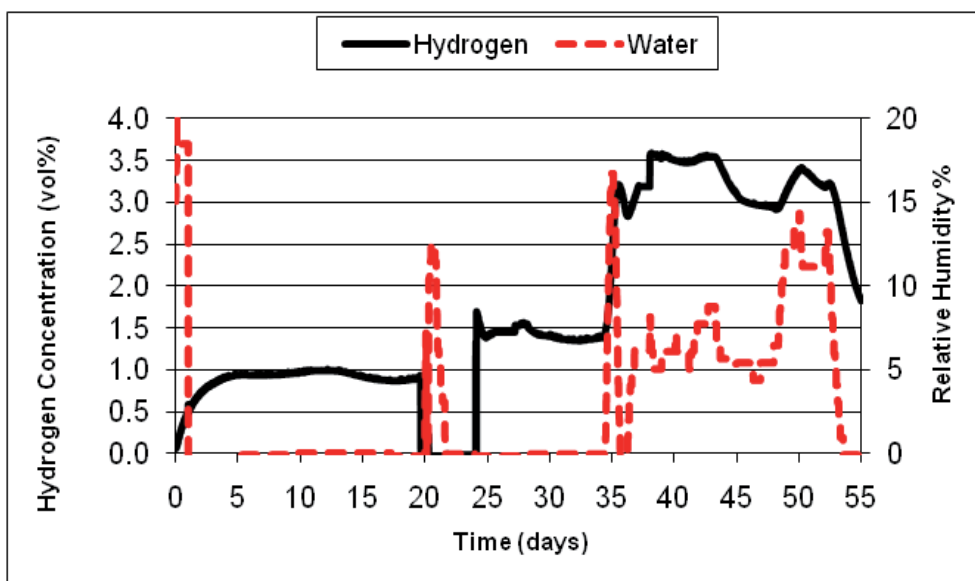


Fig. 12. Measured hydrogen concentration and relative humidity during first 55 days of treatment.

During this initial treatment period, it is estimated that approximately 150 kg of residual sodium was reacted based on the amount of water evaporated from the Humidification Cart. Although using the water tank level to determine the amount of residual sodium reacted generally produces treatment numbers that are too high, an integration of the hydrogen data for the last 30 days of this treatment period gave an even higher number than would have been possible based on a water mass balance. This discrepancy was

investigated, and two potential causes were identified: either the record of the amount of evaporated was incorrect, or the calibration on the hydrogen monitor was incorrect, and it was reading too high. No proof was found to confirm either suspicion, so it was decided to err on the side of caution and use the lower residual sodium estimate for this treatment period.

### 5.2.2 Extended system treatment

After the initial treatment period, treatment of the Primary Tank was stopped for almost two years while awaiting further funding. During this waiting period, the Primary Tank was placed in a static condition under a dry CO<sub>2</sub> blanket.

Treatment was eventually resumed using the same treatment operating conditions as used previously, and was carried out for another 600 days. The hydrogen concentration and exhaust gas mass flow rate measured during this treatment period are shown in Figure 13.

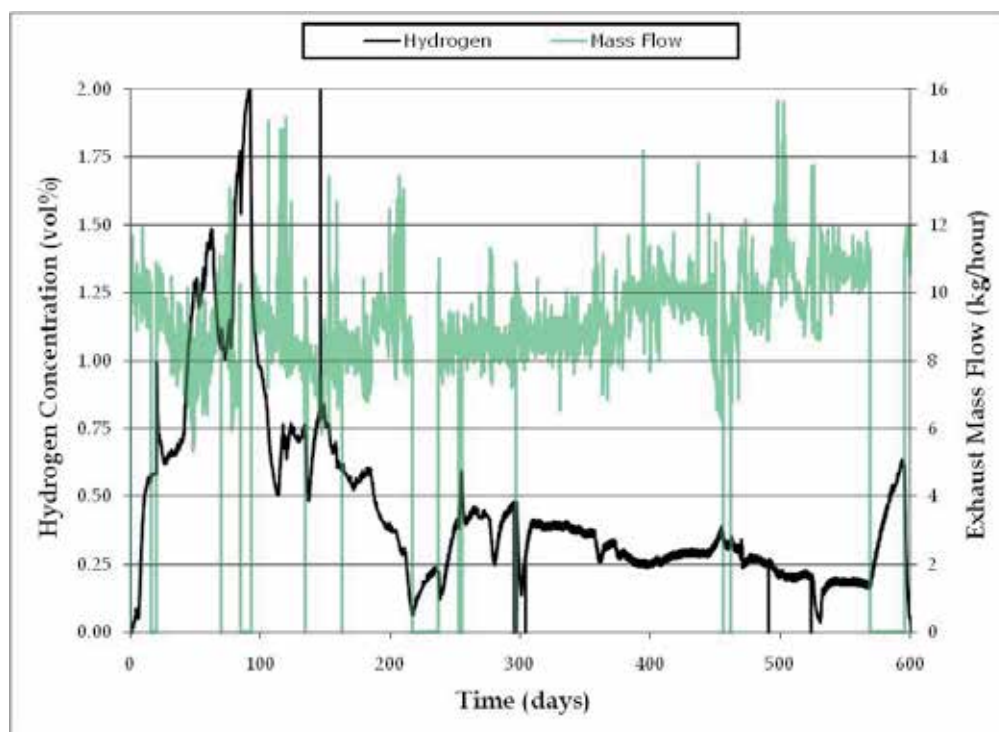


Fig. 13. Measured hydrogen concentration and exhaust gas mass flow rates during last 600 days of treatment.

In the figure, the hydrogen concentration peaked at about 2 vol% on Day 80, and then declined over the remaining treatment period to less than 0.25 vol%. The measured mass flow rate was never steady, and the variability in the measured exhaust mass flow rate is believed to arise from fluctuations in the opening of the mechanical back-pressure regulator. During this treatment period, another 630 kg of residual sodium were estimated to have been consumed.

Treatment of the Primary Tank was stopped after 600 days due to declining treatment rates, and no natural process endpoint had been reached. The decline in treatment rate was

accompanied by an increase in the humidity in the exhaust gas, and humidity levels measured greater than 70% in the exhaust gas by the end of the treatment period.

### 5.2.3 Treatment rate model and correlation to measured data

The reaction rate model was developed during the initial testing stages (Sherman et al., 2002) of the treatment method. The model is defined by a list of rules. The rules are as follows.

1. Due to uniform mixing, moisture is evenly distributed to all exposed residual sodium surfaces. Treatment of residual sodium at multiple locations occurs in parallel.
2. When the surface layer is less than 0.5 cm thick, the residual sodium reaction rate equals the moisture injection rate.
3. When the surface layer thickness is greater than or equal to 0.5 cm, the reaction rate becomes surface-limited. The flux of water vapor to the residual sodium surface is inversely proportional to the surface layer thickness, and is directly proportional to the moisture input rate. The overall residual sodium reaction rate is equal to the moisture flux times the available residual sodium surface area.
4. There is no discontinuity in the reaction rate when the surface layer thickness equals 0.5 cm, and surface-limited reaction rate equals the moisture input rate.
5. For every unit volume of residual sodium reacted, approximately 5 unit volumes of  $\text{NaHCO}_3$  are created.
6. A residual sodium deposit becomes unavailable for further reaction when it is fully consumed or the void space above a deposit becomes completely filled with the  $\text{NaHCO}_3$  (i.e., access to the residual sodium deposit by treatment gas is blocked).

Application of the model to the EBR-II Primary Tank required further definition of the physical configuration of the residual sodium deposits. The residual sodium at each location varies in depth, mass, and exposed surface area. Some deposits are relatively shallow and spread over a wide area, while other deposits are deep and have only a small area of exposed surface. Other deposits are located deep within equipment and have no exposed surface area. Table 3 provides information about the accessible residual sodium locations, and the locations are arranged in decreasing order in regard to the ability of the treatment method to react residual sodium at each location. In Table 3, the Location # corresponds to the subset of locations that are considered accessible by the Carbonation Process (see Table 1). The "Vol" column lists the residual sodium volume at each location. The "Deposit Mass" column lists the mass of residual sodium found at each location. The "Avail Area" column lists the exposed surface area of the residual sodium deposit at each location before treatment. The "Depth 1" through "Depth 6" columns provide the masses of residual sodium residing within the defined treatment depths for each location. The "Done?" column provides a logical descriptor to show whether complete treatment of a location might be achieved in a finite amount of time. The number marked "Start" shows the beginning mass of residual sodium residing at the subset of locations selected for Table 3, and the "End" number shows the total amount of residual sodium that remains after residual sodium has been reacted to a depth of 3.8 cm (Depth 6). The available surface area shows the exposed surface area at each treatment depth range, assuming that the exposed residual sodium surface area at each location remains constant until all residual sodium at a particular location is consumed or becomes blocked due to the build-up of  $\text{NaHCO}_3$ .



Location #	Vol, (L)	Deposit Mass, (kg)	Avail. Area, (m <sup>3</sup> )	Depth 1 <0.1 cm (kg)	Depth 2 0.1-0.38 cm (kg)	Depth 3 0.38-0.95 cm (kg)	Depth 4 0.95-3.18 cm (kg)	Depth 5 3.18-3.65 cm (kg)	Depth 6 3.65-3.8 cm (kg)	Done?
24	189	183	50.0	49	130	---	---	---	---	Yes
23	473	456	50.0	49	130	270	---	---	---	Yes
1	27	26	0.9	0.82	2.3	4.7	18.2	---	---	Yes
2	125	121	1.5	1.4	3.9	8.0	31.2	6.7	blocked	No
14	11	11	0.1	0.08	0.2	0.5	1.9	0.4	0.13	No
3	117	113	1.2	1.2	3.5	7.0	27.3	5.8	1.9	No
4	42	41	0.9	0.83	2.3	4.7	18.4	3.9	1.3	No
7	11	11	0.2	0.24	0.7	1.4	5.4	1.2	0.38	No
8	11	11	0.1	0.15	0.4	0.8	3.2	0.7	0.23	No
16	8	8	0.1	0.12	0.3	0.5	2.65	0.56	0.19	No
21	2	2	0.0	0.0	0.1	0.2	0.65	0.14	0.05	No
Subtotal, (kg)		Start 982		103	282	301	109	19	4	End 164
Available Surface Area, (m <sup>3</sup> )				105.0	105.0	55.0	5.0	4.1	2.6	

Table 3. Masses and available surface areas for residual sodium deposits arranged according to treatment depth.

The depth ranges are interpreted sequentially. At the start of treatment, there is no  $\text{NaHCO}_3$  surface layer, and treatment proceeds as quickly as moisture can be introduced. Once the treatment process has penetrate to a depth of 0.1 cm (Depth 1), the surface layer thickness reaches 0.5 cm (see Rule 5 above), and the water-sodium reaction rate becomes surface-controlled. At a treatment depth of 0.38 cm (Depth 2), all of the residual sodium on the bottom of the Primary Tank cover has been reacted, and the total residual sodium surface area is reduced accordingly. At a treatment depth of 0.95 cm (Depth 3), the residual sodium on the bottom of the Primary Tank has been reacted, and that surface no longer serves a moisture sink. At a treatment depth of 3.18 cm (Depth 4), the residual sodium located in the Low Pressure Plenum has been reacted, and the available residual sodium surface area is reduced again. At a depth of 3.65 cm (Depth 5), access to the residual sodium in the High Pressure Plenum becomes blocked, and that location becomes inactive. At a depth of 3.8 cm (Depth 6), the residual sodium located outside the flow baffle around the gripper/hold down becomes blocked by the build-up of  $\text{NaHCO}_3$ , and that location becomes inactive. Reaction of additional amounts of residual sodium at Locations 3, 4, 7, 8, 16, and 21 are still possible if treatment is pursued to greater depths, and the piece-wise analysis of reaction depths would need to be continued if the reaction rate model were extended to deeper reaction depths.

Interpreting the information provided in Table 3, it is clear that complete consumption of residual sodium in the Primary Tank just isn't possible using the Carbonation Process. Only about 982 kg out of the total residual sodium inventory (~1100 kg) are accessible. In addition, the treatment rate would be exceedingly slow at greater treatment depths due to loss of available surface area. At a treatment depth of 3.81 cm, for example, 97.5% of the original residual sodium surface area has been eliminated, and the overall treatment rate is reduced proportionately if a constant moisture input rate is assumed.

Average daily residual sodium treatment rates were calculated using the data shown in Figures 12 and 13, and these average treatment rates were plotted in Figure 14 as a function of the total amount of residual sodium treated. A model curve was also plotted based on the specific information provided in Table 3 and a fixed moisture input rate. During the initial treatment period, the measured data fall far below the model curve when the water tank in the Humidification Cart was unheated (first 20 days in Figure 12), but align more closely when the tank was heated (next 40 days, Figure 12). When treatment of the Primary Tank was resumed after the long hiatus, the measured points fluctuate around the model curve until approximately 400 kg of residual sodium had been consumed, and then the measured points align quite closely with the model curve. In the flat portion of the model curve (upper left), the rate is controlled by the moisture input rate, and the wide discrepancy between the measured data and the model curve is due to selection of the wrong moisture input rate for the model during the initial treatment period. Once the surface layer becomes rate-controlling, the moisture input rate becomes less critical, and the measured data follow the model curve more closely. The growth in surface layer thickness and loss of available surface area, leads to large reductions in the treatment rate at higher treatment totals, and this effect is evidenced in the plot.

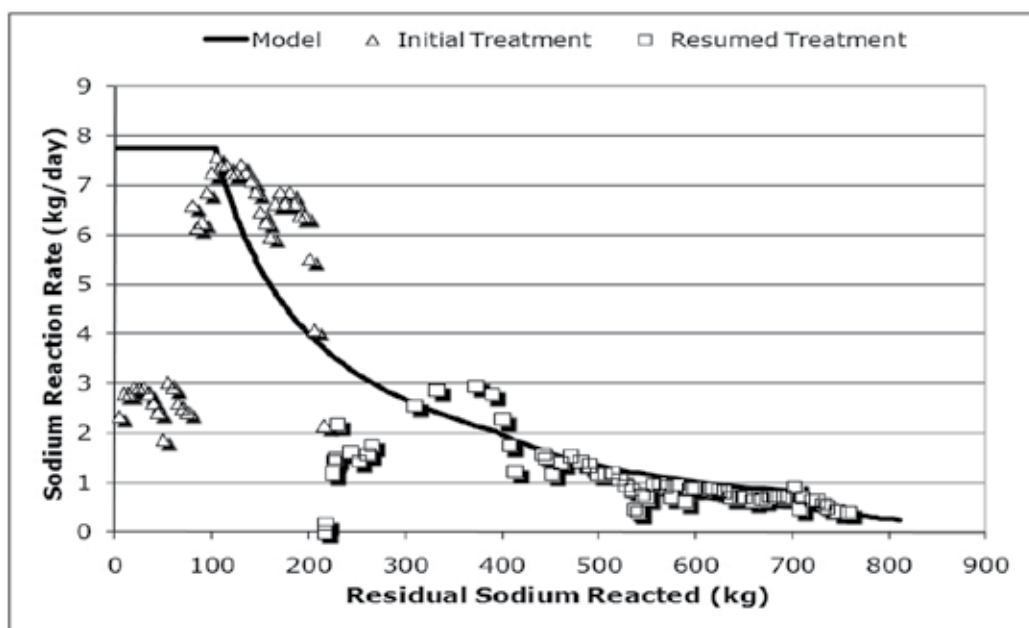


Fig. 14. Comparison of observed reaction rates versus modeled reaction rates as a function of the cumulative mass of residual sodium consumed.

#### 5.2.4 Lessons learned from treatment of EBR-II primary tank

The Carbonation Process may be stopped and started arbitrarily without causing changes in treatment performance if the system is placed in a dry, static condition in between treatment periods. The process performed smoothly over the extended treatment period without spikes in temperature or hydrogen concentration. Although complete treatment of residual

sodium within the Primary Tank was not possible, application of the treatment method did result in a great reduction in the chemical reactivity of the remaining residual sodium by elimination of the easily accessible deposits, and burial of the deeper deposits beneath a thick layer of relatively inert  $\text{NaHCO}_3$ . The treatment of residual sodium within the EBR-II Primary Tank using humidified  $\text{CO}_2$  might have been continued still further with the Carbonation Process, but the treatment process had reached the point of diminishing returns, and little further progress towards the treatment goal was anticipated if the treatment process were continued beyond the chosen stopping point.

## 6. Conclusions and future work

In one sense, application of the Carbonation Process to EBR-II in order to deactivate residual sodium was very successful. Approximately 70% of residual sodium within the EBR-II Primary Tank and 50% of residual sodium within the EBR-II Secondary Sodium System were converted into relatively benign  $\text{NaHCO}_3$  with no safety problems. The treatment method was easy to use and could be started and stopped at will with no hysteresis effects. The residual sodium that remains within EBR-II is much less chemically reactive, and the systems are much better protected against uncontrolled air and water leaks. In addition, the behavior of the treatment process appears to be well understood and can be explained and predicted using a relatively simple rule-based model.

In another sense, however, using the Carbonation Process in order to achieve a clearly defined RCRA-closed state in the EBR-II systems was not a good strategy. Complete deactivation of all residual sodium within these could never be achieved, even with very long treatment times, and an additional treatment step is still required to remove the reaction by-product.

Considering the complex geometry of the residual sodium deposits in the EBR-II Primary Tank, it is not clear that using the Steam-Nitrogen Process or the WVN Process would have been much more successful. Though these methods may have been able to achieve greater depth penetration and faster reaction rates, eventually these methods too would become surface limited due to the build-up of liquid surface layers and consumption of the easier-to-reach locations, and treatment rates would also have declined over time. In addition, achievement of a clearly defined RCRA-closed state would still have required a follow-on treatment step to remove the reaction by-products, and the desired endpoint could not be reached in a single treatment step.

At this point in time, it is still possible to meet the strict definition of RCRA closure in the Primary Tank if the tank were filled and flushed with liquid water. Filling the tank with liquid water would consume the remaining residual sodium and dissolve the reaction by-products.

Though the thought of adding liquid water to sodium metal may sound alarming, the safety aspects of the operation would be aided by the placement of the remaining residual sodium deposits. The locations still containing residual sodium reside at different heights in the Primary Tank, and the instantaneous reaction of all residual sodium would not occur if the Primary Tank were slowly filled with water. While residual sodium above the water level may react weakly in response to water vapor in the gas space above the liquid level, a strong sodium-water reaction would not occur until the liquid height reaches the height of a residual sodium deposit, or the liquid level becomes high enough to overcome a hydraulic barrier, causing water to overflow into a residual sodium location at a lower elevation. While it is certain that there would be some uncontrolled and episodic reaction behavior when liquid initially comes into contact with residual sodium, the rate of energy released

would be limited by the available surface area of the residual sodium deposit, and not all of the residual sodium at a particular location would react instantaneously due to the reduced surface area of the deposit. Also, the mass of water in the tank would serve as a heat sink and would absorb the heat of reaction as water-sodium reactions occur.

Adding water to the Primary tank would generate a large volume of waste that would need to be handled, and the costs and safety aspects of handling this waste material must be balanced against the larger need to protect the environment, which is the original intent of the RCRA permit.

If process safety is the ultimate arbiter, then the best option to pursue at this point would be to seek a risk-based closure with no further treatment of residual sodium. The relative safety and environmental risks associated with the Primary Tank were much improved by application of the Carbonation Process, and there would be little risk of any uncontrolled sodium-water reactions occurring in the Primary Tank even if moist air leaked into the Primary Tank. As an added precaution, the Primary Tank may be also filled with grout to seal and immobilize the remaining residual sodium deposits, and block all further access to them.

It is this last option that the Idaho Clean-up Project (ICP), administered by CH2M\*WG Idaho, the current organization overseeing stewardship of the EBR-II facility, has selected to pursue. By 2015, the company plans to fill the Primary Tank with grout, to further isolate the remaining reactor internals, and leave it in place. Although the Carbonation Process was not successful in reacting all of the residual sodium within the EBR-II Primary Tank, it worked well enough to allow for a risk-based closure without requiring further treatment of residual sodium.

## 7. References

- Atomics International. Report on Retirement of Hallam Nuclear Power Facility. AI-AEC-12709, May 15, 1970. Available from Library of Congress, Technical Reports and Standards, U.S.A.
- Goodman, L. Fermi 1 sodium residue clean-up. Decommissioning of Fast Reactors After Sodium Draining. IAEA-TECDOC-1633, International Atomic Energy Agency, Vienna, Austria, November 2009, p. 39-44.
- Gunn, J.B., Mason, L., Husband, W., MacDonald, A.J., Smith, M.R. Development and application of water vapor nitrogen (WVN) for sodium residues removal at the prototype fast reactor, Dounreay. IAEA-TECDOC-1633, International Atomic Energy Agency, Vienna, Austria, November 2009, p. 123-134.
- Koch, L.J. (2008). *EBR-II, Experimental Breeder Reactor-II: An Integrated Experimental Fast Reactor Nuclear Power Station*, American Nuclear Society, La Grange Park, Illinois, USA, ISBN: 0-89448-042-1.
- Sherman, S.R., Henslee, S.P., Rosenberg, K.E., Knight, C.J., Belcher, K.J., Preuss, D.E., Cho, D.H., & Grandy, C. Unique Process for Deactivation of Residual Sodium in LMFBR Systems. Proceedings of *Spectrum 2002*, American Nuclear Society, Reno, Nevada, U.S.A., August 4-8, 2002.
- Sherman, S.R. & Henslee, S.P. (2005). In-situ Method for Treating Residual Sodium. U.S. Patent 6,919,061.
- Solid Waste Disposal Act, Subtitle C, Title 42 U.S. Code Parts 6901-6992k, 2002 edition.

## **Part 3**

# **Environment and Nuclear Energy**



# Carbon Leakage of Nuclear Energy – The Example of Germany

Sarah von Kaminietz and Martin Kalinowski  
*Carl Friedrich von Weizsäcker - Centre for Science and  
Peace Research at the University of Hamburg  
Germany*

## 1. Introduction

Carbon leakage is the increase in emissions outside a region as a direct result of the policy to cap emissions in this region.

Nuclear energy is a low carbon technology but it is not emission free. Lifecycle analyses of nuclear energy find an average carbon intensity of 66g CO<sub>2</sub>/kWh of which the largest part (38%) is generated in the front end of the nuclear fuel cycle (uranium mining and milling). Besides the CO<sub>2</sub> emission there are also other environmental and health impacts that are associated with the uranium milling and mining activities.

In Germany nuclear energy use is a controversially discussed topic. In 2002 the out-phasing of nuclear energy by 2022 was decided. In 2010 a new government passed a life time extension of the 17 power plants by on average 12 years, seeing nuclear energy as an important bridging technology to reach Germany's ambitious climate goals. This chapter calculates the carbon leakage that is expected to result from the 2010 life time extension. Due to the nuclear incident in Japan in March 2011 the debate about the time plane for the out-phasing for nuclear energy started again in Germany. At the time of writing, it is unclear when and how the out-phasing process in Germany will take place. This work is therefore to be seen as an exemplary study on the issue. Uranium is not mined in Germany and it is not easy to trace the origin of the imported uranium. But it can be said that close to 100% originate from outside of Europe.

This work calculates the expected amount of carbon leakage from German nuclear energy use until 2036. The calculations are based on an energy scenario of the German government, the lifetime extension of nuclear power plants and carbon emission resolved by region for each production step from life cycle analyses.

It is important to incorporate the aspect of carbon leakage in the international discussion about climate friendly energy solutions. This assures fairness and transparency and avoids that countries with emission limits gloat over mitigation achievements whose burden has to be carried by other regions.

## 2. Carbon leakage - definition and importance

Carbon leakage is the increase in emissions outside a region as a direct result of the policy to cap emissions in this region.

International climate agreements like the Kyoto Protocol and the Copenhagen Accord apply the principle of “common but differentiated responsibility” taking into account a country's economic capability and past accumulated emissions. The Kyoto Protocol sets binding targets for 37 industrialized countries for reducing greenhouse gas emissions by on average 5% against 1990 levels over the five-year period 2008-2012 (United Nations Framework Convention on Climate Change [UNFCCC], 2010). Germany is one of the 37 countries listed in Appendix B of the Protocol which have capped emissions. In the following, countries with emission reduction targets or capped emissions are referred to as constrained countries, while the others are referred to as unconstrained countries. To reach their targets some countries have implemented or are going to implement climate policies and incentives. Carbon leakage provides a loophole in unilateral climate policies and leads to a loss of their effectiveness if viewed from a global level.

The IPCC defines carbon leakage as follows:

“Carbon leakage is the increase in CO<sub>2</sub> emissions outside the countries with emission constraints divided by the reduction in the emissions of these countries, as a result of climate policy in constrained countries.” (Intergovernmental Panel on Climate Change [IPCC], 2010)

Viewed mathematically, carbon leakage i.e. the leakage rate  $L$  is simply a ratio which is usually given as a percentage.

$$L = \frac{\text{emission increase in unconstrained country}}{\text{emission reduction in constrained country}} \quad (1)$$

$L > 100\%$  indicates an increase in total emission due to the climate policy. Here the reduction in constrained countries is less than the increase in unconstrained ones. This may be the case because energy and carbon efficiency in unconstrained countries are usually lower than in constrained countries hence more emissions are offset to produce the same amounts of goods (Babiker, 2005). This clearly counteracts the aim of the climate policy.

$0\% < L < 100\%$  represents a loss in effectiveness of the climate policy. Some of the emissions reduced in the constrained countries cannot be counted as eliminated because they caused an increase in emissions in unconstrained countries (Demailly & Quirion, 2008; Gielen & Moriguchi, 2002).

$L < 0\%$  implies negative carbon leakage, which means that constrained as well as unconstrained countries attained emission reductions. This is found to be possible due to the effect of induced technology transfer (DiMaria & van der Werf, 2008; Golombek & Hoel, 2004; Gerlagh & Kuik, 2007).

$L$  does not give information about the total change in emissions but only about the relative changes in the two countries. To make quantitative statements one still needs to know the emissions in total numbers.

Most studies about carbon leakage consider energy-intensive products as the commodity that causes the leakage. The production of those products is relocated to unconstrained countries and imports to constrained countries increase.

Theoretical studies on the topic come to a wide range of results depending on the model and assumptions. Everything from over 100% to negative carbon leakage has been found possible.

Empirical studies on carbon leakage usually investigate the effect of the European Union's Emission Trading Scheme (EU-ETS) on internationally traded, energy-intensive products



like aluminum, steel, cement and paper. The conclusion is often that there is not much empirical evidence of carbon leakage yet. Different reasons for that can be named. The probably most important one is that the EU-ETS is still a young incentive that has not yet fully developed its impacts on trade flows and production patterns in the concerned countries (Reinaud, 2008; European Commission et. al, 2006).

In this work a new commodity regarding the carbon leakage discussion is studied – the nuclear energy lifecycle.

### **3. The German energy strategy with focus on the role of nuclear energy**

Germany has high ambitions regarding German emission mitigations. But as an industrial country energy supply security and economic energy prices are two very important factors in the discussion about Germany's energy mix. Nuclear energy is a controversially discussed topic in German politics as well as in the population. In 2002 the out phasing of nuclear energy by 2022 was decided (Atomgesetz Novelle, 2002). In 2010 this decision was revised and the life times of nuclear reactors were extended by on average 12 years (Atomgesetz Novelle, 2010). The reason for that is the current government's stance that sees nuclear energy as a necessary bridging technology to reach Germany's ambitious climate goals while securing energy supply and economic energy prices. The lifetime extension can thus be seen as a climate policy. Due to the nuclear incident in Japan in March 2011 the debate about the time plane for the out-phasing for nuclear energy started again in Germany. At the time of writing, it is unclear when and how the out-phasing process in Germany will take place. All data used in this work is from before March 2011.

#### **3.1 The German nuclear law**

The German nuclear law (Das deutsche Atomgesetz (AtG)) is the legal basis for nuclear energy use in Germany. It first came into power in 1960. Since then several revisions (AtG Novells) of this law where passed. The 2002 AtG Novell introduced by the SPD/"Bündnis 90 die Grünen" government concluded the phase-out of German nuclear energy. The construction of new nuclear power plants was hereby prohibited and the lifetimes of the existing plants were limited to on average 32 years after commissioning. From this lifetime restriction and the capacity of the different power plants the rest amount of energy that each power plant can produce was calculated. These rest amounts sum up to 2620 TWh of electricity that can be produced by German reactors after 1 January 2000. It is possible to transfer parts of these rest amounts from one reactor to another if favourable. Because of this flexibility it is not possible to state exact date for the out phasing. But the estimated end of lifetime after the 2002 AtG Novell can be seen in Table 1.

In September 2010 the CDU/FDP government introduced a new energy concept for Germany; part of this energy concept is the extension of the life times of the 17 remaining nuclear power plants by on average 12 years. The lifetime extension is established in the 2010 AtG Novell. The life times of power plants which came into operation by 1980 will be extended by 8 years, all younger power plants will operate for an additional 14 years beyond 2022.

Table 1 shows a list of all German nuclear power plants, their annual capacity, the year they were expected to be shut down after the 2002 AtG Novell, the year they are expected to terminate operations after the 2010 AtG Novell. Further the table shows the life time extension and the additional amount of electricity is expected to be produced during this additional life time.

Powerplant	Capacity* [TWh/ year]	Year of operation start	End of lifetime 2002 AtG Novell**	End of lifetime 2010 AtG Novell	LT extension [years]	Capacity extension [TWh]
Neckarwestheim 1	7.36	1976	2010	2018	8	58.88
Biblis B	11.39	1977	2010	2018	8	91.12
Isar 1	7.99	1979	2011	2019	8	63.92
Biblis A	10.73	1975	2010	2018	8	85.84
Brunsbüttel	7.06	1977	2012	2020	8	56.48
Philippsburg 1	8.11	1980	2012	2020	8	64.88
Unterweser	12.35	1979	2012	2020	8	98.80
Grafenrheinfeld	11.78	1982	2014	2028	14	164.92
Gundremmingen B	11.77	1984	2016	2030	14	164.78
Gundremmingen C	11.77	1985	2016	2030	14	164.78
Philippsburg 2	12.77	1985	2018	2032	14	178.78
Krümmel	12.28	1984	2019	2033	14	171.92
Grohnde	12.53	1985	2018	2032	14	175.42
Brokdorf	12.61	1986	2019	2033	14	176.54
Isar 2	12.92	1988	2020	2034	14	180.88
Emsland	12.26	1988	2020	2034	14	171.64
Neckarwestheim 2	12.22	1989	2022	2036	14	171.08
Total						2240.66

\* Source: German Atomforum

\*\* Source: Bundesumweltministerium, 2009

Table 1. Life time extension and yearly capacity of German nuclear power plants

#### 4. Carbon emission of nuclear energy - a life cycle analysis

Nuclear energy is a low carbon technology but it is not emission free. Nuclear power does not directly emit greenhouse gas emissions, but lifecycle emissions occur through plant construction, operation, uranium mining and milling, and plant decommissioning. Life cycle analysis (LCA) is a method to account for the emissions offset during each life phase of a products lifecycle, including the production of the product and its raw material, its use and disposal.

Many life cycle analyses of nuclear energy have been conducted and they come to a wide range of emission intensities. The emission intensities used in this work are based on an analysis of Svacool (2008), who screened 103 life cycle studies of GHG emission for nuclear power plants. As a result 66g CO<sub>2</sub>/kWh is the average emission intensity. The lifecycle analysis resolves the emission intensity by steps of the life cycle. The study concludes that on average 38% of the emissions are generated in the front end of the nuclear fuel cycle (uranium mining and milling). This means that the front end of the nuclear fuel cycle which takes almost completely place outside of Europe has an emission intensity of 25.1 CO<sub>2</sub>/kWh. In the discussion about carbon leakage these front end emissions are the focus. These

emissions occur outside of Germany and outside of Europe and are due to the life time extension of German nuclear power plants.

#### **4.1 Other environmental impacts and risks in the front end of the nuclear fuel cycle**

To have a more comprehensive view on the problem, sections 4.1. will elaborate further environmental impacts and life-threatening risks connected with the front end of the nuclear fuel cycle. These factors do not fall under the issue of carbon leakage but they pose a severe disadvantage to the countries in which the uranium for German power plants is mined and milled.

Uranium mining causes a lot of different disadvantages to employees and the local population as well as to the environment besides the carbon emission from the mining, transportation, power use and building of the facilities. The mineworkers are affected by radiation contamination. The alpha radiators radium-226 and its daughter radon as well as thorium-232 can cause diseases like lung cancer. A more indirect contamination to the human population occurs from the tailings. After the milling process the wet tailings are typically stored somewhere above ground without any further protection. The drying process leads to radiating dust, which is easily spread by wind. Rainfalls sweep the radiation into the soil and groundwater. Even if there is some kind of protection it is often just an earthy coating and not really effective against heavy rainfall. A problem that could occur after the mine is abandoned is the formation of stagnate water pools from rainwater. Those could especially in Africa become hatcheries for mosquitoes that spread water-borne diseases like malaria (South Virginia Against Uranium Mining, 2008). These environmental impacts and life-threatening risks are not in the attentions of official institutions. In many countries safety guidelines for the mining companies exist on a voluntary basis. No controls or sanctions for non compliance are executed. Very little data is available on the actual impact of the problem. There are no new statistics published by governmental organisations. Most data are collected by the industries themselves and do not represent an independent assessment of the issue (Kalinowski, 2010).

### **5. Regional resolution of the German uranium imports**

Germany has terminated its domestic uranium exploration. All uranium required for German nuclear power plants is imported. To trace the origin of the material is very difficult due to intransparent accounting methods and data confidentiality of certain countries in the trading chain. However, this is required to understand to which country CO<sub>2</sub> emissions are exported. More precisely, the exact carbon leakage depends on the methods applied for uranium mining and milling and these vary significantly by country.

A study conducted by the International Physicians for the Prevention of Nuclear War (International Physicians for the Prevention of Nuclear War [IPPNW], 2010) attempted to resolve the German uranium imports by country of origin.

The largest part of the imported uranium is natural uranium (4.662 t in 2009). Only 897 t of enriched uranium were imported in 2009 (Statistisches Amt der europäischen Union / Statistisches Bundesamt, as cited in IPPNW, 2010).

The uranium demand of German nuclear power plants was 3.398 t natural uranium in 2009. (World Nuclear Power Reactors & Uranium Requirements, Website of the World Nuclear Association, as cited in IPPNW, 2010). The amount of fuel that can be produced from that is between 297 t (5% enriched) and 517 t (3% enriched). Germany is exporter of enriched

uranium. Eurostat statistics show that Germany exported 671 t enriched uranium in 2009 to mainly Belgium, France, Sweden and the USA, as well as small quantities to Brazil and South Korea. (Statistisches Amt der europäischen Union / Statistisches Bundesamt, as cited in IPPNW, 2010)

The enriched uranium Germany imported in 2009 came from: France (575t, 64%), Russia (160t, 18%), Netherlands (94t, 10%), USA (41t, 5%), UK (18t, 2%), Belgium (9t, 1%). The enriched uranium from Russia comes from dismantled nuclear weapons.

The countries Germany imports natural uranium from in 2009 are France (2109t, 45%), UK (1914t, 41%), USA (491t, 11%), Canada (134t, 3%) and Netherlands (13t, 0%) (Statistisches Amt der europäischen Union / Statistisches Bundesamt, as cited in IPPNW, 2010).

France and the UK like Germany no longer exploit own uranium resources that means they only function as trader and consumer. Information about the import countries of uranium to France are known, this information is not available for import to the UK. It is not known whether those countries are the original producers of all the uranium or if they also function as traders. Assuming France supplied the uranium in the same shares as it received, the origin of natural uranium used in German power plants in the year 2009 would look the following: Unknown (1914t, 41%), USA (597t, 13%), Australia (569t, 12%), Canada (514t, 11%), Niger (485t, 10%), Kazakhstan (190t, 4%), Uzbekistan (148t, 3%), Russia (84t, 2%), Others (148t, 3%). Since the largest fraction of uranium imports by Germany are from France and given the in-transparency of material flows the best estimate for the distribution of countries of origin is the one presented in Fig. 1.

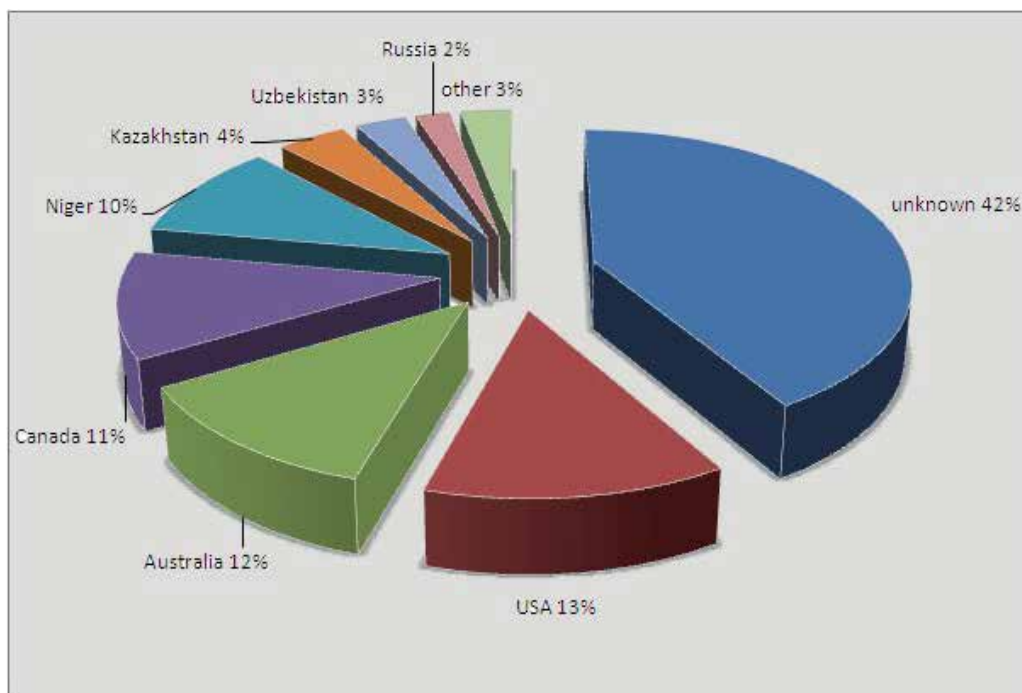


Fig. 1. Assumed origin of natural uranium used in German power plants in the year 2009

With the available data the countries from which the uranium is imported for use in Germany cannot be fully identified. It is however possible to identify the most important mining countries for uranium imports to the EU. These countries are Australia, Russia, Canada, Niger, Kazakhstan, South Africa, Namibia, Uzbekistan and USA. It can be assumed that those countries are also the countries of origin for the German imports but the shares of uranium purchased from the single countries are different between the EU and Germany.

The EURATOM Supply Agency (ESA) 2009 report identified Australia, Canada and Russia as most important suppliers for Europe. Because of the large amounts of trading the ESA has to admit that the origin of all Russian uranium cannot be definitely determined. Whether the origin of Canadian and Australian uranium can be definitely determined is unclear.

Three main conclusions can be drawn from the IPPNW investigations.

The available data are highly inconsistent and intransparent and incomplete. This makes it very hard to answer the question of where does the uranium used in German nuclear power plant originate from. IPPNW contacted the German government to provide information and the conclusion drawn from the answers of the requests was that it seems as if the government tries deliberately to obscure the origin of the uranium.

The second conclusion is that the supply security of uranium from OECD states is not provided. The USA, Australia and Canada are uranium mining countries but those countries were in the last years only responsible for less than 50% of the German uranium imports. The production in these three countries is declining (World Nuclear Association, as cited in IPPNW, 2010). If the global uranium demand rises it is probable that countries like Kazakhstan and Namibia increase their mining activities. A consequence of this is that the German supply with uranium is as unsecure and as dependent of partners outside the OECD as the supply with conventional, fossil energy sources.

The third conclusion is that Germany does not comply with its own pledge not to purchase uranium from countries like Niger in which severe human rights violations and environmental damage occur (Greenpeace "Left in the dust"; Der Spiegel "Der gelbe Fluch", 29.03.2010, as cited in IPPNW, 2010). Also in the past German companies were not able to meet its demand by import from „politically stable“ countries. One example is the import of uranium from Namibia in time of apartheid, which is not only morally unacceptable but also violated the UN-resolution *Decree No. 1 on the Natural Resources of Namibia*, which forbids the prospecting, mining, processing, selling, exporting, etc., of natural resources within the territorial limits of Namibia without permission of the Council (Dumberry, 2007). This historical evidence leads to the belief that German nuclear power plants will also in the future depend on uranium from "politically unstable" countries. Whoever runs nuclear power plants in Europe is responsible for environmental damage and health impacts in the uranium mining countries (IPPNW, 2010).

## 6. Carbon leakage calculations

In this section the amount of carbon leakage from German nuclear energy use from 2010 until 2036 is calculated based on the facts and data presented in the previous sections. The decrease in emission in Germany and the increase in emission in the uranium mining countries is based on the life time differences of the 2002 and the 2010 AtG Novell and the regionally resolved life cycle analyses.

The formula for carbon leakage is:

$$L = \frac{\text{emission increase in unconstrained country}}{\text{emission reduction in constrained country}} \quad (1)$$

The “emission increase in unconstrained countries” are the emissions that the climate policy, hence the extended lifetimes of the nuclear power plants caused outside Europe. In section 3 we calculated that the lifetime extension leads to an additional 2240.7 TWh of electricity that are produced by nuclear power. The review of the life cycle analyses in section 4 revealed the emission intensity of nuclear energy is on average 66 g CO<sub>2</sub>/kWh whereof 25.1 g CO<sub>2</sub>/kWh are emitted in the front end of the nuclear energy cycle. As has been explored in section 5, the front end of the nuclear fuel cycle for German nuclear energy does not take place in Germany. The front end emissions that are caused by the 2240.66 TWh of electricity are emissions that are offset outside Europe due to the lifetime extension of nuclear energy in Germany. These 2240.7 TWh \* 25.1 g CO<sub>2</sub>/kWh = 56.2 Mt CO<sub>2</sub> are the emission increase in unconstrained countries.

The “emission reduction in constrained countries” are the emissions that are not released due to the climate policy, hence due to the extended life times of the nuclear power plants. The extended lifetimes result in a total of 2240.7 TWh of electricity that is produced through nuclear power. As stated in section 4 life cycle analyses show that the emission intensity of nuclear energy is 66 g CO<sub>2</sub>/kWh, of these 66 g CO<sub>2</sub>/kWh only 40.9 g CO<sub>2</sub>/kWh are off set in Germany. 2240.7 TWh \* 40.9 g CO<sub>2</sub>/kWh = 91.7 Mt CO<sub>2</sub> is the amount of CO<sub>2</sub> that 2240.7 TWh of electricity produced by nuclear power offset in Germany.

It is assumed that the emission intensity with which the 2240.7 TWh would have been produced if there was no lifetime extension is the average emission intensity of the reference scenario taken from the energy scenarios of the German government (Schlesinger, 2010). The emission intensity for the electricity mix is calculated for the years 2008, 2020 and 2030. Table 2 shows the shares of the different primary energy sources for the years 2008, 2020 and 2030 and the emission intensities of those primary energy sources.

The emission intensity that result from the primary energy shares of the reference scenario of the German government after the 2002 AtG Novell is 547.6 g CO<sub>2</sub>/kWh for 2008, 520.6 g CO<sub>2</sub>/kWh for 2020 and 438.3 g CO<sub>2</sub>/kWh for 2030. The emission intensities are multiplied by the power that is after the 2010 AtG Novell produced by nuclear energy. This is 273.7 TWh in the period 2010-2015 which is multiplied by the 2008 emission intensity. The 1076.7 TWh produced in the period 2016-2025 are multiplied by the 2020 emission intensity and the 890.3 TWh produced in the period 2026-2036 are multiplied by the 2030 emission intensity. This results in 1100.6 Mt CO<sub>2</sub> that will be exhausted if the 2240.7 TWh would be produced by using the average emission intensity of the German electricity mix.

Subtracting the emissions resulting from nuclear energy from the ones resulting from the average energy mix, one ends up with the emission reduction that the life time extension of nuclear power plants caused in Germany. This is 1100.6 Mt CO<sub>2</sub> - 91.7 Mt CO<sub>2</sub> = 1008.9 Mt CO<sub>2</sub>.

An other interesting figure to look at is the percentage of emission that are causes by nuclear energy in relation to its total emission savings. 91.7 Mt CO<sub>2</sub> / 1100.6 Mt CO<sub>2</sub> = 0.09, hence 9% of the emissions that are not exhausted by other primary energy sources because they are replaced by nuclear energy are now exhausted by nuclear energy itself.

To calculate carbon leakage the emission increase in unconstrained countries is divided by the emission reduction in Germany:

$$L = 56.2 \text{ Mt CO}_2 / 1008.9 \text{ Mt CO}_2 = 0.056 \quad (2)$$

The carbon leakage ratio is often presented as a percentage. The carbon leakage for nuclear energy in Germany is 5.6%.

Primary energy sources	2008 [%]	2020 [%]	2030 [%]	Emission intensities [g CO <sub>2</sub> / kWh]
Nuclear	23.69	8.5	0	66
Hard coal	19.84	20.76	17.36	1100
Braun coal	23.98	25.08	15.01	950
Gas	13.81	6.98	16.01	600
Pumpreservoirs	0.99	1.3	1.59	15
other combustion materials	2.98	3.65	4.6	15
Hydro	3.23	4.34	4.93	10
Wind onshore	6.43	11.75	14.34	20
Wind offshore	0	4.49	9.43	20
Biomass	4.33	6.39	7.86	15
Photovoltaic	0.7	5.36	7.07	15
Geothermie	0	0.35	0.59	15
Other renewable combustion materials	0	1.07	1.22	15
Average emission intensity of the electricity mix [g CO <sub>2</sub> /kWh]	547.6	520.6	438.3	
Electricity produced by nuclear power [TWh] after 2010 AtG Novell	2010-2015 273.7	2016-2025 1076.66	2026-2036 890.3	

Table 2. Shares of different primary energy sources for the years 2008, 2020 and 2030 and their emission intensities for electricity production.

## 7. Discussion

The calculations are an estimate. Nuclear energy is substituted by the average energy mix. The average emission intensity of the German electricity mix is based on the reference scenario of the energy scenarios of the German government. The actual rate of carbon

leakage depends on the emission intensity of the primary energy source that really is replaced by nuclear energy. A replacement of coal could lead to less carbon leakage than a replacement of low carbon primary energy source. The reference scenario assumes that the policies that were in place at the time the study was conducted (August 2010), would continue. The reduction goals of the German government cannot be met with such a slow decrease in emission intensity of the energy mix. The study about the energy scenarios was conducted to develop an energy concept that can meet the reduction goals. The 2010 AtG Novell is part of this new energy concept.

For countries with large total emissions the emissions offset in through uranium milling and mining of exported uranium do not present a large share of the total emission. In countries with less total emissions countries like Niger for example this situation looks different. Niger's annual emissions are about 870 times less than the German emissions and 6500 times less than the emissions of countries like USA and China. 2009 Niger exported 485 t of natural uranium to Germany. 55.85 kWh of electricity can be produced with one g natural uranium. With a front end emission intensity of 25.1 g CO<sub>2</sub>/kWh the mining and milling of 485 t uranium result in 642,000 t CO<sub>2</sub>. Niger's total emissions in 2007 were 909,000 t (Google public data from World Bank). This data suggests that 70 % of Niger's emission were produced only from uranium produced for German use.

This is an unrealistically high number. If we assume that the front end emission intensity of 25.1 g CO<sub>2</sub>/kWh is not significantly over estimated other reasons for this high share have to be found. It is for example probable that the CO<sub>2</sub> balance of Niger is incomplete and does not include all emissions from Uranium mining.

Considering that Niger also exports to other countries, CO<sub>2</sub> emission from uranium exports seem to represent a significant share of Niger's total emissions.

## 8. Conclusion

The amount of carbon leakage from nuclear energy is not big but carbon leakage does exist. Compared to empirical studies on energy-intensive products which have often found no evidence of carbon leakage yet this is a significant finding. Besides the CO<sub>2</sub> emissions offset outside of Germany there are also other risks and environmental contaminations related to the front end of the nuclear fuel cycle. The supply security of uranium which is an often mentioned plus of nuclear energy compared to fossil fuels is eroding as shown in section 5.

The more obvious downsides of nuclear energy use like safety of operation and storage of waste material are in the centre of the public discussion. The downsides presented in this chapter have not been in the centre of attention yet. An increased awareness for those topics might increase the data availability and transparency. Focusing on climate goals without evaluating the impacts that the execution of these goals bring along is not a responsible or sustainable move and might lead to further problems as described in this chapter. In regard of all the downsides causes by uranium mining compensation should be offered by Germany to the uranium exporting countries.

## 9. Acknowledgment

We would like to thank the German Foundation for Peace Research as well as the KlimaCampus and Clisap for partly funding this project.



## 10. References

- Atomgesetz Novelle (2002). Gesetz zur geordneten Beendigung der Kernenergienutzung zur gewerblichen Erzeugung von Elektrizität, 22. April 2002, Available from: <[http://www.bgbl.de/Xaver/start.xav?startbk=Bundesanzeiger\\_BGBI](http://www.bgbl.de/Xaver/start.xav?startbk=Bundesanzeiger_BGBI)>
- Atomgesetz Novelle (2010). Elftes Gesetz zur Änderung des Atomgesetzes, 8. December 2010, Available from: <[http://www.bgbl.de/Xaver/start.xav?startbk=Bundesanzeiger\\_BGBI](http://www.bgbl.de/Xaver/start.xav?startbk=Bundesanzeiger_BGBI)>
- Babiker, M.H. (2005). Climate change policy, market structure and carbon leakage. *Journal of International Economics*, 65:421-445
- Bundesumweltministerium. Stand: March 2009 Available from: <[www.bmu.de](http://www.bmu.de)>
- Carbon Dioxide Information Analysis Center, March 2011, Available from: <<http://cdiac.ornl.gov/trends/emis/nig.html>>
- Demailly, D. & Quirion, P. (2002). European Emission Trading Scheme and competitiveness: A case study on the iron and steel industry. *Energy Economics*, 30:2009-2027
- Di Maria, C. & van der Werf, E. (2008). Carbon leakage revisited: unilateral climate policy with directed technical change. *Environ Resource Econ*, 39:55-74
- Dumberry, P. (2007). *State succession to international responsibility*, Martinus Nijhoff Publishers Leiden Boston, ISBN 978 90 04 15882 5, Netherlands
- European Comission, McKinsey & Ecofys (2006). *EU-ETS Review; Report on International Competitiveness*
- German Atomforum. January 2011, Available from: <[http://www.kernenergie.de/kernenergie/Themen/Kernkraftwerke/Kernkraftwerke\\_in\\_Deutschland/](http://www.kernenergie.de/kernenergie/Themen/Kernkraftwerke/Kernkraftwerke_in_Deutschland/)>
- Gielen, D. & Moriguchi, Y. (2002). CO2 in the iron and steel industry: an analysis of Japanese emission reduction potentials. *Energy Policy*, 30: 849-863
- Golombek, R. & Hoel, M. (2004). Unilateral Emission Reductions and Cross-Country Technology Spillovers. *Advances in Economic Analysis & Policy*, Volume 4, Issue 2, Article 3
- Google public data from World Bank. May 2011, Available under: <[http://www.google.com/publicdata/explore?ds=d5bncppjof8f9\\_&ctype=l&strail=false&nسلم=h&met\\_y=en\\_atm\\_co2e\\_kt&hl=de&dl=de#ctype=l&strail=false&nسلم=h&met\\_y=en\\_atm\\_co2e\\_kt&scale\\_y=lin&ind\\_y=false&rdim=country&idim=country:NER&hl=de&dl=de](http://www.google.com/publicdata/explore?ds=d5bncppjof8f9_&ctype=l&strail=false&nسلم=h&met_y=en_atm_co2e_kt&hl=de&dl=de#ctype=l&strail=false&nسلم=h&met_y=en_atm_co2e_kt&scale_y=lin&ind_y=false&rdim=country&idim=country:NER&hl=de&dl=de)>
- Gerlagh, R. & Kuik, O. (2007). *Carbon leakage with international technology spillovers. Workingpaper, 2007*
- Intergovernmental Panel on Climate Change IPCC (2007). *Fourth Assessment Report, Working Group III: Mitigation of Climate Change*
- IPPNW (2010). *Die Versorgung Deutschlands mit Uran, deutsche Sektion der Internationalen Ärzte für die Verhütung des Atomkrieges (IPPNW) Ärzte in sozialer Verantwortung e.V. 21.07.2010*
- Kalinowski, M. (2010). *Life-threatening risks from uranium mining, ZNF Occasional Paper No. 11*
- Reinaud, J. (2008). *Issues behind Competitiveness and Carbon Leakage Focus on Heavy Industry. IEA, 2008*

- Schlesinger, M. et al. (2010). Studie Energieszenarien für ein Energiekonzept der Bundesregierung, Projekt Nr. 12/10 es Bundesministeriums für Wirtschaft und Technologie, August 2010
- South Virginia Against Uranium Mining: How does mining affect people (2008), March 2010, Available from: <<http://sccagainsturanium.blogspot.com/2009/02/how-does-mining-affect-people.html>>
- Sovacool, B. K. (2008). Valuing the greenhouse gas emissions from nuclear power: A critical survey. *Energy Policy*, Vol. 36, (April 2008), pp. (2940-2953)
- United Nations Framework Convention on Climate Change UNFCCC (2010). Available from:<<http://unfccc.int/2860.php>>

# Effects of the Operating Nuclear Power Plant on Marine Ecology and Environment - A Case Study of Daya Bay in China

You-Shao Wang<sup>1,2</sup>

<sup>1</sup>Key Laboratory of Tropical Marine Environmental Dynamics, South China Sea Institute of Oceanology, Chinese Academy of Sciences,

<sup>2</sup>Marine Biology Research Station at Daya Bay, Chinese Academy of Sciences, China

## 1. Introduction

Bays and estuaries are known to be biologically productive and strongly influenced by human activities (Burger, 2003; Sohma et al., 2001; Tagliani et al., 2003; Zhao, 2005). Coastal bays is the region of strong land-ocean interaction, and their ecological functions are more complicated and vulnerable to the influence by human activities and land-source pollution than the open ocean (Bodergat et al., 2003; Hansom 2001; Huang et al., 2003; Yung et al., 2001). With the increase of population and rapid economic development, littoral areas are facing many ecological problems. Eutrophication and environmental pollution obviously occurred in many coastal sea areas, especially in estuaries and coastal bays (Cloern, 1996; Turner and Rabalais, 1994; Yin et al., 2001). These have directly resulted in the ecological unbalance, the decrease of biodiversity and the rapid reduction of biological resources in estuaries and coastal bays. Coastal ecosystems and the study of marine biological resources and ecological environment have attracted worldwide attention (Buzzelli, 1998; Fisher, 1991; Huang et al., 1989, 2003; Sohma et al., 2001, Souter and Linden, 2000; Zhang et al., 2001; Yung et al, 2001). Many international programs and projects have been launched to address the problems confronting the world's coastal ecosystems and biological resources (Yanez-Arancibia et al., 1999; Huang et al., 2003).

Tang et al (2003) applied AVHRR data to the study of thermal plume from power plant at Daya Bay. Satellite remote sensing can provide information on the distribution and seasonal variation of thermal plumes from nuclear power plants that discharge cooling waters to the coastal zone. Variation of phytoplankton biomass and primary production in the western part of Daya Bay during spring and summer has been reported (Song et al., 2004). Wang et al (2006) used multivariate statistical analysis to reveal the relation between water quality and phytoplankton characteristics in Daya Bay, China, from 1999 to 2002. Wu and Wang (2007) used chemometrics to evaluate anthropogenic effects in Daya Bay and found that increases in human activities alter the balance of nutrients in Chinese coastal waters, and that the human activities were the main factor to impact the ecological environment in Daya Bay.

Data collected from 12 marine monitoring stations in Daya Bay from 1982 to 2004 reveal a substantial change in the ecological environment of this region (Wang et al., 2006, 2008, 2011). The average N/P ratio increased from 1.377 in 1985 to 49.09 in 2004. Algal species

changed from 159 species of 46 genera in 1982 to 126 species of 44 genera in 2004, and the nutrients and phytoplankton are good environmental indicators which can rapidly reflect the changing water quality in Daya Bay (Wang et al., 2006). Major zooplankton species went from 46 species in 1983 to 36 species in 2004. The annual mean biomass of benthic animals was recorded at 123.10 g m<sup>2</sup> in 1982 and 126.68 g m<sup>2</sup> in 2004. Mean biomass and species of benthic animals near nuclear power plants ranged from 317.9 g m<sup>2</sup> in 1991 to 45.24 g m<sup>2</sup> in 2004 and from 250 species in 1991 to 177 species in 2004 (Wang et al., 2008). The waste warm water from nuclear power plants was the main factor influencing the ecology and environment in western areas of Daya Bay, especially for benthos near the Nuclear Power Plants in Daya Bay (Wang et al., 2011). Daya Bay is a multi-type ecosystem mainly driven by human activities (Wang et al., 2008).

As a case study of Daya Bay in China in this chapter, it is summarized long-term changes of Daya Bay and analyzed to effect of the operating Nuclear Power Plant on marine ecology & environment according to the monitoring and research data in Daya Bay obtained during 1982-2004 in China (Wang et al., 2006, 2008, 2011).

## 2. Research area, materials and methods

China is a large coastal nation located along the western Pacific Ocean with 18000 km of mainland coastline, along which there are many large and important bays (Fig.1). Daya Bay is a semi-enclosed bay. It is one of large and important gulfs along the southern coast of China. Daya Bay is located at 113°29'42"-114°49'42"E and 23°31'12"-24°50'00"N (Fig.1). It covers an area of 600 km<sup>2</sup> with a width of about 15 km and a north-south length of about 30 km, and about 60% of the area in the Bay is less than 10 m deep (Xu, 1989; Wang et al., 2006, 2008, 2011). Dapeng Cove (the investigated station 3 is in it), in the southwest portion of Daya Bay, is about 4.5 km (N-S) by 5 km (E-W). Located in a subtropical region, Daya Bay's annual mean air temperature is 22°C. The coldest months are January and February, with a monthly mean air temperature of 15°C, and the hottest months are July and August, with a monthly mean air temperature of 28°C. The minimum sea surface temperature occurs in winter (15°C) and the maxima in summer and fall (30°C) (Xu, 1989; Wang et al., 2006, 2008, 2011). No major rivers discharge into Daya Bay, and most of its water originates from the South China Sea. There are three small rivers (Nanchong River, Longqi River and Pengcheng River) that discharge into Dapeng Cove. The Pearl River is to west of Daya Bay which has a diverse subtropical habitats including coral reefs, mangroves, rocky and sandy shores, mudflats, etc. (Wang et al., 2008). The coral reefs and mangroves have special resource values and ecological benefits and are very important to the sustainable social and economical development in these subtropical coastal areas. Coral reefs and mangrove areas have important relationships to the regulation and optimization of the subtropical marine environments and have become the subject of much international attention in recent years (Mumby et al., 2004; Pearson, 2005).

Relatively few residents and industries along the cost of Daya Bay before 1980s, and there are about 239400 inhabitants living along the coast of Daya Bay at present (Fig.2). The population has nearly doubled during 1986-2002. Many factories had been built. The total industrial output value of the main towns along Daya Bay coast increased from 3.804 billion yuans of 1993 to 29.64 billion yuans of 2001(Wang et al., 2008). The total industrial output value of the main towns along the Daya Bay coast had increased 7.8 times between 1993 and 2001 (Fig.3). The Daya Bay Nuclear Power Plant (DNPP) (Fig.4) was the first nuclear power

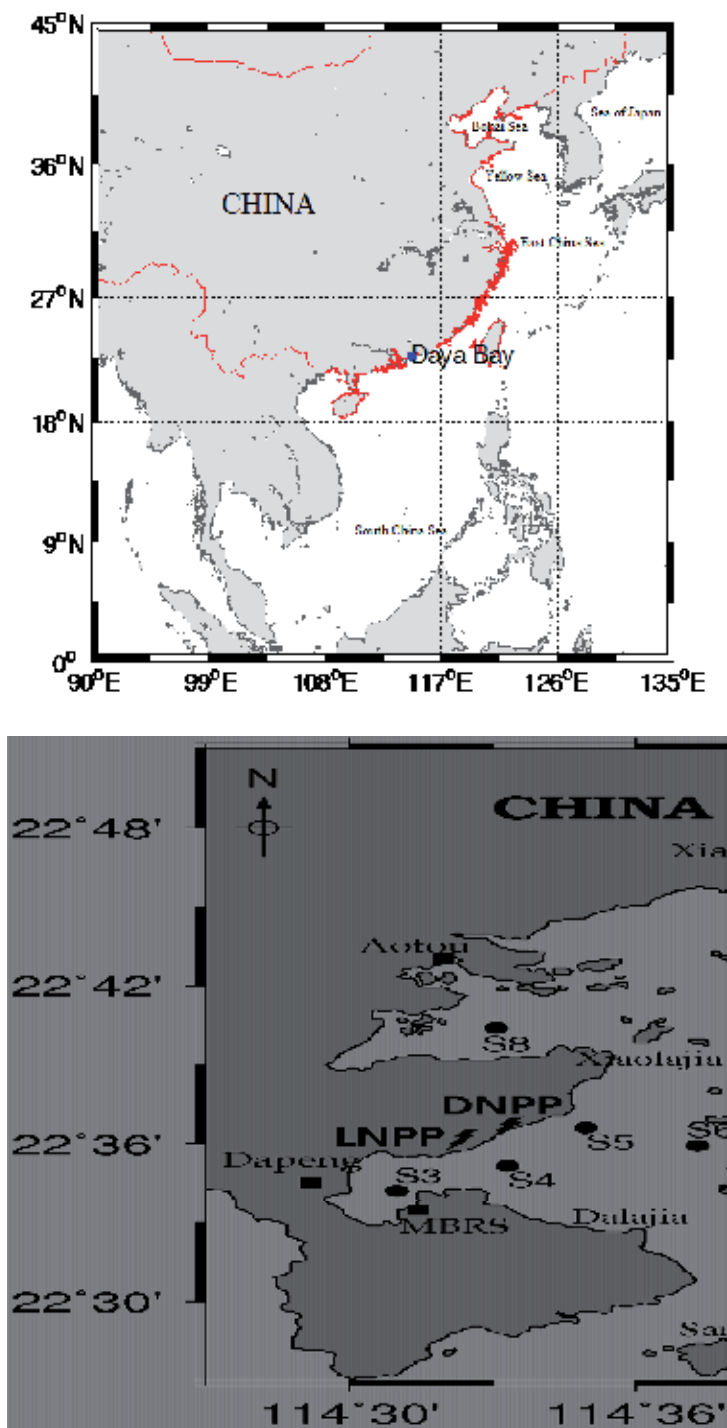


Fig. 1. Map for Daya Bay and its Locations of the 12 monitoring stations (Wang et al., 2006, 2008, 2011).

plant and the largest foreign investment joint project in China since 1982 and marked the first step taken by China in the development of large-capacity commercial nuclear power units (Zang, 1993). The sea water from the Daya Bay Nuclear Power Plant is discharged in about  $95 \text{ m}^3 \text{ second}^{-1}$  at  $65^\circ\text{C}$  since 1993, and the warm water is put into the south area of Daya Bay (Fig.4).

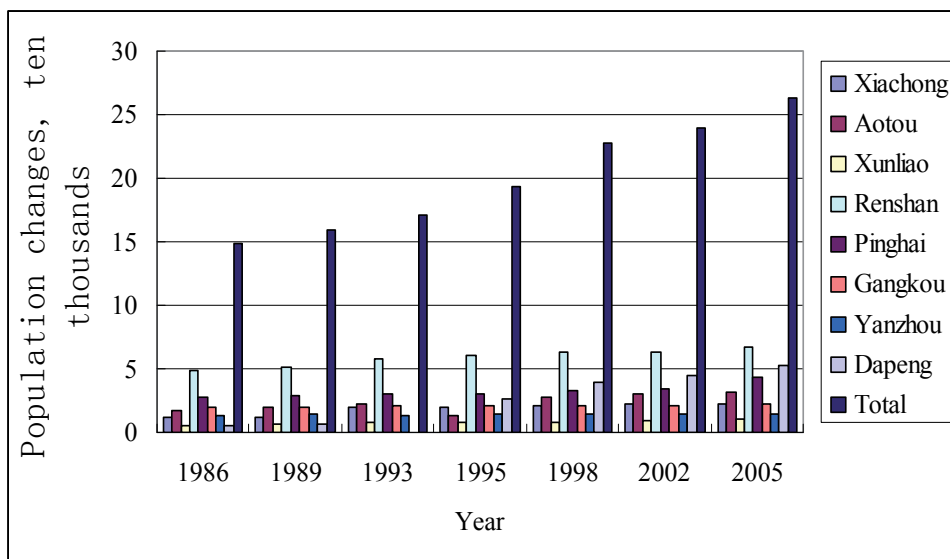


Fig. 2. Population changes of the main towns along the Daya Bay coast (unit: ten thousands).

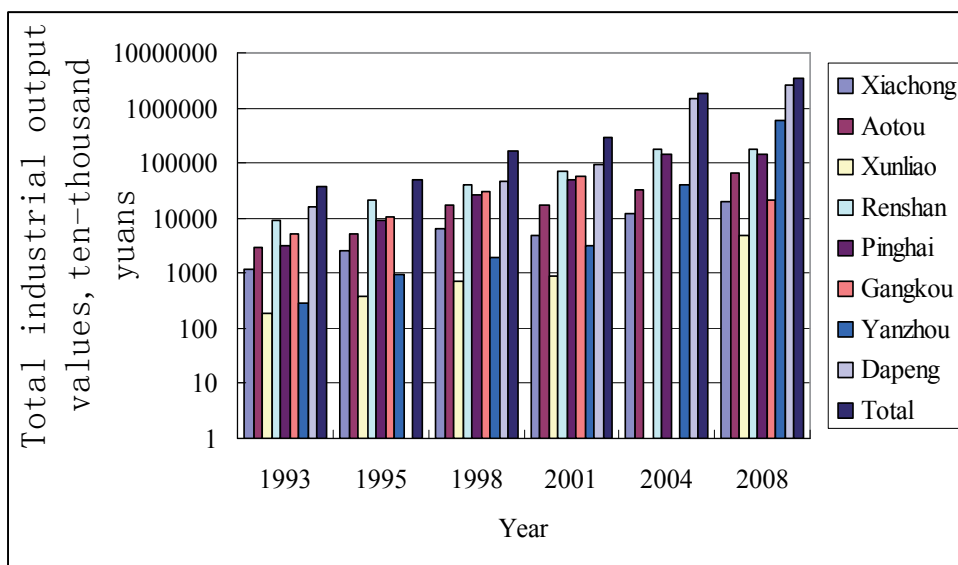


Fig. 3. Total industrial output values of the main towns along the Daya Bay coast in different year (unit: ten thousands yuans).



(1) Lingao phase I (From <http://www.google.com.hk/>)



(2) Lingao phase II (From <http://www.google.com.hk/>)

A: Lingao Nuclear Power Plant in China



B: Daya Bay Nuclear Power Plant in China (From <http://www.google.com.hk/>)



(1) Qinshan phase I (From <http://www.google.com.hk/>)





(2) Qinshan phase II (From <http://www.heneng.net.cn/>)



(3) Qinshan phase III (from <http://www.heneng.net.cn/>)

C: Qinshan Nuclear Power Plant from the first to the third investment in China



D: Tianwan Nuclear Power Plant in China (From <http://www.heneng.net.cn/>)



(1) Chinshan nuclear power plant (From <http://www.power-technology.com/>)



(2) Kuosheng nuclear power plant (From <http://www.aesieap0910.org/>)



(3) Maanshan nuclear power plant (From <http://commons.wikimedia.org/>)

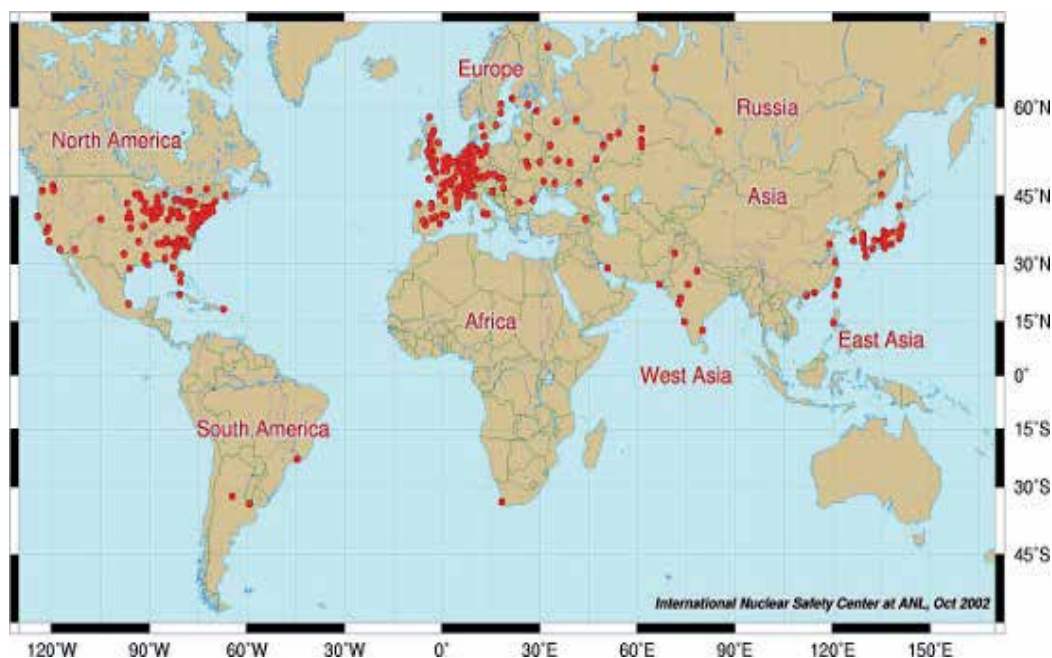




(4) Lungmen nuclear power plant (From [http:// commons.wikimedia.org/](http://commons.wikimedia.org/))  
E: Nuclear Power Plants in Taiwan of China



F: Distribution of the Nuclear Power Plants in China



G: Distribution of the Nuclear Power Plants in the world  
(From <http://www.taizhou.com.cn/>)

Fig. 4. Different Nuclear Power Plants for opening in China.

Another Nuclear Power Plant—Lingao Nuclear Power Plant (LNPP) near the Daya Bay Nuclear Power Plant has also run since 2002. These changes can also impacting on the ecological environment of Daya Bay (Zheng et al., 2001; Bodergat et al., 2003; Wu & Wang, 2007; Wang et al., 2006, 2008, 2011) (Fig.5).

The variety of ecological and environmental factors in Daya Bay has been carried out since 1982, including 12 stations with four voyages per year. All stations were occupied between 113°29'42"-114°49'42"E and 23°31'12"-24°50'00"N. The main marine monitoring investigation included the ecological environment, the ecological function of marine biological resources and the community organization etc in Daya Bay. Temperature and salinity of water were measured in the field using CTD probes. Sea-water samples for analysis of nutrients, dissolved oxygen, pH, chemical oxygen demand, chlorophyll *a* was taken using 5-L GO FLO bottles at surface and bottom layers, and other samples were collected according to the methods and sampling tools of "The specialties for oceanography survey" (GB12763-91, China). All sample analysis was carried out at National Field Station of Marine Ecosystem Research and Observation at Daya Bay, Shenzhen, China and at South China Sea Institute of Oceanology, Chinese Academy of Sciences. Analytical methods for the various physical-chemical and biological parameters are applied according to Wang et al (2006, 2008, 2011).

All these samples were collected during one day at the beginning of the first month of each season (spring-summer-fall-winter). The samples (except phytoplankton, zooplankton, benthos and fish) included those taken at the surface and the bottom, and the data for this paper are given as mean values between the surface and bottom.



Fig. 5. Daya Bay and its surrounding environments.

### 3. Statistical analysis

All statistical analysis methods were used according to Johnson & Wichern (1998). Kendall's tau-b values were used to measure the degree of association among various variables with bivariate statistical analysis. Bivariate correlations between the biomass of phytoplankton and benthos and major physical and nutrient factors were calculated for all stations. Flexible-Beta cluster analysis was used between groups transforming the measures with Flexible-Beta Distance. Factor analysis techniques were used to investigate the various factors that are present in each of the three clusters identified by cluster analysis (using PROC X16 of the SAS system) (Wang et al., 2006, 2011). All statistical analysis programs are part of the Statistical Analysis System (SAS 9.0) software package (SAS Institute Incorporation).

### 4. Results and discussion

#### 4.1 Long-term changes of Daya Bay

Spatial distribution of water temperature showed high values in the western near the nuclear power stations and low values in the mouth of Daya Bay all the years. Stratification due to temperature and salinity differences between surface and bottom waters inside the bay start to develop in June, become strongest from July to September, and disappear in November; temperature and salinity were uniformly distributed with depth from November to May in the following year (Xu, 1989; Wang et al., 2006, 2008, 2011). Changes of temperature and salinity in Daya Bay varying by seasons are shown in Fig. 6 and 7. Annual mean value of temperature was 24.04°C based on the data measured from 1982 to 2004, the highest surface and bottom water temperatures occurred in August and the lowest values were in January (Wang et al., 2006, 2008, 2011).

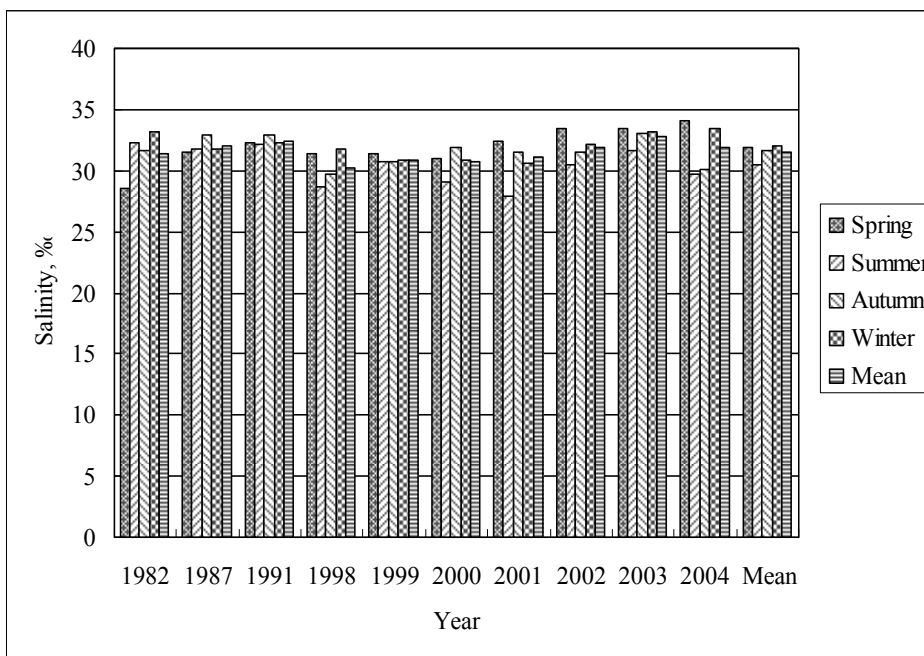


Fig. 6. Salinity of Daya Bay with different seasons from 1982 to 2004 (Wang et al., 2008) (Unit:‰).

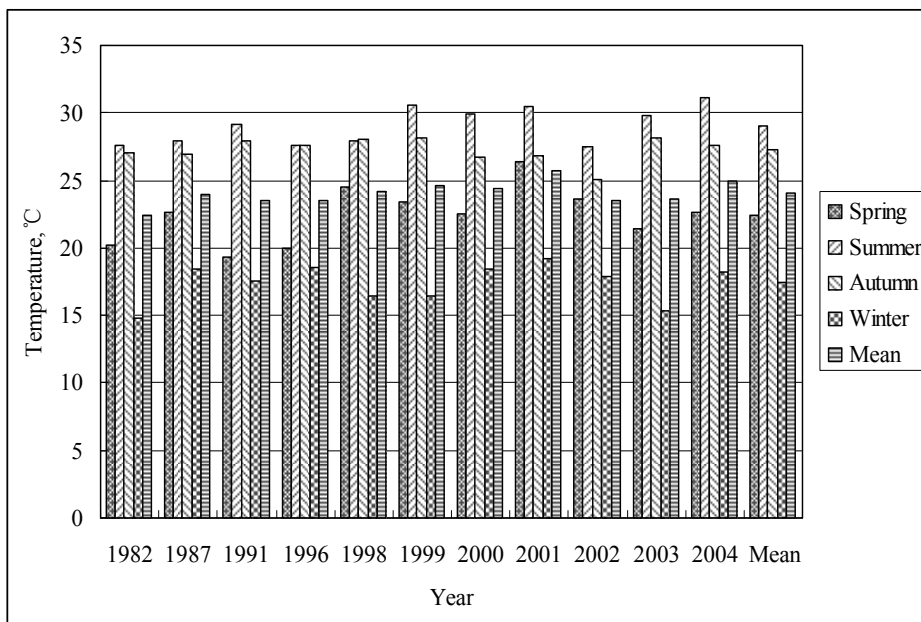


Fig. 7. Temperature of Daya Bay with different seasons from 1982 to 2004 (Wang et al., 2008) (Unit:°C).



Cold-water upwelling influenced the distribution of nutrients and temperature, fluctuates in Daya Bay. The vertical and seasonal variations and distribution of water temperature suggest that the bay is affected by the East Guangdong upwelling and a thermocline occurring during June-August (Han, 1991; Wang et al., 2006, 2008, 2011). During this time, the thermocline temperature gradient averaged  $0.5-1^{\circ}\text{C m}^{-1}$ . The depths of the thermocline are  $\sim 6-10$  m with a thickness of  $\sim 2-4$  m in Daya Bay (Wang et al., 2006, 2008, 2011). The thermocline disappeared from November to the following May due to the mixing of the seawater.

The seasonal variation of temperature of Daya Bay from 1982 to 2004 is shown in Fig.7. Annual mean temperatures were increasing from 1982 to 2004, probably due to Global Change. Climate change scenarios for the year 2100 indicates a significant increase in air temperature (by  $2.3-4.5^{\circ}\text{C}$ ) which is major factor influencing the environment of the Gulf (Kont et al., 2003). The temperature of western Daya Bay near the Nuclear Power Plants was higher than those in the other sea area in Daya Bay, by about  $1^{\circ}\text{C}$ , mainly due to waste warm water discharged to the south area of Daya Bay from the Nuclear Power Plants (Fig.8) which directly impact on the ecological environment of Daya Bay (Wang et al., 2006, 2008, 2011; Zheng et al., 2001). Assuming the temperature of the waste water from the nuclear power plant to be  $1^{\circ}\text{C}$  warmer than the surrounding seawater, then the area of Daya Bay affected by this warmer water was about  $5.51\text{ km}^2$  (Han, 1991; Wang et al., 2006).

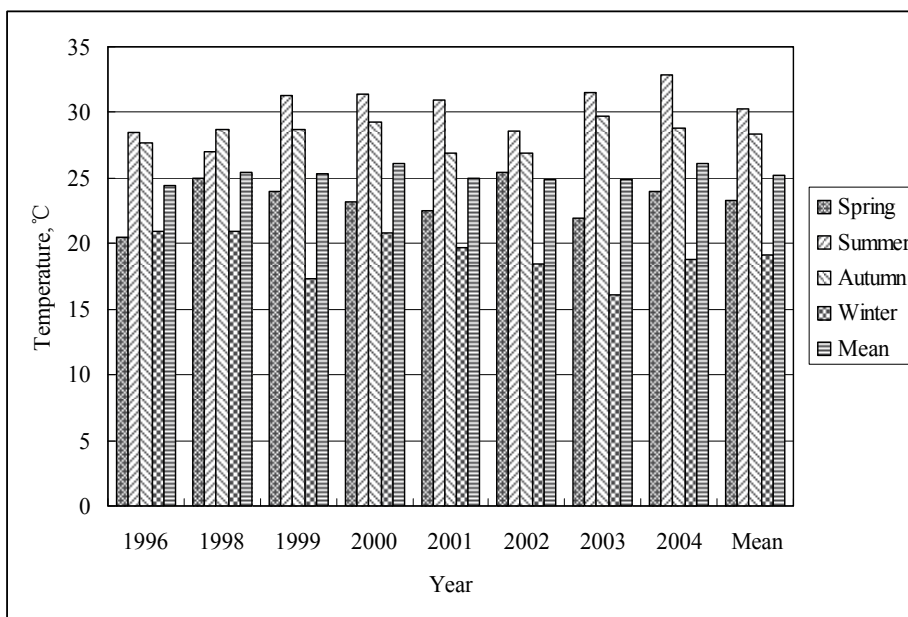


Fig. 8. Temperature of western Daya Bay with different seasons from 1996 to 2004 (Wang et al., 2008) (Unit:  $^{\circ}\text{C}$ ).

Spatial distribution of dissolved oxygen (DO) in Daya Bay was as uniform as temperature, seasonal variations were evident from 1982 to 2004 (Fig.9). Distributions of dissolved oxygen in spring and winter were higher than in summer and autumn. The highest dissolved oxygen content occurred in winter and the lowest in summer. There was a decreased from  $7.29\text{ mg l}^{-1}$  to  $7.03\text{ mg l}^{-1}$  of the dissolved oxygen from 1991 to 2002, probably due to the progressive increases in sea surface temperature increasing of Daya Bay (Fig.7). Although the results



indicate there was a small decreasing trend in the dissolved oxygen (DO), the seawater of Daya Bay was also within the First Class of National Seawater Quality Standards for China ( $>6.00 \text{ mg l}^{-1}$ , GB3097-1997) (Wang et al., 2003, Wang et al., 2006, 2008, 2011). Annual mean pH variation was at 8.15 to 8.25 from 1982 to 2004, with a little change in Daya Bay (Fig.10). The results also indicated that ocean acidification is very clear in Daya Bay (Kerr, 2010).

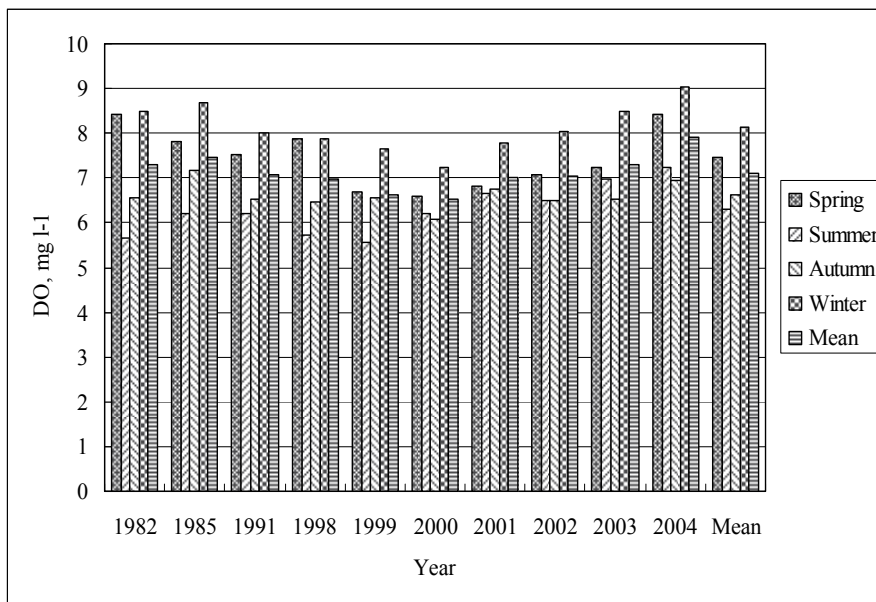


Fig. 9. Dissolved oxygen of Daya Bay from 1982 to 2004 (Wang et al., 2008) (Unit:  $\text{mg l}^{-1}$ ).

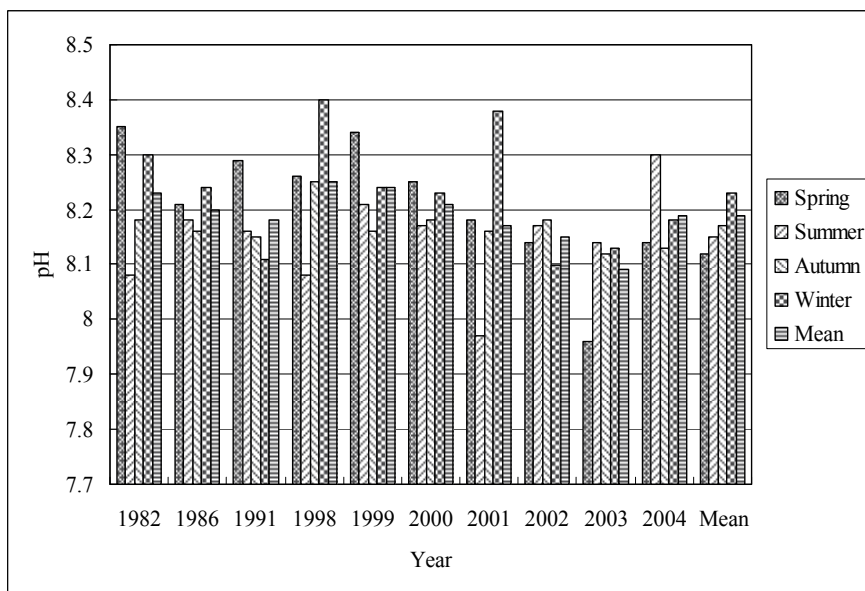


Fig. 10. pH of Daya Bay with different seasons from 1982 to 2004 (Wang et al., 2008).

The chemical oxygen demand (COD) values were 0.63-1.18 mg l<sup>-1</sup> in Daya Bay from 1989 to 2004 (Fig.11, Wang et al., 2008). The mean chemical oxygen demand values were lower than the other sea areas in China, such as the COD is between 2.90 mg dm<sup>-3</sup> and 7.50 mg dm<sup>-3</sup> in the Pearl River Estuary (Lin & Li, 2003) and from 3.32 mg l<sup>-1</sup> to 4.01 mg l<sup>-1</sup> in Rongcheng Bay in temperate zone (Mu et al., 1999). The chemical oxygen demand values also indicated that the organic pollution in Daya Bay was much lower than the other sea areas in China. The results of chemical oxygen demand in Daya Bay show that the sea water was also within the First Class of National Seawater Quality Standards for China ( $\leq 2.00$  mg l<sup>-1</sup>, GB3097-1997) (Wang et al., 2003; Wang et al., 2006, 2008, 2011).

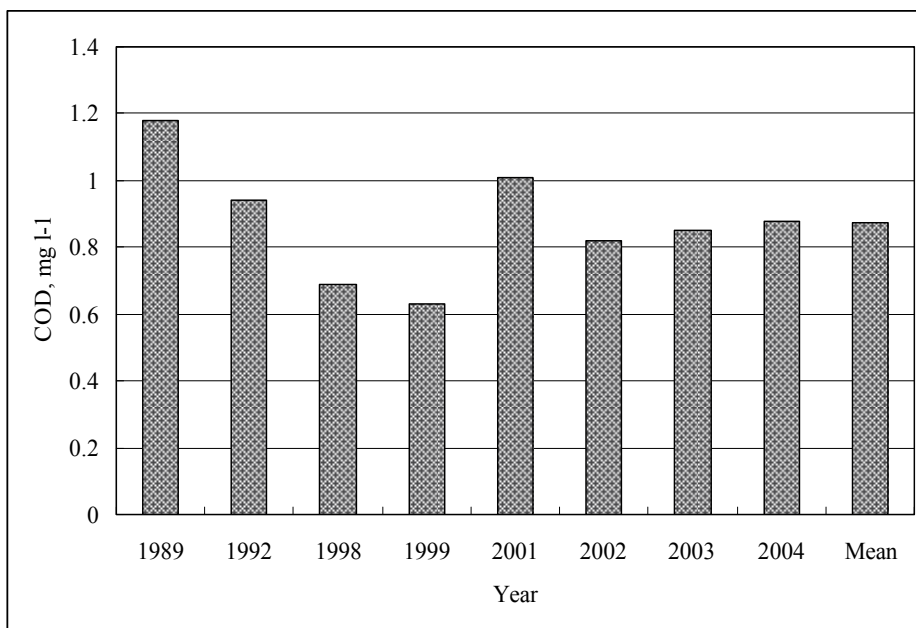


Fig. 11. Chemical oxygen demand of Daya Bay from 1989 to 2004 (Wang et al., 2008) (Unit: mg l<sup>-1</sup>).

Inorganic N and P levels were low from 1.53  $\mu\text{mol l}^{-1}$  to 5.40  $\mu\text{mol l}^{-1}$  and from 0.0945  $\mu\text{mol l}^{-1}$  to 1.12  $\mu\text{mol l}^{-1}$ , and mean values were 3.68  $\mu\text{mol l}^{-1}$  and 0.266  $\mu\text{mol l}^{-1}$  from 1985 to 2004 within the National First Class Water Quality Standards for China (Wang et al., 2003; Wang et al., 2008) (Table1). These results are similar to the inorganic N and P levels of Mirss Bay in Hong Kong (Yin et al., 2003). NH<sub>4</sub>-N (about 49%) and NO<sub>3</sub>-N (about 43%) were the dominant total inorganic nitrogen (TIN) form, which account for about 90% of the TIN and 8% of NO<sub>2</sub>-N in recent years. The NO<sub>3</sub>-N content was lower than the NH<sub>4</sub>-N, revealing a thermodynamic imbalance between NH<sub>4</sub>-N, NO<sub>2</sub>-N and NO<sub>3</sub>-N. Biological activity might be also the main factor influencing the balance (Huang et al., 2003; Wang et al., 2008), but there were different degrees of transformation of NH<sub>4</sub>-N for the different bay regions. The concentration of both N and Si were higher than inorganic P. Spatially the nutrients N increases from 1985 to 2004 in Daya Bay, probably as results of the waste water of the people lived along the coast, the land sources (such as Nanchong River, Longqi River and Pengcheng River discharge into Dapeng Cove and unclear power plants waste water

discharge into the south area of Daya Bay), seawater breed aquatics and the effect of the water from the Preal River on Daya Bay (Han, 1991). The nutrient P decreased from 1.12  $\mu\text{mol l}^{-1}$  to 0.110  $\mu\text{mol l}^{-1}$  at 1985-2004 in Daya Bay, probably as a result of the fan-used detergency powder contain-P in recent years. The average ratio of TIN/P increased from 1.377 in 1985 to 49.09 in 2004, and the highest value was 61.90 in 2003. The average ratio of Si/P increased from 35.27 to 285.82 at 1985-2004 (Wang et al., 2008). The limiting nutrients in Daya Bay has changed from N to P from 1985 to 2004 (Justice et al., 1995), and is different from those at Jiaozhou Bay which shifted from N and/or P to Si from the 1960s to the 1990s in temperate zone (Shen, 2001) and Sanya Bay which shifted from N in summer and autumn to P in winter in Sanya Bay from 1998 to 2000 in tropic zone (Huang et al., 2003).

Year	$\text{NH}_4^+$	$\text{NO}_2^-$	$\text{NO}_3^-$	TIN	$\text{SiO}_3^{2-}$	$\text{PO}_4^{3-}$	TIN/P	Si/P
1985	0.698	0.230	0.602	1.53	39.50	1.12	1.377	35.27
1989	0.607	1.10	1.52	3.23	10.85	0.377	8.560	28.78
1991	1.10	0.230	0.798	2.13	20.66	0.358	5.950	57.71
1997	1.38	0.150	2.55	4.08	14.57	0.122	33.44	119.43
1998	1.86	0.0554	0.433	2.35	5.125	0.0405	57.99	126.54
1999	1.99	0.389	2.46	4.84	9.810	0.118	40.02	76.46
2000	1.59	0.508	1.92	4.01	27.54	0.252	15.91	109.29
2001	2.28	0.134	1.93	4.33	23.21	0.229	18.91	101.35
2002	1.32	0.446	0.680	2.40	27.01	0.0945	25.40	285.82
2003	2.54	0.260	3.39	6.19	23.06	0.100	61.90	230.60
2004	3.06	0.085	2.25	5.40	12.82	0.110	49.09	116.54
Mean	1.68	0.326	1.68	3.68	19.47	0.266	28.96	117.07

\*Quality Standards of Seawater from GB3097-1997, TIN: China first class ( $\mu\text{mol l}^{-1}$ )  $\leq 14.28$ , second class ( $\mu\text{mol l}^{-1}$ )  $\leq 21.43$ ;  $\text{PO}_4\text{-P}$ : China first class ( $\mu\text{mol l}^{-1}$ )  $\leq 0.4839$ , second class ( $\mu\text{mol l}^{-1}$ )  $\leq 0.9677$ .

Table 1. Concentrations of different forms N,  $\text{SiO}_3\text{-Si}$  and  $\text{PO}_4\text{-P}$  in Daya Bay at 1985-2004 (Wang et al., 2008) (Unit:  $\mu\text{mol l}^{-1}$ ).

Phylum	1982	1983	1985	1987	1990	1994	1998	2002	2003	2004
Bacillariophyta	37/134	38/120	38/127	41/137	37/140	25/78	24/72	25/96	31/92	34/100
Pyrophyta	9/25	9/32	8/30	8/27	17/61	10/30	5/8	9/27	12/30	8/23
Cyanophyta	0	1/3	1/3	2/4	2/5	1/2	0	2/4	2/3	2/3
Total (Genera / Species)	46/159	48/155	49/160	51/168	56/206	36/110	29/80	36/127	46/125	44/126

Table 2. Species, genera of the phytoplankton of Daya Bay from 1982 to 2004 (Wang et al., 2008).

About 300 species of phytoplankton have been identified in Daya Bay since 1982 (Xu, 1989; Wang et al., 2008). They belong to *Cyanophyta*, *Bacillariophyta*, *Pyrophyta*, *Chrysophyta* and *Xanthophyta* etc. Most of them are diatoms (about 70%) and chaetocero (about 20%). Of the 183 species of diatoms, chaetoceros had many more species than other genera (45 spp), followed by *Rhizosolenia* (23 spp) and *Coscinodiscus* (22 spp) (Yang, 1990; Wang et al., 2008).

The main dominant species of Daya Bay are *Chaetoceros*, *Nitzschia*, *Rhizosolenia*, *Leptocylindrus* and *Skeletonema*, such as *Chaetoceros affinis*, *Chaetoceros compressus*, *Chaetoceros lorenzianus*, *Ch. Curvisetus*, *Ch. Pseudocurvisetus*, *Rhiz. alata f.grecillisma*, *Nitzschia delicatissima*, *Leptocylindrus danicua*, *Skeletonema costatum* and *Thalassionema nitzschioides*, the chaetocero is *Ceratium* sp. as the dominant species. The phytoplankton species have been gradually decreasing since 1990s as compared to those during 1980s (Table 2). In particular, there was only 80 species in 1998. The phytoplankton cell density has been also gradually decreasing since 1998 compared with 1985. Annual mean values of the phytoplankton in Daya Bay were between  $8.88 \times 10^5$  and  $6.63 \times 10^7$  cells  $m^{-3}$  at 1985-2004. Phytoplankton abundance peaked in spring at  $1.03 \times 10^8$  cells  $m^{-3}$  in 1985 (Table 3) and was lowest in spring at  $7.30 \times 10^4$  cells  $m^{-3}$  (1/1411) in 1999. Although the mean annual abundances of phytoplankton show a slight decrease trend from 1999 to 2004, species and values of the phytoplankton of Daya Bay were increasing that might be due to high ratios of TIN to P and Si to P occurring in recent years (Sommer et al., 2002). Annual mean values of chlorophyll *a* were 1.83-3.78  $mg\ m^{-3}$  in different seasons from 1985 to 2004, the higher values were always found in autumn and summer. The nutrient structure has become more balanced for phytoplankton growth (Shen, 2001).

Season	Production	1985	1998	1999	2000	2001	2002	2003	2004
Spring	Chl <i>a</i> ( $mg\ m^{-3}$ )	2.06	1.46	2.00	0.979	1.49	0.830	5.88	1.94
	Phytoplankton (cells $m^{-3}$ )	$1.03 \times 10^8$	$2.16 \times 10^7$	$7.30 \times 10^4$	$5.27 \times 10^6$	$6.59 \times 10^5$	$1.71 \times 10^6$	$1.53 \times 10^5$	$3.43 \times 10^6$
	Zooplankton (ind $m^{-3}$ )	109.20	28.90	-	90.00	34.97	135.29	137.58	204.67
Summer	Chl <i>a</i> ( $mg\ m^{-3}$ )	2.36	1.44	3.44	4.07	1.32	6.09	1.91	3.93
	Phytoplankton (cells $m^{-3}$ )	$9.61 \times 10^7$	$7.59 \times 10^5$	$6.28 \times 10^5$	$5.25 \times 10^7$	$9.31 \times 10^5$	$1.87 \times 10^6$	$2.45 \times 10^6$	$1.66 \times 10^7$
	Zooplankton (ind $m^{-3}$ )	578.90	82.70	-	-	404.08	248.62	191.97	131.33
Autumn	Chl <i>a</i> ( $mg\ m^{-3}$ )	1.19	3.50	4.69	3.46	2.25	2.82	1.44	1.67
	Phytoplankton (cells $m^{-3}$ )	$1.53 \times 10^7$	$6.00 \times 10^6$	$1.02 \times 10^6$	$3.86 \times 10^5$	$5.63 \times 10^5$	$3.70 \times 10^5$	$1.99 \times 10^5$	$3.49 \times 10^5$
	Zooplankton (ind $m^{-3}$ )	523.90	43.65	-	-	131.11	258.80	58.41	581.15
Winter	Chl <i>a</i> ( $mg\ m^{-3}$ )	1.70	1.77	5.01	1.85	2.81	2.98	3.32	2.06
	Phytoplankton (cells $m^{-3}$ )	$3.77 \times 10^7$	$6.73 \times 10^6$	$1.83 \times 10^6$	$8.49 \times 10^4$	$2.74 \times 10^6$	$6.21 \times 10^5$	$2.24 \times 10^6$	$3.63 \times 10^6$
	Zooplankton (ind $m^{-3}$ )	189.30	66.41	94.72	-	204.16	455.54	309.32	619.05
Mean	Chl <i>a</i> ( $mg\ m^{-3}$ )	1.83	2.04	3.78	2.63	1.97	3.18	3.14	2.40
	Phytoplankton (cells $m^{-3}$ )	$6.30 \times 10^7$	$8.77 \times 10^6$	$8.88 \times 10^5$	$1.46 \times 10^7$	$1.22 \times 10^6$	$1.14 \times 10^6$	$1.60 \times 10^6$	$6.00 \times 10^6$
	Zooplankton (ind $m^{-3}$ )	352.70	55.42	94.72	90.00	193.58	283.56	174.32	384.05

Table 3. Seasonal production measurements in Daya Bay from 1985 to 2004 (Wang et al., 2008).

Seasonal changes of chlorophyll *a* near the nuclear power plant are shown in Fig.12 (Wang et al., 2008). Annual mean values of chlorophyll *a* near Nuclear Power Plant were 1.37-2.45  $mg\ m^{-3}$  before operation and 2.46-3.34  $mg\ m^{-3}$  after operation the first Nuclear Power Plant at 1991-1997. Seasonal changes of primary productivity near the nuclear power plant are very different between before operation and after operation the first Nuclear Power Plant at 1991-1997 (Fig.13). The waste warm water can give an increase for chlorophyll *a* and primary productivity near the nuclear power plants. The waste warm water can provide extra amount of energy for phytoplankton growth (Wang et al., 2006).

265 species of zooplankton sampled from Daya Bay have been studied since 1982 (Wang et al., 2008). They can be divided into four ecological forms: estuary and inner bay type, warm coastal type and warm open sea type (Lian et al., 1990). The latter two types account for most of the species. Variations of dominant species exhibited a seasonal succession. The abundance of zooplankton varied seasonally, the maximum number of individuals occurred in autumn. Although main species of the zooplankton in Daya Bay had a decreasing trend from 46 of 60 familiar species in 1983 to 36 of 60 familiar species in 2004 (Fig.14), the annual mean individual

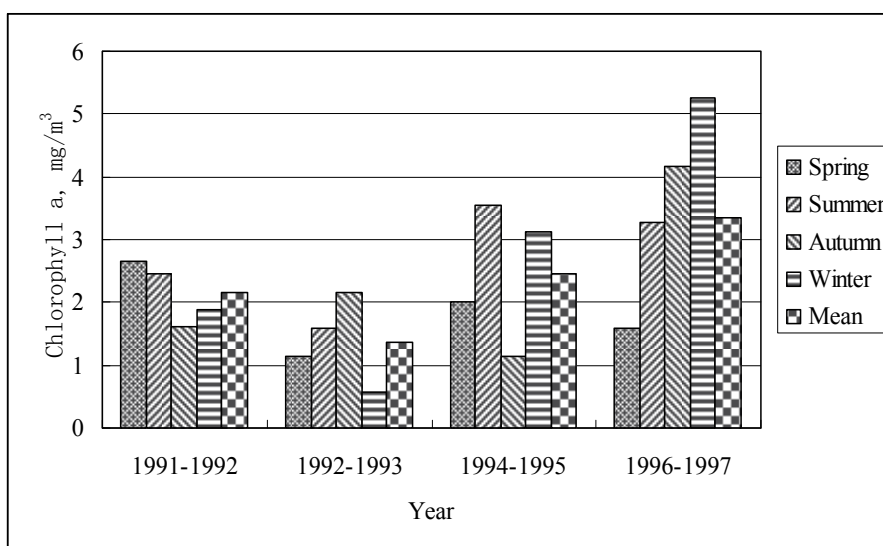


Fig. 12. Seasonal changes of chlorophyll *a* near the Nuclear Power Plant (mg/m<sup>3</sup>).

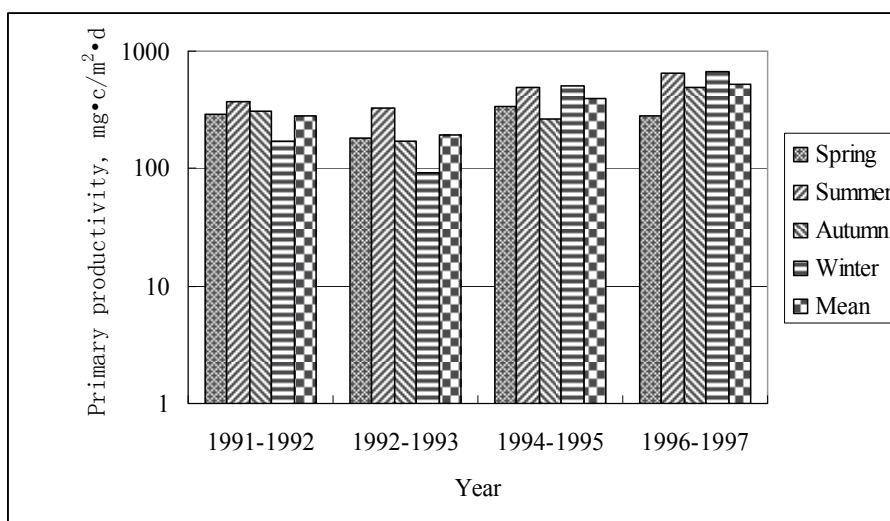


Fig. 13. Seasonal changes of primary productivity near the Nuclear Power Plant (mg c/m<sup>2</sup>·d).

number of zooplankton has been gradually increasing from 55.42 ind  $m^{-3}$  to 384.05 ind  $m^{-3}$  since 1998, and the value in 2004 has already exceeded the 352.70 ind  $m^{-3}$  level in 1985 (Table 3). One reason might be the strictly enforced regulations relating to the marine environment and fisheries from June to August in each year since 1995, and another reason might be high levels of plant nutrients and high ratios of Si to N and P, most phytoplankton falls into the food spectrum of herbivorous, crustacean zooplankton in recent years (Sommer et al., 2002, 2008).

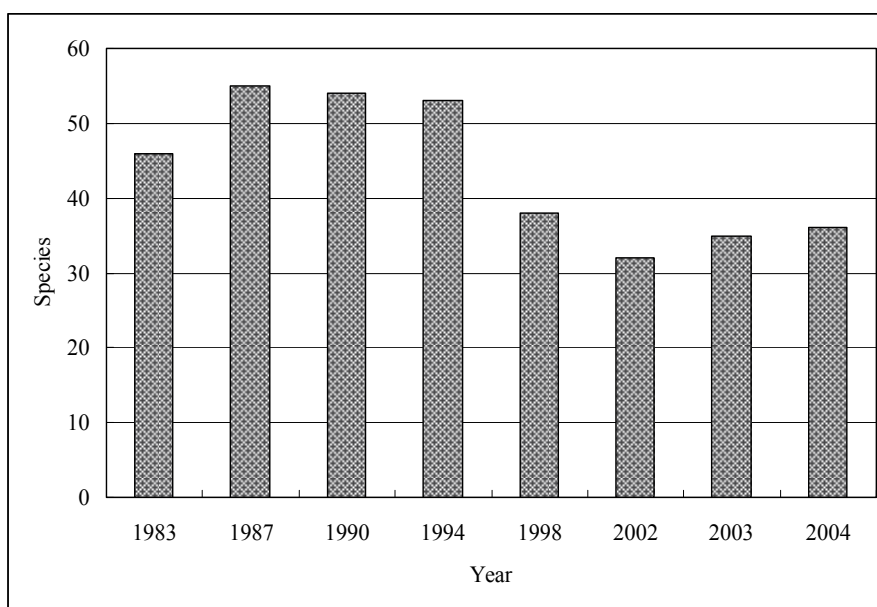


Fig. 14. Main species of the familiar zooplankton of Daya Bay changed from 1983 to 2004 (Wang et al., 2008).

Individual biomass changes of the zooplankton are shown in near the Nuclear power plant in Fig.15. Compared with the mean individual biomass of the zooplankton between 1982 to 1991 (from 392.25 ind/ $m^3$  to 680.75 ind/ $m^3$ ) before operation, it is very lower for 341 ind/ $m^3$  in 1994-1995 after the operation near the Nuclear power plant. The waste warm water is not good for zooplankton growth, especially in summer and autumn of each year. The waste warm water, which discharged to the south area of Daya Bay from the Nuclear Power Plants, directly impacts on zooplankton growth (Zheng et al., 2001).

A total of 328 species of fish were captured from 1985 to 2004, and 304 species of fishes were identified, including many edible species of high economic value such as *Sardinella jussieu*, *Clupanodon punctatus*, *Nematalosa nasus*, *Thrissa setirostris*, *Thrissa dussumieri*, *Thrissa kammalensis*, *Thrissa hamiltonii*, *Thrissa vitirostris*, *Harpodon nehereus*, *Plotosus anguillar*, *Lactarius lactarius*, *Caranx (atule) kalla*, *Pseudosciaena arcea*, *Leioganthus rivulatus*, *Pagrosomus major*, *Rhabdosargus sarba*, *Siganus oramin*, *Trichiurus haumela*, *Stromateoides argenteus*, *Stromateoides nozawae*, *Stromateoides sinensis* and *Lagocephalus lunaris spsdiceus* (Wang et al., 2008). The dominant species were perciformes including the warm-water and warm-and-temperate-water species accounted for about 90% and 10% in Daya Bay. The main fishes were about 20-28 species of 47 main species of fishes were captured in Daya Bay from 1985 to 2004 (Fig.16). Through the main species of fishes have a small change in Daya Bay from

1985 to 2004, the amount of the edible fish natural resource has decreased greatly from 1985 to 2000. The mean individual weight of the fish changed from 14.60 g tail<sup>-1</sup> in 1985 to 10.80 g tail<sup>-1</sup> in 2004 (Table 4). Although a policy to ban-fishing in the China Sea was put in practice from July to August since 1995, the amount of the fish natural resource has recovered slowly because of excessive catching and pollution, speciealy in 1987-2000. The investigation data show that Daya Bay has a sandy bottom with coral reefs and an environment suitable for growth, the fish resources are abundant as compared to those in other bays in China that have less suitable environments. For example, there were only 91 species in Jiaozhou Bay in the temperate zone of China (Zhou, 1984).

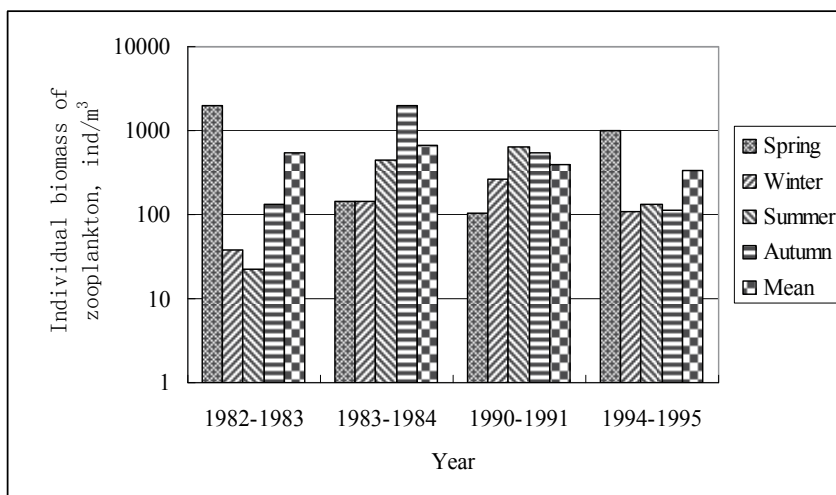


Fig. 15. Individual biomass changes of the zooplankton near the Nuclear power plant (ind/m<sup>3</sup>).

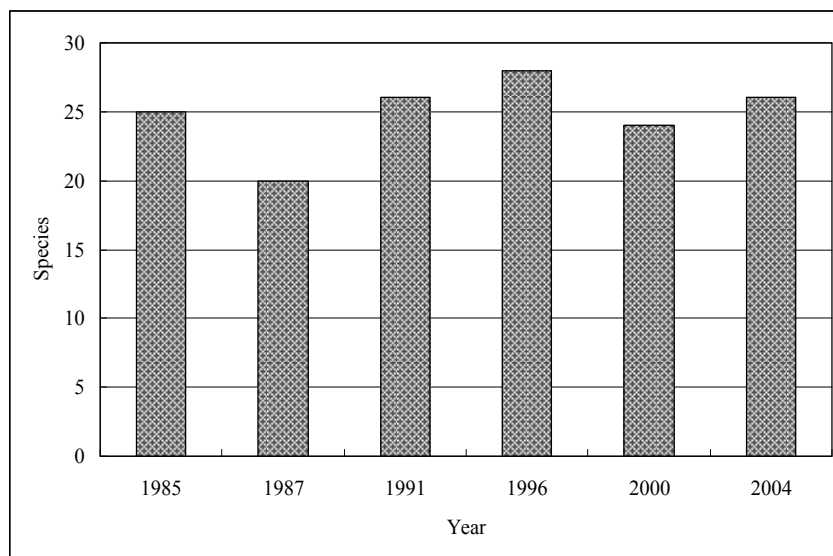


Fig. 16. Main species of fishes in Daya Bay from 1985 to 2004 (Wang et al., 2008)

In order to evaluate the potential fishery production in the sea area around the Daya Bay Nuclear Power Plant before and after the operation, the potential fishery productions were 270 t/a in 1992-1993 (before the operation) and 550 t/a in 1994-1995 (after the operation) in 45 km<sup>2</sup> sea area around the Daya Bay Nuclear Power Plant according to primary productivity and organic carbon of the phytoplankton (Peng et al., 2001).

Year	April	May	October	December	Mean
1985	9.70	6.30		27.80	14.60
1987	2.85	4.16		1.92	2.98
1996	1.08	2.51		7.39	3.66
2000		2.28			2.28
2004			10.80		10.80

Table 4. Mean individual weight of the fish (g tail<sup>-1</sup>) changed from 1985 to 2004 (Wang et al., 2008).

Daya Bay has a high diversity of natural habitats, more than 700 species of benthos were found by mud sampling and trawling since 1982 (Xu, 1989; Wang et al., 2008, 2011). Benthic plants were less than 10%, including about 60 species of diatoms which were the main benthic plants. Benthic animals were more than 90%. Besides a very few species, the benthic animals in Daya Bay were almost all warm-water species with relatively few individuals. The annual mean biomasses of benthic animals ranged from 55.70 g m<sup>-2</sup> to 148.91 g m<sup>-2</sup> ranging from 1982 to 2004 (Table 5). The lowest mean biomass of the benthic animal in Daya Bay was found to occur during 1990-1997, which was the largest foreign investment along the Daya Bay coast (Zang, 1993; Wang et al., 2006, 2008, 2011; Tang et al., 2003). The annual mean biomasses of benthic animals have increased from 1990 to 2004, and also reached the level of 1980s in recent years. The highest biomass of 1326 g m<sup>-2</sup> was collected in north region of Daya Bay in spring of 1982. Polychaeta (about 150 species account for about 21%) and molluscs (about 148 species account for about 21%) were the dominant groups, followed by crustacea (about 130 species account for about 18%) and echinoderms (about 52 species account for about 7%), the rest (about 13%, such as Spongia, Coelenterata, Bryozoa and Nemertinea etc.) exhibited the lowest biomass. 73 species of ground fishes (account for about 10%) were captured in Daya Bay at 1982-2004. Seasonal variation of biomass showed similar trends with a maximum in winter and spring minimum in autumn or summer from 2001 to 2002 (Table 6). The maximum biomass in the year mainly occurred at the northeast and middle parts of Daya Bay, those were living areas of the mollusca (Xu, 1989; Wang et al., 2008, 2011). The mean biomasses of benthic animals of western Daya Bay (near Nuclear Power Plants) have been decreasing from 317.7 g m<sup>-2</sup> in 1991 to 45.24 g m<sup>-2</sup> in 2004 (Table 7), and the number of benthic animal species was also decreasing since 1993 (Fig. 17). These results indicated that the warm water from the Daya Bay Nuclear Power Plant (since 1993) and Lingao Nuclear Power Plant (since 2002) had given great effects for this area ecology and environment, particularly for the benthos that was directly impacted marine organism (Zheng et al., 2001; Wang et al., 2008, 2011).



Year	1982	1987	1990	1996	1997	1998	2001	2002	2004
Biomass	1.9-1326	1.5-1210	5.5-99	0.1-1197	0.4-823	2-1122	0-1236.6	0-1152	2.6-506.9
Mean	123.1	123.6	55.70	74.20	78.60	152.80	148.91	117.71	126.68

Table 5. Mean biomasses of benthic animals in Daya Bay from 1982 to 2004 (Wang et al., 2008) (Unit: g m<sup>-2</sup>).

Year	Spring	Summer	Autumn	Winter
2001	256.18	88.05	47.10	248.77
2002	96.11	14.11	64.98	279.53

Table 6. Seasonal changed biomasses of benthic animals in Daya Bay changed from 2001 to 2002(Wang et al., 2008). (Unit: g m<sup>-2</sup>).

Year	1991	1993	1994	1996	1996	1997	1998	2001	2002	2004
Biomass	0.4-1651	0.4-254.10	1-120.80	1-117.5	0.1-158.0	0.4-113.0	4.4-1222	0-197.7	0-115.6	20.6-76.6
Mean	317.9	82.00	26.60	25.60	28.60	25.80	21.4.3	34.15	28.84	45.24

Table 7. Mean biomasses of benthic animals of western Daya Bay from 1991 to 2004(Wang et al., 2008) (Unit: g m<sup>-2</sup>).

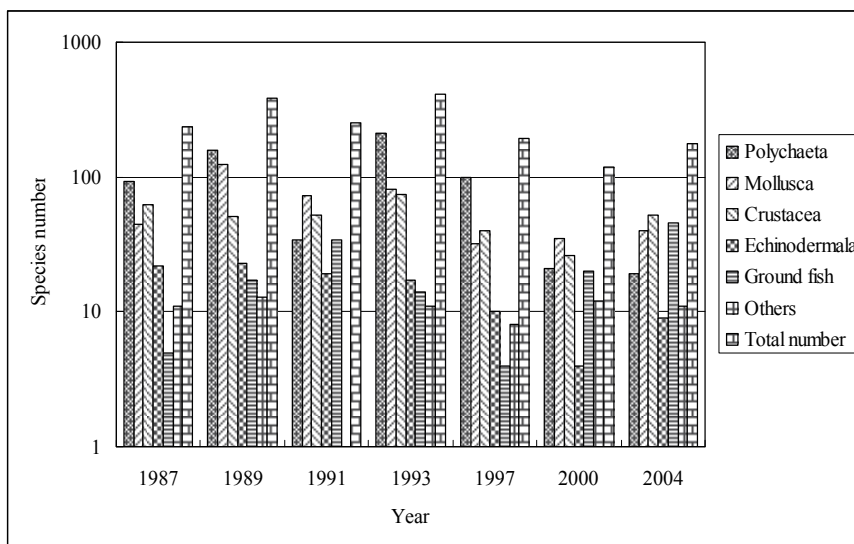


Fig. 17. Number of benthic animal species of western Daya Bay from 1987 to 2004 (Wang et al., 2008).

Coral reefs—the hermatypic coral are concentrated in the vicinity of Dalajia, Xiaolajia and west in the mouth of Daya Bay located at the northern edge of the global coral reef zone. Based on data collected in 1983-1984, there were formerly at least 19 coral species in Daya Bay (not included the part of Haotou harbour, which area was only investigated in 1964), accounting for 76.4% of the hermatypic coral from Dalajia and Xiaolajia to the mouth of the

bay (Zhang & Zhou, 1987), with *Acropora pruinosa* (Brook) as the dominant species. Only ~12-16 species were found in 1991-2002, accounting for 32% (Wen et al., 1996) and 36% of total cover rate for the hermatypic coral (Table 8). There has been a shift in the dominated species since 1990s. For example the dominated species were *Favites abdita* (Ellis & Solander) in 1991 and *Platygyra daedalea* (Ellis & Solander) in 2002, which was 7.4% of the hermatypic coral for its total cover rate. The hermatypic coral were demolished from 1984 to 2002, some of which were destroyed by men (Wen et al., 1996; Souter & Linden, 2000; Bellwood et al., 2004), such as bomb fishing, underwater coral reef sightseeing and exploitation of coral reef for making money. As one kind of sensitivity marine biology for water temperature, the coral bleaching is related to the going up of water temperature (Souter & Linden, 2000). If the seawater temperature increases by 0.5-1.5°C in several weeks, about 90-95% coral will die (Zhang et al., 2001). The hermatypic coral of Daya Bay had a little recover from 1991 to 2002 (Wang et al., 2008). The increased temperature of Daya Bay being the global change and the warm water from the nuclear power plant may be also the other reasons for decreasing the cover rate of the hermatypic coral in Daya Bay (Zheng et al., 2001).

Year	1984	1991	2002
Total species/total cover rate (%)	19/76	12/32	16/36

Table 8. Investigation results of the hermatypic coral from 1984 to 2002 (Wang et al., 2008).

Mangrove plants grow along the coast of Daya Bay, such as in Aotou, Nianshan, Dongshan, Sanmen Island and Dalajia Island etc. There were 13 species belonged to 13 families (Chen et al., 1999; Zhong et al., 1999; Wang et al., 2008). There were some herbaceous and the ornamental vine in the mangrove plants of Daya Bay, such as *Cyperus malaccensis*, *Derris trifoliata*, *Canavialamaritima*, *Ipomoea pescaprae*, *Pluchea indica*, *Sporobolus irginicus* and *Scavolahunanensis* etc. The dominant species were *Kandelia candel*, *Bruguiera gymnorrhiza*, *Aegiceras corniculatum* and *Avicennia marina*; and *Ceriops tagal*, *Lumnitzera eacemosa*, *Rhizophora stylosa* have gradually being deracinated (Chen et al., 1999). It now covers only 4% in some areas (such as in Baisha Bay of the northwest part in Daya Bay) as compared to 60-90% in 1950s, which is mainly consisted of small shrubs and bushes. A great deal of mangrove plants was felled in order to create farmland in 1970s. The total mangrove plants are about 850 hm<sup>2</sup> along the Daya Bay coast at present. In recent years, the mangrove plants were again seriously destroyed and this phenomenon is accompanied with aquatic culture, the travel and economic development (Xue, 2002; Hens et al., 2000; Zoriniet al., 2004).

Obviously, the coral reefs-the hermatypic coral and mangrove plants in Daya Bay have seriously been degraded and destroyed since 1980s and 1970s. It will be need to make a much greater effort to protect these diverse resources to maintain their ecological functions (Wang et al., 2008).

#### 4.2 Identification of water quality and phytoplankton, benthos characteristics

Water quality and phytoplankton data collected from 1999 to 2002 at 12 stations in Daya Bay are summarized in Table 9 (Wang et al., 2006).

Factors	Range	S1	S2	S3	S4	S5	S6	S7	S8	S9	S10	S11	S12
Temperature (°C)	Min-Max	18.00-28.00	17.50-27.20	16.60-31.40	18.00-32.10	16.90-30.20	16.70-30.20	16.50-29.85	14.90-31.30	16.10-30.10	16.20-30.40	14.80-30.80	15.90-30.10
	Mean	23.58	23.23	23.64	24.14	25.96	24.18	24.26	24.98	24.53	24.79	24.67	24.57
Salinity (ppt)	Min-Max	27.70-33.65	26.51-33.83	27.07-33.80	27.08-33.46	27.41-33.62	27.41-33.62	20.99-33.23	24.04-33.23	27.38-33.43	27.05-33.23	27.15-33.09	27.63-33.26
	Mean	31.67	31.92	31.78	32.21	32.61	32.70	32.33	32.33	31.73	32.28	32.05	31.58
DO (mg dm <sup>-3</sup> )	Min-Max	4.11-7.78	5.60-8.10	6.06-8.04	3.61-8.03	5.22-9.92	4.70-9.47	4.28-8.46	6.02-8.15	5.33-8.54	5.53-8.37	5.40-7.94	3.95-8.88
	Mean	6.25	6.64	7.00	6.72	6.96	6.84	7.01	7.28	7.04	7.10	6.98	6.92
pH	Min-Max	7.88-8.30	7.94-8.26	7.84-8.37	8.08-8.37	7.82-8.37	7.82-8.37	7.99-8.44	7.98-8.46	8.00-8.46	7.96-8.39	7.90-8.44	7.96-8.65
	Mean	8.12	8.13	8.19	8.19	8.18	8.19	8.20	8.24	8.22	8.21	8.16	8.20
Secchi (m)	Min-Max	2.20-5.00	1.50-3.00	1.80-5.00	1.70-4.50	1.90-3.20	1.90-3.20	1.90-3.20	1.20-4.00	1.50-5.50	1.50-4.50	1.20-4.00	1.50-5.70
	Mean	3.03	2.32	2.47	2.82	2.91	3.32	3.20	2.53	3.26	2.86	2.60	2.91
Turbidity (NTU)	Min-Max	0.27-9.08	0.77-8.13	0.57-6.26	0.17-7.77	0.27-4.72	0.12-8.84	0.12-8.84	0.17-9.31	0.07-12.15	0.17-6.24	0.17-9.31	0.12-5.30
	Mean	4.01	4.04	2.11	1.77	2.07	1.92	2.27	2.47	2.47	1.62	2.18	1.89
NH <sub>4</sub> -N (μmol dm <sup>-3</sup> )	Min-Max	0.049-4.762	0.016-4.25	0.091-6.63	0.035-3.80	0.019-6.55	0.009-16.50	0.017-3.29	0.007-8.00	0.029-7.79	0.008-8.20	0.029-9.63	0.006-3.74
	Mean	1.337	2.660	2.660	1.816	1.887	1.816	1.185	2.122	1.705	2.123	1.656	1.391
NO <sub>2</sub> -N (μmol dm <sup>-3</sup> )	Min-Max	0.015-1.400	0.009-1.41	0.2-39	0.002-1.78	0.015-2.22	0.01-4.16	0.003-3.04	0.001-1.68	0.001-1.45	0.1-1.48	0.1-1.48	0.1-1.78
	Mean	0.258	0.523	0.382	0.274	0.408	0.495	0.447	0.324	0.255	0.257	0.337	0.341
NO <sub>3</sub> -N (μmol dm <sup>-3</sup> )	Min-Max	0.06-6.05	0-5.45	0.002-4.46	0.034-26.07	0.031-5.19	0.045-5.50	0-5.45	0-27.62	0-43.7	0.004-3.38	0-27.6	0-34.3
	Mean	1.43	1.29	1.52	2.82	1.92	1.81	1.61	2.45	1.05	1.33	1.18	1.31
TIN (μmol dm <sup>-3</sup> )	Min-Max	0.125-7.85	0.054-8.76	0.071-12.10	0.071-28.22	0.069-7.90	0.067-19.19	0.033-10.49	0.021-30.05	0.040-8.60	0.012-9.10	0.038-11.27	0.006-7.04
	Mean	3.528	3.056	4.565	4.907	4.211	4.065	3.203	4.894	3.012	3.720	3.171	3.058
PO <sub>4</sub> -P (μmol dm <sup>-3</sup> )	Min-Max	0.018-0.68	0.005-0.86	0.003-0.71	0-0.38	0.011-0.65	0.007-0.64	0.06-0.37	0.009-0.53	0.001-0.38	0.04-0.42	0.003-0.45	0.002-0.37
	Mean	0.152	0.195	0.184	0.157	0.184	0.216	0.160	0.149	0.161	0.171	0.191	0.140
SiO <sub>4</sub> -Si (μmol dm <sup>-3</sup> )	Min-Max	12.83-30.00	8.81-39.38	4.60-40.40	6.06-35.71	5.18-32.00	7.17-33.75	7.72-33.71	0.33-40.00	5.38-31.30	6.01-41.65	0.83-47.50	0.93-34.38
	Mean	21.70	27.35	21.58	19.52	20.29	21.70	31.25	18.57	19.45	19.78	24.58	19.14
DIN / PO <sub>4</sub> -P	Min-Max	4.26-162.41	8.23-30.11	8.40-338.82	5.56-305.67	4.95-193.75	4.68-58.83	5.46-64.33	2.44-433.00	2.45-120.80	5.50-92.40	2.28-119.84	7.14-162.67
	Mean	23.21	15.67	24.81	31.25	22.88	18.82	20.02	32.84	32.84	21.75	16.60	21.70
SiO <sub>4</sub> -Si / PO <sub>4</sub> -P	Min-Max	37.05-1350.47	39.76-3256.17	27.75-5337.24	37.70-2442.40	33.06-2230.41	30.30-3686.64	48.12-9900.68	6.60-1377.67	23.39-5022.58	27.04-980.75	4.58-1824.37	10.33-9202.00
	Mean	142.76	140.26	117.28	124.33	110.27	100.46	195.31	124.63	120.81	115.67	128.69	136.71
BOD <sub>5</sub> (mg dm <sup>-3</sup> )*	Min-Max	0.42-6.61	0.42-5.39	0.79-3.32	0.63-3.39	0.58-2.64	0.45-7.17	0.33-6.58	0.96-4.35	0.40-4.29	0.85-1.53	0.65-2.92	0.41-5.88
	Mean	2.09	1.63	1.63	1.81	1.28	1.71	1.94	1.69	1.51	1.13	1.40	1.50
Chlorophyll <i>a</i> (mg m <sup>-3</sup> )	Min-Max	0.29-2.91	0.19-4.42	0.24-8.75	0.14-9.68	0.34-7.90	0.27-9.17	0.12-7.93	0.58-8.85	0.10-9.96	0.32-10.72	0.46-11.14	0.34-7.44
	Mean	1.34	1.63	3.78	2.69	2.45	2.53	2.76	4.14	2.52	2.88	2.98	2.44
Phytoplankton (cells m <sup>-3</sup> )	Min-Max	5.94-10 <sup>6</sup>	1.08-10 <sup>6</sup>	3.64-10 <sup>6</sup> -8.34-10 <sup>6</sup>	7.33-10 <sup>6</sup>	6.17-10 <sup>6</sup>	7.44-10 <sup>6</sup>	4.46-10 <sup>6</sup>	6.69-10 <sup>6</sup>	3.44-10 <sup>6</sup>	3.41-10 <sup>6</sup>	1.36-10 <sup>6</sup>	7.18-10 <sup>6</sup>
	Mean	6.47-10 <sup>6</sup>	1.13-10 <sup>6</sup>	6.83-10 <sup>6</sup>	8.00-10 <sup>6</sup>	4.45-10 <sup>6</sup>	6.11-10 <sup>6</sup>	4.21-10 <sup>6</sup>	2.84-10 <sup>6</sup>	2.49-10 <sup>6</sup>	2.07-10 <sup>6</sup>	2.31-10 <sup>6</sup> -2.89-10 <sup>6</sup>	6.57-10 <sup>6</sup>
Bacillarophyta (cells m <sup>-3</sup> )	Min-Max	3.59-10 <sup>6</sup>	4.77-10 <sup>6</sup>	6.83-10 <sup>6</sup>	3.76-10 <sup>6</sup>	3.76-10 <sup>6</sup>	4.70-10 <sup>6</sup>	1.12-10 <sup>6</sup>	2.03-10 <sup>6</sup>	3.96-10 <sup>6</sup>	2.24-10 <sup>6</sup>	4.13-10 <sup>6</sup>	7.00-10 <sup>6</sup>
	Mean	3.61-10 <sup>6</sup>	8.06-10 <sup>6</sup>	3.18-10 <sup>6</sup> -8.30-10 <sup>6</sup>	6.67-10 <sup>6</sup>	5.04-10 <sup>6</sup>	5.04-10 <sup>6</sup>	4.14-10 <sup>6</sup>	3.86-10 <sup>6</sup>	5.95-10 <sup>6</sup>	2.76-10 <sup>6</sup>	4.13-10 <sup>6</sup>	7.00-10 <sup>6</sup>
Pyrophyta (cells m <sup>-3</sup> )	Min-Max	1.11-10 <sup>6</sup>	1.11-10 <sup>6</sup>	1.67-10 <sup>6</sup> -4.92-10 <sup>6</sup>	2.22-10 <sup>6</sup>	5.04-10 <sup>6</sup>	4.64-10 <sup>6</sup>	3.21-10 <sup>6</sup>	3.21-10 <sup>6</sup>	3.21-10 <sup>6</sup>	3.68-10 <sup>6</sup>	1.54-10 <sup>6</sup>	1.82-10 <sup>6</sup>
	Mean	1.12-10 <sup>6</sup>	5.66-10 <sup>6</sup>	6.95-10 <sup>6</sup>	6.84-10 <sup>6</sup>	6.84-10 <sup>6</sup>	1.17-10 <sup>6</sup>	6.26-10 <sup>6</sup>	6.26-10 <sup>6</sup>	1.79-10 <sup>6</sup>	2.33-10 <sup>6</sup>	3.00-10 <sup>6</sup>	2.25-10 <sup>6</sup>
Cyanophyta (cells m <sup>-3</sup> )	Min-Max	3.42-10 <sup>6</sup>	2.02-10 <sup>6</sup>	1.27-10 <sup>6</sup>	8.08-10 <sup>6</sup>	1.04-10 <sup>6</sup>	4.05-10 <sup>6</sup>	1.44-10 <sup>6</sup>	1.44-10 <sup>6</sup>	6.80-10 <sup>6</sup>	5.41-10 <sup>6</sup>	8.26-10 <sup>6</sup>	7.02-10 <sup>6</sup>
	Mean	0.09-1.08-10 <sup>6</sup>	0.08-8.33-10 <sup>6</sup>	0.03-1.08-10 <sup>6</sup>	1.67-10 <sup>6</sup> -4.92-10 <sup>6</sup>	0.03-2.95-10 <sup>6</sup>	0.03-1.58-10 <sup>6</sup>	0.03-1.58-10 <sup>6</sup>	0.03-1.58-10 <sup>6</sup>	0.03-1.58-10 <sup>6</sup>	0.03-1.58-10 <sup>6</sup>	0.03-1.58-10 <sup>6</sup>	0.03-1.58-10 <sup>6</sup>
Others (cells m <sup>-3</sup> )	Min-Max	0.08-4.11-10 <sup>6</sup>	0.09-5.86-10 <sup>6</sup>	0.06-2.73-10 <sup>6</sup>	0.03-1.94-10 <sup>6</sup>	0.03-2.25-10 <sup>6</sup>	0.03-1.79-10 <sup>6</sup>	0.03-3.57-10 <sup>6</sup>	0.03-1.92-10 <sup>6</sup>	0.03-8.18-10 <sup>6</sup>	0.03-1.88-10 <sup>6</sup>	0.03-1.67-10 <sup>6</sup>	0.03-4.39-10 <sup>6</sup>
	Mean	1.25-10 <sup>6</sup>	1.12-10 <sup>6</sup>	1.02-10 <sup>6</sup>	1.02-10 <sup>6</sup>	1.02-10 <sup>6</sup>	1.02-10 <sup>6</sup>	1.02-10 <sup>6</sup>	1.02-10 <sup>6</sup>	1.02-10 <sup>6</sup>	1.02-10 <sup>6</sup>	1.02-10 <sup>6</sup>	1.02-10 <sup>6</sup>

\*The data of BOD<sub>5</sub> was from 2001 to 2002.

Table 9. Ranges and means of major physicochemical and biological factors in 12 stations in Daya Bay from 1999 to 2002 (Wang et al., 2006).

Cluster analysis based on the major water quality parameters measured (first column Table 10) revealed that 12 monitoring stations could be grouped into three clusters. Flexible-Beta Cluster Analysis method was used and the corresponding dendrogram using FLExible-beta method between groups transforming measures with Flexible-Beta Distance is shown in Fig.18. Cluster I consisted of stations S1, S2, S7 and S11, in the south part of Daya Bay. Cluster II consisted of stations S5, S6, S9, S10 and S12, in the middle and northeast parts of Daya Bay. Cluster III consisted of stations S3, S4 and S8, in the cage culture areas of the southwest part of Daya Bay and the northwest part nearby the Aotou harbor of Daya Bay. By the FLExible-beta's method for cluster analysis, the results could also reflect there were the different function areas in the sea of Daya Bay (Wang et al., 2006).

Factor analysis techniques were used to investigate the various factors that present in each of three clusters identified by cluster analysis. Factors were identified by the principal component method with varimax rotation (using PROC X16 of the SAS system). Eigenvalues and cumulative proportions of correlation matrix are present in Table 10. In each cluster, more than 60% of the data variance could be explained by the first two principle components. In general, pH, NO<sub>3</sub>-N, TIN and TIN/PO<sub>4</sub>-P are the most important factors in differentiating the characteristics of the three clusters as evident from the factor loadings. Cluster I with factor 1 (positive loadings for secchi, NO<sub>3</sub>-N, DIN, TIN/PO<sub>4</sub>-P and BOD<sub>5</sub>) and factor 2 (positive loadings for temperature, DO, pH and chlorophyll *a*) combined accounting for 32.61 % of the data variance. Cluster II with factor 1 (positive loadings for NO<sub>2</sub>-N, NO<sub>3</sub>-N, TIN, PO<sub>4</sub>-P, SiO<sub>3</sub>-Si, and Chlorophyll *a*) and factor 2 (positive loadings for turbidity, TIN/PO<sub>4</sub>-P and chlorophyll *a*) combined accounting for 25.31 % of the data variance. Cluster III with factor 1 (positive loadings for temperature, pH, secchi, NO<sub>3</sub>-N, TIN, TIN/PO<sub>4</sub>-P, SiO<sub>3</sub>-Si/PO<sub>4</sub>-P and BOD<sub>5</sub>) and factor 2 (positive loadings for DO, pH, turbidity, NO<sub>2</sub>-N and chlorophyll *a*) combined accounting for 43.10 % of the data variance (Wang et al., 2006).

Table 10 shows the corresponding factor loading in three clusters. It should be noted that NO<sub>3</sub>-N and TIN/PO<sub>4</sub>-P were important factors among stations in the three clusters, while concentrations of individual nutrient factors (i.e. NO<sub>2</sub>-N, NO<sub>3</sub>-N, TIN, PO<sub>4</sub>-P and SiO<sub>3</sub>-Si) were more important in Cluster II. These results were different to the research in Port Shelter, Hong Kong (Yung et al., 2001), which showed that nutrient ratios (i.e. TIN to TSi and TP to TSi) were apparently the more important factors among stations in different clusters (Wang et al., 2006).

Water quality and benthos data collected from 2001 to 2004 at 12 stations in Daya Bay are summarized in Table11 (Wang et al., 2011).

Bivariate correlations between benthos biomass and major physical and nutrient factors were calculated for all stations. The density of benthos in all stations correlated positively with temperature, DO, pH, NH<sub>4</sub>-N, SiO<sub>3</sub>-Si, SiO<sub>3</sub>-Si/PO<sub>4</sub>-P, chlorophyll *a* and negatively correlated with salinity, Secchi, COD, NO<sub>3</sub>-N, NO<sub>2</sub>-N, TIN, PO<sub>4</sub>-P, TIN/PO<sub>4</sub>-P, BOD<sub>5</sub>. Such relationship between nutrients and benthos was also found in the Lower Chesapeake Bay (Dauer & Alden, 1995). The results of the correlation analysis revealed that not only temperature, DO, pH, SiO<sub>3</sub>-Si, SiO<sub>3</sub>-Si/PO<sub>4</sub>-P, chlorophyll *a*, but also salinity, Secchi depth, NO<sub>3</sub>-N, NO<sub>2</sub>-N, TIN, TIN/PO<sub>4</sub>-P, BOD<sub>5</sub> could play an important role in determining the biomass of benthos in Daya Bay (Dauer & Alden, 1995). The results are different from those using multivariate statistical analysis to study water quality and phytoplankton characteristics in Daya Bay from 1999 to 2002 (Wang et al., 2006).

	Cluster I		Cluster II		Cluster III	
	F1	F2	F1	F2	F1	F2
Temperature (°C)	0.01249	0.99037	0.16669	0.49016	0.87157	0.49027
Salinity (ppt)	0.12846	0.02911	0.92371	-0.30711	0.26872	-0.96322
DO (mg dm <sup>-3</sup> )	0.19712	0.97137	-0.85093	0.25263	0.15601	0.98775
pH	0.07382	0.78155	-0.90136	-0.35794	<b>0.62899</b>	<b>0.77741</b>
Secchi (m)	0.90952	0.33258	0.23706	-0.94526	0.50374	-0.86386
Turbidity (NTU)	0.06313	-0.98470	0.29705	0.88071	0.17229	0.98505
NH <sub>4</sub> -N (μmol dm <sup>-3</sup> )	-0.81998	-0.57232	-0.01719	0.28781	-0.86639	0.49936
NO <sub>2</sub> -N (μmol dm <sup>-3</sup> )	-0.61670	-0.18310	0.98970	-0.09451	-0.80358	0.59520
NO <sub>3</sub> -N (μmol dm <sup>-3</sup> )	0.72416	0.01289	0.92253	0.26891	0.90624	-0.42277
TIN (μmol dm <sup>-3</sup> )	0.87689	-0.16412	0.73706	0.31524	0.98197	-0.18905
PO <sub>4</sub> -P (μmol dm <sup>-3</sup> )	-0.99369	0.01984	0.73275	-0.22751	-0.99800	-0.06318
SiO <sub>3</sub> -Si (μmol dm <sup>-3</sup> )	-0.19294	0.29027	0.81653	-0.23589	-0.98767	-0.15652
TIN/PO <sub>4</sub> -P	0.98732	-0.11482	0.03293	<b>0.92628</b>	<b>0.99951</b>	0.03141
SiO <sub>3</sub> -Si / PO <sub>4</sub> -P	0.45590	0.26096	-0.60317	0.19426	0.99274	-0.12029
BOD <sub>5</sub> (mg dm <sup>-3</sup> )*	0.89595	-0.36263	0.44634	-0.75797	0.64454	-0.76457
Chlorophyll <i>a</i> (mg m <sup>-3</sup> )	-0.23591	0.95703	-0.33466	-0.12719	-0.12588	0.99205
Cumulative % of variance explained	39.40	32.61	42.60	25.33	56.90	43.10

Table 10. Factor loadings (after varimax rotation) of first two factors for Cluster I, II and III (Wang et al., 2006).

Cluster analysis based on the major water quality parameters measured (first column Table 12) revealed that the 12 monitoring stations could be grouped into three clusters. Flexible-beta cluster analysis method was used and the corresponding dendrogram using FLExible-beta method between groups transforming measured with Flexible-beta distance, and the Flexible-beta cluster analysis result was shown in Fig.19. Cluster I consisted of the stations S1, S2, and S6 in the southern part of Daya Bay, where there are more effects from the Pearl River and South China Seas (Xu, 1989), such as the East Guangdong upwelling (Xu, 1989; Wang et al., 2006, 2008, 2011). Cluster II consisted of stations S3, S8 and S11 in the cage culture areas in the southwest part, the northwest part near the Aotou harbor and the northeast part near the Fenhe harbor of Daya Bay. The fish farming in Daya Bay has increased from an annual production of about 100 tons (~440 ha cage culture area) in 1988 to approximately 60,000 tons (~14,000 ha cage culture area) in 2005, a nearly 600-fold growth during the past 17 years (Wu et al., 2009b). Cluster III consisted of the stations S4, S5, S7, S9, S10 and S12 in the southwest, the middle and northeast parts of Daya Bay. The results of cluster analysis could also reflect the different functional areas of Daya Bay. These results are different from those reported for the water quality and phytoplankton characteristics in Daya Bay by Wang et al. (2006), and indicated also that human activities were the main factor impacting the ecological environment in Daya Bay (Wang, et al., 2008, 2011; Wu & Wang, 2007; Wu et al., 2009, 2010).

Factors	Range	S1	S2	S3	S4	S5	S6	S7	S8	S9	S10	S11	S12
Temperature (°C)	Min-Max	18.09-29.85	14.50-29.95	14.00-32.50	14.20-31.80	14.00-31.00	15.10-30.45	17.40-29.85	17.40-32.30	15.40-31.15	15.05-31.70	14.70-31.50	15.20-30.70
	Mean	23.86	23.76	24.49	24.78	23.83	23.91	23.86	24.48	24.28	24.28	24.21	23.98
Salinity (ppt)	Min-Max	28.50-33.40	28.50-33.40	26.90-33.50	27.32-33.58	25.60-33.50	30.17-33.91	28.16-34.67	26.60-33.68	27.25-34.30	27.28-34.32	27.61-34.46	28.30-33.55
	Mean	32.27	32.46	31.41	31.80	31.69	32.17	32.10	31.41	31.75	31.75	31.95	31.92
DO (mg dm <sup>-3</sup> )	Min-Max	5.36-8.11	5.63-8.81	6.66-9.51	5.04-8.66	6.23-9.76	5.22-7.71	6.09-8.81	6.25-11.04	6.31-8.64	6.31-8.64	6.34-8.64	6.23-8.93
	Mean	6.97	7.01	7.59	7.22	7.50	7.10	7.28	7.78	7.43	7.43	7.44	7.28
pH	Min-Max	7.99-8.30	7.99-8.30	7.99-8.30	8.03-8.37	7.99-8.37	7.99-8.30	7.99-8.30	7.98-8.30	8.03-8.42	7.98-8.43	7.91-8.30	7.98-8.42
	Mean	8.14	8.09	8.14	8.16	8.15	8.15	8.15	8.15	8.15	8.15	8.15	8.16
Secchi (m)	Min-Max	1.43	1.43	1.43	1.43	1.43	1.43	1.43	1.43	1.43	1.43	1.43	1.43
	Mean	1.43	1.43	1.43	1.43	1.43	1.43	1.43	1.43	1.43	1.43	1.43	1.43
COD (mg dm <sup>-3</sup> )	Min-Max	0.01-31	0.27-2.66	0.60-1.49	0.59-2.08	0.31-2.34	0.22-2.65	0.22-2.65	0.22-2.65	0.22-2.65	0.22-2.65	0.22-2.65	0.22-2.65
	Mean	1.02	0.848	0.919	0.868	0.780	0.913	0.869	0.868	0.755	0.755	1.01	1.08
NO <sub>3</sub> -N (µmol dm <sup>-3</sup> )	Min-Max	0.024-4.06	0.024-4.06	0.024-4.06	0.024-4.06	0.024-4.06	0.024-4.06	0.024-4.06	0.024-4.06	0.024-4.06	0.024-4.06	0.024-4.06	0.024-4.06
	Mean	2.747	2.245	2.282	1.809	2.061	2.354	2.088	1.759	1.591	1.621	1.547	2.153
NO <sub>2</sub> -N (µmol dm <sup>-3</sup> )	Min-Max	0.4-5.0	0.050-1.20	0.1-7.0	0.002-1.145	0.040-1.625	0.012-0.462	0.001-0.715	0.010-1.500	0.001-0.465	0.001-0.465	0.001-0.465	0.001-0.465
	Mean	0.227	0.399	0.290	0.261	0.277	0.244	0.214	0.228	0.170	0.165	0.189	0.183
NH <sub>4</sub> <sup>+</sup> -N (µmol dm <sup>-3</sup> )	Min-Max	0.019-7.611	0.028-3.670	0.080-1.770	0.010-1.002	0.030-0.589	0.030-1.007	0.135-1.684	0.031-1.436	0.011-0.505	0.021-1.436	0.021-1.436	0.010-1.418
	Mean	2.833	1.798	2.827	2.831	2.831	1.849	1.911	1.759	1.591	1.547	1.547	2.101
TIN (µmol dm <sup>-3</sup> )	Min-Max	0.124-13.6	0.010-0.85	0.010-1.0	0.010-0.85	0.010-1.0	0.010-1.0	0.010-1.0	0.010-1.0	0.010-1.0	0.010-1.0	0.010-1.0	0.010-1.0
	Mean	2.227	4.937	3.420	4.467	4.742	4.547	4.213	4.213	4.213	4.213	4.213	4.213
PO <sub>4</sub> -P (µmol dm <sup>-3</sup> )	Min-Max	0.4-5.0	0.050-1.20	0.010-0.570	0.010-0.570	0.010-0.570	0.010-0.570	0.010-0.570	0.010-0.570	0.010-0.570	0.010-0.570	0.010-0.570	0.010-0.570
	Mean	1.319	0.171	0.142	0.129	0.131	0.134	0.119	0.111	0.128	0.121	0.108	0.176
SiO <sub>2</sub> -Si (µmol dm <sup>-3</sup> )	Min-Max	9.642-30.06	8.766-38.44	6.275-39.25	4.898-35.66	6.507-43.54	5.348-33.75	7.150-34.92	2.023-35.63	8.182-38.17	5.348-40.44	6.186-47.20	36.92-27.52
	Mean	19.32	21.58	20.36	19.02	21.02	21.11	21.28	22.70	20.03	21.36	28.03	20.46
TIN/PO <sub>4</sub> -P	Min-Max	1.285-217.32	11.59-114.43	9.790-95.66	6.630-60.02	6.179-255.00	8.391-302.35	8.602-166.71	3.559-114.58	6.802-72.68	11.67-119.57	4.168-170.02	8.15-148.56
	Mean	29.81	45.79	31.36	43.13	52.07	49.16	42.39	50.02	46.80	40.11	45.30	52.07
SiO <sub>2</sub> -Si/ PO <sub>4</sub> -P (mg m <sup>-3</sup> )	Min-Max	39.81-1333.26	48.66-408.79	31.36-3802.54	45.17-1020.08	20.06-2092.74	64.77-4213.29	48.36-6993.54	56.69-729.47	35.50-16451.61	33.37-423.42	30.15-7369.72	36.92-27.52
	Mean	298.65	475.16	386.71	319.23	387.44	448.17	705.98	345.58	1250.81	233.19	720.06	418.23
Chlorophyll <i>a</i> (mg m <sup>-3</sup> )	Min-Max	0.62-7.26	0.54-0.88	0.62-1.09	0.49-0.84	0.37-1.49	0.46-2.67	0.17-2.85	0.15-1.30	0.75-10.08	0.69-11.16	0.75-10.08	0.69-11.16
	Mean	1.62	1.00	1.16	2.43	1.08	2.11	1.61	1.48	2.15	2.94	2.75	2.18
BOD <sub>5</sub> (mg dm <sup>-3</sup> )	Min-Max	0.49-1.95	0.49-1.95	0.76-3.31	0.54-3.70	0.62-2.96	0.35-1.19	0.65-2.24	0.40-1.38	0.51-2.82	0.96-3.84	0.65-3.36	0.52-5.24
	Mean	1.21	1.65	1.86	1.55	1.37	1.64	1.55	1.28	1.27	1.65	1.45	1.65
Benthos (g m <sup>-2</sup> )	Min-Max	0.115-40	0.115-40	0.790-30	0.197-74	0.150-30	0.192-70	0.448-20	0.134-10	0.115-20	0.126-60	0.528-14	0.635-30
	Mean	19.20	32.85	98.57	35.71	23.24	42.24	104.06	64.30	174.41	272.37	173.41	103.71
Polychaeta (g m <sup>-2</sup> )	Min-Max	0.17-70	0.5-20	0.8-60	0.10-254	0.16-40	0.15-30	0.26-60	0.2-20	0.5-30	0.6-60	0.1-5.0	0.1-5.0
	Mean	3.52	1.18	3.40	10.52	2.36	1.88	3.91	0.43	0.91	0.91	1.96	1.50
Mollusca (g m <sup>-2</sup> )	Min-Max	0.155-30	0.155-30	0.290-30	0.101-60	0.115-50	0.106-30	0.67-40	0.119-30	0.112-60	0.129-30	0.528-14	0.620-30
	Mean	4.68	24.84	92.34	15.35	18.09	28.06	85.58	80.16	139.54	227.32	170.28	97.56
Echinodermata (g m <sup>-2</sup> )	Min-Max	0.50-40	0.6-80	0.3-60	0.5-80	0.12-30	0.6-70	0.5-60	0.4-20	0.6-80	0.6-80	0.6-80	0.6-80
	Mean	5.71	0.81	0.30	7.75	2.04	1.63	0.56	0.025	2.71	5.15	0.072	0.64
Crustacean (g m <sup>-2</sup> )	Min-Max	0.24-30	0.4-32	0.22-30	0.3-30	0.34-30	0.1-30	0.2-30	0.4-30	0.1-30	0.1-30	0.1-30	0.1-30
	Mean	4.65	0.67	2.53	2.12	2.73	0.44	0.44	1.05	0.30	6.96	0.99	1.42
Others (g m <sup>-2</sup> )	Min-Max	0.6-50	0.80-30	0.0-40	0.1-50	0.0-40	0.126-60	0.6-60	0.5-70	0.3-30	0.5-70	0.0-40	0.38-50
	Mean	0.64	5.32	0	0.64	0.025	9.11	0.56	3.29	0.21	2.60	0	2.64

Table 11. Ranges and means of major physico-chemical and biological factors of 12 stations in Daya Bay from 2001 to 2004 (Wang et al., 2011).

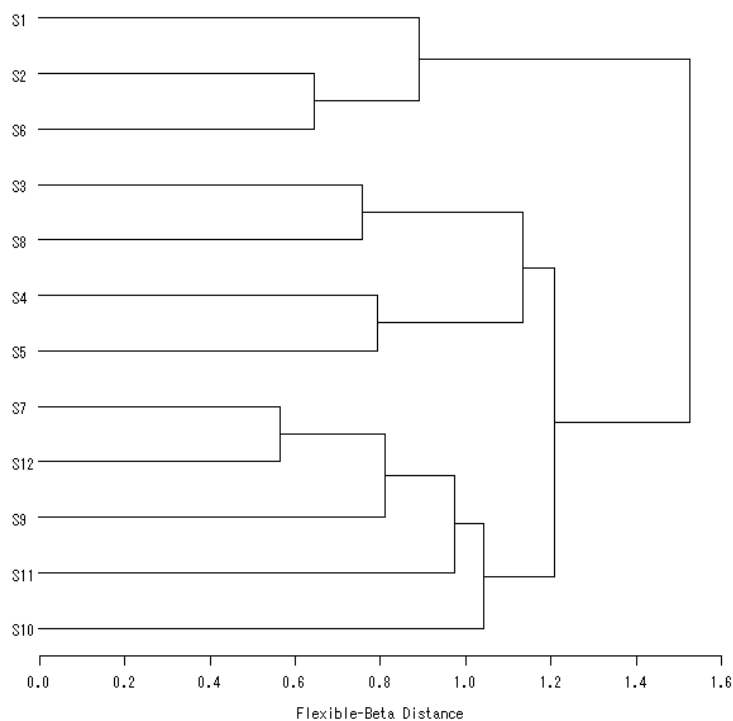


Fig. 19. Results of the FLExible-beta's method for cluster analysis showing the three clusters of all stations (Wang et al., 2011).

Factor analysis techniques were used to investigate the various factors that are present in each of three clusters identified by cluster analysis. Factors were identified by the principal component method with varimax rotation. Eigenvalues and cumulative proportions of correlation matrix are present in Table 12 (Wang et al., 2011).

In each cluster, more than 50% of the data variance could be explained by the first two principle components. In general,  $\text{NO}_3\text{-N}$ ,  $\text{NH}_4\text{-N}$  and TIN are the most important factors in differentiating the characteristics of the three clusters as evident from the factor loadings. Cluster I with factor 1 (positively with COD,  $\text{NH}_4\text{-N}$ ,  $\text{NO}_3\text{-N}$ , TIN,  $\text{TIN}/\text{PO}_4\text{-P}$  and  $\text{BOD}_5$ ) and factor 2 (positively with temperature, pH, Secchi and  $\text{NO}_2\text{-N}$ ) accounted for 45.54 % of the data variance. Cluster II with factor 1 (positively with DO, COD,  $\text{NO}_3\text{-N}$ ,  $\text{BOD}_5$  and Chlorophyll *a*) and factor 2 (positively with  $\text{NH}_4\text{-N}$ ,  $\text{NO}_2\text{-N}$ ,  $\text{NO}_3\text{-N}$ , TIN,  $\text{PO}_4\text{-P}$  and  $\text{SiO}_3\text{-Si}/\text{PO}_4\text{-P}$ ) accounted for 38.36 % of the data variance. Cluster III with factor 1 (positively with for DO,  $\text{NO}_3\text{-N}$ , TIN,  $\text{PO}_4\text{-P}$  and  $\text{SiO}_3\text{-Si}$ ) and factor 2 (positively with salinity, Secchi depth,  $\text{NO}_3\text{-N}$  and  $\text{NO}_2\text{-N}$ ) combined for 23.78 % of the data variance.

Table 12 shows the corresponding factor loading in three clusters. It should be noted that  $\text{NO}_3\text{-N}$  and  $\text{NH}_4\text{-N}$  were important factors among stations in the three clusters, whereas concentrations of individual nutrient factors (i.e.  $\text{NH}_4\text{-N}$ ,  $\text{NO}_2\text{-N}$ ,  $\text{NO}_3\text{-N}$ , TIN and  $\text{PO}_4\text{-P}$ ) were more important in Cluster II. These results were similar to the research for spatial characterization of nutrient dynamics in the Bay of Tunis (Souissi et al., 2000), for long-term changes in water quality and phytoplankton characteristics in Port Shelte (Yung et al., 2001) and also for the water quality and phytoplankton characteristics in Daya Bay (Wang et al.,

2006), which showed that the nutrients were apparently the more important factors among stations in different clusters)

	Cluster I		Cluster II		Cluster III	
	F1	F2	F1	F2	F1	F2
Temperature (°C)	-0.07402	<b>0.99726</b>	-0.91594	0.17441	0.41463	-0.84822
Salinity (ppt)	0.08681	-0.99622	-0.86609	-0.23685	-0.79031	<b>0.58854</b>
DO (mg dm <sup>-3</sup> )	-0.95422	0.29911	<b>0.90756</b>	-0.23741	<b>0.66559</b>	-0.56114
pH	0.10302	<b>0.99468</b>	0.34421	-0.88746	-0.95259	-0.18645
Secchi (m)	-0.08829	<b>0.99609</b>	-0.97061	-0.00703	-0.81068	<b>0.51100</b>
COD (mg dm <sup>-3</sup> )	<b>0.99806</b>	-0.06229	<b>0.96300</b>	0.13467	0.30587	0.37842
NO <sub>3</sub> -N (μmol dm <sup>-3</sup> )	<b>0.71192</b>	-0.70226	-0.11188	<b>0.98878</b>	0.09577	<b>0.63140</b>
NO <sub>2</sub> -N (μmol dm <sup>-3</sup> )	-0.34213	-0.93965	0.04398	<b>0.88400</b>	0.13031	<b>0.98026</b>
NH <sub>4</sub> -N (μmol dm <sup>-3</sup> )	<b>0.85008</b>	<b>0.52665</b>	<b>0.50845</b>	<b>0.85305</b>	<b>0.73916</b>	-0.65671
TIN (μmol dm <sup>-3</sup> )	<b>0.96037</b>	-0.27873	0.24975	<b>0.96593</b>	<b>0.69021</b>	0.18550
PO <sub>4</sub> -P(μmol dm <sup>-3</sup> )	-0.67938	-0.73379	-0.03668	<b>0.99788</b>	<b>0.90839</b>	-0.09308
SiO <sub>3</sub> -Si(μmol dm <sup>-3</sup> )	-0.83054	-0.55696	0.32481	-0.39576	<b>0.99190</b>	0.01782
TIN/PO <sub>4</sub> -P	<b>0.72370</b>	<b>0.69012</b>	-0.11296	0.06295	-0.09709	0.01522
SiO <sub>3</sub> -Si/ PO <sub>4</sub> -P	-0.92164	-0.38804	-0.01222	<b>0.79633</b>	0.13335	0.24584
BOD <sub>5</sub> (mg dm <sup>-3</sup> )	<b>0.99133</b>	0.13138	<b>0.98990</b>	0.09895	0.17930	0.25444
Chlorophyll <i>a</i> (mg m <sup>-3</sup> )	-0.99963	-0.02708	<b>0.99220</b>	0.02532	0.33479	-0.16112
Cumulative % of variance explained	54.46	45.54	42.63	38.56	37.04	23.78

Table 12. Factor loadings (after varimax rotation) of first two factors for Cluster I, II and III (Wang et al., 2011).

## 5. Conclusions and suggestions in the future

Daya Bay as a multi-type ecosystem including coral reef, mangrove and rock reef has a rich biodiversity. It is a good place for the reproduction and culturing of fish, shrimp, crabs and shellfish. Due to constant interaction between land and ocean area, its ecology is more complicated and vulnerable than that of the open seas. It is especially vulnerable to the effects of frequent human activities and land-based pollution. Despite the progressive increases of human activities including more domestic sewage and industrial waste water discharged as well as nutrient enrichment and toxins derived from the cage culture of the fish and seashell, the concentrations of N, P, DO and COD must not be allowed to exceed water quality standards at the risk of serious ecosystem degradation and still were within the First Class of National Seawater Quality Standards for China. The temperatures of seawater in Daya Bay were increasing from 1982 to 2004 probably due to global change. The average ratio of N/P increased from 1.377 in 1985 to 49.09 in 2004, and the limiting factor of nutrients changed from N to P. The composition of biological community has been small, with biodiversity simplified and the biological natural resource declined. For example, the species of phytoplankton decreased from 206 species of 56 genera in 1990 to 126 species of 44 genera in 2004, the warmer water from the Nuclear Power Plant can provide extra amount of energy for phytoplankton growth (Wang et al., 2006); the main species of the zooplankton of Daya Bay had decreased from 46 species of 1983 to 36 species of 2004, the



waste warm water is not a good environment for zooplankton growth, especially in summer and autumn of each year, which directly impacts on zooplankton growth (Zheng et al., 2001); the mean individual weight of the fish has changed from 14.8 g tail<sup>-1</sup> of 1985 to 10.80 g tail<sup>-1</sup> of 2004. Assessment for the potential fishery production between before and after the operation indicated that the potential fishery production after the operation was one time compared with before the operation in 45 km<sup>2</sup> sea area around the Daya Bay Nuclear Power Plant (Peng et al., 2001). More than 700 species of benthos were found, the annual mean biomasses of benthic animals increased from 72.40 g m<sup>-2</sup> in 1996 to 126.68 g m<sup>-2</sup> in 2004. The mean biomasses and species of benthic animals near the Nuclear Power Plants decreased from 317.9 g m<sup>-2</sup> in 1991 to 45.24 g m<sup>-2</sup> in 2004 and from 250 species in 1991 to 177 species in 2004, the temperature value increased about 1°C compared with the other sea areas in Daya Bay (Wang et al., 2008). The waste warm water from the Nuclear Power Plants was the main factor influencing ecology and environment in the western area of Daya Bay, particularly for the benthos that directly impacted marine organism (Wang et al., 2008, 2011; Zheng et al., 2001). Many changes had taken place in Daya Bay from 1982 to 2004, such as stony coral bleaching, changed in dominate species of coral community, seriously degraded and destroyed mangrove plants. These results indicated that the ecosystem of Daya Bay is undergoing a rapid deterioration in some areas and in some aspects. At the same time, some aspects of its ecological environment were recovering due to strategic protection and management steps for protection and management of coastal marine ecosystems in China. For example, the annual mean biomasses of benthic animals increased from 72.40 g m<sup>-2</sup> of 1996 to 1126.68 g m<sup>-2</sup> of 2004 and the nutrient P decreased from 1985 to 2004. Daya Bay is a multi-type ecosystem mainly driven by human activities (Wang et al., 2006, 2008, 2011; Wu & Wang, 2007).

The results of the present study indicated that the mean abundances of phytoplankton in all stations correlated positively with temperature, salinity, DO, pH, the ratio of TIN to PO<sub>4</sub>-P, NH<sub>4</sub>-N, NO<sub>3</sub>-N, TIN and PO<sub>4</sub>-P and negatively correlated with secchi, turbidity, SiO<sub>3</sub>-Si to PO<sub>4</sub>-P, and SiO<sub>3</sub>-Si and NO<sub>2</sub>-N by calculation with bivariate correlations. All stations could be groups into three clusters with Flexible-Beta Cluster Analysis method. Cluster I consisted of stations S1, S2, S7 and S11 in the south part and the northeast part of the Daya Bay. Cluster II consisted of stations S5, S6, S9, S10 and S12 in the middle and northeast parts of Daya Bay. Cluster III consisted of stations S3, S4 and S8 were in the cage culture areas in the southwest part of Daya Bay and in the northwest part near the Aotou harbor of the Daya Bay. The results also suggest that the nutrient and phytoplankton are good environmental indicators can rapidly image the changing water quality in Daya Bay, and this is the first attempt to analyze the water quality and phytoplankton characteristics in Daya Bay by multivariate statistics based on the investigated data in Daya Bay. The results of multivariate statistical analysis revealed that the temperature, dissolved oxygen, NH<sub>4</sub>-N and NO<sub>3</sub>-N could also play an important role in determining the density of phytoplankton in Daya Bay (Wang et al., 2006).

The results of the present study indicated that the biomass of benthos at all stations correlated positively with temperature, DO, pH, NH<sub>4</sub>-N, SiO<sub>3</sub>-Si, SiO<sub>3</sub>-Si/PO<sub>4</sub>-P and chlorophyll *a* and negatively correlated with salinity, Secchi depth, COD, NO<sub>3</sub>-N, NO<sub>2</sub>-N, TIN, PO<sub>4</sub>-P, TIN/PO<sub>4</sub>-P and BOD<sub>5</sub> by calculation with bivariate correlations between benthos and major physical and nutrient factors. All stations could be grouped into three clusters. Cluster I consisted of stations S1, S2, and S6 were in the south part of Daya Bay.

Cluster II consisted of stations S3, S4, S8 and S5 in the cage culture areas in the southwest part, the northwest part near the Aotou harbor and the northeast part near the Fenhe harbor of Daya Bay. Cluster III consisted of stations S7, S9, S10 S11 and S12 in the southwest, the middle and northeast parts of Daya Bay. The results also suggest that the nutrient and benthos are good environmental indicators that can rapidly image the changing water quality in Daya Bay. As a multi-type ecosystem Daya Bay seems to be mainly driven by human activities (Wang et al., 2008). The results revealed that temperature and nutrients could also play an important role in determining the biomass of benthos in Daya Bay (Wang et al., 2011).

The warm water from the Nuclear Power Plants and waste water from the cage culture areas had greatly influenced ecological processes and the environment in this region according to changes in biomass of benthos and water quality at different stations in Daya Bay (Wang et al., 2006, 2008, 2011). Particularly the benthos was directly impacted as marine organisms, thus there is a need for more research about waste warm water from the Nuclear Power Plants and from cage culture areas affecting the regional ecosystem of Daya Bay (Wang et al., 2006, 2008, 2011; Wu et al., 2009, 2010). Furthermore the development of fish-farming in Daya Bay should in future be controlled (Wu et al., 2009). According to the research of long-term changes of Daya Bay, regional coordination in protection and management of such vulnerable coastal marine ecosystems should be strengthened. The following strategic protection and management steps are recommended (Wang et al., 2008): (i) Enhance information dissemination and education to improve environmental protection awareness for people in the region; (ii) Strengthen the long-term monitoring of the marine environment and coastal ecosystems in Daya Bay, enhance the research of regional environmental capacity, and use that capacity to establish large-scale control of pollutant discharges; (iii) Promote the protection of coral reefs, mangroves, coastal ecosystem and regional biodiversity by carrying out scientific plans for resource use based on marine system functions; (iv) Strictly enforce regulations relating to the marine environment and fisheries from June to August in each year; (v) More research about the waste warm water from the Nuclear Power Plants for effecting the ecosystem of Daya Bay should be carried out.

## 6. Acknowledgements

This research was supported by the project of knowledge innovation program of Chinese Academy of Sciences (No. KZCX2-YW-Q07-02, No. KSCX2-SW-132, KSCX2-SW-214), the National Natural Science Foundation of China (No. 41076070), the key projects in the National Science & Technology Pillar Program in the Eleventh Five-year Plan Period (No. 2009BADB2B0606) and the National 908 project (No. 908-02-04-04).

## 7. References

- Bellwood, D. R., Hughes, T.P., Folke, C. & Nystrom, M., 2004. Confronting the coral reef crisis. *Nature*, 429, 827-833.
- Bodergat, A.M., Oki, K., Ishizaki, K., and Rio, M., 2003. Impact of volcanism, human activities, and water mass circulation on the distribution of ostracod populations in Kagoshima Bay (Kyushu Island, southern Japan). *Comptes Rendus Geosciences*, 334(14), 1053-1059.

- Burger, J., 2003. Perceptions about environmental use and future restoration of an urban estuary. *Journal of Environmental Planning and Management*, 46(3), 399-416.
- Buzzelli, C.P., 1998. Dynamic simulation of littoral zone habitats in lower Chesapeake Bay: ecosystem characterization related to model development. *Estuaries*, 21, 659-672.
- Chen, H., Miao, S., Wang, H., and Xu, Y.M., 1999. A study on syn-ecology of mangrove at Daya Bay, China. *Chinese Journal of Guangzhou Normal University*, 20(2), 90-94.
- Cloern, J.E., 1996. Phytoplankton bloom dynamics in coastal ecosystems: a review with some general lessons from sustained investigation of San Francisco Bay, California. *Reviews of Geophysics*, 34(2), 127-168.
- Dauer, D.M., Alden, R.W., 1995. Long-term trends in the macrobenthos and water quality of the Lower Chesapeake Bay (1985-1991). *Marine Pollution Bulletin* 30(12): 840-850.
- Fisher, T.R., 1991. Phytoplankton, nutrient and turbiding in the Chesapeake, Delaware and Hudson estuarine. *Estuarine, Coastal and Shelf Science*, 32, 187-206.
- Han, W.Y., 1991. Carbon cycles of Daya Bay and the Preal River. Science Press, Beijing, China, p12-42.
- Hansom, J.D., 2001. Coastal sensitivity to environmental change: a view from the beach. *CATENA*, 42(2), 291-305.
- Hens, L., Nierynck, E., Van, Y T., Quyen, N.H., Hien, L.T.T., An, L.D., 2000. Land cover changes in the extended HA long city area, North-Eastern Vietnam during the period 1988-1998. *Environment, Development and Sustainability*, 2(3-4), 235-252.
- Huang, L., Chen, Q., and Yuan, W., 1989. Characteristics of chlorophyll distribution and estimation of primary productivity in Daya Bay, China. *Asian Marine Biology*, 6, 115-128.
- Huang, L., Tan, Y., Song, X., Huang, X., Wang, H., Zhang, S., Dong, J., and Chen, R., 2003. The status of the ecological environment and a proposed protection strategy in Sanya Bay, Hainan Island, China. *Marine Pollution Bulletin*, 47(1-6), 180-186.
- Johnson, R. A., Wichern, D. W., 1998. Applied multivariate statistical analysis. Prentice Hall, New York.
- Justice, D., Rabalais, N.N., Turner, R.E., and Dortch, Q., 1995. Change in nutrient structure of river-dominated coastal waters: stoichiometric nutrient balance and its consequences. *Estuarine, Coastal and Shelf Science*, 40, 339-356.
- Kerr R.A., 2010. Ocean acidification unprecedented, unsettling. *Science*, 328, 1500-1501.
- Kont, A., Jaagus, J., Aunap, R., 2003. Climate change scenarios and the effect of sea-level rise for Estonia. *Global and Planetary Change*, 36(1), 1-15.
- Lian, G.S., Lin, Y.H., Cai, B.J., Lin, M., Dai, Y.Y., and Lin, J.H., 1990. Characteristics of zooplankton community in Daya Bay. In: Third Institute of Oceanology, State Oceanic administration (eds), Collections of papers on marine ecology in the Daya Bay (II). China Ocean Press, Beijing, China, p274-281.
- Lin, W.Q., and Li, S.Y., 2003. Three-D water quantity mathematical simulation of COD, DO, inorganic phosphorus and organic phosphorus in the Pearl River Estuary. *Acta Oceanologica Sinica* (in Chinese), 25(3), 129-137.
- Mu, X.Y., Yang, Y.L., Li, C.Y., Yin, X.C., Jia, J.J., and Xue, Y.C., 1999. Eenvironmental characteristics of seawater in the Yuehu inlet Rongcheng Bay, China. *Chinese Journal of Qingdao University*, 14(4), 57-59.
- Mumby, P. J., Edwards, A. J., Ernesto Arias-Gonzalez, J., Lindeman, K. C., Blackwell, P. G., Gall, A., Gorczyńska, M. I., Harborne, A. R., Pescod, C. L., Renken, H., Wabnitz, C.

- C. C., Llewellyn, G., 2004. Mangroves enhance the biomass of coral reef fish communities in the Caribbean. *Nature*, 427, 533-536.
- Olivieri, R.A., Chavez, F.P., 2000. A model of plankton dynamics for the coastal upwelling system of Monterey Bay, California. *Deep-Sea Research II*, 47, 1077-1106.
- Pearson, H., 2005. Scientists seek action to fix Asia's ravaged ecosystems. *Nature*, 433, 94.
- Peng, Y.H · Chen, H.R., Pan, M.X., Huang, H.H., Gao, H.L. 2001. The primary production and potential fishery production in the sea area around the Daya Bay Nuclear Power Station before and after the operation of DBNPS. *Journal of Fisheries China* (in Chinese), 25 (2), 161-165.
- Shen, Z.-L., 2001. Historical changes in nutrient structure and its influences on phytoplankton composition in Jiaozhou Bay. *Estuarine, Coastal and Shelf Science*, 52, 211-224.
- Sohma, A., Sekiguchi, Y., Yamada, H., Sato, T., and Nakata, K., 2001. A new coastal Marine ecosystem model study coupled with hydrodynamics and tidal flat ecosystem effect. *Marine Pollution Bulletin*, 43(7-12), 187-208.
- Sommer, U., Stibor, H., Katchakis, A., Sommer, F., Hansen, T., 2002. Pelagic food web configurations at different levels of nutrient richness and their implications for the ratio fish production: primary production. *Hydrobiologia*, 484(1-3), 11-20.
- Sommer, U., Lengfellner, K., 2008. Climate change and the timing, magnitude, and composition of the phytoplankton spring bloom. *Global Change Biology*, 14(6), 1199-1208.
- Souissi, S., Daly Yahia-Kéfi, O., 2000. Spatial characterization of nutrient dynamics in the Bay of Tunis (south-western Mediterranean) using multivariate analyses: consequences for phyto- and zooplankton distribution. *Journal of Plankton Research* 22(11), 2039-2059.
- Souter, D.W., and Linden, O., 2000. The health and future of coral reef systems. *Ocean and Coastal Management*, 43(8), 657-688.
- Tagliani, P.R.A., Landazuri, H., Reis, E.G., Tagliani, C.R., Asmus ML, Sanchez-Arcilla A., 2003. Integrated coastal zone management in the Patos Lagoon estuary: perspectives in context of developing country. *Ocean and Coastal Management*, 46(9), 807-822.
- Tang, D.L., Kester, D.R., Wang, Z.D., Lian, J.S., Kawamura, H., 2003. AVHRR satellite remote sensing and shipboard measurements of the thermal plume from the Daya Bay, nuclear power station, China. *Remote Sensing of Environment*, 84, 506-515.
- Turner, R.E., Rabalais, N.N., 1994. Coastal eutrophication near the Mississippi River delta. *Nature*, 368, 619-621.
- Wang, Y. S., Wang, Z.D., Huang, L.M., 2003. Changes in the ecological environment of Daya Bay and the trends in recent 20 years, [in:] Chinese Ecosystem Research Network (CERN), Center of Chinese Ecosystem Research Network (eds.), *Proc. 11th Chinese Ecosystem Research Network*, Sanya, China, 606-614.
- Wang, Y.S., Xu, J.R., Dong, J.D., Jiang, H.C., 2004. Ecological environment characteristics of thermocline and its kinetic mechanism in Daya Bay. In: Center of Chinese Ecosystem Research Network (eds), *Collections of chinese ecosystem research. Proc 12th Chinese Ecosystem Research Network*, Changsha, China, p 226-231.

- Wang, Y.S., Lou, Z.P., Sun, C.C., Wu, M.L., Han, S.H., 2006. Multivariate statistical analysis of water quality and phytoplankton characteristics in Daya Bay, China, from 1999 to 2002. *Oceanologia*, 48 (2), 193-211.
- Wang, Y.S., Lou, Z.P., Sun, C.C., Sun, S., 2008. Ecological environment changes in Daya Bay, China, from 1982 to 2004. *Marine Pollution Bulletin*. 56(11), 1871-1879.
- Wang Y.S., Sun C.C., Lou Z.P. et al. Identification of water quality and benthos characteristics in Daya Bay, China, from 2001 to 2004. *Oceanological and Hydrobiological Studies*, 2011, 40(1), 82-95.
- Wei G. F., Wang Z. D., Lian J. S., 2003. Succession of the dominant phytoplankton species in spring 2000 in at Dapeng' Ao cove, Daya Bay. *Acta Ecologica Sinica* (in Chinese), 32(11), 2285-2296.
- Wen, W.Y., Zou, R.L., Du, W.C., Huang, X.P., Zheng, Q.H., Zhang, G.X., Liang, Z.Q., Li, T.S., 1996. Impacts of warm effluent from the Dayawan nuclear power plant on stony coral community I. Stony community before the operation of the nuclear power plant. In: Pian, J.P., Cai, G.X. (eds), Annual research reports of MBRS(I). Science Press, Beijing, China, p18-22.
- Wu, M.L., Wang, Y.S., 2007. Using chemometrics to evaluate anthropogenic effects in Daya Bay, China. *Estuarine, Coastal and Shelf Science*, 72, 732-742.
- Wu, M.L., Wang, Y.S., Sun, C.C., Wang, H., Lou, Z.P., Dong, J.D., 2009a. Identification of water quality by using chemometrics in Daya Bay, China, *Oceanologia* 51 (2), 217-232.
- Wu, M.L., Wang, Y.S., Sun, C.C., Wang, H., Dong, J.D., Han, S.H., 2009b, Identification of anthropogenic effects and seasonality on water quality in Daya Bay, South China Sea, *Journal of Environmental Management*, 90, 3082-3090.
- Wu, M.L., Wang, Y.S., Sun, C.C., Wang, H., Dong, J.D., Yin, J.P., Han, S.H., 2010. Identification of coastal water quality by statistical analysis methods in Daya Bay, South China Sea. *Marine Pollution Bulletin*, 60, 852-860.
- Xue, C., 2002. The impact of human activities on mangrove coast of Kosrae Island, the federated states of Micronesia. *Transaction of Oceanology and Limnology* (in Chinese), 2, 17-23
- Xu, G.Z., 1989. Environments and resources of Daya Bay. Anhui Scientific and Technical Publishers, HeFei, China, p 8-9, 10-16.
- Yanez-Arancibia, A., Lara-Dominguez, A.L., Rojas Galaviz, J.L., Zarate Lomeli, D.J., Villalobos Zapata, G.J, Sanchez-Gil, P., 1999. Integrating science and management on coastal marine protected areas in the Southern Gulf of Mexico. *Ocean & Coastal Management*, 42,319-344.
- Yang, Q.L., 1990. Ecologic characteristics of phytoplankton community in Daya Bay. In: Third Institute of Oceanology, State Oceanic administration (eds), Collections of papers on marine ecology in the Daya Bay (II). China Ocean Press, Beijing, China, p 266-273.
- Yin, K., Qian, P.Y., Wu, M.C.S., Chen, J.C., Huang, L., Song, X., Jian, W.J., 2001. Shift from P to N limitation of phytoplankton biomass across the Pearl River Estuarine plume during summer. *Marine Ecological Progress Series*, 201, 65-79.
- Yin K., 2003. Influence of monsoons and oceanographic processes on red tides in Hong Kong waters. *Marine Ecology Progress Series*, 262, 27-41.

- Yung, Y. K., Wong, C.K., Yau, K., Qian, P.Y., 2001. Long-term Changes in Water Quality and Phytoplankton Characteristics in Port Shelter, Hong Kong, from 1988-1998. *Marine Pollution Bulletin*, 42(10), 981-992.
- Zang, M.C., 1993. Nuclear power programs in China. *Atomwirtschaft-Atometechnik* (in German), 38(6), 419-420.
- Zhao, S.J., Jiao, N.Z., Wu C.W., Liang, B., Zhang, S.Y., 2005. Evolution of nutrient structure and phytoplankton composition in the Jiaozhou Bay ecosystem. *Chinese Journal of Environmental Sciences*, 17(1), 95-102.
- Zheng, Q.H., He, Y.Q., Zhang, G.X., 2001. Impacting on the ecological environment and marine organism by waster water discharged to the sea in Daya Bay. In Pian, J.P., Wang, Z.D., Wu, X.Z. (eds), Annual research reports of MBRS (III): Science Press, Beijing, China, p10-15.
- Zhang, Q.M., 2001. Status of tropical biological coasts of China: implications on ecosystem restoration and reconstruction. *Oceanaologia and Limnologia Sinica* (in Chinese), 32(4), 454-464.
- Zhang, Y.L., Zhou, R.L., 1987. Community structure of shallow water stony corals in Daya Bay. *Chinese Journal of Tropical Oceanography*, 6(1), 12-18.
- Zhong, Z.X., Huang, Y.Y., Zhang, H.D., 1999. Research on primary productivity quantitative parameters and structure of mangrove community in Daya Bay of Guangdong Province. *Scientia Silvae Sinicae*, 35(2), 26-30.
- Zorini, L.O., Contini, C., Jiddawi, N., Ochiewo, J., Shunula, J., Cannicci, S., 2004. Participatory appraisal for potential community-based mangrove management in East Africa. *Wetlands Ecology and Management*, 12(2), 8 7-102
- Zhou, J.K., 1984. Factor analysis of the distributive relationship of the fish numbers in the Jiaozhou Bay. *Marine Science Bulletin* (in Chinese), 3(3), 58-67.

# Microbial Leaching of Uranium Ore

Hadi Hamidian

*Islamic Azad University, Qaemshahr Branch  
Iran*

## 1. Introduction

This chapter is a review of the microbiological leaching of uranium ores. Microbiological leaching has been used as an alternative approach to conventional hydrometallurgical methods of uranium's extraction. In the microbiological leaching process, iron-oxidizing bacteria oxidize pyritic phase to ferric iron and sulfuric acid, and uranium is dissolved from the ore due to sulfuric acid attack. If uranium in the ore material is reduced state and involves tetravalent form and a redox reaction is involved whereby uranium oxidized to the hexavalent form. Future sustainable development requires measures to be taken to reduce the dependence on non-renewable raw materials and the demand for primary resources. New resources for metals must be developed with the help of novel technologies. In addition, improvement of previously existed mining techniques can be resulted in metal recovery by the sources that have not been of economical interest up to today. The metal-winning processes based on the activity of microorganisms offer a possibility to obtain metals from mineral resources which are not accessible by conventional mining. Generally bioleaching is a process described as being "dissolution of metals from their mineral source by certainly and naturally occurring microorganisms" or "use of microorganisms to transform elements so that the elements could be extracted from a material when water is filtered through it". However, there are some slight differences in definition: Usually, "bioleaching" is described as the conversion of solid metal values into their water soluble forms using microorganisms. Bacterial leaching is the extraction of metals from their ores using microorganisms. The capital costs are low compared to those for a smelter. Environmental pollution caused by mineral processing is a serious problem and on the other hand, microorganisms play crucial roles in biogeochemical cycling of toxic metals and radionuclides. Recent progresses have been made to understand metal-microbe interactions and new applications of these processes to the detoxification of metal and radionuclide contamination have been developed. It also suggests an opportunity to reduce of environmental and air pollution by sulphur dioxide.

## 2. Historical review

One of the initial reports in which leaching might have been involved in mobilization of metals is given by the Roman writer Plinius Secundus. In his works on natural sciences, Plinius describes how copper minerals are derived by means of utilizing a leaching process. In cold weather during the winter the sludge freezes to the hardness of pumice. It is known

from experience that the most wanted chrysocolla is formed in copper mines, the following in silver mines. The Rio-Tinto mines in southwestern Spain are usually considered the cradle of biohydrometallurgy. These mines have been exploited since pre-Roman periods due to their copper, gold, and silver values. However, with respect to commercial bioleaching operations on an industrial scale, biohydrometallurgical techniques had been introduced to the Tharsis mine in Spain 10 years earlier. As a consequence of the ban of open-air ore roasting and its resulting atmospheric sulfur emissions in 1878 in Portugal, hydrometallurgical metal extraction has been taken into consideration in other countries more intensely. In addition to the ban, cost savings were another incentive for development: Heap leaching techniques were assumed to reduce transportation costs, allowing employment of locomotives and wagons for other services. From 1900 on, no open air roasting of low-grade ore was conducted at the Rio-Tinto mines. The researchers conducted on microbial leaching indicate an increasing rate of recovery and solubility of metals in direct, indirect, Thiosulfate and Polysulfide mechanism, due to microorganism activity. The initial work on uranium bioleaching in the early 1950s was taken to prevent solubilization, but it soon became apparent that this process could be applied for a commercial scale to extract uranium for low-grade ores. During 1952 and 1953, the plant at Urgeirica started a uranium heap leaching process on a commercial scale. This is an early turning point in the microbiological leaching of uranium ores.

Harrison et al. (1966) reported the role of the iron oxidizing *Acidithiobacillus ferrooxidans* in leaching of uranium. The uranium ore was stacked in heaps, similar to dump leaching of low-grade copper ore, and leached using an acidic ferric sulfate solution at the Elliot Lake Mine, Ontario, Canada. The presence of the bacteria in the heaps was discovered and their role in maintaining oxidizing conditions by conversion of ferrous to ferric iron for extraction of the uranium was defined. Guay's (1976) investigations showed that the effectiveness and efficiency of microorganism's influence, such as *Thiobacillus*, requires the presence of certain amount of iron. He also conducted some research on mixing level, aiersion, and oxidation rate of iron that may affect uranium's microbial leaching. He employed a specific type of microbes such as *Thiobacillus* in his study. Amongst the various parameters affecting the sufficiency of microbial leaching; he just focused upon the aforementioned parameters. Brierley (1980), one of the distinguished researchers in microbial leaching, has done a case study on uranium ore (coffinite and uraninite) in Gerantez mine in Canada. His investigation's outcomes demonstrated a promising and positive effect of *Thiobacillus ferrooxidans* in climbing recovery rate of uranium. Cerda's studies (1991) on Pitchblende ore in green-grayish shiest samples, collected from Spain's mines, revealed a close relationship of pyrite and Chalcopyrite in reduction of acid consumption in microbial leaching, in comparison with regular leaching. In continuous surveys carried out over on microbial leaching by different researchers. Gonzalez (1993) utilized column leaching, seepage and shaking table to study the effect of pyrite amount in uranium's microbial leaching. His investigation's results showed an augmenting trend of uranium recovery while there is an optimum amount of pyrite. Beyond the optimum level of pyrite, not only the pyrite presence is not beneficiary, but also it may introduce complicity in leaching process. He has also done some research on pH optimization, temperature, and stirred time. In a case study conducted by Junior (1993) on uranium ore in Figopira in Brazil, potentiality of microbial leaching in uranium recovery enhancement has been emphasized. Schipper's (1995) study on two mines in Germany indicated the identification of microbe variety in



waste materials. The waste materials (low grade black Schist) consisted of 0.05% of uranium and 0.5 to 7% of carbonate. Sampling showed the microorganisms aerobic and anaerobic were present till 1.5 to 2 meter of surface depth and more than 99% of *Thiobacillus ferrooxidans* were present within this depth. In this study, there was no investigation on microbial leaching capability and identification of microbes was just concerned. Munoz (1995), dedicated researcher in uranium's microbial leaching in Spain, has presented his research's results in many published papers in Elsevier. Bioleaching process, mineralogy of uranium ore, bearing rock type, level of toxic material, and leaching variables are among the factors which have been probed by him. He has worked on pitchblende ore with 0.097 % uranium content. Leduc, L.G. (1997) studied ten different isolated of *Thiobacillus ferrooxidans* with regard to their degree of resistance to the metals copper, nickel, uranium, and thorium. The miscellaneous isolates had different susceptibilities to the tested metals, and moreover none of the metals had a stimulus effect. Uranium and thorium were 20 to 40 times more toxic to ferrous iron oxidation than either copper or nickel. Mathur A.K. (2000) investigated the application of ferric ion as an oxidant and in combination with other anions such as ferric sulfate or chloride as a leachant is well accepted for recovery of metals, particularly from ores of copper, cobalt, nickel, zinc and uranium. Biogenically generated ferric sulfate that has been in vogue for many dump and heap leaching operations, to recover uranium and copper values. Hefnawy (2001) used fungi for Aloga uranium ore bioleaching in Egypt. The amount of uranium solubilized by *A. terreus* and *P. spinulosum* was increased by intensifying ore concentrations on the growth media, reaching its maximum at 4 % (w/v). Whereas, the highest percentage of uranium released by both fungi was obtained at 1 % (w/v), in this concentration the released uranium being 75 and 81.5% respectively for ore and 72.8 and 77.6% respectively for the second ore. The best leaching occurs when the final pH shifts toward acidity. The biosorption of released uranium by fungal Mycelium was also increased by augmenting ore concentrations on the growth media. Kalinowski and Oskarsson (2002) represented common ligand producing bacterial species (*Pseudomonas fluorescens*, *Shewanella putrefaciens* and *Pseudomonas stutzeri*) were incubated in a chemically defined medium supplemented U-ore that had been exposed to natural weathering conditions for 30 years having a content of 0.0013 % U by weight. For comparison, non-leached uranium ore (0.61 % U by weight) from the same area were incubated by *P. fluorescens* and *S. putrefaciens*. *P. fluorescens* is the only species that thrives and manages to mobilize measurable amounts of uranium from the two ores. Despite the extensive increase in pH from 4.7 to 9.3 *P. fluorescens* supplemented with ore manages to mobilize 0.001-0.005 % of the total amount of U from both ores. The release of U was interpreted to be attributed to the production of pyoverdine chelators, which is a typical ligand produced by fluorescent pseudomonades, as U could not be detected in either sterile controls or in experiments with the two other bacteria. In Sumera Saeed (2002) investigation the bioleaching behavior of rock phosphate (Jordan imported) was studied using different strains of *Aspergillus niger*. X-ray diffraction analysis revealed the presence of fluorapatite [ $\text{Ca}_2(\text{PO}_4)_3\text{F}$ ] as the main source of phosphorus. Average content of phosphorus in testing ore was 33.6% scanning electron microscope showed the presence of significant amount of phosphorus. Decrease in pH was observed due to organic acids produced by *Aspergillus niger* strains during growth on liquid media containing glucose. Akcil (2004) represented an investigation of the potential bioleaching developments in Turkey [27]. Bene Ditto (2005) in his study identified sulfur reduction bacteria in Brazil uranium mine water. This is basically

problem in Brazil nuclear industrial. Choi Moon-sung (2005), schist with 0.01 %  $U_3O_8$  content in S. Korea under study. He could reach 0.8 uranium recovery with use *Acidbacillus ferrooxidans*. Jong un lee (2005), the effects of several conditional factors on efficiency of U bioleaching via using an iron-oxidizer, *Acidithiobacillus ferrooxidans*, from U-bearing black shale (349 ppm of U) were investigated. In the case inoculated with the cells, lower pH, higher redox potential and higher amount of aqueous  $Fe^{3+}$  than those of non-inoculated reactor observed until 200h. Such development of condition, which was facilitated by microbial activity, can enhance the rate and extent of U leaching from the solid substrate.

### 3. Bioleaching mechanisms

There are two major mechanisms of bacterial leaching. One involves the ferric-ferrous cycle (indirect or non-contact mechanism), while the other involves physical contact of the organism with the insoluble sulphide (direct or contact mechanism) and is independent of indirect mechanism. Originally, a model with two types of mechanisms which are involved in microbial mobilization of metals has been proposed:

#### 3.1 Direct mechanism

Microorganisms can oxidize metal sulfides by a direct mechanism obtaining electrons directly from reduced minerals. Cells have to be attached to the mineral surface and a close contact is needed. Bioleaching of metal sulfides (MS) can be achieved in direct and indirect modes of bacterial metabolism. Figure 1 (a) shows a scheme of the reaction mechanism for the bio-oxidation of sulphide minerals-direct mechanism. The direct mechanism is given by:



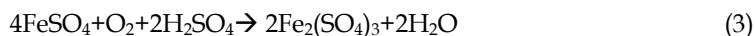
Where M is a bivalent heavy metal.

The following equations describe the "direct" mechanism for the oxidation of pyrite:



#### 3.2 Indirect mechanism

The oxidation of reduced metals through "indirect" mechanism is mediated by ferric iron ( $Fe^{3+}$ ) originating from the microbial oxidation of ferrous iron ( $Fe^{2+}$ ) compounds present in minerals. Ferric iron is an oxidizing agent and can oxidize, e.g., metal sulfides and is chemically reduced to ferrous iron which, in turn, can be oxidized microbial again. In this case, iron has a role as electron carrier. It was proposed that no direct physical contact is needed for oxidation of iron. Figure 1 (b) shows a scheme of the reaction mechanism for the bio-oxidation of sulphide minerals-indirect mechanism.



The indirect mechanisms can be demonstrated, i.e., for uranium leaching as follows:



However, the model of “direct” and “indirect” metal leaching is still under discussion. Recently, this model has been revised and replaced by another one which is not dependent upon differentiation between a “direct” and an “indirect” leaching mechanisms.

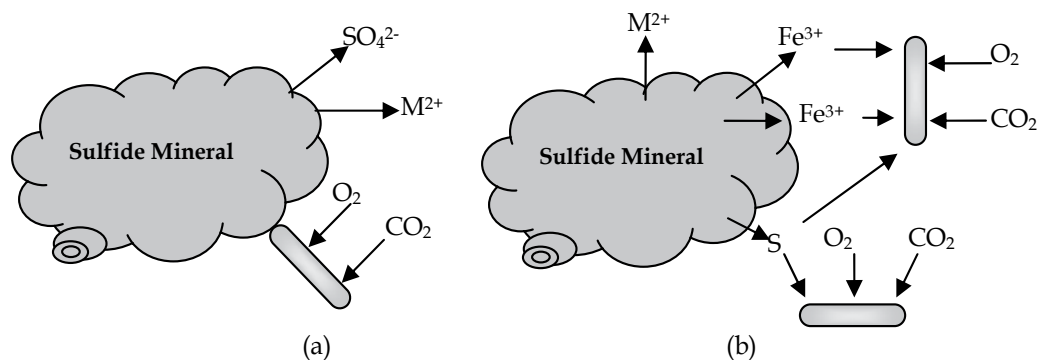
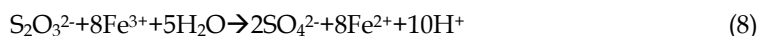
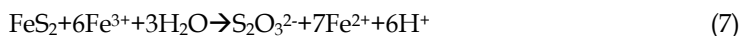


Fig. 1. The reaction mechanism for the bio-oxidation of sulfide minerals (a) Direct mechanism -, (b) Indirect mechanism

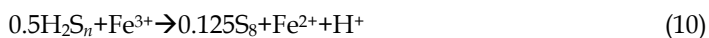
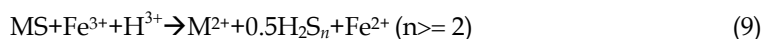
### 3.3 Thiosulfate mechanism

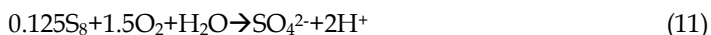
The mineral dissolution reaction is not identical to all metal sulfides and the oxidation of different metal sulfides proceeds via different intermediates. This also has been recently reviewed. Briefly, a thiosulfate mechanism has been proposed for oxidation of acid insoluble metal sulfides such as pyrite ( $\text{FeS}_2$ ) and molybdenite ( $\text{MoS}_2$ ), and a polysulfide mechanism for acid soluble metal sulfides such as sphalerite ( $\text{ZnS}$ ), chalcopyrite ( $\text{CuFeS}_2$ ) or galena ( $\text{PbS}$ ). In the thiosulfate mechanism, solubilization is through ferric iron attack on the acid-insoluble metal sulfides with thiosulfate being the main intermediate and sulfate the main end-product. Using pyrite as an example of a mineral, the reactions may be represented as [35, 36]:



### 3.4 Polysulfide mechanism

Polysulfide and elemental sulfur are the main intermediates in the “polysulfide mechanism” during oxidation of galena, sphalerite, chalcopyrite, hauerite, orpiment and realgar. The presence of iron (III) at the beginning of mineral degradation is an important prerequisite. In the case of the polysulfide mechanism, solubilization of the acid-soluble metal sulfide is through a combined attack by ferric iron and protons, with elemental sulfur as the main intermediate. This elemental sulfur is relatively stable but may be oxidized to sulfate by sulfur-oxidizing microbes such as *Acidithiobacillus thiooxidans* or *Acidithiobacillus caldus* according to reaction 11:





The ferrous iron produced in reactions (9), (10) may be reoxidized to ferric iron by iron-oxidizing microorganisms such as *Acidithiobacillus ferrooxidans* or bacteria of the genera *Leptospirillum* or *Sulfobacillus*.



The role of the microorganisms in the solubilization of metal sulfides is, therefore, to provide sulfuric acid (reaction 11) for a proton attack and to keep the iron in the oxidized ferric state (reaction 12) for an oxidative attack on the mineral.

## 4. Influenced factors on uranium microbial leaching

### 4.1 Diversity of microbial culture

In general, types of microorganisms found in heap leaching processes are similar to those found in stirred tank processes, however, the proportions of the microbes may vary depending on the mineral and the conditions under which the heaps or tanks are operate. In processes that operate from ambient temperatures to about 40°C, the most important microorganisms are considered to be a consortium of Gram-negative bacteria. These are the iron- and sulfur-oxidizing *Acidithiobacillus ferrooxidans*, the sulfur-oxidizing *Acidithiobacillus thiooxidans* and *Acidithiobacillus caldus*, and the iron-oxidizing leptospirilli, *Leptospirillum ferrooxidans* and *Leptospirillum ferriphilum*. Consortia of acidophilic thiobacilli and leptospirilli are believed to be superior to pure cultures for the biological oxidation of sulfide minerals. Microbial diversity is extensive in acid mine waters, including uranium mine leaching solutions. While moderately acidophilic thiobacili is numerous, thermo acidophilic archaea, resembling *Sulfolobus* and *Acidianus*, has been isolated from uranium-mine waste heaps.

### 4.2 Mineralization of uranium

Another important factor of bioleaching is the mineralization of the uranium. Table 1, 2 show the results of different uranium ores which are subjected to bioleaching. According to this, oxides, phosphates, sulfates and carbonates are solubilized relatively convenient, while dissolution of silicates is difficult or even impossible.

Uranium oxide	Valence	Natural form	Solution ability
UO <sub>2</sub>	IV	Uraninite	Insoluble
U <sub>2</sub> O <sub>5</sub>	IV	-	Little soluble
U <sub>3</sub> O <sub>8</sub>	IV,VI	Pitchblende	Little soluble
UO <sub>3</sub>	VI	Carnotite	Soluble

Table 1. The type of uranium oxides in nature [40]

Uranium ores	Chemical composition	Degree of bioleaching
<i>Uraninite</i>	UO <sub>2</sub>	+
<i>Gummite</i>	UO <sub>3</sub> -nH <sub>2</sub> O	+
<i>Becquerelite</i>	CaU <sub>6</sub> O <sub>19</sub> -11H <sub>2</sub> O	+
<i>Brannerite</i>	(U,Ca,Ce)(Ti,Fe)O <sub>6</sub>	+
<i>Davidite</i>	(Fe,Ce,U) <sub>2</sub> (Ti,Fe,V,Cr) <sub>5</sub> O <sub>12</sub>	+
<i>Coffinite</i>	U(SiO <sub>4</sub> ) <sub>1-x</sub> (OH) <sub>4x</sub>	-
<i>Uranophane</i>	Ca(UO <sub>2</sub> ) <sub>2</sub> Si <sub>2</sub> O <sub>7</sub> -6H <sub>2</sub> O	+ -
<i>Sklodowskite</i>	Mg(UO <sub>2</sub> ) <sub>2</sub> Si <sub>2</sub> O <sub>7</sub> -6H <sub>2</sub> O	+ -
<i>Autunite</i>	Ca(UO <sub>2</sub> ) <sub>2</sub> (PO <sub>4</sub> ) <sub>2</sub> -12H <sub>2</sub> O	+
<i>Torbernite</i>	Cu(UO <sub>2</sub> ) <sub>2</sub> (PO <sub>4</sub> ) <sub>2</sub> -8H <sub>2</sub> O	+
<i>uramphite</i>	NH <sub>4</sub> -UO <sub>2</sub> -PO <sub>4</sub> -3H <sub>2</sub> O	+
<i>Zeunerite</i>	Cu(UO <sub>2</sub> ) <sub>2</sub> (AsO <sub>4</sub> ) <sub>2</sub> -12H <sub>2</sub> O	+
<i>Carnotite</i>	K <sub>2</sub> (UO <sub>2</sub> ) <sub>2</sub> (VO <sub>4</sub> ) <sub>2</sub> -3H <sub>2</sub> O	+ -
<i>Tyuyamunite</i>	Ca(UO <sub>2</sub> ) <sub>2</sub> (VO <sub>4</sub> ) <sub>2</sub> -8H <sub>2</sub> O	+ -
<i>Zippeite</i>	(UO <sub>2</sub> ) <sub>2</sub> (SO <sub>4</sub> )(OH) <sub>2</sub> -4H <sub>2</sub> O	+
<i>Uranopilite</i>	(UO <sub>2</sub> ) <sub>6</sub> SO <sub>4</sub> (OH) <sub>10</sub> -12H <sub>2</sub> O	+
<i>Johannite</i>	Cu(UO <sub>2</sub> ) <sub>2</sub> (SO <sub>4</sub> ) <sub>2</sub> (OH) <sub>2</sub> -H <sub>2</sub> O	+
<i>Schroekingerite</i>	NaCa <sub>3</sub> UO <sub>2</sub> SO <sub>4</sub> (CO <sub>3</sub> ) <sub>3</sub> F-10H <sub>2</sub> O	+
<b>Urano-organic Compounds</b>		+
<b>+: easy , -: hard , + -: variable</b>		

Table 2. Uranium mineralization and bioleaching.

### 4.3 Country rock type

The bioleaching process also depends upon nature of the country rock. If this is alkaline, it is probable that precipitates would be formed which would lead to causing problem to natural percolation of the leaching. This issue lowers the uranium yield because some pockets of ore are not attacked. On the other hand, when the country rock is acidic, acid consumption by the rock will be low.

### 4.4 Nutrient element

The quantity of nutrient element content in the country rock is an important aspect for microbial leaching. The solid medium should supply at least adequate minerals to microorganism growth of not being stopped. The presence of organic compounds (yeast extract) inhibited pyrite oxidation from *Thiobacillus ferrooxidans*. Certain metals presented in bioleaching environments can inhibit microbial growth; therefore, these metals cause leaching efficiencies to reduce. Based on dry weight, nitrogen is the most important following element after carbon for the synthesis of new cell mass. In commercial operations, inexpensive fertilizer grade ammonium sulfate is typically added to biooxidation tanks or bioleaching heaps to ensure that sufficient nitrogen is available.

### 4.5 Toxic material and resistance to metals

Additions of copper, nickel, uranium, or thorium adversely influenced iron (II) oxidation by *Acidithiobacillus ferrooxidans* with uranium and thorium showing higher toxicities than

copper and nickel. Silver, mercury, ruthenium, and molybdenum reduced the rate of growth of *Sulfolobus* grown on a copper concentrate. Resistance to metal ions is a function of those thiobacilli tested to date. *Acidithiobacillus ferrooxidans* is resistant to a variety of metal ions such as chromium, copper, zinc, nickel, thorium, uranium and mercury. The resistance of *Acidithiobacillus ferrooxidans* to mercury is ferrous iron dependent.

#### 4.6 Temperature

Temperature is among the most important parameters influencing the diversity of the microbial communities. Use of thermophiles was found to improve metal sulfide biooxidation in at least two ways. First, reaction rates increased with increasing temperature. Second, elevated temperature increased the extent of metal extraction from certain minerals. Bioleaching processes are carried within range of temperatures from ambient to a demonstration plant that has been operated at 80°C. Temperature ranges of 2-35°C and 4-21°C, respectively, were observed. Moderately thermophiles iron-oxidizing and sulfur-oxidizing bacteria were initially cultured from mining environments and hot springs. However, psychrophiles have not been isolated from cold tailing effluents where they would be expected. The temperature used for bioleaching in most of studies is 35°C. Although *Acidithiobacillus ferrooxidans* was reported to grow most rapidly at 30°C, it oxidised iron faster at 35°C. This case has crucial implications for industrial bioleaching since the oxidation of sulphides is exothermic, and hence cooling may be essential to maintain a satisfactory industrial process. As it is expected the types of presented iron and sulfur-oxidizing microbes differentiation depending upon temperature range. The types of microbes found in processes operating from ambient to 40°C tend to be similar irrespective of mineral, as are those within the temperature ranges 45-55°C and 75-80°C. As described below, there are two broad categories of biologically-assisted mineral degrading processes. An ore or concentrate is either placed in a heap or dump where it is irrigated or a finely milled mineral suspension is placed in a stirred tank where it is vigorously aerated. In general, mineral solubilization processes are exothermic and when tanks are used, cooling is required to keep the processes that function at 40°C at their optimum temperature. At higher temperatures the chemistry of mineral solubilization is much faster and in the case of minerals such as chalcopyrite, temperatures of 75-80°C are required for copper extraction to take place at an economically viable rate. Table 3 shows a Classification of chemolithotrophic bacteria in terms of their optimum temperature ranges.

Bacterial class	Optimum temp. range /°C
Cryophiles	< 20
Mesophiles	20-40
Moderate thermophiles	40-55
Extreme thermophiles	> 55

Table 3. Classification of chemolithotrophic bacteria in terms of their optimum temperature ranges.

#### 4.7 Pyrite content

Pyrite plays a key role in many biooxidation operations. Its oxidation produces acidity, heat and dissolved iron. Pyrites vary greatly in their chemical and biological reactivity. It also is

associated with many ores, including zinc, copper, uranium, gold and silver. Pyrite is formed in a reducing environment with a continuous supply of sulphates and iron in the presence of easily decomposable organic matter. In general, microbiological leaching processes of uranium have been applied to the ores that contain accessory Fe-sulfides. The pyrite content of the ore is important and that is why this type of attack has not been widely utilized in extraction of uranium from its ores since the technology is limited to minerals with highly sulfide content. The ores from eastern Canada are especially susceptible to this kind of process since pyrites are associated with uranium. On the other hand the uranium ores along with low pyrite content are less suitable for microbial leaching. In this case, the suitable quantity of pyrite has to be added in medium.

#### 4.8 Hydrogen ion concentration (pH)

Microorganisms that biooxidize sulfide minerals at low pH are resistant to acidic conditions and most heavy metals in process solutions. Typically, microbial cultures are pre-grown or adapted to a particular ore feed in the laboratory or pilot plant. From an industrial perspective it is essential that biomining microorganisms are able to grow at low pH and tolerate high concentrations of acid. Two important reasons for this are to enable iron cycling and to permit reverse electron transportaion to take place. The optimum pH for *Acidithiobacillus ferrooxidans* is between 2-3, but when the substrate is in large part pyretic, the pH can reach extremely low values, (less than 1). This is because of the availability of abundant sulphur and the precipitation of ferric hydroxide when the solution reaches saturation. *Acidithiobacillus caldus* is a single mixotrophic species which can utilise sulphur or tetrathionate and yeast extract or glucose. Blais et al. (1993) have demonstrated that less acidophilic bacteria in sludge such as *Thermithiobacillus tepidarius*, *T. aquaesulis*, *T. denitrificans*, *T. thioparus* and other species formerly placed in *Thiobacillus*, may initiate the acidification to the point where the acidophilic species can take over. Acidophilic bacteria decreased the pH of a sulphur-containing synthetic salts medium to the level of 1.4-1.6 during 10 days. Table 4 shows pH range for *Acidithiobacillus* culture.

Microorganism	Optimum pH	pH Range
<i>Acidithiobacillus albertensis</i>	3.5-4	2-4.5
<i>Acidithiobacillus ferrooxidans</i>	2.0-2.5	1.3-4.5
<i>Acidithiobacillus thiooxidans</i>	2.0-3.0	0.5-5.5
<i>Acidithiobacillus caldus</i>	2.0-2.5	1.0-3.5

Table 4. pH range for *Acidithiobacillus* culture

Mine spoils which were alkaline in nature (pH=9), with low sulphur content and a highly concentration of chlorides tended to be free of *Acidithiobacillus ferrooxidans*. The limiting pH value for growth of *Acidithiobacillus ferrooxidans* in rock material and drainage was found to be about 7.2.

#### 4.9 Aerobic/anaerobic growth

Aeration of the solution or slurry is important in all bacterial oxidation processes using obligately acidophilic bacteria cultures. If the oxygen concentration falls to low levels, less than 0.5 to 1.0 mg L<sup>-1</sup> for processes carried out in stirred vessels, the culture will normally revert in to its lag phase and the bacterial process stop. A lack of carbon dioxide restricts the culture growth and could limit the rate and amount of reaction of the sulphide mineral.

Acidithiobacillus species are strict aerobes with the exception of Acidithiobacillus ferrooxidans, which is a facultative aerobe. In the absence of oxygen, Acidithiobacillus ferrooxidans is able to grow on reduced inorganic sulphur compounds using ferric iron as an alternative electron acceptor. The volume of air that must be supplied is based on the sulfide oxidation required. For example, at Wiluna in Western Australia, about 8 t air was supplied per tonne of concentrate, at typical oxygen utilization efficiencies of 25%. Aeration of bioheaps can accelerate biooxidation reactions, reducing leach cycle time. Air may be delivered via a network of pipes installed in a gravel layer at the base of heaps.

### 5. Microbial leaching and environmental

Environmental pollution caused by mineral processing is a serious problem; however, microorganisms play crucial roles in bioremediation of toxic metals and radionuclides, and thus are very much involved in resolving such problems. In this technology, microorganisms or their constituents such as enzymes are used to degrade or transform the soil. Much progress has been made with regard to understanding processes involving metal-microbe interactions and new applications of such processes to the detoxification of metal and radionuclide contamination have been developed. Such processes also provide an opportunity to reduce levels of sulphur dioxide polluting the environment and air (Lloyd, 2001, 2002, Morin, 2006). The Gram-negative eubacterium Acidithiobacillus ferrooxidans is important for industry and ecology because firstly, it is capable of solubilizing metals from ores, such as copper, uranium, and cobalt, and decomposing recalcitrant gold-containing ores. Secondly, this bacterium is able to remove heavy metals from contaminated industrial effluents or soils and desulfurize fossil fuels to avoid corrosion and atmospheric acid depositions (Corinne Appia-ayme, 1999). Chemical approaches are available for metal remediation, but are often expensive to apply and lack the specificity required to treat target metals against a background of competing ions. In addition, such approaches are not applicable to cost-effective remediation of large-scale subsurface contamination *in situ*. Biological approaches, on the other hand, offer the potential for the highly selective removal of toxic metals coupled with considerable operational flexibility; they can be used *in situ* in a range of bioreactor configurations (Lloyd, 2001).

### 6. Discussion and conclusions

The performed investigation into microbial leaching signifies enhancing of metals recovery particularly gold, uranium, copper and zinc, due to microorganism activity in comparison with traditional leaching method. In parallel with the recovery augmenting, utilization of microbial methods as compared with ordinary method like roasting is more environmentally friendly and its cost will be less. Hence, commercial applications in South Africa, Australia, South America, Spain, India and china are increasing in the last two decades. In most of executed operations within laboratory and commercially scale,



autotrophic bacteria's have been utilized which belong to bacillus species. Nowadays, investigation on new and other microorganism, mixed culture and fungi's is underway in order to probe their function and viability. The appropriately microbe type selection is too important in microbial leaching operations because the rate of being successful is mainly dependent upon environmental conditions, characteristics of mineralogy, country rock and the requisite technique in a way that there might be different results due to using a microbe type for two similar minerals along with divergent environmental conditions. On the other hand, microbial leaching methods include miscellaneous techniques involving; in-situ, dumps, heap, vat and stirred which making use of each of them is dependent on the metal grade, time and capacity. In order to secure the stable supply of raw materials for the industrial needs, it is necessary to develop noble recovery technology of valuable metals from refractory and low-grade mineral ore deposits, intermediate metallurgical products, and waste. Then, it is essential to find methods to treat the ores economically and environmentally to recovery valuable metal. The researches did on Microbial leaching indicating an increase in rate of metal recovery and solubility through direct, indirect, thiosulfate and polysulfide mechanism, due to microorganism activity. Generally, microbial leaching is able to process low grade and marginal ores, mining and industrial waste which couldn't be processed by other methods including gravity, electrical, magnitude and physiochemical methods. Hence this capability causes mineral ores tonnage to increase. Another advantage of microbial leaching is to use of microorganism and metal metabolically and potentially in order to decrease water and land pollution and control environmental damages. Microorganism could help to selective solution of metals through penetrating into the molecular structure of the materials, breaking existing bond and forming free ions or new compounds.

Regarding nature of uranium mineralization which are generally low grade in most cases (160 cases in the crust), and considering this fact that conventional processing methods won't be feasible for this low metal content, researches conducted to microbial leaching of uranium ores such as oxides and phosphate like Pitchblende, Uraninite, Cafinite, Gomitite, Uranium shale.

## 7. Reference

- [1] O.H, Touvinen and T.M. Bhattit, "Microbiological Leaching of Uranium Ore", Mineral Biotechnology, SME, P.P. 101-115, 2002.
- [2] Brandl Helmut, "Microbial Leaching of Metals", Zurich, Switzerland, P.P. 192-214, 2001.
- [3] Arpad E. Torma, "Mineral Bioprocessing", international Conference and Workshop Applications of Biotechnology to the Minerals Industry, South Austral, pp. 1-1 to 1-10, 1993.
- [4] Corale L. Brierley, "Biogenic Extraction of Uranium From Ores of the Grants Region", Bioextractive Applications and Optimization, PP.345-351, 1980.
- [5] Devasia P . & Natanajan K.A., " Leaching , Biotechnology in the Mining Industry " Resonance public , P.P. 24- 34 , 2004.
- [6] Liyod Jonathan R & Derek R Lovley, "Microbial Detoxification of Metals and Radionuclides", Elsevier Science Ltd. All rights reserved, Current Opinion in Biotechnology, 12:248-253, 2001.
- [7] Liyod Jonathan R., "Bioremediation of Metal; the Application of Micro-organisms that Make and Break Mieral", Microbiology Today, Vol. 29, 67-69, 2002.

- [8] Morin D., Lips A., Pinches A., Huisman J., Frias C., Norberg A., Forssberg E., "Bio-Mine Integrated Project for the Development of Biotechnology for Metal-Bearing Materials in Europe", Elsevier, Hydrometallurgy 83, PP. 69-76, 2006.
- [9] Harrison VF., Gow WA., Ivarson KC., "Leaching of uranium from Elliot Lake ore in the presence of bacteria", Can Mineral J, No. 87, PP:64-67, 1966.
- [10] Guay R., M. Silver and E. Torma, "Microbiological Leaching of a low-grade Uranium ore by Thiobacillus ferrooxidans", Applied Microbiology and Biotechnology, P.P. 157-167, 1976.
- [11] Guay R., M. Silver, A.E. Torma, "Ferrous Iron Oxidation and Uranium Extraction by Thiobacillus Ferrooxidans", Biotechnical Bioeng, 19(5), P.P. 727-740, 1977.
- [12] Cerda j., Gonzalez ,S.Rios ,J.M. and Quintana, "Uranium Concentrates Bio Productions in Spain. ( A case study )", bio hydro metallurgy 91 , Trioa, Portugal, p.p.24 ,1991.
- [13] Cerdá J., S. González, J. M. Ríos and T. Quintana, "Uranium concentrates bioproduction in Spain: A case study", Elsevier, FEMS Microbiology Reviews, Volume 11, Issues 1-3 , Pages 253-259 , 1993.
- [14] Gonzales F., J.A. Munoz, A.Ballester, M.L.Blazquez, Bioleaching of a Spanish uranium ore, FEMS Microbiology Reviews 11(1-3), PP. 109-119, 1993.
- [15] O.Garsia Junior, "Bacterial Leaching of Uranium ore from Figueira- PR, Brazil, at laboratory and pilot scale", FEMS Microbiology Reviews 11(1-3), P.P. 237-242, 1993.
- [16] Schippers A., Hallmann R. Wentzien S., "Microbial Diversity in Uranium Mine Waste Heaps", Applied and Environmental Microbiology , P.P. 2930-2935, 1995.
- [17] Schippers Axel and Wolfgang Sand, "Bacterial Leaching of Metal Sulfides Proceeds by Two Indirect Mechanisms via Thiosulfate or via Polysulfides and Sulfur", 1998.
- [18] Manoz J. A. , F. Gonzalez , M. L. Blazquez , A. Ballester, " A Study of the Bioleaching of a Spanish Uranium ore. Part I : A Review of the Bacterial leaching in the Treatment of Uranium arcs.," Elsevier , hydrometallurgy , PP. 39 - 54 , 1995.
- [19] Manoz J. A. , F. Gonzalez , M. L. Blazquez , A. Ballester, " A Study of the Bioleaching of a Spanish Uranium ore. Part II Orbital Shaker Experiments," Elsevier, hydrometallurgy, PP. 59 - 73, 1995.
- [20] Manoz J. A. , F. Gonzalez , M. L. Blazquez , A. Ballester, " A Study of the Bioleaching of a Spanish Uranium ore. Part III : Column Experiment.," Elsevier , hydrometallurgy , PP. 78 - 97 , 1995.
- [21] Klaus Bosecker, "Bioleaching: Metal Solubilization by Microorganisms", FEMS Microbiology Reviews ,Volume 20, Issues 3-4 , Pages 591-604, 1997.
- [22] Leduc, L.G., G.D. Ferroni and J.T. Trevors, "Resistance to heavy metals in different strains of Thiobacillus ferrooxidans", World Journal of Microbiology and Biotechnology 13, 453-454, 1997.
- [23] A.K. Mathur, K. Viwamohan, K.B. Mohanty, V.K. Murthy and S.T. Eshadrinath, " Uranium Extraction Using Biogenic Ferric Sulfate a Case Study on Quartz Chlorite Ore from Jaduguda, Singhbhum Thrust Belt (STB), Bihar, India", Minerals Engineering, Vol. 13, No. 5, PP. 575-579, 2000.
- [24] Hefnawy M.A. , M . El - said , M . Hussain and Maisa , A . Amin, "Fungal Leaching of Uranium from its Geological ore in Auoga Area , West Central Sinai , Egypt ",on line Journal of Biological Sciences 2 , PP. 346 - 350, 2002.
- [25] Kalinowski Birgitta E. and Oskarsson Anna, " Bioleaching of Heavy Metals from pristine and naturally Leached Uranium Ore from the Closed Mine at Ranstad, Southern sweden", Geomicrobiology, Denver Annual Meeting, Session 5, 2002.

- [26] Sumera Saeed, Haq Nawaz Bhatti and T. M. Bhatti, "Bioleaching Studies of Rock Phosphate Using *Aspergillus niger*", *OnLine Journal of Biological Sciences* 2(2): 76-78, 2002.
- [27] A. Akcil, "Potential bioleaching developments towards commercial reality: Turkish metal mining's future", *Minerals Engineering*, PP. 477-480, 2004.
- [28] Bene ditto J.S. , AL meida S.K. de, Gomes H.A. , Vazoller R.F. , Monitoring of sulfate-Reducing bacteria in acid Water from uranium mines , Elsevier , *Mineral Engineering* , PP. 1341-1343, 2005.
- [29] Choi Moon-song , cho kyung-suk , kim dung-su , Ryu Hee-wook, "Bioleaching of Uranium from Low Grade Black Schist's by *Acidithiobacillus f.* , *world journal of Microbiology and biotechnology* , volume 21, number 3 , p.p. 377-380, 2005 .
- [30] Jong un lee , Sung Min Kim , Kyoung Woong Kim , In S. Kim, "Microbial Removal of Uranium in Uranium-bearing Black Shale" , Elsevier , *Chemosphere* , PP. 147-154, 2005.
- [31] Rohwerder T, Gehrke T, Kinzler K, Sand W., "Bioleaching review part A: Progress in bioleaching: fundamentals and mechanisms of bacterial metal sulfide oxidation", *Appl Microbiol Biotechnol*, 2003.
- [32] Barrett J. , Hughes M. N. , Kaavaiko G. I. , Spencer P.A., " Metal Extraction by Bacterial Oxidation of mineral " , Ellis Harwood limited, P.P. 127-134, 1993.
- [33] Korean Geography Resource Research Center, "Study on Environment-friendly Treatment Technology of Refractory Minerals", 2003.
- [34] Sand W, Gehrke T, Hallmann R, Schippers A., "Sulfur chemistry, biofilm, and the (in)direct attack mechanism - critical evaluation of bacterial leaching", *Appl Microbiol Biotechnol*, 43:961-966, 1995.
- [35] Douglas E Rawlings, "Characteristics and Adaptability of Iron-and Sulfur-Oxidizing Microorganisms Used for the Recovery of Metals from Minerals and their Concentrates", *Microbial Cell Factories*, [http://www .microbialcellfactories.com](http://www.microbialcellfactories.com), 2005
- [36] Douglas Eric Rawlings, "Microbially Assisted Dissolution of Minerals and its Use in the Mining Industry", *Pure Appl. Chem.*, Vol. 76, No. 4, PP. 847-859, 2004.
- [37] Sand W, Gehrke T., "Analysis and function of the EPS from the strong acidophile *Thiobacillus ferrooxidans*. In: Wingender W, Neu TR, Flemming HC (eds) *Microbial extracellular polymeric substances*", Springer, Berlin Heidelberg New York, PP.127-141, 1999.
- [38] Baldi F, Clark T, Pollack SS, Olson GJ., "Leaching of pyrites of various reactivities by *Thiobacillus ferrooxidans*", *Appl. Environ Microbiol*, No.58, PP.1853-1856, 1992.
- [39] Evangelou, V.P. and Y.L. Zhang, "A review - pyrite oxidation mechanisms and acid mine drainage prevention", *Critical Reviews in Environmental Science and Technology* 25 (2), 141-199, 1995.
- [40] Habashi F., "A Text Book of Hydrometallurgy", Metallurgy Extraction Quebec Publication, Canada, 1993.
- [41] Baillet, F, J.P. Magnin, A. Cheruy and P. Ozil, "Chromium precipitation by the acidophilic bacterium *Thiobacillus ferrooxidans*", *Biotechnology Letters* 20 (1), 95-99, 1998.
- [42] Takeuchi, F., K., Iwahori, K. Kamimura and T. Sugio, "Isolation and some properties of *Thiobacillus ferrooxidans* strains with differing levels of mercury resistance from natural environments", *Journal of Bioscience and Bioengineering* 88(4), 387-392, 1999.
- [43] Sugio, T., C. Domatsu, O. Munakata, T. Tano and K. Imai, "Role of a ferric ion-reducing system in sulfur oxidation of *Thiobacillus ferrooxidans*", *Applied Environmental Microbiology* 49 (6), 1401-1406, 1985.

- [44] Iwahori, K., F. Takeuchi, K. Kamimura and T. Sugio, "Ferrous-dependent volatilisation of mercury by the plasma membrane of *Thiobacillus ferrooxidans*", *Applied and Environmental Microbiology* 66(9), 3823-3825, 2000.
- [45] Kawatra S. K. and K. A. Natarjan, "Mineral Biotechnology", *SME Publ.*, PP. 101 - 119, 2001.
- [46] Brierley JA, Brierley CL., "Microbial leaching of copper at ambient and elevated temperatures", *Metallurgical applications of bacterial leaching and related microbiological phenomena*, Academic Press, PP. 477-490, 1978.
- [47] G. J. Olson, J. A. Brierley, C. L. Brierley, "Bioleaching review part B: Progress in bioleaching: applications of microbial processes by the minerals industries", *Appl. Microbiol Biotechnol.*, No.63, PP.249-257, 2003.
- [48] Rawlings DE, Dew D., "du Plessis C: Biomineralization of metalcontaining ores and concentrates", *Trends Biotechnol.*, 21:38-44, 2003.
- [49] Brierley JA, "Thermophilic iron-oxidizing bacteria found in copper leaching dumps", *Appl Environ Microbiol*, No. 36, PP.523-525, 1978.
- [50] Brierley JA, Norris PR, Kelly DP, LeRoux NW, "Characteristics of a moderately thermophilic and acidophilic ironoxidizing *Thiobacillus*", *Eur J Appl Microbiol*, PP.291-299, 1978.
- [51] Berthelot, D., L.G. Leduc and G.D. Ferroni, Temperature studies of iron-oxidising autotrophs and acidophilic heterotrophs isolated from uranium mines. *Canadian Journal of Microbiology* 39 (4), 384-388, 1993.
- [52] Holmes, D.S., *Biotechnology in the mining and metal processing industries - challenges and opportunities*. *Minerals and Metallurgical Processing*, May, 49-56, 1988.
- [53] Schippers A., Hallmann R. Wentzien S., *Microbial diversity in uranium mine Waste heaps*, *Applied and Environmental Microbiology*, P.P. 2930-2935, 1995.
- [54] Olson GJ, Porter FD, Rubinstein J, Silver S., "Mercuric reductase enzyme from a mercury-volatilizing strain of *Thiobacillus ferrooxidans*", *J Bacteriol*, No.151, PP.1230-1236, 1982.
- [55] Hallberg, K.B. and E.B. Lindstrom, "Characterisation of *Thiobacillus caldus* sp. nov., a moderately thermophilic acidophile", *Microbiology* 140 (12), 3451-3456, 1994.
- [56] Blais, J.F., R.D. Tyagi, N. Meunier and J.C. Auclair, "The production of extracellular appendages during bacterial colonisation of elemental sulphur", *Process Biochemistry* 29 (6), 475-482, 1994.
- [57] OECD: Organization for Economic Co-operation and Development, "Consensus Document on Information Used in the Assessment of environmental Applications Involving Acidithiobacillus", *Series on Harmonization of Regulatory Oversight in Biotechnology* No. 37, PP. 16, 2006.
- [88] Twardowska, I., "The Role of *Thiobacillus ferrooxidans* in pyrite oxidation in Colliery spoil tips, I. Model investigations", *Acta Microbiologica Polonica* 35 (3-4), 291-303, 1986.
- [59] Twardowska, I., "The role of *Thiobacillus ferrooxidans* in pyrite oxidation in Colliery spoil tips II. Investigation of samples taken from spoil tips", *Acta Microbiologica Polonica* 36 (1-2), 101-107, 1987.
- [60] Pronk, J.T., J.C. de Bruyn, P. Bos and J.G. Kuenen, Anaerobic growth of *Thiobacillus ferrooxidans*. *Applied Environmental Microbiology* 58 (7), 2227-2230, 1992.
- [61] Brierley CL, Briggs AP, "Selection and sizing of biooxidation equipment and circuits. In: Mular AL, Halbe DN, Barret DJ (eds) *Mineral processing plant design, practice and control*", *Society of Mining Engineers*, Littleton, Colo., PP.1540-1568, 2002.

## **Part 4**

# **Advances in Nuclear Waste Management**



# Storage of High Level Nuclear Waste in Geological Disposals: The Mining and the Borehole Approach

Moeller Dietmar and Bielecki Rolf  
*University of Hamburg / German Czech Scientific Foundation (WSDTI)*  
Germany

## 1. Introduction

Nuclear energy is the energy in the nucleus, the core of an atom. Atoms itself are tiny particles of the universe. Nuclear energy can be used to generate electricity in nuclear power plants which currently satisfies about 35% of the European Unions' electrical energy needs. As of January, 2011 there is a total of 195 nuclear power plant units (including the Russian Federation) with an installed electric net capacity of 170 Giga Watt (GW) in operation in Europe and 19 units with approximately 17 GW are under construction in six countries [ENS, 2011]. Nuclear power can be generated from the fission of uranium, plutonium or thorium and by the fusion of hydrogen into helium. In nuclear fission, atoms are split apart to form smaller atoms, releasing energy which is used to produce electricity. Today it is almost all uranium. Uranium is non-renewable. It is a common metal found in rocks all over the world. Natural uranium is almost entirely a mixture of two isotopes, U-235 and U-238. Digging natural uranium U-235 must be extracted and processed to fission in a reactor. Compared with U-235, U-238 cannot fission to a significant extent. Natural uranium is 99.3 per centum U-238 and 0.7 per centum U-235. Therefore, nuclear power plants use enriched uranium in which the concentration of U-235 is increased from 0.7 per centum U-235 about 4 to 5 per centum U-235. This enrichment is expensive and done in a specific separation plant. The U-235 used in today's reactors seems to be available from natural uranium for a number of decades. But the key energy fact is that fission of an atom of uranium liberates about 10 million times as much energy as does the combustion of an atom of carbon from coal [McCarthy, 1995].

Nuclear power plant reactors contain a core with a large number of fuel rods. Each of which is filled with pellets of uranium oxide, an atom of U-235 fissions when it absorbs a neutron. The fission produces two fission fragments and other particles that fly off at high velocity - about 80 per centum of the neutron absorptions in U-235 result in fission; the other 20 per centum are just (n, gamma) reactions, resulting in just another gamma flying about. When they stop the kinetic energy is converted to heat [McCarthy, 1995]. The heat from the fuel rods is absorbed by water which is used to generate steam to drive the turbines that generate the electricity. The steam withdrawn and run through the turbines controls the power level of the nuclear power plant reactor. Hence, nuclear power plants use nuclear fission for producing electrical energy.

Electricity generated in nuclear power plants does not produce polluting combustion gases like traditional coal and/or gas power plants, an important fact that plays a key role helping to reduce global greenhouse gas emissions and tackling global warming especially as electrical energy demand rises in the years ahead. Hence, nuclear power is back in favor, at least in political circles. Worldwide are 436 nuclear power plants in operation, and 47 under construction. 133 nuclear power plants are planned, and 282 are proposed. In total 898 nuclear power plants will run in the near future worldwide. This could be assumed as an ideal win-win situation, but the other side of the coin is that the production of high-level nuclear waste (HLW) outweighs this advantage. Therefore, management and disposal of radioactive waste became a key issue for the continued and future use of nuclear power plants in the EU. Because the safe and sustaining disposal of HLW is not solved yet, of high political and public concern, and part of international research programmes. Thus the objective of this chapter is to highlight the state-of-the-art of possible concepts for safe and sustaining storage of HLW in geological disposals that are exist, are under construction, and/or under discussion.

## 2. Nuclear waste

Nuclear waste is a specific type of waste that contains radioactive chemical elements that do not have any practical purpose. Nuclear waste is produced as by-product of a nuclear process like nuclear fission in nuclear power plants, the radioactive left over from nuclear research projects, and nuclear bomb production. But the largest source of nuclear waste is naturally occurring radioactive material as isotopes such as carbon-14, potassium-40, uranium 238, and thorium-232. If these radioactive elements are concentrated they may become highly enriched to be treated as nuclear waste. In general nuclear waste is divided into low, medium, and high-level waste by the amount of radioactivity the waste produces. The majority of nuclear waste belongs to the so called low-level nuclear waste (LLW) which has a low level of radioactivity per mass or volume. This type of waste is all-around, and can be estimated to be approximately 80 per centum of the overall nuclear waste. It often consists of items that are only slightly contaminated but still dangerous due to radioactive contamination of a human body through ingestion, inhalation, absorption, or injection. Hence, it should not be handled by anyone without training. LLW usually includes

- material used to handle the highly radioactive parts of nuclear reactors such as cooling water pipes and radiation suits, etc.,
- low level radioactive waste from medical procedures in diagnosis and treatments or x-rays,
- industrial waste which may contain  $\alpha$ ,  $\beta$ , or  $\gamma$  emissions,
- earth exploration in order to find new sources of petroleum,
- industrial production like producing plastics,
- agricultural products, most notably for the conservation of foodstuffs, etc.

Not only LLW is still dangerous for the human body, also low-level radioactive material. Opposite to LLW nuclear power plants produce high-level nuclear waste (HLW) in their core that averages approximately 20 per centum of the total of nuclear waste. This waste depends on the rods (fuel elements) which includes large quantities of high level radioactive fission products and is generating heat. Also their extremely long half-live-time transuranic fragments (longer than 500,000 years) create extreme long time periods before the nuclear waste will settle to safe levels of radioactivity. Therefore, this nuclear waste at the very first is put in an intermediate and/or temporary storage facility, under strict safety conditions.



This facility normally is a large storage reservoir, a so called wet storage device, located next to the reactor. The wet storage reservoir is not filled with ordinary water but with boric acid, which helps to absorb some of the radiation given off by the radioactive nuclei inside the spent fuel elements. Within this large wet storage reservoir the high-level radioactive isotopes become less radioactive due to their decay and also generate less and less heat. Hence, the final disposal of HLW is delayed to allow its radioactivity to decay. Forty years after removal from the reactor less than one thousandth of its initial radioactivity remains, and it is much easier to handle. Thus canisters of vitrified waste, or spent fuel elements assemblies, are stored in large wet storages in special ponds, or in dry concrete structures or casks for at least this length of time. But this requires specific methods to handle the HLW. Some of the methods being under consideration include short term storage, long term storage, and transmutation. The longer the spent fuel element is stored in the intermediate storage facility, the easier it will be to handle. But many nuclear power plants have been holding spent fuel elements for so long that their reservoirs are getting full. They must either send the spent fuel elements off or enlarge their wet storage reservoirs to make room for more spent fuel elements. As the wet reservoirs are filled up a major problem occur. If the spent fuel elements are placed too close together, the remaining nuclear fuel could go critical, starting a nuclear chain reaction. Therefore, another method of temporary storage is used because of the overcrowding of wet reservoirs, which is the dry storage reservoir. The dry storage reservoir accommodates the HLW and putting it in reinforced casks or entombing it in concrete bunkers. This is after the HLW has already spent about 5 years cooling in a wet storage reservoir. The dry casks reservoirs are also usually located close to the reactor site. But for long-lived and HLW it is usually envisaged that this waste has to be placed in a final disposal facility, whatever this connoted. From the political perspective it seems there is no immediate economic, technical or environmental need to speed up with the construction of final geological disposal facilities for radioactive waste. Because the European Commission has prolonged the time schedule for their member states to develop their sustainable permanent HLW disposal facilities, which first were terminated for 2018. But now the year is 2030. With this in mind and from a sustainable development perspective – and if we do not want to pass the burden finding a permanent repository solution for HLW on the future generations – it has to be noticed that the temporary storage of HLW today is clearly not a satisfactory solution which with we can proceed for longer.

### **3. Options for disposing nuclear waste**

The basic idea in long-term storage of HLW that is currently preferred by international experts consists of placing the waste in a depth of at least 500 metres below the surface in a stable geological setting, that has maintained its integrity, and will maintain its integrity for millions of years. The ambition is to ensure that the HLW will remain undisturbed for the few thousand years needed for their levels of radioactivity to decline to the point where they no longer represent a danger to present and future generations. The concept of deep geological disposal is not new, it is more than 40 years old, and the technology for building and operating such repositories is now mature enough for use.

As a general concept, the natural security afforded by the chosen geological formation is enhanced by additional precautionary measures. The wastes deposited are vast immobilised in an insoluble form, in blocks of glass for example [Donald, 2010; Lutze, 1988; Weber et al., 1995], and then placed inside corrosion-resistant containers. Spaces between waste packages

are filled with highly pure, impermeable clay, and the repository may be strengthened by means of concrete structures. These successive barriers are mutually reinforcing and ensure that radioactive waste can be contained over the very long term. The main reason for relying on the deep geological disposal concept is based on the assumption that a geological environment is an entirely passive disposal system with no requirement for continuing anthropogenic involvement for its safety. It is assumed that it can be abandoned after closure with no need for continuing surveillance and monitoring. Thus, the safety of the deep geological repository system is based on multiple barriers, both engineered and natural, the main one being the geological barrier itself [OECD-NEA, 2003; Rao, 2001]. One option of disposing HLW which meets the above condition is the concept of a geological repository in the deep ocean floor, which is called seabed disposal [Carney, 2001]. It includes burial beneath a stable abyssal plain and burial in a subduction zone that slowly carry waste downward into the Earth's mantle. These option is currently not being seriously considered because of technical considerations, legal barriers in the Law of the Sea, and because in North America and Europe sea-based burial has become taboo from fear that such a repository could leak and cause widespread contamination [Nadis, 1996].

Another option of disposing HLW based on the above condition is the land-based waste disposal method of a geological repository in the deep rock, which is called the rock bed disposal. This repository concept can be realized as mined [Alexander, 2007; Loon, 2000; Miller, 2000] or borehole disposal [Anderson, 2004; Brady, 2009; Gibb, 1999; Gibb, 2005]. These repositories require as an essential boundary condition the option of recovering nuclear waste from the deep geological disposal during the initial phase of the repository, and during subsequent phases, which results in increased cost. But recovering nuclear waste provides a certain degree of freedom of choice to future generations to change waste management strategies if they wish or if there is a need for.

Based on the state-of-the-art in science and engineering [IAEA, 2001] geological repositories must be designed in such a way that it can be assumed that no radioactivity will reach the Earth's surface. Hence, environmental impact assessments must cover a 10,000 years analysis for worst-case scenarios, including geological and climate changes and inadvertent anthropogenic intrusion. These assessments maintain that even under those conditions the impact on the environment would be less than current regulatory limits, which in general are lower than natural [IAEA, 2006]. In 2007 a symposium on "Safety Cases for Deep Geological Disposal of Radioactive Waste: Where Do We Stand?" [OECD\_NEA, 2007] was organized by the Nuclear Energy Agency (NEA) of the Organization for Economic Co-operation and Development (OECD), in co-operation with the European Commission (EC) and the International Atomic Energy Agency (IAEA) to share experiences on

- developing and documenting a safety case both at the technical and managerial levels,
- regulatory requirements and expectations of the safety case,
- progress made in the last decade, the actual state of the art and the observed trends,
- international contributions in this field.

Beside the existing concepts of man-made geological disposal facilities for long-lived waste another optional solution is to reduce the mass of long-lived, high-level waste using a technique known as partitioning and transmutation. Transmutation involves isolating the transuranic elements and long-lived radionuclides in the radioactive waste and aims at transforming most of them by neutron bombardment into other non-radioactive elements or into elements with shorter half-lives. The governments in some countries are investigating this option but it has not yet been fully developed and it is not clear whether it will become

available on a large scale. This is because in addition to being very costly, partitioning and transmutation makes fuel elements handling and reprocessing more difficult, with potential implications for safety. Cost is an important issue in radioactive waste management as related to sustainable development. If the nuclear industry did not set aside adequate funds, a large financial burden associated with plant dismantling and radioactive waste disposal would be passed on to the next generations. Henceforth, in most of the OECD countries, the costs of dismantling nuclear power plants and of managing long-lived wastes are already included in electricity generating costs and billed to end consumers; in other words, they are internalised. Although quite high, in absolute terms, these costs represent a small proportion – less than 5 per centum – of the total cost of nuclear power generation.

Today different waste management and disposal strategies exist which deal with all types of radioactive waste originating in particular from the operation of nuclear power plants and back end nuclear fuel element cycle facilities. Short-lived low and intermediate level radioactive waste, generated comparatively in large volumes, have meanwhile successfully been managed from the disposal perspective world-wide. But high level radioactive waste disposal is an unsolved problem today. Worldwide it is accepted and a consensus view to dispose HLW in deep geological formations for long term and safe radioactive waste management [IAEA, 2006]. On the one hand the depth for geological disposal of nuclear waste is seen several hundred meters' below the surface in a mine, which is deemed as mined disposal concept. On the other hand the depth for a disposal zone is seen in much deeper depth. This depth can become achievable through boreholes in 1 to 6 kilometers' underground, in hard rock, which is deemed as borehole disposal concept in nuclear waste management [Brady, 2009].

#### **4. National management plans disposing nuclear waste**

The ultimate disposal of vitrified wastes, or of spent fuel elements without reprocessing, requires their isolation from the environment. The most favoured method is burial in dry, stable geological formations some 500 metres deep. Several countries in Europe, America and Asia are investigating sites that would be technically and publicly acceptable. But no country has yet established a workable, permanent and safe storage site for HLW or even a successful interim storage policy in place. A good overview on national HLW management plans can be found in [Wiki, 2011-1], to which is referred in the following paragraph, partly literally.

The United States has 104 civilian nuclear reactors in operation today, generating approximately 20 per centum of the total electricity. Beside the 104 existing nuclear reactors 1 nuclear reactor is under construction and 11 new nuclear reactors are on the immediate horizon. Nuclear fuel and HLW is currently stored in the U.S. federal states at 126 sites around the nation. In 1978 the U.S. Department of Energy (DoE) began studying Yucca Mountain, Eureka County, Nevada, to determine whether or not it would be suitable for the nation's first long-term (final) geologic repository for spent nuclear fuel and HLW. Yucca Mountain is located in a remote desert on federally protected land within the secure boundaries of the Nevada Test Site in Nye County, Nevada. The depth of the nuclear geological waste repository will be between 200 and 425 m under surface. The host rock is volcanic tuff. Signing the Joint Resolution 87 on July 23, 2002, allow the DoE to take the next step in establishing a safe repository in which to store the United States nuclear waste. The DoE is preparing an application to obtain the Nuclear Regulatory Commission license to proceed

with construction of the repository. If the DoE receives a license from the U.S. Nuclear Regulatory Commission to build and operate a repository at Yucca Mountain, Nevada, it will begin shipping nuclear waste from commercial and government-owned sites to the repository sometime after 2017. But this opening date of 2017 is a best-achievable schedule because the Yucca Mountain is years behind schedule, and according to a new economic analysis, its construction may cost more than \$50 Billion. For Yucca Mountain it is planned to use underground cavities with a connecting gallery to build up the long-term geologic repository storing the casks in horizontal galleries. The effectiveness of different technical barriers is under investigation. But the potential risk of this long-term geological repository can be seen by future trends in the global climate and earth quakes. Because it is not possible for computer models to precisely replicate all conditions of a realistic disposal facility. Thus the staffs of the U.S. Nuclear Regulatory Commission (NRC) use abstraction to simplify the information to be considered in a performance assessment. The degree of abstraction has to reflect the need to improve reliability and reduce uncertainty. Nonetheless, it is important for the model to be sufficiently detailed to ensure that it yields valid results for the performance assessment. Hence, a suitable model is a compromise between mathematical difficulties attached to complicated equations and the accuracy in the final result. In general, there are two different approaches to obtain a model of a realistic disposal facility:

1. Deductive or theoretical approach, based on the derivation of the essential relations of the disposal facility
  2. Empirical or experimental approach, based on experiment on the disposal facility
- Practical approaches often use a combination of both approaches, which might be the most advantageous way to precisely replicate conditions of a realistic disposal facility.

However, the Yucca Mountain project [Mascarelli, 2009; YUCCA, 2008] was widely opposed, with some major concerns being long distance transportation of waste from across the United States to this site, as well as the possibility of accidents, and the uncertainty of success in isolating nuclear waste from the human environment in the long term range. Yet, in 2009, the Obama Administration rejected use of the site in the United States Federal Budget proposal, which eliminated all funding except that needed to answer inquiries from the NRC (Nuclear Regulatory Commission), “while the Administration devises a new strategy toward nuclear waste disposal” [OMB, 2010]. On March 5, 2009, the Energy Secretary told in a Senate hearing “the Yucca Mountain site no longer was viewed as an option for storing reactor waste.” [Hebert, 2009].

As with many countries with a significant nuclear power program, the 18 operating nuclear power plants in Canada generated about 16 per centum of its electricity in 2006; Canada has focussed its research and development efforts for the long-term management of HLW on the concept of deep geological disposal. In 1975 the Canadian nuclear industry defined its waste-management objective as to “...isolate and contain the radioactive material so that no long term surveillance by future generations will be required and that there will be negligible risk to man and his environment at any time. ... Storage underground, in deep impermeable strata, will be developed to provide ultimate isolation from the environment with the minimum of surveillance and maintenance.” [Dyne, 1975]. In 1977 a Task Force commissioned by Energy, Mines and Resources Canada concluded that interim storage was safe, and recommended the permanent disposal of used nuclear fuel in granites, with salt deposits as a second option [Hare, 1977]. This recommendation was echoed shortly afterward by a concurrent Royal Commission on Electric Power Planning [Porter, 1978; Porter, 1980]. Many European countries have studied the deep disposal of HLW concept for a long time. In 1983, the Finnish government decided to select a site for permanent repository by 2010.

With four nuclear reactors providing 29 per centum of its electricity, Finland in 1987 enacted a Nuclear Energy Act making the producers of radioactive waste responsible for its disposal, subject to requirements of its Radiation and Nuclear Safety Authority and an absolute veto given to local governments in which a proposed repository would be located. The Finnish Parliament approved the deep geologic repository Onkalo in igneous bedrock at a depth of about 500 meters in 2010, a huge system of underground tunnels that is being hewn out of solid rock and must last at least 100,000 years [Ford, 2010]. The repository concept is similar to the Swedish model, with containers to be clad in copper and buried below the water table beginning in 2020.

In Sweden there are ten operating nuclear reactors that produce about 40 per centum of Sweden's electricity. The responsibility for nuclear waste management has been transferred in 1977 from the government to the nuclear industry, requiring reactor operators to present an acceptable plan for waste management with a so called absolute safety to obtain an operating license. The conceptual design of a permanent repository was determined by 1983, calling for a placement of copper-clad iron canisters in a granite bedrock about 1,650 feet underground, below the water table known as the KBS-3 method an abbreviation of *kärnbränslesäkerhet*, nuclear fuel safety [Wiki, 2011-2]. Space around the canisters will be filled with betonies clay. On June 3<sup>rd</sup> 2009 Swedish government choose a location for deep level waste site at Östhammar, near Forsmark nuclear power plant. A legal and institutional framework of the Swedish radioactive waste management is described in [Berkhout, 1991].

France 59 nuclear reactors contributing about 75 per centum of its electricity. France has been reprocessing its spent reactor fuel since the introduction of nuclear power. France also reprocesses spent fuel elements for other countries, but the nuclear waste is returned to the country of origin. Disposal in deep geological formations is being studied by the French agency for radioactive waste management in underground research labs. Government in 1998 approved Meuse/Haute Marne Underground Research Lab for further consideration. Legislation was proposed in 2006 to license a repository by 2015, with operations expected in 2025. Moreover, a good perspective of the French waste management strategy for a sustainable development of nuclear energy is described in [Courtois, 2005].

Nuclear waste policy in Germany is the most controversial. With 17 reactors in operation, accounting for about 30 per centum of its electricity, Germanys planning for a permanent geologic repository began in 1974, focused on the salt dome Gorleben. The site was announced in 1977 with plans for a reprocessing plant, spent fuel element management, and permanent disposal facilities at a single site. Plans for the reprocessing plant were dropped in 1979. In 2000, the federal government agreed to suspend underground investigations for three to ten years, and committed to ending its use of nuclear power, closing one reactor in 2003. Meanwhile spent fuel elements have been transported to interim storage facilities at Gorleben, Lubmin and Ahaus until temporary storage facilities can be built near reactor sites. Previously, spent fuel was sent to France or England for reprocessing, but this practice was ended in July 2005. Meanwhile the exploration of the salt dome Gorleben is carried on. Moreover, the legal and institutional framework of the German radioactive waste politics is described in [Berkhout, 1991; Wellmer, 1999].

Switzerland's four nuclear reactors provide about 43 per centum of its electricity. ZWILAG, an industry-owned organization, built and operates a central interim storage facility for spent nuclear fuel elements and HLW, for conditioning LLW and for incinerating wastes. The Swiss program is currently considering options for the siting of a deep repository for HLW disposal, and for low & intermediate level wastes. Construction of a repository is not

foreseen in this century. Research on sedimentary rock is presently carried out at the Swiss Mont Terri rock lab.

Great Britain has 19 operating reactors, producing about 20 per centum of its electricity. It processes much of its spent fuel elements at Sellafield where nuclear waste is vitrified and sealed in stainless steel canisters for dry storage above ground for at least 50 years before eventual relocate in a deep geologic disposal. In 2006 the Committee on Radioactive Waste Management (CoRWM) recommended geologic disposal in 200–1,000 meters underground, based on the Swedish model, but has not yet selected a site. Moreover, the Britain radioactive waste management politics is described in [Berkhout, 1991].

The Ministry of Atomic Energy (Minatom) in Russia is responsible for 31 nuclear reactors which generate about 16 per centum of its electricity. In the long term, Russia is planning for a deep geologic disposal. Most attention has been endowed to locations where waste has accumulated in temporary storage at Mayak, near Chelyabinsk in the Ural Mountains, and in granite at Krasnoyarsk in Siberia.

In the People's Republic of China, ten nuclear reactors provide about 2 per centum of electricity and five more are under construction. Geological disposal has been studied since 1985, and a permanent deep geological repository was required by law in 2003. Sites in Gansu Province near the Gobi desert in northwestern China are under investigation, with a final site expected to be selected by 2020, and actual disposal by about 2050.

The 16 Indian nuclear reactors produce about 3 per centum of electricity, and seven more are under construction. Interim storage for 30 years is expected, with eventual disposal in a deep geological repository in crystalline rock near Kalpakkam.

The 55 Japanese nuclear reactors produce about 29 per centum of its overall electricity. In 2000, a Specified Radioactive Waste Final Disposal Act created a new organization to manage HLW, and later that year the Nuclear Waste Management Organization of Japan (NUMO) was established under the jurisdiction of the Ministry of Economy, Trade and Industry. NUMO is responsible for selecting a permanent deep geologic repository site, construction, operation and closure of the facility for waste emplacement by 2040

## 5. Mining disposing concept of nuclear waste

Geological disposals in deep geological formations as radioactive waste repositories have been recognized since 1957 [NAS, 1957]. Such deep geological sites provide a natural isolation system that is stable over a long-term to contain long-lived radioactive waste. In practice LLW is generally disposed in near surface facilities or old mines. Compared with LLW HLW is generally disposed in host rocks that are crystalline (granite, gneiss) or argillaceous (clay) or salty or tuff. The depth of these mined repositories is in between 300 and 700 m.

In Germany, it is planned but not decided yet to dispose radioactive waste in a repository in deep geological formation several hundred metres below the surface in a salt dome. It is assumed that salt will be a natural barrier which is able to protect the environment from radiation. Rock salt possesses particularly good isolating properties for radioactive, heat-generating wastes. Henceforth, the investigation of repository sites in Germany concentrate on rock salt formations as a host rock which actually is the Gorleben project [Wellmer, 1999]. In northern Germany more than 200 salt structures are known with massive rock salt formations about 250 million years old at deep depths. Thus, the selection was quickly narrowed down to the 200 salt domes located in Lower Saxony in northern Germany. There was never a search for alternatives, such as those in granite or clay. Hence, the Gorleben salt

dome, with a mined depth of 840 m, was explored for decades. Since 1979, more than 1.5 milliards € has been conducted at Gorleben to determine whether the salt dome can be used to securely store the hot radioactive waste for hundreds of thousands of years.

The hazardousness of radioactive waste decreases in time due to the radioactive decay. Nevertheless, in case of long-living nuclides the radiation after 100,000 years requires to isolate waste from the biosphere. Therefore, in long-term analysis periods up to 1 million years and more have to be considered. 1 million years is a very long time scale but from a realistic viewpoint man-kind is unable to forecasting within the same time period in the future. But 1 million years are short compared with geological situations that can be traced back for several 10 or 100 millions of years. Therefore, the question rises whether the actual repository concepts can reliable be forecasted within the next 1 million years.

Long-term safety analyses have been performed to estimate the radiological effects of the considered repository on the biosphere for the next 1 million years. For this purpose, assumed future events and processes such as the thermal expansion of the host rock, subsrosion, gas generation or appearance of an ice-age, salt leaching in a salt dome, etc. are combined to scenarios and the consequences of these scenarios can be estimated by numerical simulation. A simulation study can be performed to test and/or optimize the behavior of engineered systems before construction. This help avoiding costly re-designs necessary due to fatal hypothetical errors, and ensuring cost-effective, high quality, and safe engineered solutions. The diversity and interdisciplinary nature and the intrinsic complexity of a conceptual approach of a geological disposal necessitate using computational modeling and simulation (CMS) to accomplish advanced and secure solutions. Using CMS in geological repository analysis requires data obtained from measurements at the real world system under test. Thus, building a model of a salt dome for scenario analysis require data sets obtained from (laser) measurements. Such data represent a scatter plot, as shown in Figure 1.

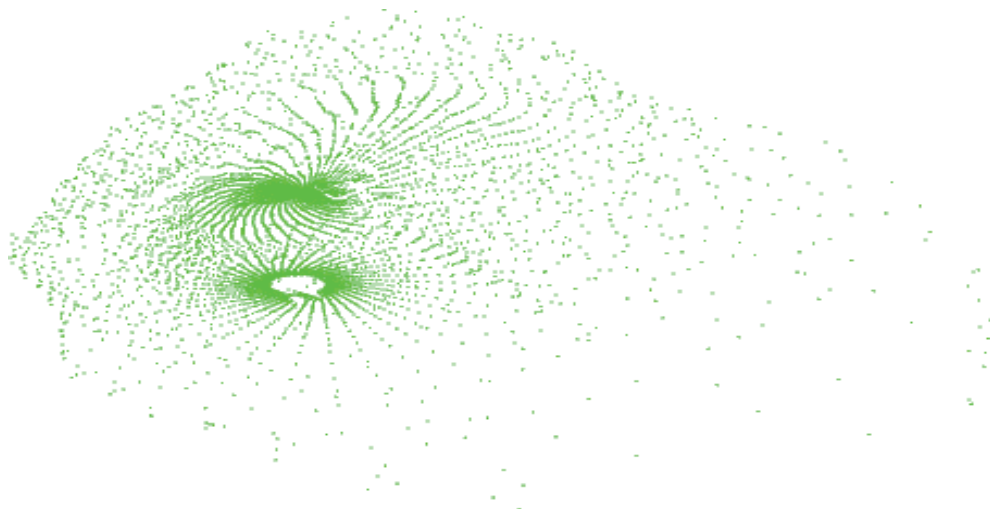


Fig. 1. Laser data obtained from a salt dome scan after (Koerber, 2004; Moeller, 2005)

The scatter plot dot distribution in Figure 1, which represents the measured data, can be applied for surface morphing in conjunction with NURBS (Non Uniform Rational B-Splines). This result in solids that are closed surfaces or more usually poly-surfaces that enclose a volume, as shown in Figure 2.

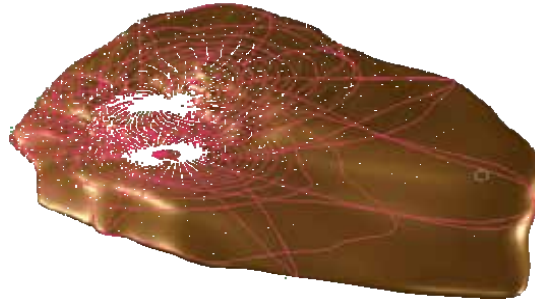


Fig. 2. B-Spline representation of laser measurements obtained from a salt dome scan after (Koerber, 2004; Moeller, 2005)

The special kind of B-Spline representation (NURBS) in Figure 2 is based on a grid of defined points  $P_{i,j}$ , which can be approximated through bi-cubic parameterized analytical functions as follows:

$$P(u, v) = \frac{\sum_{i=0}^n \sum_{j=0}^m N_{i,p}(u) N_{j,q}(v) w_{i,j} S_{i,j}}{\sum_{i=0}^n \sum_{j=0}^m N_{i,p}(u) N_{j,q}(v) w_{i,j}}, \quad 0 \leq u, v \leq 1$$

in which  $N_{i,p}$  and  $N_{j,q}$  represent the basis of a B-Spline,  $S_{i,j}$  are the weighted control points with the weights  $w_{i,j} \in \mathcal{R}$ . As the parameter values  $u$  and  $v$  can be chosen continuously, the resulting object is mathematically defined at any point, synonymic showing no irregularities or breaks. But there are several parameters to justify the approximation of the given points which change the look of the described object. Therefore, if needed, interpolation of all points can be achieved:

- First, the polynomial order describes the curvature of the resulting surface or curve, giving the mathematical function a higher level of flexibility.
- Second, the defined points can be weighted according to their dominance in accordance to the other control points. A higher weighted point influences the direction of the surface or curve more than a lower weighted. Furthermore, knot vectors  $u$  and  $v$  define the local or global influence of control points, so that every calculated point is defined by smaller or greater arrays of points, resulting in local or global deformations, respectively.

NURBS [Cottrell, 2001] are easy to use while modeling and especially modifying is achieved by moving control points, which allows adjusting the objects by simply pulling or pushing the control points. Based on this concept a methodology to interpolate given sets of points is available. Using multiple levels of surface morphing, the multi-level B-Spline approximation (MBA) adjusts a predefined surface. Constraints like the curvature or direction at special points can be given and are evaluated within the algorithm.

Mined repositories in salt often show salt deposits which have a layered structure as shown in the model of a salt mine in Figure 3, where alternating more or less potassium bearing salt rock layers appear. It is assumed that a leaching process occur in the salt mine under test which result in major structural changes in terms of instability of the cavern, erosion, and so on [Koerber, 2004; Moeller, 2005].



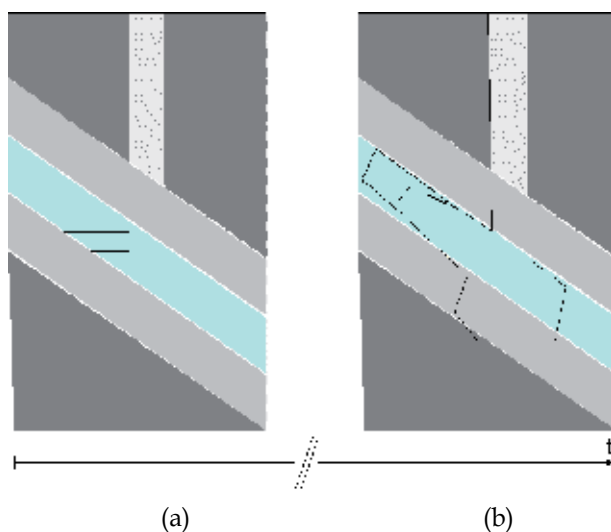


Fig. 3. Salt leaching effect in a salt mine. Figure 3.a show three different salt rock layer and the mining shaft, figure 3.b additionally show the growth of a brine body after (Koerber, 2004; Moeller, 2005)

Characteristically for potassium bearing salt is that not just salt is leached resulting in some kind of salty water the so called brine. In fact a circulation process occurs, while certain components become leached, others drop out [Sander, 1988] and accumulate at lower level, masking the leaching process in that area. The composition of the brine constantly changes over time while interactions constantly take place between salt rock and solution. These dynamic interactions can be localized along the reaction surface between brine (fluid) and rock (solid), more basically between objects with different geochemical attributes. The direction and velocity of the solution can be described by vectors, determined by an underlying process model, which integrates the relevant parameters of all involved objects (rock, fluid, reaction surface, and so on). The leaching problem in the salt mine can be approximated based on data obtained from laser measurements and modeling based on NURBS. But this approach don't optimally meet the requirements necessary to model the salt leaching process. Implicit geometry and CSG were no candidates, as well as subdivision and parametric models. It appears questionable whether the easily differentiable structure of parametric models or the arbitrary grid structure of subdivision models, justify the hassle expected from maintaining legal topology due to dynamic topology, which brings cell decomposition into the focus which fit well with the hydro-geochemical process as one cell can simply switch attributes from salt to brine without bringing topology into any trouble. One major concern in this investigation is that the reaction surface moves very slow, perhaps 1cm per cycle of the underlying process model, which would then be the required resolution for e.g. voxel. Hence, currently a model which combines cell decomposition and parametric properties by linking attributes not to voxel but to a regular grid of control points between which linearly interpolation is possible is in favor. This allows finer transition between control points/voxel without requiring more memory executing the model. Formally this is a linear solid B-Spline but since the control points lie on a regular grid, and the geometry thus is implicit, the similarities to voxel are obvious. First tests in 2D

show very good fits. Hence, Figure 4 shows the mimicked (no process model is used) leaching process in a salt mine, which does not highlight the hard edges which are typical for voxel.

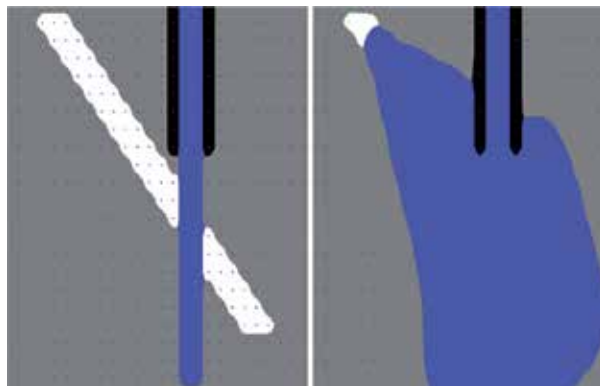


Fig. 4. Bilinear interpolating 2D cell decomposition of the investigation area in a salt mine with superposed leaching process after (Koerber, 2004; Moeller, 2005)

Some issues, like embedding different objects in one geometrical model, identifying the reaction surface and deriving its differential properties still have to be too considered while analyzing what may happen in a salt dome if water became an important fact and leaching will be became a potential risk for stability of the salt dome under test.

## 6. Borehole disposing concept of nuclear waste

Boreholes occur when using drilling technique, which has been economically developed on the basis of long-year experiences of the rotary drilling method in the petroleum industry. Moreover, petroleum drilling costs have decreased to the point where boreholes are now routinely drilled to multi-kilometer depths. Research boreholes in Russia and Germany have been drilled to 8 – 12 km which are super or ultra deep. Boreholes with a depth of 3 – 5 km are called deep and with a depth of 5 – 7 km are the very deep ones. The risk when drilling rock at medium deep up to the deep depth in between 2- 4 km is stress which may result in a hole breakout through stress. Thus, stress breakout is a feature of deep wells particularly in strong rock. Hence casing throughout the full depth of the borehole is essential. Drilling at deeper depth up to 7 km has to bear in mind temperature as a risk factor. Another important issue when drilling deep boreholes are the resulting enormous costs. In a case study it was shown for 950 deep boreholes to dispose the entire 109,300 metric tons of heavy material inventory will end up in calculated costs of around \$ 20 million per borehole, which sum up to approximately \$ 19 billion [Brady, 2009].

When drilling deep boreholes the achievable borehole diameter is depending on the drilled depth. This only allows a limited tailoring to suit the waste packaging. Because the deeper the depth the less the size of the diameter. At 8 km depth the size of the borehole will be approximately less than 0.5 m and in 1 km depth the borehole size can be more than 5 m. The foregoing mentioned drilling diameters suit with that which come up in the petroleum industry which raise the question are they adequate with the boreholes necessary for a HLW geological disposal. A deep borehole disposal of HLW which use off-the-shelf oilfield and

geothermal drilling techniques into the lower 1 – 2 km portion of a vertical borehole with a conic width of approximately 0.4 – 1.2 m diameter and 3 – 5 km deep, followed by borehole sealing, is described in [Brady, 2009]. This disposal at a depth of 3 – 5 km allows a 1 – 2 km long HLW disposal zone, as shown in Figure 5.

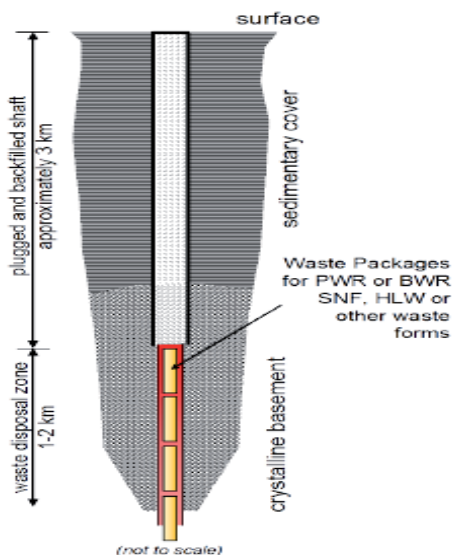


Fig. 5. Deep borehole disposal schematic after (Brady, 2009)

This 1 – 2 km long waste disposal zone can hold 200 – 400 HLW canisters. The canisters could be emplaced one at a time or as part of a canister string which represent a grouping of 10 or 20 canisters. The design concept of this borehole concept is such that the borehole allows accommodating 34 outer diameter canisters. The borehole seal system will use a combination of bentonite, asphalt and concrete, at which a top seal will consist of asphalt from 500 m to 250 m, with a concrete plug extending from 250 m to surface.

But the diameters for the borehole shown in Figure 5 are not comparable with the ones necessary to obtain a technology enhanced HLW geological disposal concept as described in the following paragraph of section 5 in this chapter. The background for the technology enhanced HLW geological disposal approach bear in mind that geological deep disposal involves sinking large diameter borehole 3 to 5 km down into the granitic basement of the continental crust, with containers of HLW in the bottom 1km or so, and scaling the hole above the deployment zone. This very deep in engineering terms is described as very deep borehole disposal [Gibb, 2005]. Thus, it is anticipated that deep borehole disposal will be on the under of 3 km deep, and necessitate at least a diameter of more than 10 m. This diameter is necessary for dumping the containers and retrieves the containers if needed. Both can be done if an elevator is embedded as part of the technology enhanced HLW geological disposal approach, because the elevator fit into the drilled diameter. The big advantages of such a deep borehole disposal, the same reason has been discussed by Brady [Brady, 2009], are that it avoid groundwater problems almost together and provides a far-field geological barrier of enormous strength. The geological barrier is the only barrier to any escape of radionuclides that can demonstrably survive on the timescale of millions of years [Gibb, 2005]. In order to

evaluate the system performance of a deep technology enhanced HLW geological disposal concept, it is necessary to adopt or develop a standard by which the performance can be measured. But the political decision in Germany to postpone the final judgment for implementation of a final HLW geological disposal only allows estimating the performance differences between the mined and the borehole geological disposal concepts.

As assumed in the preceding paragraph of the borehole geological disposal concept HLW is embedded in mineral and ceramic crystalline lattices, such as zircon, cubic zirconium and monazite, encapsulated in deep boreholes deeper than 3 kilometer and up to five kilometers' underground, in hard rock in order to overcome the uncertainties of the mined disposal concept of a few hundred meters' depth (300 – 800 m). Thus, the deep borehole disposal concept put HLW back inside the rocks from which it came as uranium. The depth of clearance of more than one to five kilometers' is the most critical as one want to get to an area where the geology is stable and there is almost no water flowing. After filling the disposal in the foregoing mentioned depth of the clearance with high radioactive waste, boreholes would be backfilled and secured by rock welding or other techniques of at least 1 – 2 kilometers height, as described by Brady [Brady, 2009]. But the drilling technique of deep boreholes as described by Brady [Brady, 2009], which use off-the-shelf oilfield and geothermal drilling techniques, is not the technical approach introduced in this section of the chapter as technology enhanced HLW geological disposal approach. It is rather a flame melts technique which melts hard rock and it is assumed that this will allow borehole diameters of approximately 10 meters and more which will limit entry of water and migration of contaminants through the borehole after it is decommissioned. It is assumed that this concept is being safe to isolate HLW from the biosphere for a very long time, protecting both mankind and environment from radiation to its best possible extent, compared with the mining approach, described in section 4 of this chapter.

Rock welding is the basic principle of a technology to sink vertical constructions or to drift horizontal driving, which has been developed at the Los Alamos Laboratories in New Mexico, U.S.A., in recent years, performing underground construction of non-specified extent. The achieved results showed that rock welding technology reached a three times higher performance than traditional drilling techniques by only causing 40% less costs [CGER, 1994]. But the staff of this research project report that this technique could not be employed near inhabited areas, since the energy source used to melt the rock was a nuclear reactor which would have contaminated the ground water in case of a disaster. To overcome this energy dependent problem, a research group with scientists from the Universities Hamburg, Germany, Košice, Slovak Republic, Brno, Czech Republic, in co-operation with the German-Czech Science Foundation (WSDTI), Germany, searched and studied an option on a rock welding technique which does not need a nuclear reactor as energy source for rock melting. The resulting technical principle is deemed as flame melting technique beneath extreme high pressure, temperature, and frequency. This approach replaces the nuclear energy source used in the borehole project using a rock welding technique in Los Alamos. This new technique is based on a cost effective high energy oxygen-hydrogen-mixture energy source. Based on this research work a first mock up assessment was carried out in support of implementation of geological disposal based on the flame melting technique concept to melt rock indicate amendatory against present mining geological disposal concepts. The necessary exploration to test the flame melting technique to melt rock material at the laboratory scale was accomplished at the Technical University Košice, and the Slovakian Academy of Science, Slovak Republic. This test site is led by the two Slovakian

Professores Felix Sekula and Tobias Lazar. For this purpose a flame jet pump system, buildup of cobalt, was developed. The crown of the flame jet pump system is covered by a 200  $\mu\text{m}$  thick ceramic coat of hafnium nitride. The head base of the jet pump system has an outflow nozzle by which the oxygen-hydrogen gas mixture flow through and melts the rock by means of the burning flame. Rock boulders with the dimension of 0.5 m<sup>3</sup> were used to melt rock by means of the burning flame. At this laboratory scale holes of approximately 70 mm diameter could be realized. The flame jet pump system melt holes in the rock boulder in such a way, that the burned waste package could disappear through the melted chambers, as shown in Figure 6. In this laboratory investigation the average penetration rate achieved was 7 mm/sec. Investigating the flame melted holes show that no disjoining pressure have occurred under the head of the jet pump system. However, radial cracks of such dimension occur that the rock boulders collapse in the final stage. Thus, the melted rock could pass through the melted chambers into the radial cracks, which has been kept in several records. Moreover, inspecting the flame melting rock boreholes show at several areas a special crust within the ambience of the melted chambers as well as at the collapsed probes. At this laboratory scale holes of approximately 70 mm diameter the radial cracks are not developed through a disjoining pressure which happened in the Los Alamos test bed in the real rock massive, rather than thermal force. Thermal force generates radial cracks in the direction of the free areas of the rock boulder.

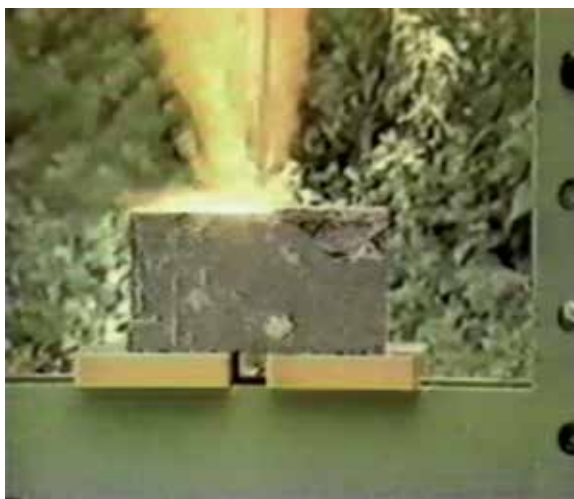


Fig. 6. Laboratory test bed of the flame melting technique (with permission of Professors Lazar and Sekula, Technical University of Košice, Slovak Republic)

The flame jet pump system injection head is shown in Figure 7.

In general, for both concepts, the mined one in salt rock and the borehole one in hard rock, it is assumed that one can thus safely isolate the higher radioactive waste from the biosphere for a very long time, protecting both man and environment from radiation to the best possible extent. Before it can be determined whether a potential location really is suitable to be a site for a long term disposal, all aspects of the overall situation regarding the geological disposal has to be investigated. Thus, one has to investigate in particular the effectiveness of the geological and geotechnical barriers and design a coherent long term management of a higher activity radioactive waste concept.



Fig. 7. Laboratory version of the flame jet pump system injection head (with permission of Professors Lazar and Sekula, Technical University of Košice, Slovak Republic)

For this reason a principle concept as basis for a repository that permit embedding elevators in the large diameter borehole and, provided that the security barriers are arranged in a suitable way, allowing retrieval from the final repository of the containers installed in the smaller boreholes, is shown Figure 8. This assumption is due to the consensus view that at first repositories will be designed for retrievable storage; but there is often a clear implication that if, after a suitable period, there are no technical difficulties and the political climate permits, the system of tunnels and access shafts will be scaled up and the repository will become a disposal. As it can be seen in Figure 8 big borehole diameters in rock massive only will melt the borehole border while the kernel will be mechanical removed.

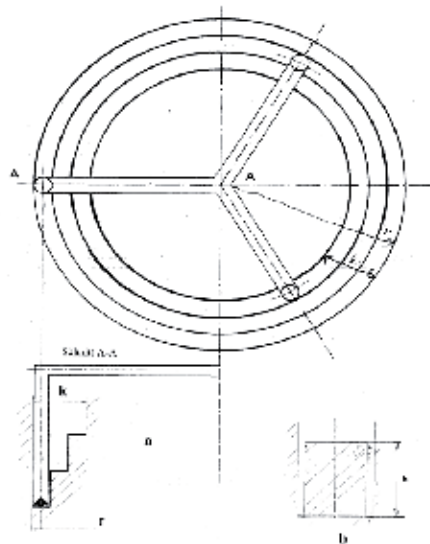


Fig. 8. Deep borehole disposal concept with borehole-border-melting dimensions

The great advantage of this type of disposal is that it prohibits groundwater problems and almost a far-field geological barrier of enormous strength. The geological barrier is the only barrier to any escape of radionuclides that can demonstrably survive on the timescale of millions of years. In contrast to the very active groundwater flows at conventional repository depth  $R$  in Figure 9, the migration of intra-rock aqueous fluids becomes increasingly sluggish with depth.

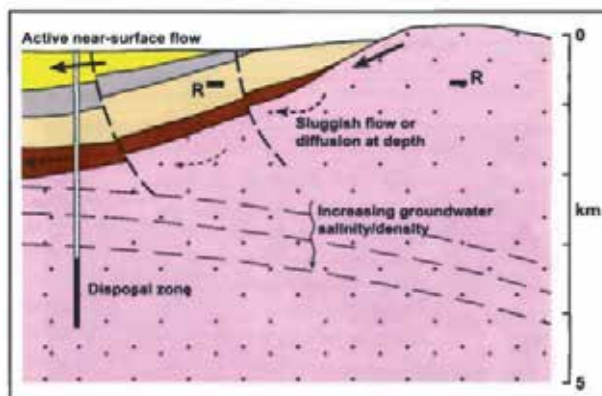


Fig. 9. Conceptual model for a very deep borehole disposal of high level radioactive waste, after Chapman and Gibb, 2005)

At depth of 4 to 5 km in the granite basement, hydraulic conductivities tend to be less, and often much less than  $10^{-11}$  meters per second, i.e. fluids migrate at most a few hundreds of meters in a million years. Due to this ultra-less risk in groundwater contamination by radionuclides one has to achieve water tightness of the storage caverns as most important ancillary condition. Assuming that a drilling techniques exist with a sufficient melting of granite than the solid rock will become individually melted in the caverns as well as in the shaft to preserve the integrity of the container and that the melt will recrystallize completely to holocrystalline granite on a time scale appropriate to the thermal decay of the high level radioactive waste. Henceforth, from the consensus point of view a proof is needed to show that the cracks already present in the host rock and the cracks created there by melting are completely closed against high pressure by the rock melt, down to sufficient depth.

Nevertheless, several main problems are unsolved to date melting solid rock like granite, based on the flame melting technique beneath extreme high pressure, temperature, and frequency, which conduct a bunch of questions. These questions refer to the knowledge gained in our previous research work and are focused on the very details to achieve such a deep borehole with the flame melt technique due to expected constraints, which we are aware. Hence, the questions are answered based on the knowledge to date.

*Whichever reactions occur if large quantities of water appear during the melting process?*

For a consensus answer at the very first it is necessary being aware that:

- before go for flame melting of solid rock like granite, precise geological and hydrogeological investigations are necessary to select the appropriate location of the geological repository.

Assuming that this has been done as part of the consensus view, the question thereafter can be answered referring to state of the art knowledge based on facts like:

- temperature of the melted rock is in between 1400 and 1800°C,
- temperature of the melting flame is approximately 2530°C,
- water has a temperature gradient of 1°C per 33 m depth; which result for a depth of 2000 m in a water temperature of 66°C; with the precondition that are no aquifers at this location,
- flame melting can be used if and when water inflow from cracks exist, which can be the case in solid rock, as well as additionally generated through the melting temperature,
- evaporating the melted product the water detract energy, but as an additive impact the water vapour pressure acts in a reinforcing manner on the melted product,
- water evaporates incremental,
- water vapour – dissociated due to the temperature of H<sub>2</sub> and O –, press the melted product into the existing fissures and cracks, while the melting flame is continuously burning (temperature approx. 2530°C) – can also burn below water surface level –,
- no chemical reaction between the water and the melting flame itself has to be considered,
- in case of substantial water inflow from cracks, additional special waterproofing procedures are needed. Thus, potential geological repository locations without cracks should be chosen as far as possible,
- high temperatures in the rock, e.g. due to aquifers, have a reinforcing impact on the melting process, because less energy is needed to melt solid rock.

*Is the vitrified rock seam around the melted hole hydraulically tight?*

A consensus answer depends on the decision on the location selected for the flame jet pump system drilled deep borehole and its depth:

- apart from the cracks, the rock seam must be hydraulically tight without the melted products, which can be determined by sample drillings on the location selected for the the flame jet pump system drilled deep borehole,
- melted products closes the cracks in the rock, and closes the pores of the rock seam,
- quantity of melted products can be regulated by the melting flame,
- thermo-shock tests are needed to determine the depth of crack closure.

*How melted holes in solid rock must be filled for hydraulic tightness?*

A consensus answer relates on both, the cracks and the bed of the flame melted hole in solid rock:

- depth of crack to be filled with melted products can be determined by non-destructive measurement devices such as sound measurements, with can additionally be supported by drillings,
- tightness of the bed of large flame melted bore holes is determined by test drillings,
- tightness of completed cavities can be determined by means of water pressure tests.

*What is the long-term behavior (ageing) of the solidified melt?*

In general, solid rock has a crystalline structure, and the melted products will recrystallize completely to holocrystalline granite on a time scale appropriate to the thermal decay of the HLW. Henceforth, from a consensus view it can be assumed that on the long scale the same long-term behaviour of the real rock massive will happen, because both of which are based on the same primary elements, what has been investigated in a previous research study [Rybar, 2004].



*What influence has the chemical milieu i.e. the chemical composition of the rock and the fissure water on the solidified melted products?*

From a consensus view it can be assumed:

- influences on the solidified melted products are the same as the influences on the real rock massive,
- aggressive substances do not influence the chemical milieu in the granite rock, since they only occur in small quantities,
- no bacteriological influences can be found at the intended depth.

*How will long-term bonding of filling material influence the vitrified rock?*

From a consensus view it can be assumed:

- bonding of the filling material of the vitrified rock seam will not occur,
- retrieving stored containers from the geological repository may have a huge impact on filling the cavities of the repository which can make this process difficult. Thus, at the very early beginning, one has to investigate the interactions that cohere with this option very carefully.

*What is the cooling behavior of the solidified rock melted products (contraction cracks)?*

From a consensus view it can be assumed:

- cool down process of the melted products is very slow because of the low thermal conductivity  $e$  ( $e = 0.25$  to  $0.73$  W(m°C)),
- thermo-shock tests will provide detailed knowledge,
- possible appearance of contraction cracks due to thermal tensions are to be closed by subsequent injections.

*How far does the melted rock penetrate into the open fracture system of the rock, and what are the factors determining the penetration depth?*

From a consensus view it can be assumed, referring to:

- published results from flame melting tests of the Los Alamos geological disposal project in the United States, show in near to the surface cavities that thermally induced cracks may have a length of up to 600 times of the drilling hole diameter ( $< 100$  mm), using the traditional rotary drilling method,
- to date knowledge that the penetration depth of melting material depends on its viscosity and the quantity which can be regulated by the flame melting process.

*Demonstrations' or estimates of radiation damages at vitrified rock?*

From a consensus view it can be assumed:

- tests at nuclear power stations reactors currently in operation show satisfactory results in their concrete structures with different rock aggregation materials (a precondition for their construction approval),
- in nuclear power stations, the kinetic energy of the neutrons is also slowed down by water – which is also possible with the cavities assembled by melted rock,
- apart from this, the radiation detection methods used in radiation measurement can also be used.

In view of the foregoing preliminary answered questions the operational improvements for supporting final radionuclide's disposal research and technological development can be estimated and valued. Furthermore, an economic assessment can be carried out to support

implementation of a geological repository for HLW based on the flame melting technique concept, as well as a mathematical risk calculation. A risk is mathematically defined by the number of potential hazards. The number of potential hazards can be described through the arithmetical average over an expectation, which represent the conjunction of products of a quantitative indication of possible consequences such as the extent of a claim and the claims amount as well as the quantitative indication of the probability, considering the de facto incidence of the consequence of a claim. The risk analysis formula is:

$$R = H * S$$

with R: risk of the expectation, H: probability of the eventuate of the incidence, S: normative dimension of claim.

This formula allows calculating possible impacts of claims quantitatively, expressed through the probability, which allow comparing potential risks.

Referring to borehole geological disposals the risk analysis allows calculating possible impacts of borehole geological disposals on the civilization quantitatively, expressed through the probability, which allow comparing potential risks, which is essential for planning safety related arrangements. The goal is to keep the potential risk as minor as possible (minimization). By means of physical simulation possible variations of initial and boundary conditions can be embedded to analyze varying safety related arrangements with their specific risk to calculate the pros and cons of technical arrangements and their costs. But the essential risk analysis for borehole geological disposals require quite more than the quantitative approach described before, it also need a qualitative approach.

The quantitative risk analysis for borehole geological disposals requires a scenario planning and analysis with adequate initial and boundary conditions, to run simulation case studies. Thus, a scenario analysis can be performed to predict possible future events of a given entity considering alternative possible outcomes, assuming changing scenarios but inherently consistent constraints, for improved decision-making, that require as prerequisite a scenario planning, a method based on simulation runs for decision making. This runs combine known facts about the future, with plausible alternative trends that are key driving forces. Hence, the quantitative risk analysis leads to the definition of scenarios with adequate constraints, which run as respective physical model of the borehole geological disposal, to predict the needs and expectations of safety related arrangements. With ongoing progress of the borehole geological repository project the physically defined scenarios can be adapted to the major information density available and being used for the whole project duration up to bringing the borehole geological disposal into service.

## 7. Conclusion

This research work demonstrate the fundamentals of the mined and borehole geological repository approaches for high level radioactive waste with reference on the actual situation of national management plans disposing nuclear waste. These plans are of interest for deciding about the structural approach developing a geological disposal and the possible disposing sites which have been taken into account. For a mining disposal concept the problem of salt leaching is described in detail, referring to NURBS as an option to model the dynamic process of salt leaching mathematically. Beside the mining concept the borehole approach is demonstrated. One borehole approach is based on deep depth but a small borehole diameter of about 1 m. The drilling technique applied is based on the long-year

experiences of the rotary drilling method in the petroleum industry. The second demonstrated borehole approach is focused on deep depth too but with a bigger diameter of about 10 m. The drilling approach used in this study is a rock welding principle to sink vertical constructions which has been developed at the Los Alamos Laboratories in New Mexico, U.S.A. But the energy source used to melt the rock in the Los Alamos project was a nuclear reactor which would have contaminated the ground water in case of a disaster. To overcome this energy dependent problem a flame melting technique beneath extreme high pressure, temperature, and frequency has been developed and is demonstrated. Based on the research work described in this chapter a first mock up assessment was carried out in support of implementation of geological disposal based on the flame melting technique concept to melt rock. The main advantages of the research work are:

- demonstration of to date existing approaches to support implementation of geological repositories,
- complementary approach to support the implementation of geological repositories in Europe,
- demonstration of a technology enhanced approach to support implementation of geological repositories,
- collaborative research work at the European level.

## 8. Acknowledgement

This project research work was conducted in part by a group of scientists from the Technical University of Košice, Prof. Dr. Felix Sekular, Slovak Republic, the Slovak Academy of Science, Prof. Dr. Tobias Lazar, Slovak Republic, the University of Hamburg, Prof. Dr. Dietmar P. F. Moeller, Germany, and the German Czech Scientific Foundation, Dr. Rolf Bielecki, Germany. Moreover the University of Sheffield, Prof. Dr. Fergus Gibb, United Kingdom, make helpful suggestions on deep borehole disposal techniques. Any opinions, findings, conclusions or recommendations expressed in this paper are those of the authors and do not necessarily reflect the views of the European Commission (EC) or the International Atomic Energy Agency (IAEA).

## 9. References

- Alexander, R. & McKinley, L. E. (2007). *Deep Geological Disposal of Radioactive Wastes*, Elsevier Science Ltd., ISBN 0 08 043852 0, Oxford, 2007
- Anderson, V. K. (2004). An Evaluation of the Feasibility of Disposal of Nuclear Waste in Very Deep Boreholes. *Dept. of Nuclear Engineering*. Cambridge, MA, MIT
- Berkhout, F. (1991). *Radioactive Waste: Politics and Technology*, Routledge, Chapman and Hall Inc., ISBN 0 0415 05492-3 and ISBN 0 0415 05493-1 (pbk), New York, 1991
- Brady, P. V., Arnold, B. W., Freeze, G. A., Swift, P. N., Bauer, S. J., Kanney, J. L., Rechar, R. P., Stein, J. S. (2009). *Deep Borehole Disposal of High-Level Radioactive Waste. SANDIA REPORT SAND2009-4401* (August 2009), Albuquerque, New Mexico 87185 & Livermore, California 94550
- Carney, S. A. (2001). Management Applicability of Contemporary Deep-Sea Ecology and Re-evaluation of Gulf of Mexico Studies, *Final Report. OCS Study MMS 2001-095*. U.S.

- Dept. of the Interior Minerals Management Service, Gulf of Mexico OCS Region Office, New Orleans, La. 174 pp
- CGER (Commission on Geosciences, Environment and Resources). (1994). *Drilling and Excavation Technologies for the Future*, National Academy Press, Washington, DC, 1994
- Cottrell, J. A., Hughes, T. J. R., Bazilevs, Y. (2009). *Isogeometric analysis: toward integration of CAD and FEA*. John Wiley and Sons (2009). ISBN- 978-0-470-74873-2
- Courtois, C., Carre, F. (2005). French waste management strategy for a sustainable development of nuclear energy. Waste Management Research Direction CEA Saclay, Gif-sur-Yvette, Cedex. Access 02.02.2011, [http://www.oecd-nea.org/pt/docs/iem/lasvegas04/04\\_General\\_Session/GS\\_03.pdf](http://www.oecd-nea.org/pt/docs/iem/lasvegas04/04_General_Session/GS_03.pdf)
- Donald, I. W. (2010). *Waste Immobilization in Glass and Ceramic Based Hosts: Radioactive, Toxic and Hazardous Wastes*, John Wiley and Sons, ISBN 978-1-444-31937-8, New York
- Dyne, P. J. (1975). Managing Nuclear Waste. *AECL Technical Report AECL-5136*, May 1975
- ENS – European Nuclear Society (January 2011). Nuclear Power Plants in Europe, January 26, 2011, Available from: [www.euronuclear.org/info/maps.htm](http://www.euronuclear.org/info/maps.htm), Access 26.01.2011
- Ford, M.(2010). Finland's nuclear waste bunker built to last 100,000 years, CNN, November 12, 2010
- Gibb, F. G. F. (1999). High-temperature, very deep, geological disposal: A safer alternative for high-level radioactive waste. *Waste Management*, Vol. 19, (1999), pp. 207-211.
- Gibb, F. G. F. (2005). Very deep borehole disposal of high level nuclear waste. *Imperial Engineer*, (2005), pp. 11-13
- Hare, F. K.; Aiken, A. M. & Harrison, J. M. (1977): The Management of Canada's Nuclear Wastes, Energy Mines and Resources', *Canada Report EP77-6*, 197
- Hebert, H. J. (2009). Nuclear waste won't be going to Nevada's Yucca Mountain, Obama officials say. Chicago Tribune, March 6, 2009, 4, Access 02.02.2011 [http://www.chicagotribune.com/news/nationworld/chi-nuke-yucca\\_frimar06,0,2557502.story](http://www.chicagotribune.com/news/nationworld/chi-nuke-yucca_frimar06,0,2557502.story)
- IAEA (September 2001). The use of scientific and technical results from underground research laboratory investigations for the geological disposal of radioactive waste. *IAEA-TECDOC-1243*, ISSN-1011-4289, Vienna
- IAEA (2006). Geological Disposal of Radioactive Waste: Safety Requirements, *IAEA Safety Standards Series No.WS-R-4*, Jointly sponsored by the International Atomic Energy Agency and the Organization for Economic Cooperation and Development Nuclear Energy Agency, (2006), Vienna.
- Koerber, C., Moeller, D. P. F., Hanusch, C. (2004). Leachable Geometry. In: Networked Simulation and Simulated Networks. Ed. Horton, G. pp. 397-401. SCS Publ. House, Ghent, (2004)
- Lutze, W., & Ewing R. C. (Eds.). (1988). *Radioactive Waste Forms in the Future*, Elsevier Science Pub., ISBN 0444871047, Amsterdam
- Mascarelli, A. L. (2009). Funding cut for US nuclear waste dump: Yucca Mountains end would leave the country with few alternatives for a long-term repository. *Nature* 458, pp. 1086-1087 (2009)
- McCarthy, J. (October 1995). Frequently asked questions about Nuclear Energy, Access 26.01.2011, <http://www-formal.stanford.edu/jmc/progress/nuclear-faq.html>

- Miller, W., Alexander, R., Chapman, N., McKinley, L. E. & Smellie, J. (2000). *Geological Disposal of Radioactive Wastes & Natural Analogues*, Elsevier Science Ltd., ISBN 0 08 045010 5, Oxford, 2000
- Moeller, D. P. F., Koerber, C., Zemke, C., Hanusch, C., Maas, K. (2005). Earth Falls as a Result of Salt Leaching Effects in the Underground – Application of Modern IT Concepts in Underground Analysis. In: *Underground Infrastructure of Urban Areas*. Eds. Madryas, C., Kolonko, B. pp. 238-253. Oficyna Wydawnicza Publ. Wroclaw (2005)
- Nadis, S. (1996). The Sub-Seabed Solution. *Atlantic Monthly*, Vol. 278, No.4, (October 1996), pp. 28-39
- NAS – National Academy of Sciences (1957). *The Disposal of Radioactive Waste on Land*.
- OECD-NEA (May 2003). *Engineered Barrier Systems and the Safety of Deep Geological Repositories: State of the Art Report*. OECD Pub., ISBN 92-64-18498-8, Paris
- OECD-NEA (January 2007). *Safety Cases for Deep Geological Disposal of Radioactive Waste: Where Do We Stand?* OECD Pub., ISBN 978-92-64-99050-0, Paris
- OMB (2010). *A New Area of Responsibility. Renewing America's Promise. Office of Management and Budget*, p. 65, 2010
- Porter, A. (1978). *A Race against Time. Interim Report on Nuclear Power in Ontario, Royal Commission on Electric Power Planning*, Queen's Printer, Ontario, 1978
- Porter, A. (1980). *The Report of the Ontario Royal Commission on Electric Power Planning: Concepts, Conclusions, and Recommendations*, Queen's Printer for Ontario, 1980
- Rao, K. R. (2001). Radioactive waste: The problem and its management. *Current Science*, Vol.81, No.12, (December 2001), pp. 1534-1546
- Rybar, P., Lazar, T., Hamrak, H. (2004). *Studium problematiky taovnia nerastnych surovin* (In Slovak language). ISBN: 80-8073-085-7
- Sander, W. (1988). Quantitative Beschreibung der Lösungs- und Metamorphose beim Eindringen von Wasser in ein Bergwerk im Zechsteinsalinar (In German language). *Kali und Steinsalz*, Vol. 10, No. 2, (1988), pp. 54-61
- van Loon, A. J. (2000). Reversed mining and reversed-reversed mining: the irrational context of geological disposal of nuclear waste. *Earth Science Reviews*, Vol. 50, (2000), pp. 269-276
- Weber, W. J., Ewing, R. C., Angell, C. A., Arnold, G. W., Cormack, A. N., Delaye, J. M., Griscon, D. L., Hobbs, L. W., Navrotsky, A., Price, D. L., Stoneham, A. M., & Weinberg, M. C. (1997). Radiation effects in glasses used for immobilization of high-level waste and plutonium disposition. *J. Mater. Res.*, Vol. 12, No. 8, (August 1997), pp. 1946-1978
- Wellmer, F.-W., Becker-Platen, J. D., Eds. (1999). *Mit der Erde leben: Beiträge geologischer Dienste zur Daseinsvorsorge und nachhaltigen Entwicklung* (In German). Springer Publ. Berlin Heidelberg New York (1999). ISBN-3-540-64947-6
- [http://en.wikipedia.org/wiki/High-level\\_radioactive\\_waste\\_management](http://en.wikipedia.org/wiki/High-level_radioactive_waste_management). Access 13.02.2011
- Wiki (2011-1). [http://en.wikipedia.org/wiki/High-level\\_radioactive\\_waste\\_management](http://en.wikipedia.org/wiki/High-level_radioactive_waste_management). Access 13.02.2011
- Wiki (2011-2). <http://en.wikipedia.org/wiki/KBS-3>. Access 04.03.2011

YUCCA (2008. *Radioactive Waste Repositories: Hanford Site, Yucca Mountain Nuclear Waste Repository, Natural Nuclear Fission Reactor*. Books LLC Publ. ISBN-13-978-1157005278

# Isotopic Uranium and Plutonium Denaturing as an Effective Method for Nuclear Fuel Proliferation Protection in Open and Closed Fuel Cycles

Kryuchkov E.F., Tsvetkov P.V.<sup>1</sup>, Shmelev A.N., Apse V.A., Kulikov G.G.,  
Masterov S.V., Kulikov E.G. and Glebov V.B.

*National Research Nuclear University "MEPhI",*

<sup>1</sup>*Texas A&M University*

Russia

<sup>1</sup>USA

## 1. Introduction

The paper addresses to the problems related with protection of the existing and advanced nuclear fuel types against unauthorized proliferation via introduction of some admixtures into their composition. So, the task may be defined as follows: these admixtures must create the barriers difficult to overcome for the use of nuclear fuels in nuclear explosive devices (NED) but, at the same time, these admixtures must preserve (or even enhance) energy potential of nuclear fuels for further peaceful use at civilian nuclear power plants (NPP). Such an approach to proliferation protection of nuclear fuels is often called as an isotopic denaturing. The term "isotopic denaturing" is used to designate any artificial changes in isotopic composition of chemical element which can give some new desirable properties to this element.

## 2. Protection of nuclear materials in fuel cycle against unauthorized applications

As is known, main raw materials for NPP are natural uranium and thorium. Natural uranium contains 0.71%  $^{235}\text{U}$ , and self-sustainable chain fission reaction (CFR) may be maintained by thermal neutrons provided rather large amounts of uranium, graphite or heavy water are available. As for natural thorium, there are no fissile isotopes, like  $^{235}\text{U}$ , in its composition at all. So, manufacturing of a small-size NED with uranium charge requires application of isotopic enrichment in order to produce highly enriched (weapon-grade) uranium (HEU, 90-95%  $^{235}\text{U}$ ). Some artificial fissile materials (plutonium or  $^{233}\text{U}$ ) can be used as a nuclear charge but they may be produced only under neutron irradiation of natural uranium or thorium in nuclear reactors.

At present, nuclear reactors apply uranium fuels of various enrichments. So, isotopic composition of uranium-based fuel for civilian NPP takes an intermediate position between

natural uranium and HEU. Conversion of civilian uranium fuel into HEU, or weapon-grade uranium, requires application of isotopic re-enrichment operations.

Plutonium, suitable element for NED, is produced by nuclear reactors in the process of their operation. As is known, weapon-grade plutonium (WGPu) consists mainly of  $^{239}\text{Pu}$  with small content of  $^{240}\text{Pu}$  (4-7%) and negligible amounts of heavier plutonium isotopes. WGPu may be produced in the special reactors with short irradiation cycle. Power reactors at NPP are operated with relatively long irradiation cycle and, thus, with high fuel burn-up. So, plutonium produced in power reactors (reactor-grade plutonium, RGPu) contains the larger amounts of heavier plutonium isotopes. Lengthy irradiation of uranium fuel can change significantly isotopic composition of uranium (in particular, isotopes  $^{232}\text{U}$  and  $^{236}\text{U}$  do appear). As an example, isotopic composition of uranium fuel (initial enrichment - 4.4%  $^{235}\text{U}$ ) after LWR operation up to fuel burn-up of 4% HM is presented in Table 1. Thus, uranium fuel may be used to produce fissile materials, suitable for NED, in nuclear reactors but it requires application of some special operations.

Composition of fresh fuel		Composition of uranium and plutonium in spent fuel, % (fuel burn-up - 4 % HM)				
4.4 % $^{235}\text{U}$	Uranium	$^{232}\text{U}$	$^{235}\text{U}$	$^{236}\text{U}$	$^{238}\text{U}$	
		$1.4 \cdot 10^{-9}$	1.26	0.59	98.15	
	Plutonium (RGPu)	$^{238}\text{Pu}$	$^{239}\text{Pu}$	$^{240}\text{Pu}$	$^{241}\text{Pu}$	$^{242}\text{Pu}$
		1.7	58.0	22.3	12.3	5.7

Table 1. Isotopic compositions of uranium and plutonium in spent LWR fuel

Artificial fissile uranium isotope  $^{233}\text{U}$ , high-efficiency material for NED, may be produced by neutron irradiation of natural thorium. However, undesirable by-products are generated in this process including other uranium isotopes, namely  $^{232}\text{U}$ ,  $^{234}\text{U}$  and  $^{236}\text{U}$ . In particular, light uranium isotope  $^{232}\text{U}$  can complicate significantly any operations with produced uranium.

Radiochemical reprocessing of spent nuclear fuel (SNF) includes extraction of radioactive fission products (FP) whose intense emission of ionizing radiation creates a protective barrier against unauthorized access to fissile materials. So, SNF reprocessing can be regarded as an operation which can remove (or, at least, weaken under incomplete purification) the radiation barrier. SNF partitioning into separate elements or groups of elements can facilitate diversion of fissile materials. In order to reduce the diversion risk, appropriate protective actions should be undertaken. In addition to the organizing measures related with physical protection of nuclear enterprises and technological control, the following barriers against diversion of fissile materials should be considered:

1. Radiation barrier mainly formed by FP. Such a barrier can be formed in the process of the reactor operation and by a special short-term irradiation of fresh fuel assemblies in the dedicated nuclear facilities. Radiation background of fissile materials is one else component of the radiation barrier.
2. Incomplete SNF purification from radioactive FP can result in intense radiation fields which make very difficult any further operations with extracted fuel.
3. Isotopic dilution of  $^{235}\text{U}$ , i.e. the use of relatively low-enriched uranium (LEU).
4. Incomplete separation of uranium from plutonium (or full exclusion of any technological procedures needed for uranium-plutonium separation) in the course of SNF reprocessing. This measure makes it impossible to use these materials directly in NED.



5. Application of automatic remote technology for fuel, fuel rods and fuel assemblies fabrication. This measure can complicate access to fissile materials.
6. Dilution (or denaturing) of fissile materials by their isotopes which can complicate the use of fissile materials in NED. A particular case of isotopic denaturing is a well-known dilution of  $^{235}\text{U}$  by  $^{238}\text{U}$ , i.e. the use of LEU fuel. Another example: neutron irradiation of mixed uranium-thorium fuel in nuclear reactors can produce fissile isotope  $^{233}\text{U}$  isotopically diluted by  $^{238}\text{U}$ .

If we consider fissile plutonium isotope  $^{239}\text{Pu}$ , then the heavier plutonium isotopes (mainly,  $^{240}\text{Pu}$ ) play the same role of isotopic diluents. In addition, light plutonium isotope  $^{238}\text{Pu}$  is an intense source of spontaneous fission neutrons and intense source of thermal energy from  $\alpha$ -decays (half-life of  $^{238}\text{Pu}$  is equal to 87.7 years).

In thorium fuel cycle the same role may be played by  $^{232}\text{U}$  (half-life – 68.9 years).

In practice, the measures listed above may be used in combinations. For example, open fuel cycle of power LWR is provided with the following protective barriers:

- Isotopic dilution (LEU fuel).
- Intense radiation background caused mainly by FP.
- SNF contains non-separated mixture of uranium and plutonium.

Just this set of protective barriers represents a basis for the USA standard on SNF proliferation protection (Spent Fuel Standard (USA National Academy of Sciences, 2000)).

As  $^{232}\text{U}$  and its neutron predecessor  $^{231}\text{Pa}$  are nuclides of low abundance, it seems reasonable to consider their properties in detail.

### 3. Nuclear properties of $^{232}\text{U}$ and $^{231}\text{Pa}$

Basic nuclear properties of main uranium isotopes are presented in Table 2 (Reilly et al., 1991; OECD Nuclear Energy Agency, 1997). As it may be seen, some nuclear properties of  $^{232}\text{U}$  make it a valuable material for proliferation protection of uranium-based nuclear fuel.

	$^{232}\text{U}$	$^{234}\text{U}$	$^{235}\text{U}$	$^{238}\text{U}$
Half-life, years	68.9	$2.45 \times 10^5$	$7.04 \times 10^8$	$4.47 \times 10^9$
Specific yield of $\alpha$ -particles, 1/(g·s)	$8 \times 10^{11}$	$2.3 \times 10^8$	$7.9 \times 10^4$	$1.2 \times 10^4$
Mean energy of $\alpha$ -particles, MeV	5.3	4.76	4.4	4.19
Specific yield of spontaneous fission neutrons, 1/(g s)	1.3	$5.02 \times 10^{-3}$	$2.99 \times 10^{-4}$	$1.36 \times 10^{-2}$
Fission cross-section ( $E_n = 0.0253$ eV), barns	77.15	0.465	583.2	$1.2 \times 10^{-5}$

Table 2. Basic nuclear properties of main uranium isotopes

$^{232}\text{U}$  is a starting isotope for chain of radioactive decays, and some  $^{232}\text{U}$  decay products ( $^{208}\text{Tl}$ ,  $^{212}\text{Bi}$ ) emit high-energy gamma-radiation (2.6 MeV and 1.8 MeV, respectively) that improves detectability of  $^{232}\text{U}$ -containing nuclear materials (Gilfoyle & Parmentola, 2001) and complicates radiation conditions, especially for any unauthorized actions. Nuclear properties of main  $^{232}\text{U}$  decay products are presented in Table 3.

Decay products	$^{228}\text{Th}$	$^{224}\text{Ra}$	$^{220}\text{Rn}$	$^{216}\text{Po}$	$^{212}\text{Bi}$	$^{212}\text{Po}$
Half-life	1.91 years	3.62 days	55.6 sec	0.145 sec	1.01 hours	$3 \times 10^{-7}$ sec
Energy of $\alpha$ -particles, MeV (relative intensity)	5.42 (71.7%) 5.34 (27.6%)	5.69 (94.9%) 5.45 (5.1%)	6.29 (100%)	6.78 (100%)	6.09 (9.7%) 6.05 (25.2%)	8.78 (100%)

Table 3.  $^{232}\text{U}$  decay products, emitters of  $\alpha$ -particles

Like  $^{238}\text{U}$ , isotope  $^{231}\text{Pa}$  can play a role of a fertile nuclide which is not split by thermal neutrons but promotes breeding of fissile materials. Dependencies of radiative capture cross-sections on neutron energy are presented in Fig. 1 for isotopes  $^{238}\text{U}$  and  $^{231}\text{Pa}$ .

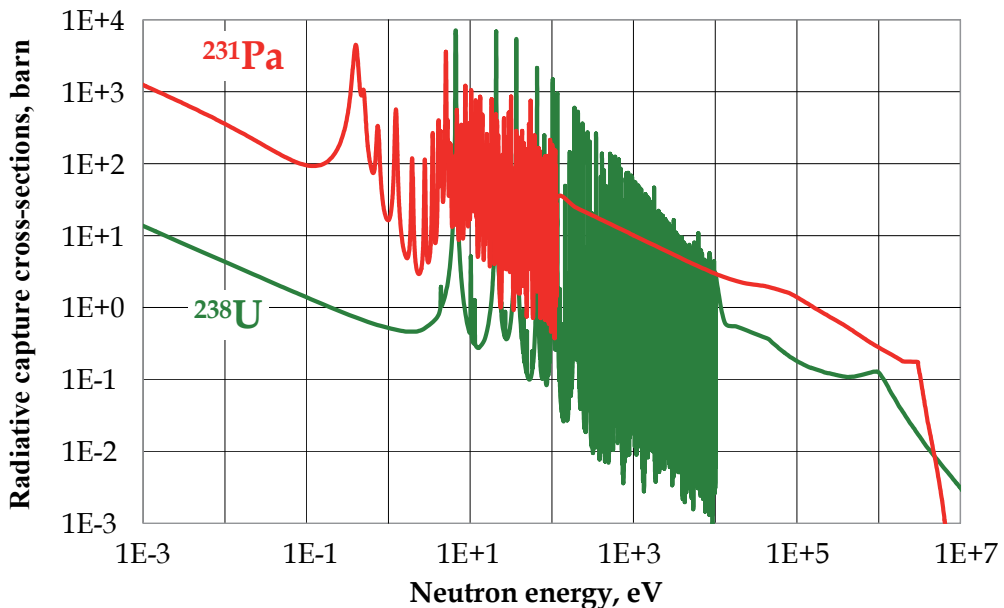


Fig. 1. Dependency of radiative capture cross-sections on neutron energy for  $^{238}\text{U}$  and  $^{231}\text{Pa}$

The following two important aspects should be noted here. Firstly, within thermal energy range,  $^{231}\text{Pa}$  is a superior neutron absorber as compared with  $^{238}\text{U}$ . For example, radiative capture cross sections of thermal neutrons ( $E_n = 0.0253$  eV) for these two isotopes are equal to:  $\sigma_c(^{231}\text{Pa}) = 227$  barns,  $\sigma_c(^{238}\text{U}) = 3$  barns. So, the presence of  $^{231}\text{Pa}$  in fuel composition can promote effective generation of fissile isotopes  $^{232}\text{U}$  and  $^{233}\text{U}$ . Secondly, there is a rather large energy distance between capture resonances of  $^{238}\text{U}$  and  $^{231}\text{Pa}$ . Capture resonances of  $^{231}\text{Pa}$  belong to relatively low energies (below 100 eV). This means the presence of  $^{231}\text{Pa}$  in fuel composition can depress thermal region in energy spectrum of neutrons (see Fig. 2).

It can be seen that, although neutron energy spectrum in VVER-1000 contains a certain fraction of thermal neutrons, introduction of  $^{231}\text{Pa}$  into fuel composition can remove the thermal fraction completely. That is why stainless steel may be used here as a structural material. Indeed, the absence of thermal fraction in neutron spectrum does not result in

additional neutron loss but fuel rods can keep their ability for working up to the higher values of fuel burn-up than with zirconium-based alloys.

Now let us consider nuclear properties of  $^{232}\text{U}$ , product of neutron capture by  $^{231}\text{Pa}$  and rapid  $\beta$ -decay of  $^{232}\text{Pa}$  ( $T_{1/2} (^{232}\text{Pa}) = 1,3$  days (Babichev et al.,1991)). Like  $^{235}\text{U}$ , isotope  $^{232}\text{U}$  is a fissile nuclide. Dependencies of fission cross-sections on neutron energy are presented in Fig. 3 for isotopes  $^{235}\text{U}$  and  $^{232}\text{U}$ .

It can be seen that, within thermal energy range, fission cross-sections of  $^{232}\text{U}$  are substantially lower than those for  $^{235}\text{U}$  while radiative capture cross-sections of these isotopes are comparable each other. For example, radiative capture cross sections of thermal neutrons ( $E_n = 0.0253$  eV) for these two isotopes are equal to:  $\sigma_c(^{232}\text{U}) = 73$  barns,  $\sigma_c(^{235}\text{U}) = 99$  barns. So, neutron-multiplying properties of  $^{232}\text{U}$  are inferior to those of  $^{235}\text{U}$  within thermal energy range.

This conclusion can be confirmed by Fig. 4 which demonstrates energy dependency of  $(\nu_{ef} - 1)$ , i.e. the number of excess fission neutrons per one absorbed neutron.

$^{235}\text{U}$  looks superior to  $^{232}\text{U}$  within thermal energy range but quite another situation takes place in resonance range. So, it may be expected that introduction of  $^{231}\text{Pa}$  into uranium-based fuel composition with aim to increase fuel burn-up will be more efficient just in resonance neutron spectrum.

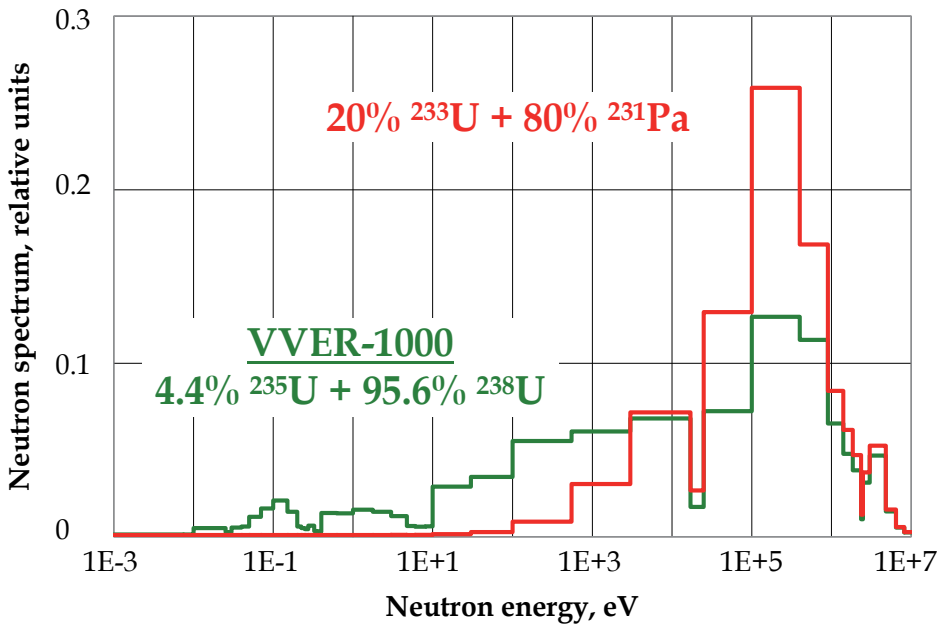


Fig. 2.  $^{231}\text{Pa}$  effect on energy spectrum of neutrons

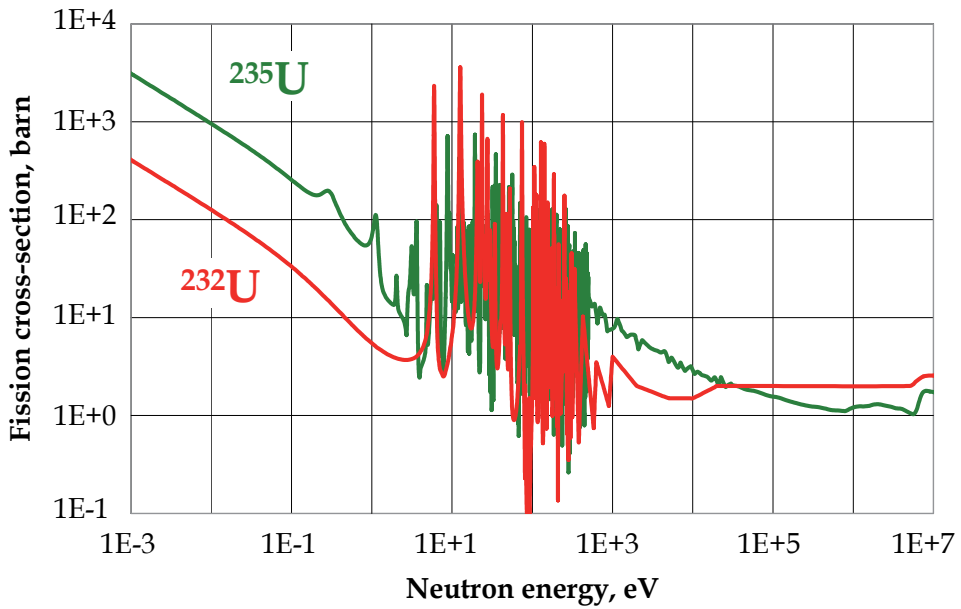


Fig. 3. Dependency of fission cross-sections on neutron energy for isotopes  $^{235}\text{U}$  and  $^{232}\text{U}$

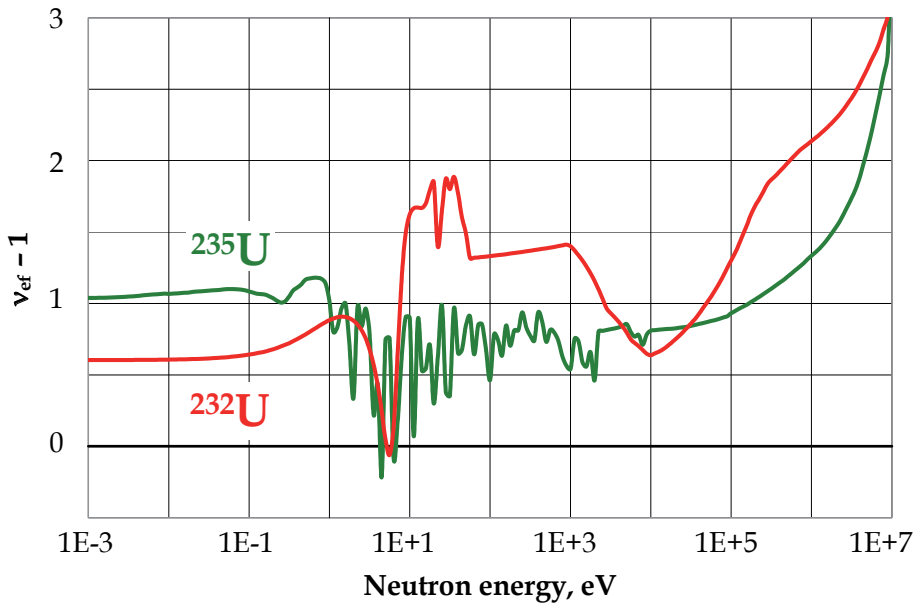


Fig. 4. Energy dependency of the number of excess fission neutrons per one absorbed neutron for isotopes  $^{235}\text{U}$  and  $^{232}\text{U}$

#### 4. Proliferation resistance of nuclear materials in open fuel cycle. The ways for closure of fuel cycle

Presently, there are different points of view on future development of nuclear fuel cycles. Some countries (USA, Canada, Germany and Sweden) are implementing in practice an open nuclear fuel cycle (Fig. 5) that does not foresee a radiochemical SNF reprocessing in the visible future. One of the reasons for this choice is a wish of decreasing a risk of nuclear weapon proliferation. SNF may be only converted into the forms suitable for long-term safe storage. However, such a strategy of nuclear power development has already resulted in large SNF stockpiles, potentially dangerous nuclear materials (NM). So, the preferable option for future development of nuclear power consists in transition to the closed fuel cycles with SNF reprocessing, separation of radioactive FP and recycling of residual fuel.

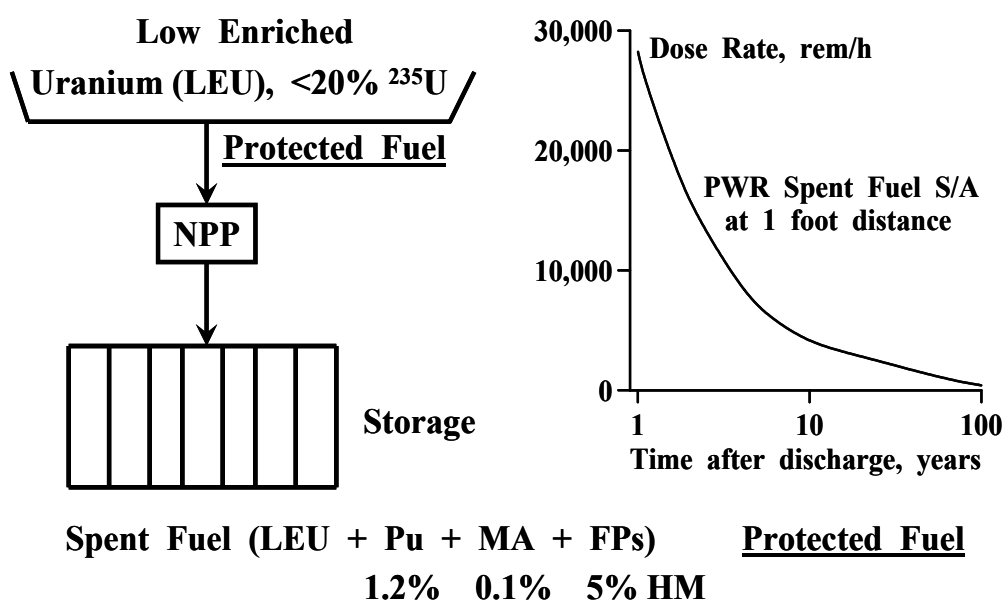


Fig. 5. Open fuel cycle

LEU is a fresh fuel for open nuclear fuel cycle. Plutonium in spent fuel assemblies is protected by intense gamma-radiation of fission products (Fig. 5). That is why unirradiated materials are more vulnerable for unauthorized proliferation.

Isotopic uranium denaturing may be regarded as an effective method for upgrading self-protection of unirradiated uranium-containing materials. The term "isotopic denaturing" is used conventionally for designation of any artificial changes in natural isotopic composition of a chemical element with aim to give him some new, desirable properties. In practice, uranium may be denatured by the following two ways: direct introduction of intense radioactive isotope  $^{232}\text{U}$  into uranium fuel composition or direct introduction of relatively weaker radioactive isotope  $^{231}\text{Pa}$  into uranium fuel composition.  $^{231}\text{Pa}$  is a neutron predecessor of  $^{232}\text{U}$ , main isotope of uranium denaturing. So, only short-term pre-irradiation of fresh fuel assemblies in the research reactors may be sufficient to produce proliferation resistant fuel assemblies, suitable even for export deliveries.

#### 4.1 Isotopic denaturing of uranium as a way for creating an internal source of $\alpha$ -particles

Along with progress in development of high-efficiency enriching technologies, potential threat of LEU diversion and re-enrichment up to the weapon-grade level excites more and more apprehensions. These reasons indicate that, besides reduction of uranium enrichment below 20%  $^{235}\text{U}$ , other measures may be also required to upgrade LEU self-protection against its unauthorized re-enrichment. Taking into consideration the growing world-wide scope of LEU utilization, including LEU with enrichment in the vicinity of the upper boundary ( $\sim 20\%$   $^{235}\text{U}$ ), high LEU vulnerability to unauthorized re-enrichment must be recognized. Particular apprehensions are related with 20%-uranium. So, some additional actions should be undertaken to protect LEU against its unauthorized re-enrichment.

The effects of  $^{232}\text{U}$  introduction into LEU are caused by the following specific properties of  $^{232}\text{U}$  (see Table 2):

- Good neutron-multiplying properties of  $^{232}\text{U}$  (Ganesan et al., 2002) and its neutron predecessor  $^{231}\text{Pa}$  make it possible to extend time period of continuous reactor operation without refueling up to the values comparable with the reactor life-time. As a result, unauthorized extraction of plutonium from spent fuel assemblies becomes unfeasible.
- It is impossible to remove  $^{232}\text{U}$  from denatured uranium without application of sophisticated and expensive isotope separation technologies.
- $^{232}\text{U}$  is a neutron source from spontaneous fission reactions and a source of high-energy  $\alpha$ -particles. Alpha-particles emitted by  $^{232}\text{U}$  are able to dissociate molecules of uranium hexafluoride and, thus, could make it practically impossible to re-enrich denatured uranium up to the weapon-grade level. Besides,  $\alpha$ -particles are able to initiate ( $\alpha, n$ )-reactions with impurities of light elements (LE) and, thus, intensify internal neutron generation. Growth of neutron background in the re-enriching process of LEU-uranium containing 0.1–0.5%  $^{232}\text{U}$  can decrease the CFR energy yield by three orders of magnitude. In essence, NED with such a re-enriched uranium is a “dirty” bomb only. Thus, export deliveries of LEU-based fuel assemblies to foreign NPP receive an additional proliferation barrier.

#### 5. Increased burn-up of proliferation protected LWR fuel containing $^{231}\text{Pa}$

One of specific features in operation of nuclear power reactors consists in a necessity to perform regular refuelings. This necessity is caused by the following effects: depletion of fissile materials, FP accumulation, potential rupture of fuel cladding with intense release of radioactive materials. LWR, the mostly spread type of power reactors, requires refueling every 1-2 years, when fuel burn-up reaches 4-6% HM.

Extension of fuel life-time up to relatively long time periods (several decades, for instance) can reduce drastically the number of refuelings or exclude them at all. Reduction or full exclusion of refueling procedures decreases the demands for fresh fuel and decreases quantity of SNF discharged per unit of produced energy. Those reactors, which are capable to operate for a sufficiently long time without any refueling, may be used as the only energy source in remote regions, at the floating NPP, as energy source for space investigations (research bases on the Moon or Mars, cosmic flights into the outer space). Our studies demonstrated that introduction of  $^{231}\text{Pa}$  into LWR fuel composition could extend significantly the fuel life-time and reach ultra-high fuel burn-up.

It should be noted that achievability of ultra-high fuel burn-up was studied here only from the standpoint of neutron-multiplying properties of advanced fuel compositions. The problems of suitable structural materials, evolution of their strength properties and durability for a long fuel life-time are not analyzed here. At present, maximal fuel burn-up (about 30% HM) was achieved in the research fast reactor BOR-60 (Grachev et al., 2003). It may be expected that the higher values of fuel burn-up could be achieved if the following operations would be multiply carried out: partial fuel burn-up (near to the practically achievable value of 30% HM), application of DUPIC-technology for removal of gaseous and volatile FP, re-fabrication of fresh fuel pellets.

**5.1 Evolution of neutron-multiplying properties in chains of isotopic transformations**

In this section we compared time evolutions of neutron-multiplying properties in two isotopic chains: traditional chain that starts from  $^{232}\text{Th}$  ( $^{232}\text{Th} \rightarrow ^{233}\text{U} \rightarrow ^{234}\text{U} \rightarrow \dots$ ) and non-traditional chain that starts from  $^{231}\text{Pa}$  ( $^{231}\text{Pa} \rightarrow ^{232}\text{U} \rightarrow ^{233}\text{U} \rightarrow \dots$ ) (see Fig. 6). Radiative capture cross-sections  $\sigma_c$  and fission cross-sections  $\sigma_f$  were calculated for a typical neutron spectrum of VVER-1000 ( $\beta$ -decays were not taken into account).

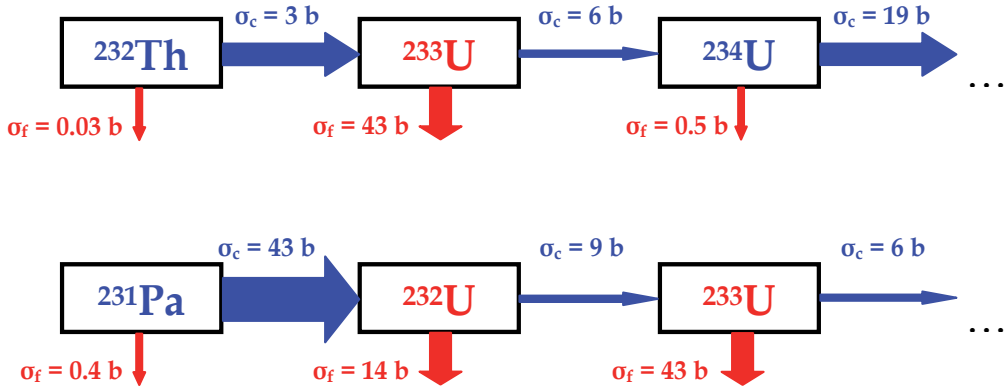


Fig. 6. Chains of isotopic transformations ( $^{232}\text{Th} \rightarrow ^{233}\text{U} \rightarrow ^{234}\text{U} \rightarrow \dots$ ) and ( $^{231}\text{Pa} \rightarrow ^{232}\text{U} \rightarrow ^{233}\text{U} \rightarrow \dots$ ) (neutron spectrum of VVER-1000)

It can be seen that neutron-multiplying properties in non-traditional chain are gradually improved: the starting isotope  $^{231}\text{Pa}$  is a neutron absorber, fission cross-section of the second isotope  $^{232}\text{U}$  prevails over its capture cross-section, and the third isotope  $^{233}\text{U}$  is a well-fissionable material. So, non-traditional chain represents the combination of two consecutive fissionable isotopes ( $^{232}\text{U}$  and  $^{233}\text{U}$ ) while, in traditional chain, the third isotope  $^{234}\text{U}$  is a neutron absorber only.

Thus, in non-traditional chain, parasitic neutron absorption by FP and depletion of fissile materials during the reactor operation can be partially compensated by  $^{231}\text{Pa}$  feeding. This makes it possible to talk about a possibility for substantial extension of fuel life-time and achievability of ultra-high fuel burn-up. By the way, in traditional LWR fuel, the negative effects caused by FP accumulation and depletion of fissile materials are compensated by  $^{238}\text{U}(n,\gamma)^{239}\text{Pu}$  chain significantly weaker than by  $^{231}\text{Pa}(n,\gamma)^{232}\text{U}(n,\gamma)^{233}\text{U}$  chain in non-traditional fuel because of lower capture cross-sections:  $\sigma_c(^{238}\text{U}) = 0.9 \text{ barns}$ ,  $\sigma_c(^{231}\text{Pa}) = 43 \text{ barns}$ .

So, it can be concluded that non-traditional chain ( $^{231}\text{Pa} \rightarrow ^{232}\text{U} \rightarrow ^{233}\text{U} \rightarrow \dots$ ) appears to be more attractive from the standpoint of neutron-multiplying properties (as a consequence, from the standpoint of extended fuel life-time or achievability of ultra-high fuel burn-up) in comparison with traditional chain ( $^{232}\text{Th} \rightarrow ^{233}\text{U} \rightarrow ^{234}\text{U} \rightarrow \dots$ ) due to the following reasons:

1. Combination of two consecutive well-fissionable isotopes ( $^{232}\text{U}$  and  $^{233}\text{U}$ ).
2. High rate of their generation from the starting isotope  $^{231}\text{Pa}$ , whose neutron capture cross-section is larger substantially than that for the starting nuclide  $^{232}\text{Th}$  in traditional chain of isotopic transformations.

It is noteworthy that  $^{231}\text{Pa}$  may be regarded, to a certain extent, as a burnable neutron poison: for fuel life-time  $^{231}\text{Pa}$  is burnt up to 80% and converted into well-fissionable isotopes, neutron capture cross-section of  $^{231}\text{Pa}$  is substantially larger than that of fertile isotope  $^{232}\text{Th}$ .

As is known, the existing LWRs are characterized by thermal neutron spectrum. In advanced LWR designs, for example, in LWR with supercritical coolant parameters (SCLWR), different regions of the reactor core are characterized by different neutron spectra depending on coolant density. Thermal spectrum prevails within the core region containing dense coolant ( $\gamma = 0.72 \text{ g/cm}^3$ ) while resonance neutron spectrum dominates within the core region containing coolant of the lower density ( $\gamma = 0.1 \text{ g/cm}^3$ ) (Kulikov, 2007).

Reasonability of  $^{231}\text{Pa}$  introduction into fuel composition for the cases of thermal and resonance neutron spectra is analyzed in the next section.

## 5.2 Reasonability of $^{231}\text{Pa}$ involvement in the case of thermal neutron spectrum

Numerical analyses of fuel depletion process were carried out with application of the computer code SCALE-4.3 (Oak Ridge National Laboratory, 1995) and evaluated nuclear data file ENDF/B-V for elementary cells of VVER-1000. The only exception consisted in the use of martensite steel MA956 (elemental composition: 74,5% Fe, 20% Cr, 4,5% Al, 0,5% Ti and 0,5%  $\text{Y}_2\text{O}_3$ ) instead of zircaloy as a fuel cladding material. Substitution of martensite steel for zirconium-based cladding is caused by the higher values of fuel burn-up.

Traditional ( $^{232}\text{Th}$ - $^{233}\text{U}$ ) and non-traditional ( $^{231}\text{Pa}$ - $^{232}\text{Th}$ - $^{233}\text{U}$ ) fuel compositions were compared for the case of thermal neutron spectrum (coolant density –  $0.72 \text{ g/cm}^3$ ). Infinite neutron multiplication factor  $K_\infty$  is shown in Fig. 7 as a function of fuel burn-up.

It can be seen that substitution of  $^{231}\text{Pa}$  for  $^{232}\text{Th}$  decreases  $K_\infty$  at the beginning of cycle, i.e. decreases an initial reactivity margin to be compensated. This effect is caused by different capture cross-sections of these isotopes -  $^{231}\text{Pa}$  is a significantly stronger neutron absorber than  $^{232}\text{Th}$ . In parallel, thanks to the larger capture cross-section of  $^{231}\text{Pa}$ , intense breeding of two consecutive well-fissionable isotopes ( $^{232}\text{U}$  and  $^{233}\text{U}$ ) takes place. So, gradual introduction of  $^{231}\text{Pa}$  into fuel composition results in the smoother relaxation of neutron multiplication factor in the process of fuel burn-up.

Acceptable fraction of  $^{231}\text{Pa}$  in non-traditional fuel composition is limited by the value of neutron multiplication factor (above unity) at the beginning of cycle. So, the effects caused by introduction of  $^{231}\text{Pa}$  may take place only in those fuel compositions where fraction of main fissile isotope is sufficiently large. For example, fraction of main fissile isotope  $^{233}\text{U}$  may be increased up to the level corresponding to the situation when neutron multiplication factor at the beginning of cycle is equal to about 1.10 at full replacement of  $^{232}\text{Th}$  by  $^{231}\text{Pa}$ . The calculations showed that this condition may be satisfied at maximal  $^{233}\text{U}$  fraction about 30%. Evolution of neutron multiplication factor in the process of fuel burn-up is presented in Fig. 8 for traditional and non-traditional fuel compositions.



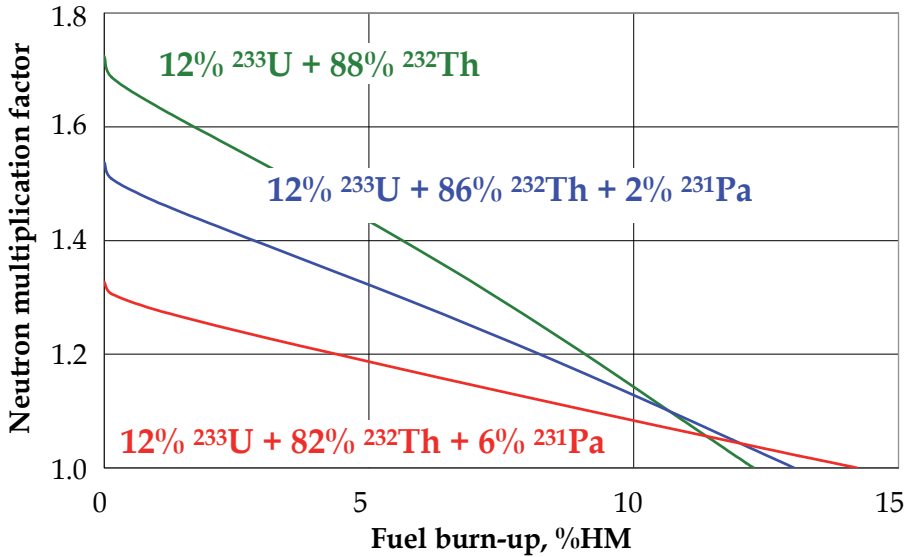


Fig. 7.  $^{231}\text{Pa}$  effects on fuel burn-up in thermal neutron spectrum

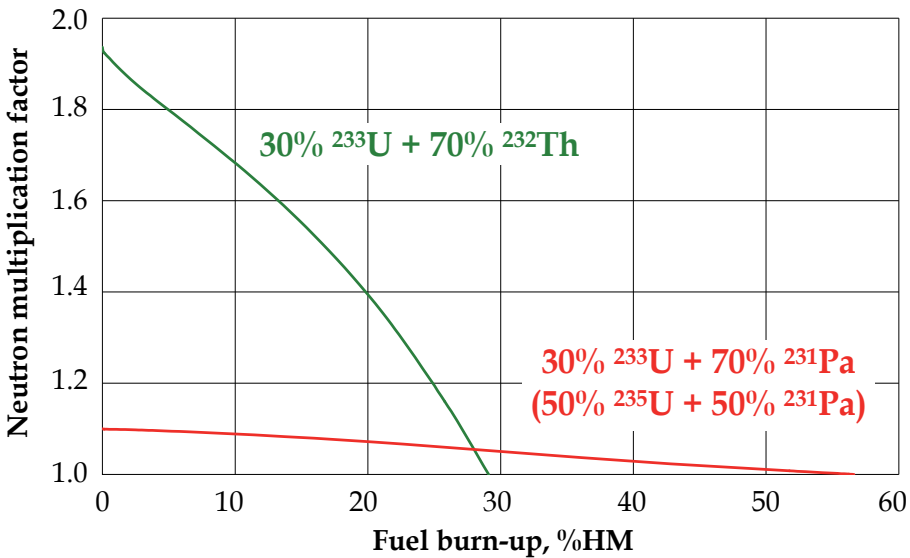


Fig. 8. Achievability of ultra-high fuel burn-up by introduction of  $^{231}\text{Pa}$  (thermal neutron spectrum)

As is seen from Fig. 8, traditional thorium-based fuel (30%  $^{233}\text{U}$  + 70%  $^{232}\text{Th}$ ) provides rather high reactivity margin ( $K_{\infty}$  (BOC)  $\approx 1.9$ ) with achievable value of fuel burn-up about 29% HM. Introduction of  $^{231}\text{Pa}$  into fuel composition decreases initial reactivity margin but, at the same time, increases fuel burn-up. If  $^{232}\text{Th}$  is completely replaced by  $^{231}\text{Pa}$ , i.e. (30%  $^{233}\text{U}$  + 70%  $^{231}\text{Pa}$ ) fuel composition is analyzed, then neutron multiplication factor remains

practically unchanged in the vicinity of unity for a full duration of fuel life-time. This means that the negative effects from neutron absorption by FP and depletion of fissile isotope are almost completely compensated by breeding of secondary fissile isotopes from  $^{231}\text{Pa}$ . In this case, about 80%-part of  $^{231}\text{Pa}$  is converted into secondary fissile isotopes which can provide ultra-high fuel burn-up (near to 57% HM).

If fuel loading in such a reactor is similar to the fuel loading of VVER-1000 (about 66 tons), then achievable value of fuel life-time is near to 40 years for the reactor power of 3000 MWt. It is interesting to note that  $^{235}\text{U}$  as well as  $^{233}\text{U}$  may be used to achieve ultra-high fuel burn-up. Moreover,  $^{235}\text{U}$  option looks very attractive because of two reasons: firstly,  $^{235}\text{U}$  resources are more available than resources of  $^{233}\text{U}$ , and, secondly, achievement of the same fuel burn-up will require lower quantity of  $^{231}\text{Pa}$ , artificial isotope to be produced in the dedicated nuclear power facilities.

### 5.3 Reasonability of $^{231}\text{Pa}$ involvement in the case of resonance neutron spectrum

Traditional ( $^{232}\text{Th}$ - $^{233}\text{U}$ ) and non-traditional ( $^{231}\text{Pa}$ - $^{232}\text{Th}$ - $^{233}\text{U}$ ) fuel compositions were compared for the case of resonance neutron spectrum (coolant density – 0.1 g/cm<sup>3</sup>). Infinite neutron multiplication factor  $K_\infty$  is shown in Fig. 9 as a function of fuel burn-up.

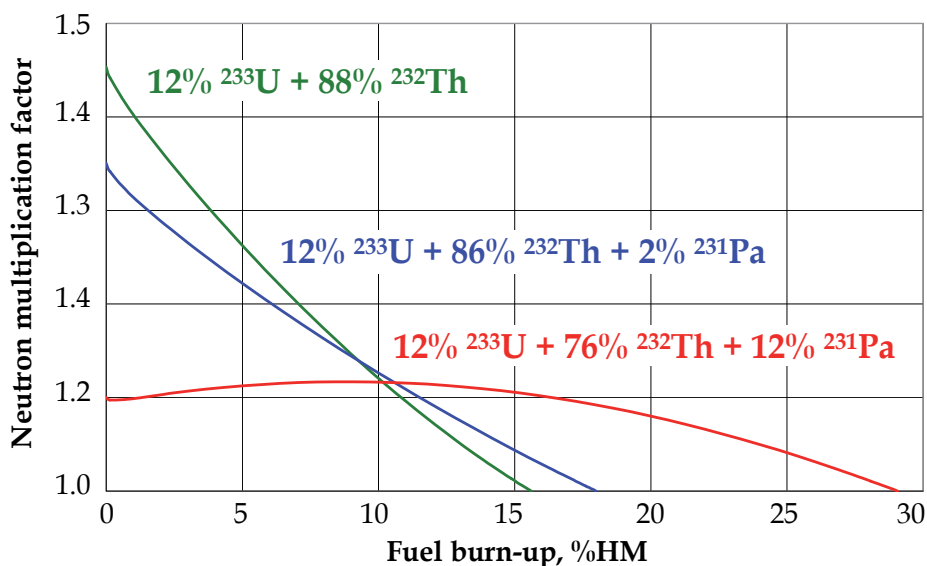


Fig. 9.  $^{231}\text{Pa}$  effects on fuel burn-up in resonance neutron spectrum

Comparison of the curves presented in Figs. 7, 9 allows us to conclude that introduction of  $^{231}\text{Pa}$  into fuel composition is more preferable from the standpoint of higher fuel burn-up in the case of resonance neutron spectrum. This conclusion can be explained by better neutron-multiplying properties of  $^{232}\text{U}$  just in resonance neutron spectrum as compared with thermal neutron spectrum (see Fig. 4).

As it follows from Fig. 9, introduction of only 12%  $^{231}\text{Pa}$  increased fuel burn-up twice. Neutron multiplication factor at the beginning of cycle increased too, i.e. neutron-multiplying properties of fuel composition became better.

Like previous analysis, fraction of main fissile isotope  $^{233}\text{U}$  may be increased up to the level corresponding to the situation when neutron multiplication factor at the beginning of cycle is equal to about 1.10 at full replacement of  $^{232}\text{Th}$  by  $^{231}\text{Pa}$ . In addition, potential use of  $^{235}\text{U}$  instead of  $^{233}\text{U}$  was analyzed to evaluate a possibility for achieving ultra-high fuel burn-up. So, numerical studies confirmed reasonability for introduction of  $^{231}\text{Pa}$  into fuel composition because this introduction results in reduction of initial reactivity margin and in substantial growth of fuel burn-up. Maximal positive effect from introduction of  $^{231}\text{Pa}$  may be observed in resonance neutron spectrum. Besides, introduction of  $^{231}\text{Pa}$  makes it possible to reach ultra-high fuel burn-up regardless of what main fissile isotope is used,  $^{233}\text{U}$  or  $^{235}\text{U}$ . In particular, (20%  $^{233}\text{U}$  + 80%  $^{231}\text{Pa}$ ) fuel composition can reach fuel burn-up of 76% HM in resonance neutron spectrum (see Fig. 10).

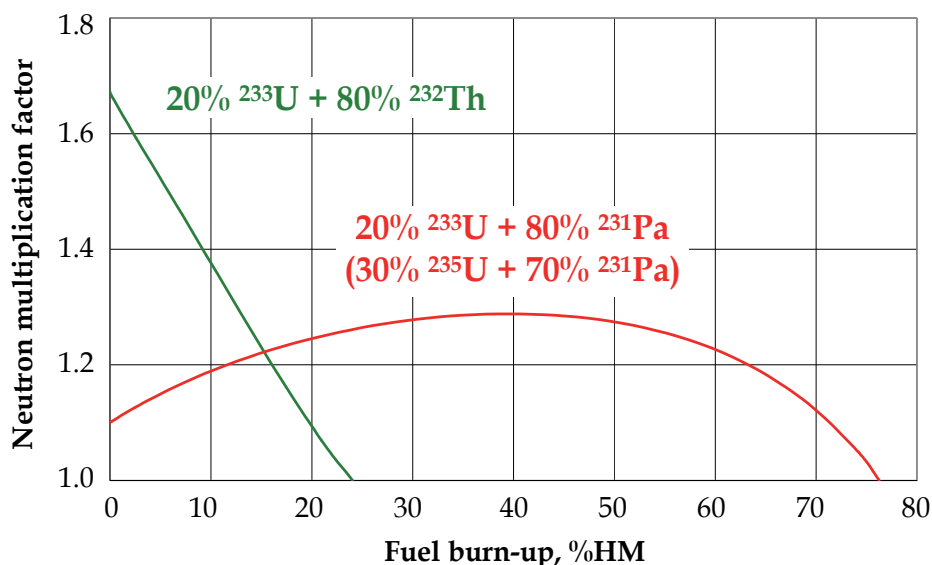


Fig. 10. Achievability of ultra-high fuel burn-up by introduction of  $^{231}\text{Pa}$  (resonance neutron spectrum)

#### 5.4 Effects of $^{231}\text{Pa}$ on safety of the reactor operation

On the one hand, introduction of  $^{231}\text{Pa}$  into fuel composition can provide small value of initial reactivity margin and high value of fuel burn-up. On the other hand, if relatively large  $^{231}\text{Pa}$  fraction is introduced into fuel composition, reactivity feedback on coolant temperature becomes positive, and safety of the reactor operation worsens.

Numerical studies demonstrated that, if maintenance of favorable reactivity feedback on coolant temperature during fuel life-time is a mandatory requirement, then, in thermal neutron spectrum,  $^{231}\text{Pa}$  fraction in fuel composition is limited by a quite certain value while, in resonance neutron spectrum, introduction of  $^{231}\text{Pa}$  is impossible at all. However, this conclusion is correct only for large-sized reactors, where neutron leakage is negligible.

So, only thermal neutron spectra should be considered to provide favorable reactivity feedback on coolant temperature. The results presented in Fig. 11 demonstrate a possibility for increasing fuel burn-up in thermal neutron spectrum by introduction of  $^{231}\text{Pa}$  into fuel composition.

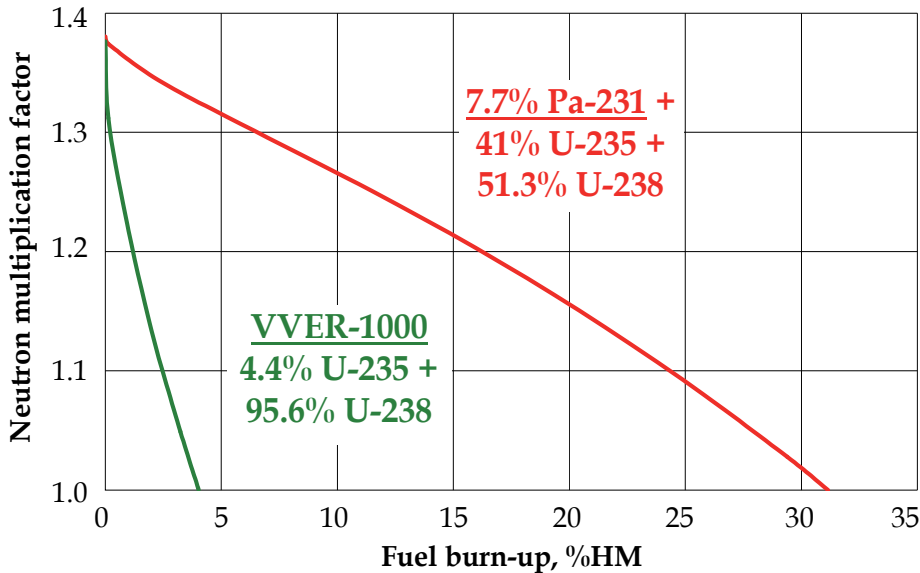


Fig. 11. Achievability of ultra-high fuel burn-up by introduction of  $^{231}\text{Pa}$  with conservation of favorable feedback on coolant temperature (thermal neutron spectrum)

As is known, fuel burn-up in VVER-1000 can reach a value about 4% HM. Introduction of  $^{231}\text{Pa}$  and higher contents of  $^{235}\text{U}$  can increase fuel burn-up by a factor of 8 with the same initial reactivity margin, i.e. more powerful system of reactivity compensation is not required.

Requirement of favorable reactivity feedback on coolant temperature completely excludes any introduction of  $^{231}\text{Pa}$  into fuel composition in the case of large-sized reactors with resonance neutron spectra. But, introduction of  $^{231}\text{Pa}$  into fuel composition of small-sized reactors does not worsen safety of the reactor operation because of relatively large neutron leakage. This indicates that the mostly attractive area for  $^{231}\text{Pa}$  applications is a small nuclear power including small-sized NPP for remote regions, for the floating NPP, for space stations on the Moon or Mars and for cosmic flights into the outer space.

The following conclusions can be made in respect of potential  $^{231}\text{Pa}$  applications:

- Application of  $^{231}\text{Pa}$  as a burnable neutron poison can reduce initial reactivity margin and increase fuel burn-up.
- Introduction of  $^{231}\text{Pa}$  into fuel composition makes it possible to reach ultra-high fuel burn-up (above 30% HM) both in thermal and resonance neutron spectra.
- The actual problem of  $^{231}\text{Pa}$  production in significant amounts should be resolved.

## 6. Proliferation protection of nuclear materials in closed uranium-plutonium fuel cycle

NPP operation in open fuel cycle results in accumulation of huge SNF stockpiles that represents a long-term hazard to the humankind. Ultimate SNF disposal is a difficult technical problem requiring large number of practically “eternal” deep underground repositories. That is why many various options for closure of nuclear fuel cycle (NFC) are

currently under research and development including extraction of residual uranium, plutonium and minor actinides from SNF.

As known, closed uranium-plutonium NFC includes reprocessing and recycling of nuclear fuel and evokes a lot of contradictory opinions with respect to potential risk of plutonium proliferation. This connected with two points:

- Although plutonium extracted from SNF of power reactors (for example, LWR or PWR, BWR or VVER type) is not the best material for nuclear weapons, nevertheless it can be used in NED of moderate energy yield (Mark, 1993).
- Recycled plutonium will be disposed at the facilities of closed NFC, and this will increase the probability of it using for illegal aims (diversion, theft).

Under these conditions, the absence of any internationally coordinated plan concerning the utilization or ultimate SNF disposal enforced the leading nuclear countries to undertake the steps directed to strengthening the nonproliferation regime (IAEA safeguards, Euratom's embargo on the export of SNF reprocessing technology). But several countries, in the first turn the USA, refused from deployment of breeder reactors which are intended for operation in closed NFC, and focused at once-through NFC. On the other hand, the social demand of solving excess fissile materials (plutonium, the first of all) problem which have both civil and military origins, stimulated carrying out the research on plutonium utilization in MOX-fuel. At the same time, the studies of advanced NFC protected against uncontrolled proliferation of fissile materials have been initiated.

### 6.1 Radiation protection of MOX-fuel. GNEP initiative

Specialists from ORNL (USA) investigated the ways for introduction of  $\gamma$ -radiation sources into fresh fuel (Selle et al., 1979). Sixty-four  $\gamma$ -active radionuclides were selected and studied as candidates for admixing into fresh fuel (see Fig. 12).

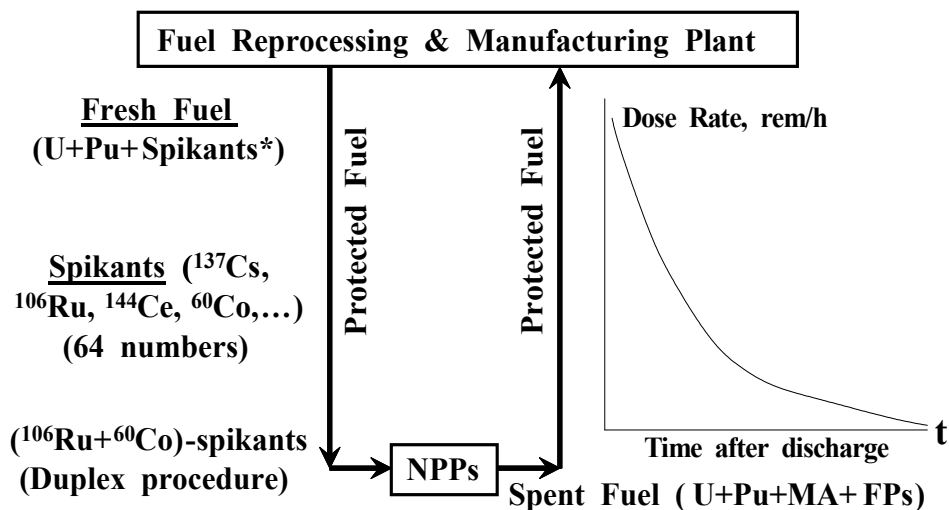


Fig. 12. Closed (U-Pu)-fuel cycle protected (ORNL, USA)\*

Radionuclides <sup>137</sup>Cs ( $T_{1/2} = 30$  years) and <sup>60</sup>Co ( $T_{1/2} = 5.27$  years) appeared the most preferable candidates. But cesium is a volatile element, and it can be easily removed from fuel by heating up. Intensity of  $\gamma$ -radiation emitted by <sup>60</sup>Co rapidly relaxes.

Specialists from LANL (USA) proposed the advanced version of the international NFC that enhances proliferation resistance of plutonium (Cunningham et al., 1997). This proposal constituted a basis for the US President's initiative on the Global Nuclear Energy Partnership (GNEP) that was supported by many countries (including Russia) with well-developed nuclear technologies (see Fig. 13).

According to the proposal, spent fuel assemblies discharged from power reactors of a country-user must be transported to the Nuclear Club countries for full-scale reprocessing. Extracted plutonium and minor actinides must be incinerated in the reactors placed on the territory of the International nuclear technology centers. Plutonium is not recycled in power reactors of a country-user. The Nuclear Club countries provide fresh LEU fuel deliveries into a country-user.

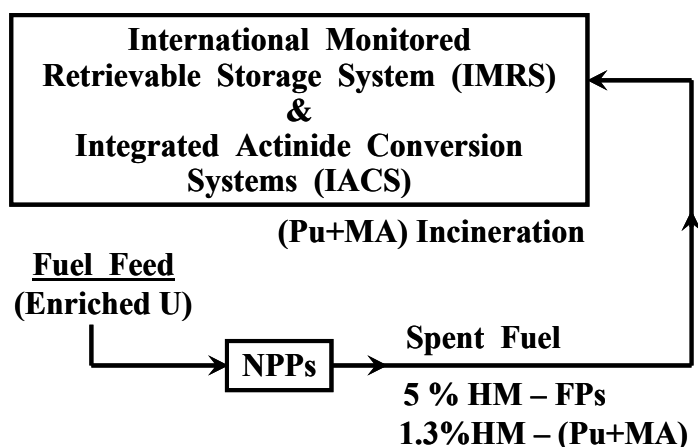


Fig. 13. Open fuel cycle protected (LANL, USA)

Upon exhaustion of rich and cheap uranium resources, nuclear power has to use artificial kinds of fresh fuel (plutonium,  $^{233}\text{U}$  or their mixtures). The GNEP initiative does not consider this opportunity. It is proposed to use such power reactors which are able to work without refueling for 15-20 years. After this time interval they must be returned to the Nuclear Club countries for SNF discharging and reprocessing and for insertion of fresh fuel. The concentrated incineration of plutonium and minor actinides in the International nuclear technology centers can lead to unacceptably large local release of thermal energy with unpredictable negative environmental and climatic effects. As for reactors with long-life cores, these are small and medium-sized power reactors. Besides, during transportation and mounting, they can be very attractive sources of plutonium in amounts large enough for manufacturing of several dozens of nuclear bombs.

## 6.2 Enhancement of LWR MOX-fuel cycle proliferation resistance by plutonium denaturing

Some nuclear properties of  $^{238}\text{Pu}$  make this isotope a valuable material for proliferation protection of uranium-plutonium fuel. Firstly,  $^{238}\text{Pu}$  is an intense source of thermal energy ( $T_{1/2} = 87$  years, specific heat generation - 570 W/kg). So, introduction of  $^{238}\text{Pu}$  into plutonium creates almost insuperable barrier to manufacturing of even primitive implosion-type NED. Plutonium heating up by isotope  $^{238}\text{Pu}$  can provoke undesirable phase transitions

and thermal pyrolysis of conventional explosives applied for compression of central plutonium charge. Secondly,  $^{238}\text{Pu}$  is an intense source of spontaneous fission neutrons, even more intense than  $^{240}\text{Pu}$ . As a consequence, probability of premature CFR initiation in NED sharply increases while energy yield of nuclear explosion drastically drops down to the levels comparable with energy yield of conventional explosives. Thus, LWR MOX-fuel cycle with ternary fuel compositions (Np-U-Pu) is characterized by enhanced proliferation resistance.

Like uranium, plutonium can be isotopically denatured by two ways: either direct introduction of intensely radioactive isotope  $^{238}\text{Pu}$  into MOX-fuel composition or introduction of relatively low intense radioactive isotope  $^{237}\text{Np}$  into MOX-fuel composition.  $^{237}\text{Np}$  is the nearest neutron predecessor of main denaturing isotope  $^{238}\text{Pu}$ . So, only short-term pre-irradiation of fresh MOX-fuel assemblies would be sufficient to produce proliferation resistant fuel assemblies, suitable even for export deliveries to any countries.

### 6.2.1 The effect of $^{237}\text{Np}$ and $^{238}\text{Pu}$ introduction on Pu protection in LWR fuel

It is proposed that the equilibrium isotope vectors are obtained for MOX-fuel circulating between LWR, spent fuel reprocessing as fuel manufacturing facilities. The fuel feed includes isotopes  $^{237}\text{Np}$ ,  $^{238}\text{Pu}$  and  $^{239}\text{Pu}$  is produced in Hybrid Thermonuclear Installation (HTI) blankets.

Using the code GETERA (Belousov et al., 1992) for cell calculations of fuel burn-up, Pu isotopic compositions of MOX-fueled PWR were determined for moments of the beginning and end of cycle.  $^{238}\text{Pu}$  fraction in plutonium was adopted to be an index of Pu protection against uncontrolled proliferation. It means that the impact of higher plutonium isotopes on neutronics of chain reaction in imploded plutonium charge of NED was not taken into account.

The fuel being loaded in PWR may be considered as material consisting of two parts: the first part includes equilibrium composition of  $^{238}\text{U}$  and plutonium isotopes produced by  $^{238}\text{U}$  while the second part ("feed part of fuel") includes equilibrium composition of  $^{237}\text{Np}$ ,  $^{238}\text{Pu}$  and other plutonium isotopes produced entirely by the feed. Equilibrium contents of  $^{238}\text{Pu}$  in plutonium of PWR fuel depending on  $^{238}\text{Pu}$  contents in plutonium of feed (with different  $^{237}\text{Np}$  fractions in "feed part of fuel") for equilibrium multi-cycle operation regime are presented in Fig. 14.

The plot region situated under the bisectrix B is a region where plutonium protection in feed is higher than plutonium protection in fuel. Respectively, the plot region situated above the bisectrix B is a region where plutonium protection in fuel is higher than that in feed. The curves of this figure characterize the correlation between plutonium protection levels in feed and fuel when the "feed part of fuel" contains  $^{237}\text{Np}$  in addition to plutonium. Basing on these data, it is possible to select the appropriate equilibrium regime of NFC.

Proper selection of the feed compositions, i.e. fractions of  $^{238}\text{Pu}$  and  $^{237}\text{Np}$ , makes it possible to attain the same level of fuel plutonium protection for various combinations of  $^{238}\text{Pu}$  and  $^{237}\text{Np}$  content in feed. For example, 32%-level of fuel plutonium protection can be attained in case of feed containing (0%  $^{237}\text{Np}$ , 52%  $^{238}\text{Pu}$ ) or (20%  $^{237}\text{Np}$ , 43%  $^{238}\text{Pu}$ ) or (40%  $^{237}\text{Np}$ , 32%  $^{238}\text{Pu}$ ). The latter option corresponds to equal level of plutonium protection both in fuel and in feed. The line "S" that connects the right ends of the curves shown in Fig. 14 may be regarded as an "ultimate option" of the (Np-U-Pu) NFC considered here. The points of this line correspond to particular option of the (Np-U-Pu) NFC where  $^{238}\text{U}$  is absent in fuel composition, and its fertile functions passed to  $^{238}\text{Pu}$  and  $^{237}\text{Np}$ . So, this NFC may be called as a (Np-Pu) NFC. In this NFC the highest fuel Pu protection level (65%  $^{238}\text{Pu}$ ) can be

reached with feed Pu protection of 90%  $^{238}\text{Pu}$ . As known, the IAEA safeguards are not applied to plutonium containing 80%  $^{238}\text{Pu}$  or more (Rolland-Piegue, 1995; Willrich & Taylor, 1974; Massey & Schneider, 1982).

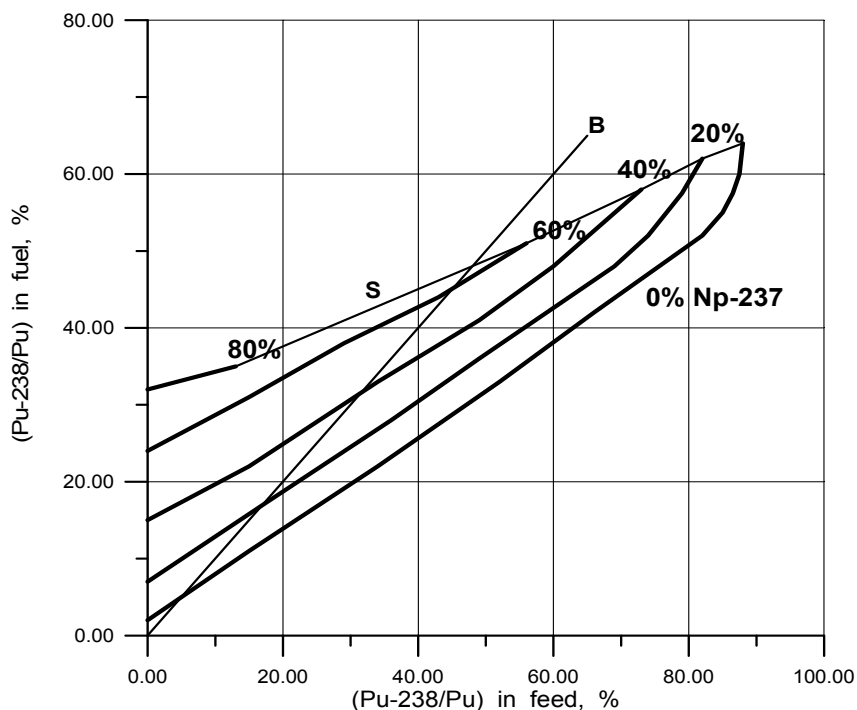


Fig. 14. Proliferation resistance of plutonium in fuel as function of proliferation resistance of plutonium in feed and  $^{237}\text{Np}$  content in "feed" part of fuel. B - bisectrix.

Inherent heat generation of plutonium is considered as a significant factor of its protection. The rates of inherent heat generation for various feed compositions are presented in Table 4. Here, the rates of specific heat generation for weapons-grade plutonium (WGPu) and reactor-grade plutonium (RGPu) are presented as well.

		$^{238}\text{Pu}/\text{Pu}$ in fuel and in feed ( $\text{Np}/(\text{Np} + \text{Pu})$ in feed)				
Generation		WG Pu	RG Pu	17% (7%)	33% (15%)	44% (19%)
$q^{\text{Pu}}$ , W/kg Pu		2.3	13.	97	186	248
$n_{\text{sf}}^{\text{Pu}}$ , $10^6(\text{n}/\text{sec})/\text{kg Pu}$		0.06	0.38	0.71	1.06	1.30
$q^{\text{fuel}}$ , W/kg fuel		---	---	14.9	41.2	99.5
$n_{\text{sf}}^{\text{fuel}}$ , $10^6(\text{n}/\text{sec})/\text{kg fuel}$		---	---	0.11	0.24	0.53
Feed $^{237}\text{Np}/^{238}\text{Pu}/^{239}\text{Pu}$ , kg/(GWe*a)		---	---	38 / 82 / 402	103 / 194 / 377	176 / 318 / 421

Table 4. Decay heat generation ( $q^{\text{Pu}}$ ) and neutron generation by spontaneous fissions ( $n_{\text{sf}}^{\text{Pu}}$ ) in LWR fuel with equal plutonium protection both in fuel and in feed.



Basing on the results shown above, it can be concluded that denatured fuel plutonium containing more than 25%  $^{238}\text{Pu}$  is characterized by the internal heat generation which exceeds that of RGPu by more than order of magnitude and, by the larger extent, that of WGPu. In addition, denatured fuel plutonium is characterized by the higher neutron background caused by spontaneous fissions. The factors mentioned above enhance plutonium protection against its utilization in NED. The same factors complicate, to certain degree, the handling procedures with such a fuel in nuclear technologies.

Values of specific heat generation and neutron emission due to spontaneous fission of MOX-fuel being loaded for the equilibrium cycle options analyzed are shown in Table 4 also. For comparison, "dry" technology for handling with spent fuel assemblies may be applied if specific heat generation does not exceed 20-35 W/kg fuel. It may be also concluded that plutonium denaturing with  $^{238}\text{Pu}$  is restricted by thermal constraints imposed on permissible specific heat generation of fuel. The same tendency exists in connection with spontaneous neutrons emission. These constraints need to be taken into account in fuel fabrication, fuel rods and fuel assemblies manufacturing and transport operations. These complications of fuel management may be considered as certain "payment" for proliferation resistance of MOX-fuel cycle.

Actually speaking, the protection of plutonium in (Np-U-Pu)-fuel cycle is supposed to be enhanced due to addition  $^{237}\text{Np}$  and  $^{238}\text{Pu}$  into fuel. The degree of fissile nuclides protection depends mainly on magnitude of  $^{238}\text{Pu}$  fraction in plutonium. Meanwhile,  $^{237}\text{Np}$  itself can be also considered as a potential material for NED. For example, critical mass of  $^{237}\text{Np}$  (metal sphere, steel reflector) is about 55 kg (Koch et al., 1997). It's ten times more than that of  $^{239}\text{Pu}$ . The magnitude of critical mass of  $^{237}\text{Np}$  is sensitive with respect of its dilution. For example, minimum critical mass of  $\text{NpO}_2$  is as much as 315 kg (Nojiri & Fukasaku, 1997; Ivanov et al. 1997). Besides, in fuel composition  $^{237}\text{Np}$  is present together with plutonium which is characterized by essential neutron source strength due to spontaneous fissions. Therefore, in order to apply extracted  $^{237}\text{Np}$  in NED it is needed to perform effective  $^{237}\text{Np}$  purification from plutonium (plutonium fraction is restricted by value of  $10^{-4}$  -  $10^{-3}$ ).

### 6.3 Increase of fuel burn-up in denatured (Np-U-Pu) fuel cycle

Good neutron-multiplying properties of  $^{238}\text{Pu}$  and its neutron predecessor  $^{237}\text{Np}$  make it possible to extend substantially time period for continuous reactor operation without refuelings. As a consequence, unauthorized extraction of plutonium from SNF becomes practically unfeasible.

Indeed, under reactor irradiation of (Np-U-Pu) fuel it is occurs the following "non-traditional" transition chain (see Fig. 15):  $^{237}\text{Np} \rightarrow ^{238}\text{Pu} \rightarrow ^{239}\text{Pu} \rightarrow \dots$ . A successive transition of these nuclides leads to enhancement of multiplication properties.

Actually, as it can be seen in Fig. 16, excess neutron generation per one absorption ( $\nu_{\text{eff}}-1$ ) in  $^{237}\text{Np}$  is negative for neutrons of all energy range (excepting fast neutrons), positive for neutrons with  $E_n > 1$  KeV for  $^{238}\text{Pu}$  and, as is known, essential positive one for  $^{239}\text{Pu}$ .

So, for (Np-U-Pu)-fuel the nuclides we are dealing with can be characterized as follows (Table 5).

At the same time, during irradiation in reactor core FP accumulation results in growth of neutron absorption. So, these tendencies can be counterbalanced and such fuel will be characterized by stabilized neutron-multiplying properties over long burning-up.

Burn-up calculations for mono-nitride fuel in cell of PWR-type reactor with heavy water as a coolant were performed by using code GETERA. The cell parameters were similar to that of VVER-1000 cell (see Table 6):

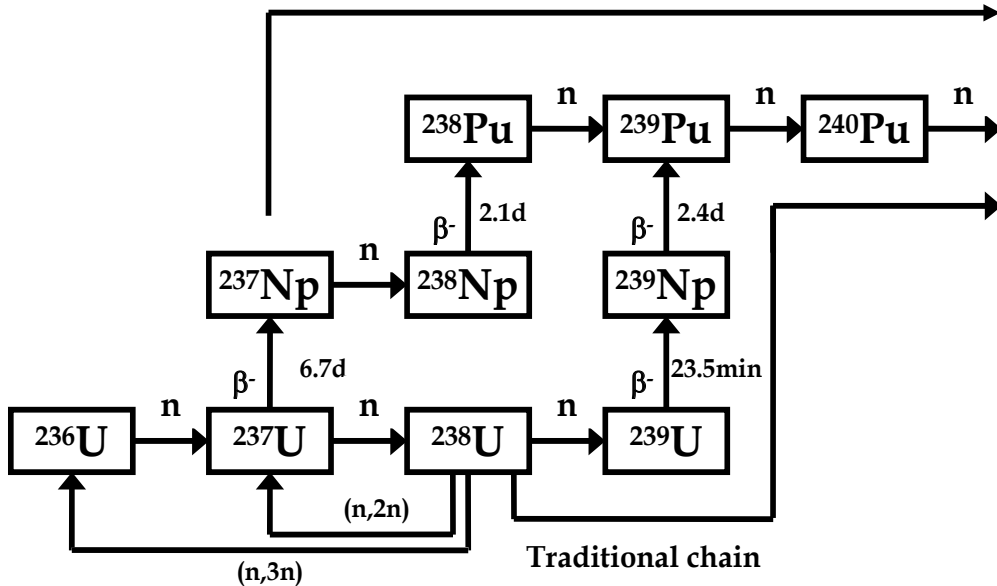


Fig. 15. Chain of isotopic transformations in uranium-plutonium fuel cycle

$^{237}\text{Np}$	$^{238}\text{Pu}$	$^{239}\text{Pu}$
"Burnable poison" nuclide	Moderate fissile nuclide ( $E_n > 1 \text{ KeV}$ )	Well-known fissile nuclide

Table 5. Characteristics of nuclides for (Np-U-Pu)-fuel

Fuel rod diameter	9.1 mm
Thickness of stainless steel cladding	0.4 mm
Coolant ( heavy water )	D <sub>2</sub> O
Water volume / fuel volume	1.6
Fuel	Mono-nitride ( porosity - 30% )
Specific heat generation	110 kW/l

Table 6. Cell parameters of PWR-type reactor

In Fig. 17 it is shown the dependence of  $K_{\infty}$  on fuel burn-up for various fuel compositions. For comparison it is demonstrated also a curve of  $K_{\infty}$  for LWR-UOX. It can be seen that, actually, there is possibility to attain fuel burn-up of 25-30%HM ( corresponding residence time is about 20-25 years.). It is worth-while mentioning that, according to papers (Ivanov et al. 1997; Bychkov et al. 1997) presented at the International Conference "GLOBAL'97", vibro-packed MOX fuel in stainless steel cladding was irradiated in fast reactor BOR-60 (Russia) and it was obtained burn-up of 26% HM on standard fuel assemblies and burn-up

of 32% HM in experimental fuel rods. No thermal-mechanical and physical-chemical fuel-cladding interaction was observed in any of the analyzed cross-sections.

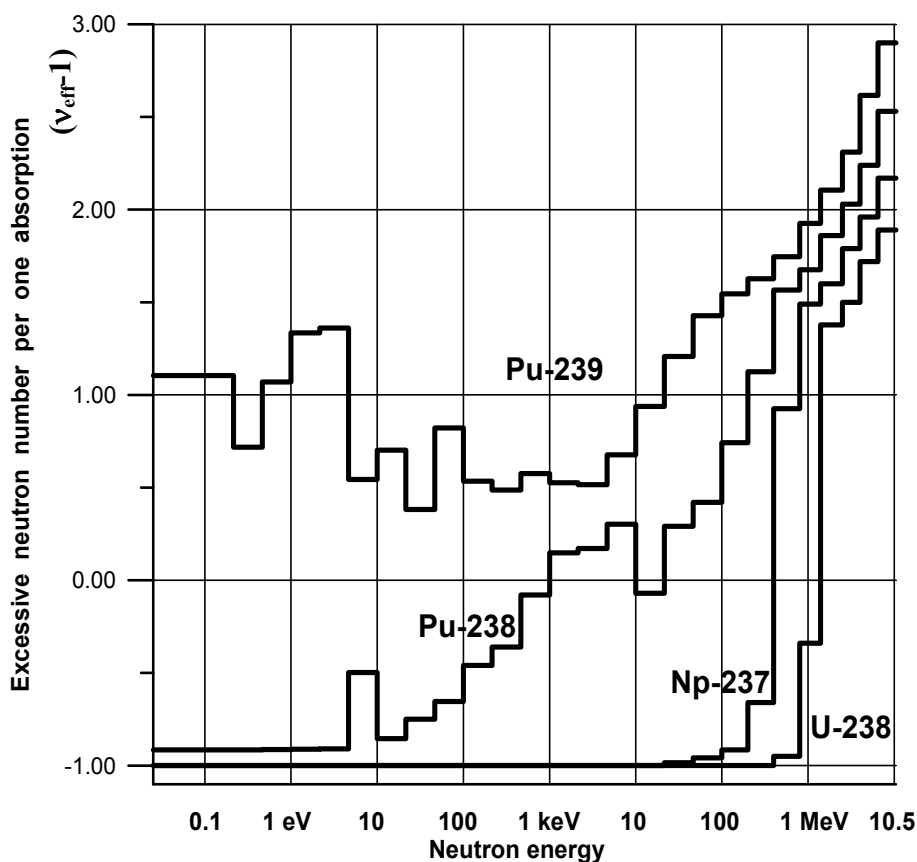


Fig. 16. Dependencies of excessive neutron number per one absorption ( $v_{eff}-1$ ) on neutron energy for nuclides of uranium-plutonium fuel cycle

The results mentioned above referred to so-called "ultimate" fuel compositions which didn't contain  $^{238}\text{U}$ . Actually speaking, these results can be considered as preliminary ones to demonstrate scale of benefit. Undoubtedly, it is needed to analyze impact of wide fuel compositions (including  $^{238}\text{U}$ ) on stabilized multiplication properties of ultra long-life cores taking into consideration reactor safety in both critical and sub-critical regime of operations. Anyway, application of ultra long-life core concepts will lead to essential decrease of SNF flow rate, reduction of reprocessing, remanufacturing and shipping operations. It's a factor for internationalization of Nuclear Energy System fuel cycle. Since fuel cycles been discussed are "rich" with respect to excess neutron generation in CFR, there is no necessity to perform fine purification of fuel being reprocessed. It's a factor of enhancement of the fuel cycles protection.

Application of NPP with ultra long-life core concepts is expected to be profitable for electricity generation in developing countries which have not improved nuclear technology infrastructure.

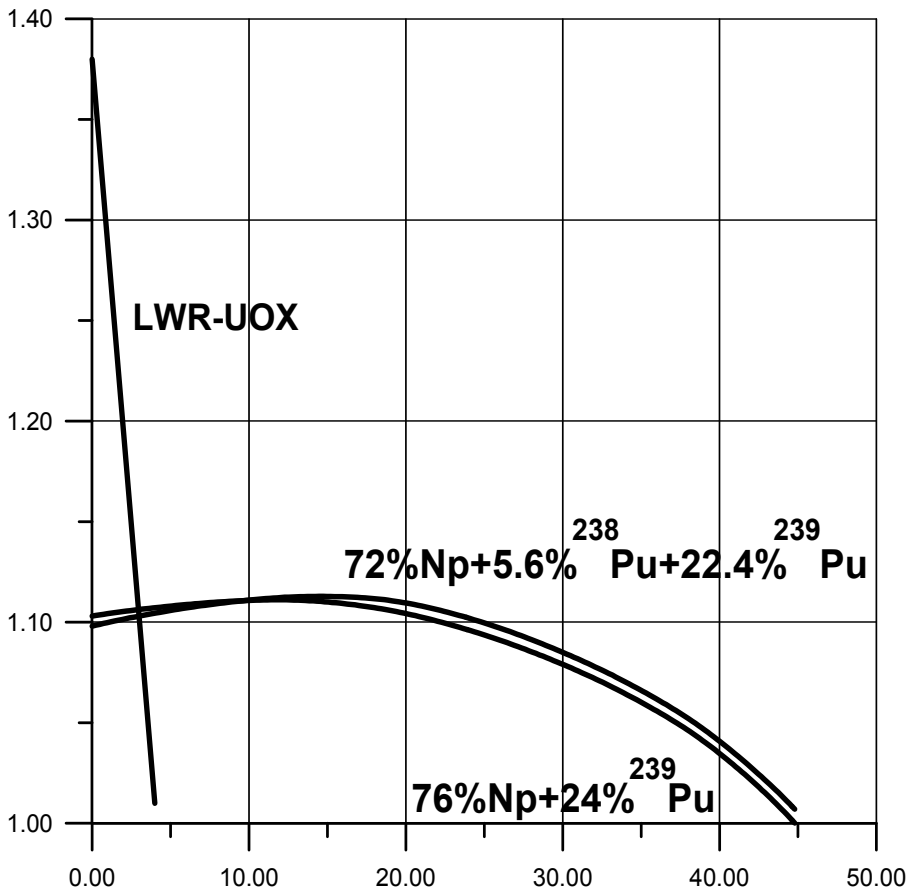


Fig. 17. Dependencies of  $K_{\infty}$  on fuel burn-up for various fuel compositions

## 7. Mixed (Th – U - Pu) fuel cycle

Plutonium has no its own “fertile” isotope. So, it is impossible to protect plutonium by isotopic dilution, like uranium. Upon exhaustion of cheap  $^{235}\text{U}$  resources, the isotope dilution principle can be applied to  $^{233}\text{U}$ - $^{238}\text{U}$  mixture. So, it seems reasonable to consider the following proliferation resistant fuel - ( $^{232}\text{Th}$ - $^{233}\text{U}$ - $^{238}\text{U}$ ) [23]. If  $^{238}\text{U}$  content is small but sufficient for low content of  $^{233}\text{U}$  in uranium fraction, then plutonium build-up may be suppressed.

In other words, the mixed ( $^{232}\text{Th}$ - $^{233}\text{U}$ - $^{238}\text{U}$ -Pu) fuel cycle should be studied along with “classical” ( $^{232}\text{Th}$ - $^{233}\text{U}$ ) and ( $^{238}\text{U}$ -Pu) cycles. In both “classical” cycles, fissile materials ( $^{233}\text{U}$  or Pu) may be figuratively called by “highly-enriched” fuel. In the mixed cycle, on the contrary, fissile isotope  $^{233}\text{U}$  is diluted with  $^{238}\text{U}$  in uranium fraction, and thus ( $^{233}\text{U}$ - $^{238}\text{U}$ ) mixture may be regarded as a “low-enriched” fuel. It is noteworthy that homogeneous mixture of two fertile isotopes  $^{238}\text{U}$  and  $^{232}\text{Th}$  is a more effective neutron absorber than both separate isotopes. This effect can improve neutron-physical properties of the mixed fuel because it can increase fuel burn-up and thus reduce flow rate of spent fuel assemblies for reprocessing (Kulikov, 2007).

In the mixed fuel cycle, the following double-strata structure may be estimated as an effective and proliferation resistant option (Figs. 18, 19): the top stratum includes full-scale reprocessing of spent fuel assemblies in the International nuclear technology centers with complete incineration of plutonium and minor actinides, the bottom stratum includes a simplified thermal-chemical (DUPIC-type) re-fabrication of fresh fuel with feeding by proliferation resistant  $^{233}\text{U}$ . Such a closed nuclear fuel cycle may be equally effective in power reactors of PWR and CANDU types.

So, if fuel contains homogeneous mixture of two fertile isotopes  $^{238}\text{U}$  and  $^{232}\text{Th}$ , the following new qualities do appear:

- Fissile isotope  $^{233}\text{U}$  produced in neutron irradiation of thorium is diluted with fertile isotope  $^{238}\text{U}$ . So,  $^{233}\text{U}$ - $^{238}\text{U}$  mixture represents, in essence, a kind of "low-enriched" uranium.
- Reduced content of  $^{238}\text{U}$  suppresses build-up rate of plutonium.
- Mixed fuel is highly effective not only in thermal but in resonant neutron spectrum too because fissile isotope  $^{233}\text{U}$  has sufficiently good neutron-multiplying properties both in thermal and resonant neutron spectra.
- Fissile isotope  $^{239}\text{Pu}$  converts rapidly into heavier plutonium isotopes with low neutron-multiplying properties because of larger  $\alpha = \sigma_c / \sigma_f$ . So, plutonium loses its attractiveness as a material suitable for NED manufacturing.

As is known (Benedict et al., 1981), fissile isotope  $^{233}\text{U}$  can be additionally protected by its denaturing with  $^{232}\text{U}$  because this isotope has the following proliferation-resistance properties (Fig. 19):

1.  $^{232}\text{U}$  is an intense source of high-energy  $\gamma$ -radiation emitted by its decay products.
2.  $^{232}\text{U}$  is an intense source of spontaneous neutrons, i.e. spontaneous fission neutrons plus neutrons from  $(\alpha, n)$ -reactions with light impurities.
3.  $^{232}\text{U}$  is an intense heat source from its own  $\alpha$ -decays and from decays of its daughter products.

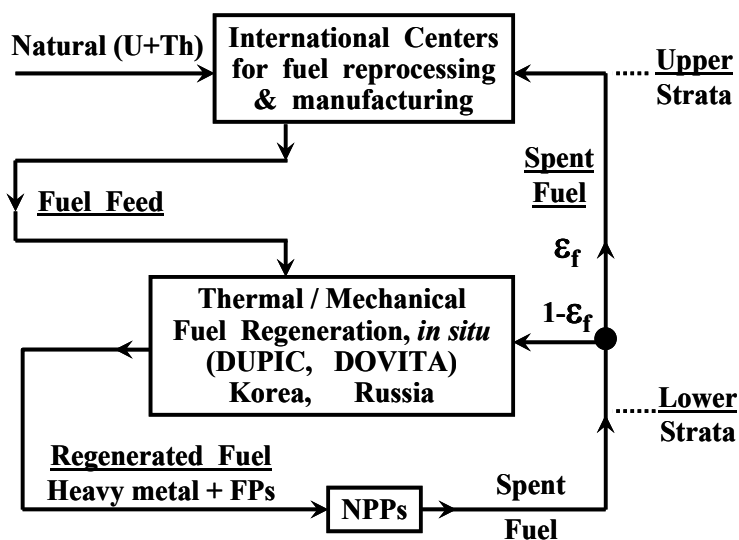


Fig. 18. Double-Strata closed fuel cycle protected

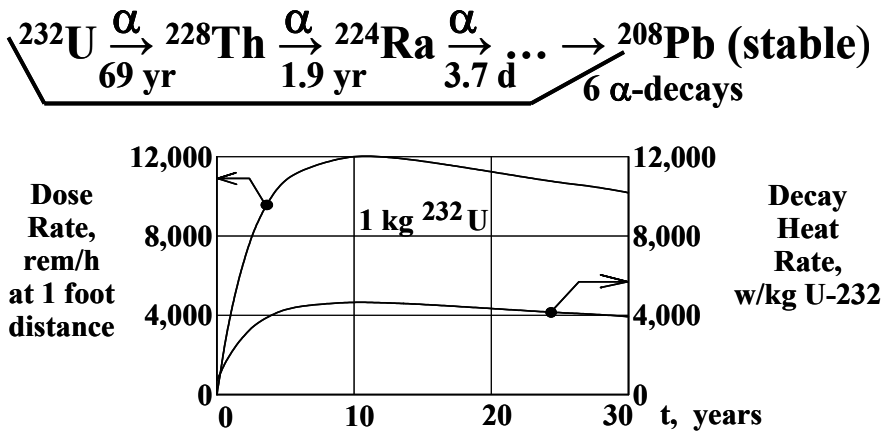


Fig. 19.  $^{232}\text{U}$  as a Spikant

$$Q_{sf} (\text{Spontaneous Fission Neutrons}) = 1.3 \cdot 10^3 \text{ n}/(\text{s} \cdot \text{kg } ^{232}\text{U});$$

$$Q_{\alpha,n} (\text{Uranium Dioxide}) = 15 \cdot 10^6 \text{ n}/(\text{s} \cdot \text{kg } ^{232}\text{U}) \quad (\cdot 20 - \text{equilibrium});$$

$^{232}\text{U}$ -leader among U isotopes as a spontaneous neutrons generator.

### 7.1 Proliferation protection of multi-isotope fuel containing uranium generate and protactinium-uranium mixture produced by Hybrid Fusion Facility

Neutron irradiation of natural thorium in blanket region of Hybrid Fusion Facility (HFF) based on (D,T)-plasma can produce many thorium, protactinium and uranium isotopes. High-energy (14 MeV) thermonuclear neutrons are able to initiate some threshold (n,xn)-reactions leading to intense generation of  $^{230}\text{Th}$ ,  $^{231}\text{Pa}$ ,  $^{232}\text{U}$ ,  $^{233}\text{U}$  and  $^{234}\text{U}$ . The longer irradiation time, the larger content of these isotopes in irradiated thorium. Content of  $^{232}\text{U}$ , for example, can reach a value of several percents.

NFC closure and SNF reprocessing can release huge amounts of fissionable materials: about 210 000 tons of uranium regenerate, RGPu and minor actinides, where uranium regenerate is a dominant fraction. Uranium regenerate may be regarded as a fertile material suitable for further use by nuclear power industry. Uranium regenerate will be released in the amounts large enough to feed NPP of total electric power at the level of 1500 GWe, i.e. 4 times higher than total power of global nuclear energy system today.

Uranium regenerate contains the following isotopes:  $^{232}\text{U}$ ,  $^{233}\text{U}$ ,  $^{234}\text{U}$  (minor fraction) and  $^{235}\text{U}$ ,  $^{236}\text{U}$ ,  $^{238}\text{U}$  (main fraction). Uranium produced in thorium blanket of HFF contains only isotopes of minor fraction, i.e.  $^{232}\text{U}$ ,  $^{233}\text{U}$  and  $^{234}\text{U}$ . So, if HFF-produced uranium is admixed to uranium regenerate, content of only minor fraction increases. Content of minor fraction can be made comparable with content of main fraction. In the extreme case, minor fraction becomes a dominant one, and NFC shifts towards  $^{233}\text{U}$ -based fuel.

Thus, uranium fraction of nuclear fuel represents a mixture of practically all significant uranium isotopes:  $^{232}\text{U}$ ,  $^{233}\text{U}$ ,  $^{234}\text{U}$ ,  $^{235}\text{U}$ ,  $^{236}\text{U}$ ,  $^{238}\text{U}$ . The following three aspects should be noted. Firstly, main fissile isotopes,  $^{233}\text{U}$  and  $^{235}\text{U}$ , are accompanied by lighter and heavier uranium isotopes, essential neutron absorbers. Secondly, if  $^{232}\text{Th}$  and  $^{231}\text{Pa}$  are introduced into fuel composition replacing partially uranium regenerate, then plutonium generation rate is suppressed. Thirdly, the presence of  $^{236}\text{U}$  in fuel composition can initiate the chain of isotopic transformations leading to accumulation of  $^{232}\text{U}$ ,  $^{233}\text{U}$ ,  $^{238}\text{Pu}$ , main isotope for plutonium denaturing (De Volpi, 1982):

$^{236}\text{U}(n,\gamma)^{237}\text{U}(\beta^-, T_{1/2} = 7 \text{ days})^{237}\text{Np}(n,\gamma)^{238}\text{Np}(\beta^-, T_{1/2} = 2.1 \text{ days})^{238}\text{Pu}$

So, produced plutonium will contain not only  $^{240}\text{Pu}$ , usually accompanying isotope to  $^{239}\text{Pu}$  in power reactors, but  $^{238}\text{Pu}$  too.

In mixed (Th-U-Pu) fuel cycle, plutonium plays an auxiliary role only while  $^{233}\text{U}$  is a main fissile isotope, and plutonium content in fuel composition may be diminished. Finally, plutonium could be removed from global nuclear energy system for peaceful utilization in the dedicated nuclear power facilities. The GNEP initiative advanced by the US President (Sokolova, 2008) foresees just a similar option. This aspect represents a special significance from the standpoint of plutonium protection against unauthorized diversion to non-energy purposes (Mark, 1993).

Uranium fraction consisting of practically all significant uranium isotopes from  $^{232}\text{U}$  to  $^{238}\text{U}$  is, in essence, low-enriched uranium with rather small content of main fissile isotopes ( $^{233}\text{U}$  and  $^{235}\text{U}$ ). Isotopic enrichment of such a multi-isotope composition will be a very difficult problem for potential proliferators in the case of its unauthorized diversion.

The presence of  $\alpha$ -emitters (mainly,  $^{232}\text{U}$ ,  $^{233}\text{U}$  and  $^{234}\text{U}$ ) in uranium fraction can initiate physical and chemical processes leading to  $\alpha$ -radiolysis of uranium hexafluoride including molecular dissociation with generation of minor fluorides, exchange reactions of recombination and coagulation. These processes can provoke serious violations in the correspondence between the order in masses of uranium isotopes and the order in masses of uranium hexafluoride molecules. This correspondence is a necessary condition for successful uranium enrichment.

So, closed mixed ( $^{233}\text{U}$ - $^{232}\text{Th}$ - $^{238}\text{U}$ ) fuel cycle can offer the following advantages in comparison with "classical" ( $^{238}\text{U}$ -Pu) and ( $^{232}\text{Th}$ - $^{233}\text{U}$ ) cycles:

- Fissile isotope  $^{233}\text{U}$  is diluted by fertile isotope  $^{238}\text{U}$  in uranium fraction of fuel composition.
- $^{238}\text{U}$  content in fuel composition may be diminished thus suppressing plutonium production. As a consequence, load of the International centers on plutonium utilization may be reduced.

General conclusion can be defined as follows: fuel of mixed (Th-U-Pu) cycle contains fissile isotopes with upgraded level of their protection against any unauthorized attempts of their diversion to non-energy purposes.

## 8. Probability analysis of risk reduction in non-energy applications of denatured uranium

Proliferation protection of uranium and uranium-plutonium fuel can be quantitatively evaluated within the frames of the concept developed for risk assessment in authorized applications of nuclear materials. The concept includes some relationships which can be used to evaluate probability for a certain chain of unauthorized actions (UAA) to occur and to evaluate damage from potential NED applications.

### 8.1 Scenarios for UAA with nuclear materials and models for UAA detection

One of main directions in nuclear non-proliferation ensuring is a formation of inaccessibility conditions for NM against any UAA. This is a main strategic function of MPC&A system at any nuclear-dangerous objects. However, the following questions arise:

1. What can occur with nuclear materials, if these conditions are violated due to some kind of reasons?

2. How can we estimate the threats?
3. What must we do under these accidental conditions? Answers to the questions are related to the threats of NM diversion including the threat of NED manufacturing from diverted NM and its military application. In order to give a correct response to these questions, two, at least, conditions must be satisfied:
  - We must know how to evaluate the threats of NED manufacturing from diverted NM and their military applications.
  - We must work out the recommendations on effective countermeasures to be undertaken against any UAA.

An important condition for successful counteraction against the use of diverted NM in NED manufacturing consists in development of the control system over illegal NM trafficking. External UAA monitoring system can apply various strategies of the searching process for potential UAA objects.

Unlike authorized activity, unauthorized actions with NM can be characterized by the following specific features:

- Secrecy of unauthorized works. The secrecy level is defined by NM properties and financial expenses to be paid by potential proliferators.
- Striving for manufacturing of NED with maximal destructive capability.
- Striving for maximal shortening of UAA time which follows from the fact that potential proliferator understands properly the threats from external UAA monitoring system.

These tendencies are the conflicting ones from position of potential proliferator who strives to reach his ultimate purpose. For example, proliferator strives for NED manufacturing with maximal destructive capability but this requires application of sophisticated nuclear technologies for processing of diverted NM. In their turn, nuclear technologies require large financial and long time expenses with appropriate reduction of the secrecy level and rising of the detection probability.

So, when analyzing various scenarios of NM diversion, we presumed a rational behavior of nuclear proliferators, i.e. the proliferator has to accept a certain compromise between his striving for manufacturing of NED with maximal destructive capability and rising of the detection probability caused by application of sophisticated nuclear technologies. In any case rather long chain of technological processes is required to manufacture NED from diverted NM.

## 8.2 Concept of risk of NM applications in destructive purposes

Potential risk of NM application for NED manufacturing and military use by terrorist groups can be evaluated as follows:  $R = P \cdot D$ , where  $P$  – probability of NED manufacturing and military use;  $D$  – potential damage from the use of NED for destructive purposes.

Probability  $P$  depends on proliferator capabilities, initial and final NM states. The probability may be written in the following form:  $P = P(F, S_I \rightarrow S_F)$ , where  $F$  – proliferator capabilities (his material and financial funds, available technological basis);  $S_I$  – initial NM state (mass, physical form, chemical composition, radioactivity, local position, etc);  $S_F$  – final NM state (design of NED, local position, chemical and isotopic compositions, radioactivity, etc). Potential damage  $D$  depends on final NM state only, i.e.  $D = D(S_F)$ .

Assumption on a rational behavior of nuclear proliferator enables us to think that proliferator will follow the well-grounded plan with proper accounting for the detection probability, if sophisticated nuclear technologies are applied for processing of diverted NM



(for example, fine NM purification with removal of all significant impurities, isotopic re-enrichment and so on). So, the risk of NED manufacturing and military use can reach a maximal point either within or on the boundaries of the domain that includes all potential UAA undertaken by nuclear proliferators. The maximal risk and its location in UAA domain depends on the level of external UAA monitoring and on financial capabilities of nuclear proliferators (see Fig. 20).

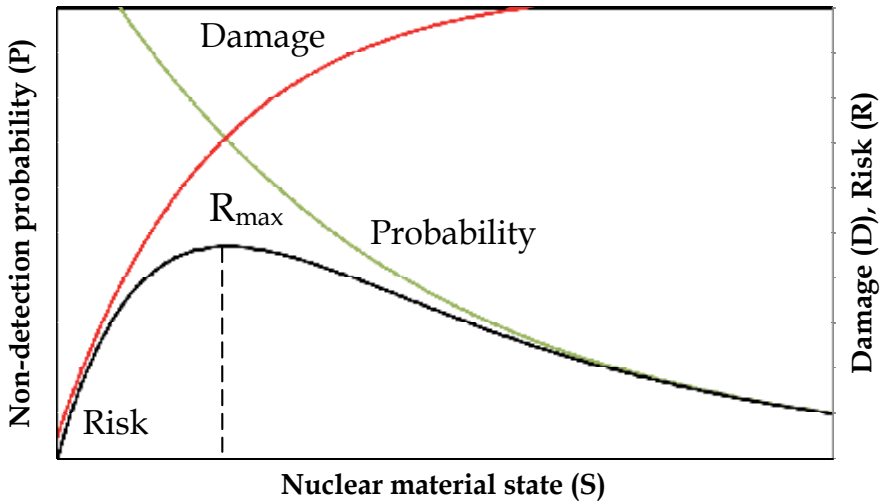


Fig. 20. Variations of the risk related with NM application in destructive purposes when sophisticated nuclear technologies are involved into NM processing

This circumstance can be used to simplify analysis by using a conservative approach to evaluating the maximal risk of NM usage for NED manufacturing. Within the frames of this approach, probability  $P$  for successful completion of UAA chain (from initial state  $S_I$  to final state  $S_F$ ) can be replaced by the following maximal evaluation:

$$R_{max}(F, S_I) = \max_{S_F} (P(F, S_I \rightarrow S_F) \cdot D(S_F)) \quad (1)$$

### 8.3 Probability to avoid UAA detection

The following problem is considered below: it is required to search for UAA object which was created on a certain territory. Let's consider a discrete limited set  $N$  consisting of  $n$  components each of them may be checked up in one identification step. If the set  $N$  contains a closed limited subset  $S$  that includes  $s$  components and characterizes dimensions of UAA object from the viewpoint of the identification process, then probability for successful identification of any component belonging to the subset  $S$  is equal to  $P_{det} = s/n$ . Naturally, non-detection probability per one identification step is equal to  $P_{undet} = 1 - P_{det} = 1 - s/n$ .

Let's assume that UAA object is not moved and UAA can be unambiguously detected by one identification procedure. If the identification rate  $V = dn/dt$  is a constant value, and UAA object is a sufficiently concealed object, i.e.  $s \ll n$ , then time dependency of non-detection probability may be presented as follows:

$$P_{undet}(t) = 1 - \frac{s}{n} V \cdot t = 1 - \lambda \cdot t \quad (2)$$

where  $\lambda = s / n \cdot V$ , parameter of successful detection, is a product of two multipliers, one of them depends on properties of UAA object only.

If UAA can not be detected for one identification step, or if UAA object moves during the identification process, then a necessity arises to perform a repeat examination of the regions which were checked up previously. In this case, time dependency of non-detection probability may be written in the following form:

$$P_{undet}(t) = e^{-\frac{s}{n} V \cdot t} = e^{-\lambda \cdot t} \quad (3)$$

#### 8.4 UAA chains. Indicators of the searching process for UAA objects

The following main links can be identified in UAA chains resulting in NED manufacturing from diverted uranium-containing NM: NM theft → chemical and physical reprocessing → isotopic re-enrichment → manufacturing of main NED components → military use of NED. Each link of UAA chain is defined by its duration  $t_i$  and mean time interval needed to detect the proliferator  $1/\lambda_i$ , which are the functions of the proliferator capability  $F$ , changes of NM properties ( $S_{i-1} \rightarrow S_i$ ) and efficiency of the searching process. In general case, detection probability is described by exponential function. So, probability  $P_i$  for successful completion of the  $i$ -th link without detection and suppression can be written in the following form:

$$P_i = P_{undet,i} \cdot P_{unsup,i} = e^{-\lambda_i t_i} \cdot P_{unsup,i}(t_i) \quad (4)$$

where  $P_{undet,i}$  – non-detection probability of diverted NM at the  $i$ -th link;  $P_{unsup,i}$  – non-suppression probability for UAA performed by detected proliferator at the  $i$ -th link. So, risk of NED manufacturing and military use is defined by the following equation:

$$R = D \cdot \prod_i P_{unsup,i}(t_i) \cdot e^{-\lambda_i t_i} = D \cdot P_{unsup} \cdot e^{-\sum_i \lambda_i t_i} \quad (5)$$

UAA object can be detected from the really existing indicators including the indicators related with consumption of energy and water resources in the unauthorized activity. The following indicators can be used in the search for UAA aimed at NED manufacturing and military use:

- Emission rate ( $A$ ).
- Resource consumption rate ( $W$ ).
- Capital expenses ( $K$ ).

When searching the UAA-object being to several independent indicators, then total non-detection probability is a product of partial non-detection probabilities for different UAA indicators, i.e.

$$P_{undet}(t) = P_{undet}^K(t) \cdot P_{undet}^W(t) \cdot P_{undet}^A(t) = e^{-\lambda_K t} \cdot e^{-\lambda_W t} \cdot e^{-\lambda_A t} = e^{-(\lambda_K + \lambda_W + \lambda_A)t} = e^{-\lambda t}, \quad (6)$$

where

$$\lambda = \lambda_K + \lambda_W + \lambda_A = \alpha_K \cdot f(K) + \alpha_W \cdot f(W) + \alpha_A \cdot f(A), \quad (7)$$

where  $\alpha$  – efficiency of the searching process for appropriate UAA indicators.

Relationship between UAA indicators and detection parameters can be derived from the following models for strategic behavior of nuclear proliferator:

1. The proliferator creates a new infrastructure for his unauthorized activity. According to equation (2), UAA detection parameter in the random searching process for new resources is proportional to the scale of new resources which were put in operation. In the simplest case, the scale is defined by the resource consumption rate  $W$  and capital expenses  $K$ . So, in this case:  $\lambda_W = \alpha_W \cdot W$  and  $\lambda_K = \alpha_K \cdot K$ .
2. The proliferator applies already available infrastructure to perform UAA. Let's assume that industrial enterprises in the search region consumes resources  $W$  in accordance with distribution  $N(W)$ , and frequency of the inspecting actions  $F_{ins}(W)$  depends on the resource consumption rate also. Optimal scheme of the searching process can be found from the following optimality criterion: efficiency of the searching process does not depend on the proliferator strategy, i.e.  $\lambda(W) \cdot T_p(W)$  is a constant value for any  $W$ , where  $T_p$  is proliferation time. Naturally, the larger available resources may be used by nuclear proliferator, the shorter time is needed to modify NM for successful NED manufacturing and military application. So, detection parameter depends on power consumed by a nuclear enterprise. Since power  $W$  consumed by nuclear enterprises and proliferation time  $T_p$  are linked by the energy  $E$  required to modify NM as  $T = E/W$ , the following equation can be written:  $\lambda(W) \cdot (E / W) = \text{const}$ , or  $\lambda(W) = \text{const} \cdot (W / E) = \alpha_W \cdot W$ .

In both models the emission rate parameter is proportional to the territorial area where abnormal emission level was observed, i.e.  $\lambda_A \sim S(A) \sim R^2(A) \sim A$ , or  $\lambda_A = \alpha_A \cdot A$ . So, each addend in equation (7) can be written as a product of two multipliers:

$$\lambda = \alpha_K \cdot K + \alpha_W \cdot W + \alpha_A \cdot A \quad (8)$$

For example, detection parameter  $\lambda^W$  is equal to the mean UAA detection frequency on the resource consumption rate  $W$ . Of course, the UAA detection frequency depends on the sensitivity of the detecting devices to the resource consumption rate  $W$ , or to  $W$ -indicator. The sensitivity defines efficiency  $a^W$  of the searching process.

### 8.5 Comparative evaluations of external UAA monitoring efficiency and enhancement of inherent proliferation protection

The following problems are considered below: it is required to analyze dependency of metal uranium proliferation protection on uranium enrichment at different efficiencies of the searching process, and it is required to analyze the effects of uranium denaturing on its proliferation resistance, if uranium is denatured by admixing small amounts of  $^{232}\text{U}$  that intensifies inherent neutron background. Nuclear proliferator does not resort to uranium re-enrichment up to the weapon-grade level, his main goal consists in a NED manufacturing.

Relative values of uranium proliferation protection were calculated for different efficiencies  $\alpha$  of the searching process including the case when  $\alpha = 0$ , i.e. the case of uranium self-protection.

Mark-Hippel-Lyman model (Mark, 1993) of CFR initiation and propagation was used to evaluate damage from NED manufacturing and military use. CFR parameters were calculated by direct mathematical simulation of neutron multiplication process with application of Monte Carlo code MCNP-4B (Briesmeister, 1997) and evaluated nuclear data

file ENDF/B-VI (National Nuclear Data Center, 2001). Mathematical model and algorithm for determination of the model parameters correspond to the approach described in paper (Kryuchkov et al., 2008).

The results obtained in calculations of relative proliferation protection (inverse value to the risk) for different monitoring efficiencies and for different levels of uranium denaturing by  $^{232}\text{U}$  are presented in Fig. 21.

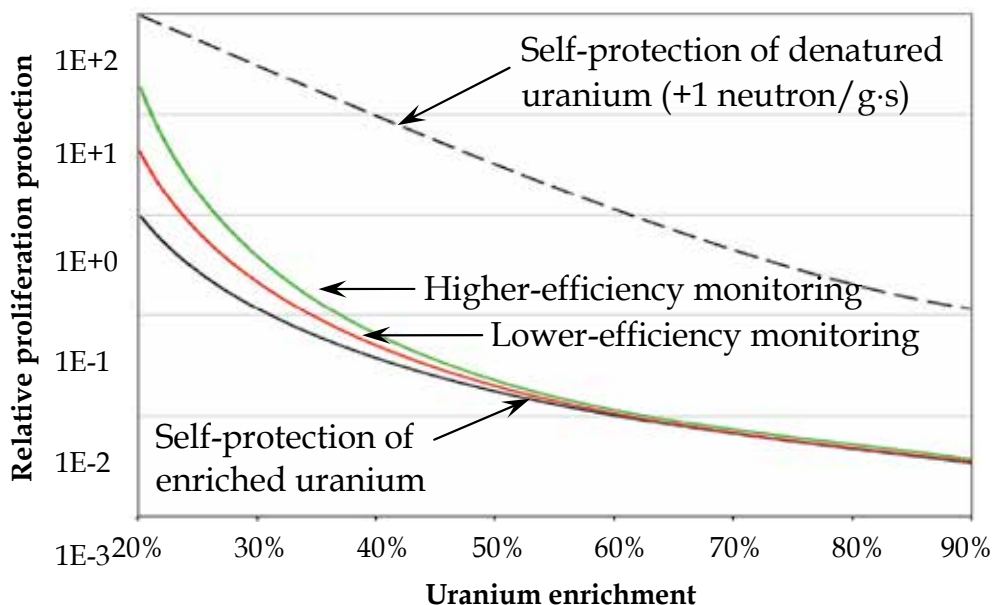


Fig. 21. Proliferation protection of metal uranium as a function of its enrichment

The following conclusions can be derived from numerical evaluations of metal uranium proliferation protection:

1. Measures of external monitoring (outside of MPC&A system) are ineffective ones in comparison with the measures aimed at upgrading of uranium self-protection for highly-enriched compositions.
2. Efficiency of external monitoring can excel efficiency of inherent self-protection for uranium enriched below 20%  $^{235}\text{U}$ .
3. Upgrading of uranium self-protection by its denaturing, i.e. by formation of internal neutron source, weakly depends on uranium enrichment and provides approximately the same effect in a rather wide range of uranium enrichments.

So, nuclear non-proliferation requires maximal restrictions to be imposed on any transactions of pure HEU while free material must be maintained in a self-protected state produced by isotopic denaturing, for instance.

## 9. References

Babichev, A.P.; Babushkina, N.A.; Bratkovsky, A.M. et al. (1991) *Physical values*. Energoatomizdat, ISBN 5-283-04013-5

- Belousov, N.; Bychkov, S.; Marchuk, Yu. et al. (1992). The Code GETERA for Cell and Polycell Calculations. Models and Capabilities, *Proceedings of the 1992 Topical Meeting on Advances in Reactor Physics*, Charleston, SC, USA, March 1992
- Benedict, M.; Pigford, T.H. & Levi, H.W. (1981). *Nuclear Chemical Engineering* (2nd Edition), McGraw-Hill, ISBN 0-07-004531-3, New York
- Briesmeister, J.F. (1997). MCNP - A General Monte Carlo N-Particle Transport Code - Version 4B. *Los Alamos National Laboratory Report, LA-12625-M*
- Bychkov, A.V.; Vavilov, S.K.; Skiba, O.V. et al. (1997). Pyro-Electrochemical Reprocessing of Irradiated FBR MOX fuel. III. Experiment on High Burn-up Fuel of the BOR-60 Reactor, *Proceedings of the International Conference on Future Nuclear Systems "GLOBAL'97"*, Yokohama, Japan, October 1997
- Cunningham, P.T.; Arthur, E.D.; Wagner, R.L. Jr. & Hanson, E.M. (1997). Strategies and Technologies for Nuclear Materials Stewardship, *Proceedings of the International Conference on Future Nuclear Systems "GLOBAL'97"*, Yokohama, Japan, October 1997
- De Volpi, A. Denaturing Fissile Materials. (1982). *Progress in Nuclear Energy*, Vol.10, No.2, (November 1981), pp. 161-220, ISSN 0149-1970
- Feiveson, H.A. (2005). In Memoriam - Ted Taylor. *Science & Global Security*, Vol.13, pp. 117-128, ISSN 0892-9882
- Ganesan, S.; Sharma, A.R. & Wienke, H. (2002). New Investigations of the Criticality Property of Pure  $^{232}\text{U}$ . *Annals of Nuclear Energy*, Vol.29, No.9, pp. 1085-1104, ISSN 0306-4549
- Gilfoyle, G.R. & Parmentola, J.A. (2001). Using Nuclear Materials to Prevent Nuclear Proliferation. *Science & Global Security*, Vol.9, No.2, pp. 81-92, ISSN 0892-9882
- Grachev, A.F.; Mayorshin, A.A.; Golovanov, V.N.; Tsykanov, V.A.; Bychkov, A.V. & Shishalov, O.V. (2003). Experience and prospects for the use of fuel rods made of vibro-packed oxide fuel, *Proceedings of the International Conference "Nuclear Power and Nuclear Fuel Cycles"*, Dimitrovgrad, Russia, December 2003
- Ivanov, V.B.; Mayorshin, A.A.; Skiba, O.V. et al. (1997). The Utilization of Plutonium in Nuclear Reactors on the Basis of Technologies, Developed in SSC RIAR, *Proceedings of the International Conference on Future Nuclear Systems "GLOBAL'97"*, Yokohama, Japan, October 1997
- Koch, L.; Betti, M.; Cromboom, O. & Mayer, K. (1997). Nuclear Material Safeguards for P&T, *Proceedings of the International Conference on Future Nuclear Systems "GLOBAL'97"*, Yokohama, Japan, October 1997
- Kryuchkov, E.F.; Shmelev, A.N.; Masterov, S.V. et al. (2008). An Approach to Quantitative Evaluation of Inherent Proliferation Resistance of Uranium Enriched up to 20%  $^{235}\text{U}$ , *Proceedings of the 30-th International Meeting on Reduced Enrichment for Research and Test Reactors*, Washington, D.C., USA, October 2008
- Kulikov, E.G.; Shmelev, A.N. & Kulikov, G.G. (2007). Neutron-physical properties of ( $^{233}\text{U}$ - $^{238}\text{U}$ ) fuel in LWR with supercritical coolant parameters. *Communications of Higher Schools. Nuclear Power Engineering*, No.2, pp. 27-39, ISSN 0204-3327
- Mark, J.C. (1993). Explosive Properties of Reactor-Grade Plutonium. *Science & Global Security*, Vol.4, pp. 111-128, ISSN 0892-9882
- Massey, J.V. & Schneider, A. (1982). The Role of Plutonium-238 in Nuclear Fuel Cycles. *Nuclear Technology*, Vol.56, No.1, pp. 55-71, ISSN 0029-5450

- National Nuclear Data Center (NNDC). (2001). <http://www.nndc.bnl.gov/nndcscr/documents/endl/endl201/>
- Nojiri, I. & Fukasaku, Y. (1997). Calculational Study for Criticality Safety Data of Fissionable Actinides, *Proceedings of the International Conference on Future Nuclear Systems "GLOBAL'97"*, Yokohama, Japan, October 1997
- Oak Ridge National Laboratory. (1995). *SCALE: A Modular Code System for Performing Standardized Computer Analyses for Licensing Evaluation*, Vols. I-III, NUREG/CR-0200, Rev. 4 (ORNL/NUREG/CSD-2/R4), Available from Radiation Shielding Information Center at Oak Ridge National Laboratory as CCC-545.
- OECD Nuclear Energy Agency. (1997). *JEF-PC, Version 2.0, A Personal Computer Program for Displaying Nuclear Data from the Joint Evaluated File Library*
- Reilly, D.; Ennslin, N. & Smith, H.Jr. (1991). *Passive Nondestructive Assay of Nuclear Materials*. Los Alamos National Laboratory, ISBN 978-999-6344-45-9
- Rolland-Piegeue, C. (1995). Safeguards and Non-Proliferation for Advanced Fuel Cycles. IAEA Safeguards on Plutonium and HEU, *Proceedings of the International Conference on Evaluation of Emerging Nuclear Fuel Cycle Systems "GLOBAL'95"*, Versailles, France, September 1995
- Selle, J.E.; Angelini, P.; Rainey, R.H. & Federer, J.I. (1979). Technical Consideration of the Use of Nuclear Fuel Spikants for Proliferation Deterrence. *Nuclear Technology*, Vol.45, No.3, (October 1979), pp. 269-286, ISSN 0029-5450
- Sokolova, I.D. (2008). Program of Global Nuclear Energy Partnership (GNEP). *Atomic Techniques Abroad*, No.3, (March 2008), pp. 3-13, ISSN 0320-9326
- USA National Academy of Sciences. (2000). *The Spent-Fuel Standard for Disposition of Excess Weapon Plutonium. Application to Current DOE Option*, National Academy Press, ISBN 0-309-07320-0, Washington, D.C.
- Willrich, M. & Taylor, T.B. (1974). *Nuclear Theft: Risks and Safeguards: A report to the Energy Policy Project of the Ford Foundation*, Ballinger Pub.Co., ISBN 0884102076, Cambridge

# **Part 5**

## **Thorium**





# Implementation Strategy of Thorium Nuclear Power in the Context of Global Warming

Takashi Kamei

*Kinugasa Research Organization, Ritsumeikan University  
Japan*

## 1. Introduction

The progress of global warming requires us to construct a sustainable society immediately. At the same time, energy demand in developing countries especially in Asian countries such as China and India is increasing rapidly and at a large scale. In the context of global warming, fossil fuels such as coal and oil should not be used as primary energy sources because they significantly increase concentration of greenhouse gases like carbon dioxide (CO<sub>2</sub>) in atmosphere. Therefore nuclear energy can be one of the candidates of carbon-free primary energy source.

However, it is also true that there are concerns relating to the use of nuclear power such as nuclear proliferation, radioactive waste and possibility of severe accident. These concerns make it difficult to apply nuclear power widely in the world even though it does not emit CO<sub>2</sub>. We are now in the end of the first commitment period of Kyoto protocol. There are mainly three mechanisms to reduce CO<sub>2</sub> emission from human activity. One of them is called "Clean Development Mechanism (CDM)", which supports implementation of technology and finance for CO<sub>2</sub> reduction in developing countries. Nuclear power is not confirmed as an option of CDM due to its concern of safety issue.

On the other hand, there are many remarkable movements on another nuclear power, which utilizes "thorium" as fuel, in the world recently. Thorium nuclear power becomes to be discussed not only by nuclear specialists but also in the field of global warming. This is because thorium nuclear power has a potential to achieve both production of electricity without emitting CO<sub>2</sub> and reduction of concerns of ordinary nuclear power at the same time. In this chapter, outline of thorium nuclear power will be introduced and its implementation scenario in the global scale from a view of global warming will be demonstrated. In addition, background of recent trend of global warming, which calls thorium nuclear power, will be shown. The focal point of above calculation is mass-balance of fissile materials because implementation amount of thorium nuclear power is mainly governed by supply amount of fissile materials.

## 2. Necessary understandings on global warming

It is indispensable to know how much CO<sub>2</sub> is emitted from different sectors in order to prepare adequate approaches in technical and economical views. 46 % of CO<sub>2</sub> is coming from energy sectors such as electricity and heat production (International Energy Agency

[IEA], 2009). Governing factor of CO<sub>2</sub> emission from electricity production is coal usage. Coal is a widely spread energy resource and its remaining resource is still large. Its price is also cheap. Recent technological progress of carbon capture and storage (CCS) is expected to reduce CO<sub>2</sub> emission from the whole life of coal usage. Most of technical elements of CCS system have been cleared and some feasibility studies are now carried in Norway, Canada and Australia. However, careful design of total system of CCS will be needed in order to avoid CO<sub>2</sub> leakage during its transportation from its production point to its final disposal area (Kamei, 2008). Solar power is also available for clean electricity supply. But it should be noted that solar power is available only in daytime and its output fluctuates due to weather condition.

One of the practical low-carbon energy sources is nuclear power. Nuclear power has been recognized as an effective way as countermeasure of global warming. But it was not counted as an option of CDM because of its several concerns. These concerns are nuclear proliferation, safety and radioactive waste. As Solana, the high representative for the common foreign and security policy of European Union (EU) said, expansion of nuclear power to developing countries in Asia will cause a concern of nuclear proliferation. We still have the memories of a severe accident of Chernobyl as a possibility relating to the use of nuclear energy. In addition, we are still facing the ongoing severe accident at Fukushima Daiichi nuclear power plant in Japan. Recently, public opinion in the USA revealed that they still have concern against radioactive waste, which contains plutonium (Pu) and trans-uranium materials (TRU).

23 % of world CO<sub>2</sub> emission is coming from transportation sector (IEA, 2009). This is the highest growing sector of CO<sub>2</sub> emission. Road transport sector occupies 73 % of all transportation (IEA, 2007). This trend is estimated to continue because transportation is essentially needed for growth in economy. Therefore, it is indispensable to reduce CO<sub>2</sub> emission from transportation sector. Though there are several candidates of low-carbon transportation, electric vehicle (EV) will rapidly expand its use because infrastructure to supply fuel to EV has already been established. Technological keys for EV and hybrid-vehicles are battery and electric motor using permanent magnet. Historically speaking, EV came to commercial phase earlier than gasoline engine cars. However EV could not obtain major position in the market because it could not have long driving range. Recent progresses of large capacity battery and high power electric motor help commercialize of EV.

Sectoral approach has been suggested by Japan at the 13<sup>th</sup> Conference of the Parties (COP13) as an effective way to reduce CO<sub>2</sub>. We should understand both advantages and disadvantages of this approach to successfully carry out. One of the advantages is that it is easy to determine each country's CO<sub>2</sub> reduction target by this approach. On the other hand, the disadvantage is that some sector's reduction has a possibility to become some other sector's imposition. The most apparent case is transportation sector, which mainly uses oil as its fuel at moment. It is easy for this sector to greatly achieve CO<sub>2</sub> reduction target by electrification. However, power generation sector will be forced to consider additional effort to reduce CO<sub>2</sub> emission, which is not their original responsibility. Therefore, it becomes very important to discuss comprehensive approach, which can avoid such phenomena of emission transition from one sector to other sector, to effectively carry this sectoral approach.

The other important information to design a suitable approach to globally reduce CO<sub>2</sub> emission is nation-based CO<sub>2</sub> emission data. China is now the biggest CO<sub>2</sub> emission country

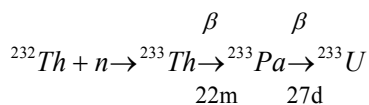
(IEA, 2009) and it is estimated to emit more CO<sub>2</sub> in near future because of its huge economic growth and its large population. The second biggest CO<sub>2</sub> emitting country is the USA. About 41% of CO<sub>2</sub> emission of the world is occupied only by these two countries. Therefore, it is also necessary to consider a way of CO<sub>2</sub> reduction, which can be applied even by these two great countries as their own countermeasure.

Present accumulation of CO<sub>2</sub> in atmosphere is mainly caused by the previous emission of CO<sub>2</sub> from developed countries such as the USA, European countries and Japan. There are only a few developing countries included in the top 15 ranking of CO<sub>2</sub> emission. However, we have to take care of the future prediction that developing countries are growing now and they will become to emit more CO<sub>2</sub>. For example, India is the fourth largest CO<sub>2</sub> emitting country in the world. India is also the second largest country in population at the same time. Therefore, it is necessary to prepare CO<sub>2</sub> emission reduction methods, which can be adopted by these developing countries, too. One of the concerns of national energy security is whether energy is stably supplied or not. From this point of view, energy resource, which can be obtained within its own land area, is most applicable. Even though there are several limitations, but renewable energy such as solar power will be nation's own energy source. Consequently, there are several points in global scale CO<sub>2</sub> reduction. CO<sub>2</sub> has to be reduced both from power generation sector and transportation sector, but some sector's reduction must not be pushed into other sector. Though there may be some effective method of CO<sub>2</sub> reduction, they should be available even by China and the US. It also should be available by developing countries such as India.

### 3. Thorium nuclear power

In spite of the concerns mentioned above, nuclear power can play a major role for providing sustainable energy with very low CO<sub>2</sub> emission. One of its advantages is that applying nuclear power will satisfy simultaneous reduction of CO<sub>2</sub> both from power generating sector and transportation sector. That is to say, if newly installed nuclear power plants supply electricity to electric vehicles, it does not disturb efforts of power generating section. China has already presented that they are going to expand use of nuclear power for providing electricity. Number of nuclear power plant under operation is 11. Number of nuclear plants under construction is 12. Number of plan is 147. Though the super-heated progress was cooled-down after the accident at Fukushima Daiichi nuclear power plant, essential trend is not changed. Even after this severe accident at Fukushima, US's president Obama said that nuclear power will also be used as clean energy source. There are still many countries planning to implement nuclear power in developing countries such as India. However, those concerns relating to nuclear power are still remaining in reality, so it is necessary to overcome these concerns if nuclear power is expanded to the world. For example, nuclear proliferation and radioactive waste must occur essentially as far as only uranium is used as nuclear fuel. Plutonium is the main production from the fertile isotope of uranium (mass number is 238) during the reaction in the nuclear reactor. If spent nuclear fuel is reprocessed, plutonium can be separated. Uranium-235, which is the fissionable isotope of uranium, becomes radioactive waste after nuclear fission. Uranium-238 changes to trans-uranium (TRU) materials such as americium and curium, which govern radioactive waste because of their long half-life. Needless to say, huge earthquakes happen again. There is a possibility to overcome these concerns relating to uranium usage by adopting thorium as nuclear fuel in parallel to uranium. In this section, outline of thorium nuclear

power will be briefly described and its recent trend in the world will be introduced. Thorium is naturally obtained fertile material. Thorium itself can not make fission reaction, but it transmutes to fissionable uranium-233 by absorbing neutron as shown below.



Thorium is a lighter element than uranium and thus it produces less amount of plutonium and TRU because more than 90 % of uranium-233 fissions without growing heavier nucleus by neutron absorption. Thorium nuclear fuel in a molten-salt reactor (MSR) produces 0.5 kg of plutonium, while uranium fuel produces 230 kg of plutonium in a light water reactor (LWR) during 1 year operation of 1 GWe capacity plant (Furukawa et al., 2008). 8 kg of plutonium is necessary at least for the minimum nuclear explosion, thus it can be said that production of plutonium in thorium MSR is very small. In addition, spent thorium fuel accompanies strong gamma ray, which makes it difficult to fabricate nuclear weapon by using uranium-233 obtained from spent thorium fuel. Tatsujiro Suzuki, a member of Japan Atomic Energy Committee, proposed a new approach toward nuclear non-proliferation and nuclear disarmament in 2009. Here, he suggested using thorium-MOX (mixed oxide) fuel in the present commercially used LWRs (Suzuki, et al., 2009).

Major factors of TRU are americium and curium. Total amount of these elements produced in the same condition mentioned above is 0.3 g from thorium MSR (Furukawa et al., 2008). This value is much smaller than the production amount being 25 kg from uranium LWR. It takes about one million years for the spent uranium fuel without reprocessing to be the same radioactive toxicity of natural uranium. Even with reprocessing, it will need about 100 thousand years. However, it is estimated to be about a few hundred years for the thorium fuel because production amount of americium and curium is very small.

Thorium is about 4 times abundant than uranium and it is widely available even in developing countries such as India, China and Brazil as summarized in Table 1. Developed countries such as Australia, Canada and Norway have large reserve of thorium, too. The U.S. Geological Survey (USGS) announced last year that the USA reserves 915 thousand tons of thorium (USGS, 2009).

We see several notifications on thorium utilization from the side of global warming, not from nuclear industry. Fritz Vahrenholt, CEO of Repower, mentioned in 2001 that conventional LWR will not come back to Germany but safe thorium reactor will be possible. Thorium utilization was recommended as one of the technical approaches to reduce CO<sub>2</sub> emission in the specialist meeting on climate change at Kyoto in 2007. Former Australian Governor-General Major General Michael Jeffrey said that “while solar has the best prospect of a clean and sustainable energy source, thorium should not be discounted, as it is cleaner and can not be used to make weapons grade materials” in 2008 (Future Summit, 2008).

9 papers discussing about thorium fuel in LWR, heavy water reactors (HWR) and MSR were seen in the ANFM IV, which is an international symposium on nuclear power. It was impressive that the general chairman of this symposium wrote as follows; “thorium fuel cycles may be unusual to many of us in the US, but they are important topics internationally, and are subjects that we must carefully study in order to ensure the future success of our industry.” Chinese Tsinghua University in Beijing organized an international workshop on thorium utilization in 2007 (TU2007) collaboratively with international atomic

energy agency (IAEA). China does not have enough amount of uranium but they have huge amount of thorium. Greneche of AREVA said, "It is important to use semi-breeding reactor with thorium fuel. Though CANDU is better than LWR, its conversion ratio (CR) is still smaller than 1. MSR has an attractive feature in this point of view." Its second workshop, TU2009, was held in Baotou, China. Baotou is the most important city of rare-earth industry, which is indispensable for manufacturing EV. Thorium has already been accumulated as by-product of rare-earth mining in a residual pool.

Country	Reserve [t]	Ratio
Turkey	380,000	14%
India	290,000	10%
Norway	170,000	6%
USA	915,000	33%
Brazil	16,000	1%
Denmark	54,000	2%
Australia	300,000	11%
Egypt	15,000	1%
South Africa	35,000	1%
Canada	100,000	4%
Greenland	54,000	2%
Liberia	1,000	0%
China	388,000	14%
Other	95,000	3%
World total	2,813,000	100%

Table 1. Thorium resource (Nishikawa, 2010)

The Ministry of Petroleum and Energy of Norway published a report of thorium utilization in 2008 (The Ministry of Petroleum and Energy of Norway, 2008). Several private companies such as "Statkraft" and "Thor Energi AS" are carrying R&D of thorium fuel. Former secretary general of IAEA Hans Blix became a board member of Thor Energi AS. In the US, one section titled "study on thorium-liquid fueled reactors for naval forces" was included in the legislation of "National Defense Authorization Act for Fiscal Year 2010". Finally the description of thorium-liquid fueled reactors was removed, but \$ 61.5 million has been assigned to Oak Ridge National Laboratory (ORNL), which is the origin of thorium-liquid fuel reactor, MSR. There were several movements between private companies of nuclear industries (Peachey, 2009). AREVA, French nuclear company, signed an agreement on collaboration of thorium nuclear fuel with US private company named Thorium Power Co. Ltd (its name has been changed to "Lightbridge" in September, 2009). Canadian nuclear company, AECL signed with Chinese companies group for testing thorium fuel rod in CANDU reactor in Qinshan nuclear power plant at Shanghai.

Many popular magazines are coming to pick up thorium issues. Newsweek presented an article entitled "The Lost Chance" to return to the road not taken 50 years ago – thorium fuel cycle in 2001 (Howard & Graham, 2007). Australian scientific magazine COSMOS reported about the thorium utilization as "green nuclear power" in 2007 (Dean, 2007). Sam Knight reported recent situations on UK's "Financial Times" in 2008 (Knight, 2008). "U.S. News & World Report" presented thorium utilization in a special issue of green economy in

2009 (Garber, 2009). An international meeting of thorium energy alliance (TEA) was held at Googleplex, the head-office of Google, in March, 2010. Wide range of thorium utilization was discussed including high temperature gas cooled reactor and molten-salt reactor called LFTR (Liquid Fluid Thorium Reactor). The 3<sup>rd</sup> conference of TEA has successfully organized in May, 2011 at Washington DC. Its sister conference was held at London in October, 2010 by international thorium energy organization (IThEO). Accelerator driven sub-critical reactor (ADSR) was also picked up as a remarkable topic of thorium utilization.

#### 4. Implementation scenario of thorium nuclear power

One of the most attractive reactor types to use thorium is MSR (Weinberg, 1997). The successful R&D program was carried in the USA on MSR for the usage of thorium since 1950's to 70's. Molten-salt reactor experiment (MSRE) was successfully operated during 1965 and 1969. Based on this success, molten-salt breeder reactor (MSBR) was started to develop for targeting commercial power reactor (Rosental et al., 1972). Furukawa et al. have proposed one design of MSR named FUJI (Furukawa, et al., 1990). MSR was chosen among 6 candidates by the Generation IV International Forum (GIF). There are aggressive activities in the US, Canada and France with different types of MSR such as LFTR or tube-in-tube reactor.

Most of MSR has a common technical background. Inner pressure of reactor vessel of MSR is only about 0.5 MPa because it applies molten-salt as coolant, which has very low vapour pressure. Therefore, there is no need to fabricate very high pressure vessel such as necessary in LWR. It reduces risks of bottleneck in its supply chain. Economy of MSR also has been examined (Roy & Robertson, 1971). Comparison between MSBR and LWR indicated that (1) capital cost will be nearly the same, (2) fuel cycle cost will be greatly reduced due to no requirement of manufacturing of fuel rods because MSR is liquid fuel and (3) maintenance cost will be also reduced because there is no necessity of fuel exchange. This is achieved by on-line re-fuelling and re-processing with liquid fuel. There is other recent work showing cost evaluation of MSR and pressurized water reactor (PWR) in view of capital cost, operations and maintenance, fuel, waste disposal and decommissioning (Moir, 2002). The result is summarized in table 2. The fuel cost of MSR was recalculated based on the use of uranium-233. Total cost of MSR will be about 30 % smaller than that of PWR.

	MSR	PWR
Capital cost	2.01	2.07
Operations & maintenance cost	0.58	1.13
Fuel cycle cost	0.12	0.74
Waste disposal cost	0.10	0.10
Decommissioning cost	0.04	0.07
Total	2.85	4.11

Table 2. Cost evaluation of MSR and PWR (cent/kWh)

The most important of thorium usage is that thorium does not contain fissile isotope. Therefore, uranium containing both fissile isotope (uranium-235) and fertile isotope (uranium-238) was used as the first nuclear fuel in the history. Uranium fuel produces fissionable plutonium and some countries are planning to use it as future nuclear fuel in fast

breeder reactor (FBR). However, there is still concern to use plutonium with uranium-238 because it has a possibility to spread plutonium to the world. Total stock amount of plutonium in the world is nearly 2,000 t and it continues increasing in the future. This plutonium can also be used as fissile material with thorium. Thorium is available in any kind of nuclear reactors and many researches are carried now on commercially used reactors, too. Thorium is still not used as nuclear fuel because it is not available for nuclear weapon. Recent global trend of nuclear disarmament also supports starting use of thorium. Disadvantage of thorium containing no fissile isotope can now be solved by applying plutonium in spent nuclear fuel of LWR (Kamei et al., 2008; Kamei et al., 2009). Though it was known that plutonium could be applied as fissile with thorium, there was not enough amount of plutonium in 1970's to start thorium reactors because plutonium is artificially produced material. Now, there is about 200 thousand t of spent nuclear fuel and 2,000 t of plutonium is accumulated. Spent nuclear fuel occurs at least 12,000 tons every year depending on the total capacity of LWR in the world. Czech, Japan and France are studying to use plutonium in spent fuel for thorium MSR. Direct fluorination facility named FERDA has been developed in order to obtain plutonium from spent nuclear fuel (Uhlir, 2008). Outline of possible implementation path of thorium utilization including different types of nuclear reactor such as LWR and new technologies including MSR can be summarized as shown in Fig. 1.

- Short term ... LWR, HWR etc. (by USA, Canada, EU, China etc.)
- Middle term ... MSR (China, US, EU, Canada and Japan)
- Long term ... Fissile breeding by ADS and nuclear fusion

In any case, the most important subject is "how to get fissile".

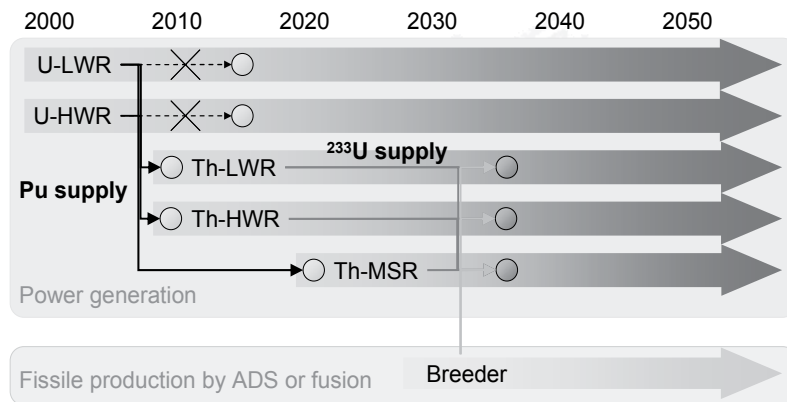


Fig. 1. Implementation path of thorium nuclear power.

The most important point to describe implementation scenario of thorium utilization is fissile supply. Plutonium will be the only fissile material having enough amounts in the very begging of world thorium utilization. Though Plutonium can be used with uranium-238, it is considered here that plutonium will be used with thorium. It is because natural uranium containing uranium-235 can be fed to uranium fuel cycle. As far as present capacity of uranium usage continues in this century, uranium resource is still enough. On the other hand, uranium-235 is also available to be used with thorium. However, it has several limitations. The first point is that in order to be used with thorium, highly enriched uranium-

235 more than 20% enrichment is necessary. This causes additional concern of nuclear proliferation. The second point is that uranium usage also should be used continuously since it is an established technology emitting no CO<sub>2</sub> during its electricity production. In addition, once uranium usage is terminated in an early stage, plutonium supply will be shortage in order to expand thorium utilization. This will be demonstrated later. Thus, parallel usage of uranium and thorium will be necessary to construct sustainable energy sources available both in developed countries and developing countries.

Once thorium is ignited by plutonium, uranium-233 is artificially produced during operation of thorium fuelled LWR and HWR. This uranium-233 can be used in the following thorium LWR and HWR. Plutonium can also be fed to start MSR. It is estimated to require about 10 years for developing proto-type MSR. Uranium-233 produced from LWR, HWR and MSR will be stored and then can be used as fissile to start following MSR. As presented in the next section, production amount of plutonium and uranium-233 is small. Therefore, production of uranium-233 from thorium by using accelerator or fusion technology will be necessary for large scale implementation. It depends on how design whole view of new nuclear power supply system.

In order to quantitatively evaluate implementation capacity of thorium fuel cycle, mass-balance of fissile material has been calculated. Calculation model is shown in Fig. 2. In this calculation, both uranium fuel cycle and thorium fuel cycle are considered as analysis targets. Fissile material for uranium fuel cycle can be obtained from natural mining. Though

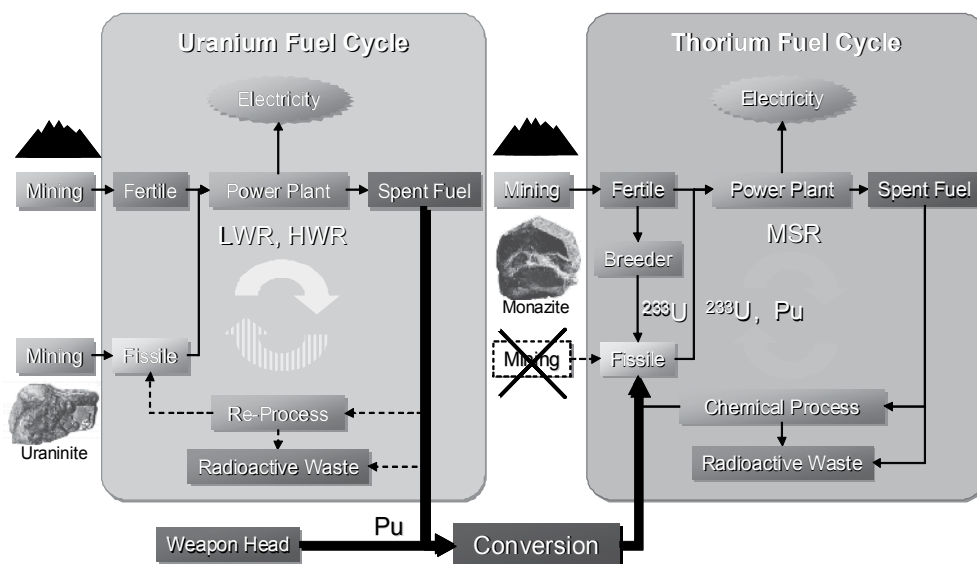


Fig. 2. Calculation model of implementation of thorium fuel cycle

recycled plutonium from spent nuclear fuel can be also fed to uranium fuel cycle as fissile, it is not considered this calculation. Because of the lack of fissile isotope in thorium, it is necessary to obtain fissile material from outside of thorium fuel cycle. Direct production of uranium-233 from thorium by using spallation neutron triggered by accelerator or nuclear fusion neutron can be available inside of thorium fuel cycle without depending on uranium fuel cycle. However, in this calculation, plutonium fed from uranium fuel cycle is considered as fissile material to start thorium fuel cycle. Capacity of uranium fuel cycle is



determined by the prediction of international energy agency (IEA) to be 680 GWe at 2030. In this case, 13 of 1 GWe LWRs will be implemented every year. 1 GWe of LWR generates about 30 t of spent fuel every year.

MSR is considered as a power reactor in thorium fuel cycle because of its high conversion ratio of fissile material. Two designs of MSR, FUJI-Pu2 and FUJI-U3, are applied in this calculation based on different initial fissile. FUJI-Pu2, which uses plutonium as fissile material, will be used for starting the thorium fuel cycle. Spent thorium fuel from FUJI-Pu2 contains uranium-233 and this can be provided to the next generation of thorium MSR. Other design of MSR, FUJI-U3, will be supported by uranium-233 obtained after termination of FUJI-Pu2. Both types of MSR have 200 MWe of electricity capacity and 30 years of lifetime. The performance of these reactors is summarized in Table 3.

	FUJI-Pu2	FUJI-U3
Electricity capacity	200 MWe	200 MWe
Lifetime	30 years	30 years
Pu inventory (initial)	5.78 t	-
Pu feed (total in life)	1.16 t	-
<sup>233</sup> U inventory (initial)	-	1.132 t
<sup>233</sup> U feed (total in life)	-	0.344 t
Batch cycle	7.5 years	7.5 years
<sup>233</sup> U production (batch cycle)	0.295 t	0.029 t
<sup>233</sup> U production (terminated)	0.295 t	1.505 t
MA production (terminated)	285 kg	5.32 kg
Th inventory (initial)	31.3 t	56.3 t
Conversion ratio	0.92	1.01

Table 3. Specification of MSR

## 5. Calculation results

Implementation capacity of thorium MSR in a global scale was calculated based on the plutonium supply from uranium fuel cycle. Calculation was carried as follows. At first, capacity of uranium fuel cycle at certain year is determined. Then production of spent nuclear fuel is obtained. It was assumed that MSR will begin to be used around 2024. Its capacity grows gradually and corresponding amount of required plutonium is calculated. This amount is reduced from spent nuclear fuel. Here, capacity of processing spent nuclear fuel to molten-salt fuel is assumed enough high. Calculation result is shown in Fig. 3.

The first Y-axis is referred by electricity capacity. The second Y-axis is referred by storage of spent fuel. Black cross line indicates growth of LWR. The gray line corresponds to the storage of spent nuclear fuel without MSR. The black chain line is the storage of spent nuclear fuel with consumption by MSR. Gray hatching is capacity of FUJI-Pu2. White dot hatching is capacity of FUJI-U3. It is assumed that FUJI-Pu2 begins to be used from 2024. Number of FUJI-Pu2 reactor at 2024 is 32. Plutonium in spent nuclear fuel is rapidly consumed with the growth of FUJI-Pu2. The growing ratio of FUJI-Pu2 decreases at 2029, when stock of spent fuel becomes almost 0. Since then, annual production of spent fuel from uranium fuel cycle is consumed within the same year for new implementation of FUJI-Pu2. After one batch cycle of fuel salt processing of FUJI-Pu2, uranium-233 is extracted and fed to

FUJI-U3. Therefore, two different designs of MSR can be used since 2029. Spent fuel salt from FUJI-U3 is also reprocessed after one batch cycle and fed to next generation of FUJI-U3. Capacity of LWR is 948 GWe and that of MSR including both FUJI-Pu2 and FUJI-U3 is 392 GWe at around 2050. Thorium MSR also produces its own spent fuel. However the amount is considerably smaller than the amount from uranium LWR. This is because spent fuel of thorium MSR comes out of reactor after its lifetime being 30 years. On the other hand, spent fuel of LWR occurs every year. It is estimated here that thorium MSR will be commercialized in 2020's. Therefore, spent fuel of thorium MSR will appear around 2050's. Its quantitative evaluation has been demonstrated in the previous work (Kamei, 2008).

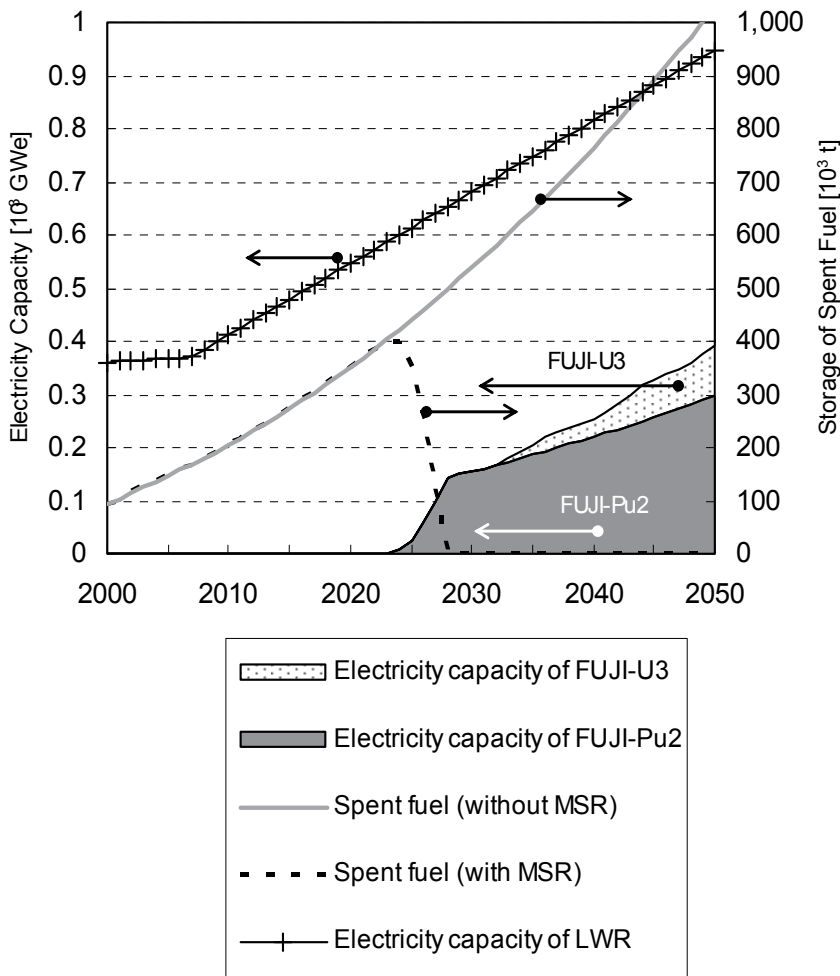


Fig. 3. Calculation result of Implementation capacity of thorium MSR (case 1)

Other result is shown in Fig. 4. It is assumed here that capacity of uranium fuel cycle will be constant within next 40 years by considering the effect of Fukushima Daiichi nuclear power plant accident. In this case, implementation capacity of thorium MSR will be about 258 GWe around at 2050, which is small because supply of fissile plutonium is reduced.

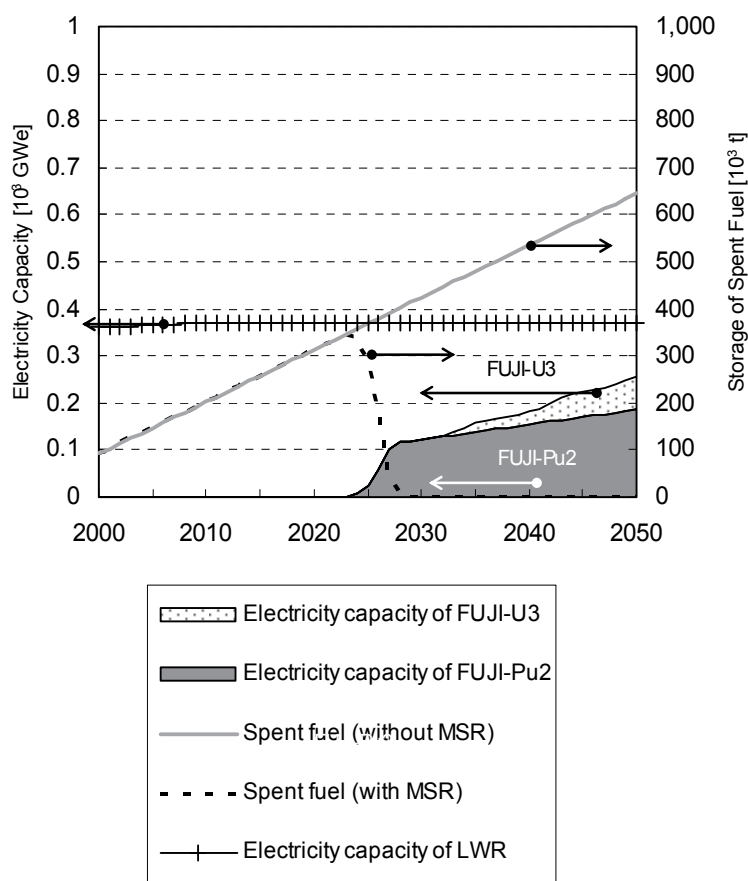


Fig. 4. Calculation result of Implementation capacity of thorium MSR (case 2)

The amount of plutonium from dismantled weapon head is estimated to be about 91.9 t and 145 t for the USA and Russia, respectively (International Panel on Fissile Materials, 2008). Additional 40 t of plutonium can be separated based on the agreement between the USA and Russia to reduce number of nuclear weapons to be 2,000. Briefly speaking, contribution of plutonium from weapon head is about 15 GWe around at 2050 to additionally implement thorium MSR to the implementation capacity by spent nuclear fuel from uranium fuel cycle.

## 6. Sustainable development with thorium utilization

In this section, relation between thorium utilization and its surroundings will be discussed in a view of comprehensive approach on sustainable development. The key issues are protection of radioactive hazard by thorium, rare-earth production accompanied with thorium, electric vehicle using lots of rare-earth and CO<sub>2</sub> reduction from human activities.

### 6.1 Production of thorium as by-product of rare-earth

One of the important sectors to reduce CO<sub>2</sub> emission is transportation sector. Many motor companies have presented to supply EV or hybrid-vehicle (HV) recently as summarized in

Table 4. Reborn GM in 2009 put EV for their new backbone like “Chevrolet Volt”. Chevrolet Volt was given the award of 2011 Green Car of the Year. Many new EV companies appeared in China, which became the world largest production and sales of cars. BYD, which was just a battery company, is one of the most famous EV companies in China.

Country	Company	Brand
Japan	Toyota	Prius (HV)
	Nissan	Leaf (EV)
	Honda	Insight (HV), CR-Z (HV)
	Mitsubishi	i-MiEV (EV)
EU	VW	New compact coupe (HV)
	Audi	e-tron (EV)
	BMW	MINI E (EV)
	Daimler	Smart EV (EV)
	Renault	Z. E. (EV)
	PSA	OEM, Mitsubishi (EV)
USA	GM	Chevrolet Volt (EV)
	Ford	Focus EV (EV)
	Tesla motors	Roadster (EV)
Korea	Hyundai	i10 electric (EV)
China	BYD	e6 (EV)
India	Tata	Indica Vista EV (EV)

Table 4. Development of Low-Carbon Vehicle

Rare-earth materials such as neodymium and dysprosium are minerals for fabricating a strong permanent magnetic of electric motor. World annual production of rare-earth materials is about 120 thousands t at 2010 (Watanabe, 2008). The production amount is expected to increase at about 3 or 5 % every year. At moment, China shares 97 % of rare-earth production in the world. These materials can be mined from other Asian countries, too. However, accompanying thorium as by-product of rare-earth mining becomes a radioactive waste having possibility to bring environmental hazard (Nishikawa, 2010).

Thorium is not commercially used as nuclear fuel until now. It has been left as radioactive waste, which become environmental and social concerns at the resource countries. Detail investigation is needed but roughly residual thorium is estimated to be produced at least 10 thousand t every year. This makes it difficult for Japanese trade companies to find rare-earth.

## 6.2 Consumption of thorium

Consumption of thorium has been simulated by using the capacity of thorium fuel cycle demonstrated in the previous section. The result is shown in Fig. 5.

Here, it is assumed that 1 % of rare-earth production corresponds to the amount of thorium. It is also assumed that initial value of thorium storage at 2005 is zero. Typical designs of thorium MSR, FUJI-Pu2 and FUJI-U3, require 31.3 t and 56.4 t of thorium as initial value, respectively. Stockpile of thorium will be about 40 thousand t around at 2024, when commercial utilization of thorium MSR begins. Though stockpile of thorium will be accumulated by production of rare-earth, thorium is also consumed and the stockpile will

be about 60 thousand t around at 2050. If there is no utilization of thorium, its stockpile will be more than 130 thousand t.

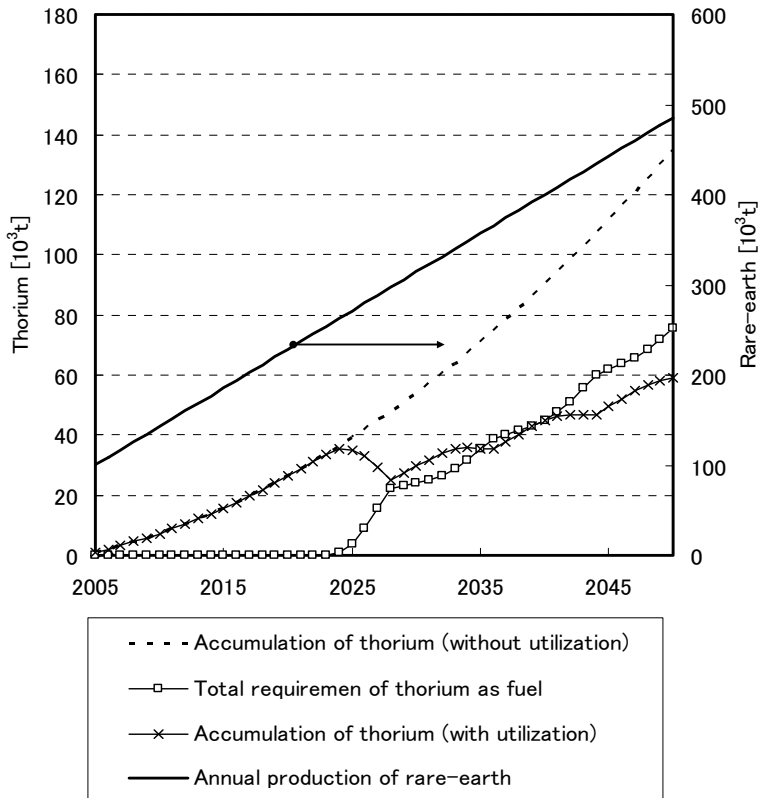


Fig. 5. Consumption of thorium.

### 6.3 CO<sub>2</sub> reduction from transportation sector

CO<sub>2</sub> emission from transportation sector has been simulated based on the prediction of capacity of thorium MSR also described in the previous section. The result is shown in Fig. 6.

It is assumed here that number of vehicles increases with 3.5% of growth rate, which is same to the recent trend (The Japan Automobile Manufacturers Association, 2009). Number of vehicle in the world around at 2005 is about 900 million. This emitted 4.5 Gt of CO<sub>2</sub>. Number of vehicle will be about 4 billion around at 2050 emitting 18.6 Gt of CO<sub>2</sub>. If 100 million EV are supplied every year since 2010, all vehicles can be replaced with EV at 2050. Even though this estimation is somewhat large, it is assumed in order to evaluate higher case of CO<sub>2</sub> reduction. 392 GWe of thorium MSR can supply electricity to 2.75 billion EV. This is obtained that EV is supplied its electricity by thorium MSR with 80 % of load factor. It is assumed that one EV can drive 10 km per 1 kWh, drives averaged 10,000 km in a year. This corresponds to 60 million t of CO<sub>2</sub> emission from thorium MSR. This was calculated that 1 kWh of nuclear power emits 0.022 kg with its load factor being 80 %. If the rest of 1.25 billion cars are also EV and supplied its electricity by coal fire plant, CO<sub>2</sub> emission is 1.23 Gt. It was assumed that coal fire plant emits 0.975 kg of CO<sub>2</sub> per 1 kWh. Total CO<sub>2</sub> emission is

1.29 Gt both from thorium MSR and coal fire plant. It can be seen that collaborative implementation of thorium MSR and EV has a great potential to CO<sub>2</sub> reduction by solving the problem of sectoral approach.

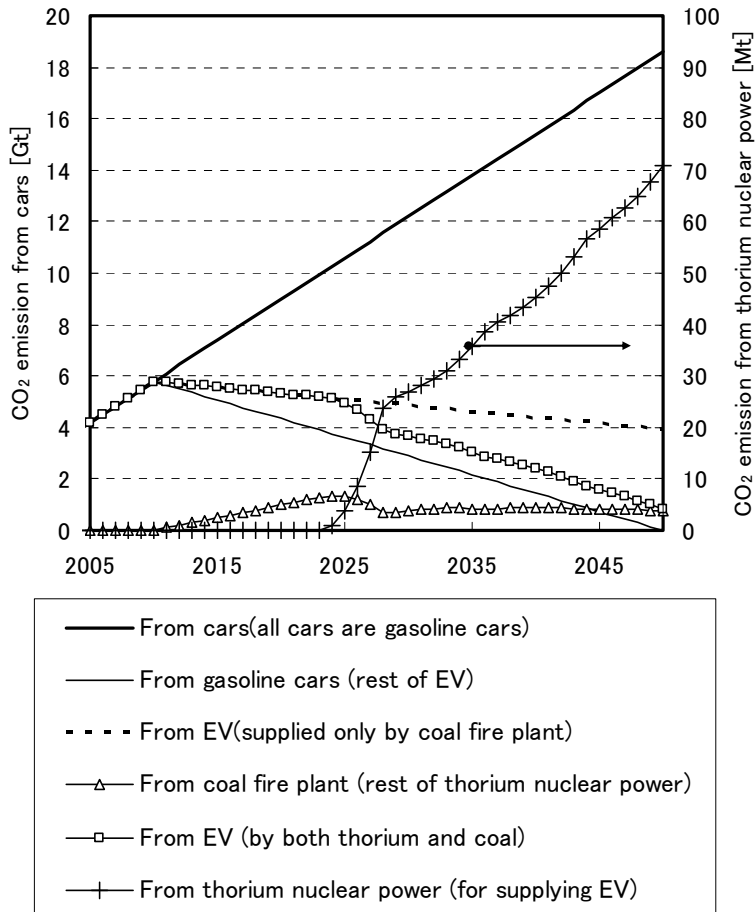


Fig. 6. CO<sub>2</sub> reduction by thorium utilization.

#### 6.4 Concept of “The Bank”

Implementation capacity of thorium MSR is limited by the amount of supply of fissile material. Thorium is recognized as radioactive waste and residual of rare-earth mining. As indicated in the Fig.5, thorium will not be necessarily completely consumed even though it is utilized as nuclear fuel. Therefore, there is a possibility that thorium, which is not managed correctly, cause environmental hazard. In order to promote progress of EV for the reduction of CO<sub>2</sub> emission from transportation sector, rare-earth mining is indispensable. Thus it is also necessary to manage thorium for keeping environment healthy. Estimation of implementation capacity of thorium MSR is based on the supply of fissile material from uranium fuel cycle since thorium does not contain its own fissionable isotope. And the other important point is that it will need more than 10 years for the first commercial implementation of thorium nuclear power. There are several countries, which hold thorium

as future energy source like India, but most of the countries have no plan to store thorium. Therefore it is necessary to store thorium. Such an idea proposed here is called "The Bank". This is named from "thorium energy bank". Outline of "The Bank" is illustrated in Fig. 7.

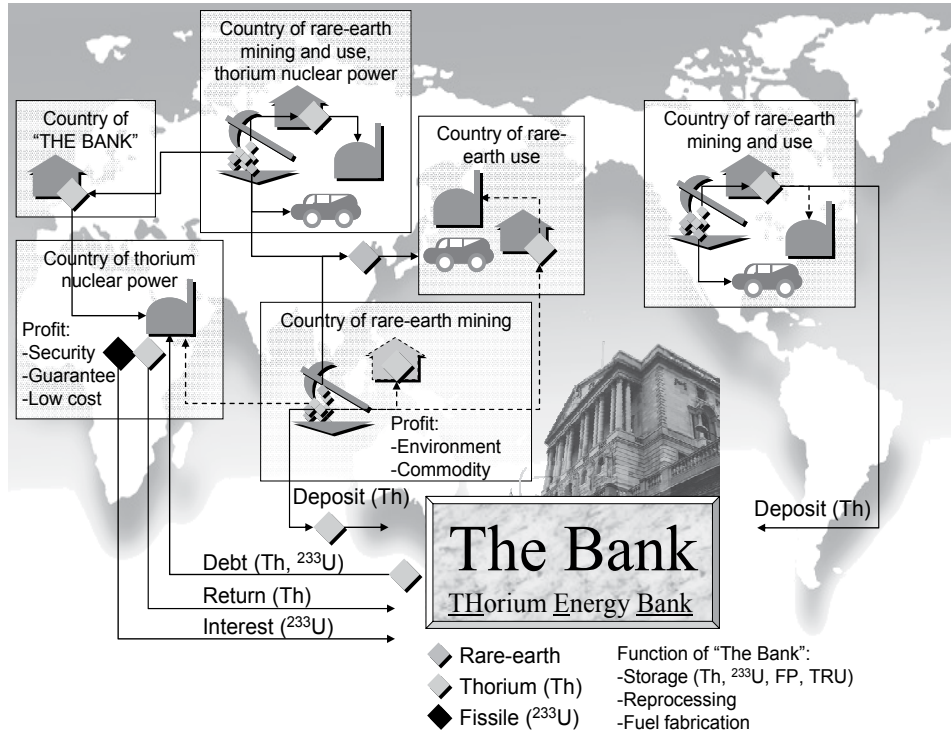


Fig. 7. Concept of "The Bank".

The most important purpose of "The Bank" is to store thorium obtained as residual of rare-earth mining. This is mainly for protecting environment of mining country of rare-earth from radioactive thorium. The other function is to lend thorium to countries, which does not own its thorium resource. Former US president Jimmy Carter proposed a concept of a nuclear fuel bank. This is to provide fissile material, enriched uranium, in order not to expand the technology of enrichment having fear of nuclear proliferation. Similar proposal was also brought from former director of IAEA, Dr. El Baradei. US President Obama also indicated at the speech in Prague, 2009 that the concept of nuclear fuel bank will be an important role to bring peace nuclear power. "The Bank" accepts both thorium and uranium-233 as fertile material and as fissile material, respectively.

However, "The Bank" will not have any uranium-233 at the beginning of its operation. Thus other fissile material such as plutonium must be provided from uranium fuel cycle. Once thorium fuel is used at some country, the spent thorium fuel will be returned to "The Bank". Uranium-233 is the interest of debt of thorium. Trend of demand toward rare-earth and thorium will be different. Rare-earth is now eagerly required but thorium is not now. "The Bank" will be an international organization. Head office of "The Bank" can be located in Norway, Sweden, Australia and Japan, which have no risk of nuclear proliferation. It will

be better that the country of the head office has an ability to handle radioactive material. The head office will have several functions. One of the functions is to store separated thorium during the refining process of rare-earth mining. The stored thorium can be lent to countries. These countries have to return both thorium and fissionable uranium-233 in the spent thorium fuel to "The Bank". Uranium-233 is produced by absorption of neutron of thorium. Uranium-233 is the interest against the debt of thorium from "The Bank". As far as the capacity of thorium nuclear power in the world is limited by the supply of plutonium from uranium fuel cycle, amount of produced thorium from rare-earth mining is larger than the consumption of thorium as nuclear fuel. Thus, price of thorium will be kept at low level. The other function of "The Bank" is reprocessing of spent thorium fuel. If LWR or HWR are used as power reactor, solid fuel rod including thorium and fissile materials (uranium-233 or plutonium) will be returned. If MSR is used, frozen fuel salt will be returned. For the former case, direct fluorination method called FERDA will be able to apply obtaining plutonium and uranium-233 from solid spent fuel. For the latter case, dry-process method using molten-salt will be available for reprocessing.

The last function of "The Bank" is to fabricate thorium fuel. If countries plan to implement thorium nuclear power, there is a possibility that it is not allowed to have fuel fabricating facility depending on the international discussion. United Arab Emirates (UAE) can be considered as such a case. UAE has signed with the USA in the agreement of nuclear power. UAE implements nuclear power plant but they do not have enrichment and reprocessing facilities. Nuclear fuel will be fed by the USA and spent nuclear fuel will be sent to France or other countries. "The Bank" will have several branch offices. The function of the branch office will just to store and lend thorium.

It is not necessarily request to all the countries to join this frame of "The Bank". Some countries such as India having thorium resource and functions of re-processing and fuel fabrication can continue their own plans. The function of "The Bank" will be attractive to the countries having rare-earth resources but having no plan to utilize thorium. Countries in the South-East Asia such as Vietnam or Myanmar will correspond to this case.

Recently, there are many researches on breeding of uranium-233 from thorium by utilizing accelerator or fusion technologies. However it is estimated to take more than 20 years to be commercialization. Therefore it is necessary to store thorium until such a wide utilization.

## 7. Conclusion

In this chapter, emerging tendency of thorium nuclear power has been introduced. It is impossible to describe all information running in the world at this time. However, outline of thorium utilization could be explained. Though thorium utilization has a very attractive feature, quantitative evaluation will be necessary to make a new energy supply vision in the near future. Implementation strategy of thorium fuel cycle discussed in this chapter will be a help for such a purpose. Several results demonstrated here based on the mass-balance of fissile materials show that thorium nuclear power will be available but still be limited. In spite of this result, it should not be said that thorium nuclear power is not enough. The concept of sustainability contains lots of different aspects. If thorium is not correctly used, it becomes an environmental hazard. However, if thorium is used, it produces clean and safe energy. We learned that present uranium LWR has a possibility of severe accident from Fukushima Daiichi nuclear power plant. However, most countries do not have huge earthquake. Therefore, uranium LWR can be used by enhancing its safety. Thorium fuel



cycle will be introduced with a collaboration of this established uranium fuel cycle which supplies plutonium as fissile material to thorium fuel cycle. Though more detailed scenario for the implementation of thorium fuel cycle will be needed including fuel reprocessing, an international frame work for nuclear safeguard, thorium fuel cycle has an attractive option to provide carbon-free primary energy source.

## 8. References

- Dean, T. (2007). New age nuclear, COSMOS, Vol. 8, pp.40-49
- Garber, K. (2009). Taking Some Risk out of Nuclear Power, *U.S.News & World Report*, Vol. 146, No. 3, pp.70-72
- Howard, M., & Graham, T. (2007). The Lost Chance, *Newsweek*, Feb., pp.63
- Furukawa, K., Lecocq, A., Kato, Y., & Mitachi, K. (1990). Summary report: thorium molten-salt nuclear energy synergetics, *Journal of nuclear science and technology*, Vol. 27, pp.1157-1178
- Furukawa, K., Arakawa, K., Erbay, L. B., Ito Y., Kato Y., Kiyavitskaya H., Lecocq A., Mitachi K., Moir R., Numata H., Pleasant J. P., Sato Y., Shimazu Y., Simonenco V.A., Sood D. D., Urban C., & Yoshioka, R. (2008). A road map for the realization of global-scale thorium breeding fuel cycle by single molten-fluoride flow. *Energy Conversion & Management*, Vol. 49, pp.1832-1848
- Future Summit Report. (2008). *Future Summit 2008*
- Honma, Y. & Shimazu, Y. (2007). Fuel Cycle Study on Pu-Th based Molten Salt Reactors for Sustainable Fuel Supply, *Proceedings of TU2007*, Beijing, China, December 4-6, 2007
- International Atomic Energy Agency. (2005). Thorium fuel cycle - Potential benefits and challenges
- International Energy Agency. (2007). *CO2 Emissions from Fuel Combustion 1971-2005*
- International Energy Agency. (2009). *World energy outlook*
- International Panel on Fissile Materials. (2008). *Global Fissile Material Report 2008*
- Kamei, T. (2008). Evaluation index of sustainable energy supply technique and its analysis, *Proceedings of 2nd international symposium on symbiotic nuclear power systems for 21st century*, Harbin, China, September 8-10, 2008
- Kamei, T., Mitachi, K., Kato Y., & Furukawa K. (2008). A new energy system suitable for the sustainable society: THORIMS-NES - fuels and radio-wastes, *Proceedings of MS8*, Kobe, Japan, October 19-23, 2008
- Kamei, T., Kato Y., Mitachi, K., Shimazu, Y., & Furukawa K. (2009). Thorium molten-salt nuclear energy synergetics for the huge size fission industry, *Proceedings of ANFM 2009*, Pittsburgh, USA, April 12-15, 2009
- Knight, S. (2008). New Power Generation, *The Financial Times*, May 31st, pp.1-7
- Mitachi, K., Yamamoto, T., & Yoshioka, R. (2007). Self-sustaining Core Design for 200 MWe Molten-Salt Reactor with Thorium-Uranium Fuel: FUJI-U3-(0), *Proceedings of TU2007*, Beijing, China, December 4-6, 2007
- Moir, R. W. (2002). Cost of electricity from molten salt reactors (MSR), *Nuclear technology*, Vol. 138, pp.93-95
- Nishikawa, Y. (2010). Thorium and Rare-earth resources, *Annual report of Metal Economics Research Institute*, No. 163
- Peachey, C. (2009). A thought for thorium. *Nuclear engineering international*, SEP., pp.33-34

- Rosental, MW., Haubenreich, PN., & Briggs, RB. (1972). The Develop. Status of Molten-Salt Breeder Reactors, *ORNL-4812*
- Roy, C., & Robertson, C. (1971). Conceptual Design Study of a Single-Fluid Molten-Salt Breeder Reactor, *ORNL-4541*
- Suzuki, T. (2009). Towards Nuclear Disarmament and Non-Proliferation:10 Proposals from Japan, 11.02.2010, Available from [http://a-mad.org/download/A-MAD\\_EN-JPN.pdf](http://a-mad.org/download/A-MAD_EN-JPN.pdf)
- The Japan Automobile Manufacturers Association, Inc. (2009). *World Motor Vehicle Statistics*
- The Ministry of Petroleum and Energy of Norway. (2008). Thorium as an energy source thorium as an energy source - opportunities for Norway, 06.05.2009, Available from <http://www.regjeringen.no/upload/OED/Rapporter/ThoriumReport2008.pdf>
- Uhlir, J., Marecek, M., & Precek, M. (2008). Progress in development of Fluoride volatility reprocessing technology, *Proceedings of ATALANTE 2008*, Montpellier, France, May 18-22, 2008
- USGS. (2009). *Thorium Minerals Yearbook*
- Watanabe, N. (2008). Rare-earth research and development, *AIST Today*, Vol.8, No. 5
- Weinberg, A. (1997). The proto-history of the molten salt system, *Journal of acceleration plasma research*, Vol. 2, pp.23-6

# Thorium Fission and Fission-Fusion Fuel Cycle

Magdi Ragheb

*Department of Nuclear, Plasma and Radiological Engineering*

*University of Illinois at Urbana-Champaign*

*216 Talbot Laboratory, Urbana, Illinois*

*USA*

## 1. Introduction

With the present-day availability of fissile  $U^{235}$  and  $Pu^{239}$ , as well as fusion and accelerator neutron sources, a fresh look at the Thorium- $U^{233}$  fuel cycle is warranted. Thorium, as an unexploited energy resource, is about four times more abundant than uranium in the Earth's crust and presents a more abundant fuel resource as shown in Table 1.

Element	Symbol	Abundance [gms / ton]
Lead	Pb	16
Gallium	Ga	15
<b>Thorium</b>	<b>Th</b>	<b>10</b>
Samarium	Sm	7
Gadolinium	Gd	6
Praseodymium	Pr	6
Boron	B	3
Bromine	Br	3
<b>Uranium</b>	<b>U</b>	<b>2.5</b>
Beryllium	Be	2
Tin	Sn	1.5
Tungsten	W	1
Molybdenum	Mo	1
Mercury	Hg	0.2
Silver	Ag	0.1
<b>Uranium<sup>235</sup></b>	<b>U<sup>235</sup></b>	<b>0.018</b>
Platinum	Pt	0.005
Gold	Au	0.02

Table 1. Relative abundances of some elements in the Earth's crust.

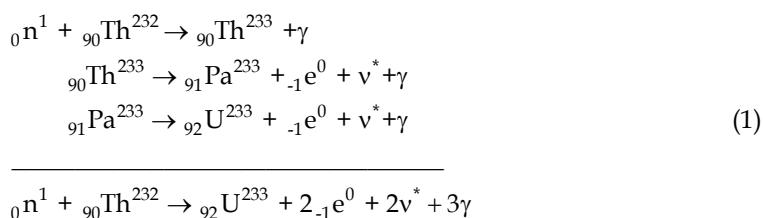


Fig. 1. Thorium dioxide with 1 percent cerium oxide impregnated fabric, Welsbach incandescent gas mantles (left) and ThO<sub>2</sub> flakes (right). Yttrium compounds now substitute for Th in mantles.

## 2. Properties of thorium

Thorium (Th) is named after Thor, the Scandinavian god of war. It occurs in nature in the form of a single isotope: Th<sup>232</sup>. Twelve artificial isotopes are known for Th. It occurs in Thorite, (Th,U)SiO<sub>4</sub> and Thorianite (ThO<sub>2</sub> + UO<sub>2</sub>). It is four times as abundant as uranium and is slightly less abundant than lead.

It can be commercially extracted from the Monazite placer deposit mineral containing 3-22 percent ThO<sub>2</sub> with other rare earth elements or lanthanides. Its large abundance makes it a valuable resource for electrical energy generation with supplies exceeding both coal and uranium combined. This would depend on breeding of the fissile isotope U<sup>233</sup> from thorium according to the breeding reactions:



Together with uranium, its radioactive decay chain leads to the stable Pb<sup>208</sup> lead isotope with a half-life of  $1.4 \times 10^{10}$  years for Th<sup>232</sup>. It contributes to the internal heat generation in the Earth, together with other radioactive elements such as U and K<sup>40</sup>.

As Th<sup>232</sup> decays into the stable Pb<sup>208</sup> isotope, radon<sup>220</sup> or thoron forms in the decay chain. Rn<sup>220</sup> has a low boiling point and exists in gaseous form at room temperature. It poses a radiation hazard through its own daughter nuclei and requires adequate ventilation in underground mining. Radon tests are needed to check for its presence in new homes that are possibly built on rocks like granite or sediments like shale or phosphate rock containing significant amounts of thorium. Adequate ventilation of homes that are over-insulated becomes a design consideration in this case.

Thorium, in the metallic form, can be produced by reduction of ThO<sub>2</sub> using calcium or magnesium. It can also be produced by electrolysis of anhydrous thorium chloride in a fused mixture of Na and K chlorides, by calcium reduction of Th tetrachloride mixed with anhydrous zinc chloride, and by reduction with an alkali metal of Th tetrachloride.

Thorium is the second member of the actinides series in the periodic table of the elements. When pure, it is soft and ductile, can be cold-rolled and drawn and it is a silvery white metal retaining its luster in air for several months. If contaminated by the oxide, it tarnishes in air into a gray then black color oxide (Fig. 1).

Thorium oxide has the highest melting temperature of all the oxides at 3,300 degrees C. Just a few other elements and compounds have a higher melting point such as tungsten and tantalum carbide. Water attacks it slowly, and acids do not attack it except for hydrochloric acid.

Thorium in the powder form is pyrophoric and can burn in air with a bright white light. In portable gas lights the Welsbach mantle is prepared with  $\text{ThO}_2$  with 1 percent cerium oxide and other ingredients (Fig. 1).

As an alloying element in magnesium, it gives high strength and creep resistance at high temperatures.

Tungsten wire and electrodes used in electrical and electronic equipment such as electron guns in x-ray tubes or video screens are coated with Th due to its low work function and associated high electron emission. Its oxide is used to control the grain size of tungsten used in light bulbs and in high temperature laboratory crucibles.

Glasses for lenses in cameras and scientific instruments are doped with Th to give them a high refractive index and low dispersion of light.

In the petroleum industry, it is used as a catalyst in the conversion of ammonia to nitric acid, in oil cracking, and in the production of sulfuric acid.

### 3. Advantages of the thorium fuel cycle

The following advantages of the thorium fuel cycle over the  $\text{U}^{235}\text{-Pu}^{239}$  fuel cycle have been suggested:

1. Breeding is possible in both the thermal and fast parts of the neutron spectrum with a regeneration factor of  $\eta > 2$ .
2. Expanded nuclear fuel resources due to the higher abundance of the fertile  $\text{Th}^{232}$  than  $\text{U}^{238}$ . The USA resources in the state of Idaho are estimated to reach 600,000 tons of 30 percent of Th oxides. The probable reserves amount to 1.5 million tons. There exists about 3,000 tons of already milled thorium in a USA strategic stockpile stored in the state of Nevada.
3. Lower nuclear proliferation concerns due to the reduced limited needs for enrichment of the  $\text{U}^{235}$  isotope that is needed for starting up the fission cycle and can then be later replaced by the bred  $\text{U}^{233}$ . The fission-fusion hybrid totally eliminates that need (Bethe, 1978). An attempted  $\text{U}^{233}$  weapon test is rumored to have evolved into a fizzle because of the presence of the  $\text{U}^{232}$  isotope contaminant concentration and its daughter products could not be reduced to a practical level.
4. A superior system of handling fission product wastes than other nuclear technologies and a much lower production of the long-lived transuranic elements as waste. One ton of natural  $\text{Th}^{232}$ , not requiring enrichment, is needed to power a 1,000 MWe reactor per year compared with about 33 tons of uranium solid fuel to produce the same amount of power. Thorium would be first purified then converted into a fluoride. The same initial fuel loading of one ton/year is discharged primarily as fission products to be disposed of for the fission thorium cycle.
5. Ease of separation of the lower volume and short lived fission products for eventual disposal.

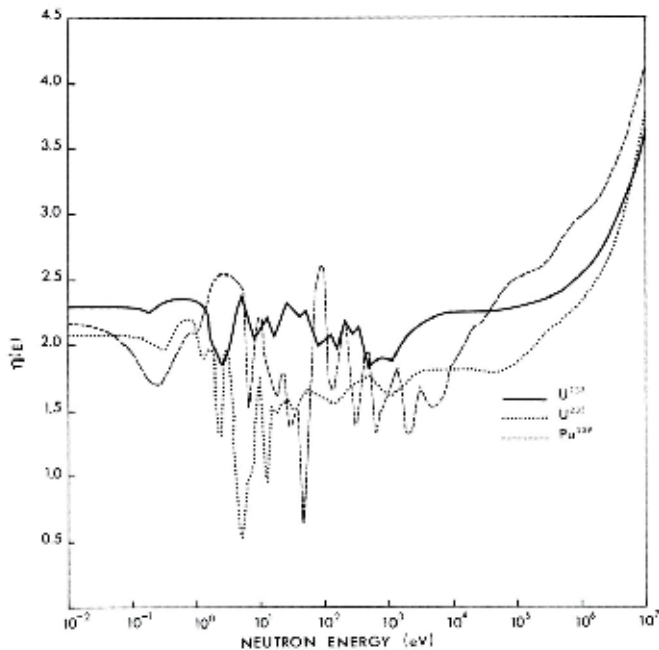


Fig. 2. Regeneration factor as a function of neutron energy for the different fissile isotopes.

6. Higher fuel burnup and fuel utilization than the  $U^{235}$ - $Pu^{239}$  cycle.
7. Enhanced nuclear safety associated with better temperature and void reactivity coefficients and lower excess reactivity in the core. Upon being drained from its reactor vessel, a thorium molten salt would solidify shutting down the chain reaction,
8. With a tailored breeding ratio of unity, a fission thorium fueled reactor can generate its own fuel, after a small amount of fissile fuel is used as an initial loading.
9. The operation at high temperature implies higher thermal efficiency with a Brayton gas turbine cycle (thermal efficiency around 40-50 percent) instead of a Joule or Rankine steam cycle (thermal efficiency around 33 percent), and lower waste heat that can be used for process heat for hydrogen production, sea water desalination or space heating. An open air cooled cycle can be contemplated eliminating the need for cooling water and the associated heat exchange equipment in arid areas of the world (Fig. 3.).
10. A thorium cycle for base-load electrical operation would provide a perfect match to peak-load cycle wind turbines generation. The produced wind energy can be stored as compressed air which would be used to cool a thorium open cycle reactor, substantially increasing its thermal efficiency, yet not requiring a water supply for cooling.
11. The unit powers are scalable over a wide range for different applications such as process heat or electrical production. Small units of 100 MWe of capacity each can be designed, built and combined for larger power needs.
12. Operation at atmospheric pressure for a molten salt as a coolant without pressurization implies the use of standard equipment with a lower cost than the equipment operated at a 1,000-2,000 psi high pressure in the Light Water Reactor (LWRs) cycle. Depressurization would cause the pressurized water coolant to flash into steam and a loss of coolant.

13. In uranium-fuelled thermal reactors, without breeding, only 0.72 percent or 1/139 of the uranium is burned as  $U^{235}$ . If we assume that about 40 percent of the thorium can be converted into  $U^{233}$  then fissioned, this would lead to an energy efficiency ratio of  $139 \times 0.40 = 55.6$  or 5,560 percent more efficient use of the available resource compared with  $U^{235}$ .
14. Operational experience exists from the Molten Salt reactor experiment (MSRE) at Oak Ridge National Laboratory (ORNL), Tennessee. A thorium fluoride salt was not corrosive to the nickel alloy: Hastelloy-N. Corrosion was caused only from tellurium, a fission product (Ragheb et. al., 1980).

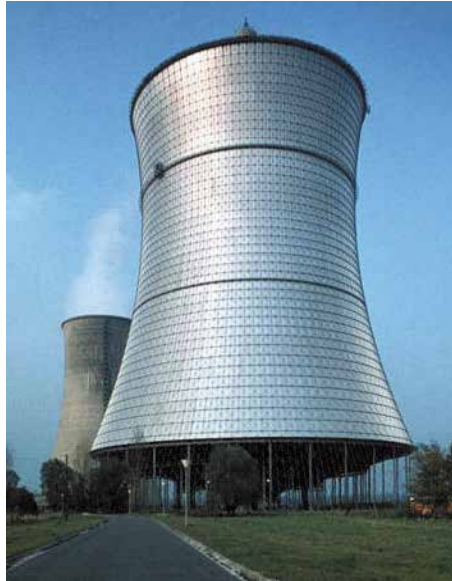


Fig. 3. Dry cooling tower in foreground, wet cooling tower in background in the THTR-300 pebble bed Th reactor, Germany.

Four approaches to a thorium reactor are under consideration:

1. Use of a liquid molten Th fluoride salt,
2. Use of a pebble bed graphite moderated and He gas cooled reactor,
3. The use of a seed and blanket solid fuel with a thermal Light Water Reactor (LWR) cycle,
4. A driven system using fusion or accelerator generated neutrons.

#### 4. Thorium abundance

Thorium is four times as abundant than uranium in the Earth's crust and provides a fertile isotope for breeding of the fissile uranium isotope  $U^{233}$  in a thermal or fast neutron spectrum.

In the Shippingport reactor it was used in the oxide form. In the HTGR it was used in metallic form embedded in graphite. The MSBR used graphite as a moderator and hence was a thermal breeder and a chemically stable fluoride salt, eliminating the need to process or to dispose of fabricated solid fuel elements. The fluid fuel allows the separation of the

stable and radioactive fission products for disposal. It also offers the possibility of burning existing actinides elements and does need an enrichment process like the  $U^{235}$ - $Pu^{239}$  fuel cycle.

Thorium is abundant in the Earth's crust, estimated at 120 trillion tons. The Monazite black sand deposits are composed of 3-22 percent of thorium. It can be extracted from granite rocks and from phosphate rock deposits, rare earths, tin ores, coal and uranium mines tailings.

It has even been suggested that it can be extracted from the ash of coal power plants. A 1,000 MWe coal power plant generates about 13 tons of thorium per year in its ash. Each ton of thorium can in turn generate 1,000 MWe of power in a well optimized thorium reactor. Thus a coal power plant can conceptually fuel 13 thorium plants of its own power. From a different perspective, 1 pound of Th has the energy equivalent of 5,000 tons of coal. There are 31 pounds of Th in 5,000 tons of coal. If the Th were extracted from the coal, it would thus yield 31 times the energy equivalent of the coal.

The calcium sulfate or phospho-gypsum resulting as a waste from phosphorites or phosphate rocks processing into phosphate fertilizer contains substantial amounts of unextracted thorium and uranium.

Uranium mines with brannerite ores generated millions of tons of surface tailings containing thoria and rare earths.

The United States Geological Survey (USGS), as of 2010, estimated that the USA has reserves of 440,000 tons of thorium ore. A large part is located on properties held by Thorium Energy Inc. at Lemhi Pass in Montana and Idaho (Fig. 5). This compares to a previously estimated 160,000 tons for the entire USA.

The next highest global thorium ores estimates are for Australia at 300,000 tons and India with 290,000 tons.

## 5. Thorium primary minerals

Thorium occurs in several minerals:

1. Monazite,  $(Ce,La,Y,Th)PO_4$ , a rare earth-thorium phosphate with 5-5.5 hardness. Its content in Th is 3-22 percent with 14 percent rare earth elements and yttrium. It occurs as a yellowish, reddish-brown to brown, with shades of green, nearly white, yellowish brown and yellow ore. This is the primary source of the world's thorium production. Until World War II, thorium was extracted from Monazite as a primary product for use in products such as camping lamp mantles. After World War II, Monazite has been primarily mined for its rare earth elements content. Thorium was extracted in small amounts and mainly discarded as waste.
2. Thorite,  $(Th,U)SiO_4$  is a thorium-uranium silicate with a 4.5 hardness with yellow, yellow-brown, red-brown, green, and orange to black colors. It shares a 22 percent Th and a 22 percent U content. This ore has been used as a source of uranium, particularly the uranium rich uranothorite, and orangite; an orange colored calcium-rich thorite variety.
3. Brocktite,  $(Ca,Th,Ce)(PO_4)H_2O$ .
4. Xenotime,  $(Y,Th)PO_4$ .
5. Euxenite,  $(Y,Ca,Ce,U,Th)(Nb,Ta,Ti)_2O_6$ .
6. Iron ore, (Fe)-rare earth elements-Th-apatite, Freta deposits at Pea Ridge, Missouri, Mineville, New York, and Scrub Oaks, New Jersey.



Ore	Composition
Thorite	(Th,U)SiO <sub>4</sub>
Thorianite	(ThO <sub>2</sub> + UO <sub>2</sub> )
Thorogummite	Th(SiO <sub>4</sub> ) <sub>1-x</sub> (OH) <sub>4x</sub>
Monazite	(Ce,La,Y,Th)PO <sub>4</sub>
Brocktite	(Ca,Th,Ce)(PO <sub>4</sub> )H <sub>2</sub> O
Xenotime	(Y,Th)PO <sub>4</sub>
Euxenite	(Y,Ca,Ce,U,Th)(Nb,Ta,Ti) <sub>2</sub> O <sub>6</sub>
Iron ore	Fe + rare earths + Th apatite

Table 2. Major Thorium ores compositions.

## 6. Global and USA thorium resources

Estimates of the available Th resources vary widely. The largest known resources of Th occur in the USA followed in order by Australia, India, Canada, South Africa, Brazil, and Malaysia.

Country	ThO <sub>2</sub> Reserves [metric tonnes] USGS estimate 2010	ThO <sub>2</sub> Reserves [metric tonnes] NEA estimate ***	Mined amounts 2007 [metric tonnes]*
USA	440,000	400,000	-**
Australia	300,000	489,000	-
Turkey		344,000	
India	290,000	319,000	5,000
Venezuela		300,000	
Canada	100,000	44,000	-
South Africa	35,000	18,000	-
Brazil	16,000	302,000	1,173
Norway		132,000	
Egypt		100,000	
Russia		75,000	
Greenland		54,000	
Canada		44,000	
Malaysia	4,500		800
Other countries	90,000	33,000	-
Total	1,300,000	2,610,000	6,970

\* Average Th content of 6-8 percent.

\*\* Last mined in 1994.

\*\*\*Reasonably assured and inferred resources available at up to \$80/kg Th.

Table 3. Estimated Global Thorium Resources (Van Gosen et. al., 2009).

The Steenkampskraal Mine in South Africa, located 350 km Northwest of Cape Town was operated by the Anglo American Company as the world's largest producer of Thorium and rare earth elements over the period 1952-1963. It was acquired by the Rare Earth Extraction Company (Rareco).

Concentrated deposits occur as vein deposits, and disseminated deposits occur as massive carbonatite stocks, alkaline intrusions, and black sand placer or alluvial stream and beach deposits.

Carbonatites are rare carbonate igneous rocks formed by magmatic or metasomatic processes. Most of these are composed of 50 percent or higher carbonate minerals such as calcite, dolomite and/or ankerite. They occur near alkaline igneous rocks.

The alkaline igneous rocks, also referred to as alkali rocks, have formed from magmas and fluids so enriched in alkali elements that Na and K bearing minerals form components of the rocks in larger proportion than usual igneous rocks. They are characterized by feldspathoid minerals and/or alkali pyroxenes and amphiboles (Hedrick, 2009).

Deposit type	Mining District	Location	ThO <sub>2</sub> reserves [metric tonnes]
Vein deposits	Lehmi Pass district	Montana-Idaho	64,000
	Wet Mountain area	Colorado	58,200
	Hall Mountain	Idaho	4,150
	Iron Hill	Colorado	1,700 (thorium veins)
			690 (Carbonatite dikes)
	Diamond Creek	Idaho	-
	Bear Lodge Mountains	Wyoming	-
	Monroe Canyon	Utah	-
	Mountain Pass district	California	-
	Quartzite district	Arizona	-
	Cottonwood area	Arizona	-
	Gold Hill district	New Mexico	-
	Capitan Mountain	New Mexico	-
	Laughlin Peak	New Mexico	-
	Wausau, Marathon County	Wisconsin	-
Bokan Mountain	Alaska	-	
Massive Carbonatite stocks	Iron Hill	Colorado	28,200
	Mountain Pass	California	8,850
Black Sand Placer, Alluvial Deposits	Stream deposits	North, South Carolina	4,800
	Stream placers	Idaho	9,130
Alkaline Intrusions	Beach placers	Florida-Georgia	14,700
	Bear Lodge Mountains	Wyoming	-
	Hicks Dome	Illinois	-
Total, USA			194,420

Table 4. Locations of USA major ThO<sub>2</sub> proven reserves (Hedrick, 2009).

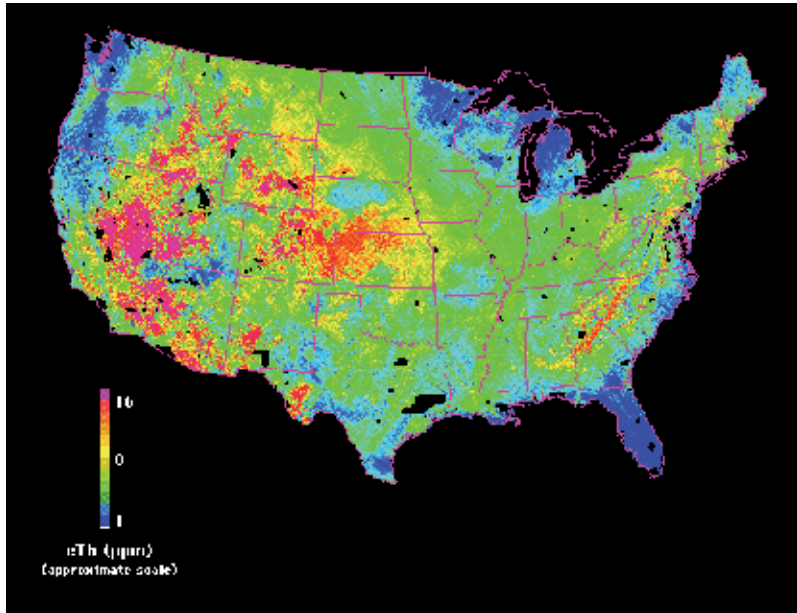


Fig. 4. Th concentrations in ppm and occurrences in the USA. Source: USA Geological Survey Digital Data Series DDS-9, 1993.



Fig. 5. Lehmi Pass is a part of Beaverhead Mountains along the continental divide on the Montana-Idaho border, USA. Its Th veins also contain rare earth elements, particularly Neodymium.



Fig. 6. Black sand Monazite layers in beach sand at Chennai, India. Photo: Mark A. Wilson (Hedrick, 2009).



Fig. 7. Thorite  $(\text{Th, U})\text{SiO}_4$ , a thorium-uranium silicate (Van Gosen, 2009).

## 7. Global and USA uranium resources

Depleting hydrocarbon fuel resources and the growing volatility in fossil fuel prices, have led to an expansion in nuclear power production. The Station Blackout accident, caused by a combined earthquake and tsunami event at the Fukushima Daiichi reactors on March 11, 2011 will lead to a reconsideration of the relative advantages and disadvantages of the existing  $\text{U}^{238}\text{-Pu}^{239}$  fuel cycle against the alternative  $\text{Th}^{232}\text{-U}^{233}$  fuel cycle.

As of 2010, there were 56 nuclear power reactors under construction worldwide, of which 21 are in China. Some are replacing older plants that are being decommissioned, and some are adding new installed capacity. The Chinese nuclear power program is probably the most ambitious in history. It aims at 50 new plants by the year 2025 with an additional 100, if not more, completed by the year 2050. Standardized designs, new technology, a disciplined effort to develop human skills and industrial capacities to produce nuclear power plant components all point to a likely decline in plant construction costs in coming years and growing interest in new nuclear projects with ensuing pressure on nuclear fuels.

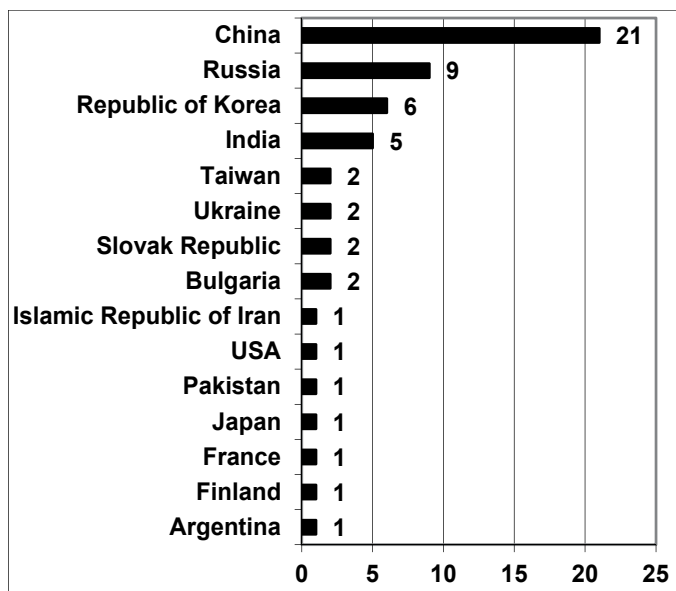


Fig. 8. Number of power reactors under construction worldwide. Total: 56. Net electrical capacity: 51.9 MWe. Data source: IAEA, 2010.

It should be noted that there are currently 150 international reactor projects in some advanced permitting stage. An additional 300 projects are in some early planning stage. Added to a significant fraction of the currently 439 operating power reactors will likely double global nuclear capacity in the coming couple decades (most countries seem willing to try to extend the operating lives of existing reactors through safety-compliant upgrades and retrofits). Building a nuclear power plant practically requires contracting its fuel supply for 40-60 years. When adding all new projects it is reasonable to conclude that fuel requirements could double in the coming couple decades.

About 30 percent of the known recoverable global uranium oxide resources are found in Australia, followed by Kazakhstan (17 percent), Canada (12 percent), South Africa (8 percent), Namibia (6 percent), and Russia, Brazil and the USA, each with about 4 percent of the world production.

The uranium resources are classified into "conventional" and "non-conventional" resources. The conventional resources are further categorized into "Reasonably Assured Resources," RAR and the believed-to-exist "Inferred Resources," IR.

The RAR and IR categories are further subdivided according to the assumed exploitation cost in USA dollars. These cost categories are given as < 40 \$/kg, < 80 \$/kg, and < 130 \$/kg.

The non-conventional resources are split into “Undiscovered Resources,” UR, further separated into “Undiscovered Prognosticated Resources,” UPR with assumed cost ranges of < 80 \$/kg and < 130 \$/kg, and “Undiscovered Speculative Resources” USR.

The USR numbers are given for an estimated exploitation cost of < 130 \$/kg and also for a category with an unknown cost.

In the twentieth century, the USA was the world leading uranium producer until it was surpassed by Canada and Australia. In 2007, Canada accounted for 23 percent and Australia for 21 percent of global production, with the USA at 4 percent. Africa is becoming a new frontier in uranium production with Namibia 7 percent, Niger 8 percent, and South Africa 1 percent. Exploration and new mine development is ongoing in Botswana, Tanzania, Jordan and Nigeria.

The federal, provincial and local governments in Australia have all unilaterally and forcefully banned the development of any new uranium mines, even though existing mines continue operation. The French company Areva was not successful in receiving approval to build a new uranium mine in Australia. It has mining activities in the Niger Republic and received exploration licenses in other countries such as Jordan.

Canadian producer Cameco rates as the first world producer of uranium oxide, followed by French Areva, and then Energy Resources of Australia (68 percent owned by Rio Tinto), which produces some 6,000 tons per year.

As of 2007, five operating uranium mines existed in the USA, with 3 in Texas, one in Wyoming and one in Northern Nebraska. The state of Texas has a positive attitude towards uranium mining, and energy production in general, with an advantageous regulatory framework that streamlines the permit process using in situ leaching of uranium. Texas, being an “Agreement State,” implies that the USA Nuclear Regulatory Commission (NRC) has delegated its authority to the state regulatory agencies such as the Texas Commission on Environmental Quality (TCEQ), and companies deal directly with the state agencies in Texas rather than with the federal government’s NRC. Most of the uranium mining operations in the USA and Kazakhstan use in situ leach methods, also designated as In Situ Recovery (ISR) methods. Conventional methods are used in 62 percent of U mining, with 28 percent as ISR and 9 percent as byproduct extraction.

By 2008, U production in the USA fell 15 percent to 1,780 tonnes  $U_3O_8$ . The U production in the USA is currently from one mill at White Mesa, Utah, and from 6 ISR operations. In 2007, four operating mines existed in the Colorado Plateau area: Topaz, Pandora, West Sunday and Sunday-St. Jude. Two old mines reopened in 2008: Rim Canyon and Beaver Shaft and the Van 4 mine came into production in 2009.

As of 2010, Cameco Resources operated two ISL operations: Smith Ranch-Highland Mine in Wyoming and Cross Butte Mine in Nebraska, with reserves of 15,000 tonnes  $U_3O_8$ . The Denison Mines Company produced 791,000 tonnes of  $U_3O_8$  in 2008 at its 200 t/day White Mesa mill in Southern Utah from its own and purchased ore, as well as toll milling.

Uranium in the Colorado Plateau in the USA has an average grade of 0.25 percent or 2,500 ppm uranium in addition to 1.7 percent vanadium within the Uravan Mineral Belt.

Goliad County, Texas has an average grade of 0.076 percent (760 ppm) uranium oxide in sandstone deposits permeated by groundwater suggesting in situ leaching methods where water treated with carbon dioxide is injected into the deposit. The leachate is pumped and passed over ion exchange resins to extract the dissolved uranium.

Country	Production [tonnes U]	Share of world production [percent]	Main owner	Extraction method	Mine
Canada	6,383	15	Cameco	Conv	McArthur River
Australia	4,527	10	Rio Tinto	Conv	Ranger
Namibia	3,449	8	Rio Tinto	Conv	Rössing
Australia	3,344	8	BHP Billiton	Byproduct	Olympic Dam
Russia	3,050	7	ARMZ	Conv	Priargunskiy
Niger	1,743	4	Areva	Conv	Somair
Canada	1,368	3	Cameco	Conv	Rabbit Lake
Niger	1,289	3	Areva	Conv	Cominak
Canada	1,249	3	Areva	Conv	McLean
Kazakhstan	1,034	2	Uranium One	ISR	Akdata
Total	27,436	62			

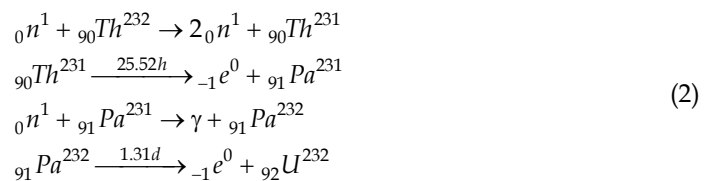
Table 5. World main producing uranium mines, 2008. Source: World Nuclear Association, WNA.

Phosphate rocks containing just 120 ppm in U have been used as a source of uranium in the USA. The fertilizer industry produces large quantities of wet process phosphoric acid solution containing 0.1-0.2 gram/liter (g/l) of uranium, which represent a significant potential source of uranium.

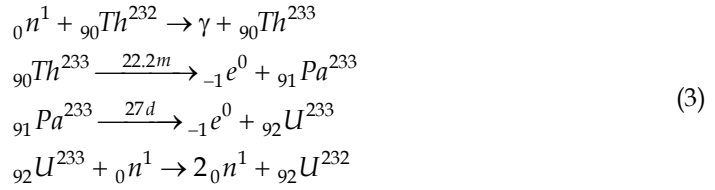
## 8. Nonproliferation characteristics

In the Th-U<sup>233</sup> fuel cycle, the hard gamma rays associated with the decay chain of the formed isotope U<sup>232</sup> with a half life of 72 years and its spontaneous fission makes the U<sup>233</sup> in the thorium cycle with high fuel burnup a higher radiation hazard from the perspective of proliferation than Pu<sup>239</sup>.

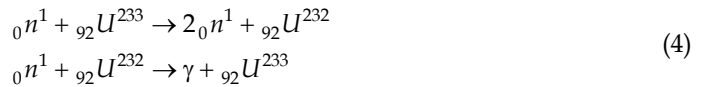
The U<sup>232</sup> is formed from the fertile Th<sup>232</sup> from two paths involving an (n, 2n) reaction, which incidentally makes Th<sup>232</sup> a good neutron multiplier in a fast neutron spectrum:



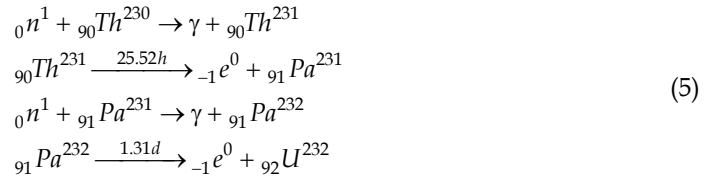
and another involving an (n,  $\gamma$ ) radiative capture reaction:



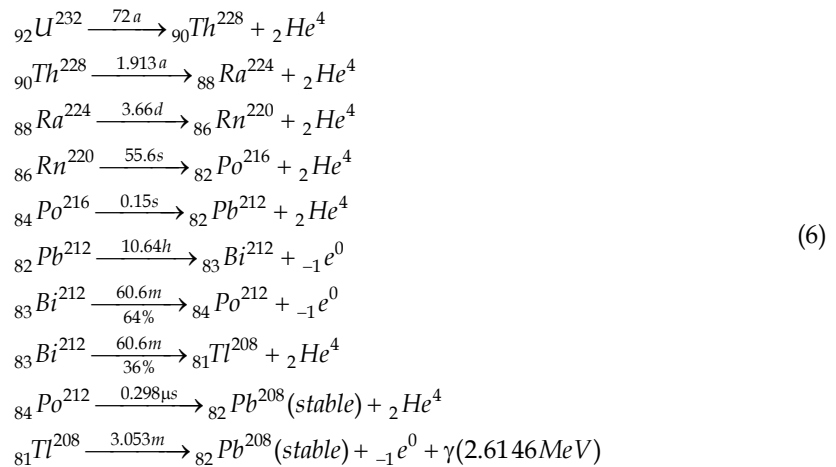
The isotope  $\text{U}^{232}$  is also formed from a reversible (n, 2n) and (n,  $\gamma$ ) path acting on the bred  $\text{U}^{233}$ :



The isotope  $\text{Th}^{230}$  occurs in trace quantities in thorium ores that are mixtures of uranium and thorium.  $\text{U}^{234}$  is a decay product of  $\text{U}^{238}$  and it decays into  $\text{Th}^{230}$  that becomes mixed with the naturally abundant  $\text{Th}^{232}$ . It occurs in secular equilibrium in the decay chain of natural uranium at a concentration of 17 ppm. The isotope  $\text{U}^{232}$  can thus also be produced from two successive neutron captures in  $\text{Th}^{230}$ :

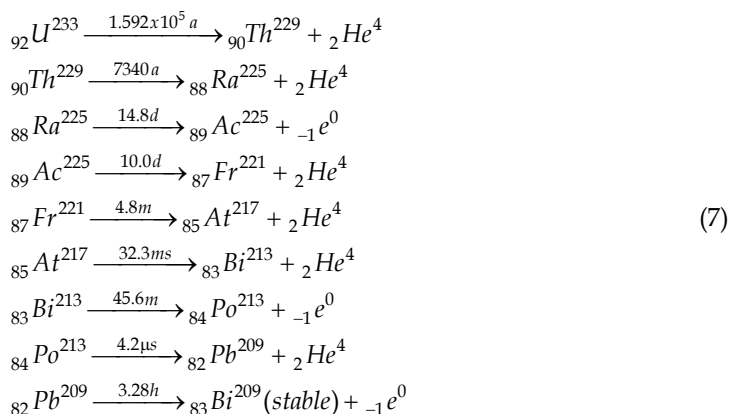


The hard 2.6 MeV gamma rays originate from  $\text{Tl}^{208}$  isotope in the decay chain of aged  $\text{U}^{232}$  which eventually decays into the stable  $\text{Pb}^{208}$  isotope:



As comparison, the  $\text{U}^{233}$  decay chain eventually decays into the stable  $\text{Bi}^{209}$  isotope:





A 5-10 proportion of  $\text{U}^{232}$  in the  $\text{U}^{232}$ - $\text{U}^{233}$  mixture has a radiation equivalent dose rate of about 1,000 cSv (rem)/hr at a 1 meter distance for decades making it a highly proliferation resistant cycle if the  $\text{Pa}^{233}$  is not separately extracted and allowed to decay into pure  $\text{U}^{233}$ .

The  $\text{Pa}^{233}$  cannot be chemically separated from the  $\text{U}^{232}$  if the design forces the fuel to be exposed to the neutron flux without a separate blanket region, making the design fail-safe with respect to proliferation and if a breeding ratio of unity is incorporated in the design.

Such high radiation exposures would lead to incapacitation within 1-2 hours and death within 1-2 days of any potential proliferators.

The International Atomic Energy Agency (IAEA) criterion for fuel self protection is a lower dose equivalent rate of 100 cSv (rem)/hr at a 1 meter distance. Its denaturing requirement for  $\text{U}^{235}$  is 20 percent, for  $\text{U}^{233}$  with  $\text{U}^{238}$  it is 12 percent, and for  $\text{U}^{233}$  denaturing with  $\text{U}^{232}$  it is 1 percent.

The Indian Department of Atomic Energy (DAE) had plans on cleaning  $\text{U}^{233}$  down to a few ppm of  $\text{U}^{232}$  using Laser Isotopic Separation (LIS) to reduce the dose to the occupational workers.

The contamination of  $\text{U}^{233}$  by the  $\text{U}^{232}$  isotope is mirrored by another introduced problem from the generation of  $\text{U}^{232}$  in the recycling of  $\text{Th}^{232}$  due to the presence of the highly radioactive  $\text{Th}^{228}$  from the decay chain of  $\text{U}^{232}$ .

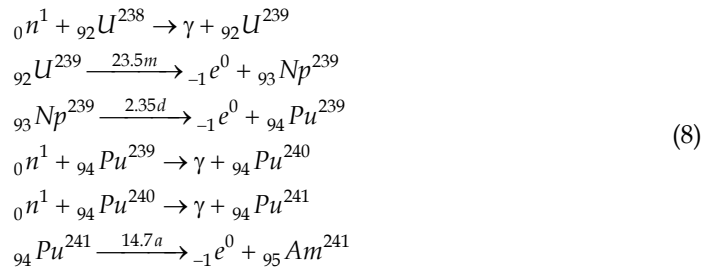
## 9. Radiation dosimetry

The International Atomic Energy Agency (IAEA) criterion for occupational protection is an effective dose of 100 cSv (rem)/hr at a 1 meter distance from the radiation source.

It is the decay product  $\text{Tl}^{208}$  in the decay chain of  $\text{U}^{232}$  and not  $\text{U}^{232}$  itself that generates the hard gamma rays. The  $\text{Tl}^{208}$  would appear in aged  $\text{U}^{233}$  over time after separation, emitting a hard 2.6416 MeV gamma ray photon. It accounts for 85 percent of the total effective dose 2 years after separation. This implies that manufacturing of  $\text{U}^{233}$  should be undertaken in freshly purified  $\text{U}^{233}$ . Aged  $\text{U}^{233}$  would require heavy shielding against gamma radiation.

In comparison, in the U-Pu<sup>239</sup> fuel cycle, Pu<sup>239</sup> containing Pu<sup>241</sup> with a half life of 14.4 years, the most important source of gamma ray radiation is from the Am<sup>241</sup> isotope with a 433 years half life that emits low energy gamma rays of less than 0.1 MeV in energy. For weapons grade Pu<sup>239</sup> with about 0.36 percent Pu<sup>241</sup> this does not present a major hazard but the radiological hazard becomes significant for reactor grade Pu<sup>239</sup> containing about 9-10 percent Pu<sup>241</sup>.

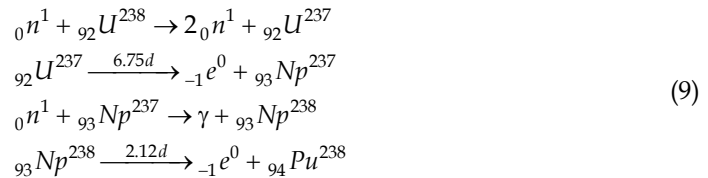
The generation of  $\text{Pu}^{241}$  as well as  $\text{Pu}^{240}$  and  $\text{Am}^{241}$  from  $\text{U}^{238}$  follows the following path:



Plutonium containing less than 6 percent  $\text{Pu}^{240}$  is considered as weapons-grade.

The gamma rays from  $\text{Am}^{241}$  are easily shielded against with Pb shielding. Shielding against the neutrons from the spontaneous fissions in the even numbered  $\text{Pu}^{238}$  and  $\text{Pu}^{240}$  isotopes accumulated in reactor grade plutonium requires the additional use of a thick layer of a neutron moderator containing hydrogen such as paraffin or plastic, followed by a layer of neutron absorbing material and then additional shielding against the gamma rays generated from the neutron captures.

The generation of  $\text{Pu}^{238}$  and  $\text{Np}^{237}$  by way of (n, 2n) rather than (n,  $\gamma$ ) reactions, follows the path:



The production of  $\text{Pu}^{238}$  for radioisotopic heat and electric sources for space applications follows the path of chemically separating  $\text{Np}^{237}$  from spent LightWater Reactors (LWRs) fuel and then neutron irradiating it to produce  $\text{Pu}^{238}$ .

Isotopic composition [percent]	$\text{Pu}^{239}$ weapons grade	$\text{Pu}^{239}$ reactors grade	$\text{U}^{233}$	$\text{U}^{233} + 1$ ppm $\text{U}^{232}$
$\text{U}^{232}$			0.0000	0.0001
$\text{U}^{233}$			100.0000	99.9999
$\text{Pu}^{238}$	0.0100	1.3000		
$\text{Pu}^{239}$	93.8000	60.3000		
$\text{Pu}^{240}$	5.8000	24.3000		
$\text{Pu}^{241}$	0.3500	9.1000		
$\text{Pu}^{242}$	0.0200	5.0000		
Density [gm/cm <sup>3</sup> ]	19.86	19.86	19.05	19.05
Radius [cm]	3.92	3.92	3.96	3.96
Weight [kg]	5	5	5	5

Table 6. Typical compositions of fuels in the uranium and thorium fuel cycles (Kang, von Hippel, 2001).

Fuel, U <sup>232</sup> /U <sup>233</sup>	Time to 5 cSv effective dose [hr]	Effective dose rate cSv/hr
0.01	0.039	127.0000
100 ppm	3.937	1.2700
5 ppm	84.746	0.0590
1 ppm	384.615	0.0130
Reactor grade Pu <sup>239</sup>	609.756	0.0082
Weapons grade Pu <sup>239</sup>	3846.154	0.0013

Table 7. Glove box operation dose rate required to accumulate a limiting occupational 5 cSv (rem) dose equivalent from a 5 kg metal sphere, one year after separation at a 1/2 meter distance(Kang, von Hippel, 2001).

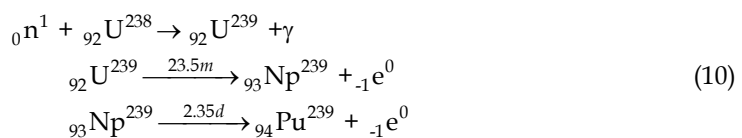
Both reactor-grade plutonium and U<sup>233</sup> with U<sup>232</sup> would pose a significant radiation dose equivalent hazard for manufacturing personnel as well as military personnel, which precludes their use in weapons manufacture in favor of enriched U<sup>235</sup> and weapons-grade Pu<sup>239</sup>.

Material	Type of radiation	Dose equivalent rate at time after separation [cSv(rem)/hr]				
		0 yr	1 yr	5 yr	10 yr	15 yr
Pure U <sup>233</sup>	γ total	0.32	0.42	0.84	1.35	1.89
U <sup>233</sup> +1 ppm U <sup>232</sup>	γ total	0.32	13.08	35.10	39.57	39.17
	γ from Tl <sup>208</sup>	0.00	11.12	29.96	33.48	32.64
Pu <sup>239</sup> , weapons grade	γ	0.49	0.71	1.16	1.57	1.84
	neutrons	0.56	0.56	0.56	0.56	0.56
	γ + neutron	1.05	1.27	1.72	2.13	2.40
Pu <sup>239</sup> , Reactor grade	γ total	0.49	5.54	16.72	28.64	37.54
	γ from Am <sup>241</sup>	0.00	3.24	14.60	26.00	34.80
	neutrons	2.66	2.66	2.65	2.64	2.63
	γ + neutrons	3.15	8.20	19.37	31.28	40.17

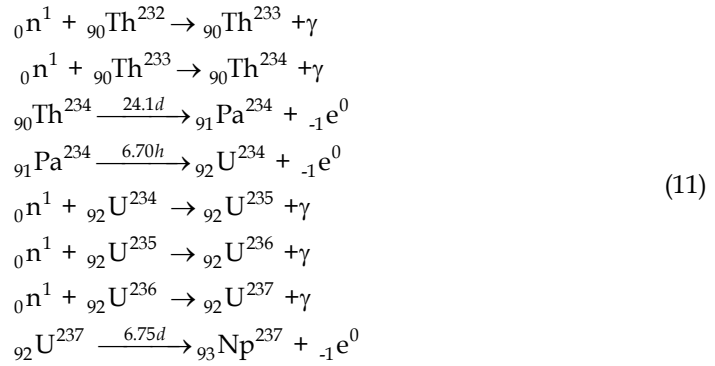
Table 8. Dose equivalent rates in cSv (rem)/hr from 5 kg metal spheres at a 1/2 meter distance for different times after separation (Kang, von Hippel, 2001).

### 10. Actinides production, waste disposal Issues

There has been a new interest in the Th cycle in Europe and the USA since it can be used to increase the achievable fuel burnup in LWRs in a once through fuel cycle while significantly reducing the transuranic elements in the spent fuel. A nonproliferation as well as transuranics waste disposal consideration is that just a single neutron capture reaction in U<sup>238</sup> is needed to produce Pu<sup>239</sup> from U<sup>238</sup>:

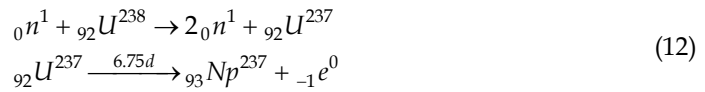


whereas a more difficult process of fully 5 successive neutron captures are needed to produce the transuranic  $\text{Np}^{237}$  from  $\text{Th}^{232}$ :

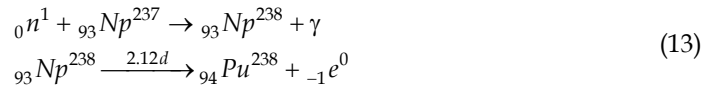


This implies a low yield of  $\text{Np}^{237}$  however, as an odd numbered mass number isotope posing a possible proliferation concern; whatever small quantities of it are produced, provisions must be provided in the design to have it promptly recycled back for burning in the fast neutron spectrum of the fusion part of the hybrid.

In fact, it is more prominently produced in thermal fission light water reactors using the uranium cycle and would be produced; and burned, in fast fission reactors through the (n, 2n) reaction channel with  $\text{U}^{238}$  according to the much simpler path:



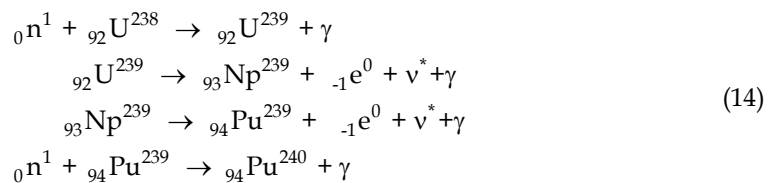
The  $\text{Np}^{237}$  gets transmuted in the  $\text{Th}^{232}$  fuel cycle into  $\text{Pu}^{238}$  with a short half-life of 87.74 years:



A typical 1,000 MWe Light Water Reactor (LWR) operating at an 80 percent capacity factor produces about 13 kgs of  $\text{Np}^{237}$  per year.

This has led to suggested designs where  $\text{Th}^{232}$  replaces  $\text{U}^{238}$  in LWRs fuel and accelerator driven fast neutron subcritical reactors that would breed  $\text{U}^{233}$  from  $\text{Th}^{232}$ .

Incidentally, whereas the  $\text{Pu}^{238}$  isotope is produced in the Th fuel cycle, it is the  $\text{Pu}^{240}$  isotope with a longer 6,537 years half-life, that is produced in the U-Pu fuel cycle:



## 11. Thorium fission-hybrid fuel cycle

The thorium fusion fission hybrid is discussed as a sustainable longer term larger resource base to the fast breeder fission reactor concept. In addition, it offers a manageable waste disposal process, burning of the produced actinides and serious nonproliferation characteristics.

With the present day availability of fissile  $U^{235}$  and  $Pu^{239}$ , and available fusion and accelerator neutron sources, a new look at the thorium- $U^{233}$  fuel cycle is warranted. Since no more than 7 percent of the  $ThO_2$  as a breeding seed fuel can be added to a Heavy Water Reactor, HWR before criticality would not be achievable; this suggests that fusion and accelerator sources are the appropriate alternative for the implementation of the Thorium fuel cycle.

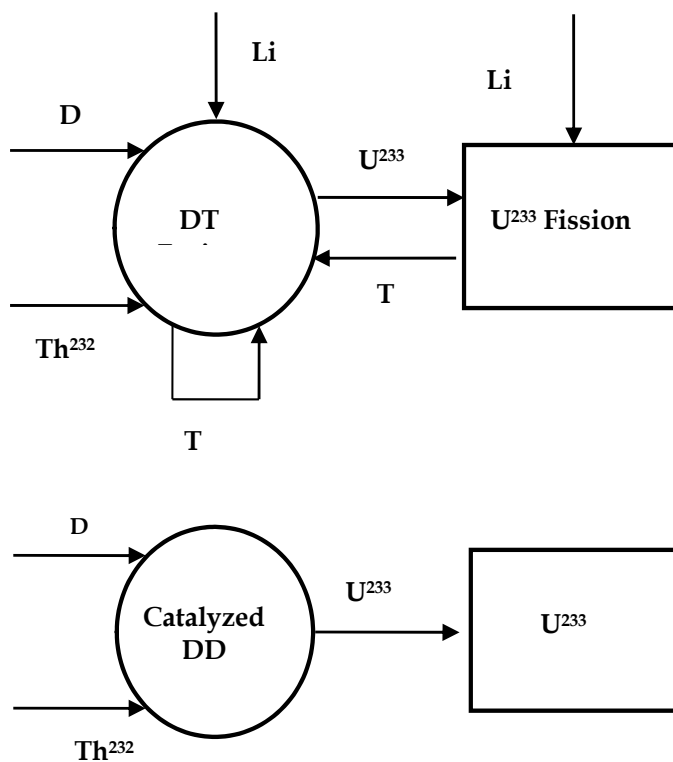
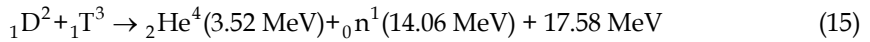


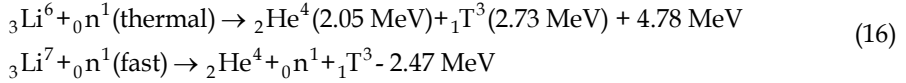
Fig. 9. Material flows in the DT (top) and Catalyzed DD fusion-fission hybrid (bottom) alternatives with  $U^{233}$  breeding from  $Th^{232}$ . The Catalyzed DD approach does not contain the Li and T paths (Ragheb, 1981).

The use of the thorium cycle in a fusion fission hybrid could bypass the stage of fourth generation breeder reactors in that the energy multiplication in the fission part allows the satisfaction of energy breakeven and the Lawson condition in magnetic and inertial fusion reactor designs. This allows for the incremental development of the technology for the eventual introduction of a pure fusion technology.

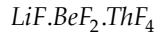
For an immediate application of the fusion hybrid using the Th cycle, the DT fusion fuel cycle can be used:



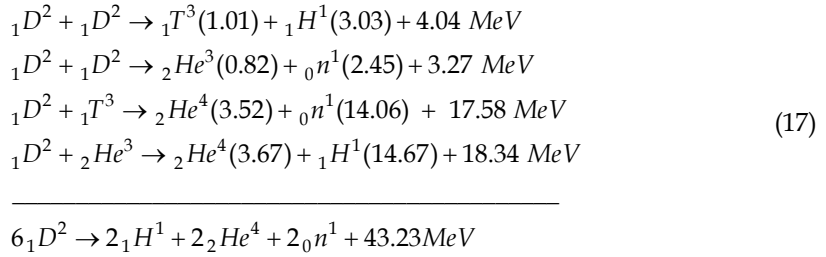
The tritium would have to be bred from the abundant supplies of lithium using the reactions with its two isotopes:



In this case a molten salt containing Li for tritium breeding as well as Th for  $U^{233}$  breeding can be envisioned:

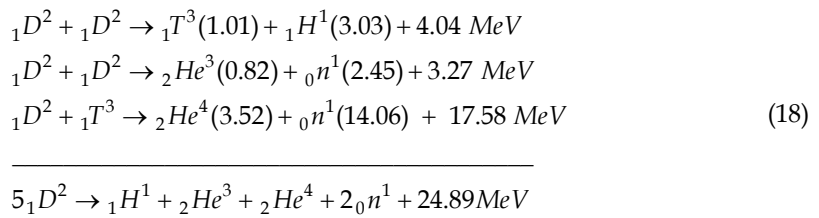


For a practically unlimited supply of deuterium from water at a deuterium to hydrogen ratio of D/H = 150 ppm in the world oceans, one can envision the use of the catalyzed DD reaction in the fusion island:

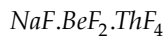


with each of the six deuterons contributing an energy release of  $43.23 / 6 = 7.205 \text{ MeV}$ .

For plasma kinetic reactions temperatures below 50 keV, the  $DHe^3$  reaction is not significant and the energy release would be  $43.23 - 18.34 = 24.89$  with each of the five deuterons contributing an energy release of  $24.89/5 = 4.978 \text{ MeV}$ .



In this case, there would be no need to breed tritium, and the lithium can be replaced by Na in a molten salt with the following composition:



With a density and percentage molecular composition of:

$$\rho = 4.52 \frac{gm}{cm^3}, (71 - 2 - 27 \text{ mol}\%)$$

## 12. Fission-fusion hybrid molten salt breeder

A system consisting of fusion fuel factories using DT or Catalyzed DD fusion and fission satellites receiving the bred fissile fuel for burning is shown in Fig. 9.

A one dimensional calculational model considers a plasma cavity with a 150 cm radius. The plasma neutron source is uniformly distributed in the central 100 cm radial zone and is isolated from the first structural wall by a 50 cm vacuum zone.

The blanket module consists of a 1 cm thick Type 316 stainless steel first structural wall that is cooled by a 0.5 cm thick water channel, a 42 cm thick molten salt filled energy absorbing and breeding compartment, and a 40 cm thick graphite neutron reflector.

The molten salt and graphite are contained within 1 cm thick Type 316 stainless steel structural shells

Computations were conducted using the one dimensional Discrete Ordinates transport ANISN code with a  $P_3$  Legendre expansion and an  $S_{12}$  angular quadrature.

The catalyzed DD system exhibits a fissile nuclide production rate of 0.880  $\text{Th}(n, \gamma)$  reactions per fusion source neutron. The DT system, in addition to breeding tritium from lithium for the DT reaction yields 0.737  $\text{Th}(n, \gamma)$  breeding reactions per fusion source neutron.

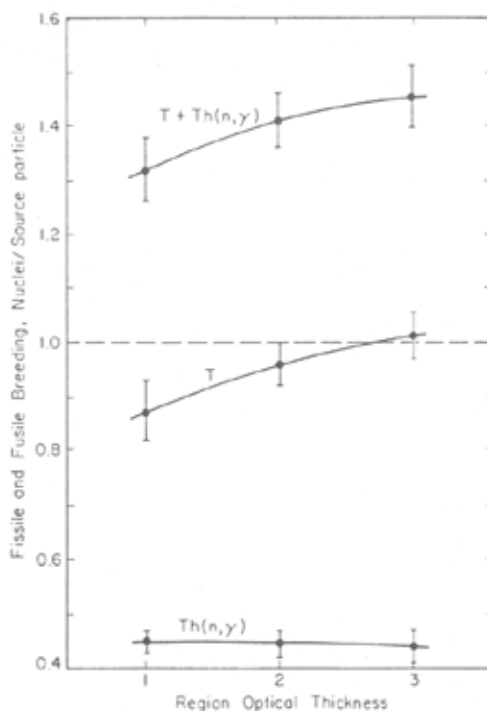


Fig. 10. Optimization of fissile  $\text{U}^{233}$  and fusile tritium (T) breeding.

Even though both approaches provide substantial energy amplification through the fusion-fission coupling process, the DT system possesses marginal tritium breeding in the fusion island of 0.467 triton per source neutron and would need supplemental breeding in the fission satellites to reach a value of unity.

The largest  $\text{Th}(n,\gamma)$  reaction rate (0.966) occurs when the sodium salt is used in conjunction with the DT reaction. For this case, however, the tritium required to fuel the plasma must be supplied to the system, since that produced in the blanket would be negligible ( $3.18 \times 10^{-3}$ ). A system of such kind has been proposed and studied by Blinken and Novikov.

A catalyzed or semi-catalyzed DD fusion cycle will not need tritium breeding. Both the DT and Catalyzed DD approaches provide substantial energy amplification through the fusion-fission coupling process. However, the DT system possesses marginal tritium breeding in the fusion island and would need supplemental breeding in the fission satellites to reach a value of the tritium breeding ratio unity.

As a first generation cycle, a DT fusion cycle needs serious consideration of its tritium breeding potential. Enhancement of the fusile breeding would require the use of neutron multipliers and optimized flux trap geometrical configurations.

### 13. Discussion

Thorium supplies constitute a yet unused energy resource (Taylor, 1964). They occur primarily in the rare earth ore mineral Monazite and the thorium mineral thorite. The size of the global resource is estimated at  $1.3 \times 10^6$  metric tonnes of  $\text{ThO}_2$ . The USA and Australia hold the world's largest known reserves with uncertain estimates ranging from  $0.19 \times 10^6$  –  $0.44 \times 10^6$  metric tonnes of  $\text{ThO}_2$ . Many of the USA reserves sizes are not known, as a result of unavailable data for lack of economical extraction attractiveness without an energy use option for thorium.

The main international rare earths processors presently opt to process only thorium-free feed materials to avoid its radioactive content, even though they still have to cope with the radioactive isotope  $\text{Ce}^{142}$  which occurs in cerium. This has been negative for the low-cost monazite ores and other thorium bearing ores. This could change in the future if thorium is adopted as a byproduct for energy use. Supplies of rare earth elements are globally available in the international trade pipeline from diverse sources without discerned immediate shortages or bottlenecks.

Thorium occurs associated with uranium in some ores such as Thorite  $(\text{Th,U})\text{SiO}_4$  and, if exploited, would help expand the known U resource base.

Other ores are associated with rare earth elements or lanthanides such as monazite  $(\text{Ce, La, Y, Th})\text{PO}_4$  which also contain other economically significant metal occurrences such as yttrium. In this case, Th as a fuel resource could be extracted for future energy applications as a byproduct of the other more important rare earth elements extraction process until such time when primary Th ores such as thorite and monazite would be exploited.

Four approaches to a thorium reactor are under consideration:

1. Use of a liquid molten Th fluoride salt,
2. Use of a pebble bed graphite moderated and He gas cooled reactor,
3. The use of a seed and blanket solid fuel with a Light Water Reactor (LWR) cycle,
4. A driven system using fusion or accelerator generated neutrons.

A concern is the potential risks to sustained economical development and of conflicts, both domestic and international, over the distribution of ever scarcer and more expensive resources. A pessimistic view maintains that the available resources cannot keep up with population and income growth, resulting in poverty and conflict for access to them. The optimistic view is that the market incentives will spur the birth of new approaches and solutions. The flaring of the first and second Gulf Wars had an element of the control of the



Middle Eastern petroleum resources. Earlier, an oil embargo of Japan by the USA was followed two months later by the attack on Pearl Harbor.

The sober way to deal with temporary resource shortages is to wait long enough for the price increases to encourage the development of new resources and/or substitutes.

The Station Blackout accident, caused by a combined earthquake and tsunami event at the Fukushima Daiichi reactors on March 11, 2011 will lead to a reconsideration of the relative advantages and disadvantages of the existing  $U^{238}$ - $Pu^{239}$  fuel cycle against the alternative  $Th^{232}$ - $U^{233}$  fuel cycle.

## 14. References

- H. A. Bethe, "The Fusion Hybrid," *Nucl. News*, Vol. 21, 7, 41, May 1978.
- S. S. Rozhkov and G. E. Shatalov, "Thorium in the Blanket of a Hybrid Thermonuclear Reactor," *Proc. U.S.-USSR Symp. Fusion-Fission Reactors*, July 13-16, 1976, CONF-760733, p. 143, 1976.
- V. L. Blinkin and V. M. Novikov, "Symbiotic System of a Fusion and Fission Reactor with Very Simple Fuel Reprocessing," *Nucl. Fusion*, Vol. 18, 7, 1978.
- Jungmin Kang and Frank N. von Hippel, "U-232 and the Proliferation Resistance of U-233 in Spent Fuel," *Science and Global Security*, Volume 9, pp. 1-32, 2001.
- M. M. H. Ragheb, R. T. Santoro, J. M. Barnes, and M. J. Saltmarsh, "Nuclear Performance of Molten Salt Fusion-Fission Symbiotic Systems for Catalyzed Deuterium and Deuterium-Tritium Reactors," *Nuclear Technology*, Vol. 48, pp. 216-232, May 1980.
- M. Ragheb, "Optimized Fissile and Fusile Breeding in a Laser-Fusion Fissile-Enrichment Flux Trap Blanket," *Journal of Fusion Energy*, Vol. 1, No.1, pp.285-298, 1981.
- M. M. H. Ragheb, G. A. Moses, and C. W. Maynard, "Pellet and Pellet-Blanket neutronics and Photonics for Electron Beam Fusion," *Nucl. Technol.*, Vol. 48:16, April 1980.
- M. Ragheb and S. Behtash, "Symbiosis of Coupled Systems of Fusion D-3He Satellites and Tritium and He3 Generators," *Nuclear Science and Engineering*, Vol. 88, pp. 16-36, 1984.
- M. Ragheb and C. W. Maynard, "On a Nonproliferation Aspect of the Presence of U232 in the U233 fuel cycle," *Atomkernenergie*, 1979.
- M. M. H. Ragheb, M. Z. Youssef, S. I. Abdel-Khalik, and C. W. Maynard, "Three-Dimensional Lattice Calculations for a Laser-Fusion Fissile Enrichment Fuel Factory," *Trans. Am. Nucl. Soc.*, Vol. 30, 59, 1978.
- M. M. H. Ragheb, S. I. Abdel-Khalik, M. Youssef, and C. W. Maynard, "Lattice Calculations and Three-Dimensional Effects in a Laser Fusion-Fission Reactor," *Nucl. Technol.* Vol. 45, 140, 1979.
- J. A. Maniscalco, L. F. Hansen, and W. O. Allen, "Scoping Studies of U233 breeding fusion fission hybrid," UCRL-80585, Lawrence Livermore Laboratory, 1978.
- L. M. Lidsky, "Fission-fusion Systems: Hybrid, Symbiotic and Auegan," *Nucl. Fusion*, Vol. 15, 1975.
- J. D. Lee, "The Beryllium/molten salt blanket-a new concept," UCRL-80585, Lawrence Livermore Laboratory, 1979.
- M. M. H. Ragheb and C. W. Maynard, "Three-dimensional cell calculations for a fusion reactor gas-cooled solid blanket," *Atomkernenergie (ATKE)* Bd. 32, Lfg. 3, 159, 1978.

- James B. Hedrick, "Thorium in the United States," "1st Thorium Energy Alliance Conference, The Future Thorium Energy Economy," Kellogg Conference Center, Gallaudet University, Washington D. C. 2002-3695, USA, October 19-20, 2009.
- Robert Hargraves, "Aim High," "1st Thorium Energy Alliance Conference, The Future Thorium Energy Economy," Kellogg Conference Center, Gallaudet University, Washington D. C. 2002-3695, USA, October 19-20, 2009.
- Bradley S. Van Gosen, Virginia S. Gillerman and Theodore J. Armbrustmacher, "Thorium Resources of the United States-Energy Resources for the Future?" Circular 1336, USA Geological Survey, USGS, Reston, Virginia, 2009.
- Magdi Ragheb, "Nuclear Age Elements," in: "Nuclear, Plasma and Radiation Science, Inventing the Future," <https://netfiles.uiuc.edu/mragheb/www>, 2010.
- Magdi Ragheb, "Uranium Resources in Phosphate Rocks," in: "Nuclear, Plasma and Radiation Science, Inventing the Future," <https://netfiles.uiuc.edu/mragheb/www>, 2010.
- WNA, World Nuclear Association, "Thorium," <http://www.world-nuclear.org/info/inf62.html>, 2009.
- James B. Hedrick, "2007 Minerals Yearbook," USGS, September 2009.
- Jungmin Kang and Frank N. von Hippel, "U-232 and the Proliferation Resistance of U-233 in Spent Fuel," *Science and Global Security*, Volume 9, pp. 1-32, 2001.
- Magdi Ragheb, "The Global Status of Nuclear Power," in: "Nuclear, Plasma and Radiation Science, Inventing the Future," <https://netfiles.uiuc.edu/mragheb/www>, 2010.
- S. R. Taylor, "Abundances of Chemical Elements in the Continental Crust: a New Table," *Geochim. Cosmochim. Acta*, 28, 1273, 1964.

# New Sustainable Secure Nuclear Industry Based on Thorium Molten-Salt Nuclear Energy Synergetics (THORIMS-NES)

Kazuo Furukawa<sup>1</sup>, Eduardo D. Greaves<sup>2</sup>, L. Berrin Erbay<sup>3</sup>,

Miloslav Hron<sup>4</sup> and Yoshio Kato<sup>5</sup>

<sup>1</sup>*Thorium Tech Solution Inc.,*

<sup>2</sup>*Universidad Simón Bolívar, Caracas,*

<sup>3</sup>*Eskişehir Osmangazi University,*

<sup>4</sup>*Nuclear research Institute Retz,*

<sup>5</sup>*International Thorium Molten-Salt Forum,*

<sup>1,5</sup>*Japan*

<sup>2</sup>*Venezuela*

<sup>3</sup>*Turkey*

<sup>4</sup>*Czech Rep.*

## 1. Introduction

### 1.1 The energy problem

In the 21st century the stress due to environmental issues like the greenhouse effect, pollution, desertification, and local climate abnormality, as well as social issues like population explosion (100 M per year), poverty and starvation, may become intolerable, leading to large-scale disorder. However, it seems that there isn't a more effective measure for averting such disorder and solving human poverty as ensuring an adequate supply of clean and cheap energy. In principle, it is impossible to predict the future. Nevertheless, a hypothetical prediction based on reliable principles, can be quite useful. A future energy scenario based on the initial work of Marchetti [Marchetti 1985, 1987, 1988, 1992], and later modified by the members of the Thorium Molten-Salt Forum [Furukawa, 2006; Furukawa, et al. 2008] is shown in Figures 1-4. The growth rate of primary energy in the world is estimated at 2.3% yearly (see Figure 1).

In Figure 2 the historical/predicted fractional contribution  $F$  from prominent sources is shown as a function of time. In the figure the "logistic function" logarithm of  $F/(1 - F)$  is plotted against the calendar year. The main sources of energy shown are wood in the past, coal, oil and natural gas at present and nuclear and solar for the future. For the solar energy two graphs are shown in view of the uncertainty in the introduction of this source for large-scale deployment. For nuclear energy two scenarios are shown, one with a total nuclear energy production measured in power times years of 900 TWe year and the other with 2000 TWe year (see Figure 3).

In the past 30 years the market share of usages of all main sources of energy (coal, oil, natural gas and fission) has been surprisingly constant as can be seen from Figure 2. This

logistic function analysis suggests that political or financial influences on the energy market have been stronger than market mechanisms resulting in non-rationality.

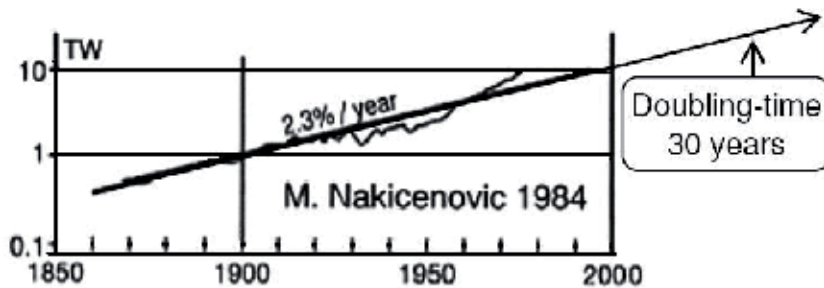


Fig. 1. Primary world energy consumption in the last 150 years.

In principle any variant of a solar-based technology could provide clean energy as it will not cause global warming or man-made abnormal weather patterns. But solar energy is low in energy density, irregular in output and it is still uneconomical and impractical for large industrial scale power plants. Even with a concentrated effort, the first industrial scale solar energy plant may only come on line after a few decades and large-scale deployment to meet projected demand would take more than 50 years after that (see Figure 2).

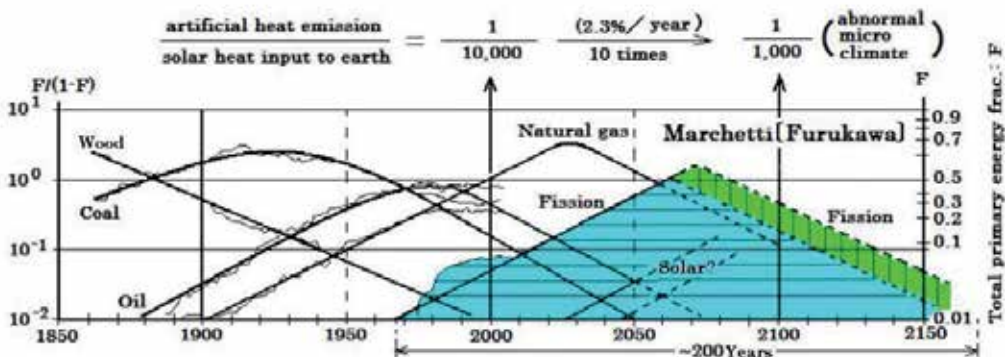


Fig. 2. Historical and predicted trends in energy usage by source in a 300 year time span.

CO<sub>2</sub> production and its attributed effect on global energy warming are expected to be a continuing problem. Even if a rapid increase in nuclear fission power generation takes place as shown in the shaded areas of Figures 2 and 3, the decrease of CO<sub>2</sub> will not be sufficient as shown in Figure 4

Other efforts such as local solar energy, eolic or wind power and hydroelectric power use etc., and in particular energy saving, are also necessary. The message of Figure 4 is that a great reduction in the use of energy will be required. Depending on the population explosion and energy demand increase, the artificial heat emission will increase tenfold in the next hundred years, based on the assumption of a 2.3 % yearly growth of world primary energy consumption as shown in Figure 1. A global warming, especially a local micro-climate abnormality will not be tolerable, and it will encourage shifting to the solar energy

era. In the long term there is no option but to curtail population growth and to reach a plateau of zero growth. Fred Hoyle [ Hoyle, 1977], has argued that at current rate of energy production, within long times for human perception (a couple of thousand years) but very short times in geological terms, the amount of predicted energy generation on the surface of planet Earth will match the energy production on the surface of the Sun! The inescapable implication is that growth has to be curtailed until a state of equilibrium is attained with no increase in energy production.

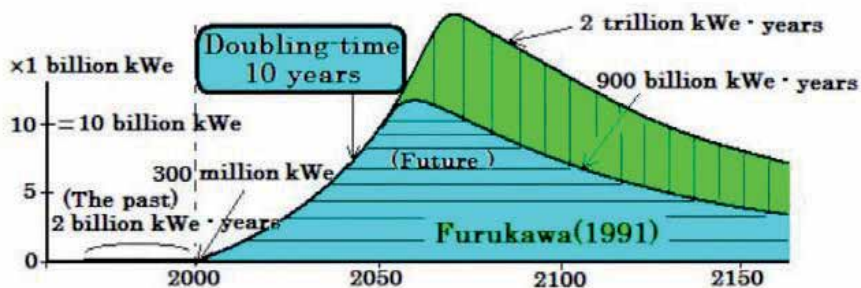


Fig. 3. Fission Energy Production

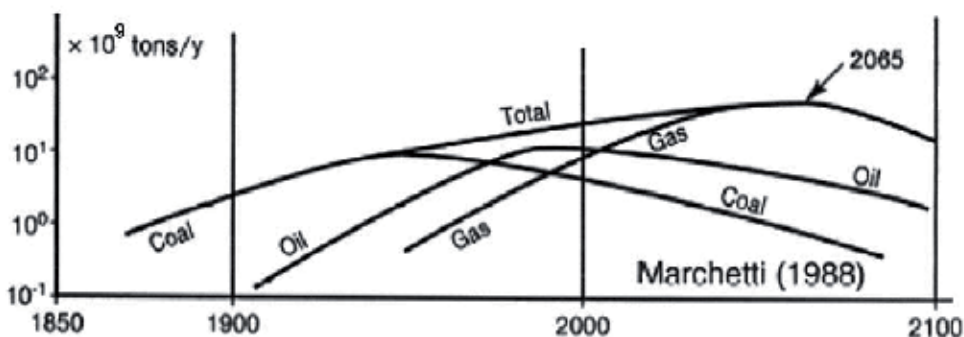


Fig. 4. Historical and predicted CO<sub>2</sub> yearly emissions. A twofold increase from the present, 50 billion tons/year is expected by 2065.

A recent technological development with influence in the future energy panorama is the introduction of electric energy for massive surface transport. It is the result of the recent developments of new batteries with greatly improved (energy /weight) ratio which are revolutionizing land transport. As fully electric vehicles supplant the internal combustion engine vehicle, the reliance on fossil fuels, petrol and gas, CO<sub>2</sub> emitting fuels, will slowly decrease. This will create an additional, increasing demand on electric utility generation which will have to supply the energy load of land transport that currently is provided by gasoline, diesel and gas.

In a final analysis, at the present time, there is no other technological choice but to rely on nuclear energy. Hence a revolution in the global energy strategy is called for by increasing the investment for fission-energy systems so that we return to a rising fission use while the market share of other energy sources falls as shown by the curves of other energy sources in Figure 2.

## 1.2 The nuclear energy problem

The current structure of the nuclear industry is inadequate to the challenges that the human society requires in the next hundred years. In spite of 60 years of development the present nuclear industry presents a number of shortcomings that require a profound reassessment for a sustainable and secure nuclear industry. In spite of the notable safety record of the nuclear power electric generation industry, compared to almost all other forms of electric generation, there is the not unjustified fear that present nuclear power technology is not safe. The safety issue is of paramount importance for society to accept nuclear power. Nuclear radioactive waste and nuclear weapons proliferation issues of current technology are also high in the agenda for the rejection of current technology by society. If the foregoing problems could be solved then the economic factors take prevalence in the selection of the energy supply system for ensuring public acceptance.

The root cause of the problems outlined lie in the extreme complexity of the solid fuel reactor, which itself is the result of the form in which the technology developed. Nuclear energy was born in the war effort of the 1940's. The huge research and development investment in nuclear science to develop the atomic bomb, before and after the war in 1945, was applied to produce and develop the nuclear reactor. In the US and elsewhere governments financed nuclear power plants for naval use and nuclear facilities designed to produce the required materials  $^{235}\text{U}$  and  $^{239}\text{Pu}$  that allowed the construction of weapons. However, this effort was not confined to the war era or its immediate aftermath. The cold war that prevailed from 1945 to the fall of the Berlin wall in 1989, continued to dictate the science and technology that was developed. Hence concepts such as economy, simplicity safety and non-proliferation characters of the nuclear technology that was developed, were the least important factors taken into consideration in the building of the industry that we have now. The technological fallout from military applications is what mostly constitutes the present nuclear industry.

Thus the compact boiling water reactor used in warships, a technological development fully paid for by governments, became, after scaling up, the current BWR for civilian use.

Thus the nuclear fuel cycle that was able to breed extra fissionable  $^{239}\text{Pu}$  for bomb production was chosen to supplant, with advantage, the production of  $^{235}\text{U}$  which needs natural uranium mining and costly enrichment.

Thus the PUREX hydrometallurgical process was developed in order to be able to extract, from spent nuclear fuel, the pure plutonium for weapons manufacture and to obtain as useful by-product uranium with the remaining concentration of  $^{235}\text{U}$  that could be used in other nuclear reactors. The nuclear energy industry that resulted from this, military biased, development has the following shortcomings:

1. The employment of discrete solid fuel elements containing either uranium enriched in  $^{235}\text{U}$  or plutonium as metal oxides (MOX) or as metal alloys clad in special zirconium alloy. They have to be built to extreme quality standards so as to withstand, during its short service life, high mechanical stress factors in the form of high temperature, thermal shock, high pressure, and extreme gamma and neutron radiation doses.
2. The employment of very high pressures in a large reactor space for the containment of the pressurised water moderator and cooling media with a pressure flange to allow periodic opening for service and fuel elements change. This dictates a reactor vessel which has to be built to extremely demanding high standards in order to provide safety against a catastrophic failure; a technology which few enterprises worldwide can supply.

3. The wasteful and inefficient use of reactor fuel elements whose contained energy usage is in the range of only 5%, and which, in the case of reprocessing, requires destroying into scrap metal, chemical acid dissolution, refining and metallurgical reconstruction into new fuel elements.
4. The production of considerable radioactive nuclear waste which although being very small in size and weight in comparison with waste from burning fossil fuels, it is of orders of magnitude of higher toxicity and, the actinide fraction of it, of extremely long lifetimes.
5. The requirement of scarce sources of natural uranium. The known amounts of this source is a matter of debate, on whether they are sufficient for providing energy for future generations.
6. The production of large amounts of plutonium, of the order of 230 kg/year for each 1000 MWe power plant. This becomes a nuclear proliferation nightmare if deployed globally, particularly in view of the present century's phenomenon of uncontrolled terrorism.
7. The inability of current technology to satisfy the world's energy demand due to its long doubling time, of the order of 20-30 years, caused by the high complexity of the technology.
8. In view of these shortcomings, the future development of nuclear energy requires a profound and fundamental reassessment if it is to supply worldwide, plentiful energy and support a clean lasting human society.

In this paper we propose and describe a thorium molten salt nuclear energy system (THORIMS-NES) which is a complete concept designed to overcome most of the stated shortcomings by the employment of several important factors: The use of thorium instead of uranium as the fertile element, the eventual use of  $^{233}\text{U}$  as the fissile element instead of  $^{235}\text{U}$  or  $^{239}\text{Pu}$ , the use of a liquid fuel instead of solid fuel elements and a stepwise chronology of introduction and development of items of technology. This system has the virtue of simplicity and will result in an affordable, sustainable, secure, clean and safe source of the required huge sized nuclear power industry and therefore will be acceptable to society so that humanity may look with optimism to a future of progress with plentiful energy for many generations.

## 2. New nuclear system THORIMS-NES

As stated above, the Thorium Molten Salt Nuclear Energy System (THORIMS-NES) is a complete fuel cycle concept which departs from current or presently employed fuel cycles. It proposes a power reactor which is radically different from current practice in the sense that: (A) - It uses a liquid fuel instead of solid fuel elements, (B) - It uses thorium instead of uranium as the as the fertile element to breed the fissile isotope  $^{233}\text{U}$ . (C) - It separates the nuclear power production from the nuclear fuel breeding by proposing a simple thorium molten salt reactor (Th-MSR) devoted exclusively for energy generation by burning initially  $^{235}\text{U}$  or  $^{239}\text{Pu}$  and eventually  $^{233}\text{U}$ . (D) - It proposes an Accelerator Molten Salt Breeder (AMSB) devoted exclusively to the production of fissile  $^{233}\text{U}$  and (E) - It will incorporate fuel reprocessing in Regional Centers. It is a "Symbiotic" system with each function optimized by its simplicity.

The THORIMS-NES concept includes a planned timetable beginning, in the first stage, with the construction of the miniFUJI, a 10 MWe small power reactor whose purpose is to recover the know-how of the Oak Ridge National Laboratory (ORNL) obtained in the period 1964-1969 during which the molten salt reactor experiment (MSRE) took place [Rosenthal et al., 1970]. The miniFUJI is a demonstration reactor that may be developed in a short time

estimated at 7 years. The second stage is the building of the FUJI reactor. This is a 150 MWe thorium molten salt reactor planned to go online in 14 years and to be deployed worldwide as a affordable, simple, safe and reliable power reactor burning either  $^{235}\text{U}$  or  $^{239}\text{Pu}$  with the purpose of using up fuel derived from dismantling nuclear weapons from spent fuel reprocessing. The third and last stage estimated some 25 years in the future is the establishment of regional Breeding and Chemical Processing Centers with production of  $^{233}\text{U}$  by thorium spallation in AMSB to supplant the use of uranium or plutonium and enter into the thorium nuclear power stage.

In the following section the properties of the various, present-day fuel cycles are summarized in order to point out how the THORIMS-NES concept is able to deal with the shortcomings and problems of current nuclear power technology for the sake of a sustainable and secure tomorrow.

## 2.1 Review of nuclear fuel cycles

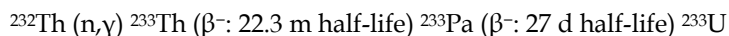
Table 1 contains a classification of Nuclear Fuel Cycles. The table is a modification of the classification introduced by W. H. Hannum, et al. 2005. It contains the following fuel cycles: 1.-Once-through route, 2.- Plutonium recycling in thermal reactor, 3.- Full recycling in fast reactor, to which we introduce a fourth class of fuel cycle: 4.- Full recycling in molten salt reactor. For each fuel cycle there is a text about the various items which characterize it allowing a comparison of the virtues and undesirable qualities and a clear idea of the differences and advantages that the proposed THORIMS-NES affords.

## 2.2 Why thorium?

Thorium-based reactor fuels have a number of advantages over uranium-based fuels.

Th is geochemically three times more abundant in the Earth than U. Resources of about 2 M tons have been confirmed with estimated amounts of about 4 M tons [IAEA, 2000]. The amount of Th necessary for production of 1,000 TWe per year required for this century, as shown in Figure 3, is estimated at only about 2 M tons, which compares with more than 1.5M tons of U already extracted from the earth. Large resources exist as heavy components of “beach sands” which can be mined with little pollution.

Natural Th has only one isotope,  $^{232}\text{Th}$ , of 100% abundance except for about 10ppm  $^{230}\text{Th}$ . (An isotope which is fairly rich in Th from U-ores). Hence in the production of a fuel no “enrichment” of the fuel is required. Chemically refined thorium is added directly to the molten salt as discussed below.  $^{232}\text{Th}$  in the reactor fuel is converted to the fissile  $^{233}\text{U}$  by the reaction:



Fissile  $^{233}\text{U}$  is suitable for thermal reactors with the advantage that with fertile  $^{232}\text{Th}$  it can largely eliminate the production of long lived trans-uranium elements (TRU, or actinides) including Pu isotopes. These elements have exceedingly long half lives of the order of 10 000 years or more. Actinide production in a thorium-fueled reactor is estimated to be 2 or 3 order of magnitude smaller than that in a uranium-fueled reactor. This is due to the lighter nature of  $^{232}\text{Th}$  against  $^{238}\text{U}$ . The negligible production of plutonium makes the thorium-fueled reactor a nuclear weapons proliferation-resistant technology. Plutonium is the ideal isotope for the manufacture of atomic bombs due to the weak accompanying radioactivity.



Name	Once-through Route	Plutonium recycling in Thermal reactor	Full recycling in Fast reactor	Full recycling in Molten salt reactor
<b>Fuel Process</b>	Solid Fuel is burned in thermal reactor. Fuel is not reprocessed in general. (Occurs in the U. S.)	Solid fuel is burnt in thermal reactor. Metallic or oxide fuel chopped. Hydrometallurgy reprocessing recovers <sup>235</sup> U, <sup>238</sup> U and <sup>239</sup> Pu with <b>Purex</b> Process	Solid fuel is burnt in advanced fast breeder reactor. Metallic or oxide fuel chopped. Reprocessing done by Pyrometallurgy (Electrorefining) or Purex process recovers <sup>235</sup> U, <sup>238</sup> U and <sup>239</sup> Pu	Liquid fuel is burnt in Molten salt reactor. Radioactive gasses removed on line. Reprocessing done by Pyrometallurgy in molten salt. Recovers <sup>233</sup> U, <sup>235</sup> U, <sup>238</sup> U and <sup>239</sup> Pu. Fissile <sup>233</sup> U produced by Accelerator Molten Salt breeder.
<b>Energy use</b>	Uses about 5 % of energy in thermal reactor fuel and less than 1 % of energy in uranium.	Uses about 5 % of energy in thermal reactor fuel in each fuel charge. Overall recovery depends on number of fuel recharges	Uses up to 15 % of energy in reactor fuel in each fuel charge. Theoretically high burn up of energy in fuel. Depends on number of fuel recharges	Continuous burning of fuel without recharge. Minor fuel chemistry adjustment. Theoretically 100% of energy in fuel
<b>Nature of fuel</b>	Solid cladded fuel elements of metal oxide or metal. Uranium enriched in <sup>235</sup> U. Burns generated <sup>239</sup> Pu.	Solid cladded fuel elements of metal oxide or metal. Uranium enriched in <sup>235</sup> U. Burns generated <sup>239</sup> Pu.	Solid fuel elements. Metallic alloy of U-Pu-Zr. <sup>238</sup> U enriched in <sup>235</sup> U, <sup>239</sup> Pu with Zircaloy cladding. Burns generated <sup>239</sup> Pu, <sup>235</sup> U and some fissionable actinides	Liquid molten salt fluoride LiF-BeF <sub>2</sub> (Flibe) with dissolved fertile <sup>232</sup> Th and <sup>235</sup> U, <sup>233</sup> U or <sup>239</sup> Pu fissile. Blanket is ThF <sub>4</sub> producing <sup>233</sup> U.
<b>Nature of cooling</b>	Pressurized or boiling Water	Pressurized or boiling Water	Liquid sodium or lead metal	Liquid molten salt fluoride LiF-BeF <sub>2</sub> (Flibe)
<b>Doubling time</b>	-	-	Greater than 20 years [1]	7 - 10 years

[1] [Furukawa K. & Erbay L. B., 2010]

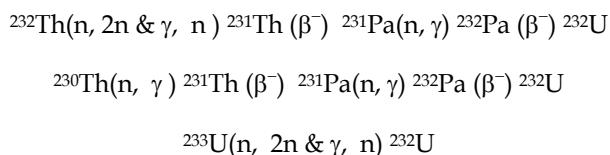
Table 1. Nuclear fuel cycle classification.

Nature of Fuel container	High pressure vessel	High pressure vessel	Low pressure vessel (low carbon steel)	Low pressure vessel (Hastealloy N steel)
Safety assessment. Major accident	High pressure vessel explosion danger. Fuel element meltdown on loss of coolant circulation. Control-rods danger.	High pressure vessel explosion danger. Fuel element meltdown on loss of coolant circulation. Control-rods danger.	No high pressure vessel explosion danger. Reduced meltdown danger. Control-rods danger.	No high pressure vessel explosion danger. No meltdown danger. No control-rod danger.
<b>Plutonium fate</b>				
Weapons proliferation assessment	Increasing inventories of Pu in used fuel. Excess weapons grade Pu	Increasing inventories of Pu and available for economic trade.	Continuous generation of Pu. Possibly on site dry-reprocessing and burn up in reactor	Burn up of Pu from weapons and spent fuel. (Decreasing Pu inventories) Eventually possible total Pu burn up and elimination.
Energy cost assessment	High pressure vessel capital cost. High fuel fabrication cost. No fuel reprocessing cost. High transport and fuel repository cost.	High pressure vessel capital cost. High fuel fabrication cost. Fuel reprocessing cost. Reduced transport and fuel repository cost.	High pressure vessel capital cost. High fuel fabrication cost. Fuel reprocessing cost. Reduced transport and fuel repository cost.	No high pressure vessel capital cost. Nill fuel fabrication cost. Single molten salt media for power reactor, for fuel reprocessing and for <sup>233</sup> U breeding in AMSB.

[1] [Furukawa K. & Erbay L. B., 2010]

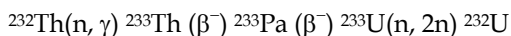
Table 1. Nuclear fuel cycle classification (continued).

$^{233}\text{U}$  can also be used to make nuclear weapons, if it were possible to get pure materials. But this is a difficult matter, as shown below. The military issue is a very confidential matter, but as was conclusively explained by Sutcliffe, a specialist of Lawrence Livermore National Laboratory (LLNL): “ $^{235}\text{U}$  is most easily made into a weapon; Pu is next most easily made into a weapon;  $^{233}\text{U}$  is hardest and least desirable for weapons.” [Sutcliffe W., 1994]. “No nuclear weapons that have ever been built use fissile  $^{233}\text{U}$ ” [Sorensen K., 2010]. The reason for this fact is that  $^{233}\text{U}$  fuel is accompanied by very strong gamma activity requiring sophisticated remote handling or a liquid-fuel technology for easy handling. The gamma activity is due to production of the  $^{232}\text{U}$  isotope which takes place in a thorium-fueled system by the following five reactions [ORNL-5132, 1976; Ganesan, et al., 2002].



These reactions occur with the initial inventory of  $^{232}\text{Th}$  and  $^{233}\text{U}$  present and  $^{230}\text{Th}$ , even though only traces are present.

$^{233}\text{U}$  is formed in situ with burn-up and thus  $^{232}\text{U}$  is also formed by a small amount through the breeding reaction from  $^{232}\text{Th}$  following the above:



The production of  $^{232}\text{U}$  is greater in a fast neutron spectrum because of the threshold nature of the (n, 2n) reactions. In other words, the production of  $^{232}\text{U}$  would be higher in a fast reactor in comparison to the production in a thermal reactor. Other possibilities exist as discussed by Ganesan, et al., 2002.

The strong gamma activities associated with  $^{232}\text{U}$  are such that detection of any diverted  $^{233}\text{U}$  is easy providing increased security and non-proliferation. [Moniz and Neff, 1978; Ganesan, et al., 2002]. Transport of significant amounts of  $^{233}\text{U}$  with more than 10 ppm level of  $^{232}\text{U}$  require remote handling operations and constitutes a high radiological hazard that requires lead or concrete shielding. This property is such as to make impractical any form of diversion for illegal purposes. Note that it is the daughter products  $^{212}\text{Bi}$  (1.8 MeV gamma) and  $^{208}\text{Tl}$  (2.6 MeV gamma) isotopes that are very strong gamma emitters and not  $^{232}\text{U}$  itself. These daughter products are formed after five successive alpha decays.

### 2.3 Why liquid fuel?

At the first nuclear reactor seminar that took place at Chicago University during World War II, in collaboration with some Nobel-prized scientists, Dr. Eugene Wigner [Weinberg A.M., 1997] argued: What is the nuclear power generator, primarily? Quite simply, it is a “Chemical Engineering Device”, since it means “equipment for utilizing the nuclear chemical reaction energy”. Wigner also predicted and recommended that in case of “Chemical Engineering Devices”, a “fluid” concept would be most desirable as reaction media for the nuclear fuel, and advocated that an ideal nuclear power reactor would probably be “the molten-fluoride salt fuel reactor”. This concept was later developed by Oak Ridge National Laboratory (ORNL), USA through the Molten-Salt Reactor Program (MSRP) during 1957-1976 [Rosenthal M.W, et al., 1972; Engel J. R. et al., 1980] under the able

guidance of his successor Dr. Alvin Weinberg. In the course of this program a Molten Salt Reactor (MSR) operated at ORNL during the four years between 1964 and 1969.

The operation was successful; it ran its course without any accident or incident and the program was fully documented. This extensive and invaluable literature is freely available in the WEB site established by Kirk Sorensen in 2010 [Sorensen K., 2010]. The operation of a power reactor with a liquid fuel as opposed to the well established practice of using solid fuel elements has a large number of advantages. These advantages are most apparent with the liquid media that was developed during the MSRP: A eutectic mixture of lithium fluoride and beryllium fluoride called FLIBE, with fertile thorium and fissile uranium or plutonium dissolved in the fluoride molten salt. ( ${}^7\text{LiF}-\text{BeF}_2-\text{ThF}_4-\text{UF}_4$  ; 73,78 -16 - 10 - 0,22 mol %) This fluid serves a triple function: 1.- as fuel element, 2.- as heat transfer medium, 3.- as fuel processing medium. Each of these functions will be described in the following.

### 2.3.1 As liquid fuel element

In a molten salt reactor the fissionable isotopes, the fertile isotopes and the products of the nuclear reactor operation: both, fission products and heavy elements resulting from neutron capture reactions, reside as ionic elements dissolved in the molten salt. The liquid is forced to circulate in such a fashion that when it enters the reaction chamber, the presence of graphite moderator material creates conditions for nuclear reaction criticality. The fuel generates heat as the fission reaction proceeds. The heated liquid fuel exits the reaction chamber and the criticality of the fuel ceases while it circulates through the pump, heat exchangers and other devices before returning to the reaction chamber.

Under reactor operation the fuel is subject to an extremely intense field of  $\alpha$ ,  $\beta$  and  $\gamma$  radiation as well as a very high neutron flux which produces damage in the reactor fuel elements. Radiation damage is well known [Olander D.R., 1976; Weber H.W., et al., 1986]. It affects the crystal structures, produces point defects and dislocations in the solids and grain boundaries, swelling due to fission gases, pore migration and fuel restructuring. Solid fuel elements are heterogeneous materials and assemblies. There are possible interactions between components and different behavior of the constituents. Extensive studies have to be done both experimentally as well as modeling of the structural behavior of fuel elements and assemblies, for radiation damage assessment, whenever a change of components is proposed. This radiation damage determines a very short life for solid fuel elements such that safety determines an obligatory exchange when only 5%, to at most 10%, of the useful energy has been burned.

On the other hand, a molten liquid fuel is free from structural radiation damage. An ionic liquid can be considered a randomly organized dynamic aggregate of ions that has no fixed structure. Any effects on the atomic level produced by radiation such as atomic displacements due to nuclear fission or reactions are inconsequential and in no way alter the basic properties or structure of the liquid. This property determines that there is **no need for fuel element replacement** during the life of the reactor. The chemistry of the liquid fuel may be monitored and may be adjusted by a very simple addition of components in an external section outside of the reactor vessel. It is easy to add additional fuel salt containing fissile  ${}^{233}\text{U}$ ,  ${}^{235}\text{U}$  or  ${}^{239}\text{Pu}$  in order to maintain an optimum fuel composition or likewise to remove some deleterious component as we discuss in the following.

An important advantage of a liquid fuel relates to radioactive gasses produced by the fission process. Radioactive gasses such as  ${}^{133}\text{Xe}$  and  ${}^{135}\text{Xe}$  in solid fuels are entrapped in the crystal

structure and produce fuel swelling. They also act as neutron poisons due to the huge cross section for thermal neutrons of  $^{135}\text{Xe}$  of  $2.6 \times 10^6$  barns [Stacey W. M., 2007]. The accumulation in the fuel represents a potential danger in the case of accidental release to the atmosphere. The presence of  $^{135}\text{Xe}$  in the fuel requires additional reactivity in order to compensate for its neutron absorption properties.  $^{135}\text{Xe}$  reactor poisoning played a major role in the Chernobyl disaster. [Pfeffer J. I. & Nir S., 2000]. A further deleterious effect of the entrapped radioactive gasses in solid nuclear fuels is the inability of a solid fuelled reactor to significantly decrease the power level. Reducing reactor power alters the equilibrium condition between  $^{135}\text{Xe}$  production as a decay product of  $^{135}\text{I}$  and its "burn up" as a result of the neutron capture reaction. A large reduction of power produces a buildup of  $^{135}\text{Xe}$  to an extent capable of shutting down the reactor. Further problems are Xenon-135 oscillations due to the interdependence of  $^{135}\text{Xe}$  buildup and the neutron flux which can lead to periodic power fluctuations [Iodine pit, 2011].

In a molten salt fuel reactor fission product gasses diffuse and are uniformly distributed in the fuel preventing these oscillations. Moreover: "Fission product Kr and Xe are virtually insoluble in the (Molten salt) fuel and can be removed, if the moderator graphite is sufficiently impermeable, by simple equilibration with an inert gas (helium)" [Grimes W. R. 1969]. Hence simple injection of an inert carrier gas such as He can continuously remove fission product poison gasses. The gasses are collected in active charcoal and can be stored and allowed to decay before final disposal. The poison gas removal and the possibility of fuel replenishment or retrieval imply that a molten salt reactor can operate at a low excess reactivity or "sub criticality" by leakage. These properties significantly reduce the possibility of any severe accidents. Furthermore, if poison gasses are removed, then the reactor power can be reduced or increased at will allowing it to follow the load demand without the limitation that  $^{135}\text{Xe}$  buildup imposes on solid fuelled reactors.

The molten salt reactor shares with liquid-metal cooled reactors some advantages: The first is that the reactor vessel may operate at low pressure. The container housing the liquid metal or molten salt only requires resisting just the necessary pressure to ensure fuel circulation. Pressure range contemplated in a MSR is about 0.5 MPascal (4.93 Atm or 72,5 PSI) which contrasts to pressures in the range of 15 MPascal (148 Atm or 2180 PSI) as are used in PWR. Hence no large pressure sealing flange is required. This constitutes a significant safety and cost advantage. The possibility of catastrophic reactor vessel failure completely disappears in a liquid fuel reactor.

The second advantage shared by the molten salt reactor and liquid-metal cooled reactors is the feasibility of high temperature operation which is several hundred degrees higher than any water cooled reactor. This implies significantly higher thermal efficiency for electrical energy production as well as the possibility of using the high temperature for hydrogen production. Development of less expensive methods of production of bulk hydrogen is relevant to the establishment of a hydrogen economy which is being currently considered. [Häussinger P., et al., 2002].

A molten salt fuelled reactor has the property that increasing operating temperature in the reactor vessel produces a volumetric expansion of the liquid. This has the consequence of a corresponding exit from the reactor of an amount of liquid reactant fuel. This produces a decrease in the overall reactivity and hence an inherent automatic mechanism of power reduction. This negative reactivity coefficient with temperature is universally recognized as a most desirable safety feature for power reactors.

Among engineering circles a very popular dictum is: “Simple is beautiful”. Perhaps the most attractive feature of a fluid fuel reactor is the beauty of its **simplicity**. This connects tightly with ECONOMY in general. Economy in capital costs, economy in fuel manufacturing costs and economy in operational costs. Economy is closely related to the possibility of nuclear energy deployment in lesser developed or underdeveloped countries. Bringing nuclear power to an economy level to make it competitive with coal fired power plants is the most powerful mechanism to replace fossil fuel utilization and meet greenhouse gas emission standards required by international agreements.

### 2.3.2 FLIBE as the fluid fuel medium

ORNL made a choice of a fuel-salt based on the  ${}^7\text{LiF}\text{-BeF}_2$  (FLIBE) solvent [Rosenthal M.W., et al., 1972; Engel J. R., et al., 1980; Yoyuenn & Zousyyokuro. 1981; Furukawa, K. et al., 2005], on the basis of its very low thermal neutron cross-section, but also on the structural-chemical properties which make it very similar to  $\text{MgO-SiO}_2$ , which is a main component of the earth mantle and has a deep correlation with silicate slag useful in the metal refining furnace. Furthermore, it has very promising properties as a chemical processing medium [Furukawa K. & Ohno H., 1978].(see below).

A comprehensive data-book of FLIBE has been prepared [Furukawa K.& Ohno H., 1980]. The important thermo-physical properties of molten FLIBE are shown in Table 2 and are compared with other technologically important molten-salts and liquid Na. This solvent salt has significant and useful characteristics. It dissolves fertile  $\text{ThF}_4$  and fissile  ${}^{233}\text{UF}_4$  (and/or  ${}^{239}\text{PuF}_3$ ) salts as shown in Table 3. Its flexibility is significant for the selection of fuel-salt composition. Suitable combination sets of fuel-salt compositions for obtaining a melting point (MP) lower than 773K [500°C] (lower zone in  $\text{BeF}_2$ ) are:

${}^7\text{LiF}$	73 -	73 -	74 -	74 -	72 -	69 mole %
$\text{BeF}_2$	19 -	18 -	16 -	15 -	16 -	16 mole %
$\text{ThF}_4$	8 -	9 -	10 -	11 -	12 -	15 mole %
${}^{233}\text{UF}_4$	0.2 ---- 0.4 mole %,					

and for obtaining a melting point lower than 798K [525°C] are:

${}^7\text{LiF}$	73----53	74---58	74---63	74---64 Mole %
$\text{BeF}_2$	20---40	16---32	13---24	12---21 mole %
$\text{ThF}_4$	7	10	13	15 mole %
${}^{233}\text{UF}_4$	0.2 ---- 0.4 mole %.			

It is necessary to predict the viscosity coefficient of the fuel salt. This is easily obtained with the known semi-empirical method using the huge experimental data available [Cantor S. 1968] and applying the mutual replacement ability of  $\text{UF}_4$  and  $\text{ThF}_4$  due to the similar ionic

size. This is also supported by the good similarity of phase diagrams in LiF-BeF<sub>2</sub>-UF<sub>4</sub> and LiF-BeF<sub>2</sub>-ThF<sub>4</sub>.

- a. (i) In UF<sub>4</sub> (+ThF<sub>4</sub>) < 30 mole %, viscosity will decrease until 15 mole % BeF<sub>2</sub>.  
 (ii) In UF<sub>4</sub> (+ThF<sub>4</sub>) > 30 mole %, viscosity will increase by an increase of BeF<sub>2</sub>.
- b. UF<sub>4</sub> (+ThF<sub>4</sub>) < 25 mole %, and 10 mole % < BeF<sub>2</sub> < 30 mole %, which is the most interesting region in MSR.

### 2.3.3 As heat transfer medium

The important thermo-physical properties of molten FLIBE and the characteristics of FLIBE-based fuel salt seen in Table 2 and 3, respectively, indicate that this solvent salt has significant and acceptable characteristics as a working fluid and coolant. Such excellent characteristics are based on (1) low pressure coolant, (2) highest heat capacity due to the main constituent ions being the smallest possible, (3) low viscosity fluid, and (4) suitable Prandtl number of 10-20 in the fuel-salt. Especially the parameter for heat-transfer per unit pump power has the highest value for FLIBE among the others included in the Table 2.

	NaNO <sub>3</sub> -KNO <sub>3</sub> -NaNO <sub>2</sub> [HTS]	NaBF <sub>4</sub> -NaF	Li <sub>2</sub> CO <sub>3</sub> -Na <sub>2</sub> CO <sub>3</sub> -K <sub>2</sub> CO <sub>3</sub>	LiF-NaF-KF [FLINAK]	LiF-BeF <sub>2</sub> [FLIBE]	Na
Chemical composition. (mol%)	7 44 49	92 8	41 36 23	46.5 11.5 42	66 34	-
Melting point (K) [°C]	415 [142]	657[384]	672 [399]	727 [454]	732[458.9]	371[98]
Volumetric heat capacity C (J/m <sup>3</sup> K) x10 <sup>-6</sup>	2.79	2.82	3.49	4.01	4.80	1.05
Density d (Kg/m <sup>3</sup> ) x 10 <sup>3</sup>	1.79	1.87	2.02	2.17	2.05	0.83
Thermal conductivity. h (W/mK)	0.59	0.35	0.55	1.2	1.00	66.
Kinematic viscosity. k (m <sup>2</sup> /s)x10 <sup>6</sup>	2.26	0.8	11.8	4.2	7.44	0.29
heat-transfer capability (C/k) <sup>0.4</sup> h <sup>0.6</sup> x 10 <sup>-3</sup>	49.7	55.7	25.2	69.4	52.8	1.264
heat-transfer per unit pump - power C <sup>3</sup> /d x 10 <sup>-15</sup>	12.1	12.1	21	29.4	53.8	1.39

The viscosity coefficients are about (6-7) x 10<sup>-3</sup> Pa s and do not depend strongly on composition. More detailed physical properties data was summarized by Cantor (1968), although it should be supplemented by several reports of ORNL. The phase diagrams of binary and ternary fluoride systems are comprehensively collected by Thoma (1975) and Janz G. J., et al., 1978.

Table 2. Thermo-Physical Properties of Molten-Salts and Sodium (At about 770K [500°C]).

This parameter represents the power requirement for pumping the fluid through a channel, which is related to the design of the pump for a molten salt as working fluid and coolant in the power cycle. Since there will be no phase change during the process, it will enable the design of an effective and simple coolant loop. In the power - heat generation system the main design studies will depend on the thermal aspects of the heat generating fluid flow

system in the core and heat exchanger group (see Figure 5). There are no doubts about the FLIBE-based fuel salt being a suitable heat transfer medium.

Fuel-salt FLIBE: ${}^7\text{LiF} - \text{BeF}_2 - \text{ThF}_4 - ({}^{233}\text{UF}_4 - {}^{239}\text{PuF}_3)$ Weak nuclear chemical reaction of solvent* Ideal ionic liquid with stable ions. Large heat-capacity & high fluidity.*,**  Low melting-point (480-530°C). **,***  Chemically inert, low aqueous solubility.**  Compatible with Hastelloy-N (Ni-Mo-Cr) alloy. High (flexible) solubility for multiple ions.*** Solubility for nuclear fission/spallation products. Easy prediction of physico-chemical behavior.*** Very limited radioactivity release in accident.  Easy reactor operation.	[mole %] [72-74]-[15-18]- [13-9] - [0.2-0.8] Very small thermal neutron cross-section Immune to radiation damage* Transparent, ambient pressure liquid** *** Single phase fluid: High Boiling point about 1400°C, no need to pressurize the system. Good compatibility with structural materials.**,** Compatible with graphite (no wetting)  Solubility for nuclear capture reaction materials (actinides). No-solubility for Xe/Kr/T *,***  If released it solidifies as a stable glass*** With trapping of radioactivity and no dissemination. Easy on maintenance/repair/dismantling
★ Triple-functional medium for * NUCLEAR-ENGINEERING, ** HEAT-TRANSFER MEDIUM *** CHEMICAL-ENGINEERING purposes	

Table 3. Summary of Characteristics of FLIBE-Based Fuel Salt

### 2.3.4 As fuel processing medium

Most present day spent fuel reprocessing is by a hydrometallurgical procedure called PUREX (Plutonium and Uranium Recovery by EXtraction). This is the most developed and widely used process in the industry at present. A number of variations of this basic process (UREX, TRUEX, DIAMEX, SANEX, UNEX) have been developed all of them being variations of the organic solvent extraction from aqueous solutions which result from acid dissolution of spent fuel. Alternative procedures that do not use water or organic liquids are high temperature processes called by the generic terms “Pyroprocessing or Dryprocessing” In this case solvents are molten salts (e.g.  $\text{LiCl}+\text{KCl}$  or  $\text{LiF}+\text{CaF}_2$ ) and molten metals (e.g. cadmium, bismuth, magnesium) rather than water and organic compounds.

In the THORIMS-NES concept the reprocessing media is FLIBE, the same media that is used as a molten salt fluid fuel. Although less developed than hydrometallurgical methods these high temperature procedures have a number of advantages. Among them 1.- They do not use solvents containing hydrogen and carbon, which are neutron moderators creating risk of criticality accidents, 2.- They are more compact than aqueous methods, 3.- They can separate many or almost all of the elements contained in spent fuel: remaining fertile or fissile uranium and plutonium, fission products and transuranic actinides, 4.- Simplicity of the separating equipment, 5.- No radiation damage is expected on the processing media, the liquid molten salt.



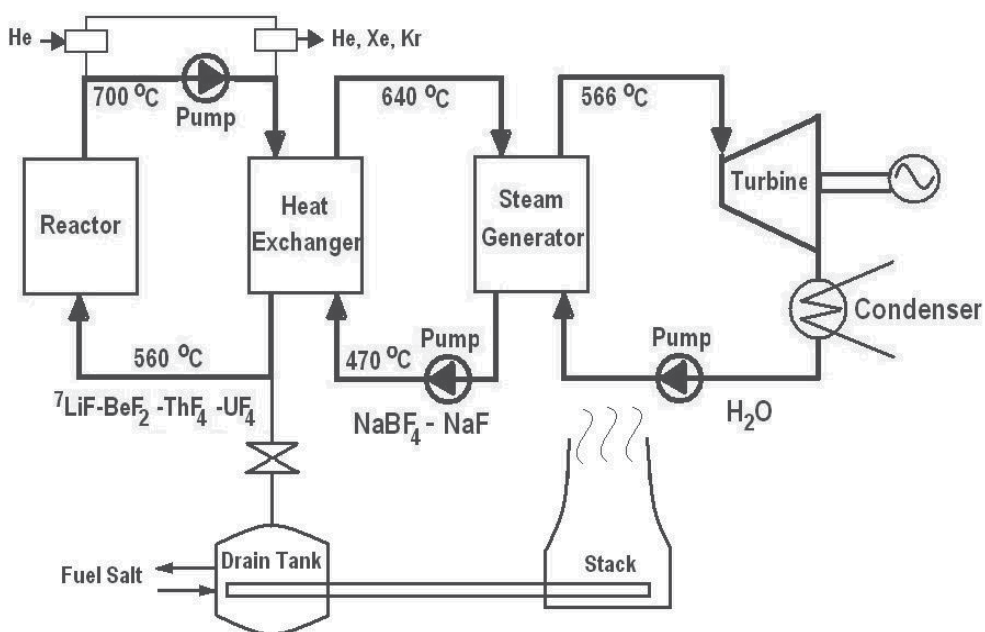


Fig. 5. Block diagram showing the three heat exchange loops in the FUJI series reactors

Separation of components in a molten salt can be achieved by a number of chemical processes such as: 1.- Electro deposition in a liquid or solid electrode [Kennedy J. W. 1950; Yang H., et al., 2010]; 2.- Absorption into a liquid metal cathode (cadmium or bismuth) [Delpech S. et al., 2008]; 3.- By the production of volatile compounds which can be separated by fractional distillation [ORNL-4577, 1971] or 4.- By selective precipitation of oxides [Rosenthal M.W et al., (1972)]. Pyroprocessing is the ideal procedure for processing fuel from a molten salt reactor. All the materials to be processed, separated or recovered are already in a suitable molten salt medium which can be used for the recovery process.

The Oak Ridge National Laboratory (ORNL) Molten Salt Reactor Program (MSRP) included on-line fuel processing of the fuel salt. Additionally, an intense R & D for chemical processing of spent fuel salts was done by ORNL [Whatley M.E (1970)]. One of the most significant advantages in THORIMS-NES is the elimination of the continuous chemical processing of the molten salt fluid during reactor operation. This deviation from the ORNL-MSRP is performed in order to achieve the greatest simplification of the reactor. The chemical processing of spent reactor fuel is considered in the THORIMS-NES concept as a separate operation from reactor operation. Fuel processing at the reactor during power operation is limited to removal of gaseous products.

Spent fuel reprocessing is to be performed under strict supervision at regional centers where chemical treatment of spent fuel takes place, breeding of fissile <sup>233</sup>U is carried out by an Accelerator Molten Salt Breeder (AMSB) and new molten salt fuel is produced. (see 4.2 below)

#### 2.4 Construction materials: Hastelloy N and graphite

The FUJI reactor vessel and all components in contact with the molten salt as well as the AMSB are constructed exclusively by a structural Ni alloy, Hastelloy N, and graphite.

### 2.4.1 Structural alloy

Structural alloy Hastelloy N (Ni- 15~18% Mo- 6~8% Cr- 5% Fe) [Rosenthal M.W. et al., 1972; Engel J.R. et al., 1980; Zousyokuro Y., 1981; Haynes International, Inc., 2002] is used as a main container material. It is composed of Ni, Cr, Fe, Mo and other minor alloying elements. To improve high temperature embrittlement due to He of fission products (f.p.), two modified Hastelloy N have been developed where Mo, Si and B were reduced and Ti (1.5~2.0%) and Nb (2%) added.

Less noble Cr is the most reactive among the alloy constituents. A Cr depleted zone was observed on the surface exposed to MSRE fuel salt after 22,000 hr at 650°C (923K) [McCoy H. E. Jr., 1967], but the depth of the degraded zone did not propagate above 0.2 mil (= 5Wm). Advanced corrosion tests simulating non-isothermal dynamic conditions had been performed by thermal and forced convection test loops. The weight change of standard and modified Hastelloy N after over 22,000 hr exposure to MSBR fuel salt at maximum 704°C (977K), and temperature difference 170°C [Koger J.W., (1972)] have been measured. The corrosion specimens in the hot legs resulted in weight loss and weight gain in the cold legs. The estimated corrosion rate of Hastelloy N was 0.02 mil/y, and modified Hastelloy N exhibited higher corrosion resistance. These corrosion levels are acceptable to the reactor design, although careful dehydration of salt and graphite is essential.

Standard Hastelloy N exposed to fuel salt under irradiation revealed material embrittlement due to inter-granular attack, where grain boundaries were degraded due to the existence of Te (f.p.) although not penetrating deeply. To solve this problem the following action was taken: [A] Hastelloy N was modified adding 1 to 2% Nb significantly reducing the Te attack. [B] The redox potential, that is the  $U^{4+}/U^{3+}$  ratio, control is essential for preventing Te attack [Keiser J. R., 1977]. The extent of cracking appeared very weak at a  $U^{4+}/U^{3+}$  ratio  $\leq 60$ , and extensive at the ratio  $> 80$ . The experience of the Molten-Salt Reactor Experiment (MSRE) at ORNL suggested that Te possibly converts to innocuous telluride (e.g. "CrTe") by a reaction:  $CrF_2 + Te + 2UF_3 \rightarrow 2UF_4 + CrTe$ , where the equilibrium of the reaction is controlled by varying the  $U^{4+}/U^{3+}$  ratio, that is, the redox potential by adding Be (reducing) or  $NiF_2$  (oxidizing). The potential should be kept within the region of stable Te compound ( $U^{4+}/U^{3+} < 60$ ) and beyond that of U-carbide deposition on graphite ( $U^{4+}/U^{3+} > 6$ ). The Te problem will be solved by applying both measures [A] and [B]. Alternatively, Russian work developed candidate materials for the MSR. Under similar test conditions the alloy showed a maximum corrosion rate  $\approx 6Wm/y$  [Ignatyev V. et al., 1993], and no trace of Te attack in the promising material. The development of monitoring techniques is necessary for ensuring sound/efficient reactor operation.

The reactor system does not need continuous monitoring of major fuel constituents such as Li, Be, Th, F and U [Rosenthal M.W. et al., 1972], because the chemical composition drift is very slow. Electrochemical in-line monitoring of the redox potential has been developed: the  $U^{4+}/U^{3+}$  ratio, which responds to the corrosive atmosphere and the distribution of f.p. and tritium in the reactor system. In-line monitoring of the  $U^{4+}/U^{3+}$  ratio in MSRE showed that the observations agreed well with the result of thermodynamic and spectroscopic analyses, accompanied with a Ni/ $NiF_2$  reference electrode [Rosenthal M.W. et al., 1972]. The  $U^{4+}/U^{3+}$  ratio can be easily kept in the suitable region by varying dissolution of Be into the salt. Preparation of modified Hastelloy N data for ASTM standard and ASME coding (Tensile test data, Ductility data, Creep test data, Toughness data, on base and weld metals) should be carried out as the first step of the miniFUJI project.

### 2.4.2 Graphite

Graphite is used as neutron moderator and reflector with the Th and fuel molten salt directly immersed in it. The basic requirements were dictated by the research in the MSBR at ORNL. [Rosenthal M.W et al., 1972; Engel J.R et al., 1980; Zousyokuro Y., 1981]. The graphite used should be stable under neutron irradiation, not penetrable by the fuel salt, and immune to absorption of Xe and Kr.

Under irradiation, point defects are formed and they tend to be agglomerated with each other in crystallites causing growth in the c-axis direction and a small shrinkage in the other two directions [Reynolds W. N., 1966] resulting in material distortion. The lifetime is determined by the failure criterion, and by the degradation of thermal conductivity. The volume change for monolithic graphite has been concluded to be the best criteria of quality after irradiating with fast neutrons ( $> 50$  keV) at  $715^{\circ}\text{C}$  (988K). Such results obtained at ORNL were supported by R&D of EdF-CEA and the former USSR.

Although the core graphite in the MSBR should have to be replaced every 4 years, the graphite in FUJI does not need be replaced in its full life. The effective seal of graphite against fuel salt penetration is resolved by choosing a pore-diameter less than  $1\ \mu\text{m}$  due to the surface tension of the salt. It means that graphite presents no serious problem for the MSR, although large size homogeneous graphite is not easy to fabricate.

If the irradiation dose limit of graphite can be increased, the electric generation cost of FUJI will be improved significantly. Toyo Tanso Co. (Japan) holds the top share of isotropic graphite in the world, having supplied reactor grade IG-110, for the High-Temperature Gas Reactor (HTGR) at the Japan Atomic Energy Research Institute (JAERI) and HTR-10 at China Tsinghua University. They promised to cooperate with the FUJI development, in the basic research. Irradiation with energetic particles, including carbon ions and high-energy electrons will be performed to understand more precisely the damage mechanism and to develop better materials.

### 2.5 Separation of power generation and fissile production process

At the early days of nuclear power it was realized that the operation of a nuclear reactor produced additional fissile material via the capture reaction on “fertile” isotopes: mainly  $^{238}\text{U}$  or  $^{232}\text{Th}$ . This realization opened the door to the dream of producing fuel in the same amount or even exceeding the amount of burnt fuel and opening a practically inexhaustible source of energy. This possibility gave birth to the concept of breeder reactors used in nuclear power plants to produce nuclear power and more fissile nuclear fuel than it consumes. Breeder reactors have been built and operated in the USA, UK, France, Russia, India and Japan. A breeding ratio substantially larger than 1 can only be obtained in a fast neutron spectrum. Hence water as cooling media is precluded and a substantial amount of experience has been obtained in fast breeder reactors cooled by liquid metal, either liquid sodium or liquid lead.

After considerable effort in breeder reactor development the “Fission Breeding Power Stations” has become a sophisticated, huge-size complex system. However, still insufficient in its breeding capacity and with a doubling-time longer than 30 years in the Fast Breeder Reactor (FBR) and 20 years even in the Molten-salt Breeder Reactor (MSBR) proposed by ORNL. [ORNL WASH-1222, 1972]. In order to overcome the breeding limitation of the power reactor and to ensure the required design simplicity, the THORIMS-NES system separates into distinct operations the power producing function and the fuel breeding function. THORIMS-NES is composed of simple power generation stations: Molten Salt

Reactors (MSR), named FUJI-series (See 3 FUJI Reactor, 4.1 miniFUJI Reactor; ) and fissile producing stations Accelerator Molten Salt Breeder (AMSB). (See 4.2 AMSB). These two, power and breeding stations are complemented by batch-type process-plants (See 4.4 Regional Center) establishing a **Symbiotic** Th Breeding Fuel-cycle System. This separation recognizes that the fission reactors are neutron-poor and are best for producing energy and that fission power stations themselves should be simpler and size-flexible. They should be extremely reliable power producing units for continuous uninterrupted operation deployed in the neighborhood of population centers.

This separation also recognizes that the fuel breeding, neutron-rich fissile producer power plant does not need continuous operation. It may operate producing, in a batch-wise manner, the required fuel. This separation will be essential for establishing a huge-size breeding fuel cycle, growing with a doubling time of 10 years. The THORIMS-NES system also recognizes that at the present time there are considerable weapons grade  $^{235}\text{U}$  and  $^{239}\text{Pu}$  inventories resulting from the Cold War era. Also there are at the present time  $^{235}\text{U}$  enrichment facilities as well as facilities under construction or operation which are issues of international concern. The weapons grade fuel is being used for power plant fuel manufacture [Megatons to Megawatts, 2010] and the MSR is an ideal platform for its burn up. This resource is not estimated to last very long. Another source of fissile material is the considerable amounts of spent nuclear fuel at repositories containing remaining  $^{235}\text{U}$  and  $^{239}\text{Pu}$  which can be accessed by reprocessing and recovering operations as discussed below.

The U.S. and Germany have abandoned reprocessing, and the plants in the UK, France, Russia, Japan, China and Pakistan can process only a fraction of the spent nuclear fuels accumulating all over the world. The reprocessing could be performed by a fluorination molten-salt chemical-processing Method. [Uhlir Jan., 2011]. France laid the foundation for this method. The former Soviet Union, with the cooperation of France and the former Czechoslovakia, nearly completed it by about 1988. [Novy, I., et al., 1989; Furukawa K., 2001]. In this method, the spent oxide fuels are pulverized and made to react instantaneously in fluorine gas (Called a "flame reaction" because of the high-temperature combustion). The fluorination flame reactor technology used as the basis of this method has been put into practical use on a large scale at Pierrelatte in southern France to produce uranium hexafluoride gas for uranium enrichment from uranium oxide. The former Soviet Union called it the "FREGATE" project. By eliminating the last process of solid nuclear fuel production from the original FREGATE process and aiming only at supplying molten-salt nuclear fuel, the resulting modified process becomes surprisingly simple. Further, the solid spent nuclear fuel around the world can be processed economically. The best and most economical solution is to utilize the FREGATE process all over the world to prepare plutonium-containing molten-salt to be burnt in a thorium molten-salt reactor. If FLIBE is added to the molten-salt resulting from the modified FREGATE process allowing the fluorides of various fission products to contaminate the salt, then a molten-salt nuclear fuel containing plutonium can be easily prepared. Plutonium and other nuclear wastes retained in the salt gradually disappear owing to neutron absorption reactions and radioactive decay while the molten-salt reactor is operated.

These resources depend on the economics of reprocessing against the production of fresh fuel from mining and enrichment operations. The existence of these two sources of nuclear fuel implies that, within the THORIMS-NES system, the deployment of the AMSBs (See 4.2 AMSB) and associated process-plants is only required some 25 years in the future.

### 3. FUJI reactor

#### 3.1 FUJI reactor description

The FUJI-series power reactors are modeled on the successful molten salt reactor program (MSRP) carried out at ORNL [ORNL reports 2010]. However important differences are incorporated: FUJI Power reactors should be simpler, size-flexible and fissile-fuel self-sustaining, which allows a most simple/stable operation and requiring minimum maintenance work. Such idealistic performance was almost realized by the FUJI concept, eliminating the continuous chemical processing in situ and periodical core-graphite replacement, both of which were needed for the Molten Salt Breeder Reactor (MSBR). [Furukawa K., et al., 1985; 1989; 1990]. Figure 6 shows a vertical cross section of the primary fuel salt system of FUJI. A standard conceptual design of FUJI [Furukawa K., et al., 1987; 1992] is 350 MW thermal and 160 MW electric. The reactor-vessel is cylindrical 5.4 m diameter and 4.0 m high, inside of which it is filled only by graphite (93.9 vol.%) and fuel-salt as shown in Figure 6. The reactor-vessel is weld-sealed in the factory and does not need opening during its entire life. The core is constituted by liquid fuel directly immersed inside central hexagonal graphite rods surrounded by a graphite neutron reflector. Graphite inventory is 161 tons and spatially arranged to get a best performance attaining an initial conversion-ratio of 1.002.

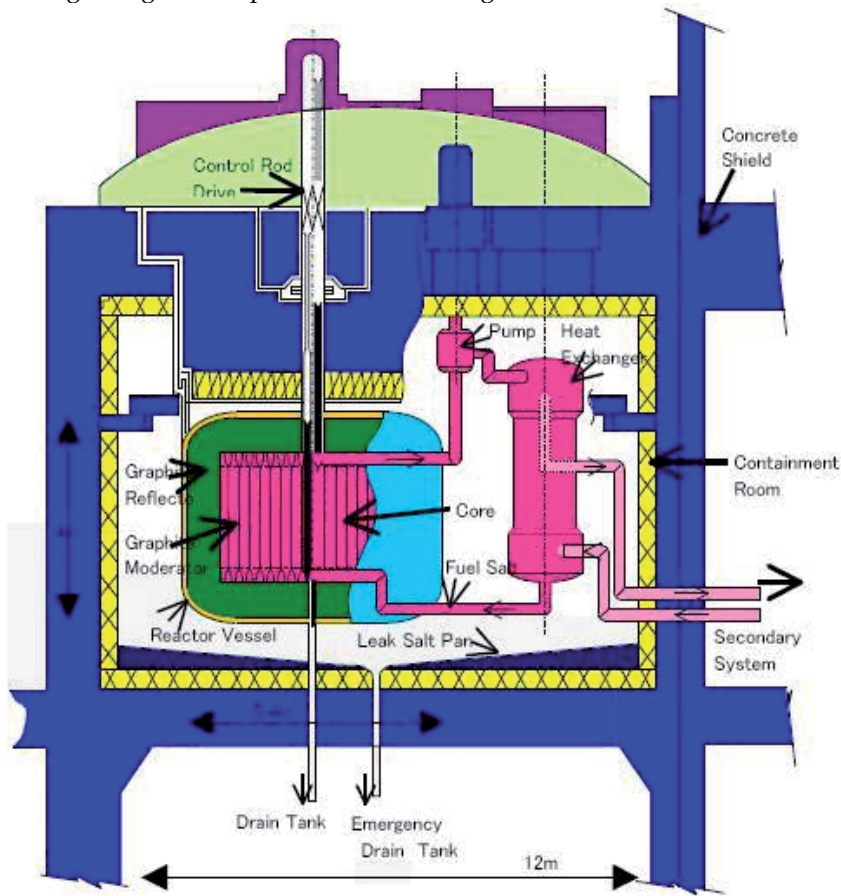


Fig. 6. Cross section of the primary system of Molten-Salt Power Reactor (FUJI)

The standard fuel salt of FUJI is  ${}^7\text{LiF}\text{-BeF}_2\text{-ThF}_4\text{-UF}_4$  (69.78-18-12-0.22 mol%). (See 2.3.2) The total volume of fuel salt is  $13.7\text{ m}^3$  flowing upward at a rate of  $33.2\text{ m}^3/\text{min}$ . The inner diameter of the main fuel piping is 25 cm. The structural Ni alloy, Hastelloy N (See 2.4.1) is appropriate for up to 1170K or more. Hence it can operate as industrial-heat supply up to 930K, and in the future 1030K will be feasible. As such it allows for hydrogen production, as well as cogeneration, desalination, and district heating. Centrifugal pumps transfer the outlet fuel salt to heat exchangers, where the heat is transferred to a secondary coolant salt of  $\text{NaBF}_4\text{-NaF}$ , which transports the heat to a super-critical steam generator for electric generation, resulting in a thermal efficiency of more than 44%.

Several analyses have been carried out to establish nuclear characteristics of FUJI series cores which use several kind of fissile materials ( ${}^{233}\text{U}$ ,  ${}^{235}\text{U}$  and  ${}^{239}\text{Pu}$ ) with denominations such as FUJI-233U or FUJI-Pu [Mitachi K., et al., 1994; Mitachi K. & Furukawa K. 1995] and several output powers. A full schematic image of the FUJI molten salt reactor is shown in Figure 7. It includes the reactor containment building, primary heat transfer and cooling circuit, secondary cooling salt circuit, supercritical steam generator, turbines and electrical generators.

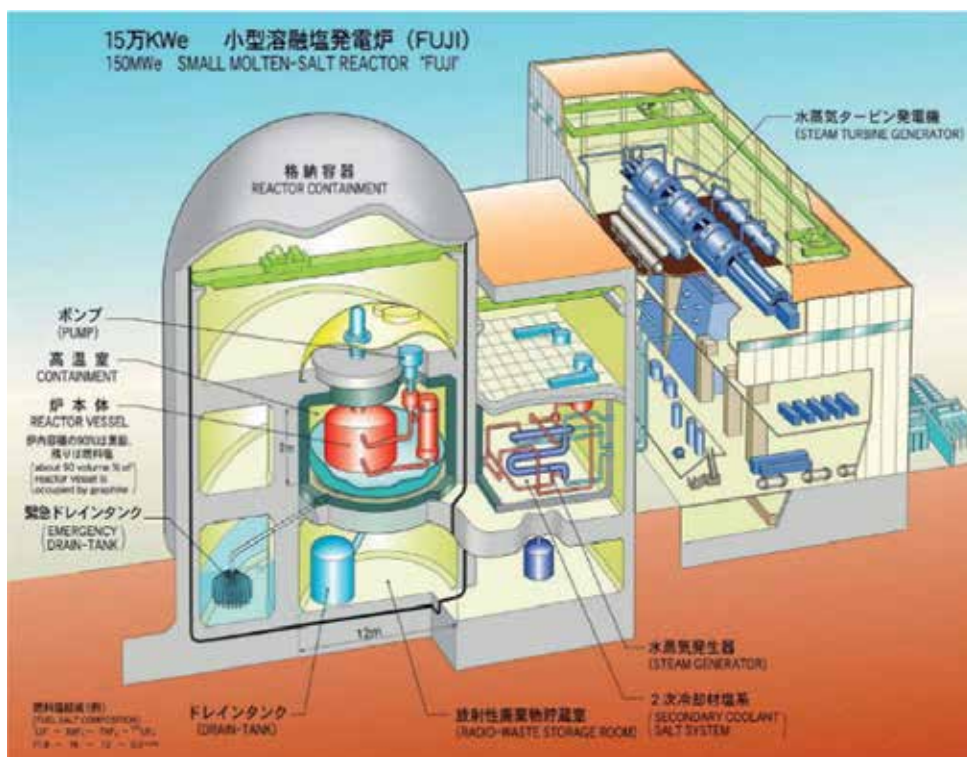


Fig. 7. Full view of FUJI molten salt reactor.

The reactor design has a three level containment security: The reactor core is contained in a primary Hastelloy N vessel which is inside the high-temperature containment. The tertiary level is the reactor containment building. The design is extremely safe as the fuel is only critical inside the core. In the unlikely event of reactor fuel salt leakage the molten salt will be caught by a spill pan and flow into a drain tank preventing any release of radioactive

material. Full power failure results in a freeze-valve melting and releasing all the fuel to a passively-cooled emergency drain tank surrounded by borated water.

### 3.2 Coolant salt

In the experimental reactor MSRE at ORNL, ortho-FLIBE ( ${}^7\text{Li}_2\text{BeF}_4$ , MP: 732K, see Table 2) was used as a coolant salt. In spite of its higher melting point, it has a high price, and was replaced by sodium-fluoroborate (92 mole %  $\text{NaBF}_4$  - 8 mole%  $\text{NaF}$ , MP: 653K, see Table 2). The detailed physico-chemical data have been summarized [Cantor S., 1968; Ohno H. and Furukawa K., 1972]. This molten salt has a satisfactory good compatibility with Hastelloy N, and its contact with the fuel-salt would not induce any serious result. It has a slight higher vapour pressure over  $\text{BeF}_3$ , but only 174 Torr (23.2 kPa) at 873K. This salt has about 30 ppm hydrogen, which is useful for the collection of tritium penetrating from the fuel salt. Collected tritium (T) is extracted as water vapor (HTO) in the He cover gas, and the environment release will be less than the regulation limit. The T management has been successful in the MSR system.

### 3.3 Reactor chemistry

#### Reactor Fuel and the Behavior of Fission Products (f.p.)

FUJI will consume 400 g/day of  ${}^{233}\text{U}$  including 350g/day by fission, meaning that 1920 kg (8300 moles) of  ${}^{233}\text{U}$  are converted to f.p. in its full life. [Furukawa K., et al., 1989; 1990; Rosenthal M. W., et al 1972; Engel J.R., et al., 1980]. This behaviour will be explained by dividing the f.p. in the following three groups. Their crude amounts in full life operation were estimated as shown in Table 4.

Group I: Noble-gas f.p. and tritium (Kr, Xe and T). Kr and Xe have practically no solubility, and more than 99 % can be easily separated to cover-gas, reducing their huge neutron absorption to achieve a fuel self-sustaining condition. 210 g in total of T will be produced at the rate of about 380 Ci (14TBq)/day, decaying with the half-life of 12.36 y. From the experimental examination of ORNL [Engel J. R., et al., 1980; Houtzeel A. & Dyer F. F., 1972] the environmental release of T in FUJI will be less than 1 Ci (37GBq)/day (See 3.2)

Group II: Soluble/stable fluorides (Rb, Cs, Sr, Ba, Y, the Lanthanides, Zr, Br, I, etc.) Almost all isotopes of Rb, Cs, Sr, Y, Ba have noble-gas precursors, which will be isolated to gas-phase of off-gas lines, and finally deposited in beds, except the short half-life isotopes: 32s  ${}^{90}\text{Kr}$  (final daughter: Sr), 3.1m  ${}^{89}\text{Kr}$  (Y), 3.8m  ${}^{137}\text{Xe}$  (Cs), 14.1m  ${}^{138}\text{Xe}$  (Ba), and some parts of their daughters will remain in the fuel salt. These fluorides are stably dissolved in fuel salt owing to the low concentrations (See Table 4), and will not have any severe problems in reactors. I and Br will be soluble as I and Br ions in the reducing condition containing an appreciable  $\text{UF}_3$ .

Group III : Noble and Semi-noble f.p. (Ge, As, Nb, Mo, Ru, Rh, Pd, Ag, Cd, Sn, Sb, etc.) They will exist in the elemental state in the reductive fuel salts. In the MSRE, the deposit of such elements mostly occurred as an accumulation of finely divided well-mixed materials rather than "plating" [Houtzeel A. & Dyer F. F., 1972]. Some part will escape as aerosol to off-gas phase.

The total amount of trivalent fluorides in fuel salt including  $\text{U}^{+3}$ , the lanthanides and  $\text{Y}^{+3}$  should not exceed 1.3 mole% of the solubility limit. In FUJI it will be safely about 0.63 mole % or less in the final stage. FUJI can soundly and simply be operated without any chemical processing except fission gases and T separation for its full life. The detailed examination of f.p. behavior in MSRE was reported by ORNL [Houtzeel A. & Dyer F. F., 1972; Rosenthal M.W, et al., 1972].

	production from $^{233}\text{U}$		amount dissolved in fuel salt	separated to gas phase
I	Xe	27.6 a/o		312.0 Kg
	Kr	6.5 a/o		45.9 Kg
	T			0.1 Kg
II	I	2.6 a/o	27.6 Kg [0.032m/o]	
	Br	0.42 a/o	2.8 Kg [0.005m/o]	
	Te	4.1 a/o	43.5 Kg [0.050m/o]	
	Cs	17.8 a/o	56.0 Kg [0.060m/o]	144.0 Kg
	Rb	7.2 a/o	0.5 Kg [0.001m/o]	51.0 Kg
	Sr	11.8 a/o	28.1 Kg [0.047m/o]	60.5 Kg
	Ba	6.3 a/o	0.3 Kg [0.005m/o]	72.0 Kg
	Ce	14.1 a/o	166.0Kg [0.170m/o]	
	Nd	16.4 a/o	199.0Kg [0.200m/o]	
	Y	5.9 a/o	1.5-7.5Kg [0.003-0.013m/o]	42-37 Kg
	Zr	30.0 a/o	232.0Kg [0.370m/o]	2-10 Kg(?)
III	Mo	21.6 a/o	[deposit 175.9Kg]	2-10 Kg(?)
	Se	0.9 a/o	6.1 Kg [0.010m/o]	
	Sn	0.3 a/o	3.0 Kg [0.004m/o]	

Table 4. Predicted amount of fission products accumulated at the life-end of “FUJI-II” (in (atomic %), (mole %) and kg)

### 3.4 The reactor moderator

The reactor moderator is graphite (See Table 5) which fills a very large portion of the reactor vessel. [Furukawa K., et al., 1987] As shown in Figure 8, it is mostly built up of perforated graphite vertical rods of hexagonal shape. As shown in the figure, the rods have a varying size perforation. The core is divided in various sections: The central section houses the control rods. They are surrounded by Zone I of hexagonal graphite rods with the smaller diameter perforations. Zone II occupies the largest area and contains intermediate size perforations. In the outer, blanket zone of the core, the perforations are larger. The core is surrounded on sides, top and bottom by a graphite reflector.

The radial moderator-fuel variation has been designed in order to ensure the flattest neutron flux distribution in the core. A graphite density of  $1.8 \text{ g/cm}^3$  was assumed in calculations. The graphite moderator is not expected to be replaced in the life of the reactor. To prevent damage, a neutron irradiation limit of  $3 \times 10^{22} \text{ nvt}$  is selected ( $<50 \text{ keV}$ ). [Op cit.]. Therefore the maximum core flux should be less than  $6 \times 10^{13} \text{ n cm}^{-2}\text{s}^{-1}$  in a 30 year life with 60% load as a local power station. High quality graphite with high irradiation resistance and small pore size ( $< 1 \mu\text{m}$ ) is used.



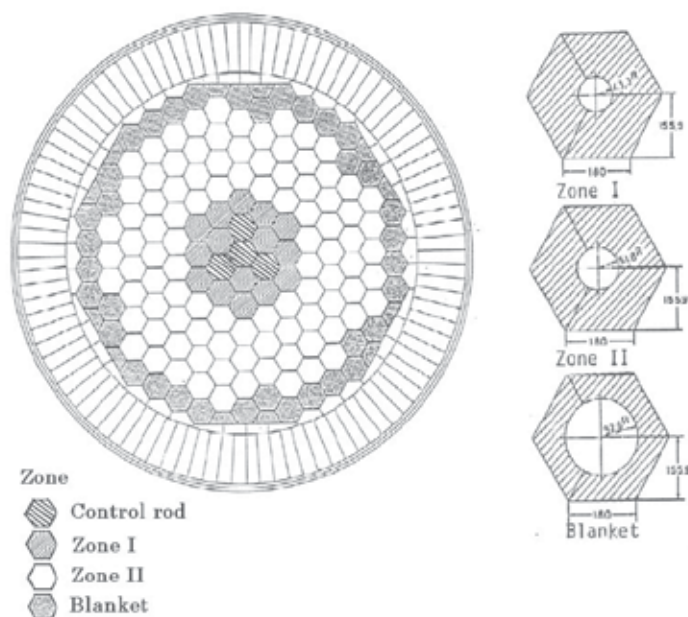


Fig. 8. Geometry of the FUJI reactor graphite moderator. Molten fuel flows through the circular channels in the graphite.

### 3.5 The reactor control system

The MSR FUJI has very high safety and reliability owing to the very small excess reactivity, due to the fuel-salt loss and other several advantages, and has essentially no possibility of a severe accident. [IAEA, 2007].

The MSR uses control rods which are made of graphite for the control of power. It employs shut-down control rods using  $B_4C$ , which are always withdrawn when the reactor is in operation. When inserting the graphite control rod into the core, this graphite functions as a moderator which promotes the fission reaction, contrary to the scram control rods. Graphite rods will be drawn by floating power in a fail-safe mode.

### 3.6 The Reactor fuel chemistry control

The chemical valence shift by the fission of  $^{233}U$  fuel salt is quite small. However, the development of a monitoring technique is necessary to ensure sound and efficient operation of the FUJI. Fortunately, the reactor system does not require continuous monitoring of the major fuel constituents such as Li, Be, Th, F and U [ORNL-4812, 1972]. Therefore, an electrochemical on-line monitoring of the redox potential has been developed; it only depends on the  $U^{4+}/U^{3+}$  ratio, which responds to the corrosive atmosphere and to the distribution of fission products and tritium in the reactor system. On-line monitoring of the  $U^{4+}/U^{3+}$  ratio in the MSRE has proven the results previously obtained in thermodynamic and spectroscopic analyses. These have shown that observations agreed with those from thermodynamic and spectroscopic analyses, in the presence of a Ni/NiF<sub>2</sub> reference electrode [ORNL-4396, 1969]. The  $U^{4+}/U^{3+}$  ratio can easily be kept within the suitable region by varying the time during which beryllium (Be) is dissolved in the melt.

	Experimental Reactor ORNL (Operated 1965-1969) MSRE	Pilot plant miniFUJI	Standard power station FUJI-II (Fuel self sustaining)
Heat capacity (MWTh)	7,3	16,7	350,0
Electric power (netMWe)	-	7,0	155
Thermal efficiency (%)	-	42 <sup>b</sup>	44,3 <sup>b</sup>
Reactor vessel size (m) (diameter x height)	1,45 x 2,2	1,8 x 2,1	5,5 x 4,1
Core: Max diameter (m)	1,14	0,6	1,4; 3,4 <sup>a</sup>
Graphite frac. (Vol%)	77,5	90	93,90 <sup>a</sup>
Blanket: Thickness (cm)	-	20	35
Graphite frac. (Vol%)	-	70	65
Reflector: Thickness (cm)	7?	40	68
High temp. Containment (m) Diameter x height	(5,8 x 7,2)	3,7 x 3,2	12,0 x 8,0
Core/blanket Power density Average-Peak (KWth/l)	2,9-6,6	16,4-24,9	9,5-17,5
Neutron flux: (n/cm <sup>2</sup> s) Maximum thermal	0,5 x 10 <sup>14</sup>	0,58 x 10 <sup>14</sup>	2,4 x 10 <sup>14</sup>
Max graphite (>50 keV)	0,3 x 10 <sup>14</sup>	0,75 x 10 <sup>14</sup>	0,8 x 10 <sup>14</sup>
Fuel conversion ratio	-	0,58 <sup>c</sup>	1,002 <sup>c</sup>
<sup>233</sup> U inventory (kg)	32,0	27,0	370,0
[Per 1 GWe] (Ton)	[-]	[6,4]	[2,4]
<sup>232</sup> Th (Ton)	-	0,65	20,1
Fuel salt: <sup>233</sup> UF <sub>4</sub> (mol %)	0,14 <sup>c</sup>	0,47 <sup>d</sup>	0,22 <sup>d</sup>
Total volume (m <sup>3</sup> )	2,1	0,45	13,7
[Reactor](m <sup>3</sup> )	[0,54]	[0,30]	[9,7]
Flow rate (m <sup>3</sup> /Min)	4,5	1,59	33,2
Temperature (°C)	632-654	560-700 <sup>b</sup>	585-725 <sup>b</sup>
Main piping (inn. dia.cm)	15,0	8,0	25,0
Graphite inventory (ton)	3,7	8,8	161,6

a The second core-zone.

b 2% up by "Ultra-ultra supercritical steam-turbine cycle [593 oC, 317 Atm]" at a fuel temperature of 725°C.

c In the stationary state after 500 days from start up.

d 7LiF - BeF<sub>2</sub> - ThF<sub>4</sub> - <sup>233</sup>UF<sub>4</sub> = (72-x) - 16 - 12 - x (mol%)

e 7LiF - BeF<sub>2</sub> - ZrF<sub>4</sub> - UF<sub>4</sub> = 64,5 - 30,2 - 5,2 - 0,154 (mol%) (91% <sup>233</sup>U)

Table 5. Main design parameters of three molten salt reactors: the MSRE at ORNL, the miniFUJI and the FUJI Power reactor. [Furukawa K., et al., 1992]

## 4. Technological description of THORIMS-NES

THORIMS-NES depends on the following three principles: [Furukawa K, et al., 1990; 2005] (I) Thorium utilization (See 2.2). (II) Application of molten-fluoride fuel technology (See 2.3). (III) Separation of fissile-producing breeder's process plants: Accelerator Molten-Salt Breeder (AMSB) from power generating fission-reactors: utility facilities Molten-Salt Reactor (MSR). This separation will be essential for the global establishment of breeding-cycle applicable over the world. This separation is dictated by the need for a doubling time of the fission industry to be 10 years or less as mentioned in section 2.

The THORIMS-NES concept is composed of: simple power stations Molten Salt Reactors (MSR) named FUJI-series, fissile-producers Accelerator Molten salt Breeders (AMSB), and batch-type process plants establishing a symbiotic Th breeding fuel-cycle system. The THORIMS-NES concept also includes a detailed timetable for development [Furukawa 2008]. It includes a Short Term Program estimated in 7 years during which the prototype miniFUJI reactor would be built, a Middle Term Program, estimated in 14 years from the initial start of the miniFUJI, during which the small molten salt power station FUJI would be built, and a Long Term Program, estimated 25 years from the start of the miniFUJI, during which the AMSB and regional fuel processing center would be constructed in order to complete the Symbiotic Thorium Breeding fuel cycle capable of satisfying the huge electric energy demand (see Figure 1). In the following sections the main features of each of these programs will be described.

### 4.1 miniFUJI reactor

The development program begins with the Pilot-plant: miniFUJI followed with the FUJI power reactor. The development of FUJI-series MSR is based on the reliable R&D at ORNL [Rosenthal M.W et al., 1972; Engel J.R et al., 1980; Zousyokuro Y., 1981]. Almost all reactor engineering problems were clarified and/or solved. Their experimental reactor 7 MWth MSRE successfully operated 17.655 hrs without any accident (1965-69). The operation time of molten-salt loops was 26.076 hrs corresponding to just 3 years. However, it was about 40 years ago, and such technology experience should be rebuilt by the operation of the pilot-plant (miniFUJI) [Furukawa K., et al., 1987; 1989; 1990].

The fuel salt does not need any irradiation test, and the development of the structural steel Hastelloy N was essentially finished and is currently on the phase of performing an endurance test of modified Hastelloy N. The time and expenditure required for the development of FUJI would be short and small. The "miniFUJI" will differ from the ORNL-MSRE, in that it will generate electricity of 7 MWe. The design contemplates a reactor-vessel of 1.8m in diameter and 2.1m in height [Harms A.A. & Heindler M., 1982] and with piping of 8 cm in diameter. Figure 9 shows a cross section of the miniFUJI. This facility could be commissioned in about 7 years. The demonstration reactor "FUJI" which will follow will be started with the detailed design work in parallel. [Furukawa, et al., 1983; Furukawa, et al., 1985] Table 5 provides comparative information of the main design parameters for the experimental MSRE operated at ORNL, the miniFUJI and the FUJI power reactor. [Furukawa, et al., 1992]

### 4.2 Production of $^{233}\text{U}$ in accelerator molten-salt breeder (AMSB)

During the 1980s, the technical feasibility of an accelerator-based nuclear fuel breeding facility AMSB [Baes C. F., 1969; 1974; McCoy Jr. H. E., 1967], was established based on a

“single-fluid target/blanket concept” using the same kind of molten salts as FUJI, except with a higher  $\text{ThF}_4$  content to establish an idealistic single-phase molten-fluoride fuel cycle. AMSB is composed of three parts: (1) a 1 GeV and 200–300 mA proton accelerator, (2) single-fluid molten-fluoride target/blanket system and (3) heat transfer and electric power recovery system. A diagram of the system is shown in Figure 10. The size of target/blanket salt bath is 4.5 m in diameter and 7 m in depth. The Hastelloy N vessel is protected by a graphite reflector.

The salt is introduced at the top forming a vortex of about 1 m in depth. The proton beam is injected in an off-centered position hitting near the bottom of the vortex to minimize the neutron leakage and to improve the generated heat dissipation. This target/blanket molten-salt system is sub-critical and is not affected by radiation unlike similar systems based on solid targets. This makes heat removal easy, and does not need target shuffling.

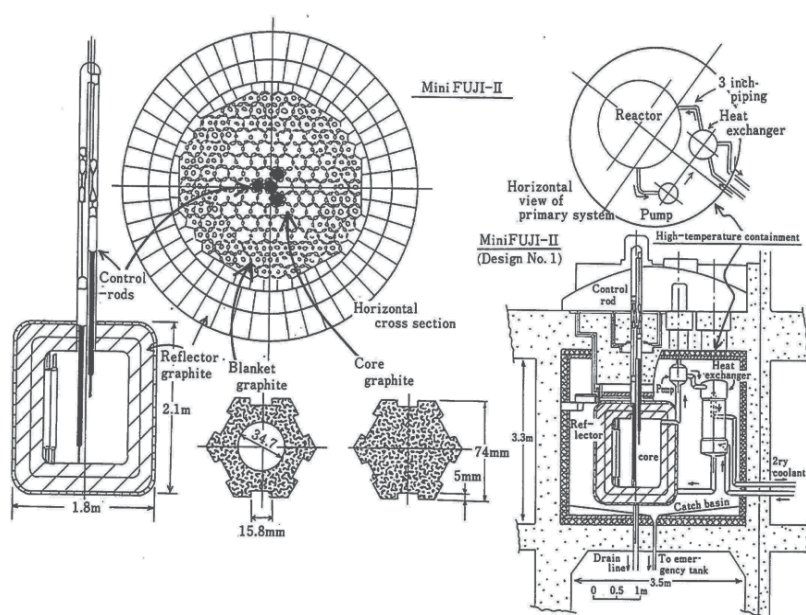


Fig. 9. Cross section of the miniFUJI reactor vessel and secondary containment housing the primary cooling circuit, control rod and the path for gravity fuel drainage.

The design of the beam injection port will be aided by improved gas-curtain technology. Engineering of this simple configuration, based on the MSR technology, will be manageable. The high proton current accelerator will utilize multi-beam funneling. The spallation neutrons transmute Th to  $^{233}\text{U}$  and also cause fission in the target. The following two items need to be considered. (i) Suppression of the fission of produced  $^{233}\text{U}$ , (ii) Utilization of the fission energy in the target/blanket salt for electric-power feedback for the operation of the AMSB. A heat output of about 1400MWth is required to achieve the power for the accelerator proton beam of 1 GeV, 300 mA. The above two requirements will be satisfied by adding Pu to the target salt composition; for example:  $\text{LiF}-\text{BeF}_2-\text{ThF}_4-^{233}\text{UF}_4-^{239}\text{PuF}_3$ : 64–18–17.15–0.3–0.55 mol%. The role of the Pu component is the same as FUJI-Pu, that is, burning itself and increasing the net production rate of  $^{233}\text{U}$ .

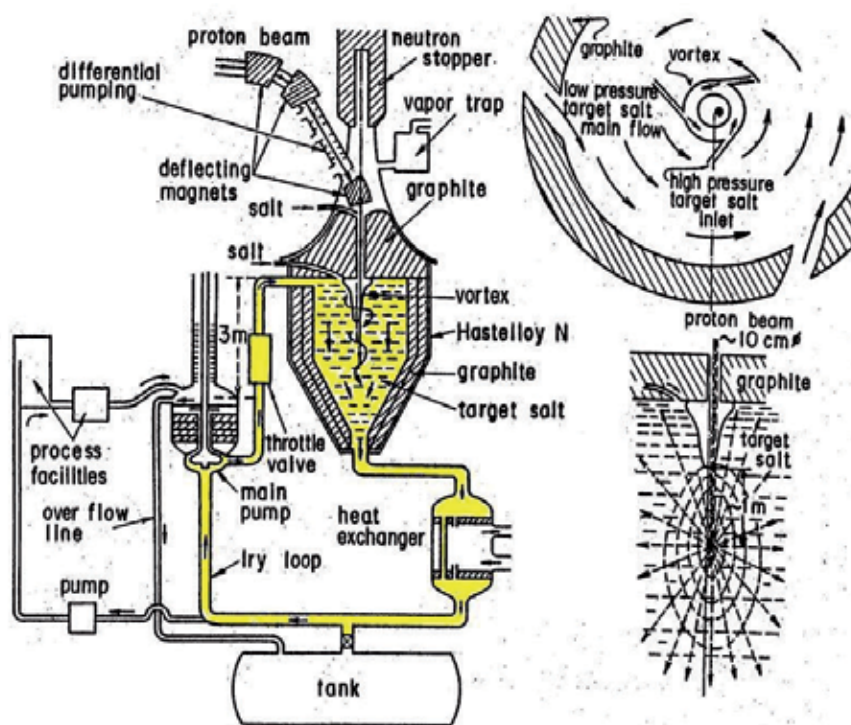


Fig. 10. Schematic diagram of single-fluid molten-salt target/blanket system in accelerator molten-salt breeder (AMSB).

The annual net production rate of  $^{233}\text{U}$  is about 700 kg/y under the following beam and target conditions: [Koger J.W., 1972] Proton beam: (1 GeV, 300 mA), Target/blanket size: 4.5 m in diameter, 6 m in depth; Initial fissile/fertile inventory: ( $^{233}\text{U}$ : 2.240 kg), ( $^{239}\text{Pu}$ : 4.200 kg), ( $^{232}\text{Th}$ : 28.000 kg). This performance can be improved by in situ chemical processing.

#### 4.3 Regional center chemical processing and fissile production

As mentioned previously the THORIMS-NES program contemplates three consecutive time terms leading to a global deployment opening of the Thorium Era in nuclear power utilization. The long term program, some 25 years after the initiation with the miniFUJI reactor (See 4.1), implies the building of medium and large size molten salt FUJI power stations (See 3.1), the establishment of fissile production: the Accelerator Molten Salt Breeder (See 4.2) (AMSB, AMSB-Pu), as well as the establishment of molten salt fuel processing units to supply the power stations.

These last two operations are highly sensitive about the issue of weapons proliferation as it implies the handling of tonnage quantities of sensitive  $^{233}\text{U}$ ,  $^{235}\text{U}$  and  $^{239}\text{Pu}$  fissile material as well as highly radioactive fission products and extremely long lived actinides for treatment or waste disposal. Hence these facilities should be built in specially planned, 20–30 bases or “Regional Centers”, heavily safeguarded under international supervision throughout the world. [Furukawa K., et al., 2008] Figure 11 shows in a block diagram the units, relationships and functions that the regional center would house.

As shown, after finishing the FUJI reactor life, the spent fuel-salt will be sent back to the “Regional Centers”. The salt is processed in batch mode for removal of  $^{233}\text{U}$ , other remaining fissile and some fission products (f.p.). Which elements are removed will be decided on the basis of optimization, material compatibility, neutron economy, cost economy, etc. [Harms A.A. & Heindler M., 1982]. The decontaminated diluents salt is adjusted to make-up to a suitable  $\text{ThF}_4$  content and charged to AMSB to keep constantly a 0.5 mole% in  $^{233}\text{U}$  content for the target/blanket salt. After starting the operation of AMSBs the thorium breeding cycle system will gradually be achieved. In the AMSBs (See 4.2), 1GeV/300mA proton accelerators produces about 400 kg/year of  $^{233}\text{U}$ .

The initial  $^{233}\text{U}$  inventory of FUJI-233U (160MWe) is about 800 kg, so each of the AMSB can support the commissioning of one FUJI-233U every two years. Also, high gain type AMSB with Pu can produce more  $^{233}\text{U}$  possibly resulting in an effective doubling-time of about 2~3 years and generate sufficient thermal output power to make the AMSB a self-sustained system, which will be able to start up sufficient numbers of FUJI reactors to meet the steep growth of energy demand.

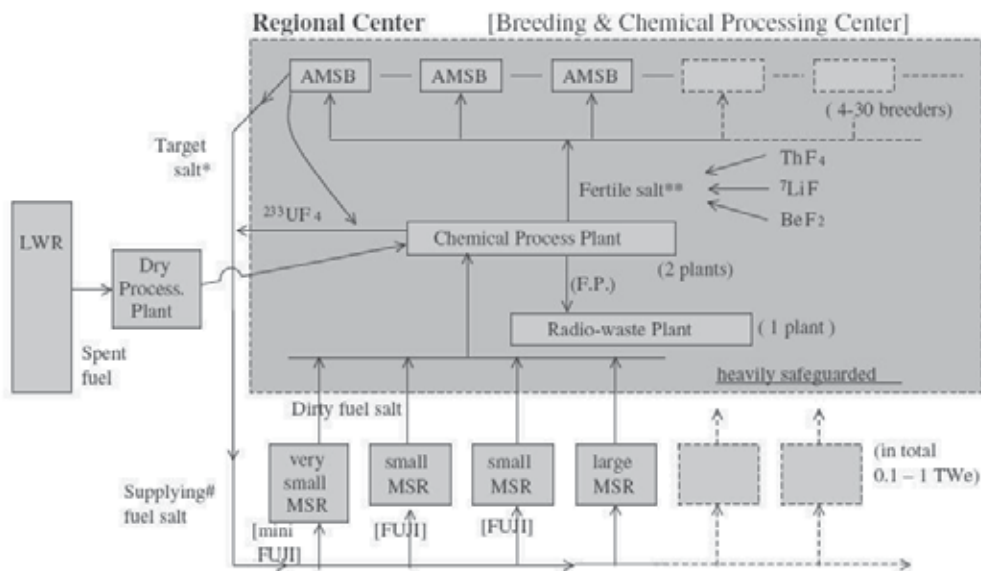


Fig. 11. Breeding & Chemical Processing Regional Center. Accommodating the AMSBs, chemical-processing plant and radio-waste plant. External input and output units are: Molten salt power reactors coupled by molten salt. The connection with the U-Pu cycle systems is shown via external or internal fuel processing plants.

The significant aspects of this fuel cycle are the followings: The total system is simply integrated by a single phase of molten fluorides based on  $^7\text{LiF}\text{-BeF}_2$  solvent, after doing some make-up in each component facilities. Each “Breeding & Chemical Processing Regional Center” (See Figure 11) will accommodate 4 to 10 AMSBs, two Chemical Processing Plants and one Radio-Waste Managing Plant. It is contemplated that on the long term several tens of centers will be built in different locations in the world.



## 5. Technical advantages of FUJI

### 5.1 Safety

FUJI and the AMSB are significantly safe reactors, and there is no possibility of "Severe accidents". [Furukawa K., et al., 2002] The most important safety properties are due to the following:

1. The system pressure is lower than 0.5 MPa (72 psi, 5.1 kg/cm<sup>2</sup>)
2. The fuel salt is chemically inert, is not reactive with air or water, and suffers no radiation damage.
3. The boiling point of the fuel salt is 1673K, much higher than the operation temperature 973K.
4. The fuel will only become just critical when it coexists with the graphite moderator. Therefore, leaked fuel salt will not be able to introduce re-criticality.
5. FUJI has a large negative prompt temperature reactivity coefficient. The temperature-coefficient of graphite is slightly positive, but controllable due to the slow temperature increase due on its large heat capacity.
6. The delayed-neutron yield of <sup>233</sup>U fission is smaller than that of <sup>235</sup>U, but it is controllable due to longer neutron lifetime, and large negative prompt temperature coefficient.
7. The fuel composition can be adjusted at any time if necessary. The excess reactivity is very small and the control-rod worth is also small. A large reactivity shift by control-rods is not required due to the very small excess reactivity in a MSR.
8. Gaseous fission products such as Xe, Kr and T are permanently removed from the fuel salt, and their leakage in accidents are minimized.
9. Provision for loss of coolant circulation: In an event of a catastrophic accident in which total power failure prevents power delivery to the fuel pumps, so that fuel circulation and residual heat removal from the reactor is interrupted, such as the accident at the Fukushima I power plant in Japan due to the earthquake and tsunami on March 11, 2011 [Fukushima, 2011] the reactor automatically shuts down without operator intervention. In FUJI reactors the fuel is already in the molten state and quite fluid. If fuel circulation stops, the temperature inside if the reactor would increase. The Freeze Valve will automatically melt open by lack of valve-cooling due to electric-power loss. The molten fuel salt will drain to the Emergency Drain Tank (see Figure 5) covered by a big borated water pool, which will be cooled by a NaK Heat-Pipe. Re-criticality cannot occur in such an event.
10. The triple confinement of radioactivity is ensured in FUJI like in the other solid-fuel reactors. The reliability of each barrier in FUJI is much higher depending not only on the above (1), (2), (3), (8) and (9), but also on the soundness of the first barrier, which is composed of a simpler reactor-vessel, piping and intermediate heat-exchanger that have very thick tube-walls working at low pressure and without any serious irradiation and thermal-stresses. The event of a "severe accident" will never occur in FUJI even assuming full stoppages of primary and secondary pumps resulting in a reactor scram.

Even in the case of "severe reactor destruction" by military attack or sabotage, FUJI might be the safer reactor compared with any other ordinary Solid Fuel Reactors owing to the following: 1.- Only a weak release of gaseous radioactivity due to the continuous fission-gas removal. 2.- No core melt down, and no re-criticality due to the separation of graphite and fuel, which might be drained automatically and/or leaked. Leaked fuel-salt is solidified as a

stable glass confining radioactivity, and does not produce any troublesome aerosol (See 5.4). 3.- Graphite (MP: 4000K) with large heat-capacity and thermal conductivity is not easily fired by virtue of inexistence of high temperature heat-sources. Even if a fire started, simple suffocation extinction will be enough, because graphite is not wetted by the fuel salt.

## 5.2 Nuclear proliferation and terrorism resistance

The present  $^{238}\text{U}$ -Pu fuel cycle is difficult to protect, not only from nuclear proliferation but also from nuclear terrorism [Semenov B.A. and Oi N., 1993]. For example, an article in the US newspaper New York Times, 11<sup>th</sup> August, 2004, discussed that an "American Hiroshima" could take place by a 10-kiloton weapon at New York killing half a million people. Such a weapon could supposedly be stolen from Russia and transported undetected. This is because concealment of  $^{239}\text{Pu}$  or  $^{235}\text{U}$  is easy due to the very weak gamma activity.

On the other hand a weapon made from the Th -  $^{233}\text{U}$  fuel cycle is very difficult to conceal due to the very strong gamma activity of  $^{232}\text{U}$  associated with fissile  $^{233}\text{U}$  as explained below. (see also 2.2). Deputy-Director General, IAEA, Semenov and Oi (1993) stated that "Another way is to revisit the thorium/uranium cycle that is free of the stigma associated with plutonium."  $^{233}\text{U}$  in fuel salt inevitably contains small amount of  $^{232}\text{U}$  (about 500 ppm) and its daughter nuclides, produce very high radiation dose rates due to the high-energy gamma ray of 2.6 MeV from the daughter  $^{208}\text{Tl}$ .

Even if fuel salt is withdrawn from the core, Pa separation should be done in a short time, because the decay of  $^{233}\text{Pa}$  producing pure  $^{233}\text{U}$  is fast, with a half-life of 27 days. The separation is very difficult, because spent fuel salt has very high radiation, and about 50 tons of fuel salts are necessary for getting 1 SQ (Significant Quantity for a weapon): 8 kg of pure  $^{233}\text{U}$  from  $^{233}\text{Pa}$ . The required 50 tons of salt is more than the fuel inventory of FUJI. The theft of 1 SQ : 8 kg of ordinary (dirty)  $^{233}\text{U}$  is also very difficult due to the very low fissile concentration (about 1 wt%) and the reactor would stop. It would cause a lethal dose (about 1 Sv/h at 50 cm distance) of  $^{208}\text{Tl}$  to the possible criminals. To shield this substance for handling, lead of about 20 cm in thickness is necessary, resulting impossible to transfer and fabricate the nuclear explosives, and very easy to detect by the high gamma radiation. FUJI produces negligible Trans-U elements (TRU: Np, Pu, Am and Cm) by virtue of the lower nuclear mass of fertile  $^{232}\text{Th}$ , six units smaller than  $^{238}\text{U}$ . This fact will greatly contribute to the non-proliferation and an effective incineration of TRU by the Th-U cycle system. In general the weapon usability of  $^{233}\text{U}$  is classified information. But the specialist of proliferation issues of Lawrence Livermore National Laboratory (LLNL), W.G. Sutcliffe advised that " $^{235}\text{U}$  is most easily made into a weapon, Pu is next easily made into a weapon, and  $^{233}\text{U}$  is hardest and least desirable for a weapon", and "any of the above can be made into 'any old-type weapon' but a dedicated arsenal builder would prefer  $^{235}\text{U}$  or Pu rather than  $^{233}\text{U}$ . Therefore  $^{233}\text{U}$  is less "weaponizable." [Sutcliffe, W., 1994]

## 5.3 Radioactive waste management

The difficult radioactive waste management becomes significantly easier owing to negligible TRU production in THORIMS-NES [Furukawa K., et al., 1991; David S., et al., 2007]. The production of Pu and Am + Cm in FUJI are 0.5 kg and 0.3 g Am + Cm for every 1 GWe y, respectively, i.e. very small compared to about 230 kg Pu and 25 kg Am + Cm in Light Water Reactors. Furthermore, avoiding solid fuel fabrication results in a lower production of low level radioactive waste and the need for maintenance.



In the long term after about year 2070, the recession age of the Thorium Era as shown in Figure 1, some very long-lived radioactive wastes should be transmuted to stable isotopes using the neutron capture reaction. Such work is not easy within the ordinary fuel-cycle. However in THORIMS-NES huge amounts of low-cost neutrons could be easily obtained, because excess fissile fuels could be burned out generating neutrons for this purpose. The circulating molten-fluoride system is the “best medium” for transmutation work due to the high solubility of several kinds of ions, good reaction-heat reservoir and no radiation damage. This is the case for both circulating systems: FUJI, a thermal neutron system, and AMSB, a fast neutron system. Considering this scheme, managing the radioactive waste becomes not a “Million Years” issue but rather a “Hundred Year” problem. This argument is shown in Figure 12 where the radio toxicity of nuclear waste is presented as a function of storage time. [Adapted from David S., et al., 2007]

On the issue of management of non-nuclear materials at the end of reactor life: All components would be sent back to the regional centers for reuse or disposal. (see 2.5) Hastelloy N would mostly be re-melted and recycled and graphite, that has received low irradiation levels, would be reused after grinding the surface to 0.1 mm depth thus minimizing production of low level radioactive waste.

#### 5.4 Operation and maintenance

Reactor systems in THORIMS-NES are quite safe (See 5.1), and their operation and maintenance simple and easy. Some additional evidence of this are: 1.- The reactor vessel is not opened in its life, and the control rods are very few (or no rods might be feasible). The reactor vessel is a simple welded tank without any big flange or fuel-handling machine. 2.- The primary circuit system is confined inside a high-temperature containment at about 810K, which results in a simpler reactor configuration without any heater, insulator, neutron shield or instrumentation with the exception of some flow-meters and surface-level meters, etc. Therefore, fully remote maintenance, inspection and repairing would be easier, without any worker’s exposure. The recent advances of robot technology are a great benefit. 3.- In the unlikely case of leakage of fuel salt, the bottom of the high-temperature containment is a spill-pan, whereby leaked salt is guided to the drain-tank. (See Figure 5) If necessary, the salt can be washed out by clean carrier salt ( ${}^7\text{LiF}\text{-BeF}_2$ ). 4.- A MSR has excellent load-following ability by virtue of the liquid fuel and the removal of poison gas  ${}^{135}\text{Xe}$ . The output power can be controlled by the fuel salt flow rate due to its negative temperature coefficient of reactivity not using the control rod. In the event of a lowering of temperature the salt freezes as a water-insoluble glassy matter stably sticking on the walls. The reactor building will be negligibly contaminated not as in an “Aqueous Homogeneous Reactors” [Lane J.A., et al., 1958], where radioactive aerosol will be dissipated after fuels dry up.

As MSR (FUJI-233U or FUJI-Pu) are self-controllable, the operational work is simple comprising the following main items: (a) off-gas management, (b) redox electrochemical potential control of the fuel salt, and (c) semi-periodical additions of Th, Pu and/or U in the eutectic-salt forms: [Th]  ${}^7\text{LiF}\text{-29 mole } \% \text{ ThF}_4$  (MP: 838 K), [Pu]  ${}^7\text{LiF}\text{-19.5 mole } \% \text{ PuF}_3$  (MP: 1016 K), and [U]  ${}^7\text{LiF}\text{-27 mole } \% \text{ UF}_4$  (MP: 763 K). Th is added once per year holding the variation to less than 1 wt %. The chemical balance due to the fission reaction of  ${}^{233}\text{UF}_4$  will introduce some excess free F atoms, which is controlled by Be addition. But in FUJI-Pu the main fission depends on  ${}^{239}\text{PuF}_3$ , and neutrality will nearly be held. By the above additions of fuel components,  ${}^7\text{LiF}$  content will increase, which will be corrected by  $\text{BeF}_2$  addition. Component additions are achieved by the use of the above eutectic salts.

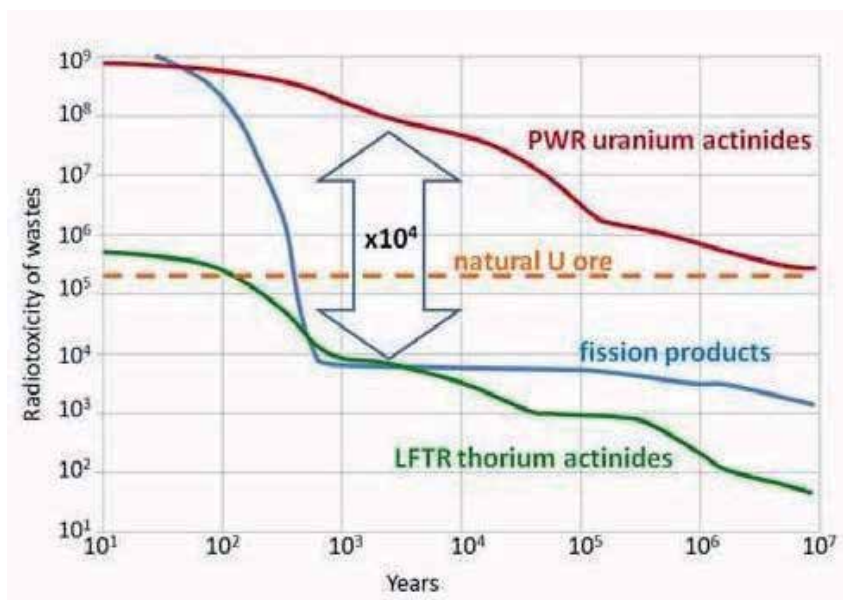


Fig. 12. Comparison of the radio toxicity of nuclear waste produced by a uranium-based PWR to that produced by a Liquid Fueled Thorium Reactor (LFTR) as a function of years of decay time. [Adapted from David S., et al., 2007].

## 6. Conclusion

One of the most promising philosophical and technical strategies for the world survival in this century has been presented. Although many more detailed design and optimization studies are needed and should proceed with international cooperation, we have to start from the very simple pilot-plant, miniFUJI, to rapidly demonstrate the rational technological integrity of THORIMS-NES and to make the initial step into the Thorium era.

We hope that our work will be valuable as a reply to the sincere wish of David E. Lilienthal [Lilienthal D. E., 1980] a most significant American/Human of the 20th century, given on the final sentence of his last book "Atomic Energy: A New Start": "What I have reflected upon and written about is not merely a new source of electrical energy, nor energy as an economic statistic. My theme has been our contemporary equivalent of the greatest of all moral and cultural concerns—fairness among men and the endless search for a pathway to peace."

For such purpose, "I have proposed that we make a new start toward a safer peaceful atom, using a technology that will not, as the present technology does, produce bomb material in the process of creating the peaceful atom." And he recommended to us that "We need to back away from our present nuclear state in order to find a better way, a route less hazardous to human health and to the peace of the world and its very survival."

One of the authors (K.F.) deeply benefited from the strong support of Bernal [Brown A., 2005] in his early scientific work on inorganic liquid structure chemistry as a base of this work. Bernal was also one of the scientists who were most concerned to achieve a "World without War" [Bernal J. D., 1958], and was the first to use the phrase "weapons of mass

destruction". On his birthday towards the end of his life he wrote: "I am sure that you share my hope that in the not too distant future science may come to be used for the benefit of all mankind"

## 7. Acknowledgements

In order to create this work we received a lot of cooperation, support and encouragement from a large number of people worldwide in the past 40 years. While I cannot mention all the names, I would like to express sincere and deep thanks for all their help, partially presenting some names eliminating the title as the followings: Japan: E. Nishibori, S. Kaya, K. Kamei, E. Takeda, N. Husimi, N. Saito, T. Ishino, N. Watanabe, K. Tsukada, Y. Nakahara, A. Furuhashi, K. Mitachi, R. Yoshioka, Y. Shimazu; USA: A.M. Weinberg, H.G. MacPherson, L. Lidsky, M.W. Rosenthal, A.W. Trivelpiece, W.R. Grimes, F.C. Reicle, D.R. deBoisblanc, J.R. Engel, U. Gat, R. Moir, J. Pleasant, A. Bromley, J. Gibbons; France: A. Lecocq, C. Bienvenu, M. Chemla, M. Gaune-Escard; USSR, Russia: V.N. Novikov, I.V. Chuvillo, G.V. Kiselev, E.N. Avrorin, V.A. Simonenco; Belarus: S. Chigrinov, A. Kievitskaya; Czech: I. Peka, P. Hosnedl, O. Matal, J. Uhlir, M. Fiala; India: P.K. Iyengar, D.D. Sood, A.K. Kakodkar; Canada: A.A. Harms, G.A. Bartholomew, etc.

## 8. References

- Oak Ridge National Laboratory (ORNL) reports in this reference list, accessed March 2011, are available at <http://energyfromthorium.com/pdf/>
- Baes Jr. C.F. (1969) *The Chemistry and Thermodynamics of Molten Salt Reactor Fuels* In: P. Chiotti, Editor, *Nucl. Metal, Symposium on the Reprocessing of Nuclear Fuels*. 15 (1969), p. 617 USAEC-Conf.-690801.
- Baes Jr. C. F., (1974) *The chemistry and thermodynamics of molten salt reactor fuels*. *J. Nucl. Mat.*, 51, (1) 149-162
- Brown A. (2005) J.D Bernal. *The sage of science*. Oxford University Press.
- Bernal JD. (1958). *World without war*. London: Routledge & Kegan Paul Ltd.
- Cantor S. Ed. (1968) *Physical Properties of M. S. Reactor Fuel, Coolant, and Flush Salts* ORNL-TM-2316.
- David S., Huffer E., & Nifenecker H. (2007). Revisiting the thorium-uranium nuclear fuel cycle. *Europhysics news*, 38(2), (March-April 2007) 24-27 DOI: 10.1051/EPN:2007007
- Delpech S., Merle-Lucotte E., Heuer D., Allibert M., Ghetta V., Le-Brun C., Doligez X. & Picard G.. (2008) *Reactor physic and reprocessing scheme for innovative molten salt reactor system*. *Journal of Fluorine Chemistry* 130 (2009) 11-17. doi:10.1016/j.jfluchem.2008.07.009
- Engel J. R., Grimes W.R., Bauman H. F., McCoy E. H. Dearing J. F. & Rhoades W. (1980) A. *Conceptual design Characteristics for a Denatured Molten-Salt Reactor with Once-Through Fueling*. ORNL/TM-7207 July 1980.
- Fukushima. (2011) Accessed March 2011. Available at: [http://en.wikipedia.org/wiki/Fukushima\\_I\\_Nuclear\\_Power\\_Plant](http://en.wikipedia.org/wiki/Fukushima_I_Nuclear_Power_Plant)

- Furukawa K. & Ohno H. (1978) Establishment of Corresponding-state Principle in Molten Fluoroberyllates and Silicates and Its Application. *Trans. J. Inst. Met.* 19, 553-561;
- Furukawa K. (1980) *Koubutugaku-zasshi*, 14 (2), 34 (in Japanese)
- Furukawa K. & Ohno H. (1980) *Data-Books Molten Materials:1. Molten  ${}^7\text{LiF-Bef}_2$  (Flibe) System*, Japan Nucl. Ene. Information Center.
- Furukawa K., Kato Y., Ohmichi T. & Ohno H. (1985) [Japan-US Seminar on Th Fuel Reactors (Oct.1982, Nara)] *Th Fuel Reactors*, Atom. Ene. Soc. Japan, p.271. [Russian Trans.:Atomnaja Teknikaza Rubezom, 1983 [6] 23 (1983) ]
- Furukawa K., Minami K., Oosawa T., Ohta M., Nakamura N., Mitachi K. & Kato Y., (1987). *Emerg. Nucl. Ene. System (Proc. 4th ICENES)*, World Sci., p.235.
- Furukawa K., Minami K., Mitachi K. & Kato Y. (1987) Molten Salts (Ed. G. Mamantov), PV87-7, p.896 *The Electrochem. Soc. Proc. Ser.*, Pennington, NJ.
- Furukawa K., Minami K., Oosawa T., Ohta M., Nakamura N., Mitachi K. & Katoh Y. (1987) Design study of small molten-salt fission power station suitable for coupling with accelerator molten-salt breeder. *Emerg. Nucl. Ene. System (Proc. 4th ICENES)*, World Sci., p. 235
- Furukawa K. Minami K., Mitachi K. & Kato Y. (1989) *High-safety and economical small Molten-salt Fission Power Stations and their developmental program--Th Molten-salt Nuclear Energy Synergetics (THORIMS-NES)*. *Alternative Energy Sources VIII, Vol.2*, Hemisphere Pub. p.2.
- Furukawa K. Lecocq A. Kato Y. & Mitachi K. (1990) Summary Report: Thorium Molten-Salt Nuclear Energy Synergetics. *J. Nucl. Sci.Tech.*, 27, 1157-1178
- Furukawa K., Lecocq A., Kato Y. & Mitachi K. (June, 1991). Radiowaste management in global application of Thorium Molten-Salt Nuclear Energy Synergetics with Accelerator Breeders. *Saltsjobaden, SWEDEN, LA-12205-C, 686 (1991); UC-940, p.686 (1991)*.
- Furukawa K., Mitashi K., Kato Y. (1992) Small molten-salt reactors with a rational thorium fuel cycle. *Nuclear Engineering and Design*. 136, 157-165.
- Furukawa K., Mitachi K. & Kato Y. (1992) Design study of small MS fission power station *Nucl. Engine. & Design*, 136, 157-65
- Furukawa K. (2001) "*The Revolution in Nuclear Power Plants (Gennpatsu Kakumei)*", Bunsyun-Sinsyo No.187 Bungei-syunjyuu Pub.Co. (in Japanese)
- Furukawa K., Simonenko V., Mitachi K., Furuhashi A., Yoshioka R., Chigrinov S.E., Lecocq A. & Kato Y. (2002) *Th Fuel Utilization: Options and Trends*. IAEA-TECDOC-1319. p.123.
- Furukawa K., Numata H., Kato Y., Mitachi K., Yoshioka R., Furuhashi A., Sato Y. & Arakawa K., (2005) New Primary Energy Source by Thorium Molten-Salt Reactor Technology. *Electrochemistry*, 73, No. 8. 552-563
- Furukawa K., Numata H., Kato Y., Mitachi K., Yoshioka R., Furuhashi A., Sato Y. & Arakawa K. (2005). New Primary Energy Source by Thorium Molten-Salt Reactor Technology. *Electrochemistry*. 73:552-63.
- Furukawa K. (2006). *New nuclear energy system advantages for nuclear nonproliferation THORIMS-NES: thorium molten-salt nuclear energy synergetics*. In: The 22nd Eisaku Sato (Nobel Pease Prize Laureate) Memorial Prize Essay, June

- Furukawa K., Arakawa K., Erbay L. B., Ito Y., Kato Y., Kiyavitskaya H., Lecocq A., Mitachi K., Moir R., Numata H., Pleasant J., Sato Y., Shimazu Y., Simonenco V. A., Sood D. D., Urban C & Yoshioka R. (2008) A road map for the realization of global-scale thorium breeding fuel cycle by single molten-fluoride flow. *Energy Conversion and Management* 49, 1832–1848
- Furukawa K. & Erbay, L. B. (2010) A Study On A Global-Scale Symbiotic Thorium Breeding Fuel Cycle. 2<sup>nd</sup> International Conference on Nuclear and Renewable Energy Resources. 7 July 2010 Ankara TURKEY
- Ganesan S. Sharma, Amit Raj & Wienke, H. (2002). New investigations of the criticality property of pure <sup>232</sup>U. *Annals of Nuclear Energy* 29, 1085–1104.
- Grimes W. R.(1969) *Molten-Salt Reactor Chemistry* Oak Ridge National Laboratory. Accessed March 2011. Available at:  
[http://energyfromthorium.com/pdf/NAT\\_MSRchemistry.pdf](http://energyfromthorium.com/pdf/NAT_MSRchemistry.pdf)
- Hannum, W. H., Marsh G. E. & Stanford G. S. (2005). Smarter use of nuclear waste. *Scientific American* Special subscriber edition: Energy's Future, breaking the boundaries. Scientific American Inc. pp. 14-21
- Harms AA, & Heindler M. (1982) *Nuclear energy synergetics*. New York: Plenum Press; [trans. Japanese by K. Furukawa et al. (1986) Kakuenerugi Kyoudousisutemu Gairon, Baifuukann.
- Häussinger P., Lohmüller R. & Watson A. M. (2002) "*Hydrogen*" Ullmann's Encyclopedia of Industrial Chemistry, Wiley-VCH, Weinheim.
- Houtzeel A. & Dyer F. F. (1972) A study of fission products in the Molten-Salt Reactor Experiment by Gamma. Spectrometry. August 1972. ORNL-TM-3151
- Haynes International, Inc. (2002) *HASTELLOY® N alloy*. Kokomo, Indiana 46904-9013 (USA). Accessed March 2011. Available at: <http://www.haynesintl.com/>
- Hoyle Fred (1977). *Energy or Extinction? Case for Nuclear Energy* (ISBN: 0435544306 / 0-435-54430-6 ) Heinemann Educational Publishers. UK.
- IAEA (2000) *Th based fuel options in the 1990s*, IAEA-TECDOC-1155, p.7.
- IAEA (2007) *Status of Small Reactor Designs Without On-Site Refueling*. IAEA-TECDOC-1536, 2007, ISBN 92-0-115606-5, p.821-856.
- Ignatyev V., Novikov V. M., Surenkov A. I. & Fedulov V. I., (1993) IAE-5678/11, Kurchatov Inst.
- Iodine Pit (2011). Accessed March 2011. Available at:  
[http://en.wikipedia.org/wiki/Iodine\\_pit](http://en.wikipedia.org/wiki/Iodine_pit)
- Janz G. J., Allen C. B., Downey J. R. & Tomkins R. P. T. (1978) Physical Properties Data compilations relevant to energy storage. 1. Molten salts. Eutectic data. NSRDS US Department of Commerce. National Bureau of Standards. March 1978. Accessed March 2011. Available at: <http://www.nist.gov/data/nsrds/NSRDS-NBS-61-1.pdf>
- Keiser J. R., (1977) Status of Tellurium–Hastelloy N Studies in Molten Fluoride Salts. ORNL/TM-6002.
- Kennedy Joseph W. (1950) *Lithium Isotope Separation By Electrolysis*. Los Alamos Scientific Laboratory L.A-1156 September 4, 1950

- Kightower J. R., Jr. McNeese L. E., Hannaford B. A. & Cochran H. D., Jr (1971) *Low-pressure distillation of a portion of the fuel carrier salt from the Molten Salt Reactor Experiment* ORNL-4577. August 1971
- Koger J.W. (1972) Salt corrosion studies. p.124 in Rosenthal M. W., Briggs R. B., Haubenreich P. N. (1972) *Molten Salt Reactor Program Semiannual Progress Report for Period Ending August 31,1972*. Oak Ridge National Laboratory ORNL-4832
- Lane J.A., MacPherson H.G. & Maslan F. Eds (1958) *Fluid Fuel Reactors*. Addison-Wesley Publishing Co. p.1.
- Lilienthal D. E. (1980). *Atomic energy: A new start*. New York: Harper & Row Publ;
- Marchetti C. (1985) Nuclear plant and nuclear niches: on the generation of nuclear energy during the last twenty years. *Nucl. Sci. Eng.*; 90:521–6; Marchetti C & Nakicenovic (1987) *The Dynamics of Energy Systems and the Logistic Substitution Model*. Research Report-79-13, Laxenburg, Austria: *Int. Inst. Appl. System Anal.*; Marchetti C. (1988) In: 7th World hydrogen conf, Moscow, September; Marchetti C. (1992) *Perspect Energy*;2:19–34.
- McCoy H. E. Jr., (1967) An evaluation of the molten salt Reactor Experiment Hastelloy N Surveillance Specimens –First Group. ORNL-TM-1997.
- Megatons to Megawatts (2010). The Megatons to Megawatts™ Program is a commercially financed US government-industry partnership in which bomb-grade highly enriched uranium (HEU) from dismantled Russian nuclear warheads is being recycled into low enriched uranium (LEU) used to produce fuel for American nuclear power plants. USEC, is the executive agent for the U.S. government, and Techsnabexport (TENEX), acts for the Russian government. It is a 20-year program. To date (Dec., 2010) 412 metric tons of bomb-grade HEU has been recycled into 11,905 metric tons of LEU, equivalent to 16,494 nuclear warheads eliminated. Natural uranium is delivered by USEC to TENEX. The program's total value is approximately \$12 billion. Accessed March 2011. Available at <http://www.usec.com/megatonstomegawatts.htm>
- Mitachi K., Furukawa K., Murayama M. & Suzuki T. (1994) Emerging Nuclear. Energy Systems *ICENES'93*, World Sci., p.326;
- Mitachi K. & Furukawa K. (1995). Neutronic Examination on Plutonium Trans mutation by a Small Molten-Salt Fission Power Station IAEA-TECDOC-840, p.183
- Moniz E.J. & Neff, T.L., 1978. Nuclear power and nuclear weapons proliferation. *Physics Today*, April 1978, p. 42.
- Novy I. Peka, I. Chochlovsky, (1989) *The Technological Project of the Fluoride Volatility Process for the Reprocessing of the Spent Fuel from FBR* (in Czech), NRI Report-9081 Ch, T, NRI Rez. Czech Republic.
- Ohno H. & Furukawa K. (1972) *Alkali-fluoroborates*, JAERI-M 5053, 61pp, Japan Atom. Ene. Res. Inst. (Oct.1972).
- Olander D.R. (1976) *Fundamental aspects of nuclear reactor fuel elements*. Technical Report TID-26711-P1. 624 Pages. California Univ., Berkeley (USA).
- ORNL (1969) Rosenthal M. W., Briggs R. B. & Kasten P. R. *Molten salt Reactor Program Semiannual Progress Report*. February 28, 1969. ORNL-4396. USA. p.200

- ORNL WASH-12 2 2.(1972) *An Evaluation Of The Molten Salt Breeder Reactor*. September 1972
- ORNL (1972) Rosenthal M. W., Haubenreich P. N. & Briggs R. B.. *The Development Status of Molten-Salt Breeder Reactors. MSR Program Semiannual Progress Report*, August 1972. ORNL-4112. USA. p.146.
- ORNL-5132, (1976). *Molten-salt Reactor Program, Semiannual Progress report for Period ending February 29, 1976*, 7-12
- ORNL reports (2010) A collection of the reports of work related to nuclear energy and the Molten Salt Reactor Project at ORNL may be found. Accessed March 2011. Available at: <http://energyfromthorium.com/pdf/>
- Pfeffer J. I. & Nir S. (2000). *Modern Physics: An Introductory Text*. Imperial College Press. pp. 421 ff. ISBN 1860942504. Accessed March 2011. Available at: [http://en.wikipedia.org/wiki/Iodine\\_pit](http://en.wikipedia.org/wiki/Iodine_pit)
- Reynolds W. N., (1966). In: *Chemistry and Physics of Carbon*. Edited by: P. L. Walker Jr. Marcel Dekker New York Vol. 2 , p121 (1966)
- Rosenthal M. W., Briggs R. B. & Haubenreich P. N. *Molten-Salt Reactor Program Semiannual Progress Report. Period Ending August 31, 1970* ORNL-4622 8
- Rosenthal M.W. , Haubenreich P. N. & Briggs R. B. (1972) *The Developmental Status of Molten-Salt Breeder Reactors*, ORNL-4812
- Schutcliffe William G. (1994) Private communication.
- Semenov B.A. & Oi N. (1993). Nuclear fuel cycles: Adjusting to new realities IAEA Bulletin, 1993 – Vol. 35, Issue 3, p. 2-7.
- Sorensen K. (2010). Accessed March 2011. Available at: <http://energyfromthorium.com/pdf/>
- Sorensen, Kirk (2010) Remark during the “Media Session” at the Thorium Energy Conference 2010, London, UK, October 17 – 20. Hosted by itheo.org. Accessed March 2011. Available at: <http://itheo.org/>
- Stacey, W. M. (2007). *Nuclear Reactor Physics*. Wiley-VCH. p. 213. ISBN 3527406794.
- Thoma R. E (1975) *Advances In Molten Salt Chemistry*. Vol.3, p.275.
- Uhlir Jan. (2011) *An Experience On Dry Nuclear Fuel Reprocessing In The Czech Republic*. Accessed March 2011. Available in : <http://www.oecd-nea.org/pt/docs/iem/mol98/session2/SIIpaper9.pdf>
- Yang H, He N., Tang G., Li Y. & Zhang Y.; (2010) Growth kinetics of boride layer by molten salt electrodeposition. Mechanical and Electrical Technology (ICMET), 2010 2nd International Conference. : Singapore 10-12 Sept. 2010. ISBN: 978-1-4244-8100-2 pp 323 - 326
- Yoyuenn Zousyokuro (1981) (MSBR) Rev. Ed., Atom. Ene. Soc. Japan (in Japanese).
- Weber, H.W., Böck, H., Unfried E. & 31 Greenwood L.R. (1986). Neutron dosimetry and damage calculations for the TRIGA MARK-II reactor in Vienna. *Journal of Nuclear Materials*. 137, Issue 3, February, 236-240
- Weinberg A.M. (1997) The proto-history of the molten salt system. *J. Accel. & Plasma Research*, 2(1) 23-26.

Whatley M.E., McNeese L.E., Carter W.L., Ferris L.M. & Nicholson E.L., 1970, Engineering development of the MSBR fuel recycle", *Nuclear Applications and Technology*, vol. 8, 170-178.

Zousyokuro Yoyuuenn (1981) Rev. Ed., Atom. Ene. Soc. Japan (in Japanese).



## **Part 6**

# **Advances in Energy Conversion**



# Water Splitting Technologies for Hydrogen Cogeneration from Nuclear Energy

Zhaolin Wang and Greg F. Naterer

*Clean Energy Research Laboratory, Faculty of Engineering and Applied Science,  
University of Ontario Institute of Technology (UOIT), Ontario,  
Canada*

## 1. Introduction

Currently, nuclear energy is mainly utilized for the generation of electricity that is distributed to end users via power transmission networks. However, there are also other distribution forms. For example, hydrogen produced from nuclear energy is a promising future energy carrier that can be delivered to end users for purposes of heating homes, fuel supply for hydrogen vehicles and other residential applications, while simultaneously lowering the greenhouse gas emissions of otherwise using fossil fuels [Forsberg, 2002, 2007]. Current industrial demand for hydrogen exists in the upgrading of heavy oils such as oil sands, refineries, fertilizers, automotive fuels, and manufacturing applications among others. Hydrogen production is currently a large, rapidly growing and profitable industry. The worldwide hydrogen market is currently estimated at about \$300 billion per year, growing at about 10% per year, growing to 40% per year by 2020 and expected to reach several trillions of dollars per year by 2020 [Naterer et al., 2008]. This chapter will examine the usage of nuclear energy for the cogeneration of electricity and hydrogen with water splitting technologies.

In section 2 of this chapter, various hydrogen production methods will be briefly introduced and compared. The potential economics and reduction of greenhouse gas emissions with nuclear hydrogen production are examined. In section 3, matching the heat requirements of various thermochemical hydrogen cycles to the available heat from nuclear reactors (especially Generation IV) will be studied from the aspects of heat grade, magnitude, and distribution inside the cycles. The requirement of an intermediate heat exchanger between the nuclear reactor and hydrogen production plant is discussed. Long distance heat transport is examined from the aspects of the performance of working fluids, flow characteristics, and heat losses in the transport pipeline. In section 4, layout options for the integration of nuclear reactors and hydrogen production plants are discussed. In section 5, modulations of nuclear energy output and hydrogen cogeneration scales are studied, regarding the increase of the nuclear energy portion on the power grid through the adjustment of the hydrogen production rate so as to lower the needs for fossil fuels. The options for keeping the total nuclear energy output at a constant value and simultaneously varying the electricity output onto the power grid in order to approach a load following profile for peak and off-peak hours are discussed. In section 6, conclusions are provided for the cogeneration of hydrogen with nuclear heat.

## 2. Environmental and economic benefits of nuclear hydrogen production methods

The growing demand for hydrogen will have a significant impact on the economy. However, currently the major production methods for hydrogen are not clean, although its usage is clean. More than 95% of the global hydrogen is directly produced from fossil fuels, i.e., about 48% from steam methane reforming (SMR), 30% from refinery/chemical off-gases, and 18% from coal gasification [NYSERDA, 2010; IEA, 2010]. Water electrolysis accounts for less than 4%, and even this 4% is not “clean” because the electricity used is not fully generated from clean sources. The usage of fossil fuels to produce hydrogen has been resulting in major greenhouse gas emissions and other hazardous pollutants. Table 1 shows the CO<sub>2</sub> emission levels of various production methods [Wang et al., 2010]. On average, the CO<sub>2</sub> emissions are 19 tonnes per tonne of hydrogen production, which results in 959 million tonnes of CO<sub>2</sub> emissions per annum. Therefore, the future hydrogen economy must be based on clean production technologies.

Scientists and engineers have been attempting for years to develop new technologies for clean and efficient hydrogen production. Among the technologies, photoelectrochemical water splitting, water electrolysis with off-peak hours electricity, high temperature electrolysis (HTE), and thermochemical water splitting are promising clean options. To evaluate these options, the clean extent of the energy source, thermal efficiency and economics are the three major criteria. In terms of the clean extent, photoelectrochemical water splitting utilizes sunlight to split water into hydrogen and oxygen [Sivula et al., 2010]. However, due to the intermittent nature of sunlight, this production method cannot deliver a continuous flow of hydrogen production at night and other times when sunlight is not available. Water electrolysis can utilize off-peak hour electricity from the power grid that can improve the hydrogen production economics, due to the lower price of electricity at off-peak hours. However, it may not be clean production because the power sources contributing to the power grid are not fully clean. As shown in Table 1, water electrolysis cannot even provide a better scenario than steam methane reforming and coal gasification if using the existing power grid. To make the water electrolysis “clean”, the electricity must be derived from a clean source. Regarding high temperature electrolysis and thermochemical water splitting methods that utilize some heat as a portion of energy input, the same situation exists because the heat must also be derived from clean sources so as to deliver a clean production method. Solar, wind, and nuclear energy are sustainable options for energy sources [Steinfeld, 2005; Schultz et al., 2003; Kreith et al., 2007]. Among these options, nuclear energy is more mature and widespread than solar and wind in current industry. Overcoming the intermittency of solar and wind energy is a long-term challenging task. Therefore, to integrate nuclear power with hydrogen production is a promising option.

Method	SMR	Coal gasification	Water electrolysis
CO <sub>2</sub> emissions <sup>(a)</sup> CO <sub>2</sub> /H <sub>2</sub> (Moles /mole)	0.51	1.21	1.00 <sup>(b)</sup>
(a) Heat from fossil fuel combustion and electricity from the existing power grid. (b) 84% of the electricity from fossil power generation (Alberta, Canada [Government of Alberta, 2008]).			

Table 1. CO<sub>2</sub> emissions with current production methods and energy sources

In terms of production efficiency, the thermal efficiency of a hydrogen production cycle can be defined as follows:

$$\varepsilon = \frac{\Delta H_f}{\Delta H_{NetInput} + \Delta E_{Electrolysis}} \times 100\% \quad (1)$$

where  $\Delta H_f$  is the formation enthalpy of water with the value of 286 kJ/mol  $H_2O$ ,  $\Delta E_{Electrolysis}$  is the electrical energy required for the process of electrolysis, and  $\Delta H_{NetInput}$  is the net heat input to the cycle. Equation (1) can apply to conventional electrolysis, high temperature electrolysis, and thermochemical (either fully thermal or hybrid) water splitting cycles. If the value of  $\Delta H_{NetInput}$  is zero, then it indicates pure electrolysis. Conversely, if  $\Delta E_{electrolysis}$  is zero, it means a purely thermal water splitting process that only uses heat. If neither is zero, it is a hybrid process. The power generation process can be subdivided into three stages: (1) heat is generated from a nuclear reactor; (2) heat converts to mechanical energy by driving a steam or gas turbine, which makes an electric generator rotate; (3) rotation of electric generator produces AC electric power. Each stage inevitably experiences some heat loss. To produce hydrogen from conventional water electrolysis, all three stages are experienced, plus an additional stage of converting AC to DC. Therefore, although the conversion efficiency from DC electrical to chemical energy in a water electrolyzer could reach 80~90% [Forsberg, 2002, 2003], the overall thermal efficiency is only around 30%. The power generation efficiency of future nuclear reactors will be increased significantly, e.g., utilizing Generation IV nuclear reactors [WNA, 2010].

In terms of the economics of various hydrogen production methods, lower costs lead to better economics. In this chapter, the word "cost" is discussed in terms of monetary spending per unit of hydrogen, e.g., US\$/tonne  $H_2$ , in order to avoid confusion with the term "efficiency" because "cost" is often used interchangeably in place of efficiency in cost-effectiveness analyses and efficiency assessments.

Table 2 lists the thermal efficiencies and costs of various hydrogen production methods with nuclear energy on a comparative basis. Detailed thermal efficiency calculations and cost analyses were reported in past studies [Wang et al., 2010; Jean-Pierre Py et al., 2006; de Jong et al., 2009; Kreith et al., 2007]. In Table 2, the cost of steam methane reforming that utilizes the combustion heat of methane is also shown for a comparison since it is today's major production method. The S-I and Cu-Cl cycles are selected as typical thermochemical hydrogen production cycles that will be studied in subsequent sections. It can be found that the costs of various hydrogen production technologies with nuclear energy are similar to that of steam methane reforming, especially, thermochemical cycles integrated with Generation IV nuclear reactors, e.g., supercritical water-cooled reactor (SCWR). The cycles have the potential to deliver lower production costs than other methods.

Regarding the  $CO_2$  emissions of thermochemical cycles, as discussed previously, a hybrid cycle utilizes a portion of electricity for its electrolytic step. If the electricity is not derived from non-fossil fuel sources, then  $CO_2$  emissions will be generated. Table 3 shows the emission comparison for the current power grid and nuclear power plant. According to the structure of energy sources on the power grid, the emissions were estimated [Wang et al., 2010]. Comparing Tables 3 and 1, it can be observed that hydrogen production with thermochemical cycles and nuclear energy can lower the  $CO_2$  emissions by at least one order, regardless of the energy sources for electricity.

Condition \ Production	Thermochemical		HTE	Electrolysis	SMR
	S-I cycle	Cu-Cl cycle			
pricing year	2003	2003	2003	2003	2003
Nuclear reactor	VHTR	SCWR	GenIV	GenIII+	methane <sup>(a)</sup>
T, °C	950	650	800	650	700-- 1100
Price ratio $E_{\text{electricity}}/E_{\text{heat}}$	3	3	3	3	3
production efficiency	52%	52%	52%	41%	65~75%
ratio (capital recovery / operating cost)	0.77	0.40	N/A <sup>(b)</sup>	0.32	0.46
production scale (tonnes H <sub>2</sub> /day)	200	200	208		200
		(10)		10	
Cost, US \$/ kgH <sub>2</sub>	1.85	1.60	2.25		
		(2.31)		2.52	2.67

Note:

(a) Current SMR uses the combustion heat of methane.

(b) Not reported in literatures for industrial scale hydrogen production.

**Acronyms of nuclear reactors:**

GenIII+ (Advanced Generation III reactor), GenIV (Generation IV nuclear reactor), SCWR (Supercritical water reactor), VHTR (Very high temperature reactor).

**Acronyms of hydrogen production methods:**

Cu-Cl cycle (copper-chlorine thermochemical cycle), HTE (high temperature electrolysis), S-I cycle (sulfur-iodine thermochemical cycle), SMR (steam methane reforming).

Table 2. Costs of various nuclear powered hydrogen production methods.

Thermochemical cycle	S-I, fully thermal <sup>(a)</sup>	Cu-Cl, hybrid	
CO <sub>2</sub> emissions, CO <sub>2</sub> /H <sub>2</sub> (Moles /mole)	0	0	0.07 <sup>(b)</sup>

(a) Energy source for electricity generation has no influence on CO<sub>2</sub> emissions.  
(b) 84% of the electricity from fossil power generation [Government of Alberta, 2008].

Table 3. CO<sub>2</sub> emissions with nuclear powered thermochemical production methods

### 3. Thermal integration of thermochemical cycles and nuclear reactors

#### 3.1 Matching the temperatures of thermochemical cycles and nuclear reactors

Many thermochemical hydrogen production cycles have been developed to split water thermally through auxiliary chemical compounds and reactions. About two hundred thermochemical cycles were reported to produce hydrogen by thermochemical water splitting [Sadhankar et al., 2005; Forsberg, 2003]. Different cycles have various inputs of temperatures that must be provided by nuclear reactors. Table 4 shows the temperatures of some thermochemical cycles and nuclear reactors. Among these cycles, the sulfur-iodine (S-I) cycle is a leading example of purely thermal cycles that has been scaled up from proof-of-principle tests to a large engineering scale by the Japan Atomic Energy Agency (JAEA,

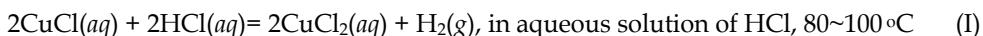
[Kubo et al., 2004]). Among the hybrid thermal cycles, the copper-chlorine (Cu-Cl) cycle is a leading example and its scale-up is underway at the University of Ontario Institute of Technology [Wang et al., 2010] in collaboration with its partners that include Atomic Energy of Canada Limited (AECL). The maximum temperature required by thermochemical cycles can be met by Generation IV nuclear reactors. The temperature requirement of the Cu-Cl cycle is much lower than that of other cycles. Therefore, the Cu-Cl cycle can more readily link with the heat output of various nuclear reactors due to its lower temperature requirement.

Cycle name	T, °C	Development status
M <sub>2</sub> SO <sub>4</sub> -NH <sub>3</sub> (metal sulphate - ammonia) cycles M: Zn, Mg, Ca, Ba, Fe, Co, Ni, Mn, Cu	1,100	Proof-of-principle
Mn-C (carbon dioxide - Manganese oxide) cycle	977	Proof-of-principle
Mn-Cl (manganese - chlorine) cycle	900	Proof-of-principle
S-Br (sulfur - bromine), Cr-Cl (chromium - chlorine), and V-Cl (vanadium - chlorine) cycles	850	Proof-of-principle
S-I (sulphur - iodine) cycle	850	Under scale-up
Ni-Fe (nickel - ferrite) cycle	800	Proof-of-principle
Mn-Na (manganese - sodium) cycle	800	Proof-of-principle
Fe-Ca-Br (ferrite-calcium-bromine) cycle	750	Proof-of-principle
Fe-Cl (ferrite - chlorine) cycle	650	Proof-of-principle
Hg-HgO (mercury - mercury oxide) cycle	600	Proof-of-principle
Cu-Cl (copper - chlorine) cycle	530	Under scale-up
<b>Reactors</b>		
Generations II and III	<450	Commercialized
Generations III+ and IV	>450	Under development

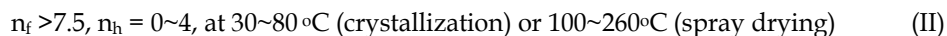
Table 4. Temperatures of thermochemical cycles and nuclear reactors

There are several types of Cu-Cl cycles with various numbers of steps from 2 to 5 depending on reaction conditions. Due to the lower efficiency and more engineering challenges of two-, three- and five-step cycles, the following cycle with 4 steps will be considered in this chapter [Wang et al., 2009]:

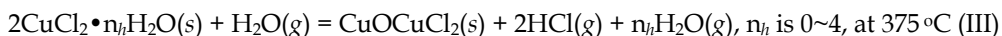
**Step 1.** Hydrogen production step (electrolysis)



**Step 2.** Drying step (endothermic)



**Step 3.** Hydrolysis step (endothermic)



**Step 4.** Oxygen production step (endothermic)



### 3.2 Matching the nuclear heat and hydrogen production requirements

Even if the temperature of a nuclear reactor can reach the maximum temperature requirement of 530°C, it may not match the heat distribution that is regulated by different temperatures at different steps. Table 5 shows the heat requirements of the Cu-Cl cycle [Wang et al., 2009]. It can be found that different steps occupy different heat percentages. If the heat source does not match the required distribution, then one or two steps may not be supplied with sufficient heat and simultaneously another one or two steps may be supplied with surplus heat. Therefore, the temperature of the heat source should cover the maximum temperature requirement of the Cu-Cl cycle, as well as provide a similar heat requirement structure.

Step	T, °C	Net heat input <sup>(a)</sup> kJ/mol H <sub>2</sub>	Compared with the total net heat input, %
I	<100	0	0%
II	<200	122.2	26.9%
III	≥375	181.8	40.1%
IV	≥530	149.4	33.0%
<b>Sum<sup>(b)</sup></b>		453.4 (226.7MJ/kg H <sub>2</sub> )	100%
(a) 50% of the heat released by exothermic processes of Cu-Cl cycle is recovered.			
(b) The sum includes all unlisted auxiliary processes for each step.			

Table 5. Heat requirements of the Cu-Cl cycle

The distribution of heat inputs depends on the temperatures of the working fluid, i.e., heat transfer fluid, entering and exiting the Cu-Cl cycle. The nuclear heat must be transported over a distance through a heat transfer fluid to the thermochemical hydrogen production plant. Due to the design and operation complexity of dealing with phase change heat transfer fluids, only sensible heat is considered in this chapter for the heating purposes of the Cu-Cl cycle. In this chapter, 250°C is selected as the maximum temperature of heat transfer fluid exiting the Cu-Cl cycle, which is about 100°C lower than most of the inlet temperatures of Generation IV nuclear reactors, so as to have a sufficient temperature difference for heat exchange between the heat transfer fluid and the nuclear reactor coolants. Later sections of this paper will discuss further details of the temperature selection criteria based on the calculations of heat losses. Since only sensible heat of the heat transfer fluid is provided to the Cu-Cl cycle, the delivered heat requirement of the heat transfer fluid can be estimated by variations of the fluid temperature passing through each step of the Cu-Cl cycle, assuming the heat capacity of the heat transfer fluid does not vary significantly in the temperature range of interest. The matching criterion is that higher grade heat should be met at a higher priority since lower grade heat may be met by the exiting heat of higher grade steps.

Figure 1 shows the matching extent for various maximum delivered temperatures of the heat source. It can be found that 600°C can cover the maximum temperature requirement 530°C of step IV of the Cu-Cl cycle, but it does not have a sufficient heat percentage for step IV, yet it provides surplus heat for steps 2 and 1. To satisfy the heat requirement of step IV, the mass flow rate of heat transfer fluid must be increased. However, this may also deliver surplus heat to other steps. As a result, the temperature exiting the Cu-Cl cycle will be



increased and the overall thermal efficiency of both nuclear and hydrogen production plants is hence decreased. Therefore, to increase the temperature entering the Cu-Cl cycle could be a better option for satisfying the requirement. Figure 1 shows that the temperature of the heat from the nuclear reactor entering the Cu-Cl cycle after a distant transport must be around 650°C to match the heat requirements of the Cu-Cl cycle. In addition, the temperature of heat transfer fluid leaving the nuclear reactor should be sufficiently high to offset the heat losses in the transport pipeline between the nuclear and hydrogen production plants, and also to avoid condensation or solidification on the inner wall of pipeline after leaving the Cu-Cl cycle if the heat transfer fluid is steam or molten salt. An intermediate heat exchanger that can heat a transfer fluid by the nuclear reactor coolant is suggested for the heat supply to the hydrogen production plant due to the safety considerations of both the nuclear reactor and hydrogen production plant, because the nuclear reactor coolant has a risk to be contaminated by the chemicals of the Cu-Cl cycle if there is any leak in the pipe.

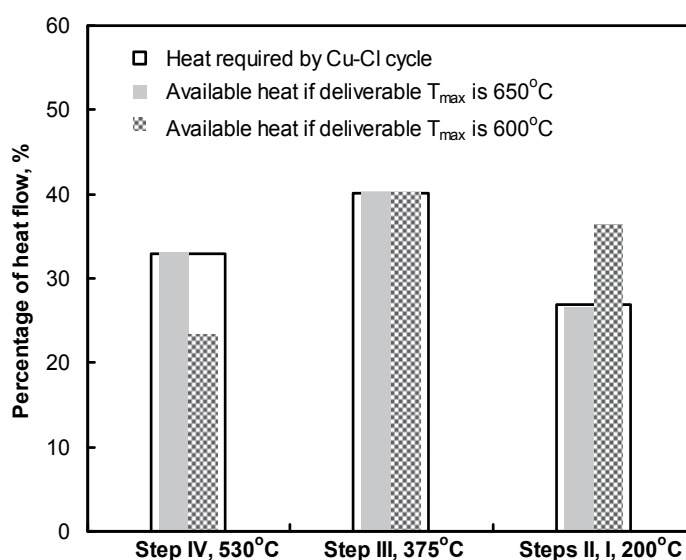


Fig. 1. Heat distribution of Cu-Cl cycle and nuclear heat source at various temperatures

### 3.3 Evaluation and selection of heat transfer fluids for heat transport in pipeline

Heat must be transferred by a heat transfer fluid flowing in a pipeline and transported from a nuclear power station to a thermochemical hydrogen plant. On the basis of the heat requirement per kilogram of hydrogen production shown in Table 5, the heat load can be estimated according to the hydrogen production scale. Table 6 shows the estimate, where  $Q_T$  is the heat load in the pipeline in units of  $MW_{th}$ , i.e., megawatts of thermal energy.

When using sensible heat of the heat transfer fluid, the performance of the fluid can be evaluated by the required flow rate for per unit heat quantity transported in the pipeline:

$$X_T = \frac{Q_T}{\int_{T_L}^{T_H} C_p dT} \text{ at } Q_T = 1 MW_{th} \quad (6)$$

where  $X_T$  has the units of  $\text{kg}\cdot\text{s}^{-1}/\text{MW}_{\text{th}}$ , and  $T_L$  and  $T_H$  are the inlet and outlet temperatures of the heat transfer fluid that extracts heat from nuclear reactor coolant in the intermediate heat exchanger. The values of  $T_L$  and  $T_H$  should prevent phase change and at the same time allow a portion of heat losses in the transport pipeline. Also,  $C_p$  is the heat capacity of the heat transfer fluid that could be thermal oils, molten salts, supercritical water, steam, or helium. To transport supercritical water, the transport pipeline must withstand a high pressure ( $>22\text{MPa}$ ), which is an engineering challenge for pipeline manufacturing and maintenance. Thermal oil may experience coking and decomposition at a high temperature. Solidification may occur in molten salt at low temperature spots. Steam may condense after a distance of transport if the pressure is higher than its saturation point. The condensation of steam indicates the need for an intermediate steam generator and two-phase flow in the transport pipeline. This may significantly increase the construction capital and operating cost. Therefore, in this chapter, the pressure of the steam is not suggested to be sufficiently high such that the steam can remain in a gaseous state during circulation.

<b>H<sub>2</sub> production scale, tonnes/day</b>	100	200	400
<b>Heat requirement by Cu-Cl cycle , MW<sub>th</sub></b>	263	525	1050
<b>Heat transport load (Q<sub>T</sub>) in pipeline, MW<sub>th</sub></b>	316	630	1260

Table 6. Heat requirement and heat load in pipeline for various hydrogen production scales

Since step II of the Cu-Cl cycle has a temperature range of 80 - 200°C, it is assumed the heating fluid exiting the step is 230°C. To avoid condensation, the pressure of the heating fluid is 2 MPa, which is slightly lower than the saturation pressure of steam in case steam serves as the heating fluid. For a comparable study, helium is designed to have the same temperature and pressure as steam. Table 7 gives the values of  $X_T$ , the suggested operating parameters for the heat transfer fluids (helium, superheated steam, and molten salt), and the thermodynamic properties of the fluids [Petersen, 1970; Wang, 2010]. Among the three fluids of Table 7, both steam and molten salt have a phase change issue in the transport pipeline, and molten salt has an issue of chemical stability when the temperature is high. Therefore, helium is a comparatively good option for working as the heat transfer fluid.

Fluid in pipeline		Thermodynamic properties <sup>(a)</sup>				$X_T$ kg s <sup>-1</sup> /MW <sub>th</sub>
		P MPa	C <sub>p</sub> kJ/kg·K	ρ kg/m <sup>3</sup>	k w/m·K	
Helium	T <sub>L</sub> = 230°C	2	5.196	1.916	0.238	0.520
	T <sub>H</sub> = 600°C	2	5.196	1.100	0.330	
Steam	T <sub>L</sub> = 230°C	2	2.735	9.495	0.042	1.189
	T <sub>H</sub> = 600°C	2	2.247	5.010	0.081	
Molten salt <sup>(b)</sup>	230 -- 600°C	0.1	1.549	1794	3.635	1.745

(a) C<sub>p</sub> – heat capacity; ρ – density; k – thermal conductivity.  
(b) Averaged values for the properties are used here due to the condensed state of molten salt. For comparison purposes: 60% NaNO<sub>3</sub> and 40% KNO<sub>3</sub>; Melting point: 222°C; Boiling point: 704°C.

Table 7. Values of  $X_T$ , suggested operating parameters, and thermodynamic properties of heat transfer fluids

### 3.4 Flow characteristics of the heat transfer fluids in the transport pipeline

The heat loss of the transport pipeline is greatly influenced by the flow characteristics. The flow parameters such as flow velocity and pressure loss must be controlled in an acceptable engineering range in the pipeline. The velocity is determined by the flow rate and pipe diameter. The flow rate can be calculated from  $X_T$  and the heat load. Figure 2 shows the dependence of helium flow velocity on the heat load and pipeline diameter. It can be found that the velocity depends strongly on the pipeline diameter. Utilizing a smaller diameter pipeline can reduce the construction cost. However, a smaller pipeline diameter may lead to a higher velocity and larger pressure drop, which requires an increased pressure boosting for the pipeline transport.

To estimate the pressure drop, the following equation is adopted:

$$\frac{\Delta P}{L} = f \cdot \frac{1}{D} \cdot \frac{\rho u^2}{2} \quad (7)$$

where  $\Delta P/L$  is the pressure drop per unit length (Pa/m),  $D$  is the pipeline inside diameter,  $\rho$  is the helium density (values given in Table 7),  $u$  is the helium velocity (values given in Fig. 2),  $f$  is the friction factor determined by the Reynolds number and the pipeline inner wall roughness. Then from equations (6) and (7), the pressure loss can be calculated by:

$$\frac{\Delta P}{L} = \frac{1}{2} \left( \frac{4}{\pi} \right)^2 \frac{f}{\rho} \cdot X_T^2 \cdot D^{-5} \cdot Q_T^2 \quad (8)$$

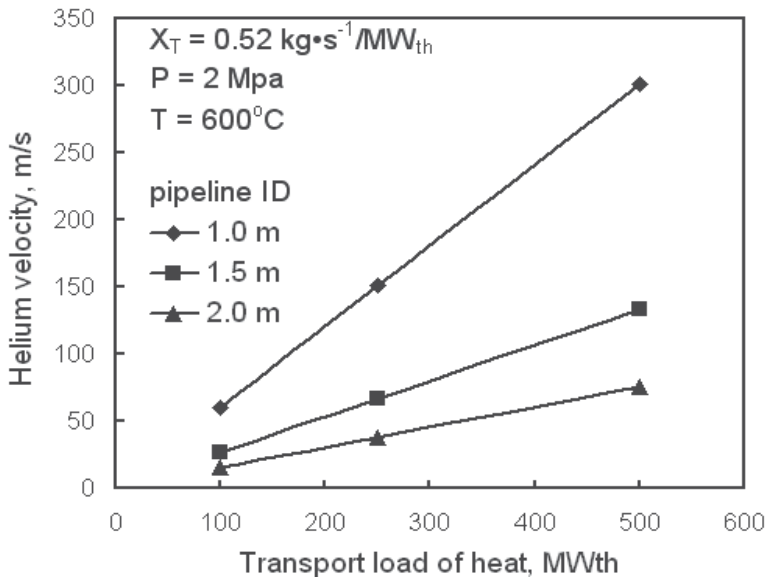


Fig. 2. Dependence of helium flow velocity on the heat load and pipeline diameter

Figure 3 shows the dependence of pressure drop on heat load and pipeline diameter. For the pipeline diameter of 1.0 m, the pressure loss may reach 500 kPa/km (5 bars/km) when the heat load is 500 MW<sub>th</sub> (about 150 tons H<sub>2</sub>/day). To pump helium 10 km away, the pressure

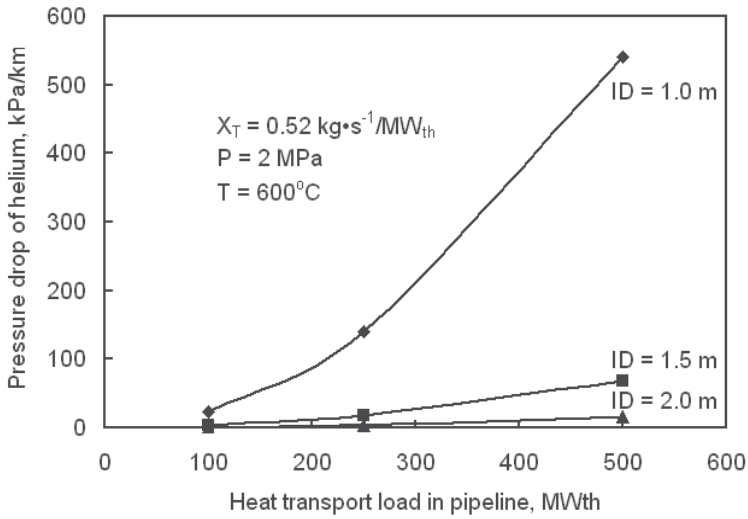


Fig. 3. Dependence of helium pressure drop on the heat load and pipeline diameter

loss is about 50 bars (5 MPa). This is a large pressure loss that may need significant compressor work. To lower the pressure loss, the pipeline diameter must be increased or multiple pipelines must be utilized.

### 3.5 Heat transport load and heat loss in the transport pipeline

When heat is transported by helium from a nuclear station to a hydrogen plant, it will experience heat losses. The influencing parameters include the helium flow rate, heat load, temperature, pipeline diameter, insulation, and weather conditions, among others. The heat loss is transferred from helium to the pipeline wall mostly through convection, and then through the conduction of the insulation of the pipeline, and lastly to air through convection and radiation if the pipeline is on the ground surface. If the pipeline is buried underground, the heat loss mostly goes to the soil. Since the thermal conductivity of metal is usually at least one order larger than most types of soils, the soil can also serve as insulation if the soil moisture is not significant. Due to the variations of soil types, buried depth and transport length of pipeline, the investigation of the heat loss for underground pipelines is not discussed in detail here. To simplify the evaluation, this paper will mainly examine the heat loss of the surface pipeline.

Since the pipeline is sufficiently long compared with its diameter, the axial flow effect can be neglected. The heat transfer can be approximated as a one-dimensional flow in the radial direction. The heat loss per unit length of the pipeline can be calculated with the following equation [Lienhard et al., 2008]:

$$\frac{Q}{L} = \frac{2\pi(T_{He} - T_{air})}{\frac{1}{R_i h_{conv}^{He}} + \frac{\ln(R_o / R_i)}{k_{pipe}} + \frac{\ln[(R_o + \theta) / R_o]}{k_{insu}} + \frac{1}{(h_{conv}^{air} + h_{rad})(R_o + \theta)}} \quad (9)$$

where  $Q/L$  is the heat loss per unit length,  $T_{He}$  is the average helium temperature in the pipeline,  $T_{air}$  is the air temperature varying with days and seasons,  $R_i$  and  $R_o$  are the pipeline inside and outside radius (not including the insulation),  $k_{pipe}$  is the thermal conductivity of

the pipeline material,  $\theta$  is the insulation thickness,  $h_{convec}^{He}$  and  $h_{convec}^{air}$  are the convection heat transfer coefficients of helium flow in the pipeline and wind outside the insulation, and  $h_{rad}$  is the radiation heat transfer coefficient.

To have a safe design approximation, the upper value of the thermal conductivity of insulation for a very high temperature environment (600°C) is adopted. It is also assumed that the outer surface of the insulation will be oxidized after use of some time so that the emissivity coefficient is higher than that of a well maintained condition. In addition, extreme cold weather conditions may take place occasionally. Table 8 shows the parameters of the pipeline, insulation and weather conditions for the calculation of heat losses.

Pipeline	Insulation		Air	
Thermal conductivity	Thermal conductivity	Emissivity	T	Wind speed
15 w/m·K	0.25 w/m·K	0.31	-50°C	6.0 m/s
Stainless Steel AISI 304L [Assael et al., 2003]	Ceramic fiber blanket wrapped by heavily oxidized aluminum foil [Desjarlais et al., 2002; Engineeringtoolbox, 2010]		Ontario, Canada [Ontario Government Data, 2010]	

Table 8. Parameters of pipeline, insulation and weather conditions for heat loss estimate

Figure 4 shows the estimated heat losses for the heat transport loads of 200 - 700MW<sub>th</sub>. It can be found that the heat loss can be controlled to below 2 MW<sub>th</sub>/km if the insulation thickness

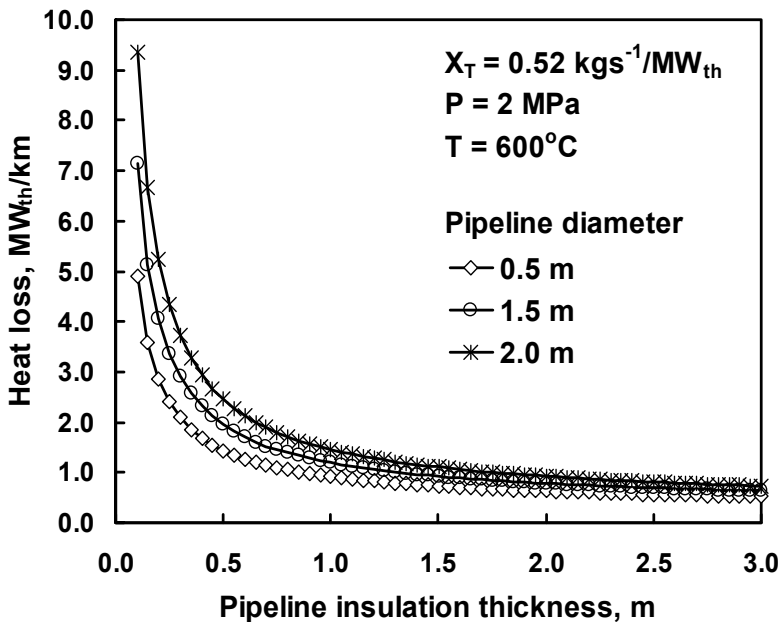


Fig. 4. Heat losses of pipeline for the heat transport loads of 200 - 700MW<sub>th</sub>

is larger than 1.0m. This suggests the key importance of the pipeline insulation. If considering both the pipeline diameter (e.g. 1.0m) and insulation thickness (1.0m), the total

diameter would be about 3.0m, which creates a barrier for animals and human activities if the pipeline is constructed on the ground surface. To bury the pipeline underground is another option. An underground pipeline will increase construction and maintenance costs. Assume the cost of insulation is much lower than the pipeline so that the insulation thickness can be constructed larger than 1.0 m. Then the heat loss of 2.0 MW<sub>th</sub>/km can be considered as a typical value for the transport. When the heat load is higher, the heat loss percentage is lower. When the pipeline length is 10 km, then the heat loss is 20 MW<sub>th</sub>. If the heat load is 500 MW<sub>th</sub> (about 150 tonnes H<sub>2</sub>/day), the two-way heat loss is then about 12.5%. However, Fig. 4 also shows the limit of heat loss reduction by insulation: to increase the insulation thickness does not always have a significant heat loss reduction effect when the thickness is larger than 1.5m. Considering the heat loss through pumps and other components such as valves and expansion joints, the heat loss for a two-way transport pipeline design is assumed below 20% when the transport distance from a nuclear reactor to a hydrogen plant is within 10 km. The analysis shown in Table 6 of the former section is based on this value.

#### 4. Layout options for the integration of nuclear and hydrogen production plants

When a nuclear reactor is coupled with a hydrogen production plant, the layouts for the heat and fluid flows are important for safety and economics. The layout options depend strongly on the reactor types. Since the indirect or reheat cycle nuclear reactors have a secondary coolant or circulation that can provide heat to the heating fluid of a hydrogen plant through an intermediate heat exchanger, the integration of a hydrogen production plant with an indirect or reheat cycle nuclear reactor may provide safer and more flexible layout options. Therefore, the focus of this section will examine the direct cycle nuclear reactors, which are represented by SCWR in this chapter.

Figure 5 shows the arrangement of a supercritical water-cooled nuclear reactor (SCWR) and a hydrogen cogeneration plant with the Cu-Cl thermochemical cycle. The values of temperatures and pressures of the flowchart were calculated according to the water stream enthalpy change and expansion ratio that were reported in the past [Yamaji et al., 2005; Naidin et al., 2009]. The streamlines for the supercritical water are based on existing fossil fuel power plants that use a supercritical water turbine after changing the fossil fuel combustion chamber and supercritical water tank to SCWR [Yamaji et al., 2005; Naidin et al., 2009; Buongiorno et al., 2002]. The water stream circulation passing the lines A-B-C-D-E and A-B-F-E in Figure 5 has the typical features of a no-reheat system that uses a preheater and two types of turbines, i.e., high pressure (HP) and low pressure (LP) turbines. From the temperatures shown in Figure 5, it can be found that point A, i.e., the location downstream of the nuclear reactor but upstream of the turbines, can provide around 100 °C of a driving temperature difference for step IV of the Cu-Cl cycle that requires 530 °C. At this location, a bypass line of the supercritical water stream passing points A and N can be designed for heat extraction from supercritical water to the Cu-Cl cycle. An intermediate heat exchanger can be arranged on the line A-N-B to provide heat to helium that is used to heat the hydrogen cycle through the circulation of H-I-J-K-L. For step III of the Cu-Cl cycle, the temperature requirement is 375 °C. The heat for this step can be supplied by the helium stream exiting step IV that still has a temperature higher than 530°C at point I. The helium stream exiting step III at point J still has a temperature higher than 375°C, so it can be used for step II. Since step I of the Cu-Cl cycle needs electricity for electrolysis, the electricity can

be conducted from the generator to the Cu-Cl cycle, as shown by the line passing points O and M.

As to the water stream for the power generation, there could be a number of preheaters, or the water stream circulation could be designed as a multiple reheat cycle. The details of these layouts will not be discussed in this chapter since these designs can provide multiple options for the heat extraction bypass lines and the water stream circulation layout. Also, a single reheat cycle layout, including its steam turbines and generator, is most widely employed in current BWR and PWR technologies that can be applied to SCWR so as to reduce the design complexity.

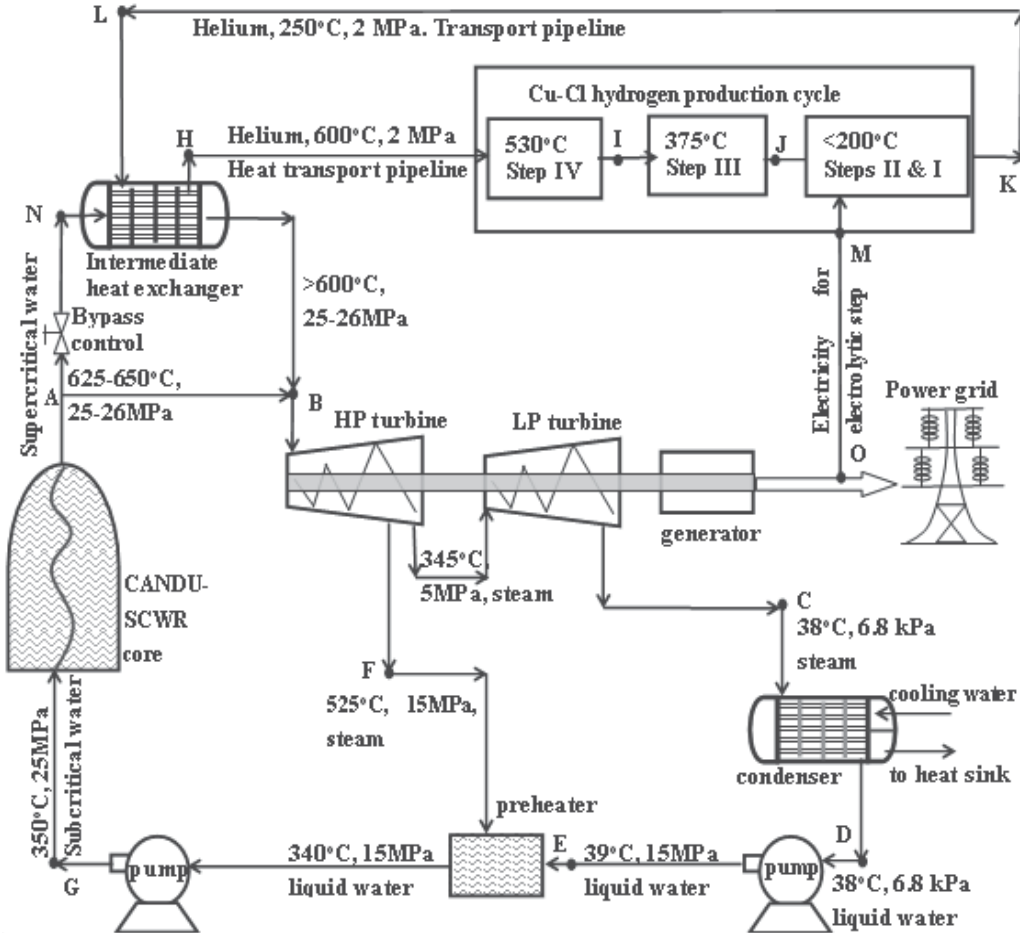


Fig. 5. Layout options for the integration of SCWR and Cu-Cl cycle (coolant passing through high pressure and low pressure turbines in series)

## 5. Modulation of nuclear energy output and hydrogen cogeneration scale

The demand on power varies hourly, daily, monthly and seasonally on the power grid. Figure 6 shows an actual power load profile on the power grid of a day (January 18, 2010) in

Ontario, Canada [IESO, 2010]. It can be found that the power demand varies significantly at different hours. The gap between peak and off-peak hours can even reach 70% of the base power load. Since the power grid comprises various energy sources such as nuclear, fossil fuels, hydro, solar and wind, the modulation of the power output from these sources is very

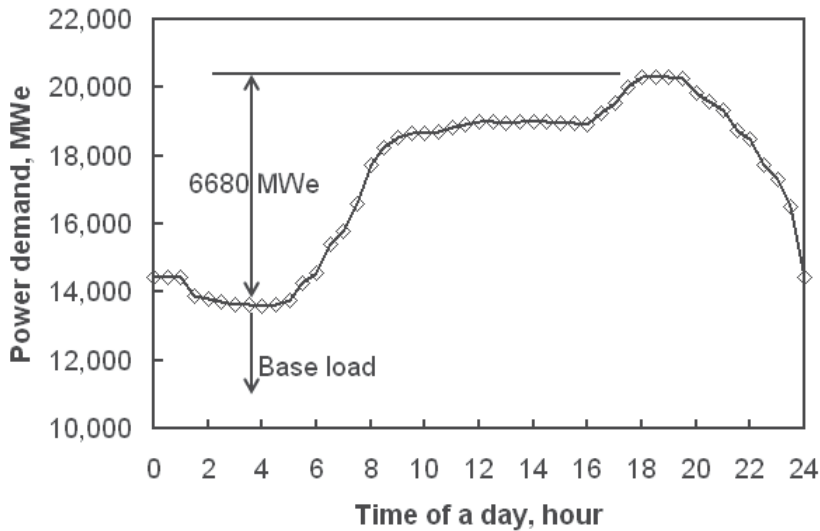


Fig. 6. Typical power load profile of a day in Ontario, Canada (January 18, 2010).

important. This means some power plants cannot operate at a constant power output. The selection of energy sources to be adjusted upward to meet the peak power demand will influence the amount of greenhouse gas emissions. To increase the nuclear power output for the peak hour demand can reduce the greenhouse gas emissions, so there are some countries employing and developing nuclear modulation technologies to adjust the power output. The modulation technologies include the adjustment of control rod insertion depth, the velocity of circulation steam, new types of grey rods, or a combination thereof [WNA , 2011; Gilbert et al., 2004]. However, the adjustment of nuclear power output may directly influence the operation of the nuclear reactor and introduce more safety issues than a constant power output, so most countries use other energy sources such as fossil fuel and hydroelectric power to follow the power demand on the grid. The percentage of nuclear power in the base load in Figure 6 is maximized to lower the portions of other energy sources. However, the base load varies monthly and seasonally, so the nuclear power plant can rarely operate at its full design capacity of power generation, except if the nuclear portion in the base load is small.

Using nuclear energy (either in the form of electricity or heat) to produce hydrogen at off-peak hours and surplus generation capacity is a promising option. As shown in Figure 7, both the heat and electricity outputs are controlled to be constant. The electricity delivered to the power grid can follow the power load profile on the grid (either fully or partly), and the rest of the electricity goes to conventional water electrolysis. This option has no requirement of modulating the heat and electricity output of the nuclear reactor, but the hydrogen production facilities must be able to accommodate the modulation of production rate.

Figure 8 shows another option that has no requirement of modulating the heat but must modulate the electricity generator to accommodate varying heat input, and at the same time



to modulate the hydrogen production rate. In both options, the total heat output from a nuclear reactor is constant, so it is anticipated to be safer than the measure of varying heat output. In comparison, option 1 is safer and more simple in principle, but the hydrogen production efficiency with water electrolysis is lower than with thermochemical cycles in option 2, which may influence the hydrogen production scale and economics.

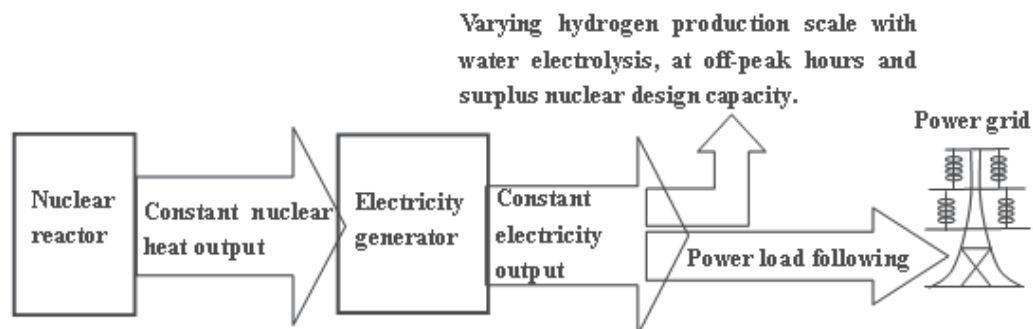


Fig. 7. No modulation of both nuclear heat and electricity with water electrolysis

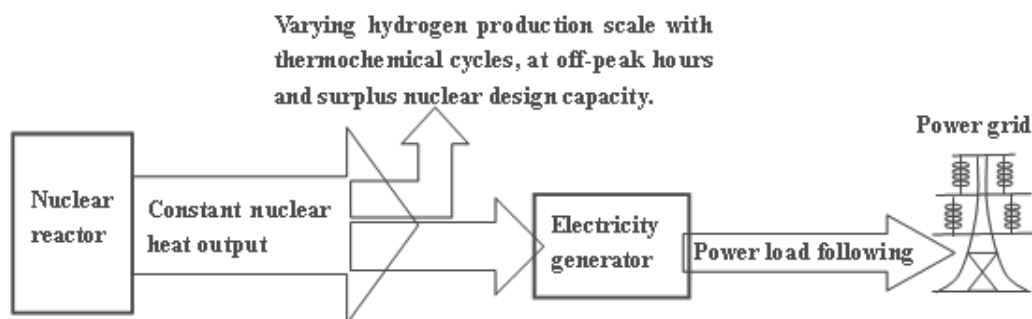


Fig. 8. No modulation of nuclear heat with thermochemical cycles

Table 9 shows the hydrogen production rate at different hours of a day. The values are calculated on the basis of the design capacity of 1,000 MWe for a Generation IV single supercritical water-cooled nuclear reactor (SCWR). The SCWR operates at its maximum capacity with cogeneration of hydrogen. The available heat for hydrogen production is the difference between the design capacity of the SCWR and the power generated that is following the power demand profile of the power grid shown in Figure 6. The heat supplied to the Cu-Cl cycle from SCWR for the thermochemical Cu-Cl cycle is assumed to have a loss of 20% within 10 km, as discussed in the former section. The data in Table 5 is used to determine the heat requirements of the Cu-Cl cycle. The overall efficiencies of water electrolysis and the Cu-Cl cycle are assumed to be 30% and 45% respectively, which suggests a smaller efficiency gap than shown in Table 2 so as to have a conservative estimate. It can be found that a single SCWR at off-peak hours and surplus design capacity can produce at least 100 tonnes of hydrogen each day. This production rate is equivalent to the production capacity of an industrial plant with steam methane reforming, which is the major technology employed today.

Time hour	Generated power and design capacity, MW <sub>e</sub>		Available heat for H <sub>2</sub> production, MW <sub>th</sub>		H <sub>2</sub> production rate Tonnes/day	
	% of full design capacity	Generated power	Unused power capacity	Unused heat quantity <sup>(a)</sup>	Water electrolysis	Cu-Cl cycle
1-5am	53%	530	470	1044	265	318
5-6am	56%	560	440	844	248	298
6-7am	62%	620	380	978	215	257
7-8am	66%	660	340	756	192	230
8-9am	70%	700	304	676	172	206
9am-16pm	74%	740	260	578	147	176
16-17pm	75%	750	250	556	141	169
17-18pm	78%	780	220	489	124	149
18-19pm	80%	800	200	444	113	136
19-20pm	78%	780	220	489	124	149
20-21pm	74%	740	260	578	147	176
21-22pm	66%	660	340	756	192	230
22-23pm	60%	600	400	889	226	271
23pm-1am	54%	540	460	1022	260	312

(a) The thermal efficiency of power generation is assumed to be 45% for SCWRs [Kirillov, 2008, Yamaji, 2005; Naidin, 2009; Buongiorno, 2002].

Table 9. Hydrogen production scale and quantity with nuclear energy at various hours

## 6. Conclusions

This chapter examined the usage of nuclear energy for the cogeneration of electricity and hydrogen with water splitting technologies, so as to improve the economics of power plants and at the same time reduce greenhouse gas emissions. The hydrogen economy is discussed and the reduction of greenhouse gas emissions by use of nuclear generated hydrogen as a substitute of fossil fuels is quantified. The thermal efficiencies and economics of various hydrogen production methods with nuclear energy are examined. The methods include thermochemical water splitting cycles, conventional electrolysis, and high temperature electrolysis. Among these methods, thermochemical cycles have the most promisingly high efficiency and economics. It is found that the relatively high temperature requirements of

numerous thermochemical cycles are the common threshold of utilizing nuclear heat to produce hydrogen. The copper-chlorine (Cu-Cl) cycle has a minimum temperature requirement (about 530°C) that can be met by most Generation IV nuclear reactors. The temperature of a nuclear reactor should not only meet the threshold, but it should also match the heat distribution of the thermochemical cycle. Also, the nuclear reactor temperature must be high enough to offset the heat losses in the heat transport pipeline. The future studies of thermochemical hydrogen production can be conducted toward lowering the temperature requirements. An intermediate heat exchanger is suggested between the nuclear reactor and thermochemical cycle so as to minimize the mutual influence between the plants and improve the safety and operating flexibility.

Various heat transfer fluids for the heat exchange and transport pipeline were compared and evaluated. Considering the heat transport complexity in the pipeline and the importance of being chemically inert, phase change fluids and thermal oils are not suggested. Pressurized helium is a promising option for serving as the long distance heat transport fluid in the pipeline. A challenge of the heat transport in a pipeline is the pressure boosting requirement to overcome the considerable pressure losses if the pipeline diameter is smaller than one meter or the heat transport load is too large. Another challenge is the large diameter of the pipeline and thermal insulation. In order to control the two-way heat loss below 20%, the diameter must be larger than 3 meters (thermal insulation inclusive), which is a challenge for either underground or surface transport. The overall layout options for the integration of nuclear reactors and hydrogen production plants are also discussed, including the distant heat transport from nuclear reactors to a hydrogen production plant. Direct cycle nuclear reactors are discussed in more detail due to less flexibility than indirect cycle reactors.

The modulations of nuclear energy output and hydrogen cogeneration rates are also discussed in this chapter. The energy output modes of nuclear reactors include constant and variable output. Similarly, the hydrogen production scales also have two modes that are determined by the modulated heat availability of the nuclear reactors. It is concluded that a constant total heat output can be approached if the hydrogen is produced from thermochemical cycles. A constant total electricity output can also be approached with conventional water electrolysis. The constant energy output (either in the form of heat or electricity) from a nuclear reactor can provide a load following pattern that can meet the power load profile on the grid, so as to reduce the usage of fossil fuels for peak hours. The thermal energy of a single Generation IV nuclear reactor at off-peak hours and surplus design capacity are sufficient to power an industrial hydrogen plant with a thermochemical cycle or water electrolysis.

## 7. Acknowledgements

Support of this research from Atomic Energy of Canada Limited and the Ontario Research Excellence Fund is gratefully acknowledged.

## 8. References

- Assael, M. J. & Gialou, K. (2003). Measurement of the Thermal Conductivity of Stainless Steel AISI 304L up to 550 K. *International Journal of Thermophysics*, Vol. 24, pp. 1145-1153

- Buongiorno, J. (2002). The Supercritical-water-cooled Reactor (SCWR). *American Nuclear Society (ANS) Winter Meeting*, Washington DC, US, November 18, 2002.
- de Jong, M; Reinders, A. H. M. E.I.; Kok, J. B. W. & Westendorp, G. (2009) Optimizing a Steam-methane Reformer for Hydrogen Production. *International Journal of Hydrogen Energy*, Vol. 34, pp. 285 – 292
- Desjarlais, A. O. & Zarr, R. R. (2002) Insulation Materials. Printed in Bridgeport, NJ, US. ISBN 0-8031-2898-3. 2002, Vol. 4, pp. 122-128
- Engineeringtoolbox (2010). The Radiation Heat Transfer Emissivity Coefficient of Some Common Materials as aluminum, Brass, Glass and Many More. Available from (Accessed on Oct 4, 2010): [http://www.engineeringtoolbox.com/emissivity-coefficients-d\\_447.html](http://www.engineeringtoolbox.com/emissivity-coefficients-d_447.html)
- Forsberg, C. W. (2007). Future Hydrogen Markets for Large-scale Hydrogen Production Systems. *International Journal of Hydrogen Energy*, Vol. 32, pp. 431-439.
- Forsberg, C. W. (2003). Hydrogen, Nuclear Energy, and the Advanced High-temperature Reactor. *International Journal of Hydrogen Energy*, Vol. 28, pp.1073-1081
- Forsberg, C. (2002). Hydrogen, electricity, and nuclear power. *Nuclear news*, September 2002, pp. 30-31
- Gilbert, M. M. (2004) Renewable and Efficient Electric Power Systems. ISBN: 978-0-471-28060-6. Wiley-IEEE Press, August 11, 2004, pp. 135-148
- Government of Alberta (2008). Electricity statistics. Available from (Accessed on May 20<sup>th</sup>, 2010): <http://www.energy.alberta.ca/Electricity/682.asp>
- IEA (International Energy Agency) (2010). Hydrogen Production & Distribution. *IEA Energy Technology Essential.*, Available from (Accessed on December 20, 2010): <http://www.iea.org/techno/essentials5.pdf>
- IESO (Independent system operator) (2010). Ontario Demand on MW. Available from (Accessed on November 26, 2010): <http://www.ieso.ca/imoweb/monthsYears/monthsAhead.asp>
- Jean-Pierre Py & Capitaine, A. (2006) Hydrogen Production by High Temperature Electrolysis of Water Vapour and Nuclear Reactors. *16th World Hydrogen Energy Conference (WHEC16, 2006)*, June 13-16, Lyon, France.
- Kirillov, P. L. (2008). Supercritical Water Cooled Reactors. *Thermal Engineering*, Vol. 55, pp. 361-364
- Kreith, F & Yogi Goswami, D. (2007). Handbook of Energy Efficiency and Renewable Energy. Publisher: CRC press, ISBN: 9780849317309, ISBN 10: 0849317304, Chaper 6
- Kubo, S.; Kasahara, S.; Okuda, H; Terada, A; Tanaka, N.; Inaba, Y.; Ohashi, H.; Inagaki, Y.; Onuki, K. & Hino, R. (2004). A Pilot Test Plan of the Thermochemical Water-splitting Iodine-sulfur Process. *Nuclear Engineering and Design* , Vol. 233, pp. 355–362
- Lienhard IV, J. H.; Lienhard V, J. H. (2008) A Heat Transfer Textbook. 3<sup>rd</sup> edition, Phlogiston Press, Cambridge, Massachusetts, USA, 2008, Chapters III and IV, pp. 341-594
- Naidin, M., Mokry, S., Baig, F. & Gospodinov, Y. (2009). Thermal-Design Options for Pressure-Channel SCWRS With Cogeneration of Hydrogen. *Journal of Engineering for Gas Turbines and Power*, Vol. 131, pp. 012901-1~80

- Naterer, G.F. ; Fowler M.; Cotton J. & Gabriel K. (2008). Synergistic Roles of Off-peak Electrolysis and Thermochemical Production of Hydrogen from Nuclear Energy in Canada. *International Journal of Hydrogen Energy*, Vol. 33, pp. 6849 – 6857.
- NYSERDA (New York State Energy Research and Development Authority) (2010). Hydrogen Fact Sheet: Hydrogen Production -- Steam Methane Reforming (SMR). *Technical report - Clean Energy Initiative.*, Available from (Accessed on May 1<sup>st</sup>, 2010):  
<http://www.getenergysmart.org/files/hydrogeneducation/6hydrogenproductionsteammethanereforming.pdf>
- Ontario government data (2010). Available from (Accessed on Oct 4, 2010):  
<http://www.omafra.gov.on.ca/english/engineer/facts/03-047.htm#f13>
- Petersen, H (1970). The Properties of Helium: Density, Specific Heats, viscosity, and Thermal Conductivity at Pressures from 1 to 100 bar and from Room Temperature to about 1800 K. *Risø Report No. 224. Danish Atomic Energy Commission Research Establishment Risø*. September, 1970.
- Sadhankar, R. R.; Li, J.; Li, H.; Ryland, D. & Suppiah, S. (October 2005). Hydrogen Generation Using High-temperature Nuclear Reactors. *55th Canadian Chemical Engineering Conference*, Toronto
- Schultz, K. (2003) Thermochemical Production of Hydrogen from Solar and Nuclear Energy. Presentation to The Stanford Global Climate and Energy Project. 14 April, 2003. General Atomics, San Diego, California, US. Also available from:  
[http://gcep.stanford.edu/pdfs/hydrogen\\_workshop/Schultz.pdf](http://gcep.stanford.edu/pdfs/hydrogen_workshop/Schultz.pdf)
- Sivula, K.; Zboril, R.; Le Formal, F.; Robert, R.; Weidenkaff A.; Tucek, J.; Frydrych, J. & Grätzel, M. (2010). Photoelectrochemical Water Splitting with Mesoporous Hematite Prepared by a Solution-Based Colloidal Approach. *Journal of American Chemical Society*, Vol. 132, pp. 7436–7444
- Steinfeld, A. (2005). Solar Thermochemical Production of Hydrogen – A Review. *Solar Energy*. Vol. 78, pp. 603–615
- Wang, Z. L. & Naterer, G. F. (2010). Greenhouse Gas Reduction in Oil Sands Upgrading and Extraction Operations with Thermochemical Hydrogen Production. *International Journal of Hydrogen Energy*, Vol. 35, pp. 11816-11828
- Wang, Z.L.; Naterer G. F.; Gabriel, K.S.; Gravelsins, R. & Daggupati, V.N. (2010). Comparison of Sulfur-iodine and Copper-chlorine Thermochemical Hydrogen Production Cycles. *International Journal of Hydrogen*, Vol. 35, pp. 4820 – 4830
- Wang, Z. L.; Naterer, G. F.; Gabriel, K. S.; Gravelsins, R. & Daggupati, V. N. (2009). Comparison of Different Copper-chlorine Thermochemical Cycles for Hydrogen Production. *International Journal of Hydrogen Energy*, Article in Press, Vol. 34, pp. 3267-3276
- WNA (World Nuclear Association). Generation IV Nuclear Reactors. Available from (accessed on December 20, 2010) <http://www.world-nuclear.org/info/inf77.html>
- WNA (World Nuclear Association) (2011). Nuclear Power in France. Available from (Accessed on March 20, 2011): <http://www.world-nuclear.org/info/inf40.html>.

Yamaji, A.; Kamei, K.; Oka, Y. & Koshizuka, S. (2005). Improved Core Design of the High Temperature Supercritical-pressure Light Water Reactor. *Annals of Nuclear Energy*, Vol. 32, pp. 651-670

# Reformer and Membrane Modules (RMM) for Methane Conversion Powered by a Nuclear Reactor

M. De Falco<sup>1</sup>, A. Salladini<sup>2</sup>, E. Palo<sup>3</sup> and G. Iaquaniello<sup>3</sup>

<sup>1</sup>*Faculty of Engineering, University Campus Bio-Medico of Rome,*

<sup>2</sup>*Processi Innovativi, L'Aquila,*

<sup>3</sup>*Tecnimont KT S.p.A., Rome,*

*Italy*

## 1. Introduction

In the last few years, significant developments in membrane science and the vision of process intensification by multifunctional reactors have stimulated the academic and industrial research focused on membrane reactor application to chemical processes (Mendes et al., 2010, Dittmeyer et al., 2001, Basile et al., 2005a, De Falco et al., 2007). From these works, the increase of the reactants conversion above the equilibrium values appears to be possible when a reaction products at least is removed through the membrane. As stated in the following, the integration of selective membrane in a chemical process can be twofold:

- directly inside the reaction environment (Integrated Membrane Reactor – IMR);
- after the reaction step (Reaction and Membrane Module – RMM).

In this chapter a methane steam reforming (MSR) RMM pre-industrial plant, designed and tested to investigate at an industrial scale level the plant performance, is presented.

A major benefit of the proposed RMM configuration is the shift of steam reforming reactions chemical equilibrium by removing the hydrogen produced at high temperature, thanks to the integration of highly selective Pd-based membranes and enhancing the final product yield. By this way, the process can operate at a temperature as low as 600-650°C in comparison to 850-880°C needed in conventional plants, and enable the use of low temperature heat source as helium heated in a nuclear reactor.

This chapter reports, firstly, membrane reactor concept, selective membrane typologies and integration strategies; then it discusses the experimental data gathered over 1000 hours of testing on an industrial pilot unit in terms of feed conversion at different operating parameters and elaborates such data in order to optimize the overall architecture, defining the maximum achievable feed conversion under different scenario of heat integration. Finally, a membrane reactor perspectives analysis, mainly focused on integration with nuclear reactors for steam reforming reactor heat duty supplying, is reported in order to understand which technical and economical targets have to be reached in the next future for a commercial diffusion.

The plant discussed in this chapter, placed in Chieti Scalo (Italy), is characterized by a H<sub>2</sub> design capacity of 20 Nm<sup>3</sup>/h and it operates with three Pd and Pd/Ag based membranes for

hydrogen separation. It was developed in the framework of the Italian FISR Project “Pure hydrogen from natural gas reforming up to total conversion obtained by integrating chemical reaction and membrane separation”, which grouped Italian universities, and the engineering society Tecnimont KT (TKT), cooperating in the development of each critical point of this innovative technology, such as membrane manufacture and assembling and catalyst optimization, resulting in the plant design and operation finally carried out by TKT. This installation, the first of this type and size, makes it possible to completely understand the potential of selective membrane application in industrial high-temperature chemical processes.

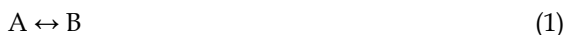
## 2. Membrane reactor concept and benefits

A membrane reactor (MR) is a system coupling reaction and separation of one or more products, with the separation operation performed by a selective membrane. Although not yet very used at industrial scale, MRs are attracting the attention of scientists and engineers in the last two decades and many interesting papers have appeared in the literature on their performance and possible applications in many fields of chemical and biochemical industries. An excellent review about these topics has appeared in 2002 by Sanchez Marcano & Tsotsis (Sanchez Marcano & Tsotsis, 2002). Moreover, the Italian company Tecnimont-KT has developed and fabricated a membrane reactor methane steam reforming pre-industrial prototype with a pure hydrogen production capacity of 20 Nm<sup>3</sup>/h (De Falco et al., 2011a) and described in paragraph 3.

MR concept is based on the removal of a reaction product in order to avoid the reaction equilibrium conditions to be achieved and promoting reaction kinetics.

Most of industrial chemical reactions are reversible reactions, thermodynamically limited since equilibrium conditions cannot be overcome in the reacting mixture. From a thermodynamic point of view, equilibrium is represented by a constraint, i.e. equilibrium constant, on mole concentrations, temperature and pressure, derived from the second principle of thermodynamics. When equilibrium conditions are achieved, no net change in state variables is observed.

From a kinetics point of view it means that at equilibrium the reaction rate of the direct reaction is equal to the reaction rate of the inverse reaction. Taking as reference an elementary reversible reaction:



the kinetics scheme is characterized by a direct reaction rate ( $A \rightarrow B$ ) and an inverse reaction rate ( $B \rightarrow A$ ). Initially, if only component A is fed to the reactor, the direct reaction is promoted. Then, as the concentration of component B increases, the inverse reaction is supported as far as the direct reaction and inverse reaction rates assumes a similar value (equilibrium conditions) and reaction stops.

Integrating a selective membrane into the reaction environment allows to remove the reaction product (B), avoiding the increase of inverse reaction and promoting the direct reaction kinetics. By this way, two main benefits are reached:

- removing one or more reaction products as they are generated allows to obtain conversions higher than equilibrium values;
- if the membrane is very selective with regard to a specific product, it is possible to support reaction and product separation in one single compact device, obtaining a very pure compound.



In this paragraph, the two main MR configurations are described and compared; then properties of selective membranes, suitable to be integrated in industrial chemical processes, are reported.

## 2.1 MR configurations

A selective membrane can be integrated in a chemical process by two different configurations:

- when the selective membrane is integrated directly in the reaction environment and the reaction product is removed as it is produced, the system is called Integrated Membrane Reactor (IMR);
- if the selective membrane is placed outside the reactor, in a proper unit located downstream, the system is called Staged Membrane Reactor (SMR) or Reactor and Membrane Module (RMM).

### 2.1.1 Integrated membrane reactor

An Integrated Membrane Reactor (IMR) is a compact device in which a selective membrane is directly assembled inside the reaction environment. The simplest configuration is composed by two concentric tubes, where catalyst pellets are packed in annular zone (Fig. 1) or in the inner tube (Fig.2), which is the membrane itself. Therefore, the reactor is composed by two zones:

- the reaction zone, where the catalyst is packed;
- the permeation zone, where the product permeated through the selective membrane is collected and carried out by a sweeping gas fed co-currently or counter-currently.

The membrane integration can be made also assembling many smaller tubes, so thus increasing the specific membrane surface on reactor volume and consequently the global permeated hydrogen flow.

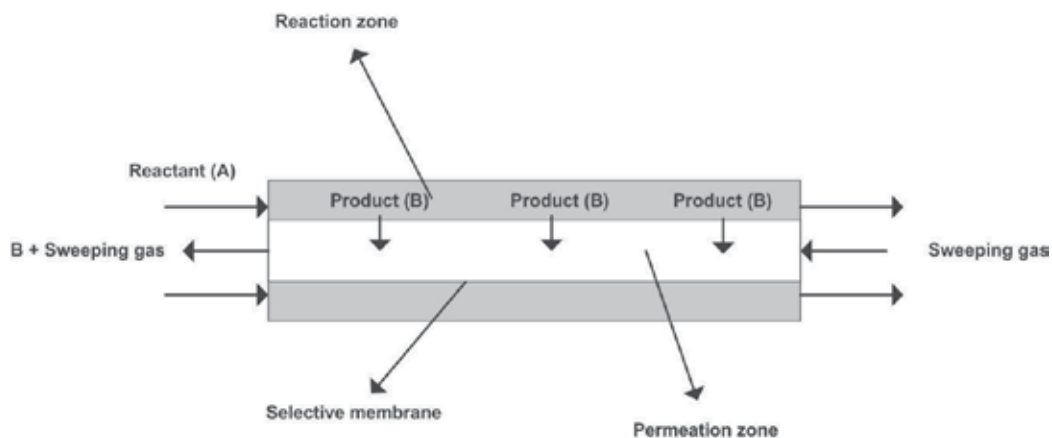


Fig. 1. IMR with catalyst packed in the annular zone.

### 2.1.2 Reactor and membrane module

The RMM configuration is composed by steps of reaction followed by steps of products separation through selective membranes. Fig. 3 shows a two reaction-separation modules

process layout: taking as reference the reaction (1), the reactant A is fed to the first reaction step where it is partially converted in the product B; then, the mixture A+B is sent to the separation module where component B is partially separated and recovered. The A-rich mixture is then fed to the second reaction step where the direct reaction is further promoted and the B produced is separated again in the second membrane module.

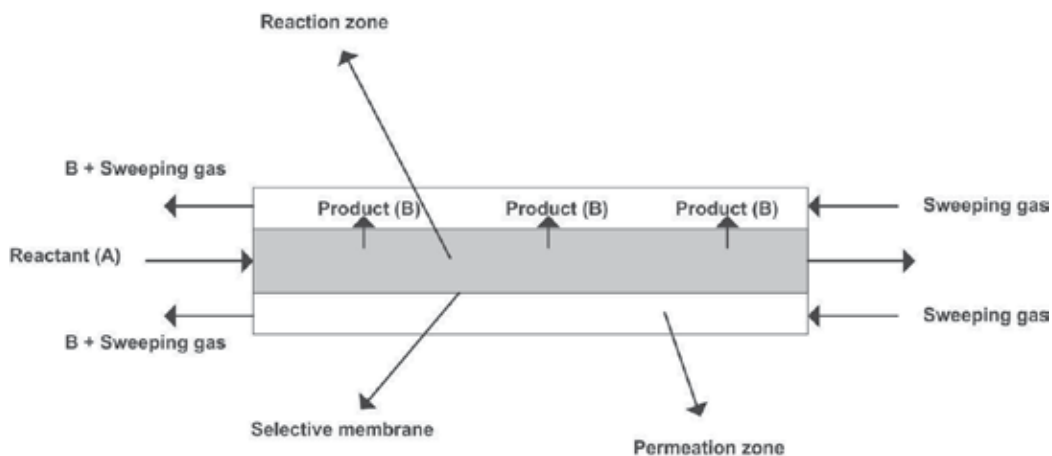


Fig. 2. IMR with catalyst packed in the inner tube.

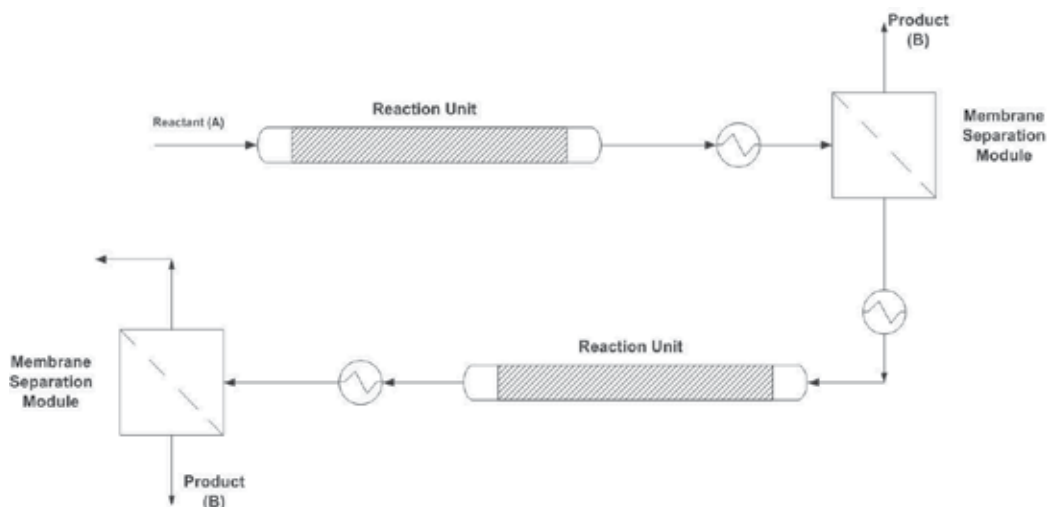


Fig. 3 RMM configuration.

### 2.1.3 MR configurations comparison

Both MR configurations assure crucial benefits in respect to the traditional technology. In order to compare the traditional technology and the membrane based one, we take as an example the methane steam reforming, which is the most applied process for industrial production of hydrogen. The conventional steam methane reforming system is composed of

a steam reformer, a shift converter and a hydrogen purifier based on the pressure swing adsorption (PSA).

The reactions that occur during this process are the following (2-4):



Steam reforming process is highly endothermic and equilibrium limited. To sustain global endothermic reaction and achieve high feed conversion, it is necessary to burn a part of methane feedstock in furnaces and operate at high temperature (800-850°C). This implies a reduced process global efficiency, increased greenhouse gas (GHG) emissions and a stronger dependence of hydrogen cost on the natural gas cost. Thus, on these bases the integration of a hydrogen selective membrane would allow:

- a strong reduction of the reaction temperature to about 450-650°C, since a high temperature is not required to reach natural gas conversion to hydrogen > 90%. The lower operating temperature leads to: a higher efficiency of the heat transfer from the external source to the reactor; a lower exergy of the heating fluid in comparison with the high temperature combustion gas used in the furnace, which means a lower heating cost; the possibility to use different heating fluids, depending on their availability; the possibility to fabricate tubular reactor by cheaper alloy steels.
- Process efficiency increase. The global process efficiency increases from the 65-80% of the traditional technology up to 85% and more for all the plant sizes.
- Combustion fuel saving. Reduction of reaction temperature leads to the reduction of process heat duty. The heat flux from the external source to the catalytic bed should be 30-40 kW/m<sup>2</sup> instead of 80 kW/m<sup>2</sup> about of the traditional process (Dybkjaer, 1995).

To make a comparison between IMR and RMM configurations (De Falco et al., 2011b), it is a worth assessment that:

- at the same operating conditions, IMR leads to better performance, since an integrated membrane reactor is equivalent to an infinite series of reactor + separator modules.
- On the other hand, in the RMM configuration, reaction and separation operating conditions can be optimized separately. In some cases it could be a crucial benefit. For example, in a methane reforming process, dense supported membranes (as Pd-based membranes on ceramics or Porous Stainless Steel) are assembled to selectively remove the hydrogen produced by the reactions. These membranes have to respect a stringent temperature threshold ( $T < 500^\circ\text{C}$ ) in order to guarantee a proper selective layer – support adherence. But a too low temperature limits the endothermic reaction thermodynamic conversion and the reaction rates. If an IMR is applied, a compromise solution has to be found, while in a RMM process the operating conditions of reaction and separation units can be imposed separately.

At the actual selective membrane state-of-the-art, RMM seems to be the leading architecture for membrane safety, for the multi-optimization potentiality and for its maintenance easiness. Surely, a future improvement of membrane performance, mainly for operating stability, would promote the applications of IMRs.

## 2.2 Selective membranes properties

Figure 4 shows a general classification of membranes, based on their nature, separation regime and geometry.

The classification based on the membrane nature distinguishes them into biological and synthetic ones, differing completely for functionality and structure.

Biological membranes are easy to be fabricated but they present many drawbacks such as limited operating temperature (below 100 °C) and pH range, problems related to the clean-up and susceptibility to microbial attack due to their natural origin (Xia et al., 2003).

Synthetic membranes can be subdivided into organic (polymeric) and inorganic (ceramic, metallic). Polymeric membranes operate between 100 - 300 °C, inorganic membranes above 200 °C. Surely, for industrial chemical process, the inorganic membranes are the most interesting.

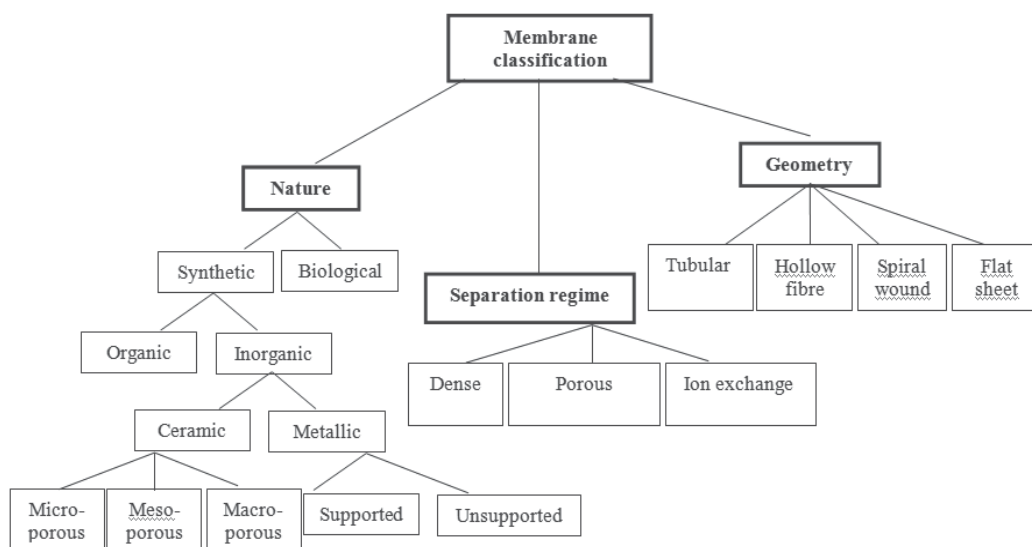


Fig. 4. Scheme of a general classification of the membranes (De Falco, 2011b).

Concerning with separation mechanism, there are three mechanisms depending on specific properties of the components (Mulder, 1996):

- separation based on molecules/membrane surface interactions (e.g. multi-layer diffusion) and/or difference between the average pore diameter and the average free path of fluid molecules (e.g. Knudsen mechanism);
- separation based on the difference of diffusivity and solubility of substances in the membrane: solution/diffusion mechanism;
- separation due to the difference in charge of the species to be separated: electrochemical effect.

In the following paragraphs, a pre-industrial application of selective membrane is described: the membrane applied is a Pd-alloy based supported membrane (dense inorganic membrane) for the separation of the hydrogen produced in a methane steam reformer. The Pd-based membranes are characterized by much high hydrogen selectivity and follow a solution/diffusion mechanism, composed by the following steps (Fig. 5):

- dissociation of molecular hydrogen at the gas/metal interface;
- adsorption of the atomic hydrogen on membrane surface;
- dissolution of atomic hydrogen into the palladium matrix;
- diffusion of atomic hydrogen through the membrane;
- re-combination of atomic hydrogen to form hydrogen molecules at the gas/metal interface;
- desorption of hydrogen molecules.

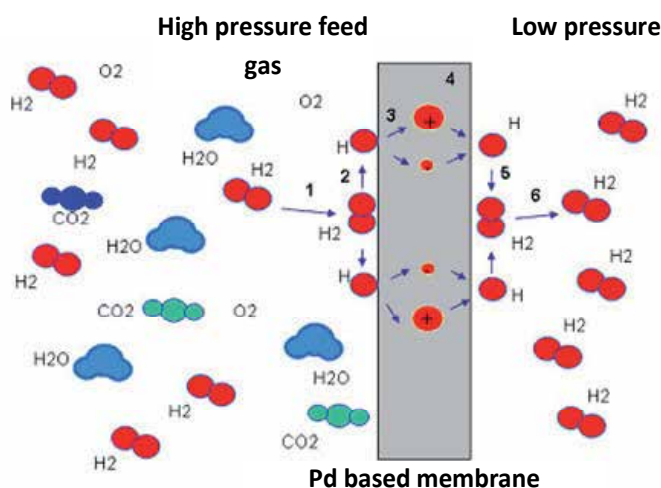


Fig. 5. Mechanism of permeation of hydrogen through metal membranes: 1) dissociation, 2) adsorption, 3) ionization, 4) diffusion, 5) recombination, 6) desorption (De Falco, 2011b).

When the pressure is relatively low, the diffusion is assumed to be the rate-limiting step and the permeation flux is described by Sieverts-Fick's law (5):

$$J_{H_2, \text{Sieverts-Fick}} = P_{e_{H_2}} / \delta \cdot (p_{H_2, \text{ret}}^{0.5} - p_{H_2, \text{perm}}^{0.5}) \quad (5)$$

where  $\delta$  is the membrane thickness,  $p_{H_2, \text{ret}}$  and  $p_{H_2, \text{perm}}$  are the hydrogen partial pressure in the retentate and permeate respectively,  $P_{e_{H_2}}$  is the membrane permeability calculated by Arrhenius law thus defined (6):

$$P_{e_{H_2}} = P_{e_{H_2}}^0 \exp(-E_a/RT) \quad (6)$$

where  $P_{e_{H_2}}^0$  is the pre-exponential factor,  $E_a$  the apparent activation energy,  $R$  the universal gas constant and  $T$  the absolute temperature.

Although a strong effort has been devoted to Pd-based membrane development by research and industrial institutions during these years, these membranes have not yet reached a commercial stage due to some technical issues as long term permeance and selectivity stability, but also to the cost related to their manufacture. In the following paragraphs, the pre-industrial plant fabricated by Tecnimont-KT in Italy is described and experimental tests results are reported. Then, the concept of coupling membrane reactors to nuclear reactors is analyzed from a technical and an economic point of view.

### 3. Reformer and membrane modules (RMM) plant

#### 3.1 Plant description

As reported above, a pre-industrial natural gas steam reforming RMM plant has been developed by Tecnimont-KT in Chieti Scalo. The plant process scheme is reported in Figure 6a together with a bird-eye view (Figure 6b) of the constructed industrial test plant which covers an area of 1000 m<sup>2</sup>.

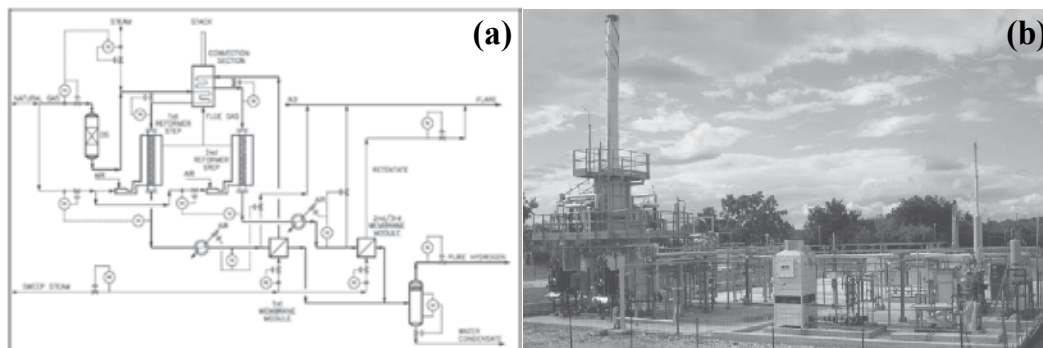


Fig. 6. Process scheme (a) and bird-eye view (b) of the industrial test plant

The plant is composed by two-step reformers and two membrane modules working respectively in the temperature range 550-650°C and 400-450°C.

Natural gas is supplied from battery limits or from cylinders at 20 barg. A portion of natural gas is fed through a flow controller to the desulphurisation reactor (DS) for sulphur compounds removal to content lower than 0.1 ppm. The residual is used as fuel gas, reduced at 0.3 barg. The desulphurised feed is mixed with steam, produced separately by a real hot oil boiler, preheated in the convection section and fed to the first reforming stage. More specifically, each reformer module is composed by two main sections: (i) a radiant tube, charged with the catalyst and (ii) a convection section, where heat is recovered from the flue gases, having a temperature higher than 800°C, for preheating and superheating feed and steam.

The design of the radiant chamber differs from the conventional one for the heated length of the reformer tube which is around 3 meter, the tube metallurgy and the contained catalyst. In particular, it must be observed that, owing to the lower operating temperature relevant to the use of this innovative architecture, a low cost stainless steel instead of exotic and quite expensive material as HP25/35 chromium/ nickel alloy was employed.

The reformed gas product from the first reformer is cooled down at the temperature chosen for membrane module operation and enters the first separation module. A retentate, recycled to the second reformer stage and a mixture of H<sub>2</sub> plus sweeping steam, are produced. The second reformer stage is cooled down from 650°C to the temperature chosen for membrane operation and routed to the second separation module. H<sub>2</sub> from both modules are mixed together and sent to final cooling and condensate separation. Retentate from the second stage is sent to the flare. The pressure of both shell and permeate sides are controlled using a back pressure regulators. Both membrane modules are protected using a pressure relief regulator installed on the income lines. All the vent points are connected to main vent system and routed to the flare. Heat of reaction in both reforming steps is provided by two independent hot gas generators in order to set the reforming temperatures as required by the tests.

The main parameters such as the temperatures and pressures before and after each reformer and separation step as well as the pressure drop along the catalytic tube were monitored respectively with K-type thermocouples and differential pressure sensors. A constant flow of the exhaust stream is sent through a cold trap maintained at fixed temperature (0°C) to NDIR analyzers (Uras 14, ABB) for real-time CH<sub>4</sub>, CO, CO<sub>2</sub> measurements, while the concentration of H<sub>2</sub> was performed with a thermoconductivity analyser (Caldos 17, ABB). Three different membrane separators, Pd and Pd/Ag based, able to work at high temperatures (480°C for ECN and Japanese membranes, 500°C for MRT), were planned for installation on the prototypal plant. Their main features are summarised in Table 1.

Developer	Substrate/support	Membrane selective layer	Thickness selective layer, $\mu\text{m}$	Geometry
ECN	Al <sub>2</sub> O <sub>3</sub>	Pd	3-9	Tubular
MRT	SS	Pd/Ag	25	Planar
Japanese	Al <sub>2</sub> O <sub>3</sub>	Pd/Ag	2-3	Tubular

Table 1. Main characteristics of the employed membranes (De Falco et al., 2011a)

Figure 7 show the installed membrane modules. The relevant permeation surfaces (A) are also reported.

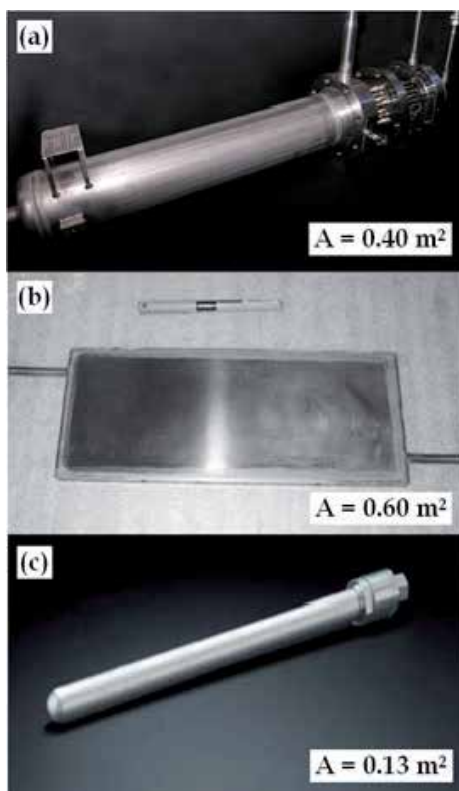


Fig. 7. ECN (a), MRT (b) and Japanese (c) membranes

Another innovation of this work is represented by the catalyst employed for the catalytic activity tests. Typically, methane steam reforming catalysts for industrial production of hydrogen and synthesis gas are based on pellets shaped nickel/nickel oxide or cobalt compositions on refractory alumina or supports such as magnesium alumina spinel, often promoted with alkali or alkali-earth compounds to accelerate carbon removal (Faur Ghenciu, 2002). However, also noble metals based catalysts are often employed. Furthermore, the consideration that in the steam reforming process, the kinetics, and therefore the throughput, is limited by the rate at which the heat generated in external burners can be transferred to the catalytic bed where the endothermic reforming reactions take place, led for this plant to the choice of open cells foam structured catalysts, whose particular irregular network may greatly contribute to an intensification of heat and mass transfer along the catalytic bed in both axial and, more important, radial directions. In particular, the catalytic activity tests performed at the University of Salerno in collaboration with TKT in the framework of the above mentioned FISR project, on a pre-pilot scale autothermal reforming reactor showed how such structured supports, in particular when fabricated with high thermal conductivity materials, may contribute to an enhancement of heat transfer along the catalytic bed resulting in a flattening thermal profile (Palo, 2007; Ciambelli et al., 2007). More specifically, the catalyst loaded in the industrial steam reformer in Chieti Scalo was characterized by a commercial formulation Rh-Pt based (SR10, BASF) deposited on high thermal conductivity SiC open cells foams. Each cylindrical shaped element was 150 mm long with a diameter of 60 mm and twenty-one elements were loaded in each reformer.



Fig. 8. Structured steam reforming catalyst

The catalytic activity tests were carried out in the following operating conditions:  $3.8 < (H_2O/CH_4)_w < 4.8$ ,  $550^\circ C < T_{\text{reformer}} < 680^\circ C$ ,  $P = 10 \text{ barg}$ ,  $4,300 \text{ h}^{-1} < \text{GHSV} < 6,900 \text{ h}^{-1}$  where the GHSV value is defined as the ratio between the total gaseous flow rate fed to the reactor (referred to  $0^\circ C$  and 1 atm) and the total catalytic bed volume. For membrane characterization in terms of hydrogen flux and permeability, the following syngas composition was employed (Table 2).

H <sub>2</sub> , vol%	CH <sub>4</sub> , vol%	CO <sub>2</sub> , vol%	CO, vol%	H <sub>2</sub> O, vol%
24-30	6-9	6-9	1-2	54-59

Table 2. Typical syngas composition used for membranes characterization (De Falco et al., 2011a)



### 3.2 Plant performance

The first preliminary catalytic activity tests without membrane integration were performed aiming to evaluate the effect of the main parameters, i.e. reformer outlet temperature, steam to carbon feed ratio and gas hourly space velocity, on  $\text{CH}_4$  conversion. The obtained results are reported in Figure 9.

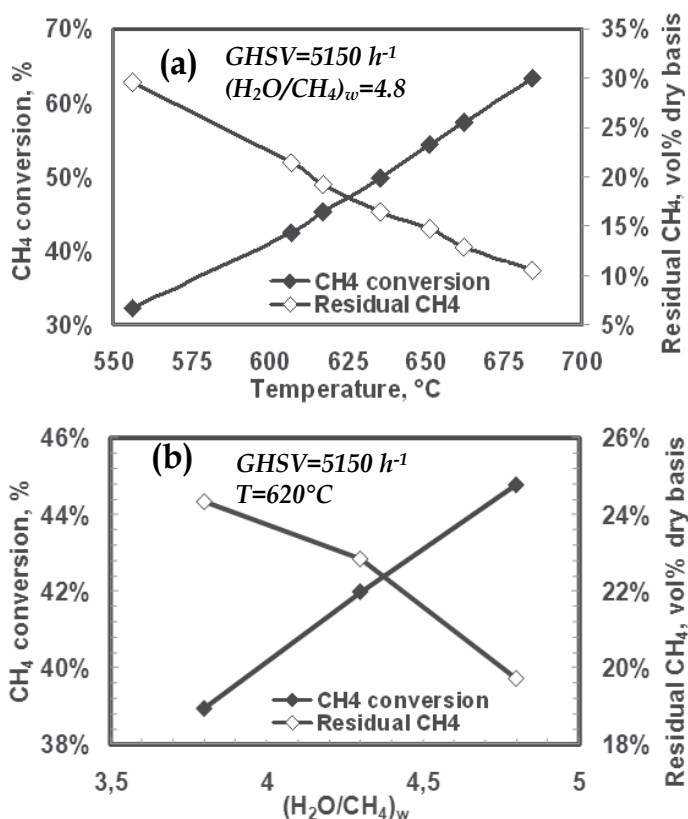


Fig. 9. Effect of reformer outlet temperature (a) and steam to carbon ratio (b) on  $\text{CH}_4$  conversion and residual  $\text{CH}_4$

It can be observed a decrease in the residual methane at the reactor outlet and a corresponding increase in methane conversion at increasing both the reformer outlet temperature (from 32% at 550 °C to 64% at 680 °C) and the steam to carbon feed ratio (from 39% at  $S/C=3.8$  to 44.8% at  $S/C=4.8$ ). A detrimental effect was on the contrary noticed upon changing the GHSV value in the range 4,300-6,900  $\text{h}^{-1}$  since a decrease in methane conversion from 48.7% to 46.5% was observed (De Falco et al., 2011a, De Falco et al., 2011b). However, in time on stream tests performed over 1000 h, any catalyst deactivation occurred, as evidenced by stable methane conversion over the entire test period (De Falco et al., 2011a).

Membrane integration resulted in an enhanced overall plant performance. A comparison of methane conversion obtained in the absence or in the presence of membranes for hydrogen separation is reported in Figure 10 as a function of GHSV values. The results are collected

over 200 h of operation at 10 barg, at a reformer outlet temperature ranging between 610-620°C and at a steam to carbon ratio of 4.8 (De Falco et al., 2011a).

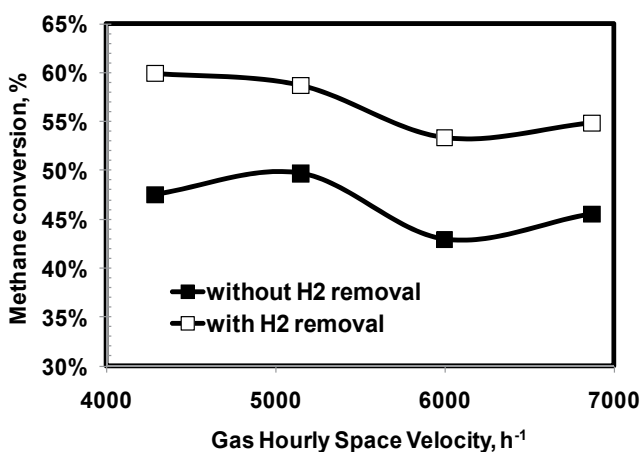


Fig. 10. Effect of hydrogen removal on plant performance at changing the gas hourly space velocity

All these catalytic activity tests enabled for a membranes permeability characterization. In particular, by assuming the Arrhenius law for the dependence of permeability from temperature and the Sievert-Fick's law for hydrogen flux expression (Ockwig and Nenoff, 2007), the following results were obtained for the tested three membranes (Table 3, De Falco et al., 2011a):

Membrane	Pre-exponential factor, kmol/(m h kPa <sup>0.5</sup> )	Activation energy, kJ/mol	Permeability at 450°C, kmol/(m h kPa <sup>0.5</sup> )
ECN	$1.72 \times 10^{-1}$	77.0	$4.67 \times 10^{-7}$
MRT	$5.75 \times 10^{-4}$	35.3	$1.61 \times 10^{-6}$
Japanese	$9.31 \times 10^{-2}$	80.4	$1.44 \times 10^{-7}$

Table 3. Permeability membranes characterisation results (De Falco et al., 2011a)

Furthermore, starting from permeability expression above reported, for ECN membrane several parametric studies were performed, enabling to predict the overall CH<sub>4</sub> conversion with both: (i) a larger membrane surface (De Falco et al., accepted for publication) and (ii) a higher membrane thickness as parameters. In both cases, the experimental operating conditions were the following:  $P_{ref}=10$  barg,  $(H_2O/CH_4)_w=4.8$ ,  $P_{perm}=0.4$  barg,  $T_{mem}=430$ °C. The CH<sub>4</sub> conversion evaluation was carried out by commercial process flow modeling (PRO II) integrated with a subroutine to simulate membrane behaviour.

The first case was more specifically developed by assuming in the calculations the same permeance of  $30 \text{ Nm}^3/\text{m}^2 \text{ h bar}^{0.5}$  obtained at 430°C. The CH<sub>4</sub> conversion was found to be enhanced with an increase in the reforming temperature and membrane area. In particular, the membrane area can be increased to achieve the same conversion at lower reformer temperature (methane conversion of 60% can be achieved at 603°C with  $A=1.2\text{m}^2$ , at 623°C with  $A=0.4\text{m}^2$ ). Methane conversion increases more slowly when the membrane area

exceeds 0.8m<sup>2</sup>. By comparing such data with those obtained in the absence of membrane, it was possible to evaluate the conversion increase with such open architecture. At 620°C such increase ranges from 11 to 19 point percent respectively, with a membrane surface of 0.4m<sup>2</sup> and 0.8m<sup>2</sup>.

In the second case, the membrane permeance was extrapolated at different selective layer thicknesses ranging between 2.5 and 100 micron. The results are reported in Figure 11, as well as those obtained from literature review.

Obviously, the thickness of the separation layer greatly affects the membrane permeance which resulted lowered from  $2.12 \times 10^{-4}$  to  $5.3 \times 10^{-6}$  at 350°C and from  $7.85 \times 10^{-3}$  to  $1.96 \times 10^{-4}$  at 550°C by increasing the thickness of the separation layer from 2.5 to 100 micron. The obtained results pointed out on the continuous industrial efforts aiming to develop composite membrane made of a very thin Pd layer. It is worth nothing that reducing the selective layer thickness allows membrane cost to be decreased (decreasing the Pd thickness by a factor two reduces the total Pd cost by a factor four) and increasing the hydrogen flux, which is in inverse proportion with the film thickness. On the other side, a too high decrease in the selective film thickness may result in an excessive embrittlement of the membrane which becomes too mechanically fragile for the condition of high temperature catalytic processes.

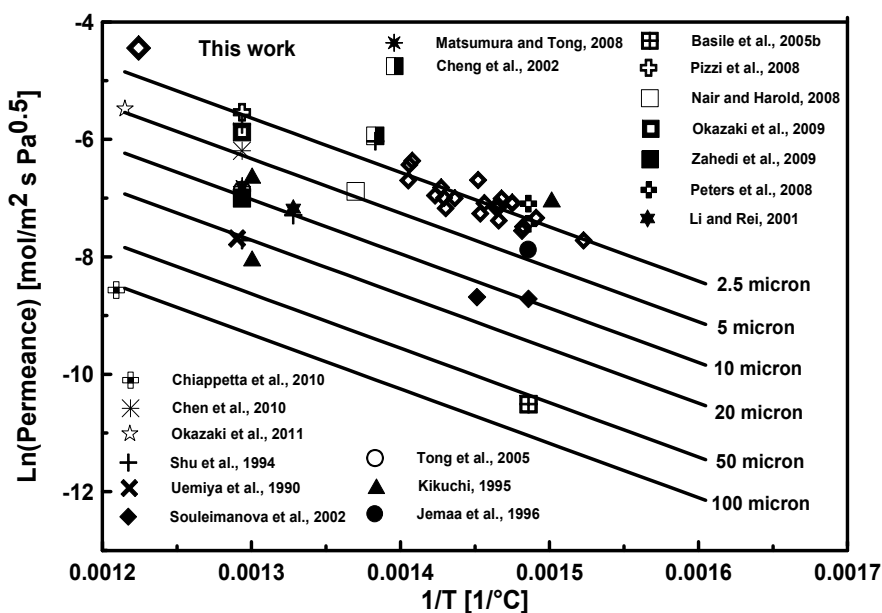


Fig. 11. Effect of membrane thickness on ECN membrane permeance

In terms of CH<sub>4</sub> conversion, the influence of the selective layer thickness is reported in Figure 12, even at lower value than those reported in Figure 11.

At each operating temperature investigated, the decrease of membrane thickness resulted in higher methane conversion. In particular, at 630°C, a reduction of membrane thickness from 2.5 micron to 0.5 micron may enhance methane conversion of 10% due to the higher hydrogen removal. It is interesting to note that thickness thinner than 0.5 micron have no more significant effect on the overall performance. Such a thickness could be considered as

the technological limit to be overcome. Globally it is possible to reach  $\text{CH}_4$  conversion higher than 90% with a permeated  $\text{H}_2$  flux of  $300 \text{ Nm}^3/\text{m}^2 \text{ h bar}^{0.5}$ .

The achievement of this goal shows the industrial feasibility of this option up to now demonstrated only on a laboratory scale, even if the last gap to be overcome for the technology commercialization is represented by the optimization of membrane preparation procedure with enhancement of their stability.

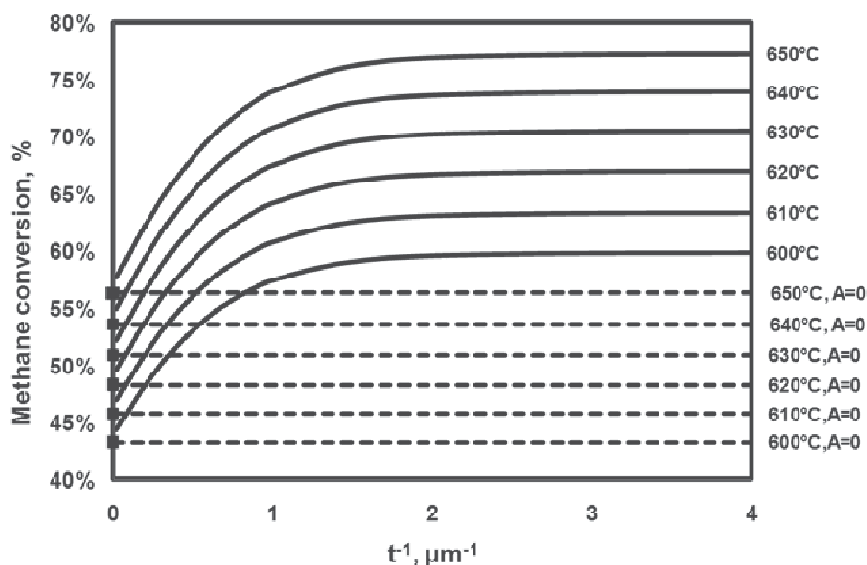


Fig. 12. Effect of membrane thickness on  $\text{CH}_4$  conversion with ECN membrane

### 3.3 Application to nuclear power

In order to sustain the global endothermic steam reforming reaction, a part of the methane feedstock must be burned in a fired heater. To reduce this consumption, purge gas coming from PSA unit or retentate from the membrane separation unit have to be burned. The calorific value of these streams is a function of composition and consequently of the achieved conversion. A self-balance of heat exits with a fixed external natural gas supply, at an appropriate level of feed conversion. Therefore, conversion should not exceed the point closing the heat balance (around 60%).

Furthermore, it must be considered that owing to the high process temperature, the thermal efficiency of this process is about 65 to 75%. Also, a substantial amount of greenhouse gases (GHG) is emitted as  $\text{CO}_2$  produced along with hydrogen. Moreover, carbon dioxide is also emitted during the burning of a part of methane feedstock in order to sustain the global endothermic balance of the steam reforming reaction. In total, a typical steam reforming process emits up to 8.5 – 12 kg  $\text{CO}_2$  per 1 kg  $\text{H}_2$ . To prevent the emitted  $\text{CO}_2$  to be released into the atmosphere, it needs to be captured. Presently, all commercial  $\text{CO}_2$  capture plants use processes based on chemical absorption with amine solvents as monoethanolamine (MEA) or (methyldiethanolamine) MDEA, which is a considerably energy intensive step and thus is unfavourable to the overall process energy efficiency.

Therefore, a higher methane conversion is required to reduce the carbon dioxide emission per unit of hydrogen produced. This could be achieved by using heat from an external

source such as a high temperature nuclear reactor. Replacing the burning of natural gas by nuclear heat allows avoiding, at least partially, all the CO<sub>2</sub> production related to fuel burning (De Falco et al. accepted for publication, Iaquaniello and Salladini, 2011).

High temperature helium-cooled reactors are the best understood nuclear technology that can supply high temperature heat for thermal processes for producing hydrogen. Nuclear reactor designers became interested in high-temperature helium-cooled reactors more than 40 years ago because of the new possibility for heating the helium at the reactor exit up to 1000°C and the enhanced safety of the reactor (Mitenkov et al., 2004).

The synergistic production of hydrogen using fossil fuels and nuclear energy is considered to be extremely advantageous, especially when performed through a recirculation-type membrane reformer (Hori et al., 2005).

In particular, even assuming an idealistic case, in which all the heat generated by combustion of hydrocarbon is used for the heat of endothermic reaction of steam reforming as well as a portion of the heat released by exothermic water gas shift reaction, the consumption of methane for the nuclear-heated steam reforming reaction is 17% less of that of the conventional steam reforming reaction for producing the same amount of hydrogen. In the actual case of conventional steam reforming as the heat utilization and the reaction yield are limited, the efficiency of the process will be around 80%, that is 2.7 mol of hydrogen produced from 1 mol of methane feed. In the case of nuclear-heated recirculation-type membrane reformer, as no methane is consumed for combustion and the yield of hydrogen is nearly stoichiometric, the nuclear-heated SMR reaction will produce 4 mol of hydrogen from 1 mol of methane. Therefore, this process scheme will save about 30% natural gas consumption, or reduce 30% carbon dioxide emission, comparing with traditional process (Hori et al., 2005). Furthermore, typical merits of this process are: (i) nuclear heat supply at medium temperature around 550°C, (ii) compact plant size and membrane area for hydrogen production, (iii) efficient conversion of a feed fossil fuel, (iv) appreciable reduction of carbon dioxide emission, (v) high purity hydrogen without any additional process and (vi) ease of separating carbon dioxide for future sequestration requirements.

Figure 13 reports a plant configuration of hydrogen and pressurized CO<sub>2</sub> production coupled with a nuclear reactor cooled by He.

Natural gas is compressed, heated and mixed with hydrogen recycle before entering the hydro desulphurizer reactor (HDS). The desulphurised feed is mixed with steam, preheated in the convective section CC-01 and fed to the first reforming step (R-01). The reformed gas reaction mixture at 600-650°C is cooled down to a proper temperature for membrane separation, i.e. 450-470°C, before entering the first separation module. Sweeping steam is sent to the permeate side of the membrane to reduce the hydrogen partial pressure with a consequent improvement of hydrogen permeation. The permeate side stream, composed of hydrogen and sweeping steam, is sent to the cooling and water condensing section. The retentate from the first membrane module is sent to the second reforming reactor (R-02) for further methane conversion.

A part of the final retentate is recycled to the post combustion chamber. The hydrogen permeated is separated from water stream by condensation and routed to a compression section and to a PSA unit where final purification is carried out. A portion of the H<sub>2</sub> produced is recycled to the feed where it is needed to keep the catalyst in the first part of the reformer in an active state.

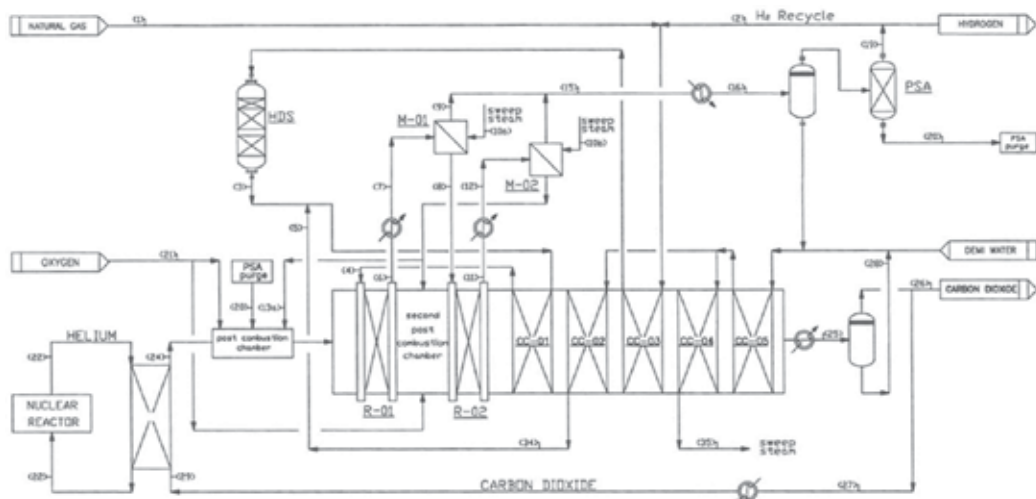


Fig. 13. Process scheme of hydrogen and pressurised CO<sub>2</sub> production coupled with a nuclear reactor cooled by He

Thermal fluid used to transfer thermal energy from the nuclear cycle to reforming reactors is CO<sub>2</sub> circulating within a closed loop. CO<sub>2</sub> is firstly heated up by the heat exchange medium of a nuclear plant in an intermediate heat exchanger. Its temperature is further increased in the post-combustion chamber where all the purge gas from the PSA unit together with a portion of retentate are burned to achieve a correct temperature. Thus, the thermal fluid is a pressurized mixture of only CO<sub>2</sub> and H<sub>2</sub>O due to the use of pure oxygen in post combustion. After heat recovery, thermal fluid is cooled down to separate water from CO<sub>2</sub>. The latter is recycled back to the nuclear reactor while a portion, corresponding to that produced in post combustion, is removed from the closed loop. Water, produced in post combustion, can be recycled to the process. This kind of separation is much simpler and less energy intensive than a traditional physical absorption process with amine solutions. Moreover, providing the reformer duty through pressurized carbon dioxide instead of, e.g., air allows to achieve a higher heat transfer coefficient due to the higher heat capacity and gas emissivity.

By applying the proposed scheme, hydrogen and pressurized carbon dioxide are produced with a nuclear heat source and with a reduced carbon dioxide emission. In this way, the major portion of the heat required for the steam reforming reaction is not provided by the combustion of fresh hydrocarbons but is supplied from a separate unit without carbon dioxide emissions.

The scheme presented in Figure 13 realises a feed conversion of 90% with a carbon dioxide production equal to 6 kgCO<sub>2</sub>/kgH<sub>2</sub> corresponding to 0.55 kgCO<sub>2</sub>/Nm<sup>3</sup>H<sub>2</sub>. From the energy point of view, using a RMM architecture allows to produce hydrogen with a higher overall energy efficiency. The reduced reforming temperature achievable only by membrane application, allows performing the exothermic water gas shift reaction simultaneously with the endothermic steam reforming reaction reducing in this way the net heat duty. The proposed scheme achieves a hydrogen production with an overall energy efficiency of more than 85%. Such a scheme could be also considered a first step in producing ammonia and urea by reacting ammonia with CO<sub>2</sub> recovered (Figure 14).

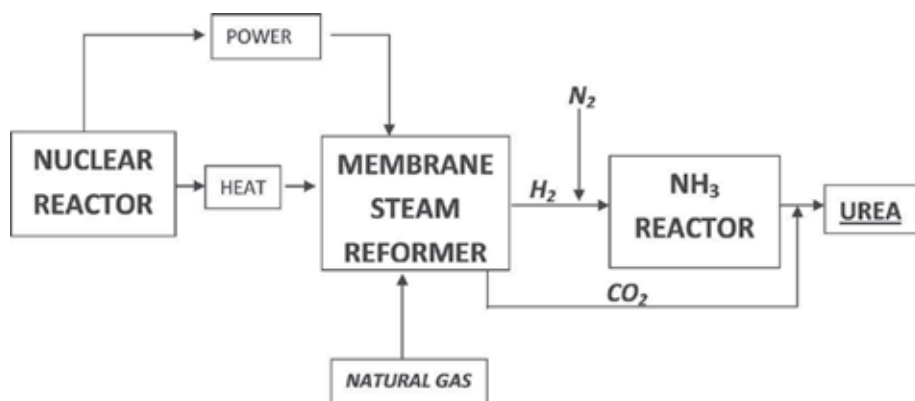


Fig. 14. Process scheme for urea production coupling a membrane steam reformer with a nuclear reactor

#### 4. Economic analysis

An economic analysis was performed at first focusing attention on membrane production costs, further the analysis was extended to the coupled process scheme proposed in the previous section.

In order to tackle this issue and to be able to forecast a production cost for thin Pd-based membranes, it is important to introduce the concept of “economics of learning” in understanding the behaviour of all added costs of membranes as cumulative production volume increased. Such economics of learning or law of the experience may be expressed more precisely in an algebraic form (7):

$$c_n = c_1 n^{-a} \quad (7)$$

where  $c_1$  is the cost of the unit production (square meter of membrane for instance),  $c_n$  is the cost of the  $n^{\text{th}}$  unit of production,  $n$  is the cumulative volume of production, and  $a$  is the elasticity of cost with regard to output.

Graphically, the experience curve is characterized by a progressively declining gradient, which, when translated into logarithms, is linear. The size of experience effect is measured by the proportion by which costs are reduced with subsequent doublings of aggregate production.

Constructing an experience curve is a simple matter once the data are available. Of course for the Pd-based or ceramic membrane such dates are limited to minimal surface (less than 1 m<sup>2</sup>), which can, however, be used as starting point of the curve. The other issue associated with drawing an experience curve is that cost and production data must be related to a “standard product”, which is not the case due to the fact that in the membrane technology no standard is yet emerged and there is a lot of discussion on the membrane composition and preparation method, supporting matrix and other mechanical and construction details.

It is, however, a fact that costs decline systematically with increases in cumulative output. The assumptions made in the following are that  $c_1=50,000$  € and  $a=0.25$ , where  $c_1$  value derived by Tecnimont-KT recent experience in building a pilot unit, meanwhile the “ $a$ ” factor was assumed as average value typically between 20 and 30%.

Using such a data is possible to forecast the cost for m<sup>2</sup> of membrane module versus the cumulative value of production, expressed in terms of m<sup>2</sup>. Table 4 shows such data.

Cumulated production m <sup>2</sup>	€ cost per m <sup>2</sup>
1,000	8,900
10,000	5,000
100,000	2,800
1,000,000	1,600
10,000,000	900

Table 4. Cost per m<sup>2</sup> of membrane module versus cumulated production

From the drawn experience curve, some implications for the membranes market business strategy can be extracted. The first and more important question to answer is when a 1,000,000 m<sup>2</sup> of membrane module cumulative production could be reached in order to have a unit cost around 1.600 € per m<sup>2</sup> of membrane.

In order to answer such a question, further considerations need to be developed, to relate surface to membrane module to the H<sub>2</sub> production and to the introduction of such a new technology in the market.

On previous published data, Iaquaniello et al. (2008) were calculating for a open membrane reactor architecture a surface of 1,000 m<sup>2</sup> for an installed capacity of 10,000 Nm<sup>3</sup>/h of hydrogen. The envisaged installed capacity in the hydrogen market is today around 1 MM Nm<sup>3</sup>/h of capacity per year, which translated into a production of 100,000 m<sup>2</sup> of membrane year, once the new technology will supersede the conventional one.

To derive the rate of membranes technology introduction in the market a Volterra equation was considered (8):

$$x = A/(1+e^{(Bx)}) + C \quad (8)$$

where A, B, C are constants and x is the cumulative production.

Such equation, also called “S logistic curve” is used to describe a process with a low growth which accelerate with time to seem an exponential growth. A 10-year period (2012–2022) is considered to achieve 50% substitution in the conventional market starting from 2012, which roughly implies that over the next decade half a million of square meters of membranes modules could be produced. With such cumulative production around year 2020, the membrane cost per m<sup>2</sup> could reach the target of 1.600 € per m<sup>2</sup> and the overall market will have a size of 1 billion of € per year.

Figure 14 represents the cumulative production coupled to the “S” curve.

The approach used to determine the growth of the membranes market, together with the cumulative production does not, however, identify the real factors that determine its dynamics. As matter of fact, the experience curve combines four sources of costs reduction: learning, economics of scale, process innovation, and improved production design.

Economics of scale, conventionally associated with manufacturing operations, is probably the most important of these costs drivers and exists wherever as the scale of production increases unit costs fall. A plant capacity has then an economic sense if a minimum efficiency plant capacity is reached.

This will imply that to reach the required reduction in the membrane cost, not only a few specialized technologies must emerge, but the production market will be concentrated in few highly specialized production plants.

Regarding the proposed process scheme coupling a membrane based steam reformer with a nuclear reactor, a preliminary investigation was carried out under the basic assumption that the cost of electric power from nuclear source is 0.03€/kWh (Romanello et al., 2006). Thus, in



order to produce 1000 kWh<sub>e</sub> the total costs amount is 30€. Considering an efficiency equal to around 34%, so that 3000 kWh<sub>th</sub> (or 2580000 kcal) should be produced to obtain our power target, this will translate into a cost of 12€/MMkcal against more than 30€ for heat produced from natural gas. The variable costs of producing H<sub>2</sub> are then reduced of more than 20% without considering the beneficial effects of reduced CO<sub>2</sub> emissions in the atmosphere.

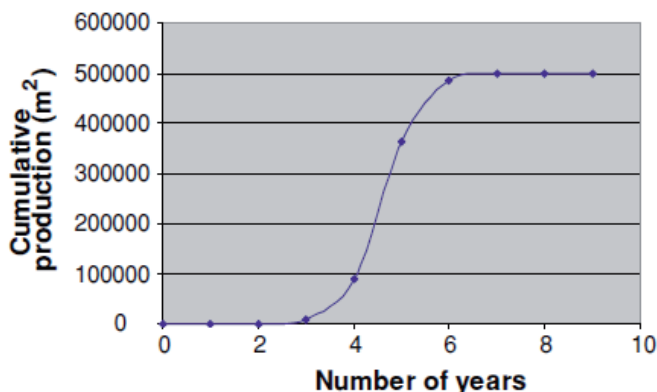


Fig. 15. Cumulative production coupled to the “S” curve

Compared to the thermochemical processes, hydrogen production by nuclear-heated steam reforming of natural gas is considered to be much closer to commercialization and is viewed as an intermediate step to nuclear-driven hydrogen production from water.

Alternatively such process could be modified to produce urea without any additional CO<sub>2</sub> emissions.

## 5. Conclusions and future perspectives

Membrane reforming with recirculation of reaction products in closed loop configuration is a particularly promising nuclear application, even if one of the last gap to be overcome for the technology commercialization of membrane reformers is represented by the optimization of membrane preparation procedure with enhancement of their stability. Because the nuclear heat is needed at below 600°C, it employs a compact membrane and reformer, and gives efficient conversion of the hydrocarbon feed and high-purity hydrogen without additional processing. With all these benefits, the synergistic blending of fossil fuels and nuclear energy to produce hydrogen, ammonia and urea, can be an effective solution for the world until large-scale thermochemical water splitting processes, which may benefit from economy of scale, are available. For both the fossil fuels industry and the nuclear industry, this approach offers a viable symbiotic strategy with the minimum of impact on resources, the environment and the economy.

## 6. Acknowledgment

The pre-industrial natural gas steam reforming RMM plant was developed within the framework of the project “Pure hydrogen from natural gas reforming up to total conversion obtained by integrating chemical reaction and membrane separation”, financially supported by

MIUR ( FISR DM 17/12/2002)-Italy. The authors are grateful to Prof. Luigi Marrelli and Prof. Diego Barba for their support.

## 7. References

- Basile, A.; Gallucci, F. & Paturzo, L. (2005a). A dense Pd/Ag membrane reactor for methanol steam reforming: Experimental study. *Catalysis Today*, Vol. 104, No. 2-4, (June 2005), pp. 244-250, ISSN 0920-5861.
- Basile, A.; Gallucci, F. & Paturzo, L. (2005b). Hydrogen production from methanol by oxidative steam reforming carried out in a membrane reactor. *Catalysis Today*, Vol. 104, No. 2-4, (June 2005), pp. 251-259, ISSN 0920-5861.
- Chen, W. ; Hu, X. ; Wang, R. & Huang, Y. (2010). On the assembling of Pd/ceramic composite membranes for hydrogen separation. *Separation and Purification Technology* Vol. 72, No. 1, (March 2010), pp. 92-97, ISSN 1383-5866.
- Cheng, Y.S.; Pena, M. ; A., Fierro J. L. ; Hui, D.C.W. & Yeung, K.L. (2002). Performance of alumina, zeolite, palladium, Pd-Ag alloy membranes for hydrogen separation from town gas mixture. *Journal of Membrane Science*, Vol. 204, No. 1-2, (July 2002), pp. 329-340, ISSN 0376-7388.
- Chiappetta, G.; Barbieri, G. & Drioli, E. (2010). Pd/Ag based membranes reactors on small scale: assessment of the feed pressure and design parameters effect on the performance. *Chemical Engineering and Processing: Process Intensification*, Vol. 49, No. 7, (July 2010), pp. 722-731, ISSN 0255-2701.
- Ciambelli, P.; Palma, V.; Palo, E.; Iaquaniello, G.; Mangiapane, A. & Cavallero, P. (2007). Energy sustainable development through methane autothermal reforming for hydrogen production. *AIDIC Conference Series*, Vol. 8, pp. 67-76, ISBN 0390-2358.
- De Falco, M. ; Di Paola, L. ; Marrelli, L. & Nardella, P. (2007). Simulation of large-scale membrane reformers by a two-dimensional model. *Chemical Engineering Journal*, Vol. 128, No. 2-3, (April 2007), pp. 115-125, ISSN 1385-8947.
- De Falco, M. ; Iaquaniello, G. & Salladini, A. (2011a). Experimental tests on steam reforming of natural gas in a reformer and membrane modules (RMM) plant. *Journal of Membrane Science*, Vol. 368, No. 1-2, (February 2011), pp. 264 - 274, ISSN 0376-7388.
- De Falco, M. ; Marrelli, L. & Iaquaniello, G. (2011b). Membrane Reactors for Hydrogen Production Processes. Springer Ed., ISBN 978-0-85729-150-9.
- De Falco, M. ; Salladini, A. & Iaquaniello, G. (accepted for publication). Reformer and membrane modules (RMM) for methane conversion : experimental assessment and perspectives of said innovative architecture. *ChemSusChem*, ISSN 1864-564X.
- Dittmeyer, R. ; Höllein, V. & Daub, K. (2001). Membrane reactors for hydrogenation and dehydrogenation processes based on supported palladium. *Journal of Molecular Catalysis A: Chemical*, Vol. 173, No. 1-2, (September 2001), pp. 135-184, ISSN 1381-1169.
- Dybkjaer, I. (1995). Tubular reforming and autothermal reforming of natural gas - an overview of available processes. *Fuel Processing Technology*, Vol. 42, No. 2-3, (April 1995), pp. 85-107, ISSN 0378-3820.
- Faur Ghenciu, A. (2002). Review of fuel processing catalysts for hydrogen production in PEM fuel cell systems. *Current Opinion in Solid State & Materials Science*, Vol. 6, No. 5, (October 2002), pp. 389-399, ISSN 1359-0286.

- Hori, M.; Matsui, K.; Tashimo, M.; Yasuda, I. (2005). Synergistic hydrogen production by nuclear-heated steam reforming of fossil fuels. *Progress in Nuclear Energy*, Vol. 47, No. 1-4, (December 2005), pp. 519-526, ISSN 0149-1970.
- Iaquaniello, G.; Giacobbe, F.; Morico, B.; Cosenza, S.; Farace, A. (2008). Membrane reforming in converting natural gas to hydrogen: Production costs, Part II. *International Journal of Hydrogen Energy*, Vol. 33, No. 22, (November 2008), pp. 6595-6601, ISSN 0360-3199.
- Iaquaniello, G. & Salladini, A. (2011). Method for hydrogen production. *European Patent Application* EP11150491.
- Jemaa, N. ; Shu, J. ; Kaliaguine, S. & Grandjean, B. (1996). Thin palladium film formation on shot peening modified porous stainless steel substrates. *Industrial & Engineering Chemistry Research*, Vol. 35, No. 3, (March 1996), pp. 973-977, ISSN 0888-5885.
- Kikuchi, E. (1995). Palladium/ceramic membranes for selective hydrogen permeation and their application to membrane reactor. *Catalysis Today*, Vol. 25, No. 3-4, (August 1995), pp. 333-337, ISSN 0920-5861.
- Li, Y.M. & Rei, M.H. (2001). Separation of hydrogen from the gas mixture out of catalytic reformer by using supported palladium membrane. *Separation and Purification Technology*, Vol. 25, No. 1-3, (October 2001), pp. 87-95, ISSN 1383-5866.
- Matsumura, Y. & Tong, J. (2008). Methane steam reforming in hydrogen-permeable membrane reactor for pure hydrogen production. *Topics in Catalysis*, Vol. 51, No. 1-4, (October 2008), pp. 123-132, ISSN 1022-5528.
- Mendes, D. ; Mendes, A. ; Madeira, L. M. ; Iulianelli, A. ; Sousa, J. M. & Basile, A. (2010). The Water-Gas Shift Reaction: From Conventional Catalytic Systems to Pd-based Membrane Reactors – a Review. *Asian-Pacific Journal of Chemical Engineering on Membrane Reactors*, Vol. 5, No. 1, (August 2009), pp. 111-137, ISSN 1932-2143.
- Mitenkov, F.M. ; Kodochigov, N.G. ; Vasyaev, A.V. ; Golovko, V.F. ; Ponomarev-Stepnoi, N.N. ; Kukharkin, N.E. & Stolyarevskii, A.Ya. (2004). High-temperature gas-cooled reactors-energy source for industrial production of hydrogen. *Atomic Energy*, Vol. 97, No. 6, (December 2004), pp. 829-840, ISSN 1063-4258.
- Mulder, M. (1996). *Basic Principles of Membrane Technology*. Kluwer Academic: Dordrecht pp. 564.
- Nair, B. K. R & Harold, M. P. (2008). Experiments and modeling of transport in composite Pd and Pd/Ag coated alumina hollow fibers. *Journal of Membrane Science*, Vol. 311, No. 1-2, pp. 53-67, ISSN 0376-7388.
- Ockwig, N.W. & Nenoff T.M. (2007). Membranes for hydrogen separation. *Chemical Reviews*, Vol. 107, No. 10, (October 2007), pp. 4078-4140, ISSN 0009-2665.
- Okazaki, J. ; Ikeda, T. ; Pacheco Tanaka, D.A. & Sato, K. (2011). An investigation of thermal stability of thin palladium-silver alloy membranes for high temperature hydrogen separation. *Journal of Membrane Science*, Vol. 366, No. 1-2, pp. 212-219, ISSN 0376-7388.
- Okazaki, J. ; Ikeda, T. ; Pacheco Tanaka, D. A. ; Suzuki, T. M. & Mizukami F. (2009). In situ high-temperature X-ray diffraction study of thin palladium- $\alpha$ -alumina composite membranes and their hydrogen permeation properties. *Journal of Membrane Science*, Vol. 335, No. 1-2, pp. 126-132, ISSN 0376-7388.
- Palo, E. (2007). *Structured catalysts for hydrogen production by methane autothermal reforming*. PhD Thesis, University of Salerno.

- Peters, T. A.; Stange, M.; Klette, H. & Bredesen R. (2008). High pressure performance of thin Pd-23%Ag/stainless steel composite membranes in water gas shift gas mixture: influence of dilution, mass transfer and surface effects on hydrogen flux. *Journal of Membrane Science*, Vol. 316, No. 1-2, pp. 119-127, ISSN 0376-7388.
- Pizzi, D.; Worth, R. ; Baschetti, M. G. ; Sarti G. C. & Noda K. (2008). Hydrogen permeability of 2.5  $\mu\text{m}$  palladium-silver membranes deposited on ceramic supports. *Journal of Membrane Science*, Vol. 325, No. 1, pp. 446-453, ISSN 0376-7388.
- Romanello, V.; Lomonaco, G.; Cerullo, N. (2006). I veri costi dell'energia nucleare. NT1127(2006). Università di Pisa.
- Sanchez Marcano, J.G. & Tsotsis, T.T. (2002). Catalytic membranes and membrane reactors. Wiley-VCH Verlag, Weinheim.
- Shu, J.; Grandjean, B. & Kaliaguine, S. (1994). Methane steam reforming in asymmetric Pd- and Pd-Ag/porous SS membrane reactors. *Applied Catalysis A : General*, Vol. 119, No. 2, (November 1994), pp. 305-325, ISSN 0926-860X.
- Souleimanova, R.S.; Mukastan, A.S. & Varma, A. (2002). Pd membranes formed by electroless plating with osmosis: H<sub>2</sub> permeation studies. *AIChE Journal*, Vol. 48, No. 2, (February 2002), pp. 262-268, ISSN 1547-5905.
- Tong, J.; Matsumura, Y. ; Suda, H. & Haraya, K. (2005). Thin and dense Pd/CeO<sub>2</sub>/MPSS composite membrane for hydrogen separation and steam reforming of methane. *Separation and Purification Technology*, Vol. 46, No. 1-2, (November 2005), pp. 1-10, ISSN 1383-5866.
- Uemiya, S.; Sato, N.; Ando, H. ; Matsuda, T. & Kikuchi, E. (1990). Steam reforming of methane in a hydrogen-permeable membrane reactor. *Applied Catalysis*, Vol. 67, pp. 223-230.
- Xia, Y.; Lu, Y.; Kamata, K.; Gates, B. & Yin, Y. (2003). Macroporous materials containing three-dimensionally periodic structures. *Chemistry of Nanostructured Materials* (Ed.: Yang, P.), World Scientific 69-100.
- Zahedi, M.; Afra, B.; Dehghani-Mobarake, M. & Bahmani, M. (2009). Preparation of a Pd membrane on a WO<sub>3</sub> modified Porouys Stailless steel for hydrogen separation. *Journal of Membrane Science*, Vol. 333, No. 1-2, (May 2009), pp. 45-49, ISSN 0376-7388.

# Hydrogen Output from Catalyzed Radiolysis of Water

Alexandru Cecal and Doina Humelnicu  
*"Al.I. Cuza" University, Department of Chemistry, Iasi,  
Romania*

## 1. Introduction

Energy is the source of the vitality of industrial civilization and a necessary condition to save the world from poverty.

Current methods of generating energy for the industrial civilization undermine local, regional, global environmental conditions, and are based mainly on the processing of fossil resources.

Nowadays, the dawn of a new renewable energy revolution is occurring. It is the use of hydrogen instead of using oil and its derivatives. The stakes are global. The fight against the greenhouse effect requires finding a solution for the production of green energy.

The relatively new method of producing electricity is based on conversion, in fuel cells, of heat and energy of certain chemical substances, in electricity.

Since fuel cells convert fuel directly in electricity two to three times more efficiently than the thermodynamic conversion, the fuel cell is, by definition, a very efficient technology and, being a potential source of high energy still, clean and, compatible with renewable energy policy, reliable and sustainable over time (does not contain moving parts).

Hydrogen is the key to the future of energy having the highest energy content per unit weight of all known fossil. When burned in an engine, hydrogen produces zero issues; when the power source in a fuel cell, clean waters it is the only residue at 250-300 °C (International Atomic Energy Agency, [IAEA], 1999; Ohta&Veziroglu, 2006; Veziroglu, 2000). Combined with other technologies, such as carbon capture and storage, renewable energies, fusion energy, it is possible that the fuel cell will generate in future energies without harmful programs. Hydrogen is the only energy carrier making it possible to drive an aircraft using solar energy.

At the beginning of the XXIst century it is assumed that fuel cells will become a pervasive technology; hydrogen as fuel is becoming increasingly presented as the "solution", also by carmakers, ecologists, and governments who do not want to impose unpopular measures to limit car traffic.

The use of hydrogen will extend from cell phones to electric power plants.

Implementing the "hydrogen economy" will lead to changes not seen in the XIX century and early XX century when the world went through the experience of the last energy revolution.

Environmentalists argue that there is no alternative to a hydrogen based energy system because the reserves of exploitable oil and natural gas, indispensable resource materials not

only in energy industry, but also in petrochemicals (holds might miss today plastics), will be completely exhausted in less than a century.

T. N. Veziroglu summarizes some properties that recommend the use of hydrogen as energy carrier produced from unconventional technologies, because hydrogen is a concentrate (energy) sources of primary energy, presented to the consumer in a convenient form, having a relatively cheap production cost as a result of technological refinements. Moreover hydrogen has a high efficiency of converting in various forms of energy and represents an inexhaustible source, considering that it is obtained from water, and by use it becomes water.

Hydrogen production and consumption is a closed cycle, that maintains constant power production – water, and represent a classic cycle of raw material recycling – it is the easiest and cleanest fuel. Burning hydrogen is almost without polluting emissions, excepting  $\text{NO}_x$ , which can also be removed by proper adjustment of combustion conditions. It has a gravimetric "energy density" higher than any other fuel.

Hydrogen can be stored in several ways: gas at normal pressure or high pressure, as liquid or solid form of hydrides and can be transported long distances in any one of the above mentioned forms.

Assessing the effects of global economic shift to energetic system based on hydrogen it can be established that environmental pollution through energy production will not be a problem and hydrogen economy will lead to industrial transformations comparable to those produced in the microelectronics industry;

Moreover economic resources, financial, intellectual, intended for energy today and environmental and ecological problems, will be geared towards solving, for the good of mankind, other productive tasks. Life will get better. The literature state that the idea of a "hydrogen economy" would have been born and developed under the impact of oil shock, using hydrogen as fuel being presented as the last cry of modernity. In fact, however, using hydrogen as a "universal fuel" devoid of pollutant emissions appeared long before the oil shock in 1973.

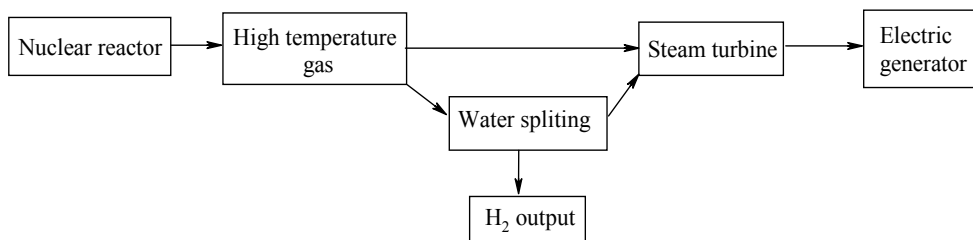
The literature state that the idea of a "hydrogen economy" would have been born and developed under the impact of oil shock, using hydrogen as fuel being presented as the last cry of modernity. In fact, however, using hydrogen as a "universal fuel" devoid of pollutant emissions appeared long before the oil shock in 1973.

## **2. Hydrogen production using the heat resulted in nuclear reactors after splitting the U-235 or Pu-239 nuclei**

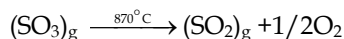
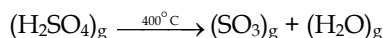
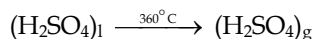
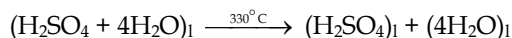
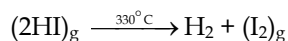
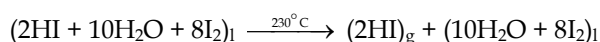
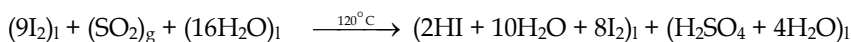
A series of tests are known to produce hydrogen by water splitting by making calls to the thermochemical cycles (hybrid) initiated by heat inside the reactor cores from fission of U-235, Pu-239, etc. (Besenbuch et al. 2000; Rahier et al., 2000; Tashimo et al., 2003, Verfondern, 2007)

An outline of such a plant for water decomposition through cycles of thermochemical reactions initiated by heat from inside a nuclear reactor is presented below:

To this end it used a series of thermochemical cycles or hybrid cycles that have been developed in different types of specialized research institutes or companies with business in areas of nuclear energy: General Atomics (USA) JAEA, Julich JRC, NRC -Ispra and other units from France, China, South Korea, Russia etc.



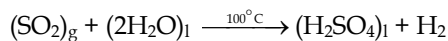
- a. *Sulfur-iodine cycle* is shown by the sequence of reactions that occur at different temperatures:



At first, through the Bunsen reaction, there result two-phase nemiscible acids: HI and  $\text{H}_2\text{SO}_4$ .

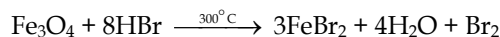
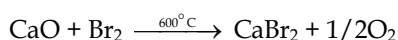
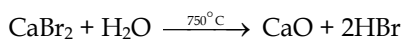
These oxides, under the influence of high temperature, will decompose releasing hydrogen (and oxygen), and  $\text{I}_2$  and  $\text{SO}_2$ , which will restore (as reactants) the Bunsen reaction.

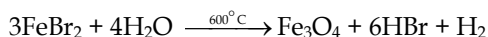
- b. *Westinghouse cycle* takes place through two reactions, due to sulfuric acid:



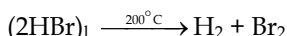
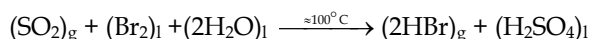
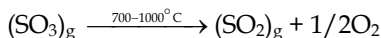
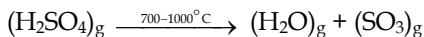
The second reaction takes place in an electrolytic cell at low temperature when there result hydrogen and sulfuric acid in the aqueous phase at a potential of 0.17 V and at a pressure of about 1 MPa. Then the cycle is repeated with gaseous  $\text{H}_2\text{SO}_4$ .

- c. *UT-3 cycle*, developed in Japan, is represented by the following reactions:

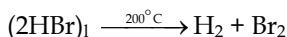
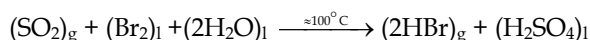
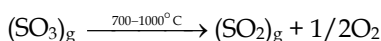
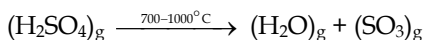




on the account of salts or metal oxides in solid form, as "spherical pellets". Due to the  $\text{CaBr}_2$  high melting point, the efficiency of the hydrogen production process is of only 40%.

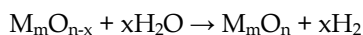


d. *The Mark-13 or the cycle of  $\text{H}_2\text{SO}_4$  -  $\text{Br}_2$* , is described by the following chemical transformations:



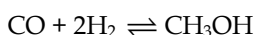
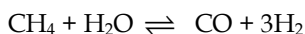
Here hydrogen is released by decomposing electrolytic HBr, with an efficiency of 37 %.

e. *Metal-metal oxide cycle* developed at PSI, Switzerland, schematically as follows:



If water splitting occurs at  $650^\circ\text{C}$ , the reduction of the metal oxide is at a temperature of  $2000^\circ\text{C}$ . The research was done on the system:  $\text{Fe}_3\text{O}_4/\text{FeO}$ ;  $\text{Mn}_3\text{O}_4/\text{MnO}$ ,  $\text{ZnO} / \text{Zn}$ ;  $\text{Co}_2\text{O}_3/\text{CoO}$  or  $\text{MFe}_2\text{O}_4$ , where  $\text{M} = \text{Cu}, \text{Ni}, \text{Co}, \text{Mg}, \text{Zn}$ .

f. *Thermochemical cycle methane- methanol - iodomethane* was tested in South Korea and can be played as follows:

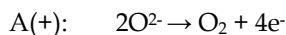
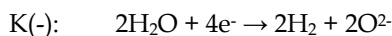


Transformations occur at  $150^\circ\text{C}$  and a pressure of 1.2 MPa.

There are also known other hydrogen production processes based on thermochemical cycles, such as another one, HHLT and others.



- g. *High-temperature electrolysis.* Hydrogen can be produced by electrolysis of water vapor at 750-950 ° C, by the reactions:



### 3. Radiolytic split of water molecules in several experimental conditions

In this sense, it know a number of studies respecting the hydrogen obtaining by catalyzed decomposition of water under the influence of nuclear radiation emitted by some sources, including fission products recovered from spent nuclear fuel.

Thus, Maeda and co-workers have studied obtaining of molecular hydrogen by irradiation with  $\gamma$  radiations of silicagels and metal oxides dispersed in water.

They found that a higher radiolytic yield was obtained in the silicagels case with pore diameter of about 2 nm, and the most active area against water decomposition under the action of  $\gamma$  radiation was the SiO<sub>2</sub> dried at 100 °C (Maeda et al., 2005).

Yamamoto and collab. have used in their investigations nanoparticles of TiO<sub>2</sub> and  $\alpha$ - and  $\beta$ -Al<sub>2</sub>O<sub>3</sub> noting that the radiolytic yield of molecular hydrogen production when irradiated with  $\gamma$  radiation of aqueous solutions with  $\alpha$ - and  $\beta$ - Al<sub>2</sub>O<sub>3</sub> is 7-8 times higher than water irradiation without catalyst (Yamamoto et al., 1999)

Jung and collab. studied the effect of adding EDTA on the reaction of water radiolysis containing TiO<sub>2</sub> and noted that the presence of this organic compound increased the radiolytic yield of molecular hydrogen (Jung et al., 2003).

Rotureau and collab. studied the obtaining molecular hydrogen from water radiolysis in presence of SiO<sub>2</sub> and of mesoporous molecular sieves obtaining a value of radiolytic yield of molecular hydrogen  $G_{H_2} = 3$  (Rotureau et al. 2006).

Recently, Kazimi and Yildiz studied the obtaining of hydrogen through alternative nuclear energy, including radioactive wastes that result from nuclear plants (Yildiz & Kazimi, 2006).

Brewer and colleagues have used complex supramolecular of ruthenium and rhodium in the study of water decomposition under the action of radiant energy (Brewer & Elvington, 2006).

Masaki and Nakashima studied the gamma-irradiation of Y zeolites both in form Na (NaY) and form H (HY). Discussions on obtaining H and H<sub>2</sub> were based on comparing values  $G_{H_2}$  and  $G_H$  between systems NaY- and HY-water. They obtained higher values of radiolytic yield of H<sub>2</sub> due to energy transfer from zeolite to absorbed water (Nakashima & Masaki, 1996).

The  $G(H_2)$  values of HY system were 3 times higher than those of system NaY.

Seino and co-workers observed that the nanoparticles of TiO<sub>2</sub> and Al<sub>2</sub>O<sub>3</sub> dispersed in water would lead to a significant increase of radiolytic yields of hydrogen to radiolytic yield of pure water. They also noted that radiolytic yield of hydrogen depends on gamma radiation dose absorbed and metal oxide particle size (Seino et al., 2001; Seino et al., 2001).

Yoshida and collab. proposed to get hydrogen by gamma irradiation of water in the presence of Al<sub>2</sub>O<sub>3</sub> particles of different diameters. The maximum amount of hydrogen produced was 3.48  $\mu\text{mol}/\text{cm}^3$  for water containing Al<sub>2</sub>O<sub>3</sub> particles with diameter of 3  $\mu\text{m}$ , value three times higher than the one obtained for the systems with pure water (Yoshida et

al., 2007). Hydrogen produced from catalyzed reactions of water radiolysis was determined by gas chromatography.

Cecal and others (intended to obtain hydrogen through water radiolysis in the presence of solid catalysts, in different experimental conditions, under the action of gamma rays emitted by a source of  $\text{Co}^{60}$ ). The produced hydrogen was determined by a device specially adapted for mass spectrometer (Cecal et al., 2001; Cecal et al., 2003; Cecal et al., 2004). This study may be accomplished using as irradiation  $\gamma$  source so called spent nuclear fuel elements extracted from nuclear plants as high level radioactive wastes, instead of the  $\beta$ - $\gamma$   $\text{Co-60}$  or  $\text{Cs-137}$  radionuclides.

#### 4. Irradiation characteristics

Qualitative and quantitative effects of phenomena suffered by substances after interaction with ionizing radiation are determined by the characteristics of the irradiation process.

Irradiation process is characterized by the following quantities (Arnikor, 1987; Ferradini & Pucheault, 1983):

- radiation intensity,
- absorbed dose,
- absorbed dose rate,
- dose equivalent,
- linear energy transfer radiation (LET).

*Radiation intensity*: This feature expresses the amount of energy emitted by source, and expressed in J/s.

*Absorbed dose*, denoted  $D_a$ , represents the amount of energy transferred by incident radiation to unit mass of matter, energy absorbed by matter, respectively. In I.S. absorbed dose is expressed as *Gray (Gy)*:

$$1 \text{ Gy} = 1 \text{ J/kg} = 6, 24 \cdot 10^{13} \text{ eVg}^{-1}.$$

*Absorbed dose rate* represents the energy received by the unit of mass per unit time. It is usually expressed in Gy/s, but there are also used kGy/h, Mgy/h, as well as rad/s, rad/min, rad/day if necessary.

*Equivalent dose* represents the radiation effect on the organism. Even at the same absorbed dose biological effects on living organisms may be different. This differential action is quantified by introducing a quality factor of incident radiation. As unit of measurement in I.S. there is used *Sievert (Sv)*, which is defined as equivalent dose to the body (tissue) exposed to radiations with quality factor equal with unit when absorbed dose is 1 Gy.

$$1 \text{ Sv} = v \times 1 \text{ Gy}, \text{ where:}$$

$v$  – coefficient which depends on radiation quality, for X or  $\gamma$ ,  $v=1$ .

*Linear energy transfer radiation (LET)*

As a result of interaction with matter, electromagnetic radiations continuously lose energy, photon beam intensity gradually decreasing as they penetrate matter. The phenomenon is called linear energy transfer noted LET, and it is expressed quantitatively by the radiation energy loss per unit length,  $\text{LET} = -dE/dx$ , with the unit keV/ $\mu\text{m}$ .

Linear energy transfer should increase as the particle slows down towards the end of the journey so that much of the ionization and excitation produced by fast electrons is produced on the path of gamma radiation, where linear energy transfer value is much higher than average.

With the linear energy transfer there can be characterized, by a number the „quality” of a radiation, not always describing the type of radiation and its energy.

## 5. Water radiolysis

### 5.1 General considerations

A permanent presence of water and ionizing radiation in nature, show the appearance of water radiolysis on Earth and outside it. Laboratory experiments and computer simulations of the processes induced by radiolysis relate to radioactive action of  $^{40}\text{K}$  in the ocean 3800 Ma (1 Ma= 1 000 000 years ago) and natural radiation from the groundwater nuclear reactor of the Earth in its infancy.

Radiation-induced decomposition of water molecules, water radiolysis, is carefully studied for several authors, as Debiern, Marie Skłodowska Curie, O. Fricke, J. Franck, J. Weiss, Hart, Boag using different experimental conditions.

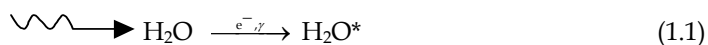
### 5.2 Mechanism of water radiolysis

As a result of water radiolysis with a beam of high-energy radiation as  $\gamma$  radiation or an accelerated electron beam, it occurs excitation and ionization of water molecules, phenomenon that leads to the formation of various ion species, radicals and new molecules – radical theory of water radiolysis (Belloni & Mostafavi, 2001; Kiefer, 1989; Majer, 1982).

According radicals’ theory, radiolysis of water flows in three distinct phases:

#### a. Physical stage

A few pico-seconds after irradiation it is discovered the occurrence of excited molecules,  $\text{H}_2\text{O}^*$  and ionized  $\text{H}_2\text{O}^+$  as of secondary electrons with high kinetic energy:



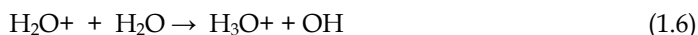
Secondary electrons, Compton or photoelectric are fast slowed down and thermalised, after which they are promptly captured by water molecules, hydrating themselves, ( $e_{\text{aq}}^-$ ). Highlighting the hydrated electron is of great importance in the development of radiation chemistry. Electron hydration corresponds to the stabilization phase through dipole of solvent molecules:



At *physico-chemical* stage, which takes about  $10^{-13}$  s, absorbed energy is redistributed through interactions with other stable or excited molecules and ions by splitting olyatomic molecules or through ion-molecule reactions.

It is noticeable that ion-molecule reactions do not necessarily imply ionized molecule movement; interactions can take place in liquid and at a distance of order of several interatomic distances:





Ionized molecule can be neutralized by an electron:



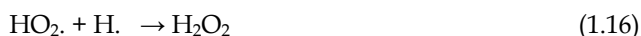
which quickly dissociates:



Formed radicals can combine with each other, forming molecules:



*Chemical stage*, which takes about  $10^{-10}$  s is the phase in which there occur reactions between species formed in previous steps: recombination between radicals, ions, molecules and free electrons:

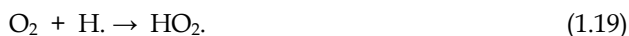


reaction which allows to explain the increase concentration of  $\text{H}_2\text{O}_2$ .

Molecular oxygen is produced through the following reactions:



In the presence of dissolved molecular oxygen reaction takes place:



Hydrated electron  $\text{e}_{\text{aq}}^-$  has both properties:



Therefore, a few nano-seconds after irradiation, in water there are present the following species ionic, radicalics and molecules:

$\text{H}_3\text{O}^+$ ,  $\text{HO}^-$ ,  $\text{H} \cdot$ ,  $\cdot\text{OH}$ ,  $\text{HO}_2 \cdot$ ,  $\text{H}_2$ ,  $\text{O}_2$ ,  $\text{H}_2\text{O}_2$ , of which the following are stable:  $\text{H}_2$ ,  $\text{H}_2\text{O}_2$ ,  $\text{H}_3\text{O}^+$ , and short-lived free radicals  $\text{e}_{\text{aq}}^-$ ,  $\text{H} \cdot$ ,  $\cdot\text{OH}$ ,  $\text{HO}_2 \cdot$ .

### 5.3 Physical and chemical properties of primary species formed in water radiolysis

The properties of some primary species formed in water radiolysis are presented in Table 1.

Property	$e^-_{aq}$	H·	·OH
Absorption maximum(nm)	720	<200	225
$\epsilon$ , molar extinction coefficient, (L/mol·cm)	19.000 (720nm)	1620 (188nm)	240 (240nm)
Diffusion coefficient ( $cm^2s^{-1} \times 10^5$ )	4.9	8	2.3
Mobility ( $cm^2V^{-1}s^{-1} \times 10^3$ )	1.98	-	-
$\Delta H$ ionization, kJ/mol	-	9.6	11.9
Electrons affinity (eV)		0.776	1.83

Table 1. Properties of some primary products of water radiolysis.

1. *The hydrated electron  $e^-_{aq}$* , is present in system a few milliseconds in the most favorable case. The hydrated electron is considered as a chemical species with a very high reactivity being a very strong reductant; it attaches immediately to radicals molecules or to meet ions. The formed new product containing an extra electron is generally unstable and dissociates forming new radicals or ions in an unstable valence state. Except s block metals other metal, cations are reduced as following:



Anions  $F^-$ ,  $Cl^-$ ,  $Br^-$ ,  $I^-$ ,  $CN^-$ ,  $OH^-$ ,  $SCN^-$ , with complete electronic layers and oxoanions  $(SO_4)^{2-}$ ,  $(PO_4)^{3-}$ ,  $(ClO_4)^-$ ,  $(CO_3)^{2-}$  do not react with the hydrated electron.

Organic molecules, aliphatic hydrides, alcohols, ethers and amines practically do not react with  $e^-_{aq}$ , while aliphatic carbonyl compounds such as aldehydes and ketones present a high reactivity.

Redox potential of water has high value  $E^0(nH_2O/e^-_{aq}) = -2.87 V$  and it is not annihilated by any other species present in the system except the hydrated electron ( $e^-_{aq}$ ) within dismutation processes.



2. *Hydrogen atom, H*

The hydrogen atom or atomic hydrogen is a strong reductant, almost as vigorously as the hydrated electron, with the standard potential  $E^0(H_3O^+/H) = -2.3V$ , at  $pH=0$ .

It can uproot hydrogen from a C-H link from an organic compound to form  $H_2$ . It may also be a supplement to a double link.

Radical  $HO\cdot$

Radical  $HO\cdot$  is a strong oxidant, extremely energetic with standard potential  $E^0(HO/H_2O) = -2.76 V$ ; it is a species considered very dangerous for living cells in radiobiology. Oxidant properties of radical  $HO\cdot$  depend on the pH of the medium. It is considered that at  $pH > 9$ , the radical is completely dissociated:



Radicals  $\cdot OH$  may participate in reactions with various components of the system:





Radical  $\text{HO} \cdot$  reacts with organic compounds as it follows:

- extracting a hydrogen atom;
- can addition to a double bond;
- oxidizes primary alcohols to aldehydes in aqueous solutions;
- oxidizes aldehydes to acids, acids from peroxyacids etc.

In favorable conditions it can strip an electron from one molecule to form a cation.

#### 4. Radical $\text{HO}_2$ .

$\text{HO}_2$  radicals are obtained by the reaction of  $\text{HO} \cdot$  With  $\text{H}_2\text{O}_2$  in general on the radiation trajectory or, possibly, in mass solution, if there are no  $\text{HO} \cdot$  Radical traps and, of course, with a considerable concentration of  $\text{H}_2\text{O}_2$ . In accordance with this, the yield of these radicals would be higher in the case of low specific ionization radiation. Indeed, it was found that when water radiolysis with  $\alpha$  radiation of  $^{210}\text{Po}$ , radiochemical yield of  $\text{HO}_2$  radicals is 0.23, while at the  $\gamma$  radiolysis  $G_{\text{HO}_2}=0.02$ . Also,  $\text{HO}_2$  radicals are obtained from radiolysis of aqueous solutions containing  $\text{O}_2$ , according to the reaction:



The presence of these radicals in aqueous solutions was highlighted both by indirect methods and direct methods. Indirectly, there was studied the variation of the conductivity of irradiated water containing  $\text{O}_2$ , in which case it has been detected the presence of some intermediate products with a lifetime in excess of 0.1 s and was attributed to  $\text{O}_2^-$  -ions radical, which could come from  $\text{HO}_2$ .  $\text{HO}_2$  radicals were revealed by direct methods using pulse radiolysis of water containing  $\text{O}_2$ .

Due to the complexity of the phenomenon taking place in a watery liquid system when it interacts with  $\gamma$  radiations this methodology was used for many purposes. This way, a new practical method for obtaining the most diverse products appeared, known as *radiolytic method*.

Within the research required in this paper, the radiolytic method is used to obtain hydrogen in the presence of different catalysts, using high-activity nuclear radiation about  $5 \times 10^4$  Ci, emitted by spent nuclear fuel or  $^{60}\text{Co}$  sources, process studied by other researchers, too.

### 5.4 Radiolytic yield

*Radiolytic yield concept was introduced in order to quantify the effect of radiation, i.e. in order to calculate the amount of products formed depending on the dose of radiation absorbed.*

There can be distinguished:

- *Ionic-yield, g*, also called ion pair yield, which is the ratio between the number of equivalents turned, the number of molecules that interact and the number of the formed ions.
- *Radiolytic yield, G* is the number of molecules (M) transformed by an energy equivalent to 100 eV absorbed

$$G = \frac{M}{100\text{eV}} \quad (1)$$

This definition does not conform to International System units.

A new definition expresses G yield, as expressed in mol J<sup>-1</sup>, equivalent to 9.65 × 10<sup>6</sup> molecules/100 eV, so that the defined value can be converted in I.S. units through multiplication with the 0.36 × 10<sup>-7</sup> factor.

To determine the yield of radiolysis products there are considered the maximum yields of radiolytic decomposition of water in which:

- W<sub>a</sub> - the average ionization potential of water in the gas phase (30eV);
- I<sub>a</sub> - minimum ionization potential of water (12.56 eV)
- E<sub>a</sub> - the minimum excitation potential of water molecules (6.5 eV)

100 eV absorbed will form 100 / W<sub>a</sub> water molecules ionized.

Formation of an ion consumes excitation energy equal to (W<sub>a</sub>-I<sub>a</sub>) eV, so, for 100/W<sub>a</sub> ions, at absorption of 100eV there results an excitation energy of 100/W<sub>a</sub> (W<sub>a</sub>-I<sub>a</sub>) eV.

In this way, due to excitation, there will be radiolysed 100(W<sub>a</sub>-I<sub>a</sub>) / W<sub>a</sub> E<sub>a</sub> = water molecules.

$$G_a = \frac{100}{W_a} + \frac{100(W_a - I_a)}{W_a I_a} = \frac{100}{W_a} \left[ 1 + \frac{W_a - I_a}{E_a} \right] \text{ molecules/100eV} \quad (2)$$

G<sub>a max</sub> = 12 molecules/100eV.

In liquid phase G<sub>a max</sub> is approximately two times smaller.

In neutral aqueous solutions deaerated and irradiated with gamma radiation from a <sup>60</sup>Co source, the primary yield for radicals and molecules, in μmol/J and atoms/100eV is shown in Table 2.

On the other hand, (Majer, 1982) radiolytic yield depends not only on the concentration (C<sub>x</sub>) of the transformed reactant or on the reaction product occurred, but also on the irradiation time (t) with nuclear radiations having a rate dose (D):

$$G_x = \frac{C_x \cdot N}{D \cdot t} \cdot 100 \quad (3)$$

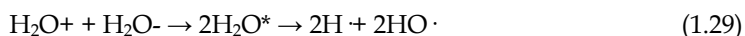
N - Avogadro's number. Product D t = D<sub>a</sub> is dose of absorbed energy, expressed in eV L<sup>-1</sup> mol<sup>-1</sup>. Radiolytic yield for different species stable or unstable: H ·, HO ·, HO<sub>2</sub> ·, H<sub>2</sub>O<sub>2</sub>, H<sub>2</sub>, etc. is determined from the slope obtaining by plotting the previous relation (3) in coordinates C<sub>x</sub> = f (D<sub>a</sub>).

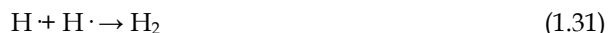
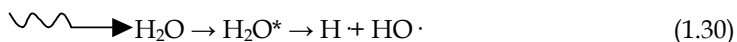
The concentrations of chemical species encountered by primary irradiation (H · and HO ·) or subsequent reactions (HO<sub>2</sub> ·; H<sub>2</sub>O<sub>2</sub>, H<sub>2</sub>..) can be determined by physico-chemical methods such as: electron paramagnetic resonance (EPR), the pulse radiolysis, spectrophotometry etc. or from measurements of luminescence or radical capture.

Henglein proposed a similar formula to determine the radiolytic yield (Heinglein et al., 1969):

$$G_x = \frac{C_x \cdot N \cdot 100}{D_a \cdot g \cdot 1000 \cdot 6.24 \cdot 10^{13}} = \frac{C_x}{D_a \cdot g} \cdot 9.66 \cdot 10^8, \text{ mol J}^{-1} \quad (4)$$

Given the sequence of chemical reactions initiated by nuclear radiation:





It appears that the formation of a single pair of radicals  $\text{H}\cdot$  and  $\text{HO}\cdot$  (reaction 1.30) decomposes with a single molecule of water. For the appearance of molecular hydrogen (the stable product of radiolysis – reaction 1.31) two molecules of water will decompose, while producing a molecule of hydrogen peroxide (as a stable product) needed also two molecules of water (reaction 1.34).

The balance equation becomes:

$$G_{(-\text{H}_2\text{O})} = G_{(\text{H}\cdot)} + 2G_{(\text{H}_2)} = G_{(\text{HO}\cdot)} + 2G_{(\text{H}_2\text{O}_2)} + 3G_{(\text{HO}_2\cdot)} \quad (5)$$

Type of $\gamma$ radiation, 0.1-10MeV	Linear energy transfer, keV/ $\mu\text{m}$	$G_{(\text{H}_2)}$ $\mu\text{mol/J}$	$G_{(\text{H}_2\text{O}_2)}$ $\mu\text{mol/J}$	$G_{(e_{aq}^-)}$ $\mu\text{mol/J}$	$G_{(\text{H}\cdot)}$ $\mu\text{mol/J}$	$G_{(\text{HO}\cdot)}$ $\mu\text{mol/J}$	$G_{(\text{HO}_2)}$ $\mu\text{mol/J}$
pH=3-11	0.20	0.047	0.073	<b>0.28</b>	0.06	<b>0.28</b>	0.0027
pH=0.46	0.20	0.041	0.081	0	0.378	<b>0.301</b>	0.0008
		$G_{(\text{H}_2)}$ at/100eV	$G_{(\text{H}_2\text{O}_2)}$ at /100eV	$G_{(e_{aq}^-)}$ at/100eV	$G_{(\text{H}\cdot)}$ at/100eV	$G_{(\text{HO}\cdot)}$ at/100eV	$G_{(\text{HO}_2)}$ at/100eV
pH=3-11	0.20	0.45	0.704	<b>2.7</b>	0.579	<b>2.79</b>	0.026005
pH=0.46	0.20	0.39	0.78	0	3.64	<b>2.9</b>	0.0077

Table 2. Primary radiolytic yield values for ions and radicals from irradiated water at 25 °C.

The values from Table 2 show that the prevalent species are the solvated electron and the OH radical.

In the range of pH = 3-12, forming efficiency of primary species does not vary, but the radicals may be located in various chemical forms depending on pH.



These existing acid-base equilibria are characterized by constant acidity / basicity. For example, at pH = 7, HO<sub>2</sub>·, over 99 % of the radicals formed according to the reaction:



are represented as oxide, O<sup>2-</sup>.

Table 3 shows acidic and basic forms of data and pK radicals.

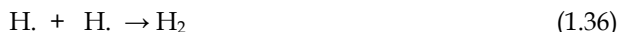
Radicals	Acidic form	Basic form	pK
H·	H·	e <sup>-</sup> <sub>aq</sub>	9.6
e <sup>-</sup> <sub>aq</sub>	H·	e <sup>-</sup> <sub>aq</sub>	9.6
·OH	·OH	O·	11.9
HO <sub>2</sub> ·	HO <sub>2</sub> ·	O <sub>2</sub> <sup>-</sup>	4.8

Table 3. pK values for acidic and basic forms of the radicals formed from water radiolysis.

Among the primary species formed in the radiolysis reactions, important are the reactions of free radicals and radical solution.

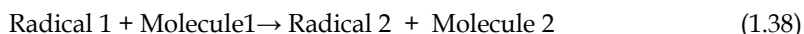
*Free radical reactions:* the most species of free radicals are unstable in solution and hence highly reactive. They quickly recombine with each other to form stable molecular products.

As shown above, most of the molecular species formed during irradiation are formed by recombination of free radicals:



Radical reactions take place, generally, in solution and have fast kinetics.

Free radicals can react with molecules to form other molecules or free radicals, according to the general equation:



### 5.5 Considerations on the radiolytic yield (G<sub>H<sub>2</sub></sub>)

Mass spectrometer was calibrated before measurements of irradiated samples on the basis of resulted hydrogen in a total chemical reaction:



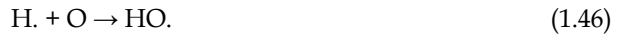
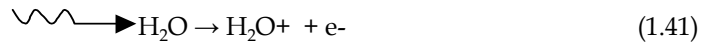
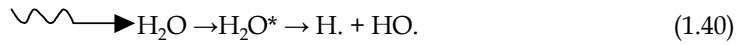
From 1.08 g Zn → 0.01 mol H<sub>2</sub> → the spectrogram corresponds in the table to a bit of 1.58 ·10<sup>6</sup> a.u. intensity (for anionic and cationic clays) and 2.68 ·10<sup>7</sup> a.u. for the species with mass number 2, respectively.

Schematic diagram of the measurements performed is given below:

**Sample → Mass spectrometer → PC → Mass spectrometer**

Before each measurement, to avoid any contamination of samples by chemical species remaining from the previous sample, the mass spectrometer was ensured a vacuum of 2.10<sup>-6</sup> Torr. Mass spectrogram was recorded by a computer in coordinates peak intensity = f (Mass number), and recorded data were processed with chemistry program Origin 7.1.

It is well known that radiolysis of water through two stages, primary and secondary, leads to the formation of various chemical species such as:  $H_2$ ,  $O_2$ ,  $H_2O_2$ ,  $HO\cdot$ ,  $O$ ,  $HO_2\cdot$ , etc. through a series of reactions with excited species, ionized and free radicals:



Considering that energy transfer from the catalyst to water molecules plays an important role in the decomposition of water in the presence of catalyst, radiolysis can be expressed as:



To calculate the *radiolytic yield* of hydrogen, Henglein's formula:

$$G = \frac{c \cdot N_A \cdot 100}{D_a \cdot \rho \cdot 1000 \cdot 6.25 \cdot 10^{13}} = \frac{c}{D_a \cdot \rho} \times 9.66 \cdot 10^8 \quad (6)$$

where:

$D_a$  - absorbed dose Gy ( $1J/kg$  or  $6.24 \cdot 10^{13}$  eV/g ) representing the product of dose debit ( $D$ ) and irradiation time ( $t$ )

$\rho$  - density of irradiated material ( $g/cm^3$ )

$N_A$  -Avogadro number

Considering that:

$$c = b \cdot \frac{I_x}{I_{et}} \quad (7)$$

*Radiolytic yield* of hydrogen resulted from radiolysis are calculated with the expression derived:

$$G_{H_2} = \frac{b \cdot I_x}{D \cdot t \cdot \rho \cdot I_{et}} \cdot 9.66 \times 10^6 \quad (8)$$

where:

$$D \cdot t = D_a - \text{is absorbed dose in Gy} \quad (9)$$

$\rho$  – density of irradiated material (g/cm<sup>3</sup>)

$b$  – amount of hydrogen resulting from the spectrometer calibration (mol H<sub>2</sub>/1kg H<sub>2</sub>O)

$I_{et}$  – intensity peak corresponding to molecular hydrogen from the reaction mass spectrometer calibration

$I_x$  – intensity peak corresponding to molecular hydrogen from the reaction of catalyzed radiolysis

Radiolytic yield was calculated for:

$b = 1.53 \text{ mol H}_2 / 1\text{kg H}_2\text{O}$ ,  $I_{et} = 2.68 \cdot 10^7$  arbitrary unit (cationic and anionic clays)

$b = 1.556 \text{ mol H}_2 / 1\text{kg H}_2\text{O}$ ,  $I_{et} = 1.58 \cdot 10^7$  arbitrary unit (catalyst with and double perovskitic oxides)

In mass spectrograms there have identified a number of species (H<sub>2</sub>, O<sub>2</sub>, H<sub>2</sub>O<sub>2</sub>, HO·, O·, HO<sub>2</sub>·), but radiolytic yield was established only for molecular hydrogen, which is a stable product of radiolysis. The other identified species (HO·, HO<sub>2</sub>·...) may occur in the ionization source mass spectrometer from the decomposition of molecules of water (as vapor), whereas as free radicals, disappear immediately.

## 6. Experimental part

In order to study the catalyzed radiolysis of water under the action of nuclear radiation, with hydrogen release, there were used two types of catalysts:

### a. *Clays.*

In this case natural anionic clays have been used, such as: (MgZn<sub>2</sub>Al, Zn<sub>2</sub>Al, Zn<sub>2</sub>CuAl, Mg<sub>2</sub>Al) and cationic R<sub>1</sub> and C<sub>1</sub> pillared with: Cr, Fe, Al and Ti.

Raw clay (R<sub>1</sub>, C<sub>1</sub>) have a complex mineralogical composition: SiO<sub>2</sub> – 69.61 %, Al<sub>2</sub>O<sub>3</sub> – 19.7 %, MgO – 2.41 %, Fe<sub>2</sub>O<sub>3</sub> – 1.27 %, Na<sub>2</sub>O – 1.31 %, K<sub>2</sub>O – 0.18 % etc. The cation exchange capacity (CEC) of 82 mEq/100 g clay was determined with ammonium acetate, and the specific surface area is between 140-142 m<sup>2</sup> / g.

At first there were prepared clays of the type C<sub>1</sub>-Na and R<sub>1</sub>-Na by cations exchanges naturally present, by dispersing those raw solid mass skins in a solution of 1M NaCl at a temperature of 22 °C and a contact time of 12 hours.

After that, the solid clay was separated by centrifugation as C<sub>1</sub>-Na or R<sub>1</sub>-Na of the remaining solid solution and dried at 110 °C. Clay particle size range was 0.2-0.8 mm (Van Olphen, 1963).

To obtain a microporous material with increasing interlamelare space and volume of pore, was performed Keggim inserting of the polications Al<sub>13</sub><sup>7+</sup> between the layers of clay, resulting in pillared samples (C<sub>1</sub>-Al and R<sub>1</sub>-Al) with a specific surface of 280 m<sup>2</sup>/g and 320 m<sup>2</sup>/g, respectively. Pillars of the cationic clays C<sub>1</sub>-Na and R<sub>1</sub>-Na with other cations were obtained by ion exchange Na-M<sup>n+</sup> where M<sup>n+</sup> is Cr<sup>3+</sup>, Fe<sup>3+</sup> and Ti<sup>2+</sup> (Asaftei et al., 2002; Popovici et al., 2006).

### b. *Site zeolites and mesoporous silica MCM-41.*

The Pt<sup>2+</sup>-ZSM-5 samples with different SiO<sub>2</sub>/Al<sub>2</sub>O<sub>3</sub> ratios were prepared by ion exchange: H<sup>+</sup>-ZSM-5-Pt<sup>2+</sup> in a solution of H<sub>2</sub>PtCl<sub>6</sub> (10<sup>-3</sup>M) at a temperature of 22 °C and at a time 10 contact hours. Afterwards, the zeolitic precipitate was washed with distilled water and dried at 110 °C. Platinum content was 1-2%. The same process was applied to NH<sub>4</sub> - ZSM-5.

In order to prepare mesoporous silica MCM-41, there was made a mixture of: 27.3 % SiO<sub>2</sub> and 10.8 % NaOH, hexadecyl-trimethyl ammonium bromide, C<sub>16</sub>H<sub>33</sub>N(CH<sub>3</sub>)<sub>3</sub>Br and H<sub>2</sub>SO<sub>4</sub> (95 %), having the following molar ratio: 1m SiO<sub>2</sub>: 0.297 m NaOH: 0.414m C<sub>16</sub>H<sub>33</sub>N(CH<sub>3</sub>)<sub>3</sub>Br: 0.277m H<sub>2</sub>SO<sub>4</sub>: 82.54m H<sub>2</sub>O. After a contact time of 30 minutes, there has been obtain a gel which was then placed in an autoclave at 105 °C for 48 hours. After that, the resulting solid product was washed and dried at room temperature (Mastalir et al., 2008; Zholobenko et al., 1997).

The experiments proceeded as it follows (Cecal et al., 2008; Hauta et al., 2009): different amounts of each catalyst were weighed and introduced in 50 ml bottles, over which 30 ml distilled water were added. Then the glass vials were sealed with rubber cork, paraphyned outside and subjected to various doses of radiation energy. The stable radiolysis product, H<sub>2</sub>, resulted in the above reactive systems, was determined quantitatively by a mass spectrometer, previously calibrated. The relationship between the irradiated sample and mass spectrometer was performed with a special device, which had at one end a chromatographic syringe needle that pierced the rubber stopper.

The obtained experimental results are represented in the following figures:

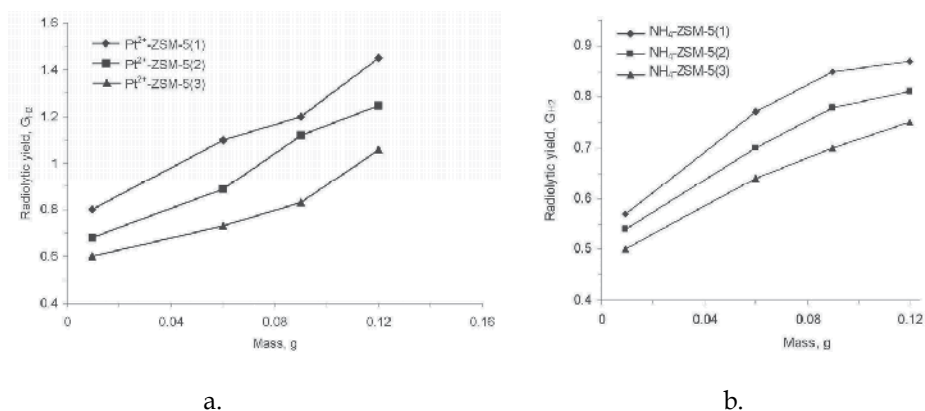


Fig. 1. Plots of radiolytic yield vs catalyst mass for a) Pt<sup>2+</sup>-ZSM-5 and b) NH<sub>4</sub><sup>+</sup>-ZSM-5 with different SiO<sub>2</sub>/Al<sub>2</sub>O<sub>3</sub> ratios SiO<sub>2</sub>/Al<sub>2</sub>O<sub>3</sub> = 140, (2) SiO<sub>2</sub>/Al<sub>2</sub>O<sub>3</sub> = 80, (3) SiO<sub>2</sub>/Al<sub>2</sub>O<sub>3</sub> = 15.

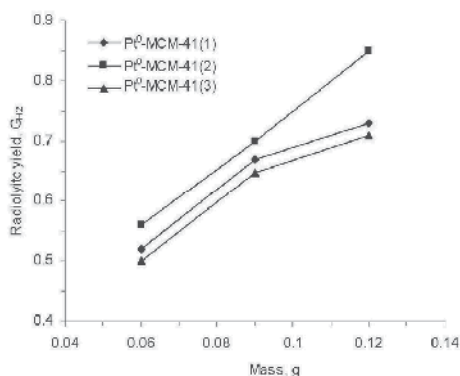
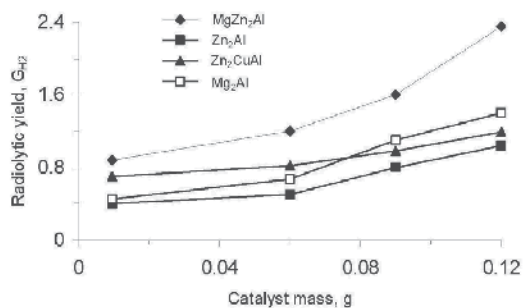
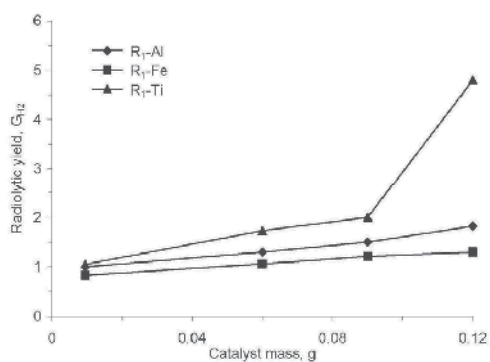


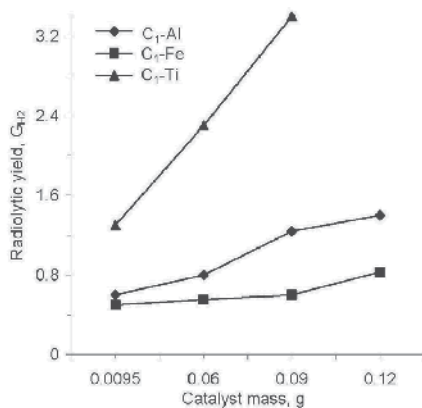
Fig. 2. Plots of radiolytic yield vs. catalyst mass for Pt<sup>0</sup>-MCM-41 impregnated for 1) short temps 2) long temps, 3) before irradiation.



3.1

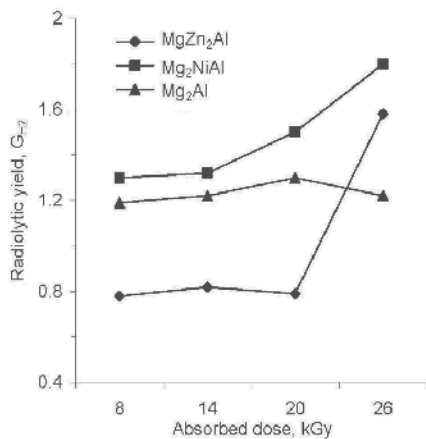


3.2

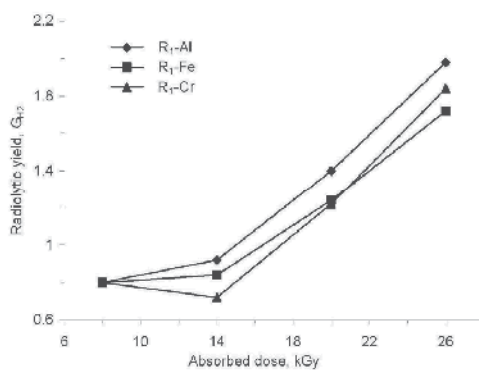


3.3

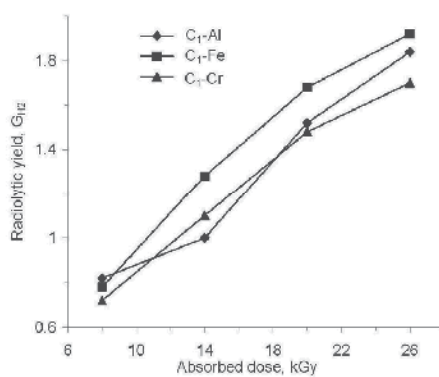
Fig. 3. Dependence of radiolytic yield of molecular hydrogen on the catalyst amounts for: (3.1) anionic clays; (3.2) R<sub>1</sub>-clays and (3.3) C<sub>1</sub>-clays.



4.1



4.2



4.3

Fig. 4. Variation of radiolytic yield ( $G_{H_2}$ ) vs. absorbed dose for: (4.1) anionic clays, (4.2) R<sub>1</sub>-clays and (4.3) C<sub>1</sub>-clays.

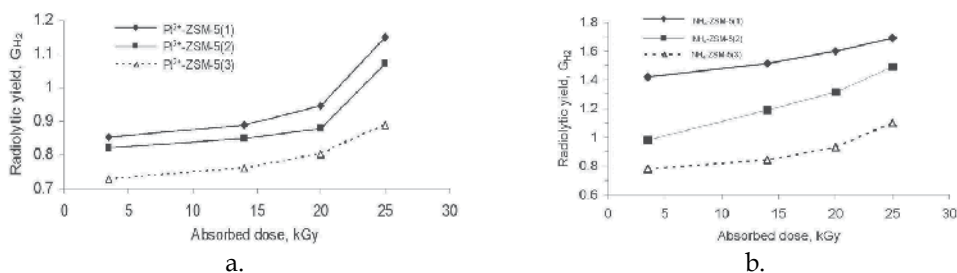


Fig. 5. Plots of radiolytic yield vs. absorbed dose for: a) Pt<sup>2+</sup>-ZSM-5 and b) NH<sub>4</sub>-ZSM-5 with different SiO<sub>2</sub>/Al<sub>2</sub>O<sub>3</sub> ratios (1) SiO<sub>2</sub>/Al<sub>2</sub>O<sub>3</sub> = 140, (2) SiO<sub>2</sub>/Al<sub>2</sub>O<sub>3</sub> = 80, (3) SiO<sub>2</sub>/Al<sub>2</sub>O<sub>3</sub> = 15.

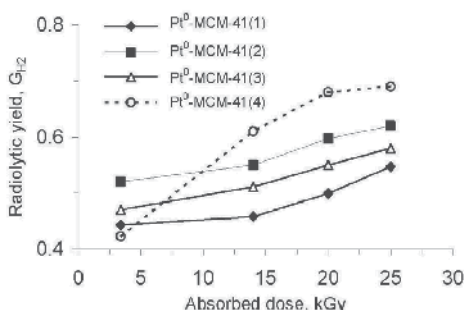


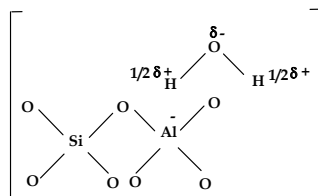
Fig. 6. Plots of radiolytic yield vs. absorbed dose for: a) Pt<sup>0</sup>-MCM-41 impregnated samples for 1) short temps 2) long temps, 3) before irradiation, 4) after irradiation.

It is worth mentioning that the release of hydrogen was obtained only in the catalyst samples, previously subjected to irradiation with  $\gamma$  radiations.

Explanations of the catalytic effects could be: the catalytic role of clay could be explained by facilitating the appearance of intermediate structures.

In the case of clays studied as catalysts in water radiolysis, it can be considered that in active status, the catalyst creates a structural availability so that dipole water molecules can penetrate its pores.

In this excited configuration of the catalyst, water molecules are subjected to Coulomb forces of attraction-repulsion of the ionic species in the clay structure.



Under the action of gamma radiation, H-OH bonds in water molecules adsorbed on the catalyst surface will be easier to split towards non-adsorbed water molecules.

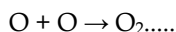
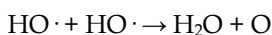
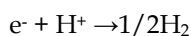
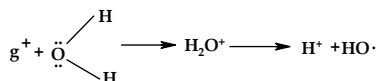
It has been noticed an increasing amount of hydrogen resulted from water radiolysis in the presence of clays in comparison with the reference sample, irradiated under the same experimental conditions. In the case of pillared clays, greater efficiency in the decomposition of water have the pillared with Ti. Pillared clays R<sub>1</sub>-metal had an important catalytic effect

towards C<sub>1</sub>-metal, probably due to SiO<sub>2</sub>/Al<sub>2</sub>O<sub>3</sub> different ratio and the presence of 3d series microelements. Ionic species in the composition of clay acts as Coulomb attraction-repulsion forces on the dipole water molecules, facilitating H-OH bonds break under the action of nuclear radiation.

In the case of zeolites, through the interaction of nuclear radiation on the surface, there might appear “charge carriers” e<sup>-</sup> and g<sup>+</sup>, namely:



Water molecules can be broken down as it follows:



The differences reported in the radiolytic yields are due to the respective catalyst involved in the radiolytic splitting of water (Chemerisov et al. 2001; Gondal et al. 2004).

## 7. References

- Arnikar Jeevan, H. (1987) *Essential of Nuclear Chemistry*, J. Wiley, ISBN 81-224-0712-9, New York, USA, pp.302-317
- Asaftei, I.; Balba, N. & Iofcea, Gh. (2002). *Elements of catalysis*. CERMI, ISBN 973-8188-08-3, Iasi, Romania, pp.172-183
- Belloni, J. & Mostafavi, M. (2001). *Radiation chemistry, present status and future trends*, in C.D. Jonah, B. M. Rao (eds), Elsevier, ISBN 0-444-82902-4, Amsterdam, Netherlands
- Besenbuch, G. E.; Brown, L. C.; Funk, J. F. & Sowalter, S. K. (2000). High Efficiency Generation of Hydrogen Fuels using nuclear power, in *Nuclear production of hydrogen, First information. Exchange Meeting*, Paris, France, 2-3 oct., pp. 205-218
- Brewer, K. J. & Elvington, M. (2006). *Supramolecular Complexes as Photocatalysts for the Production of Hydrogen from Water*, U. S. Patent, 7 pp.122
- Cecal, Al.; Paraschivescu, A.; Popa, K.; Colisnic, D.; Timco, G. & Singorean L. (2003). Radiolytic splitting of water molecules in the presence of some supramolecular compounds, *Journal of Serbian Chemical Society*, Vol.68, No. 7, pp. 593-598, ISSN 0352-5139
- Cecal, Al.; Goanta, M.; Palamaru, M.; Stoicescu, T.; Popa, K.; Paraschivescu, A. & Anita, V. (2001). Use of some oxides in radiolytical decomposition of water, *Radiation Physics and Chemistry*, Vol.62, No.4 pp. 333-336, ISSN 0969-806X
- Cecal, Al.; Colisnic, D.; Popa, K.; Paraschivescu, A.; Bilba, N. & Cozma, D. (2004). Hydrogen yield from water radiolysis in the presence of zeolites. *Central European Journal of Chemistry*, Vol.2, No.2, pp. 247-253, ISSN 1895-1066



- Cecal, Al.; Hauta, O.; Macovei, A.; Popovici, E.; Rusu, I. & Puica Melniciuc, N. (2008). Hydrogen Yield from water radiolysis in the presence of some pillared clays. *Revue Roumaine de Chimie*, Vol. 53, No. 9, pp. 875-880, ISSN 0035-3930
- Chemerisov, S.C.; Werst, D. W. & Trifunac, A. D.; (2001). Formation, trapping and kinetics of H atoms in wet zeolites and mesoporous silica. *Radiation Physics and Chemistry*, Vol. 60, No.4-5, pp. 405-410, ISSN 0969-806X
- Ferradini, C. & Pucheault, J. (1983). *Biologie de l'action des rayonnements ionisants*, Messon, ISBN 2-225-78859-6, Paris, France, pp.6-22
- Gondal M. A.; Hameed, A.; Yamani, Z. N. & Suwaiyan, A. (2004). Production of hydrogen and oxygen by water splitting using induced photo-catalysis over Fe<sub>2</sub>O<sub>3</sub>. *Applied Catalysis A:General*, Vol. 268, No.1-2, pp. 159-167, ISSN 0926-860X
- Hauta, O.; Macovei, A.; Apostolescu, G.; Ganju, D. & Cecal, Al. (2009). Radiolytic output of hydrogen as environmentally friendly energy vector. *Environmental Engineering and Management Journal*, Vol. 8, No. 1, pp. 91-95, ISSN 1582-9596
- Henglein, A; Schnabel, W & Wendenburg, J. (1969). *Einführung in die Strahlenchemie*, Verlag Chemie, GmbH, Weinheim, Germany, pp.20-25
- Jung, J.; Jeong, S.; Chung, H. H.; Lee, M. J.; Jin, J. H. & Park, K. B. (2003). Radiocatalytic H<sub>2</sub> production with gamma-irradiation and TiO<sub>2</sub> catalysts, *Journal of Radioanalytical and Nuclear Chemistry*, Vol.258, No.3, pp. 543-546, ISSN 0236-5731
- Kiefer, J. (1989). *Biologische Strahlenwirkung*, Birkhauser Verlag, ISBN 3-7643-2266-7, Basel, Germany, pp.105-107
- Majer, V. (1982). *Grundlagen der Kernchemie*, C. Hanser Verlag, ISBN: 3-446-13377-1 München, Germany, pp. 369-396
- Maeda, Y.; Kawara, Y.; Kawamura, K.; Hayami, S.; Sugiuhara, S. & Okai, T. (2005). Hydrogen Gas Evolution from Water Included in Silica Gel Cavity and on Metal Oxides with gamma-Ray Irradiation, *Journal of Nuclear and Radiochemical Sciences*, Vol.6, No.2, pp. 131-134, ISSN 1345-4749
- Mastalir, A.; Rac, B.; Kraly, Z.; Tasi, G. & Molnar, A. (2008). Preparation of monodispersed Pt nanoparticles in MCM-41 catalytic applications, *Catalysis Communicatios*, Vol.9, No.5, pp. 762-768, ISSN 1566-7367
- Nakashima, M. & Masaki, N. M. (1996). Radiolytic hydrogen gas formation from water adsorbed on type Y zeolites, *Radiation Physics and Chemistry*, Vol.47, No.2, pp. 241-245, ISSN 0969-806X
- Ohta, T. & Veziroglu, T. N. (2006). Energy carriers and conversion systems with emphasis of hydrogen, in *Energy Carriers and Conversion Systems*, [Ed. Tokio Ohta], in *Encyclopedia of Life Support Systems (EOLSS)*, Developed under the Auspices of the UNESCO, Eolss Publishers, Oxford, UK, [<http://www.eolss.net>]
- Popovici, E.; Humelnicu, D. & Hristodor, C. (2006). Retention of UO<sub>2</sub><sup>2+</sup> ions from simulated residual waters on Romanian pillared clays. *Revue Chimie (Bucharest)*, Vol. 57, No. 7, pp. 675-678, ISSN 0034-7752
- Rahier, A.; Fonteyne, A.; Klein, M.; Ponnet, M.; Pirard, J. P. & Germain, A. (2000). Hydrogen production associated to the treatment of nuclear wastes, in *Nuclear production of hydrogen, First information. Exchange Meeting*, Paris, France, 2-3 oct., pp. 197-204
- Rotureau, P.; Renault, J. P.; Lebeau, B.; Patarin, J. & Mialocq, J.-C. (2006). Radiolysis of Confined Water: Molecular Hydrogen Formation, *ChemPhysChem*, Vol.6, pp. 1316-1323, ISSN 439-4235

- Seino, S.; Yamamoto, T. A.; Fujimoto, R.; Hashimoto, K.; Katsura, M.; Okuda, S. & Ohitsu, K. (2001). Enhancement of Hydrogen Evolution Yield from Water Dispersing Nanoparticles Irradiated with Gamma-Ray, *Journal of Nuclear Science and Technology*, Vol. 38, No.8, pp. 633-636, ISSN 0022-3131
- Seino, S.; Yamamoto, T. A.; Fujimoto, R.; Hashimoto, K.; Katsura, M.; Okuda, S.; Okitsu, K. & Oshima, R. (2001). Hydrogen evolution from water dispersing nanoparticles irradiated with gamma-ray/size effect and dose rate effect, *Scripta materialia*, Vol.44, No.8-9, pp. 1709-1712, ISSN 1359-6462
- Tashimo, M.; Kurasawa, A. & Ikeda, K. (2004). Role of nuclear produced hydrogen for global environment and energy, in *Nuclear Production of Hydrogen – Second Information Exchange Meeting* Argonne, Illinois, USA, 2-3 oct. 2003, pp. 43-47
- Van Olphen, H. (1963). *An introduction to Clay Colloid Particle Technology*, 1<sup>th</sup> edition, Micromeritics Instrument Corp, Norcross, Georgia, USA, pp.67-89
- Verfondern, K. (Editor).(2007).*Nuclear energy for hydrogen production*, Schriften der Forschungszentrum Jülich: Reihe Energietechnik/Energy Technology, Vol. 58, ISBN 978-3-89336-468-8, Zentralbibliothek Verlag, D-52425 Jülich, Germany, pp.91-110
- Veziroglu, T. N. (2000). Quarter century of hydrogen movement 1974-2000, *International Journal of Hydrogen Energy*, Vol.25, No.12, pp. 1143-1150, ISSN 0360-3199
- Zholobenko, V. L.; Holmes, S. M.; Cundy, C.S. & Dwyer, J. (1997). Synthesis of MCM-41 materials an in situ FTIR study, *Microporous Materials*, Vol. 11, No.1-2 , pp. 83-86, ISSN 1387-1811
- Yamamoto, T. A.; Seino, S.; Katsura, M.; Okitsu, K.; Oshima, R. & Nagata, Y. (1999). Hydrogen gas evolution from alumina nanoparticles dispersed in water irradiated with  $\gamma$ -ray, *Nanostructured Materials*, Vol.12, No.5-8, pp. 1045-1048, ISSN 0965-9773
- Yildiz, M. & Kazimi, S. (2006). Efficiency of Hydrogen Systems using Alternative Nuclear Energy Technologies, *International Journal of Hydrogen Energy*, Vol.31, No. 1, pp. 77-92, ISSN 0360-3199
- Yoshida, T.; Tanabe, T.; Sugie, N. & Chen, A. (2007). Utilisation of gamma-ray irradiation production from water, *Journal of Radioanalytical and Nuclear Chemistry*, Vol.272, No.3, pp. 471-476, ISSN 0236-5731
- <http://satyen.baindur.org/>. IAEA TecDoc-1085, Hydrogen as an Energy carriers and its production by nuclear power, May 1999, Safety issues in Nuclear Hydrogen production with the VHTR
- <http://www.top-alternative-energy source.com/hydrogen-from-water.html>. Hydrogen from water



*Edited by Pavel Tsvetkov*

We are fortunate to live in incredibly exciting and incredibly challenging time. Energy demands due to economic growth and increasing population must be satisfied in a sustainable manner assuring inherent safety, efficiency and no or minimized environmental impact. These considerations are among the reasons that lead to serious interest in deploying nuclear power as a sustainable energy source. At the same time, catastrophic earthquake and tsunami events in Japan resulted in the nuclear accident that forced us to rethink our approach to nuclear safety, design requirements and facilitated growing interests in advanced nuclear energy systems. This book is one in a series of books on nuclear power published by InTech. It consists of six major sections housing twenty chapters on topics from the key subject areas pertinent to successful development, deployment and operation of nuclear power systems worldwide. The book targets everyone as its potential readership groups - students, researchers and practitioners - who are interested to learn about nuclear power.

Photo by ktsimage / iStock

**IntechOpen**

